ORNL-5306

PHYSICS Division - Annual PROGRESS REPORT

Period Ending June 30, 1977

ORNL-5306
Distribution Category
UC-34

Contract No. W-7405-eng-26

PHYSICS DIVISION
ANNUAL PROGRESS REPORT
for Period Ending June 30, 1977

P. H. Stelson, Director

SEPTEMBER 1977

OAK RIDGE NATIONAL LABORATORY
Oak Ridge, Tennessee 37830
operated by
UNION CARBIDE CORPORATION
for the
ENERGY RESEARCH AND DEVELOPMENT ADMINISTRATION

Reports previously issued in this series are as follows:

ORNL-2718	Period Ending March 10, 1959
ORNL-2910	Period Ending February 10, 1960
ORNL-3085	Period Ending February 10, 1961
ORNL-3268	Period Ending January 31, 1962
ORNL-3425	Period Ending May 21, 1963
ORNL-3582	Period Ending January 31, 1964
ORNL-3778	Period Ending December 13, 1964
ORNL-3924	Period Ending December 31, 1965
ORNL-4082	Period Ending December 31, 1966
ORNL-4230	Period Ending December 31, 1967
ORNL-4395	Period Ending December 31, 1968
ORNL-4513	Period Ending December 31, 1969
ORNL-4659	Period Ending December 31, 1970
ORNL-4743	Period Ending December 31, 1971
ORNL-4844	Period Ending December 31, 1972
ORNL-4937	Period Ending December 31, 1973
ORNL-5025	Period Ending December 31, 1974
ORNL-5137	Period Ending December 31, 1975

Contents

1. Accelerators

HOLIFIELD HEAVY ION RESEARCH FACILITY—PHASE I

J. B. Ball
J. A. Martin
J. A. Biggerstaff
B. J. Casstevens[1]
R. S. Lord
D. L. Haynes[2]
C. M. Jones
R. C. Juras[1]
R. L. Robinson
J. K. Bair
R. M. Beckers[3]
E. Eichler[4]
K. N. Fischer[1]
C. D. Goodman
E. D. Hudson
J. W. Johnson
R. F. King[5]
J. D. Larson[5]
B. Lieberman[2]
L. B. Maddox[1]
M. L. Mallory[6]
J. E. Mann
J. W. McConnell[7]
G. S. McNeilly
W. T. Milner
S. W. Mosko
J. A. Murray[2]
J. D. Rylander[2]
R. O. Sayer[1]
J. A. Steed[2]
N. F. Ziegler

PROJECT STATUS

Holifield Heavy Ion Research Facility—Phase I (HHIRF) includes a 25-MV folded tandem electrostatic accelerator, two new experimental areas for use with beams from the tandem, and a beam transport and injection system to couple the tandem to the Oak Ridge Isochronous Cyclotron (ORIC), which allows use of the cyclotron as an energy booster. The facility is scheduled for completion in the fall of 1979.

Site preparation was completed in February 1976, and building construction began in April 1976. On May 1, 1977, the building construction was 36% complete. The most obvious part of the construction is the tower, which now rises over 80 ft above the ground-floor level. Figure 1.1 shows the artist's conception of the appearance of the completed facility; Figs. 1.2 and 1.3 show photographs of construction progress taken April 20, 1977.

The present schedule calls for completion of the tower to about the 140-ft level by mid-July, to be followed by installation of the accelerator pressure vessel and completion of the tower and building about one year later. Installation of the tandem is scheduled to begin in July 1978, with completion of installation and testing in October of the following year.

Design is complete for the radiation safety system, the SF_6 and O_2 monitoring systems, the operational and research intercom, and the beam and signal transport systems; much of this equipment has been ordered.

Construction of the 25-MV folded tandem accelerator by the National Electrostatics Corporation (NEC) proceeded with only minor deviations from the original schedule. Major achievements during this period include completion of all components requiring electrode-insulator bonding operations (column support posts, acceleration tubes, and corona tubes), receipt by NEC of most purchased components, and assembly of the basic injector and accelerator column structure in the NEC plant at Madison, Wisconsin. Figure 1.4 is a photograph of the lower one-fourth of the column structure.

The tandem accelerator control system is based on two Interdata 7/32 computers interfaced by NEC to four CAMAC Serial Highways. NEC received the computers and CAMAC equipment, and the interface was designed, built, and tested. The overall structure of the software control system was developed; software modules fitting this framework are now being developed. Some testing of components was carried out with ad hoc software. Testing of light links for transmission of data to the high-voltage terminal and to points along the accelerating column is under way.

All the components of the SF_6 transfer and storage system were delivered to Oak Ridge. The two 450-hp SF_6 compressors and the three 2000-ft[3]

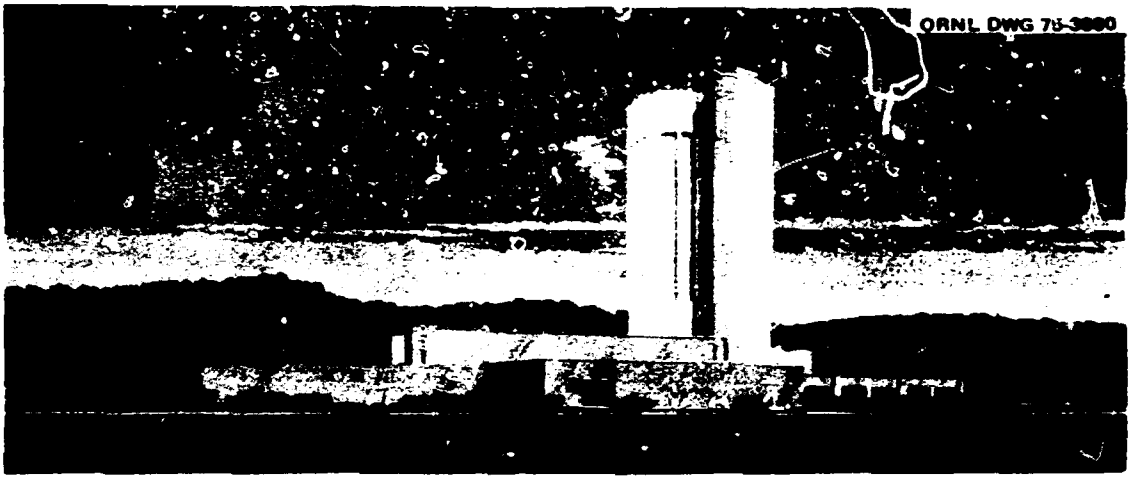

Fig. 1.1. Artist's conception of the ORIC building with the addition of the tower for tandem.

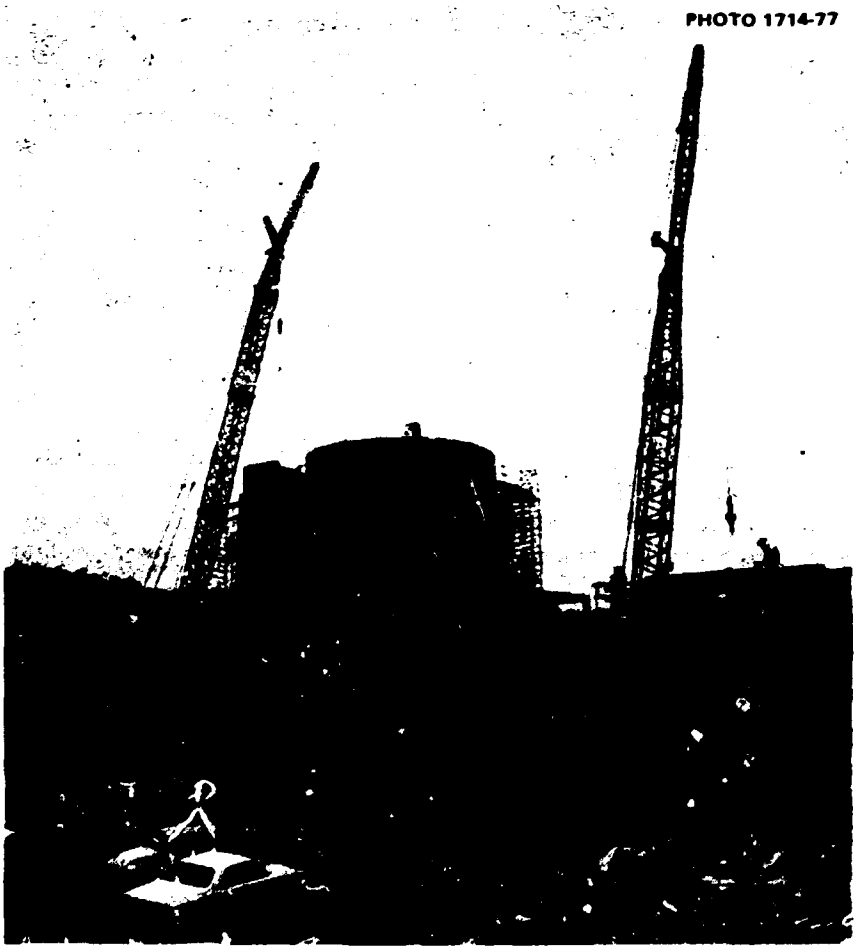

Fig. 1.2. Construction site on April 20, 1977. Concrete walls and roof of the first floor, which is predominantly below the elevation of the street, are complete. Steel structure for the remaining two floors is in place to the right of the tower. The corner of the gas-compressor building is shown on the right. This building will house two 450-hp compressors used in transferring the SF_6 and three SF_6 storage tanks.

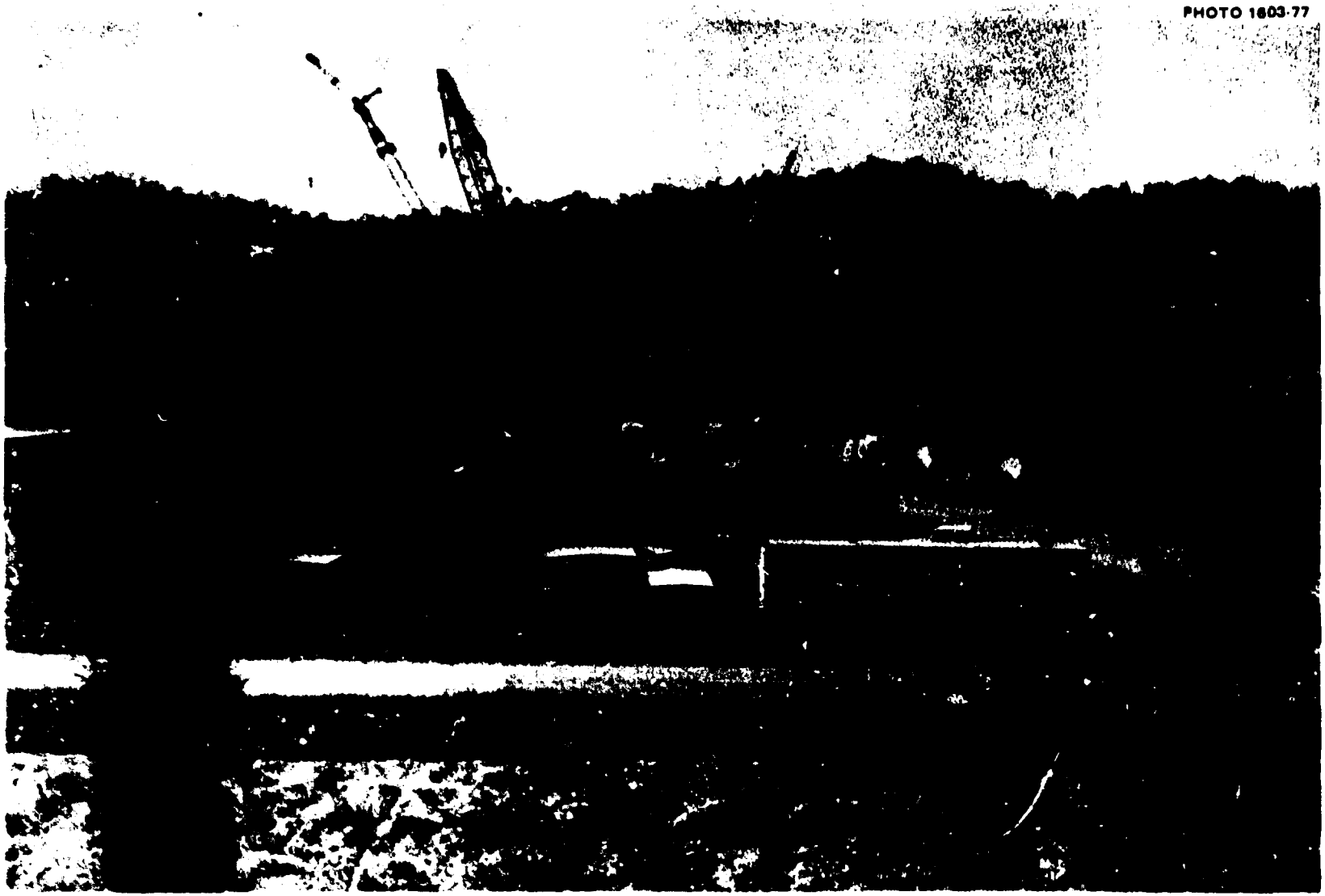

Fig. 1.3. In the foreground are fabricated sections of the pressure vessel for the tandem accelerator. In the background, the tower that will house the tandem accelerator can be seen under construction above the ORIC building. A concrete pour and storage tank installation are in progress.

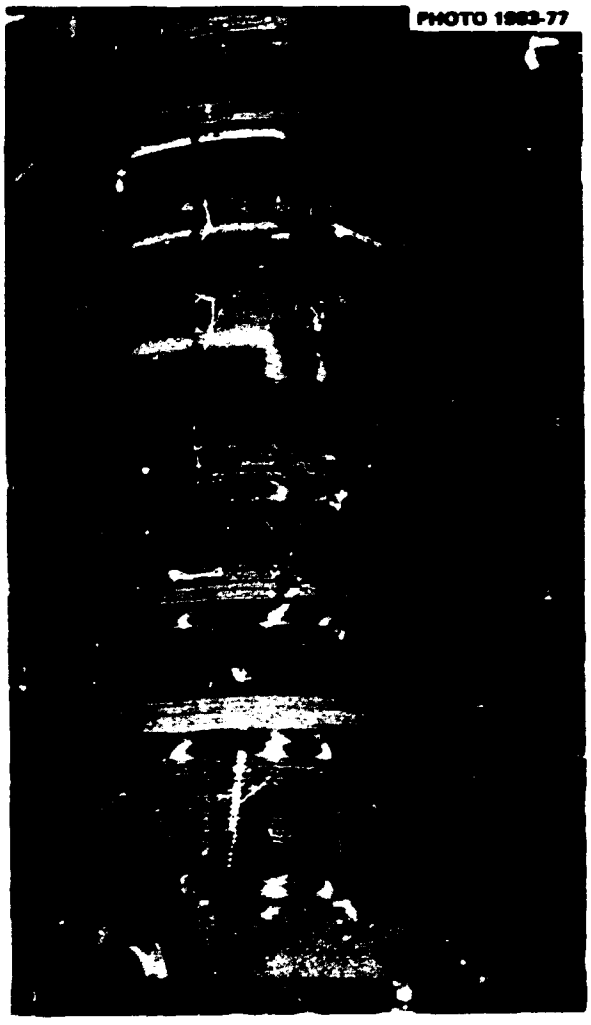

Fig. 1.4. Photograph of the lower one-fourth of the tandem accelerator column structure taken at the NEC plant in Madison, Wisconsin, in February 1977. In ascending order are the forged steel support ring, four 24-in. modules, the first minor dead section, and three 24-in. modules. The equipotential hoops have been placed in their final position only on the first module.

liquid SF_6 storage vessels were installed in the building. Field erection of the accelerator pressure vessel began in Oak Ridge in January 1977. All the vessel assembly work that could be done prior to installation in the tower was completed in April.

A number of activities are also in progress within the Physics Division in preparation for operation of the new tandem accelerator. These activities include negative-ion source development, buncher and buncher control system development, stripping and ion-optics studies, and development accelerator diagnostic techniques and computer-based models for SF_6 transfer processes. Most of these activities are discussed in other sections of this report.

The first major installation of beam injection hardware on the ORIC was made during the period from January to May 1977. During this time, the ORIC was shut down and the new dee and rf trimmers were installed (Figs. 1.5 and 1.6).

Fig. 1.5. New dee mounted on the ORIC dee stem. The copper surface of the dee stem is brazed to the copper dee.

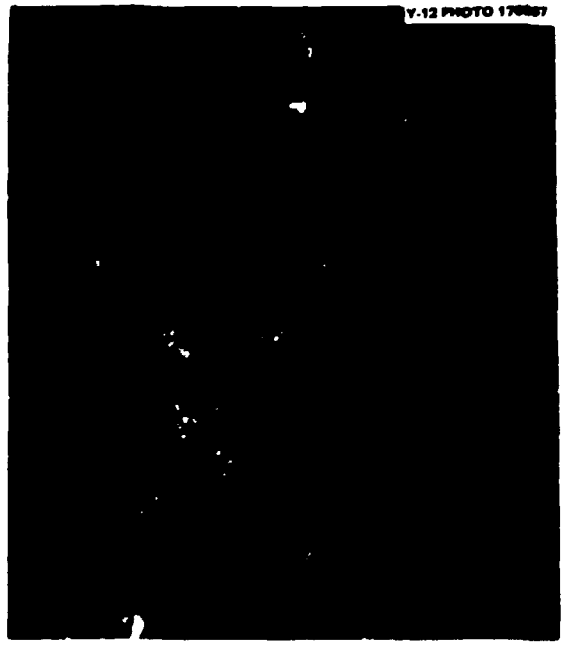

Fig. 1.6. New rf trimming capacitors. The surface that faces the dee is at the top, and the slot for the injected beam can be seen in this surface.

the rf liner was modified to be compatible with the dee and to fit the foil positioner, and the rails for the inflection magnet were installed in the dee stem. The dee and trimmers are slotted on the periphery to provide a passage for the injected beam as it crosses the pole edge. Improved voltage-holding characteristics, dimensional stability, and frequency range are also expected with the new system. Start-up is now scheduled for about June 1. Engineering is about 80% complete, with 160 of 214 drawings and 39 of 65 data sheets completed. Orders were placed for many of the major hardware items. These include the foil positioner, the inflection magnet and power supply, the quadrupoles and power supplies, the steering magnets, and, of course, the dee and trimmers. The major items not yet on order include the two magnets which make the 90° bend from the vertical tandem beam line to the horizontal injection line and a number of smaller injection line components.

1. UCC-ND Computer Sciences Division.
2. UCC-ND Engineering Division.
3. Instrumentation and Controls Division.
4. Chemistry Division, deceased.
5. Consultant.
6. On temporary leave at Michigan State University, East Lansing.
7. Neutron Physics Division.

EXPERIMENTAL FACILITIES

R. L. Robinson

Figure 1.7 illustrates the planned layout for HHIRF. Beam lines 23, 33, 35, and the first leg of 31 are to be built as part of the heavy-ion project. Beam line 31 will be extended in the future so that, by means of three bending magnets, beams from both accelerators can be brought through lines 61, 62, 64, and 65.

The time-of-flight system was completed and installed on beam line 53. A conceptual design was developed for a large multipurpose scattering chamber. Criteria are being developed for a gamma-ray spectrometer system and recoil mass spectrometer. Possible upgrade of the broad-range spectrometer and development of a new magnetic spectrometer are under study.

In an attempt to ensure a smooth-running operation appropriate for a national facility, we initiated a system in which there will be a resident scientist responsible for each major experimental device and/or beam line. The tasks of each "mentor," as presently envisioned, are (1) to assure that the beam lines and experimental apparatus available to users-at-large are maintained in good condition; (2) to be involved with equipment that is or will be a part of the mentor's beam line (this could range from one extreme where the resident scientist has primary responsibility for design of a device to the other extreme where he is aware that the device is being planned but his involvement is only to ensure that the device is compatible with the facility); (3) to approve any modifications to the beam lines and experimental devices located permanently at the facility; and (4) to assist in providing a liaison between the users and the resources and services available at HHIRF.

This mentor system will not be fully realized until there is formation of an experimental support group, which, according to present planning, is to be initiated in 1978. However, mentors are already being selected in areas where there are clearly defined needs in 1977. Those who have agreed to serve as mentors and their areas of responsibility (refer to Fig. 1.7 for beam-line numbers) are:

J. Ford assisted by J. G. del Campo—The broad-range Elbek magnetic spectrometer, the Enge split-pole magnetic spectrometer, and associated beam lines 52 and 33.

C. Goodman—A large new multipurpose scattering chamber.

M. Halbert—The existing 30-in.-diam scattering chamber and associated beam line 51.

N. Johnson—Germanium gamma-ray spectrometer systems and associated beam lines 41 and 23.

R. Mlekodaj—The beam lines (31 and 62) between the tandem accelerator and University Isotope Separator at Oak Ridge (UNISOR).

C. Moak—Beam line 35 for atomic and solid-state physics apparatus.

R. Stokstad and T. Obenshain—The new time-of-flight system and the associated beam lines 53 and 54.

F. Plasil—A new recoil mass spectrometer.

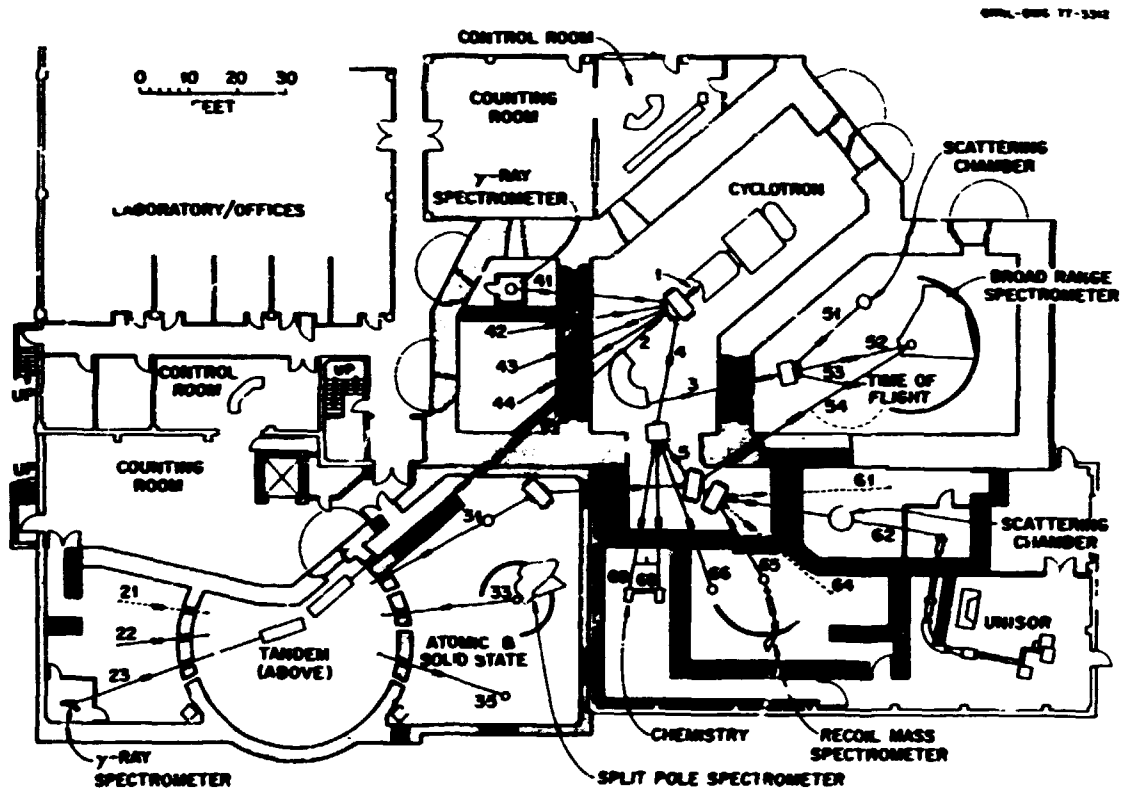

Fig. 1.7. Planned experimental layout of HHIRF.

DATA ACQUISITION

J. A. Biggerstaff R. C. Juras[1]
N. F. Ziegler J. W. McConnell[2]

We intend to provide dual data acquisition systems in each of the two counting rooms (cyclotron and tandem) for a total of four systems. Systems not in use on-line will be used for setup of upcoming experiments, postcalibrations, and off-line data reduction. The systems will have large amounts of disk storage and core storage; emphasis is being placed on capabilities for real-time and "nearly-real-time" data processing of multiparameter data requiring several million channels of storage. All interfacing to experimental equipment will be via high-speed CAMAC data channels. We acquired two 300-megabyte disk systems and interfaced them to an existing data acquisition computer. Software drivers for these units were completed, but development of a file management system is being impeded by demands for use of the computer for ongoing experimental programs. Funds were approved for purchase of a minimal set of hardware to permit development of the software and hardware (interface) for the new systems.

1. Instrumentation and Controls Division.
2. Neutron Physics Division.

USERS ACTIVITIES

E. Eichler[1] R. L. Robinson

The HHIRF Users Group has a membership of 254. Another 169 people have requested that they be sent information on the project, particularly the HHIRF Newsletter, which is published three times a year. The primary effort of the Users Group during 1976, as expressed through its six-person Executive Committee, has been to study the experimental needs of the users at the facility. This study was made by eight Working Groups made up of members of the Users Group. These Working Groups investigated the following areas: Atomic Physics Apparatus, Computer Systems, Gamma-Ray Spectrometers, Magnetic Spectrometers, Neutron Spectrometers,

Recoil Mass Spectrometers, Scattering Chambers, and Time-of-Flight Systems.

The efforts of these Working Groups were brought to a focus at a one-day meeting held October 4, 1976, at ORNL. From this meeting came the following list of recommendations:

1. Undertake design study of a recoil mass spectrometer;
2. Acquire computer hardware immediately and begin software development;
3. Begin design of a large (about 60-in.-diam) scattering chamber;
4. Determine needs for a gamma-ray spectrometer system;
5. Design a buncher/chopper system for producing pulsed beams for experimental studies using only the tandem accelerator;
6. Move the split-pole magnetic spectrometer now located at the EN tandem site to the east experimental room of HHIRF;
7. Study the possibility of modifying the broad-range spectrometer to a split-pole design;
8. Defer commitment to a new magnetic spectrometer until the usefulness of the existing spectrometers is established;
9. Select beam lines 31, 33, 35, and 23 as those funded as part of the project (see Fig. 1.7);
10. Consider alternate configurations for the use of space in the existing south experimental hall;
11. Develop more complete data to evaluate needs for atomic physics.

Implementation and study of these recommendations are being actively pursued at ORNL.

Attendees of this one-day session on October 4 also generated a four-year equipment priority list. The years in which they recommended that funds be requested are listed in Fig. 1.8.

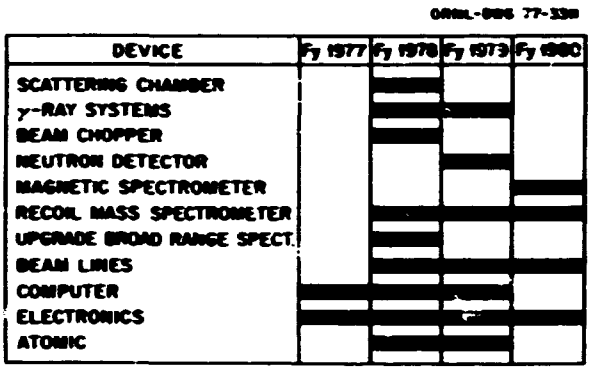

Fig. 1.8. Schedule proposed by users for fabrication and procurement of new experimental apparatus and beam lines.

HOLIFIELD HEAVY ION RESEARCH FACILITY—PHASE II

J. B. Ball
J. A. Martin
R. M. Beckers[1]
D. A. Dyslin[1]
L. E. Eckert[1]
S. E. Hamblen[1]
E. D. Hudson
D. R. Wallace[1]
F. Irwin
R. S. Lord
J. E. Mann
G. S. McNeilly[2]
J. A. Murray[1]
R. L. Robinson
J. A. Steed[1]

A complete redesign of the Phase II addition to HHIRF was completed, and a conceptual design report[3] was prepared. The new Phase II facility features a higher-energy separated-sector cyclotron (SSC) and a more efficient arrangement of beam transport systems and experiment areas. The emphasis in the design of the new facility was to provide balanced performance for high-energy light ions and for very heavy ions and to take full advantage of the high-intensity capability of ORIC as a light-ion injector. An additional goal was to reduce the electrical power consumption wherever possible.

Cyclotron

The basic criteria for the SSC were developed in 1975[4] and refined in 1976. The present design has an energy rating of 400 q^2/A MeV, where q is the charge number and A the mass number of the accelerated ion, to give energies up to 100 MeV/amu for fully

1. Chemistry Division, deceased.

stripped light ions and up to 12 MeV/amu for very heavy ions such as uranium. Figure 1.9 shows the energy-mass characteristics of the cyclotron, using the 25-MV tandem as the injector.

The principal characteristics of the cyclotron are given in Table 1.1. The facility plan giving the locations of the ORIC, the 25-MV tandem, and the Phase II booster cyclotron is shown in Fig. 1.10.

Magnet design. The magnet design was evaluated with a 0.15-scale model.[5] The measurements show that the focusing characteristics were essentially as designed, with ν_r and ν_z away from significant resonances over the full operating range of the accelerator.

The magnetic field between adjacent poles is large enough to require cancellation along the injected beam path if a nearly fixed path were to be used. However, using a special magnet outside the cyclotron, a solution was found that accommodates the trajectories of ions of differing rigidities. This is illustrated in Fig. 1.11.

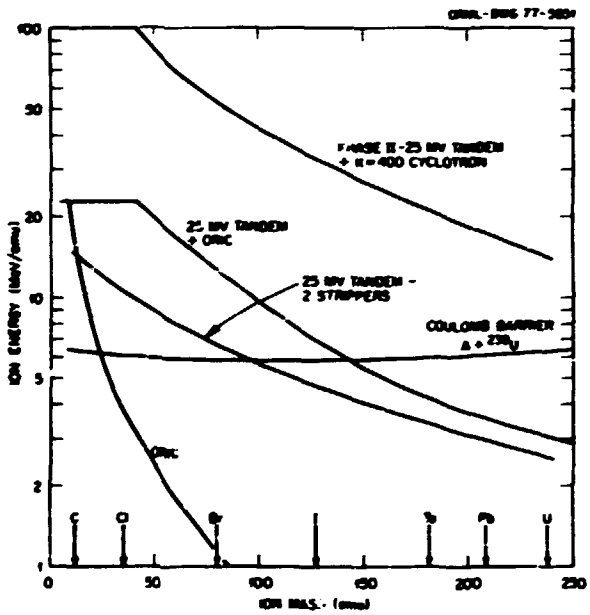

Fig. 1.9. Energy-ion mass characteristics of Oak Ridge heavy-ion accelerators. Phase I of the Holifield Heavy-Ion Research Facility, the 25-MV tandem, and the transport/injection system to use the ORIC as an energy booster will be completed in 1979. *Phase II is proposed for completion in 1983.*

Table 1.1. Principal SSC characteristics

Energy constant, K ($E = Kq^2/A$) (MeV)	400
Energy for U^{42+} (MeV/amu)	12
Energy for C^{6+}, O^{8+}, Ca^{20+} (MeV/amu)	100
$B\rho$ (kG-cm)	2957
Magnet fraction (52° hills)	0.58
Energy ratio, E_f/E_i	8–16
Injection mean radius (m)	1.07–0.75
Extraction mean radius (m)	3.01
Rf system frequency range (MHz)	9–20

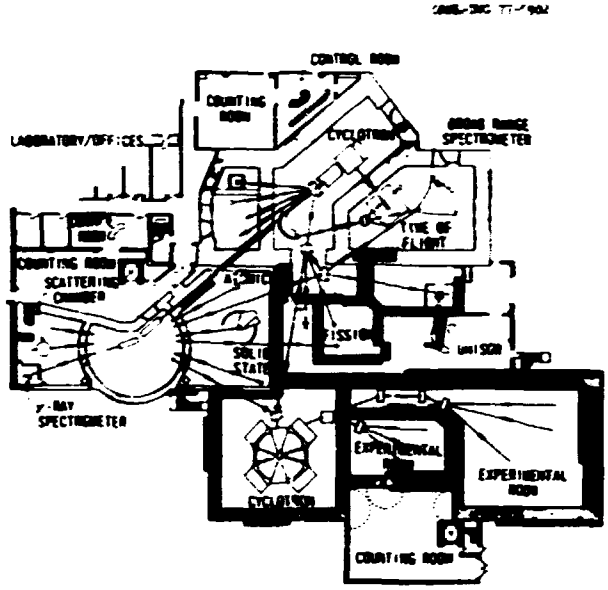

Fig. 1.10. Holifield Heavy-Ion Research Facility. Phase II is the portion housing the separated-sector cyclotron and associated experiment areas.

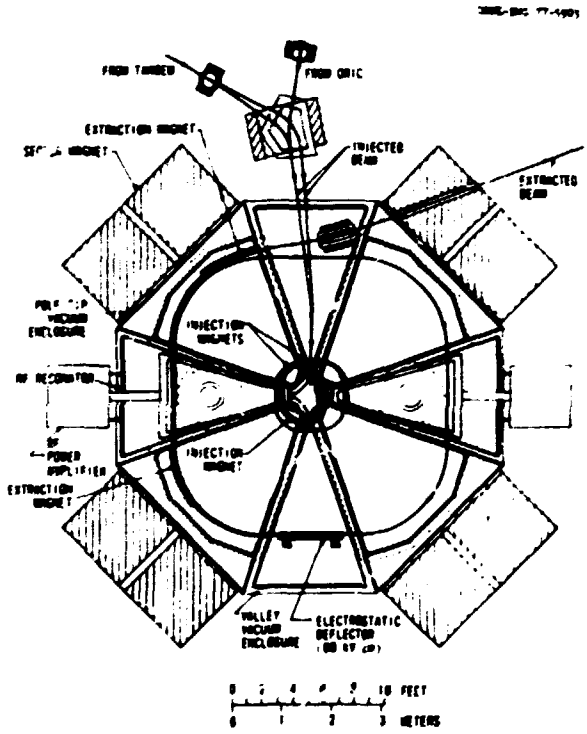

Fig. 1.11. Plan view drawing of the cyclotron. The injected beam is seen at the top of the figure entering the injection magnet.

The radial profile of the average magnetic field is free of significant saturation effects but exhibits a roll-off of several percent near the center and at the outer edge. To adjust the magnetic field, a constant-width shim section is provided along the center of the pole tip, as shown in Fig. 1.12. The shim section is contoured to provide the appropriate correction; the result is illustrated in Fig. 1.13. With the approximate field correction provided by the shim system, the maximum trimming coil power required is only 80 kW.

Rf system. The previous rf system design using radial quarter-wave resonators was tunable over the frequency range of 7 to 14 MHz. With this range, it is not possible to use the ORIC as the injector above about 45 MeV amu. Above that energy, the SSC must be operated on the second harmonic, but the ORIC cannot accelerate on even-numbered harmonics because of the 180° dee design. To eliminate this basic incompatibility, the SSC rf system range would have to be extended to 20 MHz. The new system (Fig. 1.14), uses vertical half-wave resonators to achieve a frequency range of 9 to 20 MHz and provides complete compatibility with the ORIC as the injector. For example, 100 MeV amu oxygen ions can be obtained by accelerating O^{4+} ions in the ORIC to 5.6 MeV amu, stripping to O^{6+}, and accelerating in the SSC to 100 MeV amu. The new design eliminates second-harmonic flat-topping resonators. Acceleration of 6°-wide beam pulses without flat-topping resonators gives the same resolution, ($\Delta E/E \sim 10^{-3}$) that is achieved with 20° phase width with flat-topping. A buncher efficiency of more than 50% for 6° bunches is predicted for the two-gap bunching system being developed for the 25-MV tandem.[6,7]

The 250-kW rf power amplifier systems use high-gain tetrodes driven directly by broad-band solid-state amplifiers.

Mechanical design. For the heaviest ions with a charge-exchange cross section of about 10^{-16} cm^2, a pressure of 10^{-7} torr is required to keep beam losses less than 10%. The present design uses cryogenic

Fig. 1.12. Contoured shim to adjust the magnetic field contour fits in a slot in the middle of the face of the pole tip. Lower pole of one sector of 0.15-scale model is shown.

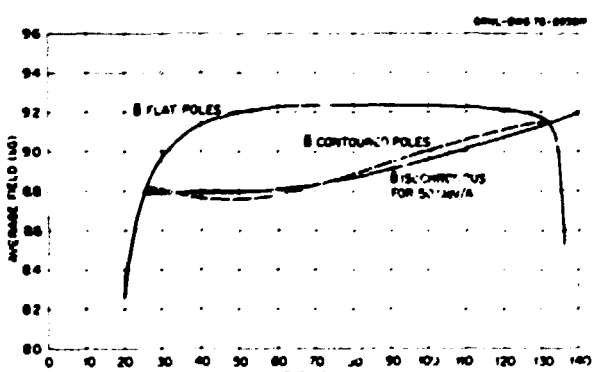

Fig. 1.13. Average magnetic field produced by the contoured poles approximates the isochronous magnetic field for 50 MeV/A.

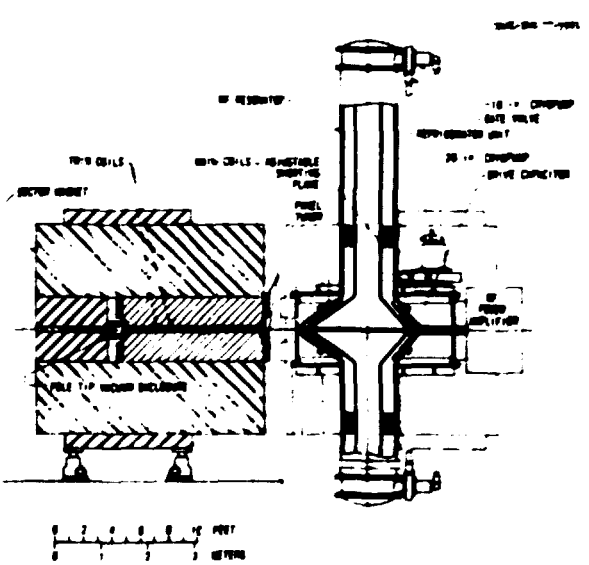

Fig. 1.14. Elevation section of the cyclotron, showing the vertical stem half-wave resonator.

pumps and blower mechanical pumps, and the system can be pumped from atmospheric pressure to 10^{-7} torr in approximately 15 hr.

To reduce residual gas loads and to improve reliability, elastomer seals have been eliminated wherever possible. Thin metal welded seals are used between the magnet poles and pole-tip vacuum chamber and between the pole-tip chambers and the valley vacuum chambers. Soft metal (indium) seals are used between the valley vacuum chambers and the rf resonator assemblies.

Building and Facilities

The cyclotron vault, beam transport corridor, and two experiment rooms are to be in a new structure located south of the existing cyclotron building and Phase I project, as shown in Fig. 1.10. Shielding is provided by a combination of poured concrete walls and solid concrete blocks. Extra shielding is provided on the forward direction of beams in positions where high-intensity beams will be used. The experiment areas were designed to facilitate future expansion by providing more experiment stations or adding additional areas. The facility incorporates a large counting room adjacent to both experimental rooms. Control of the facility will be from either of the existing control rooms, that is, the ORIC control room or the new control room for the 25-MV tandem.

1. UCC-ND Engineering Division.
2. UCC-ND Computer Sciences Division.
3. *Holifield Heavy-Ion Research Facility—Phase II Conceptual Design Report*, X-OE-28 (May 1977).
4. S. W. Mosko et al., "A Separated-Sector Cyclotron Post-Accelerator for the Oak Ridge Heavy-Ion Laboratory," *Proceedings of Seventh International Conference on Cyclotrons and Their Applications*, Birkhauser, Basel (1975), p. 600.
5. E. D. Hudson et al., "Magnet Model Studies for Separated-Sector Heavy-Ion Cyclotrons," *Proceedings of Seventh International Conference on Cyclotrons and Their Applications*, Birkhauser, Basel (1975), p. 197.
6. W. T. Milner et al., "Transport of DC and Bunched Beams through a 25-MV Folded Tandem Accelerator," *IEEE Trans. Nucl. Sci.* NS-22, 1697 (1975).
7. See this report, W. T. Milner and N. F. Ziegler, "Beam-Bunching and Pulse-Detection Test Facility."

EXPERIMENTAL APPARATUS AND ACCELERATOR DEVELOPMENT

CHARGED-PARTICLE TIME-OF-FLIGHT FACILITY

J. L. C. Ford, Jr. F. Plasil
J. W. Johnson R. G. Stokstad
F. E. Obenshain A. H. Snell
J. E. Weidley

The time-of-flight (TOF) facility now approaching completion consists of a 36-cm-diam scattering chamber joined by a sliding seal to an arm that allows a flight path of up to 3 m in length. The angular range possible is ±135°, with one port allowing an angular range of −10 to +70°. A layout of the TOF facility is shown in Fig. 1.15. The detector system will consist of two channel plate detectors for the start and stop signals, followed by a gas ionization chamber and silicon surface barrier detector as a $\Delta E \times E$ counter. All of the necessary electronics for this system have either been built or purchased.

The chamber has four 10-cm-diam removable ports on which detector holders can be mounted so that large area counters or other types of large detectors can be used separately or in coincidence with the detectors in the TOF arm. Two rotating wheels within the scattering chamber can also be used to mount solid-state counters or other devices. The vacuum system will have cryopumps, and the pump-out time will be approximately 45 min. Because the TOF system is supported on a gun mount, it will be possible to add a quadrupole to the system to increase the solid angle, if there is demand for it in the future. Figure 1.16 presents the floor plan of the HHIRF and indicates the location of the TOF station, which will be accessible to beams from either the new tandem or the ORIC cyclotron.

Figure 1.17 is a photograph of the system taken in March 1977. The sliding seal mechanism has proven to be very successful, and the scattering angle can be varied while maintaining a pressure of about 2×10^{-7} torr in the scattering chamber. This instrument, which will be an important tool for investigating heavy-ion collisions, will be available for the research programs sometime in the summer of 1977.

ORNL DWG 76-17283

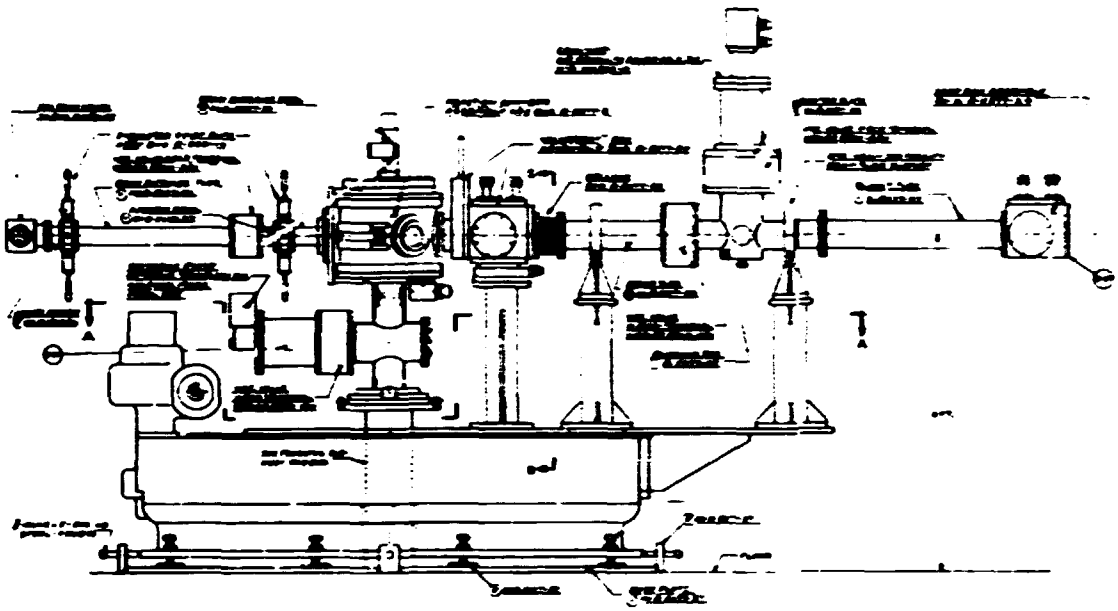

Fig. 1.15. Layout of the time-of-flight facility.

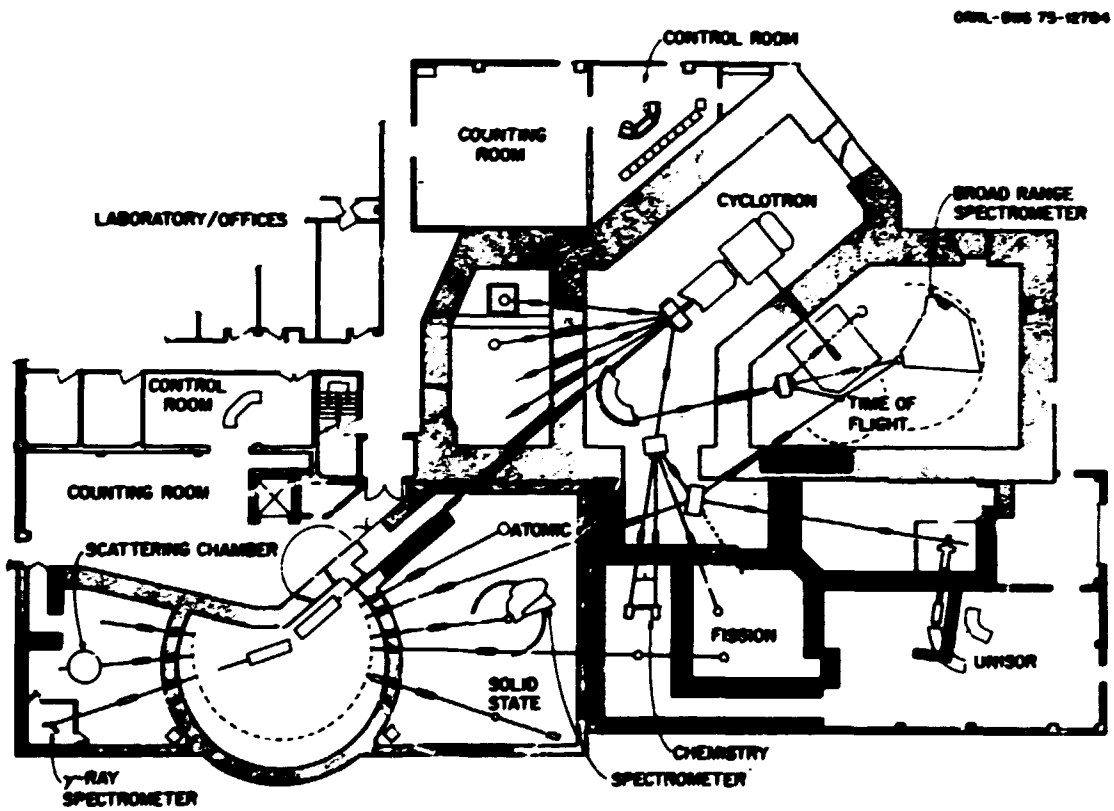

Fig. 1.16. General HHIRF floor plan showing the location of the TOF facility, where it will be accessible to beams from both the tandem and the cyclotron.

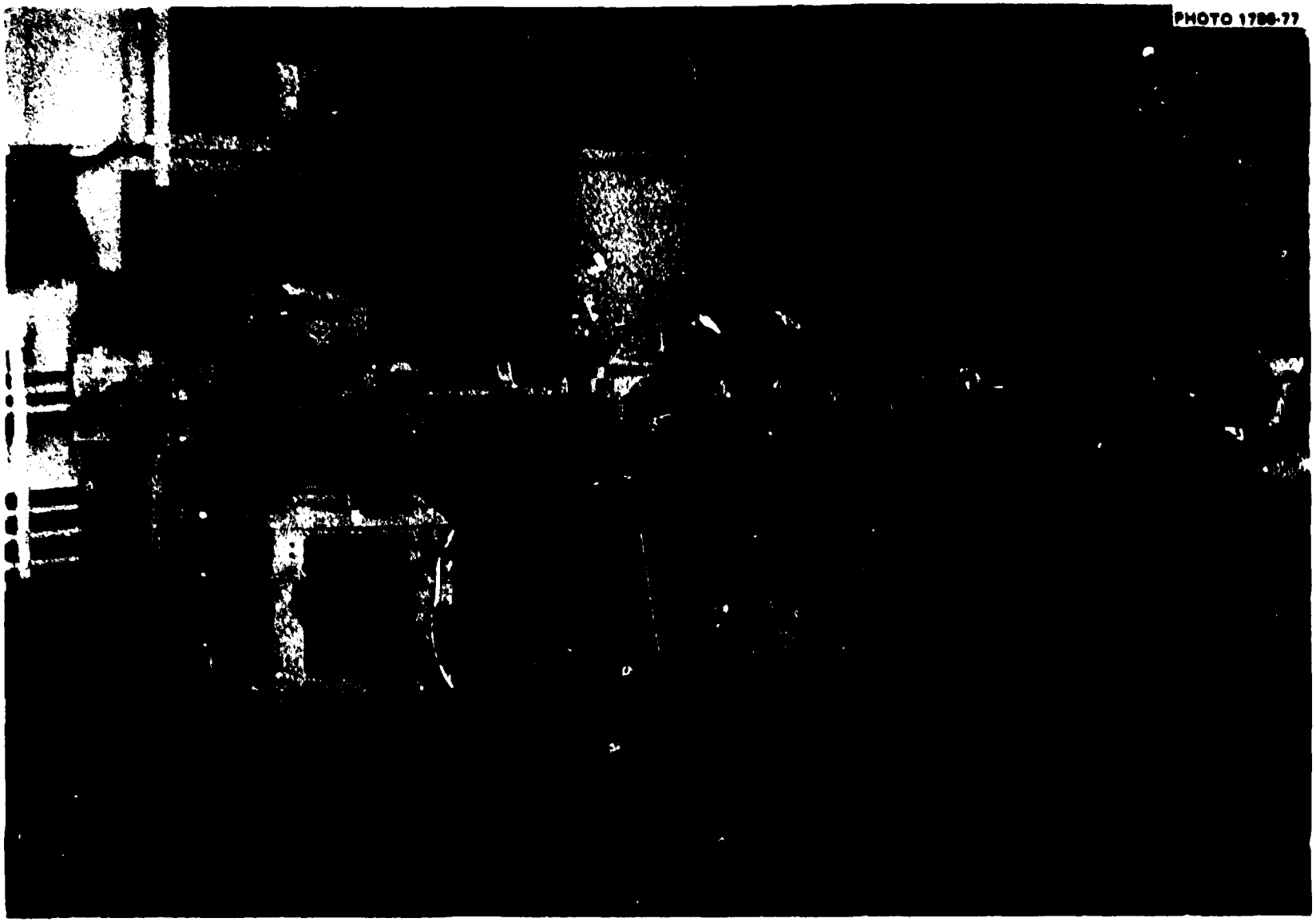

Fig. 1.17. Status of the TOF facility as it appeared in March 1977.

VACUUM SYSTEM FOR HHIRF BEAM LINES

J. W. Johnson R. L. Robinson

The program to evaluate and select vacuum system components for the HHIRF beam transport lines has now been completed. This selection should provide beam line pressures in a range of 1 to 5×10^{-8} torr after pumping about 12 hr and without baking.

The main components will be closed-cycle cryogenic vacuum pumps, ConFlat (copper gasket) flange joints, stainless steel valves with Viton gate seals, and mechanically or chemically cleaned stainless steel beam tubing.

The pump and beam tubing selection was based on an evaluation program reported earlier,[1] which tested on a prototype beam line the following state-of-the-art ultra-high-vacuum (UHV) pumps: (1) cryogenic, (2) electrostatic ion-getter, (3) magnetic ion-getter, (4) turbomolecular, and (5) oil diffusion with an LN_2 trap. Pumps were compared for pump-down time of a beam line initially at atmospheric pressure, for throughput, for base pressure, and for general operating conditions. A comparison of the pump-down time is illustrated in Fig. 1.18. The beam tubes were compared for pump-down time and base pressure.

1. J. W. Johnson, "Recent Vacuum Work at Oak Ridge," *Proceedings of the Symposium of Northeastern Accelerator Personnel, Nov. 3 5, 1976, Florida State University, Tallahassee.*

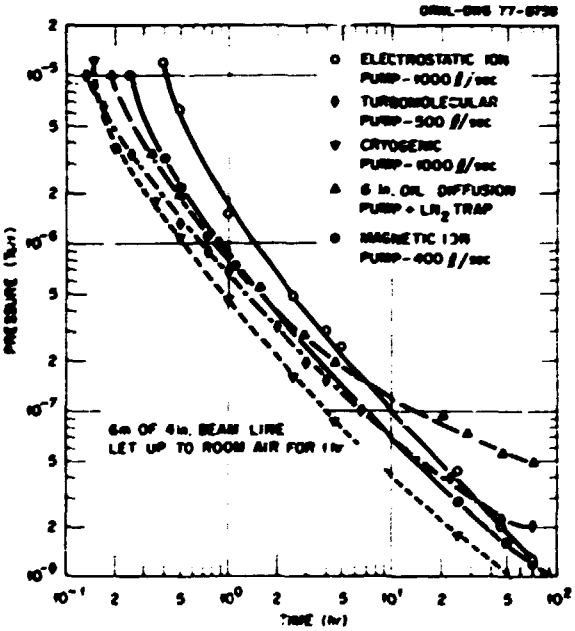

Fig. 1.18. Comparison of pump-down time for several UHV pumps.

BEAM-BUNCHING AND PULSE-DETECTION TEST FACILITY

W. T. Milner N. F. Ziegler

A beam-bunching and pulse-detection test facility has been implemented on the EN tandem accelerator. The bunching system, a two-harmonic double-drift klystron type, is designed to operate over a frequency range of 4.5 to 14.5 MHz and will eventually be used to produce bunched beams of ions (in the mass range 12 to 240 amu) from the 25-MV Pelletron accelerator for injection into ORIC.

Figure 1.19 illustrates the bunching system diagrammatically as it exists today. The beam encounters the first harmonic buncher, is somewhat "overbunched," drifts to the second harmonic buncher (operating at twice the frequency of the first buncher and 180° out of phase), is again energy modulated, drifts to the accelerator, is accelerated by the tandem, and finally comes to a "time focus" at the pulse detector.

Preliminary tests with three ion beams (22.5-MeV ^{16}O, 25-MeV ^{32}S, and 30-MeV ^{63}Cu) were carried out with observed results very close to those predicted. Beam pulses were detected with a capacitive pickup unit (CPU) and a fast Faraday cup and were observed with a sampling oscilloscope as well as a 500-MHz (TEK 7904) oscilloscope. In the case of the ^{16}O beam, a time-to-amplitude converter (TAC) spectrum was

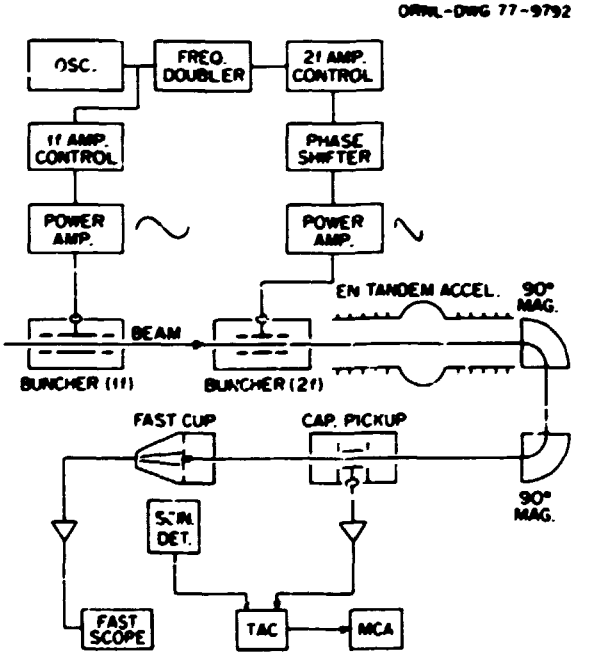

Fig. 1.19. Block diagram of the beam-bunching and pulse-detection test facility being used for system development.

obtained by using timing pulses derived from the CPU and a plastic scintillator that detected Coulomb excitation gamma rays produced in the stainless steel beam stop of the fast Faraday cup.

Pulse widths of 1.1 and 1.6 nsec were observed with a sampling oscilloscope for the ^{16}O and ^{32}S beams respectively. The ^{63}Cu beam was too weak [less than 10 electrical nanoamperes (enA)] for an accurate pulse width estimate, but pulses were observed. The TAC spectrum (see Fig. 1.20) shows that about 55% of the ^{16}O beam was bunched into 6° of the first harmonic klystron phase (the acceptance window of the ORIC).

Pulses from the CPU and the fast Faraday cup were amplified by wide-band rf preamplifiers (HP-8447F, gain = 48 db) prior to being fed into the time-pickoff unit (ORTEC-260) and the sampling oscilloscope. By using such equipment, we should be able to reliably detect the phase of pulses with average beam currents as small as 50 to 75 enA. The $^{16}O^{4+}$ beam (1.4 MeV/amu, averaging 300 (enA) that we used corresponds closely in velocity to a 225-MeV ion of mass 150. We expect that most bunched beams from the 25-MV Pelletron will have intensities greater than 300 enA.

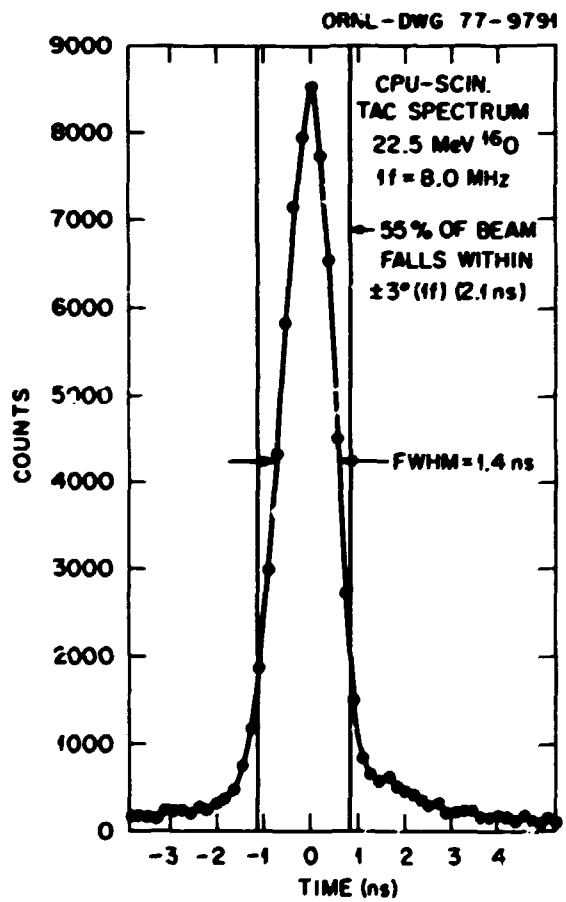

Fig. 1.20. Time profile of an ^{16}O ion-beam pulse produced by the double-drift klystron bunching system.

In addition to continued work on buncher evaluation with other ions and conditions, future work will also include the development of rf amplitude and phase stabilization circuits, pulse phase detectors, an ORIC-to-buncher phase monitor and control system, and an overall CAMAC-based control system that will be compatible with the HHIRF system.

COMPILATION OF EQUILIBRIUM CHARGE-STATE DISTRIBUTION DATA

R. O. Sayer[1] L. B. Maddox[1]

A data base containing information on charge-state distributions has been established at ORNL. Included are experimental values of mean charge, width, skewness, and charge-state fractions for energetic ion beams that have traversed gaseous and solid strippers of thicknesses near equilibrium or greater.

With the exception of a few corrections and deletions, all data in the compilation of Wittkower and Betz[2] for projectiles of energy 2 MeV and higher are contained in our data file.[3] More than 90 charge-state distributions from recent measurements (post-1972) are also included, and the total number of distributions in the data file exceeds 930. Periodic additions are planned as new experimental results become available.

We have written a computer code that reads data from the file and produces plots of charge-state distributions measured at various energies for a specified projectile and target. A sample plot for ^{127}I in krypton is reproduced in Fig. 1.21.

Inspection of the data reveals differences of 0.5 to 1.0 unit in the values of mean charge reported by different experimenters for identical projectile energies and target materials. These variations may be attributed to effects such as the angular acceptance of the apparatus, insufficient target thickness for equilibrium, and the "density effect" in gases. Such ambiguities make it difficult to assign errors without complete details of the experimental configuration. Therefore, caution is advised in the use of a particular result from one experimental group. For heavy ions, an uncertainty of one unit in the mean charge may be

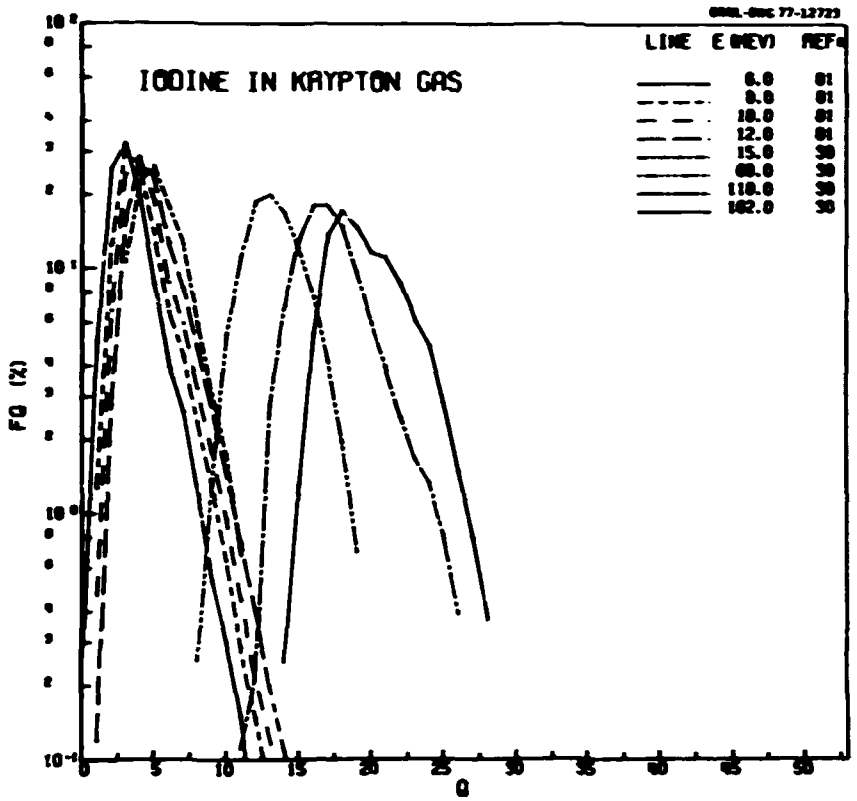

Fig. 1.21. A sample plot for ^{127}I in krypton.

assumed until comparison of independent measurements and/or examination of the original literature indicates otherwise.

1. UCC-ND Computer Sciences Division.
2. A. B. Wittkower and H. D. Betz, *At. Data* 5, 113 (1973).
3. The authors are indebted to Dr. Betz for sending us a tape containing data reported in his compilation.

DEPENDENCE OF ^{12}C AND ^{16}O CHARGE-STATE YIELDS AT 20 MeV ON STRIPPER GAS FLOW IN THE BROOKHAVEN MP-7 TANDEM VAN DE GRAAFF ACCELERATOR

R. O. Sayer[1] E. G. Richardson
P. Thieberger[2]

Injection of carbon and oxygen beams from the 25-MV tandem into the ORIC will require tandem acceleration of low charges at relatively high terminal voltage, V_t. Previous measurements[3] at ORNL indicated that ample intensities of charges 3 and 4 at V_t = 6 MV could be obtained at reduced gas pressures.

To investigate the situation at higher V_t, we have measured charge-state distributions using the three-stage operating mode of the two MP tandem Van de Graaff accelerators at Brookhaven National Laboratory to produce 20-MeV negatively charged ions at the terminal of MP-7, the second machine. Ions from a Middleton sputter source in the terminal of MP-6 were accelerated to 7.5 MeV, injected into MP-7, and accelerated to 20 MeV before entering the terminal gas stripper. Analyzed currents for charges 2, 3, 4, 5, and 6 were measured as a function of pressure at the entrance of MP-7, which was assumed to be proportional to the amount of N_2 gas in the stripper canal.

The observed yields in particle nanoamperes (pnA) are shown in Figs. 1.22 and 1.23. Injected intensities were 720 nA for ^{12}C and 1900 nA for ^{16}O. Overall maximum transmissions of 14% for ^{12}C and 19% for ^{16}O were obtained by summing the observed yields with estimates for the unobserved 0+ and 1+ yields.

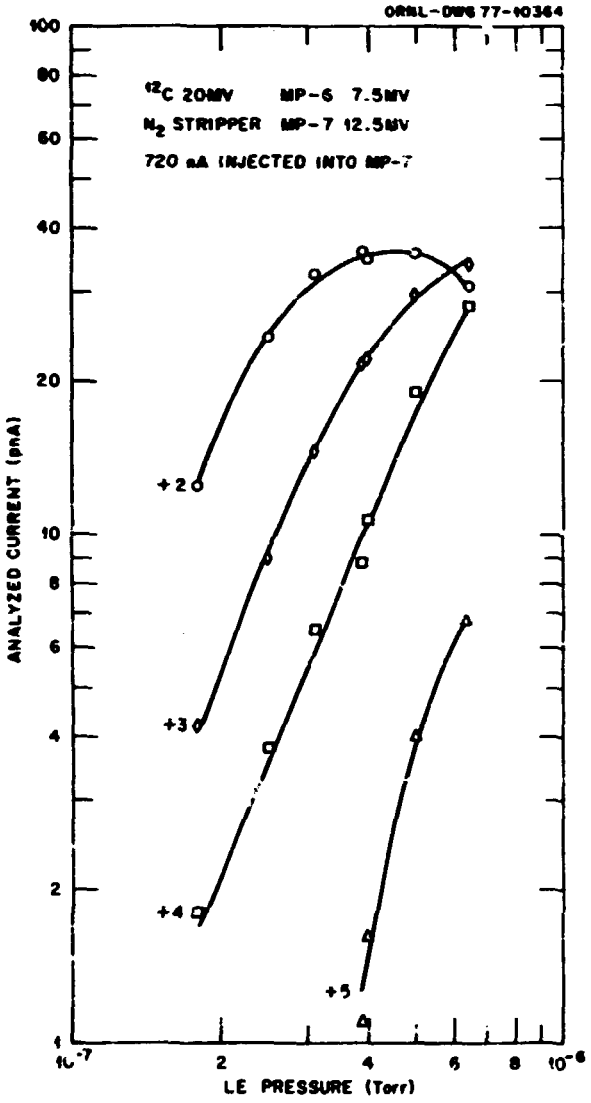

Fig. 1.22. Analyzed current in pnA vs pressure at the low-energy end of MP-7 for ^{12}C ions of charge 2, 3, 4, and 5.

Yields at the three highest pressures were normalized to the maximum observed transmission (about 3×10^{-7} torr) to compensate for the rapid falloff in transmission with increasing pressure, presumably caused primarily by charge-changing collisions in the high-energy accelerator tube.

Although insufficient gas could be introduced to achieve peak yields of $^{12}C^{3+}$ and $^{16}O^{4+}$, peak yields of 36 pnA of $^{12}C^{2+}$ and 110 pnA of $^{16}O^{3+}$ at lower pressures were measured. These beams would be more rigid and, thus, easier to inject into the ORIC than the marginally rigid 3+ and 4+ beams. Therefore, the salient results from our data are those shown below:

Ion	Injected current (pnA)	Total transmitted current (pnA)	Charge	Maximum analyzed current (pnA)
^{12}C	720	103	2+	36
^{16}O	1900	348	3+	110

These 20-MeV data indicate that, with a suitable flow of stripper gas, about one-third of the total transmitted beam can be obtained in the desired charge state (2+ for ^{12}C or 3+ for ^{16}O).

What currents might be expected from the 25-MV accelerator? If the machine delivers 1000 pnA in the most probable charge state at 20 MV, our data

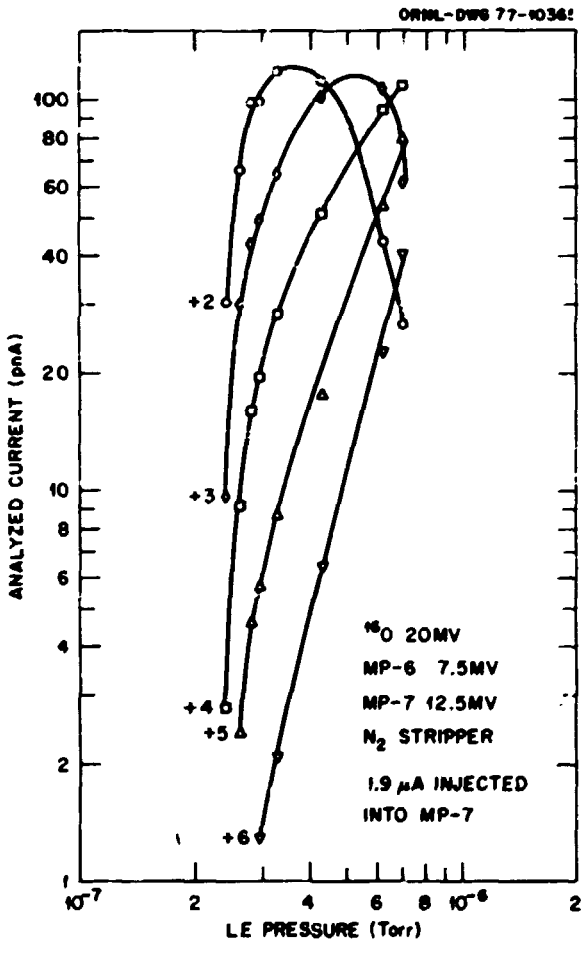

Fig. 1.23. Analyzed current in pnA vs pressure at the low-energy end of MP-7 for ^{16}O ions of charge 2, 3, 4, 5, and 6.

suggest that it will deliver at least 300 pnA of $^{12}C^{2+}$ or $^{16}O^{3+}$. Of course, the MP inclined field tubes produce larger excursions from the optic axis for higher charge states. This effect may bias our yields in favor of low charge states. On the other hand, the equilibrium charge fraction is about two-thirds at 20 MeV for the most probable charge; thus, our intensity estimate should be increased to about 500 pnA.

The present data indicate that quite adequate intensities of $^{12}C^{2+}$ and $^{16}O^{3+}$ beams at $V_t = 20$ MV can be obtained with a suitable flow of stripper gas. These beams are lower by one charge than those used in calculation of ORIC injection orbits, and the higher rigidity should considerably improve the chances for successful injection of ^{12}C and ^{16}O into the ORIC.

---

1. UCC-ND Computer Sciences Division.
2. Brookhaven National Laboratory, Upton, N.Y.
3. R. O. Sayer and E. J. Richardson, *Phys. Div. Annu. Prog. Rep. Dec. 31, 1975*, ORNL-5137, p. 113.

SF_6 GAS TRANSFER STUDIES

W. T. Milner

We have carried out an extensive study of the transfer of the SF_6 insulating gas from the accelerator vessel (volume of 80,000 ft^3) to the "liquid" storage tanks (three tanks of 2000 ft^3 each) in order to predict the performance of the transfer system for any realistic set of operating parameters. This transfer is accomplished using two Cooper-Penjax three-stage piston compressors. Figure 1.24 shows a simplified diagram of that part of the system with which we are concerned (only one of the two compressors is shown). Compression is done in three stages, with SF_6 gas from the first and second compression stages (CL1 and CL2) being passed through heat exchangers (HEX1 and HEX2) prior to injection into subsequent stages. Gas from the third stage (CL3) is cooled and/or liquefied by an after-cooler (HEX3) before being transferred into the storage tanks. Heat is removed from each heat exchanger by a circulating bath of cooling water.

The most important objectives of this study were to determine what conditions can lead to liquid SF_6 being injected into a compressor cylinder (which is to be avoided) and to determine the SF_6 temperature, pressure, and liquid fraction at any point in the system at any time during the transfer.

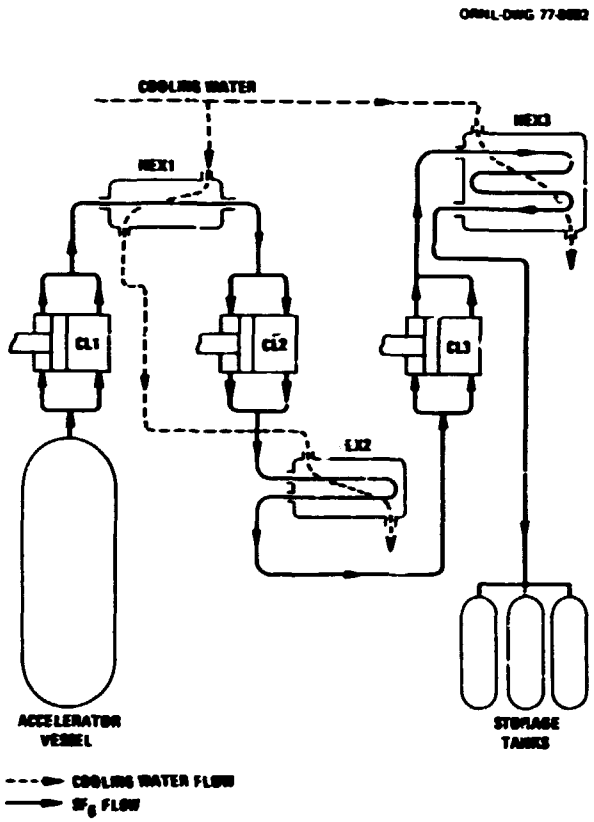

Fig. 1.24. Simplified diagram of the system for transferring the SF_6 insulating gas from the accelerator vessel to the storage tanks. Only one of two three-stage compressors is shown.

"Realistic" thermodynamic quantities (enthalpy, entropy, specific heat, and density) were used in all calculations. Stage compression ratios and SF_6 flow rates were calculated from "first principles." The heat transfer in HEX1 and HEX2 was calculated using standard engineering formulas, while the after-cooler (exchanger/condenser) was treated numerically.

Figure 1.25 displays the SF_6 temperature at four points in the system (at the discharge of HEX1, HEX2, and HEX3 and inside the storage tanks) as a function of the percentage of total inventory of SF_6, which has been transferred to storage for a typical set of operating conditions.

As a result of this study, we have recommended that the discharge cooling water from HEX1 be used as the input for HEX2 (as shown in Fig. 1.24) in order to eliminate the possibility of interstage condensation of the SF_6 in cases where the cooling water temperature is between 45 and 60°F. In addition, we have determined that the performance of the system

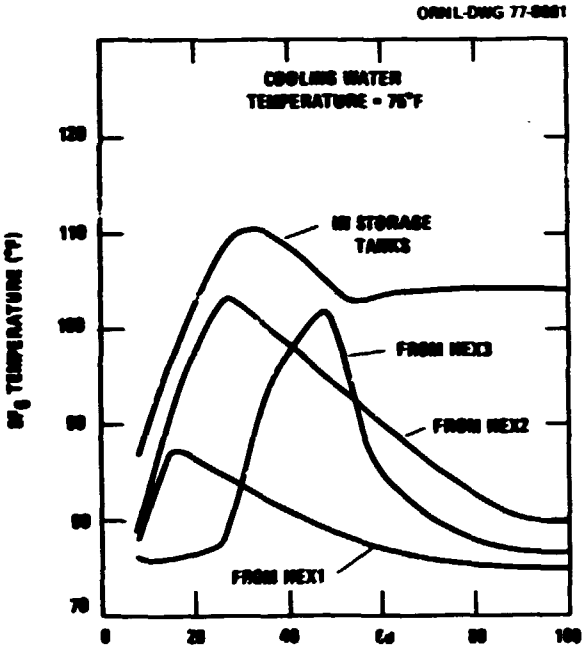

Fig. 1.25. Temperature of SF_6 at several locations in the system as a function of the percentage of the total SF_6 inventory, which has been transferred into storage.

should be adequate for cooling water temperatures less than or equal to 75° F with up to 40% degradation of all exchanger heat transfer coefficients.

NEGATIVE-ION-SOURCE DEVELOPMENT

G. D. Alton

Negative-Ion Spectra and Yields from the ORNL Sputter Source

The ORNL negative-sputter ion source, in conjunction with the negative-ion-source test facility,[1,2] was used during 1976 to study systematically the negative-ion yields from most of the naturally occurring elements, excluding, of course, radioactive elements and the noble gases. The study was initiated to determine the negative-ion-yield capabilities of the ORNL source and to establish preferred methods for generating ion beams of adequate intensity for tandem accelerator applications. Hopefully, the results of the study will serve as a valuable aid to tandem users in selecting the best method for producing the negative ions of interest from sputter sources of this type.[2,3]

The yields and spectra were recorded from elemental or compound materials with and without certain reactant gases, such as H_2, N_2, NH_3, and O_2, which were fed at a controlled rate onto the sample surfaces during the sputtering process. The choice of a particular reactant gas was made on the basis of the chemical reactivity of the sample with the particular gas. The source arrangement used during the study is illustrated in Fig. 1.26.

The Group II elements, which do not form stable atomic negative ions, can be produced more effectively by using NH_3 to form their hydrides, while most other elements are more effectively generated in molecular negative oxide form by using O_2 as the reactant gas. The form of the molecular oxide from which most intense beams can be generated depends on the element and usually varies from the monoxide to the trioxide, with uranium producing slightly more intense beams of UO_4^-. Elements possessing high electron affinities (e.g., Au, Br, C, Cl, F, I, O, P, Pt, S, Se, and Si) usually can be produced readily in elemental atomic form. The period-5 elements of tin, antimony, and tellurium form more intense di- and triatomic, rather than monoatomic, negative beams. Cluster negative-ion formation is characteristic of many elements other than those listed above (e.g., As, C, Se); however, the atomic negative ion usually predominates.

Typical examples of the negative-ion spectra from a Group II element such as calcium are shown in Fig. 1.27. The spectra were obtained by feeding NH_3 and

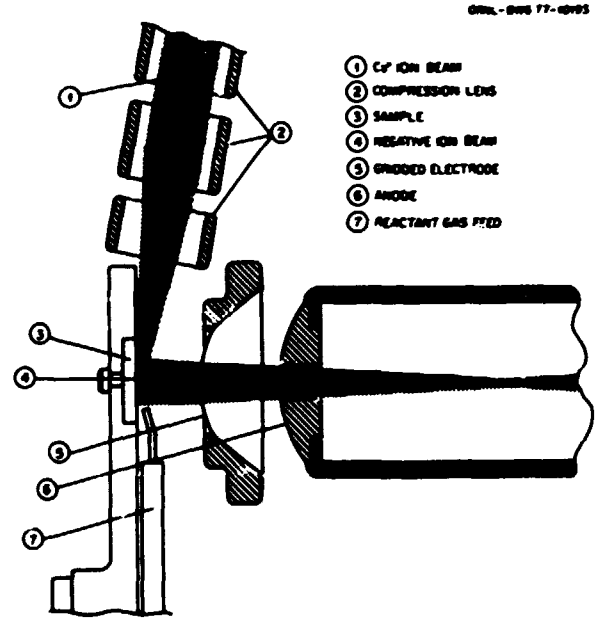

Fig. 1.26. Ion generation and extraction regions of the ORNL negative-sputter source.

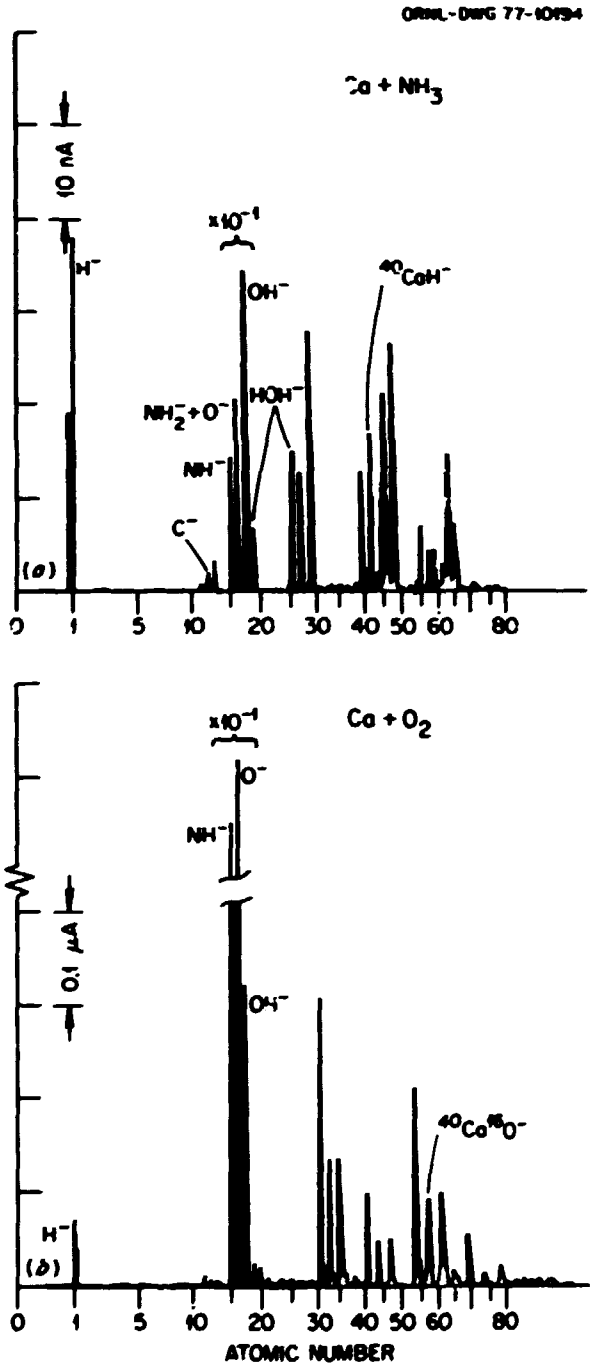

Fig. 1.27. Negative-ion spectra obtained by feeding (1) NH_3 and (2) O_2 onto elemental calcium.

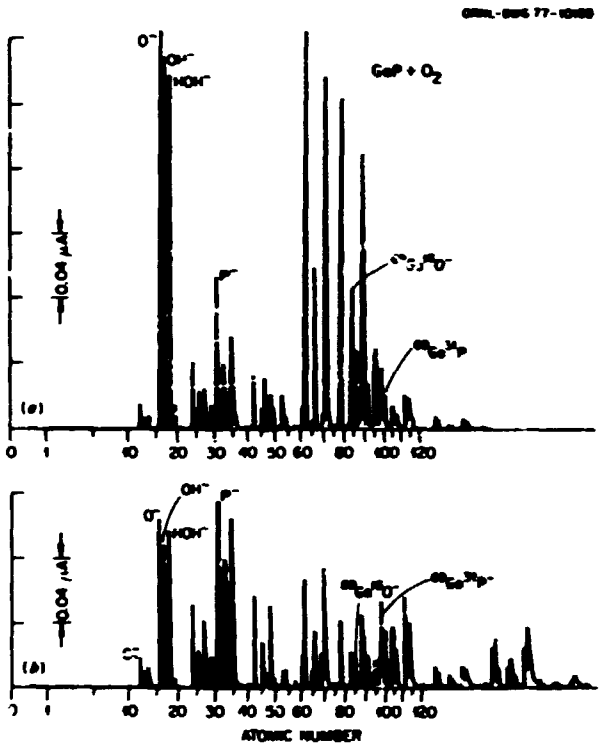

Fig. 1.28. Negative-ion spectra obtained with and without O_2 on GaP.

O_2 onto the surface of elemental calcium. Figure 1.28 illustrates how a diatomic molecular compound material such as GaP may be used to generate negative ions from both constituents, neither of which could be used in elemental form as a sputtering sample. The figure shows the spectra obtained from GaP with and without the reactant gas O_2.

Surface-Ionization Source for Production of UF_6^-

Preliminary investigations were initiated in 1976, in collaboration with S. Datz and P. Dittner of the Chemistry Division, to study the production of UF_6^- negative-ion beam by surface ionization, using the negative-ion-source test facility.[1] The source arrangement, which is extremely simple, is illustrated in Fig. 1.29. A sample of UF_6 is fed at a controlled rate onto a heated platinum ribbon maintained at about 1000 to 1500°C. The UF_6 is subsequently reevaporated from the filament and efficiently surface-ionized to form UF_6^-. The ions formed are then accelerated by the same ion extraction system used in the ORNL sputter source.[2] Datz and Dittner, who made a fundamental study of this phenomenon, found the efficiency of the process to be sensitively dependent of the presence of carbon on the platinum surface. While only preliminary attempts have been made and problems still exist, the technique has yielded mass-analyzed beams of UF_6^- up to 15 μA.

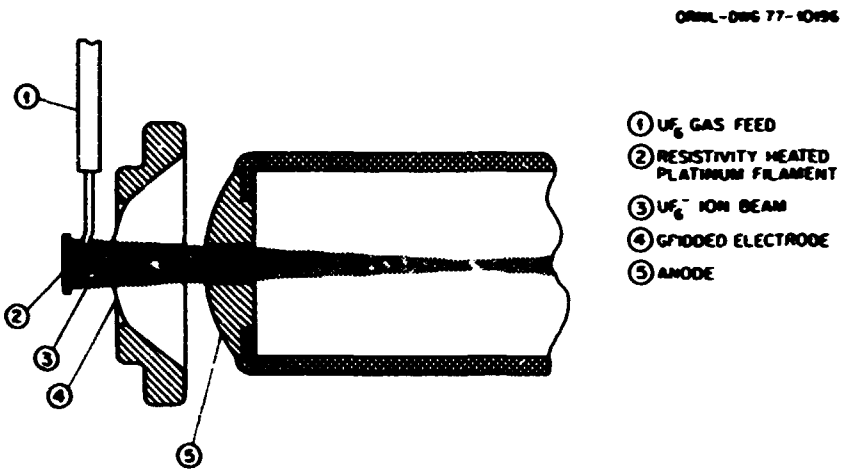

Fig. 1.29. Surface-ionization source for the production of UF_6^-.

Negative-Ion Source for Acceptance Testing of the 25-MV Accelerator

The specifications for the 25-MV tandem accelerator require that the source used in the acceptance testing of the accelerator be capable of producing a 7.5-μA negative-ion beam of mass greater than or equal to 195 within a transverse-phase space area (emittance) $\epsilon = 1\pi$ cm·milliradians·MeV[1,2,4]. The only source that can readily meet the intensity and emittance requirements to date is one based in principle on the design by the University of Aarhus.[5] A modified source of this type has been designed at ORNL and will undergo evaluation during 1977. The source is shown in Fig. 1.30.

1. G. [illegible] Alton et al., *Phys. Div. Annu. Prog. Rep. Dec. 31, 1974*, ORNL-5025, p. 192.
2. G. D. Alton, *IEEE Trans. Nucl. Sci.* NS-23, 1113 (1976).
3. R. Middleton and C. T. Adams, *Nucl. Instrum. Methods* 118, 329 (1974).
4. C. M. Jones et al., *Technical Specification for a 25-MV Tandem Electrostatic Accelerator*, ORNL TM-4942 (August 1975), pp. 130-32.
5. P. Tykesson, H. H. Anderson, and J. Heinemeier, *IEEE Trans. Nucl. Sci.* NS-23, 1104 (1976).

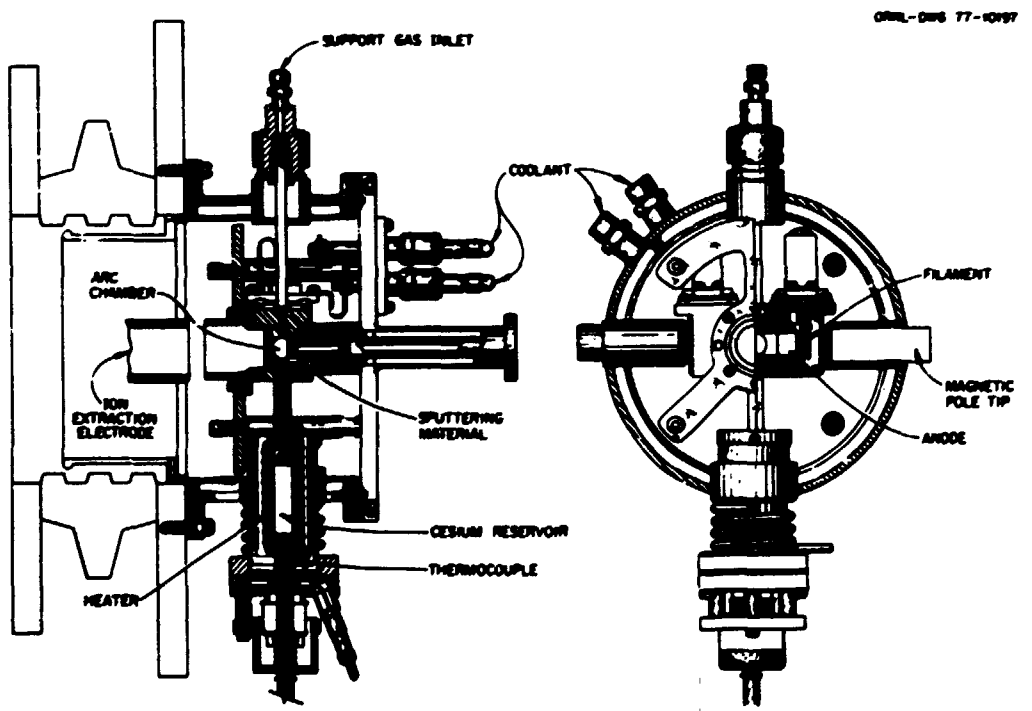

Fig. 1.30. Modified ORNL version of the University of Aarhus negative-ion source.

ORIC HEAVY-ION-SOURCE SUPPORT-GAS MIXING EXPERIMENTS

E. D. Hudson M. L. Mallory[1]

Experiments on mixing an easily ionized support gas with the primary ion-source gas have produced large beam enhancements for high-charge-state light ions (masses less than or equal to 20).

In the ORIC, the beam increase has been a factor of 5 or greater, depending on ion species and charge state. Approximately 0.1 cc/min of the easily ionized support gas (Ar, Kr, or Xe) is supplied to the ion source through a separate gas line, and the primary gas flow is reduced by about 30%. The proposed mechanism for increased intensity is as follows: The heavier support gas ionizes readily to a higher charge state, thus providing increased cathode heating. Increased heating permits a reduction in primary gas flow (lower pressure) and the subsequent beam increase. Effects in the source and near the cyclotron central region that are pressure dependent may then vary as different gases are used because less gas flow would be needed for the heavy-mass gases.

Another ion-source characteristic that is known (but not understood) is that different cold cathode-ion-source geometries require different amounts of gas flow for source operation. For example, the present ion source of the ORIC[2] requires about 3 to 4 cc/min gas flow for normal operation, whereas the ion source of some other laboratories requires a flow of 0.5 to 1 cc/min.[3] Central-region pressure effects and ion-source gas-usage effects would then be expected to be more readily detectable in the large gas-flow source of the ORIC.

Support gas is now used routinely. Normally, the gases are fed to the ion source through separate gas lines and are mixed in the plasma chamber. Mixing the gases external to the ion source and feeding through one gas line have produced substantially the same results. Results from mixing of krypton with neon for an extracted beam of $^{20}Ne^{6+}$ at 163 MeV is shown in Fig. 1.31. As krypton gas was added to the ion source, the neon gas flow was decreased until the arc voltage started to rise. The neon beam intensity increased by approximately a factor of 5 for a krypton gas flow of 0.15 cc/min. A further increase in krypton flow resulted in a decrease in the neon beam intensity. In Fig. 1.32, the cyclotron internal beam intensity of an $^{14}N^{5+}$ beam is plotted against the radius squared for xenon gas mixing. The internal beam attenuation slope for gas mixing and without gas mixing is the same and indicates that the internal pressure in the cyclotron is the same and does not account for the increase in beam intensity that occurs with gas mixing.

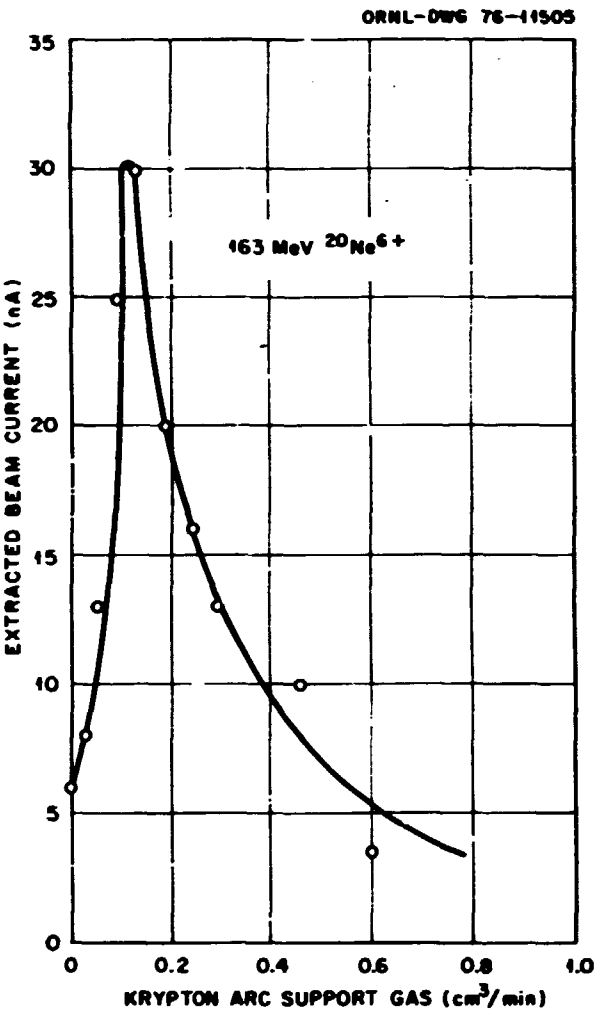

Fig. 1.31. The $^{20}Ne^{6+}$ extracted beam intensity vs the support-gas flow (krypton). For each point, a small amount of krypton was supplied to the arc and then the primary gas (neon) was decreased until the arc voltage started to increase, an indication that the arc was about to drop out. A maximum beam enhancement occurred at 0.15 cc/min of krypton.

The intensity of the $^{20}Ne^{6+}$ beam with gas mixing and without gas mixing indicates that the charge distribution in the source plasma is shifting to the higher charge states.

The effects of different support gases (Ar, Kr, and Xe) indicate that the maximum beam improvement obtained is about the same for the three gases; the $\bar{q}$ values of these gases are approximately equal.[4] Xenon and krypton gas-mixing experiments with an $^{40}Ar^{8+}$ beam have not shown an increase in intensity with gas mixing.

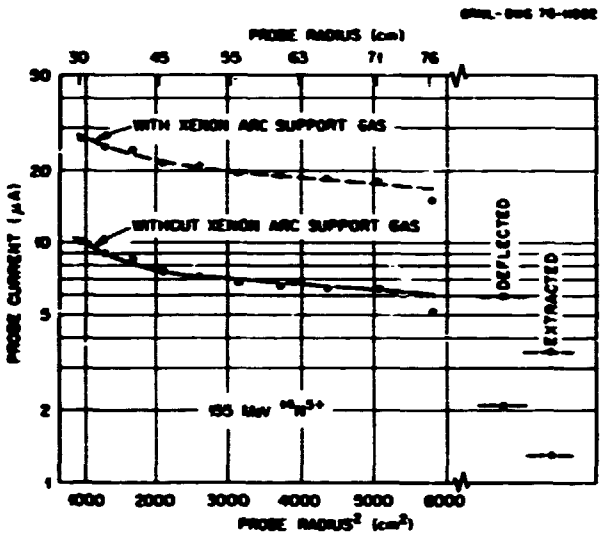

Fig. 1.32. The $^{14}N^{5+}$ beam attenuation with radius as measured on a cyclotron probe, with and without xenon support gas. The slopes of the curves are equal, indicating equal pressure attenuation in the cyclotron.

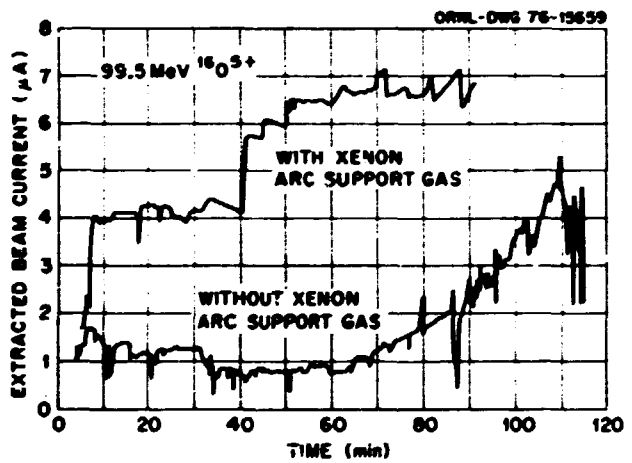

Fig. 1.33. The extracted beam intensity for an $^{16}O^{5+}$ beam vs time. The intensity of oxygen without support gas tends to increase slowly over a period of hours. The beam intensity with xenon support gas reaches an even higher level in a few minutes and is more stable.

In Fig. 1.33, the extracted beam intensity of an $^{16}O^{5+}$ beam is recorded as a function of time with and without mixing. The increase in beam intensity at 40 min was obtained by adjusting the xenon gas flow. The data indicate that the large beam intensity for the oxygen is obtained from the beginning of the ion-source lifetime. An important side effect is that the xenon gas mixing markedly improves the stability of the oxygen beam performance of the ion source.

---

1. On temporary leave at Michigan State University, East Lansing.
2. E. D. Hudson, M. L. Mallory, and R. S. Lord, *IEEE Trans. Nucl. Sci.* NS-23, No. 2, 1065-68 (1976).
3. M. L. Mallory and D. H. Crandall, *IEEE Trans. Nucl. Sci.* NS-23, No. 2, 1069-72 (1976).
4. J. R. J. Bennett, *IEEE Trans. Nucl. Sci.* NS-19, No. 2, 48 (1972).

ORIC MAGNETIC FIELD MEASUREMENTS[1]

R. M. Beckers[2] F. Irwin
J. A. Biggerstaff N. Lane
B. J. Casstevens[3] R. S. Lord
H. L. Dickerson C. A. Ludemann
K. M. Fischer[3] L. B. Maddox[3]
H. D. Hackler M. B. Marshall
C. L. Haley J. W. McConnell[4]
D. L. Haynes[2] G. S. McNeilly[3]
D. C. Hensley S. W. Mosko
E. D. Hudson G. A. Palmer
J. D. Rylander[2]

In preparation for beam injection from the tandem, the magnetic field of the ORIC was remapped during the shutdown for installation of the new dee. Remapping was required because we now routinely operate at main coil currents up to 30% higher than the highest one for which previous measurements were available and because we needed data on the fringe field through which the injected beam passes. The latest measurements were much more extensive than the original ones. The effect of the main coils was measured at 28 levels (vs 10 in the original measurements); the effects of the 10 trim coils, 9 harmonic coils, 3 valley coils, and the fringe field were measured at 15 of these 28 levels. In all, about 5 million data points were measured in ten weeks (vs 260,000 originally).

Such an extensive program was possible only because of significant advances in instrumentation technology. Field measurements were made using 39

search flip coils mounted at 1-in. increments on a common shaft. The output of each coil was fed to a separate electronic integrator, and the integrator outputs were scanned by a relay matrix and digitized by a 16-bit ADC with 1-G resolution. The data were fed directly to one of the SEL 840A computers, which also exercised process control over the acquisition system and the probe positioner. The probe positioner was a 180-tooth, 80-in. precision gear used in the previous measurements that had been modified to receive the 39 flip coils (Fig. 1.34). A complete map of 7059 points required less than 1 hr. Use of the computer provided a large amount of flexibility in the process. The coils were used in a combination search/flip mode, with flipping sometimes occurring only at every fourth azimuth. Time delays for eddy-current decay and vibrational settling could be readily changed in the program, and additional information such as flipping time, integrator drift, and magnet coil currents could be monitored. A series of data analysis programs was employed to check the data for inconsistencies shortly after the data were recorded. Error-checking programs identified out-of-tolerance data points, and display programs gave radial and azimuthal plots of the basic data and of differences between runs with a coil on and then off. Fourier analysis displays of the harmonic content of the data were also available. By use of this "instant analysis" system, we were able to keep a close check on the accuracy of the data, quickly identify equipment failure, and repeat any runs that looked suspicious. Reproducibility of the

PHOTO 6987-76

Fig. 1.34. The 80-in. precision gear with the probe arm in the extended position as it would be for fringe field measurements.

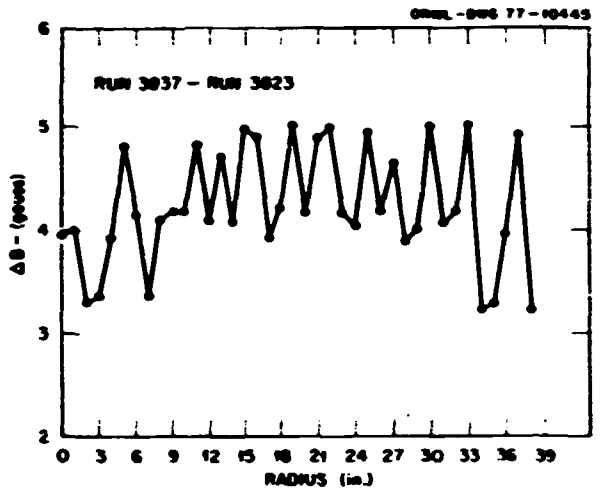

Fig. 1.35. Radial plot of the point-by-point difference between two field maps having identical currents but made on different days. Except for a small offset, agreement is within ±1 G.

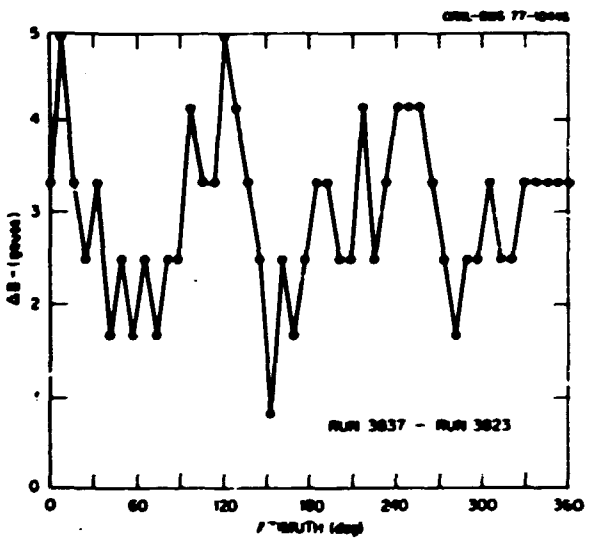

Fig. 1.36. Azimuthal plot of the same data as in Fig. 1.35. The larger variation is due to the small errors in azimuthal positioning of the probes in the high-gradient regions of the field (1200 G in).

data is illustrated in Figs. 1.35 and 1.36, which are plots of point-by-point differences between two runs having identical settings but made on different days.

1. S. W. Mosko et al., "Magnetic Field Measuring System for Remapping the ORIC Magnetic Field," *IEEE Trans. Nucl. Sci.* NS-24, No. 3 (1977).

2. UCC-ND Engineering Division.
3. UCC-ND Computer Sciences Division.
4. Neutron Physics Division.

ORIC RF SYSTEM DEVELOPMENT[1]

S. W. Mosko J. D. Rylander[2]
G. K. Schulze[3]

A new dee was designed, fabricated, and installed in conjunction with HHIRF-related modifications to the ORIC. This new dee features an open periphery for transmission of injected ion beams from the HHIRF tandem accelerator to the ORIC. The 2.5-cm beam aperture of the new dee is smaller than that of the original dee (4.8 cm) but still adequate for good beam transmission. The dee-to-ground clearance was decreased from 3.8 cm to 2.5 cm for increased capacitive loading, which extends to lower the end of the rf tuning range to about 7.0 MHz. These dimensional changes permitted a considerable increase in structural bracing in the dee walls for improved dimensional stability and some geometric improvement in the dee edges which raise the rf-voltage breakdown threshold from about 44 kV to 66 kV.

A broadband solid-state rf power amplifier was added to the main power amplifier driver circuit. The new driver unit eliminates the former 4CX50000A driver and several other tuned amplifier stages. The power-amplifier plate circuit and the main rf resonator are the only tuned circuits remaining in the rf system. A new rf voltage regulator was designed and built as a companion to the new driver.

The rf transient detection and level limiter system was rebuilt to include monitoring of vital parameters on the broadband driver and to replace existing circuitry with improved designs. The new system uses interchangeable level sensor modules that can be individually removed for servicing without interrupting cyclotron operation. The transient detectors and limiter system have TTL compatible output circuitry, which will permit a future tie-in to the ORIC control computer.

1. S. W. Mosko et al., "ORIC Rf System Preparation for HHIRF," *IEEE Trans. Nucl. Sci.* NS-24, No. 3 (1977).

2. UCC-ND Engineering Division.
3. Instrumentation and Controls Division.

ORIC OPERATIONS

S. W. Mosko
R. S. Lord
C. A. Ludemann
M. B. Marshall
N. R. Johnson
C. L. Viar
H. L. Dickerson
H. D. Hackler
G. A. Palmer
N. Lane
A. D. Higgins[1]
E. W. Sparks[1]
W. F. Ohnesorge[1]
C. L. Haley

The ORIC operated on a 15-shift-per-week schedule throughout 1976. A shutdown period of approximately six months duration began on January 3, 1977, to permit major equipment modification and magnetic field measurements in preparation for ion beam injection from the HHIRF electrostatic tandem accelerator.

Experiments using accelerated ions heavier than helium accounted for 87% of total machine-operable time. The most used beams of 25 to 172 MeV carbon, 90 to 180 MeV nitrogen, 43 to 170 MeV oxygen, and 70 to 213 MeV neon accounted for 78% of total machine-operable time.

Table 1.2 is a summary of research bombardments conducted during 1976; Table 1.3 shows a summary of beam time according to the particle used; and Table 1.4 is a time analysis of machine operation during the same period.

A new broadband solid-state driver amplifier array was installed in the rf system. A multitude of tuned components in the former driver amplifier stages was eliminated. The plate circuit of the main power amplifier and the dee resonator are the only tuned components remaining in the rf system. A new rf dee voltage regulator loop, which incorporates the new driver amplifier, was installed. New fault detection circuitry that features computer-compatible logic-level outputs for a future tie-in with the ORIC control computer was also included. These modifications have greatly simplified the rf system and improved the overall reliability of the ORIC.

The ion source of the ORIC benefited from recent developmental work with xenon arc support gas. A small amount of xenon added to the source gas for ions below mass 20 results in improved arc stability.

Table 1.2. Research bombardments at the ORIC in 1976

Research activity	Investigators	Cyclotron time (8-hr shifts)
UNISOR[a]	Spejewski, Mlekodaj, Carter, et al.	64
Heavy-ion fusion, fission, and transfers	Plasil, Ferguson, Pleasonton, Hahn, Obenshain, Snell, Bemis, Silva, Webb, Caretto,[b] Kaplan[b]	66
Materials research	Horak, Saltmarsh, Wiffen, Bloom, Washburn, Ullmaier, Jenkins, Noggle, Reiley, Auble, Ludemann, Roberto, Kalbunde, Coltman, Williams, Jung,[c] Duncan[d]	30
Accelerator development and machine research	Ludemann, Mallory, Hudson, Lord, Martin, Hale	52
Doppler-shift lifetime measurements	Johnson, Eichler, Yates,[e] Simms,[f] Riedinger,[d] Popick,[f] Daly,[f] Huppi,[f] Saha,[f] Kahler[d]	18
Coulomb-nuclear interference	Hillis,[d] Gross, Riedinger,[d] Bingham,[d] Halbert, Hensley, Scott,[g] Martin,[h] Baker,[g] Guidry,[d] Johnson, Kahler,[d] Vrba[d]	23
Isotope production	Mackey, Ottinger, Ratledge, Gross, Ludemann, Johnson	22
Excitation of giant resonances	Bertrand, Kocher, Gross, Goodman, Auble	4
Atomic physics	Sellin, Mowatt,[d] Pegg,[d] Griffin, Haselton,[d] Peterson,[d] Laubert,[d] Datz, Thoe[d]	5

Table 1.2. (continued)

Research activity	Investigators	Cyclotron time (8-hr shifts)
Backbending of rotational bands	Riedinger,[d] Stelson, Robinson, Johnson, Sayer, Eichler, Yates,[c] Ronningen,[h] Kahler,[d] Hichwa[h]	18
^{6}Li-induced reactions	Halbert, Hensley, Goodman, Wharton,[b] Debevec[i]	6
Heavy-ion transfer reactions and heavy-ion elastic scattering	Ford, Toth, Hensley, Thornton,[j] Gross, Bull, Gustafson,[j] Riley,[k] Snell, DeVries,[l] Cleary, Cramer,[m] Goldberg,[n] Halbert	28
Proportional-counter tests and miscellaneous experiments	Hensley, Gross, Stokstad, Snell, Dayras, Cleary, Goodman	10
Transfer-reaction studies with recoil nuclei	Hahn, Toth, Huberi,[o] Fleury,[o] Delaunge[o]	11
Properties of elements 104, 105, 106	Dennis, Silva, Hensley, Hahn, Tarrant, Hunt, Hulet,[p] Lougheed[p]	13
Deep inelastic scattering	Stokstad, Hensley, Halbert, Sarantites,[q] Westerberg,[q] Dayras, Robinson, Fulmer, Snell	37
Limits on fusion cross sections	Stokstad, Biggerstaff, Snell, Stelson, Dayras, Gomez del Campo	24
Search for short-lived isomers	Gross, Cleary, Hensley, Toth, Hungerford,[r] Bingham,[d] Burt[r]	9
Multiplicity measurements	Sarantites,[q] Gronemeyer,[q] Burke,[s] Halbert, Eichler, Johnson, Beene, Hensley, Westerberg,[q] Jastrebski[t]	39
(^{6}Li,^{6}He) charge exchange reaction	Goodman, Hensley, Stokstad	5
Nuclear spectroscopy with helium-jet techniques	Toth, Bingham, Carter	5
High-intensity neutron source	Saltmarsh, Fulmer, Ludemann, Greenwood,[f] Heinrich,[f] Kennerley,[f] Styles[u]	9

[a]UNISOR is a consortium of 12 universities, Oak Ridge National Laboratory, and Oak Ridge Associated Universities.
[b]Carnegie-Mellon Institute, Pittsburgh, Pa.
[c]Kernforschungsanlage, Jülich, Germany.
[d]University of Tennessee, Knoxville.
[e]University of Kentucky, Lexington.
[f]Purdue University, Lafayette, Ind.
[g]University of Georgia, Athens.
[h]Vanderbilt University, Nashville, Tenn.
[i]Indiana University, Bloomington.
[j]University of Virginia, Charlottesville.
[k]University of Texas, Austin.
[l]Rochester University, Rochester, N.Y.
[m]University of Washington, Seattle.
[n]University of Maryland, College Park.
[o]University of Bordeaux, France.
[p]Lawrence Livermore Laboratory, Livermore, Calif.
[q]Washington University, St. Louis, Mo.
[r]University of Houston, Houston, Tex.
[s]St. Louis University, St. Louis, Mo.
[t]Argonne National Laboratory, Argonne, Ill.
[u]Berry College, Mt. Berry, Ga.

Table 1.3. Analysis of ORIC beam use by type of particle (1976)

Particle	Energy (MeV)	Total hours assigned	Percent
	Nuclear research		
Lithium	90–62	108	3.2
Boron	107–80	108	3.2
Carbon	172–25	754.4	22.2
Nitrogen	180–90	583.2	17.1
Oxygen	170–63	488.0	14.3
Neon	213–70	816.0	24.0
Argon	159–36	88.0	2.6
Titanium	48	12.0	0.3
Total, heavy-ion experiments		2957.6	86.9
Protons	65	16.0	0.5
Deuterons	40–22	136.0	4.0
^{3}He	70	32.0	1.0
Alphas	95–35	260.0	7.6
Total, light-ion experiments		444.0	13.1
Total, nuclear research experiments		3401.6	100.0
	Machine research		
Carbon	195–130	96.0	23.5
Oxygen	208–100	156.8	37.6
Neon	165–131	64.0	15.4
Nitrogen	171–132	24.0	5.8
Titanium	47	24.0	5.8
Argon	200	16.0	3.8
Lithium	90	8.0	1.9
Total, heavy-ion experiments		388.8	93.3
Protons	65–62	20.0	4.8
Deuterons	40	8.0	1.9
Total, light-ion experiments		28.0	6.7
Total, machine research experiments		416.8	100.0

Table 1.4. Time analysis of ORIC operations for 1976

	Hours	Percent
Beam on target	2539	42.3
Beam adjustment	195	3.2
Target setup	73	1.2
Start-up and machine shutdown	555	9.3
Machine research	438	7.3
Total machine-operable time	3800	63.3
Source change	361	6.0
Vacuum outage	41	0.7
Rf outage	161	2.7
Power supply outage	96	1.6
Electrical-component outage	80	1.2
Mechanical-component outage	251	4.2
Water-leak outage	43	0.7
Radiation outage	1	0
Total unscheduled outage	1034	17.1
Scheduled maintenance	621	10.4
Scheduled engineering	555	9.2
Total scheduled downtime	1176	19.6
Total time available	6010	100

reduced gas flow, and improved vacuum. Sources with xenon support gas can operate with maximum ion output over most of their lifetime, rather than requiring several hours of conditioning prior to a short period of good performance.

1. Plant and Equipment Division.
2. Instrumentation and Controls Division.
3. Health Physics Division.

TANDEM VAN DE GRAAFF OPERATIONS

G. D. Alton J. L. C. Ford, Jr.
R. P. Cumby[1] J. W. Johnson
F. A. DiCarlo E. G. Richardson
N. F. Ziegler

The EN tandem operated very reliably during the year; in fact, no tank entry was made during the first nine months. In August a new charging belt was installed replacing a belt that had operated for almost 9000 hr. During the belt installation period, the accelerator was thoroughly cleaned and inspected, and damaged components were replaced. In November the tank was entered twice. One entry was necessitated by a loose screw in the bottom of the tank and the second by a broken belt guide and spring.

A spark, or transient, recording system has been developed on the EN tandem for possible use on the 25-MV machine. High-speed information is obtained from a capacitive pickup mounted opposite the terminal in the tank wall. Transient signals from the device trigger a storage oscilloscope and camera,

Table 1.5. Research activities on the tandem Van de Graaff accelerator

Type	Projectile	Investigators	Approximate percent of utilized beam time
X-ray studies	^{10}B,^{12}C,^{14}N	Miller, Bashe,[a] Duggan,[a] McDaniel,[a] Gossett,[b] Johnson,[b] Payne,[b] Pepper,[b] Rice,[b] Toten,[b] Tricomi,[b] Chatterjee,[c] Wheeler,[c] Elliott,[d] Krumhold,[d] McCoy,[d] Zander,[e] Rayburn,[f] Lin,[g] Cipolla,[h] Lapicki[i]	9
Atomic physics	^{9}B,^{12}C,^{16}O,^{19}F,^{27}Al, ^{28}Si,^{35}Cl,^{48}Ti,^{56}Fe	Griffin, Sellin,[j] Pegg,[j] Thoe,[j] Elston,[j] Forester,[k] Vain,[k] Pearson,[l] Hayden,[j] Wright,[m] Groeneveld,[n] Schumann,[n] Bashkin,[o] Jones,[p] Knox,[q] Pinno,[p] Lambert,[j]	9
High-charge-state stripping studies	^{56}Fe,^{127}I	Alton, Jones, Mouk, Miller, Bridwell,[r] Kessel,[s] Scott,[t] Wehring[r]	9
Energy-magnet heavy-ion reaction studies	^{10}B,^{15}N,^{16}O	Ford, Gomez del Campo, Robinson, Shapiro, Thornton[u]	6
Atomic collisions in solids	^{12}C,^{14}N,^{16}O,^{63}Cu,^{127}I	Datz,[v] Biggerstaff, Miller, Mouk, Dittner,[v] Gomez del Campo,	6
Charge-exchange cross sections	p	Bayfield,[w] Gardner,[x] Koch,[x] Sellin,[j] Pegg,[j] Thoe,[j] Hayden,[j] Forester,[k] Kim	6
Charge-exchange cross sections	Fe	Bayfield,[w] Kim, Stelson	6
Radiation damage effects	^{27}Al	Noggle,[y] Appleton,[y] Mouk	6
Compound nucleus studies	^{13}C,^{14}N	Thornton,[u] Cordell,[u] Dennis,[u] Schweizer,[u] Ford, Gomez del Campo	6
Coulomb excitation and lifetime measurements	^{4}He	Hamilton,[z] Ronningen,[z] McGuire,[z] Piercey,[z] Ramayya,[z] Riedinger,[j] Sayer[aa]	6
Coulomb excitation	^{4}He	Dagenhart,[bb] Stelson	6
In-beam gamma-ray studies	$^{6,7}Li$,^{12}C	Robinson, Sayer,[aa] Milner, Lin,[g] Wells,[g] Hamilton,[z] Ronningen,[z] Ramayya,[z] Piercey,[z] Kawakami,[z] deLima[z]	6
(^{7}Li,^{6}He) reactions	^{7}Li	Maguire,[z] Ramayya,[z] Ford, Gomez del Campo	5
Heavy-ion-produced neutron cross sections	$^{12,13}C$,^{16}O	Bair, Miller, Gomez del Campo	5
(^{15}N,α) reaction	^{15}N	Andrade,[cc] Ducal,[cc] Ortiz,[cc] Menchaca-Rocha,[cc] Ford, Gomez del Campo	3
Radiation damage studies	^{16}O,^{19}F	Clark,[dd] Biggerstaff, Appleton,[y] Mouk, White[y]	3
Beam-foil spectroscopy	^{56}Fe	Bashkin,[o] Sellin,[j] Pegg,[j] Griffin, Groeneveld,[n] Forester[j]	3
In-beam gamma-ray spectroscopy	^{6}Li	Raman, Walkiewicz,[ee] Kim, Miller	2

[a]North Texas State University, Denton.
[b]Thesis student, North Texas State University, Denton.
[c]State University of New York, Cortland.
[d]Tulsa University, Tulsa, Okla.
[e]East Texas State University, Commerce.
[f]University of Texas, Arlington.
[g]Tennessee Technological University, Cookeville.
[h]Creighton University, Omaha, Nebr.
[i]New York University, New York.
[j]University of Tennessee, Knoxville.
[k]Thesis student, University of Tennessee, Knoxville.
[l]University of Connecticut, Storrs.
[m]University of New Hampshire, Durham.
[n]Institut für Kernphysik der Universität, D-6, Frankfurt/M. 90, W. Germany.
[o]University of Arizona, Tucson.
[p]Brookhaven National Laboratory, Upton, N.Y.
[q]Rutgers University, New Brunswick, N.J.
[r]Murray State University, Murray, Ky.
[s]Cornell University, Ithaca, N.Y.
[t]University of Illinois, Urbana-Champaign.
[u]University of Virginia, Charlottesville.
[v]Chemistry Division.
[w]University of Pittsburgh, Pittsburgh, Pa.
[x]Yale University, New Haven, Conn.
[y]Solid State Division.
[z]Vanderbilt University, Nashville, Tenn.
[aa]UCC-ND Computer Sciences.
[bb]Isotopes Division.
[cc]University of Mexico, Mexico City.
[dd]Solid State Division on assignment from Mineral Research Laboratory, CSIRO, Sydney, New South Wales 2113, Australia.
[ee]Edinboro State College, Edinboro, Pa.

providing photographs of terminal voltage during a spark. A spark also triggers the data logger, producing a printout at 0.1-sec intervals of operating parameters just preceding and following the spark.

Other minor additions and modifications to the EN system include a light link from terminal to ground, a data link from the experimenters' data acquisition computer to the operating data logger, a CAMAC crate for the data logger, and new gaskets for reduction of gas leakage.

The research activities on the EN tandem for 1976 are listed in Table 1.5, together with the principal ions accelerated and approximate beam-time utilization for each activity. Typically, for the last several years, the research time was about equally divided between nuclear physics research and atomic or solid-state research. The experimental programs are almost entirely devoted to heavy-ion research.

1. Instrumentation and Controls Division.

5.5-MV VAN DE GRAAFF OPERATIONS

F. K. McGowan N. H. Packan[1]
G. F. Wells R. A. Buhl[1]
M. B. Lewis[1] Martha Inman[1]
R. P. Cumby[1]

The 5.5-MV Van de Graaff continues to be used routinely for heavy-ion-induced radiation damage studies by the Radiation Effects Group of the Metals and Ceramics Division. The 4-MeV ^{58}Ni ion beam was used to irradiate 108 specimens requiring 352 hr of ion beam on target. The heavy-ion-induced radiation damage ranged from less than about one displacement per atom (dpa) to 600 dpa per specimen. The average irradiation per specimen corresponded to a dose of 120 dpa, which was produced at a rate of 35 to 50 dpa hr (70 dpa is equivalent to a fluence about 10^{23} neutrons cm^{-2}).

The model 910 Danfysik ion source was refurbished 23 times. For an initial charge of 200 mg of ^{58}Ni in the ion source, the average useful lifetime is about 75 hr, when operating with a normal beam of 1.5 pμA on target. A summary of the use of the ^{58}Ni ion beam is given in Table 1.6.

A number of modifications to the facility have been completed during this reporting period:

1. Upgrading the E × H crossed-field analyzer at the terminal by tilting the magnetic pole pieces to correct the astigmatism.
2. Replacement of most of the heavy-ion beam line with electropolished stainless steel tubing and ultrahigh-vacuum joints.
3. Implementation of a multistation radiation damage chamber and a profilometer chamber.
4. Installation of cryogenic pumps on the heavy-ion beam line and damage chamber.
5. Implementation of simultaneous helium-ion injection through a 400-kV Van de Graaff.

The new radiation damage chamber contains six stations for mounting specimens. At each station, an array of nine disk specimens may be loaded. This makes possible at least six irradiations before breaking vacuum to unload and reload specimens. The profilometer chamber, which is adjacent and upstream to the damage chamber, contains a Physicon model MS-10 beam scanner, beam-defining apertures for the heavy-ion and the helium-ion beams, a

Table 1.6. Use of the ^{58}Ni ion beam

Activity	Total hours	Percent
Irradiation of 108 specimens (11,000 dpa)	352	27
Loading and removing specimens from damage chamber (3.5 hr/sample)	378	28
Start-up time after refurbishing the ion source (12 hr)	276	21
Calibration of beam profile monitor and microaperture scans	216	16
Preparation of beam for an irradiation	108	8
Total	1330	100

mask and microaperture strip drive, and viewing ports for an infrared pyrometer. The mask drive permits the experimentalist to cover part of the 3 × 3 specimen array during an irradiation. The microaperture strip scans the beam cross section at the target site for uniformity. This system is coupled to a Faraday cup, a current digitizer, and a signal-averager analyzer operating in the multichannel scaling mode. With the new damage-chamber system, the fraction of the beam intercepted by the vanes of the beam profilometer may be calibrated prior to and checked immediately after an irradiation. The value of the total ion-flux incident on the target specimen is believed known to within ±10%.

He^+ Ion Injector

The He^+ ion injector is now operative and capable of implanting helium in targets concurrently with the $^{58}Ni^{2+}$ ion beam. The He beam is injected at a 15° angle with respect to the Ni^{2+} beam. The He^+ energy is varied continuously at a rate of 60 sec/cycle from 200 to 400 keV. Beam intensities from 0.1 to 100 nA are available, with uniformity of beam intensity maintained within ±10% over the entire energy range and ±3% over 80% of the energy range.

The system is driven by a master ramp generator producing a triangular signal at the rate of 60 sec/cycle. Its primary function is to vary the analyzing magnet power supply. Unbalanced signals from the analyzed beam slits drive the accelerator corona control tube to vary terminal loading, thereby increasing or decreasing the accelerator terminal voltage. Because this method of energy variation drives the corona amplifier to its limits to achieve the desired 200–400-kV range, a small signal from the ramp generator is used to vary the belt charge power supply synchronously with the corona signal. This allows the corona amplifier to operate comfortably over about one-half its range.

Two focusing devices are utilized to maintain beam intensity uniformity. An electrostatic lens in the accelerator terminal provides primary focusing of the beam prior to acceleration. A magnetic quadrupole singlet lens in the beam line after mass analysis determines ultimate beam intensity and uniformity on target. The terminal lens is operated by a servomotor-driven control rod. This servomotor receives its signal from a beam-shape sensing device located at the analyzing magnet entrance, and this control accounts for the major deviations from uniformity in beam intensity due to its slow response at the maximum and minimum energy points. A faster-responding control for the terminal lens will be required for faster cycle times.

The quadrupole lens power supply is driven from the master ramp generator and may be adjusted to give constant target current at a variety of intensity levels. At present, intensity levels from 1 to 50 nA may be obtained at an ion-source current of 20 μA by adjusting the focusing controls. Higher or lower intensities require different ion-source production. A total range from 0.1 to 100 nA on target is available.

---

1. Metals and Ceramics Division.
2. Instrumentation and Controls Division.

OAK RIDGE ELECTRON LINEAR ACCELERATOR

J. A. Harvey[1] T. A. Lewis[2]
H. A. Todd[2] J. G. Craven[3]

Operation

During this report period, the Oak Ridge Electron Linear Accelerator (ORELA) was operated on the average of 400 hr/month. Because of a limitation of funds, the level of operation was maintained at 29 shifts per two-week period, except for two two-week shutdowns. Because the neutron experiments are operated on many flight paths simultaneously (up to 11), the actual number of experimenter hours per month averaged 2000, five times the actual number of electron beam hours. Table 1.7 shows the distribution of accelerator operating conditions. The wide-pulse operation is appropriate for neutron measurements below about 10 keV, but narrow pulses are needed for high-resolution measurements at higher energies. The low-repetition-rate operation is needed for measurements down to thermal neutron energies.

One klystron developed a vacuum leak during the period, but the leak was small enough that a temporary repair was made with vac-seal around the Vaclon pump ceramic. This klystron was operated for an additional 2800 hr after repair of the leak. Klystron lifetimes have averaged about 15,000 hr.

The electron-gun fabrication facility was transferred from the Y-12 site to ORELA. From the very beginning, we have had trouble with leakage developing at a rotating flange where the slow valve attaches to the gun. This flange has been changed so that it is now a fixed flange, and we anticipate that this will decrease the occurrence of leaks in that area. There

Table 1.7. Distribution of accelerator operating conditions

Repetition rate (pps)	Pulse width (nsec)			Total (%)
	3–6	10–20	30–45	
25			1.5 kW – 4%	4
200–350			20 kW – 12%	12
600			33 kW – 4%	4
800–1000	10 kW – 36%	25 kW – 8%	55 kW – 36%	80
Total, %	36	8	56	100

are now three spare guns that have been rebuilt since the facility was moved to ORELA. Procedures for gun fabrication and cathode preparation are still being improved.

A report[4] has been prepared that summarizes most of the recent information concerning the performance of ORELA that would be of interest to experimenters. Included are characteristics of the beam (in terms of both time and intensity) and descriptions of systems routinely used to monitor these beam characteristics.

Improvements

The major goal of the linac improvement programs is to increase the accelerator output in short pulses (3 to 5 nsec). Results from calculations and hardware tests have been encouraging and support the value of the original plans, which included a buncher system using klystron bunching, an improved electron gun, and modified focusing along the early part of the electron path.

The tests of critical-hardware items being conducted by D. W. Bible[2] and T. A. Lewis[3] and the three-dimensional calculations being conducted by R. G. Alsmiller,[5] F. S. Alsmiller,[6] and J. Barrish[6] have led to a final design of nine buncher gaps. There is also a solenoidal magnetic confinement field starting at 1 kG and increasing to 3 kG for the part of the beam path just before injection into the linac.

Data Processing and Analysis

A data-file operating program has been written for the PDP-10 to enable the user to operate on his data sets through mathematical equations that are input at run time. The program can do what most of the short programs have done, thus reducing the amount of information the user must know to operate on his data sets. Operations such as listing, plotting, displaying, and dumping can be accomplished with a single equation. Plotting can be as automatic, simple, or complicated as the user desires. The program also allows the user to operate on his data sets through short FORTRAN programs that are input at run time. All input and output is handled by the program. The user treats his data file as data arrays, specifying where to start in the array by giving element number, element time, or element energy. Documentation is being edited for distribution.

As part of the ORNL PDP-10 computer upgrade, the existing PDP-10 has been moved to ORELA. The ORELA PDP-10 consists of a CPU, 2 disk controllers, 10 disk drives, 16 terminal slots, and a PDP-15 communications computer. The PDP-10 is used to process and analyze data at ORELA through interactive display programs. The dedicated PDP-10 will result in the user having better response to his interactive programs.

1. Codirector of ORELA (with R. W. Peelle, Neutron Physics Division).
2. Instrumentation and Controls Division.
3. UCC-ND Computer Sciences Division.
4. T. A. Lewis, *ORELA Performance*, ORNL TM-5112 (April 1976).
5. Neutron Physics Division.
6. UCC-ND Computer Sciences Division.

2. Nuclear Physics Research

INTRODUCTION

This chapter describes experimental nuclear physics research in separate reports organized into four sections according to the nature of the bombarding projectile: (1) heavy ions ($A > 4$), (2) light ions (*n*, *p*, *d*, ^{3}He, alpha), (3) neutrons, and (4) pions.

The most intense concentration is in basic research on reactions induced by heavy ions. These experiments are done mainly with the Oak Ridge Isochronous Cyclotron (ORIC) and the EN tandem accelerator. Over 85% of ORIC time during 1976 was devoted to heavy-ion beams.

The Oak Ridge Electron Linear Accelerator (ORELA) continues to excel as a facility for accurate high-resolution neutron cross-section measurements. The nuclide ^{208}Pb was studied in detail by all possible neutron techniques. A striking example of a "doorway" state was discovered.

Members of other divisions of the Laboratory are involved in some of the research programs reported here. Some work not reported here is carried out by other divisions (principally the Chemistry Division) on accelerator facilities operated by the Physics Division. Scientists from at least 23 institutions outside ORNL also participate in research with Physics Division accelerators. The University Isotope Separator at Oak Ridge (UNISOR) on-line isotope separator project serves as the focus of the largest collaborative effort of this type.

Applied research is carried out on ORIC in collaboration with other ORNL divisions and outside users. Brief reports are given in the section of this chapter on light-ion reactions.

During one-third of the period covered by this report, ORIC was dismantled for measurements and modifications required for its role as energy booster in the new Holifield Heavy-Ion Research Facility (HHIRF). The heavy-ion time-of-flight facility is nearing completion and is expected to be used for experiments during the summer of 1977.

HEAVY-ION NUCLEAR RESEARCH

Nuclear reactions induced by heavy ions fall into three broad categories: peripheral collisions, strongly damped collisions, and fusion reactions. These may also be thought of as successive stages in the time development of a single reaction, because complete fusion must be preceded by some peripheral processes and then by strong damping. The research program outlined in the reports below provides new information on all three aspects of heavy-ion reactions. Their interconnection is clearly shown in some of the reports where the same apparatus provides information on elastic scattering, deep inelastic reactions, and fusion.

A brief survey of selected results follows. One of the inelastic-scattering measurements is expected to resolve the existing conflict in the value of the ^{20}Ne deformation parameters as obtained from Coulomb excitation and light-particle scattering studies. The previously observed discrepancy between distorted-wave Born approximation (DWBA) theory and experiment for single-proton transfer from ^{12}C to ^{208}Pb has also been shown to exist with ^{12}C on ^{206}Pb.

In an experiment designed to define shielding needs for heavy-ion accelerators, the spectrum of charged particles from iron bombarded by 16 MeV nucleon ^{12}C ions was measured. As predicted by a theoretical calculation, protons of very high energy (up to 70 MeV) were observed at forward angles.

In the measurements of gamma-ray multiplicity with rare earth targets, clear evidence for pre-equilibrium decay was found, and the transition from statistical to nonstatistical behavior was demonstrated. The multiplicity apparatus was combined with a heavy-ion detector to provide a more complete picture of the energy and angular momentum transfer in deep inelastic collisions. These results indicate that for the low-Z products from ^{20}Ne + ^{63}Cu at 165 MeV, the angular momentum transfer is less than that expected for complete sticking but is greater than that caused if the nuclei merely roll on each other.

The fusion cross section for $^{14}N + ^{12}C$ was found to decrease at 248 MeV, which is contrary to its increasing trend at energies up to 178 MeV. This appears to be the result of having reached the liquid-drop limit for the ^{26}Al compound nucleus. The ^{27}Al compound nucleus at about 30 MeV has been studied exhaustively, and the average coherence width of the overlapping states has been determined. On the other hand, nonstatistical structures in the excitation functions, which may be due to nonoverlapping high-spin levels, have been discovered. Studies of compound nuclei formed with ^{40}Ar and $^{84,86}Kr$ beams on a number of different targets were carried out at the Super-Heavy-Ion Linear Accelerator (Super-HILAC).

A great deal of spectroscopic information was obtained in a variety of other experiments. Data from in-beam gamma-ray measurements were used to deduce lifetimes in ^{192}Pt, ^{194}Pt, and ^{150}Nd. Other in-beam experiments elucidated the structure of the band-crossing region of ^{164}Er responsible for its backbending and provided data on ^{185}Au and odd-A thallium isotopes. Much new data for nuclei with A = 64 to 74 have been obtained.

Studies of radioactive decay, principally of short-lived activities separated by UNISOR, provided a wealth of information on nuclei between A = 182 and 201. Particularly notable was the three-pronged attack on the A = 184 mass chain involving studies of alpha, beta, and gamma rays. Other decay studies provided data on ^{116}Sn and $^{149,150,151}Ho$.

Reports on developments in instrumentation useful for spectroscopic studies are given at the end of this section.

ELASTIC SCATTERING OF ^{12}C BY ^{28}Si AT 131 MeV

J. G. Cramer[1] R. M. DeVries[3]
D. A. Goldberg[2] R. G. Stokstad
M. L. Halbert

An extensive survey of elastic scattering of heavy ions, particularly ^{16}O, by ^{28}Si has been made in various laboratories,[4] including a measurement at ORIC.[5] This work was extended by measuring the elastic scattering of the 131.5-MeV ^{12}C beam from ORIC by an ^{28}Si target. The detection method employed in ref. 5 was used (multiple-slit collimator with a position-sensitive silicon detector).

The results are shown by dots in Fig 2.1. It is

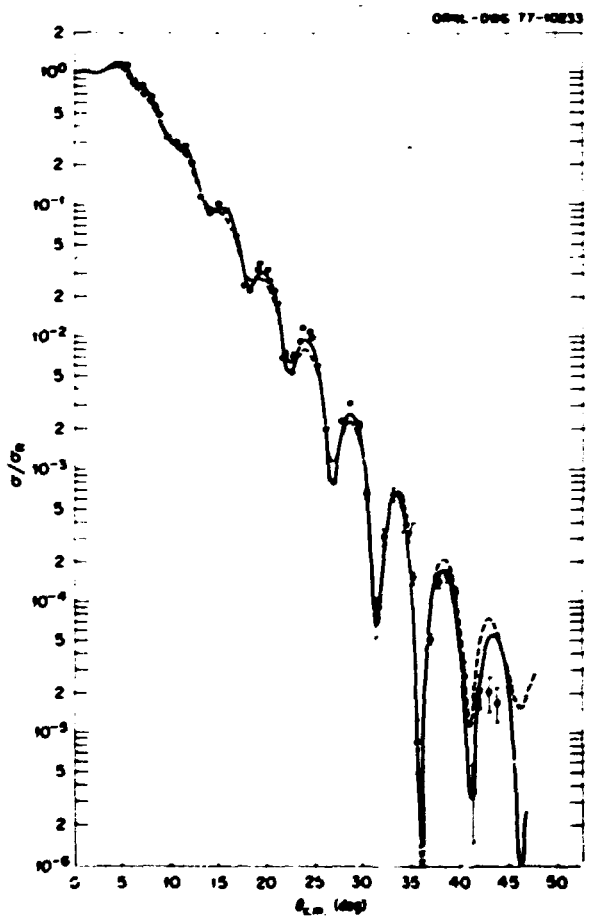

Fig. 2.1. Elastic-scattering cross section relative to the Rutherford cross section for 131.5-MeV ^{12}C on ^{28}Si. The dots are the experimental points. The full curve is an optical-model calculation based on the *E18* Woods-Saxon potential of ref. 4; the parameters are V_0 = 10, r_0 = 1.32, a = 0.653, W_0 = 22.7, r' = 1.20, a' = 0.599. The dashed curve is a calculation using a folding-model real potential derived from *M3Y* of ref. 5, with normalization N = 0.79; the imaginary well is of Woods-Saxon shape with W_0 = 62.0, r' = 0.9, a' = 1.030.

notable that the measurements extend over nearly six decades in σ/σ_R. The curves are preliminary fits with two optical-model potentials. The solid curve is derived from the energy-independent six-parameter Woods-Saxon potential *E*18 of ref. 4, while the dashed curve is a modification of the folded potential *M*3*Y*.[5] With further adjustments, good fits to the data will be obtained with both of these potentials.

1. University of Washington, Seattle.
2. University of Maryland, College Park.
3. University of Rochester, Rochester, N.Y.
4. J. G. Cramer et al., *Phys. Rev. C* 14, 2158 (1976).
5. G. R. Satchler et al., to be published in *Nuclear Physics*.

INELASTIC SCATTERING

The use of heavy-ion probes to explore nuclear shapes has four distinct advantages over conventional light-ion inelastic scattering.

1. The small de Broglie wavelengths of heavy-ion projectiles yield a greater sensitivity to the nuclear shape.
2. Inelastically scattered heavy ions probe only the surface region, while light-ion scattering may include effects of the interior.
3. The large amount of angular momenta brought into the nuclear system by the heavy-ion projectile gives a greater emphasis to the higher-order moments of the matter distribution.
4. Coulomb and nuclear reorientation effects associated with the static quadrupole moments of excited nuclear states are enhanced.

In a comprehensive study of ^{12}C scattering on a series of neodymium targets, Hillis et al.[1,2] demonstrated that heavy-ion inelastic scattering, when analyzed in a coupled-channels formalism, can be used to consistently and reliably extract nuclear structure information for targets ranging in shape from nearly spherical to extremely deformed. Efforts have been made during the past year to exploit these techniques for studying the shapes of transitional nuclei and extending such reaction studies to cases where projectile excitation is a dominant component in the excitation of the system.

1. D. L. Hillis et al., *Phys. Rev. Lett.* 36, 304 (1976).
2. D. L. Hillis et al., *Phys. Div. Annu. Prog. Rep. Dec. 31, 1975*, ORNL-5137, p. 46.

Inelastic Scattering of 78-MeV ^{12}C from ^{194}Pt

F. T. Baker[1] J. L. C. Ford, Jr.
A. Scott[1] E. E. Gross
T. P Cleary D. C. Hensley

The recent results of Hillis et al.[2] have clearly shown the importance of reorientation effects in the inelastic scattering of heavy ions. Before heavy-ion inelastic scattering can be used confidently to actually measure quadrupole moments, one must be certain that the reaction mechanisms assumed in the coupled-channels (CC) calculations will yield results consistent with previously measured quadrupole moments for a variety of nuclei. An obvious choice to test the CC theory is an oblate nucleus whose 2^+ quadrupole moment (Q_2) differs in sign from those of the neodymium isotopes studied by Hillis et al.[2] We have chosen ^{194}Pt for such a test. Not only has Q_2 been accurately measured using Coulomb excitation,[3,4] but ^{194}Pt has been studied using inelastic alpha-particle scattering[5,6] where standard CC calculations can be performed confidently.

Although the analysis of the data is not yet complete, the findings to date are: (1) The data for the first 2^+ state are better fitted by CC calculations, assuming an oblate intrinsic shape rather than a prolate intrinsic shape. (2) Values of β_4 extracted from our data for the 4^+ state are in good agreement with the alpha-scattering results.[6] There is substantial sensitivity to the sign of β_4. (3) The sign of the interference term $P_4 = M_{02}M_{22}M_{22}'M_{02}'$ is unambiguously determined to be positive, as was found in the alpha-scattering experiments.[5,6] Therefore it appears that the results of this experiment will lend credence to our methods of analysis of heavy-ion inelastic scattering.

1. University of Georgia, Athens.
2. D. L. Hillis et al., *Phys. Rev. Lett.* 36, 304 (1976).
3. J. E. Glenn and J. X. Saladin, *Phys. Rev. Lett.* 20, 1298 (1968).
4. J. Sprinkle et al., *Bull. Am. Phys. Soc.* 22, 545 (1977).
5. F. T. Baker et al., *Phys. Rev. Lett.* 37, 193 (1976).
6. F. T. Baker et al., *Nucl. Phys.* A266, 377 (1976).

^{20}Ne + ^{208}Pb Elastic and Inelastic Scattering at 131 MeV

E. E. Gross J. L. C. Ford, Jr.
T. P. Cleary D. C. Hensley
K. S. Toth

Because the ^{20}Ne deformation parameters derived from light-ion[1-3] and Coulomb excitation[4] experiments are in disagreement, measurements were made of inelastic scattering of ^{20}Ne on ^{208}Pb at 131 MeV to study the shape of ^{20}Ne. Angular distributions for elastic and inelastic scattering to the ^{20}Ne 2^+ state at 1.63 MeV, the ^{208}Pb 3^- at 2.62 MeV, and a broad group of levels corresponding to excitation of the ^{20}Ne 4^+ (4.25 MeV), ^{208}Pb 2^+ (4.09 MeV), and ^{208}Pb 4^+ (4.32 MeV) states was measured by means of a large solid-angle spectrograph.[5] More detailed angular distributions for the elastic and ^{20}Ne 2^+ transitions were obtained by means of a position-sensitive solid-state detector, which was adjusted to simultaneously provide data in 1° steps at 15 angles.[6]

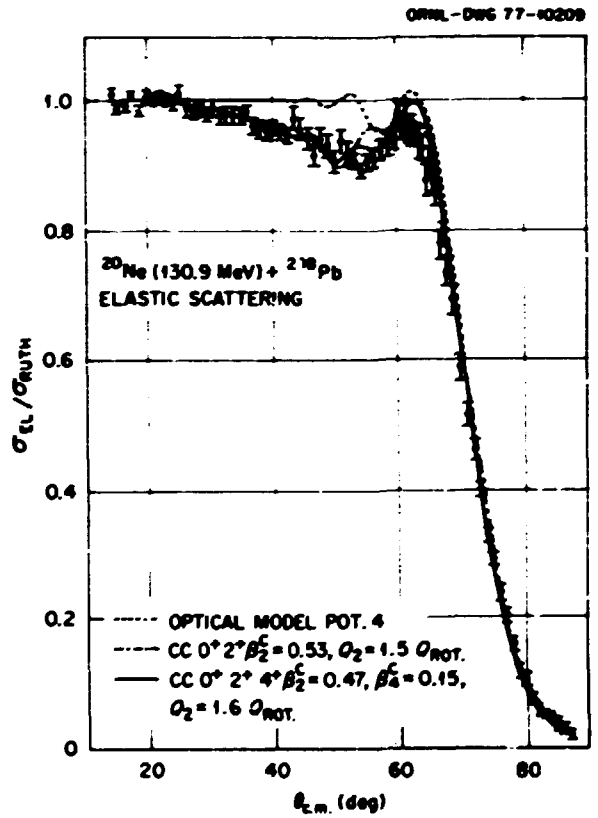

Fig. 2.2. Ratio of elastic scattering to Rutherford scattering for 130.9-MeV ^{20}Ne incident on ^{208}Pb. The dotted curve is an optical-model calculation with the parameters of Table 2.1. The dot-dash curve is a 0^+-2^+ CC calculation employing the rotational model. The solid curve is a similar calculation including the 4^+ state with the parameters shown and the potential of Table 2.1.

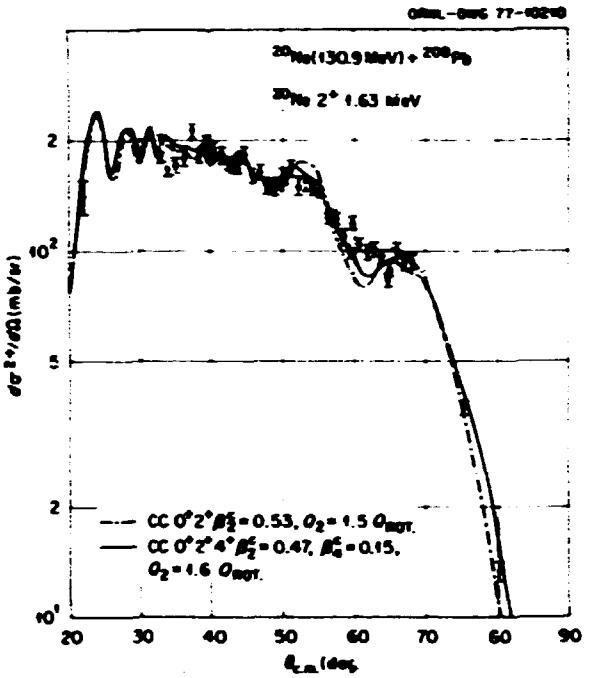

Fig. 2.3. Differential cross section for exciting the ^{20}Ne 2^+ state (1.63 MeV). The curves are CC calculations corresponding to the ground-state calculations shown in Fig. 2.2.

The results from these two measurements for the elastic and 1.63-MeV transitions are shown in Figs. 2.2 and 2.3. The strong coupling of the elastic and ^{20}Ne 2^+ reaction channels, signified by the dramatic falloff of the elastic data from Rutherford scattering beyond 20°, cannot be simulated by any reasonable parameter variation of the traditional optical-model potential. However, CC calculations[7] employing the rotational model and including the coupling to the ^{20}Ne 2^+ state are found to provide a much better description of the data. Of particular significance is the surprising sensitivity of the elastic calculations to the inclusion of the ^{20}Ne 4^+ channel. The effects of coupling to the 4^+ are even more pronounced in the angular distribution for the 2^+ transition (Fig. 2.3). Indeed, the region of the distribution associated with the grazing collision, approximately 65°, seems to be extremely crucial in determining the value of β_4. While the small-angle region ($30° < \theta < 50°$) of the 2^+ calculation depends predominantly on the value of β_2^c, the large-angle region ($70° < \theta < 80°$) depends most sensitively on the value of Q_2. This partial separation of the different aspects of the excitation process allows for the possibility that a final fit to these data will result in a unique set of parameters.

Preliminary attempts to achieve a simultaneous fit to the data for the elastic scattering, for inelastic scattering to ^{20}Ne 2$^+$, and for transitions to the group of levels above 4.0 MeV excitation (not shown) with the potential given in Table 2.1 yield the following results: $\beta_2' = 0.47$, $\beta_4' = 0.15$, and $Q_2 = 1.6\ Q_{rm}$. The

Table 2.1. Potential parameters[a]

	V_r	r_r	a_r	W	r	a
Optical model	22.5	1.33	0.44	15.2	1.29	0.67
Coupled channels	22.5	1.29	0.51	5.0	1.43	0.30

[a]All depths in MeV and geometrical factors in fm.

nuclear deformations (β'') were determined from the Coulomb deformations (β'), using the Hendrie scaling procedure.[8]

1. R. de Swiniarski et al. *Nucl. Phys.* A261, 111 (1976).
2. H. Rebel et al., *Nucl. Phys.* A182, 145 (1972).
3. F. Hinterberger et al., *Nucl. Phys.* A115, 570 (1968).
4. K. Nakai et al., *Nucl. Phys.* A150, 114 (1970).
5. E. E. Gross, *Nucl. Instrum. Methods* 121, 297 (1974).
6. J. B. Ball et al., *Nucl. Phys.* A252, 208 (1975).
7. J. Raynal, computer code ECIS73 (unpublished).
8. D. L. Hendrie, *Phys. Rev. Lett.* 31, 478 (1974).

Mutual Excitation of ^{22}Ne and ^{126}Te in Inelastic Scattering

T. P. Cleary, D. C. Hensley, J. L. C. Ford, Jr., C. R. Bingham[1], E. E. Gross, J. Vrba[1]

One aspect of heavy-ion collisions that might afford us new insight into nuclear shapes is the possibility of achieving simultaneous excitation of both target and projectile nuclei in inelastic scattering. This phenomenon has been observed only in the scattering of heavy ions from light-mass targets.[2] In order to search for such excitations in collisions between heavy systems, measurements were made for the inelastic scattering of ^{22}Ne from ^{126}Te at 93.5 MeV. The presence of strongly collective 2$^+$ states in both of these nuclei and the energy spacing of the low-lying levels made this an ideal system in which to look for such excitations.

A magnetic spectrograph was used to measure angular distributions for transitions to the ground states, the ^{126}Te 2$^+$ state at 0.666 MeV, the ^{22}Ne 2$^+$ at 1.27 MeV, and a weak transition at a Q value of −1.94 MeV. This last transition is identified with the mutual excitation of both ^{126}Te and ^{22}Ne to their 2$^+$ states. The results obtained for the ^{126}Te 2$^+$ and ^{22}Ne 2$^+$ transitions are shown in Fig. 2.4, and the angular distribution for the mutual excitation is shown in Fig. 2.5. While the overall shapes of the angular distributions for the 2$^+$ transitions are similar, with Coulomb excitation dominating the forward angle

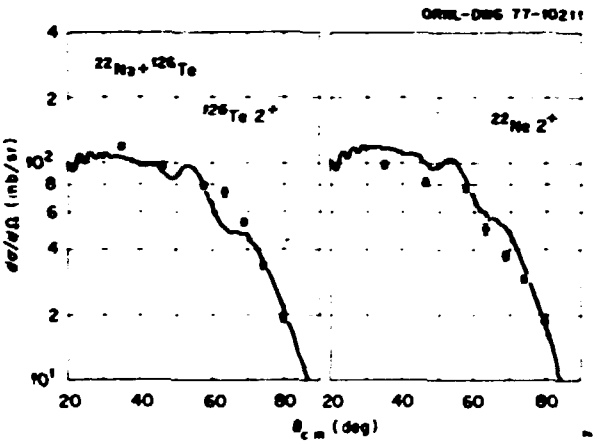

Fig. 2.4. Angular distributions for transitions to the ^{126}Te 2$^+$ state at 0.666 MeV and the ^{22}Ne 2$^+$ state at 1.27 MeV. The curves represent the results of CC calculations that include couplings to each of the 2$^+$ channels.

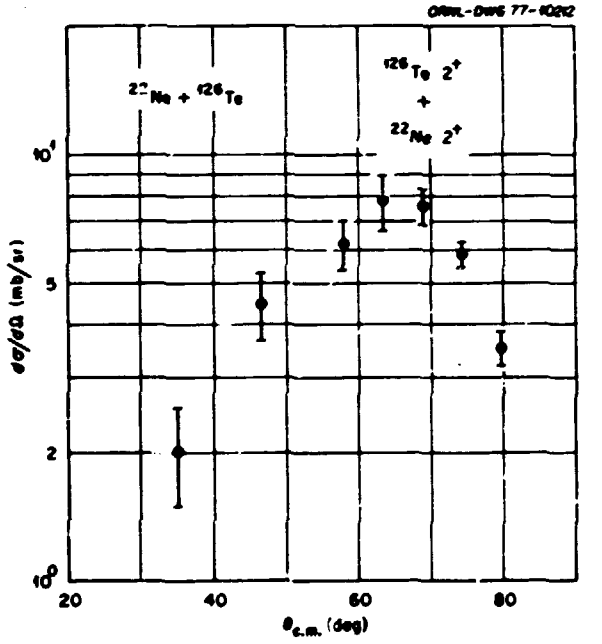

Fig. 2.5. Angular distribution for the transition to the mutual excitation at an energy of excitation of 1.94 MeV in the composite system.

data and nuclear processes dominating the back angles, the shapes do differ near the angles corresponding to grazing orbits (about 65°). In sharp contrast to these results, the angular distribution for the mutual excitation exhibits a bell shape centered about the grazing angle. This shape is the signature for a reaction that takes place when the nuclear surfaces come in contact; thus the magnitude of the cross section could provide a sensitive measure of the nuclear surface deformations of the two colliding systems. Initial CC calculations,[3] which include only couplings to the ^{126}Te 2^+ and ^{20}Ne 2^+ states, are shown in Fig. 2.4. Efforts are under way to incorporate the mutual excitation channel into the calculation.

1. University of Tennessee, Knoxville.
2. G. T. Garvey, A. M. Smith, and J. C. Hiebert, *Phys. Rev.* **130**, 2397 (1963).
3. P. D. Kunz, Computer Code CHUCK (unpublished).

SINGLE-PARTICLE TRANSFER REACTIONS INDUCED BY ^{12}C ON ^{208}Pb

T. P. Cleary, E. E. Gross, J. L. C. Ford, Jr., D. C. Hensley, J. Gomez del Campo, K. S. Toth, S. T. Thornton[1]

As part of a continuing effort to explore the systematics of ^{12}C-induced reactions in the lead region, initiated by work[2] on a ^{208}Pb target, we have measured angular distributions for the ^{206}Pb(^{12}C,^{11}B) and (^{12}C,^{13}C) reactions. The measurements were carried out with magnetic spectrograph at an incident energy of 95 MeV. Spectra obtained at a lab angle of 46° (near the maxima in the angular distributions) are shown in Fig. 2.6. Spectroscopic transition strengths derived from analogous light-ion transfer experiments are indicated for each of the reactions, and the general distributions of strength are closely reflected in the measured spectra.

The DWBA calculations, including full finite-range and recoil effects, were made with the code LOLA,[3] and the results obtained are in excellent agreement with the angular distributions for the (^{12}C, ^{13}C) reaction. This is consistent with the agreement observed in the analysis of the ^{208}Pb(^{12}C,^{13}C) data. However, the systematic discrepancy between calculation and experiment that was originally

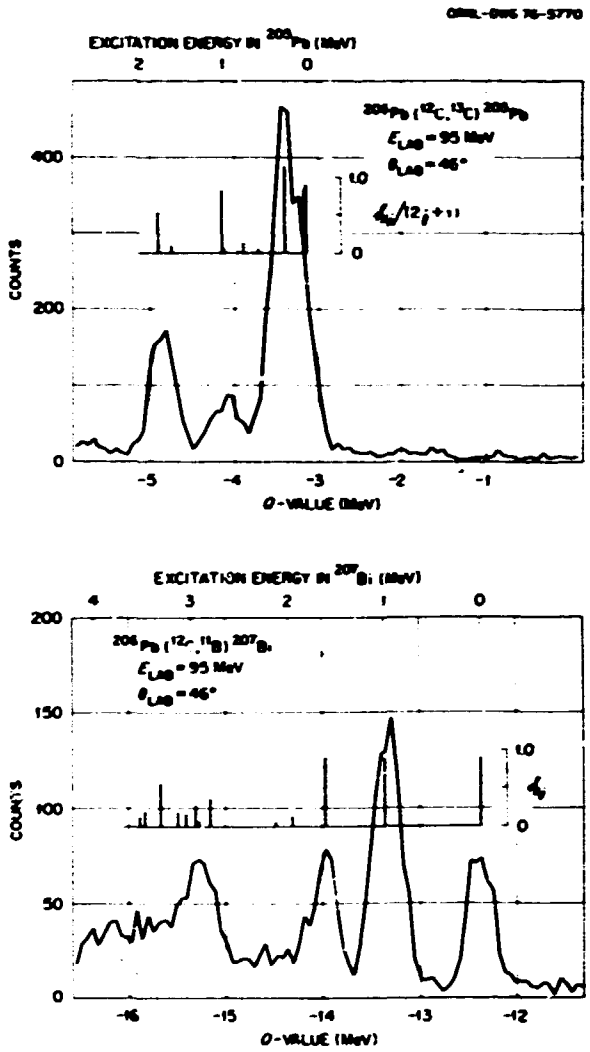

Fig. 2.6. Spectra of ^{13}C and ^{11}B obtained from ^{12}C-induced reactions on ^{208}Pb.

observed[2] for the ^{208}Pb(^{12}C,^{11}B) reaction is found to persist for the present study on ^{206}Pb. The angular distributions for both of these reactions and the corresponding LOLA calculations are presented in Fig. 2.7. While the calculations predict that the peak in the angular distributions should move back in angle as the Q value becomes more negative, the maxima in the data remain relatively constant in angle. Coupled-channels calculations are in progress to determine if multistep processes might play a

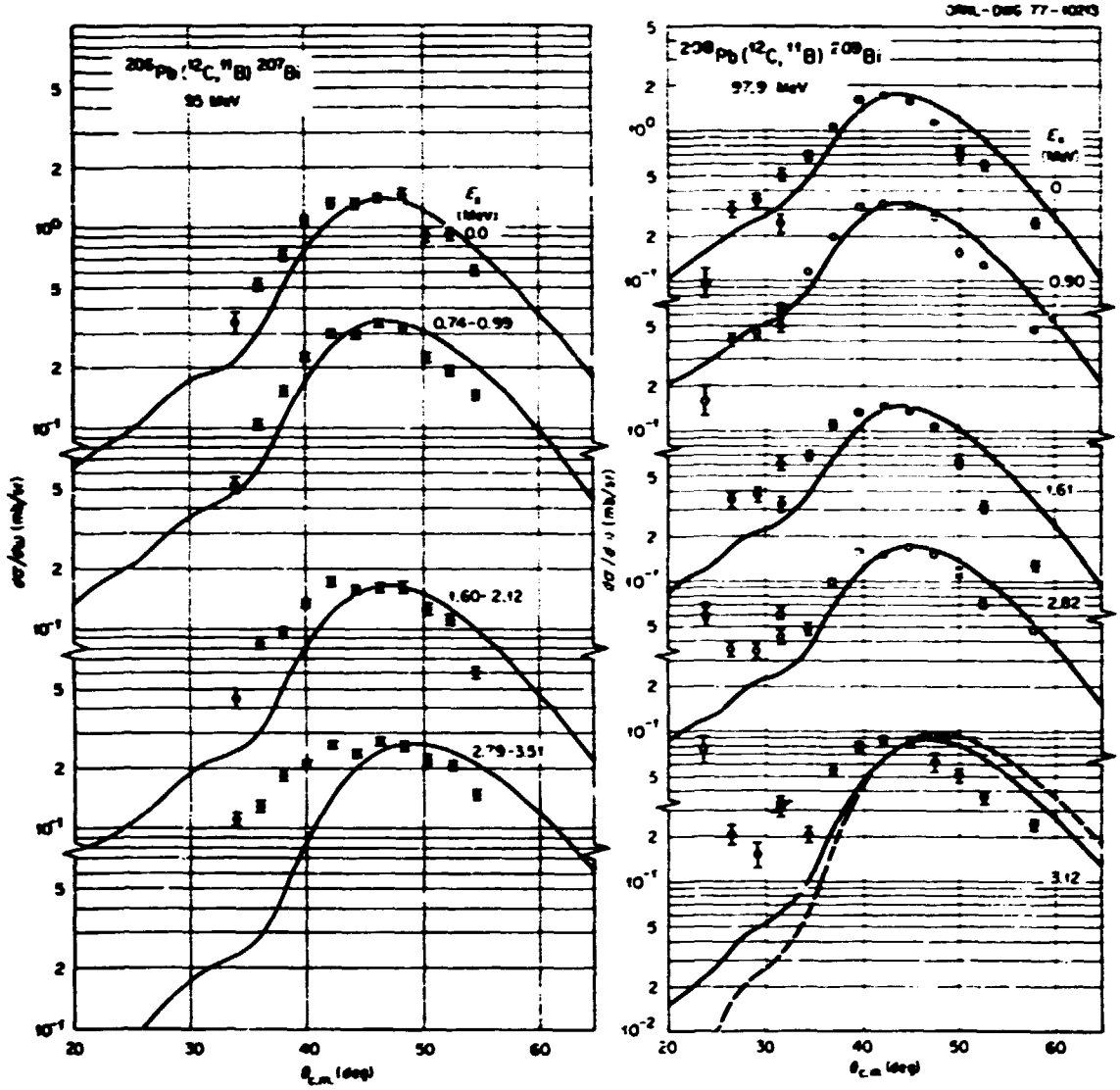

Fig. 2.7. Comparison of the angular distributions from the present $^{208}Pb(^{12}C,^{11}B)$ measurement with the previous study on ^{208}Pb of ref. 2. The solid curves are DWBA calculations made with the code LOLA.

significant role in the reaction process and thus account for this discrepancy.

1. University of Virginia, Charlottesville.
2. K. S. Toth et al., *Phys. Rev. C* 14, 1471 (1976).
3. R. M. DeVries, *Phys. Rev. C* 8, 951 (1973).

HIGH-ENERGY PARTICLES FROM HEAVY-ION-INDUCED REACTIONS

J. B. Ball C. B. Fulmer
R. L. Robinson

Recent calculations by Bertini et al.[1] of nucleon spectra emitted from ^{12}C reactions with iron targets at several incident particle energies ranging from 16 to 75 MeV/nucleon predict appreciable numbers of nucleons with energies greater than the energy per nucleon of the incident projectile. The calculations are based on a model[2] that treats heavy-ion reactions as the interaction of two Fermi gases. According to these calculations, these energetic nucleons are due to evaporation from the excited projectile-like nuclei which, after the interaction, are moving in the forward direction. These results are in contrast to experimental measurements of heavier fragments ($A \geq 4$) from fragmentation of 29-GeV ^{14}N ions on a variety of targets,[3] where the most energetic fragment energies were of the same energy per nucleon as that

of the incident projectile. Experimental results are of interest to elucidate mechanisms of energetic fragment cooling and, particularly, to compare with the calculations of Bertini et al. as a test of the evaporation-cascade model. Experimental measurements are also of practical interest for determining shielding requirements of heavy-ion accelerators such as the proposed phase II booster for the Holifield Heavy-Ion Research Facility (HHIRF).

We used a beam of 194-MeV ^{12}C ions from ORIC to bombard an ^{56}Fe target and measured energy spectra of protons and other charged particles at a number of angles between 8 and 65°. Particles were detected by a ΔE-E telescope to provide particle identification and energy spectra. An energy calibration of the detector was obtained by measuring elastically scattered proton recoils from a polyethylene target at a number of angles.

Figure 2.8 presents energy spectra of protons, deuterons, and tritons observed at a laboratory angle of 15°. The proton energy spectra extend to 70 MeV, which is more than a factor of 4 times the energy per nucleon of the incident beam. Surprisingly, the deuteron and triton spectra also extend to energies per nucleon that are appreciably higher than that of the incident projectile. Qualitatively similar results were also obtained with beams of ^{14}N and ^{16}O ions and other target materials.

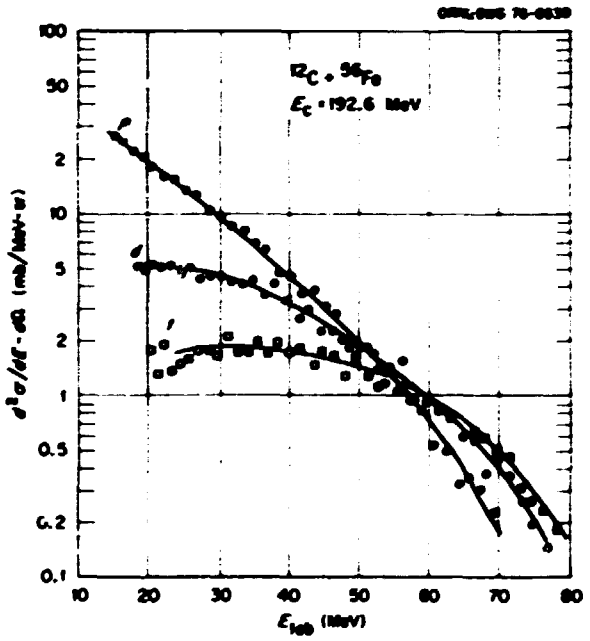

Fig. 2.8. Energy spectra of protons, deuterons, and tritons from 16-MeV/nucleon ^{12}C-induced reactions on an iron target. These data were obtained at 15° laboratory angle.

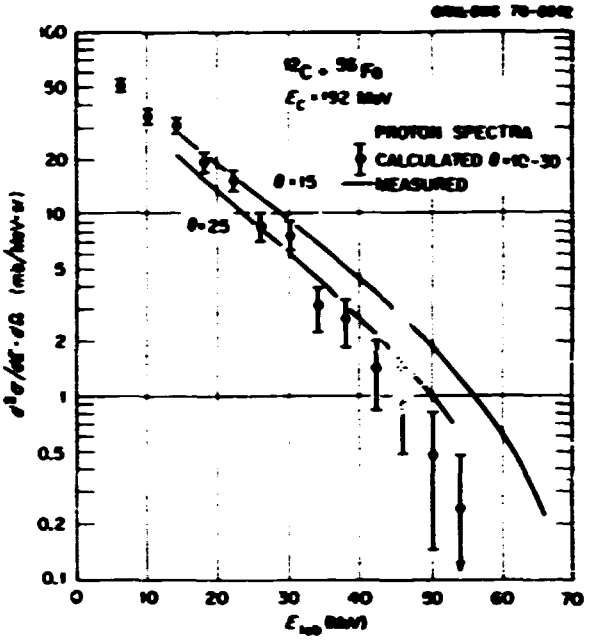

Fig. 2.9. Comparison of experimental and calculated proton energy spectra from ^{12}C + ^{56}Fe reactions at 192 MeV. The calculated spectrum is from ref. 1.

In Fig. 2.9, we compare proton energy spectra with yields obtained from the calculations of Bertini et al.[1] There is reasonable agreement between the experimental and the calculated results. It is obviously desirable to obtain data at higher incident particle energies. We plan to obtain such measurements at the Indiana University Cyclotron Facility, using incident projectile beams of 25 to 30 MeV/nucleon.

1. H. W. Bertini, R. T. Santoro, and O. W. Hermann, *Phys. Rev. C* 14, 590 (1976).
2. H. W. Bertini, T. A. Gabriel, and R. T. Santoro, *Phys. Rev. C* 9, 522 (1974).
3. H. H. Heckman et al., *Phys. Rev. Lett.* 14, 926 (1972).

POSSIBLE ANOMALY IN THE $^{13}C(^7Li,^6He)^{14}N$ TRANSFER REACTION

C. F. Maguire[1] R. B. Piercey[1]
A. V. Ramayya[1] J. L. C. Ford, Jr.
R. M. Ronningen[1] J. Gomez del Campo

One of the more disturbing failures of the DWBA approach to the analysis of heavy-ion-induced transfer reactions is the so-called "$l = l$ anomaly." First seen by DeVries et al.[2] in the $^{12}C(^{14}N, ^{13}N)^{13}C^*$ ($^1/_2^+$, 3.09 MeV) neutron transfer reaction, the

anomaly refers to the predicted uniquely allowed $l = 1$ angular distribution having an oscillatory shape that is almost exactly out of phase with the experimental data. The anomaly has since been seen in other such reactions,[3] although there are a few known cases for which the predicted uniquely allowed shape is in phase with the data. No satisfactory explanation is available for this effect.

In all the reported studies, the anomaly shows up when the transferred particle goes from or into an odd-odd nucleus, but the anomaly does not appear otherwise. In order to test whether this is an accidental correlation, we decided to look at the $^{12,13}C(^7Li,^6He)^{13,14}N$ reactions, especially at those final states representing uniquely allowed $l = 1$ transfers. With the ^{12}C target, no odd-odd system is present for the location of the transferred proton, while for the ^{13}C target, the final state is odd-odd. The object of this experiment was to determine if the anomaly would appear in the latter reaction, while not appearing in the former. These reactions were performed previously by Schumacher and collaborators[4] at 36 MeV, using solid-state detectors, which, however, did not resolve the groups of interest here.

The experiment was performed on the EN tandem accelerating sputter-source-produced ^7Li ions to the near maximum energy of 25 MeV. Reaction products were momentum-analyzed by the Enge magnetic spectrometer and detected in the 60-cm-long double-chambered gas proportional counter, which yielded position (*momentum*) and dE/dx (Z identification). Figure 2.10 illustrates the data obtained for the ^{13}C target, leading to the ground 1^+ (predominantly an $l = 2$ transfer), the 4.92-MeV 0^- (uniquely $l = 1$), and the 5.69-MeV 1^- (also uniquely $l = 1$) residual states. Fits to these data were generated, with the full-recoil code NICOLE employing the potential well-matched optical-parameter set derived by Schumacher. The highly oscillatory ground-state group is extremely well fit in this reaction. By comparison, the fits to the $l = 1$ transfer groups are markedly inferior. The predicted local maximum at about 24° c.m. appears as a local minimum in the data of these groups. However, the angular distributions are not structured enough to conclude that the anomaly is definitely present.

The second part of the experiment, the comparison of a similar transition to ^{13}N, was not successful. The

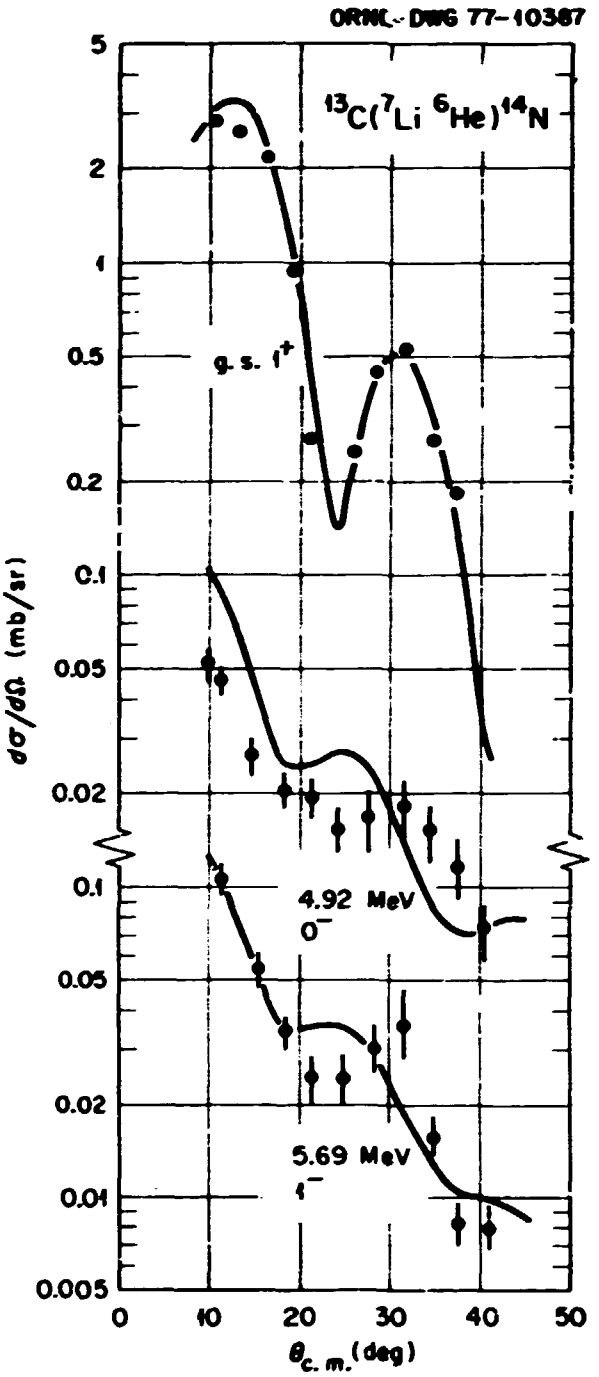

Fig. 2.10. Differential cross sections for the $^{13}C(^7Li,^6He)^{14}N$ reaction populating the ground and the $2s_{1/2}$ fragments in ^{14}N. The solid lines represent the predicted shapes according to the exact-finite-range DWBA theory and have been normalized to the data.

^{4}He background in dE/dx was too strong for the weaker ^{6}He groups to be resolved. This was all the more unfortunate because of the possible anomaly in the transitions to ^{14}N. In this regard, future experiments at higher energies where the angular distributions become much more structured are now under consideration elsewhere.

---

1. Vanderbilt University, Nashville, Tenn.
2. R. M. DeVries et al., *Phys. Rev. Lett.* 32, 680 (1974).
3. K-I Kubo, K. G. Nair, and K. Nagatani, *Phys. Rev. Lett.* 37, 222 (1976).
4. P. Schumacher et al., *Nucl. Phys.* A212, 573 (1973).

STRONGLY DAMPED COLLISIONS INVOLVING MEDIUM-MASS TARGETS

R. A. Dayras, R. L. Robinson, C. B. Fulmer, D. G. Sarantites[1], M. L. Halbert, A. H. Snell[2], D. C. Hensley, R. G. Stokstad, L. Westerberg[1]

Strongly damped collisions have been studied mainly by measuring the energy, mass, and angular distributions of the projectile-like fragments. Such measurements characterize the gross features of these reactions (i.e., the energy damping, the mass transfer, and the time scale of the interaction). More detailed and complete measurements of the reaction products are necessary, however, in order to obtain information on the transfer of angular momentum of relative motion to the internal degrees of freedom and information on the dissipation of the energy removed from relative motion. These two aspects of strongly damped collisions are under investigation at ORIC, using several reactions involving medium-mass targets.

Multiplicity and Energy of Gamma Rays

The average number, M_γ, and the average energy, E_γ, of the gamma rays accompanying strongly damped collisions are measured as a function of the atomic number Z and the energy of the projectile-like fragments. A set of nine NaI(Tl) detectors (2 by 3 in.) is operated in coincidence with a heavy-ion telescope consisting of a ΔE gas ionization chamber and a 1500-μm surface-barrier E detector subtending a solid angle of 12 millisteradian (msr). The front faces of the individually shielded NaI detectors are located 10 cm from the target, and their thresholds are set at 100 keV. The digitized ΔE and E signals are stored on-line in one of five 200 by 300 channel arrays according to whether 0, 1, 2, 3, 4, or more NaI detectors record gamma rays in coincidence with the heavy-ion telescope. Simultaneously, and in coincidence with the heavy-ion telescope, the linear signals from three of the NaI detectors are recorded event by event on magnetic tape.

A list of the reactions under investigation and the experimental conditions are given in Table 2.2. Some of the experimental results are shown in Fig. 2.11 for the ^{20}Ne + ^{63}Cu reaction. The energy spectrum for the reaction products with $Z = 11$ exhibits a quasi-elastic component and a strongly damped component. The energy spectra for the reaction products with $Z = 7$ and $Z = 12$ (further removed from the Z of the beam) are dominated by the strongly damped component. For the ^{20}Ne + ^{63}Cu reaction, the average gamma-ray multiplicity $\bar{M}_\gamma$ measured in coincidence with all the observed reaction products increases with the inelasticity of the collision to reach a maximum near the optimum Q value for strongly damped collisions. As the energy dissipated in the collision continues to increase, $\bar{M}_\gamma$ appears to drop sharply (dotted line). The value of $\bar{M}_\gamma$ nearly equal to 10.5 for the lowest energy reaction products (shaded area in Fig. 2.11) represents the average multiplicity for the evaporation residues.

The decrease in $\bar{M}_\gamma$ for large energy loss is still under experimental investigation. Fusion reactions by ^{20}Ne bombarding carbon and oxygen contaminants on the target can produce evaporation residues in the same mass range as the projectile-like fragments from the ^{20}Ne + ^{63}Cu deep inelastic reaction. Such light evaporation residues would have a very low gamma-ray multiplicity. The presence of a sufficiently large amount of carbon and/or oxygen on the target surface, therefore, could contribute to the apparent drop in $\bar{M}_\gamma$ in an energy region where the yield of products from the strongly damped collision decreases rapidly. Further experiments will clarify this. If verified, the observed decrease in $\bar{M}_\gamma$ at large energy loss would be evidence for the emission

Table 2.2 Deep inelastic reactions for which gamma-ray multiplicity is being investigated

Target	Projectile	Incident energy (MeV)	Laboratory angle of the heavy-ion telescope (°)
^{63}Cu (1 mg/cm^2)	^{12}C	130	16, 20, 30
		86	28
	^{20}Ne	165	26
^{156}Gd (1.5 mg/cm^2)	^{12}C	195	23, 33

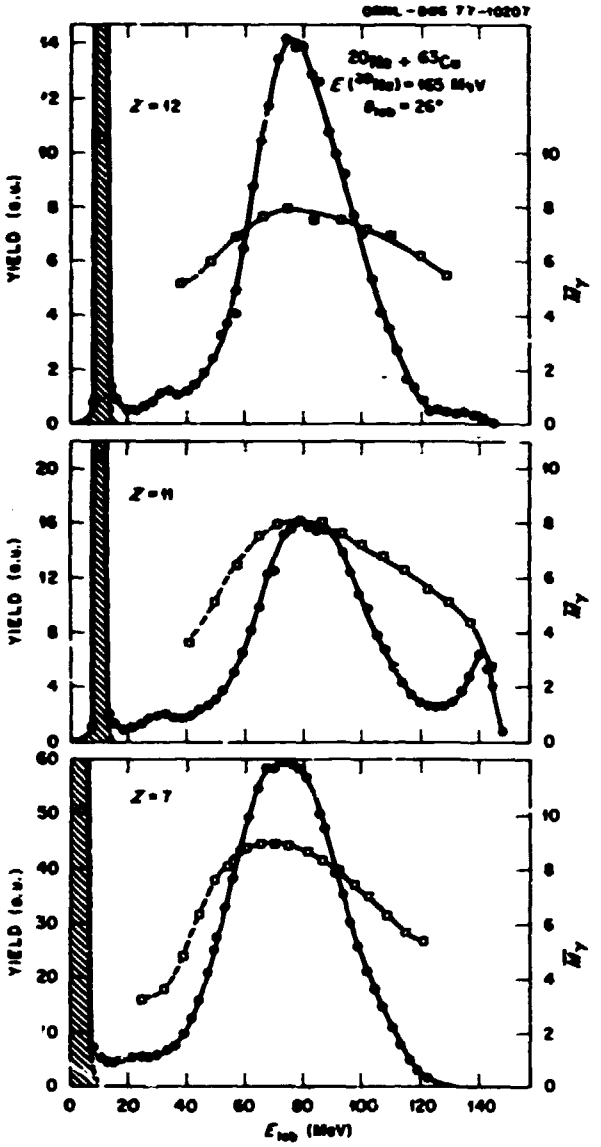

Fig. 2.11. Particle yields (circles) and average gamma-ray multiplicities (squares) for products with $Z = 7$, 11, and 12 produced in the reaction $^{20}Ne + ^{63}Cu$. The lines connecting the data points are to guide the eye. The shaded region in the lowest energy portion of the spectra corresponds to low-energy heavy particles (mainly evaporation residues) which have an energy loss in the gas comparable to that of the light fragment.

of particles prior to the scission of the intermediate system into projectile- and target-like fragments.

From the measured average gamma-ray energy $\bar{E}_\gamma$ equal to about 2.0 MeV and from the values of $\bar{M}_\gamma$ equal to about 8 to 10 obtained in the main portion of the strongly damped spectrum, we deduce that only about 25% of the energy absorbed in the collision is dissipated by gamma-ray emission. Consequently, the main portion of this energy has to be dissipated by the emission of light particles such as protons, neutrons, and alpha particles.

From the multiplicities $\bar{M}_\gamma$, one may attempt to deduce the internal angular momentum I imparted to the two fragments resulting from strongly damped collisions. Light-particle emission, which carries away both angular momentum and excitation energy, complicates this task. The results of such an analysis are shown in Fig. 2.12, where the internal angular momentum I imparted to the fragments during the collision is plotted as a function of the Z of the projectile-like fragment. It has been assumed that each gamma ray carries two units of angular momentum. Correction for light-particle emission has been applied in a way described by Albrecht et al.[3] For comparison, the angular momentum I imparted to both fragments has been calculated,

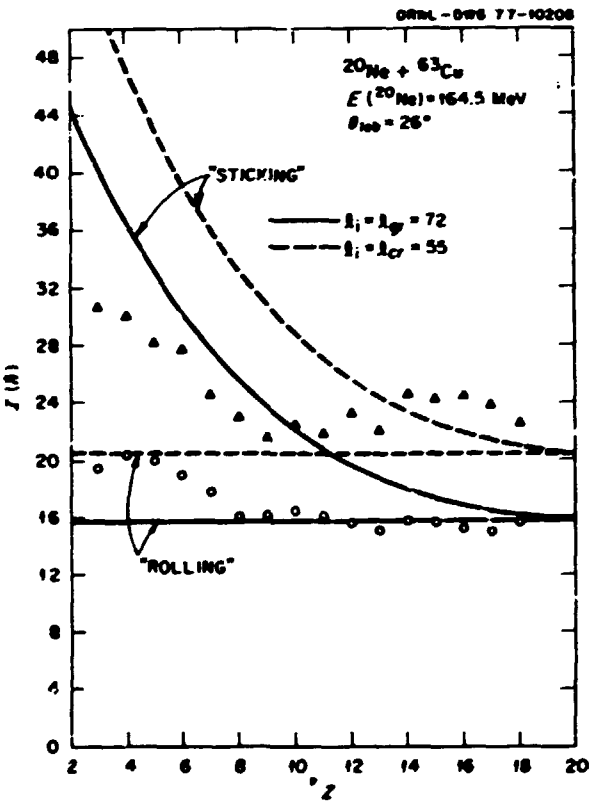

Fig. 2.12. Intrinsic angular momentum I imparted to the fragments at scission vs Z for the strongly damped components, assuming $I = 2M_\gamma$ (circles) and $I = 2M_\gamma + L_p$ (triangles). L_p is the correction for light-particle emission. The curves are the predictions from a classical friction model in the limiting cases of rolling and sticking.

assuming that transfer of angular momentum of relative motion into internal degrees of freedom occurs under the action of frictional forces between two spherical nuclei. In the initial stage of the collision, the two nuclei slide on each other. The action of viscous forces sets them into rotation. When the peripheral velocities are matched, the system reaches the rolling stage. Finally, under the action of rolling friction, the fragments reach a sticking configuration and rotate as a rigid body. Two limiting cases are considered: first, the nuclei roll on each other; or second, the nuclei stick rigidly at their point of contact. These calculations have been done for two values of the entrance channel angular momentum: the critical angular momentum for fusion $l_c = 55\ \hbar$ and the grazing angular momentum $l_g = 72\ \hbar$, which constitute the limiting l values for strongly damped collisions. Within the uncertainty of the corrections for particle emission, it appears that frictional forces lead to a sticking condition for fragments heavier than the beam. A situation intermediate between rolling and sticking is indicated for fragments with atomic numbers less than 10.

Gamma-Ray Identification of Reaction Products

In the bombardment of ^{63}Cu with 130-MeV ^{12}C projectiles, as one additional technique for obtaining information on deep inelastic process and other non-fusion reaction mechanisms, gamma rays were detected in a 50-cc Ge(Li) detector at 90° from the beam direction, in coincidence with the heavy-ion telescope positioned at 20°. The gamma-ray spectra in coincidence with each element with $Z = 2$ to $Z = 14$ were analyzed. In spite of poor statistics, a number of gamma rays were tentatively identified on the basis of their energy and their coincidence relation with the various elements.

The data indicate that the reactions can be categorized into three groups:

1. Reactions in which nucleons are emitted by the target and the ^{12}C projectile remains intact. The gamma rays observed in coincidence with carbon nuclides suggest the presence of five isotopes which can result from emission of one to three protons and/or neutrons.
2. Reactions in which some nucleons are transferred to the target nucleus and some additional nucleons are emitted by the system. There is evidence for 11 different reactions in which one to three particles (neutrons, protons, alphas) are transferred to the target nucleus, and one to three particles are emitted. In these reactions, the residual heavy fragment is equal to or heavier than the target nucleus ^{63}Cu.
3. Reactions in which nucleons are transferred to the target nucleus and the target emits more mass than has been transferred to it. In the five cases identified as having this process, all but one emit only an alpha particle. The fifth case emits an alpha and a neutron.

---

1. Washington University, St. Louis, Mo.
2. Consultant with the Physics Division.
3. R. Albrecht et al., *Phys. Rev. Lett.* 34, 1400 (1975).

DEEPLY INELASTIC AND OTHER REACTIONS OF ^{20}Ne WITH ^{48}Ti AND ^{94}Zr

R. L. Ferguson[1] F. Pleasonton
H. Nakahara[2] A. H. Snell
F. E. Obenshain M. P. Webb
F. Plasil

Studies of the reactions ^{20}Ne on ^{48}Ti and ^{94}Zr extend our systematic survey of neon-induced reactions in the medium-mass region.[3] There are no reaction models that have been specifically applied to this mass region, and we plan to investigate whether models designed for heavy nuclear systems will be applicable. However, the diversity of reaction products is qualitatively the same in the two regions. For example, fission of the compound system may be expected to occur in this region, but it has become clear from our measurements that other modes of decay of the composite system dominate.

For the two systems discussed here, as well as for ^{20}Ne on ^{60}Ni reported earlier, we have chosen to obtain data for all three systems at equal energies above the Coulomb barrier as shown in Table 2.3. In

Table 2.3. Estimate of the range of l-values populating direct reactions

Target	E_c (MeV)[a]	σ_R (mb)	$\sigma_{r,r}$ (mb)	Elastic-scattering quarter-point angle ($\sigma/\sigma_R = 4$)(°)	l_{max}	l_{cr}
^{48}Ti	155	1913	1342	21.33	66	55
^{60}Ni	166	1903	1163	24.25	72	58
^{94}Zr	166	2430	1576	27.2	91	75

[a]The projectile was ^{20}Ne in each case with the laboratory energy as listed.

[b]The angle given here was obtained from the elastic-scattering curve and converted to the c.m. system in order to calculate the total reaction cross section in column 3.

order to compare our results with reaction models, it will probably be necessary to make measurements as a function of excitation energy.

The experimental setup consisted of several gas-filled ionization chambers with silicon surface-barrier detectors mounted in the rear of the chambers. These were mounted on movable arms in a scattering chamber. The gas serves as a variable-thickness ΔE detector and the solid-state detector as an E-ΔE detector. For our systems, atomic numbers (Z) produced in the reactions may be resolved up to $Z = 24$. As a result, individual Zs for evaporation-residue products cannot be resolved. These products do form a well-defined mountain in the E-ΔE plane, and the number of events is observed to decrease exponentially with increasing angle. The neon elastic-scattering data are obtained at the same time as the evaporation-residue products, and one may extract both the evaporation-residue and the total-reaction cross sections. Table 2.3 gives a list of targets, the cross sections, and other related information. The nickel target data are included for completeness.

The angular distributions for a number of reaction products of ^{20}Ne and ^{48}Ti are shown in Fig. 2.13. The products with atomic numbers near that of the projectile show a strong forward peaking, and the angular distributions for those far from the projectile become nearly 1/sine in $\theta_{c.m.}$. Figure 2.14 shows contour plots of the relative yield as a function of the c.m. energy E and the c.m. angle $\theta_{c.m.}$. The $Z = 8$ map shows a peak between 50 and 60 MeV which is due to the quasi-elastic reaction. The deeply inelastic events do not form a distinct peak in this case. However, the map for $Z = 12$ does show a peak near 25 MeV which is due to the deeply inelastic events.

One of the striking differences between the nickel and titanium data on the one hand, and the zirconium data on the other, is that the yield for products with Z less than 10 is relatively much higher in the zirconium case than in the other two. Figure 2.15 shows the Z distributions at two angles for the Ne + Ni and Ne + Zr systems, where the yields are arbitrarily normalized at $Z = 10$. The yield for reaction products with Z greater than that of the projectile decreases relatively more quickly in the Ne + Zr system than in the Ne + Ni case. This feature can be qualitatively explained by examining the liquid-drop potential-energy surface as a function of both the mass asymmetry and the angular momentum. If it is assumed that the stripping and pickup reactions (leading to projectile-like light-reaction products) are projectile-like and are dominated by the higher

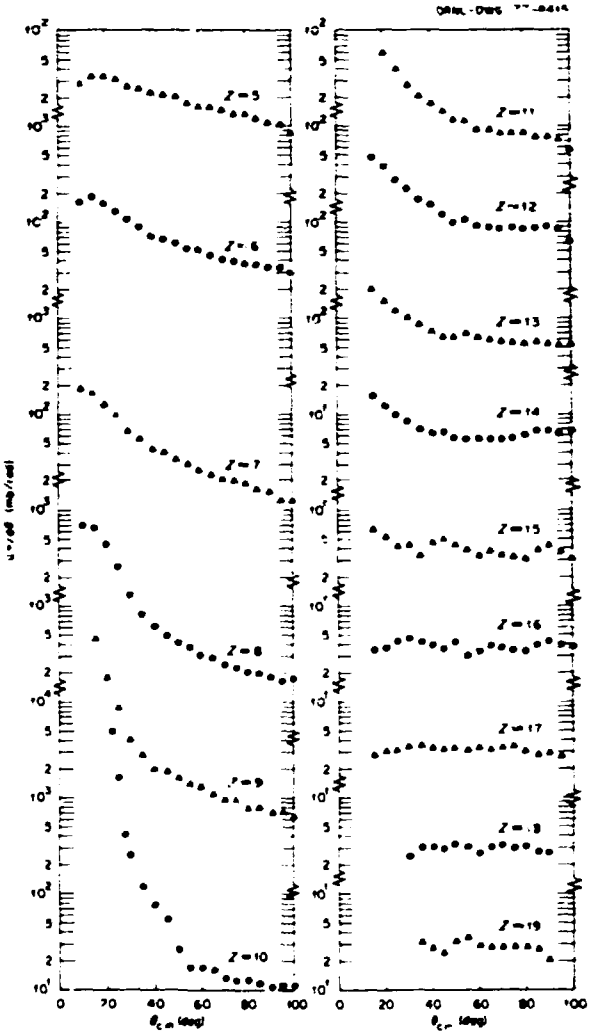

Fig. 2.13. Differential cross sections $d\sigma/d\Omega$ plotted vs $\theta_{c.m.}$ for various reaction products from 155-MeV ^{20}Ne on ^{48}Ti.

partial waves, we can estimate the range of l values populating these reactions from estimates of the total reaction and complete fusion cross sections. From the elastic-scattering quarter-point angle (where $\sigma/\sigma_R = 1/4$), the total reaction cross section and grazing angular momentum were calculated and are shown in Table 2.3. Neglecting a contribution to the complete-fusion cross section from fusion-fission reactions (analysis of the data suggests that this is a small cross section), the angle-integrated evaporation-residue cross section provides an estimate of the complete-fusion cross section for zirconium, which was found to be 1570 mb. The critical angular momentum (that l value below which complete fusion is assumed to be the only reaction) may then be estimated to be $l_{cr} = 75$ $\hbar$. Thus the range of l values populating the direct

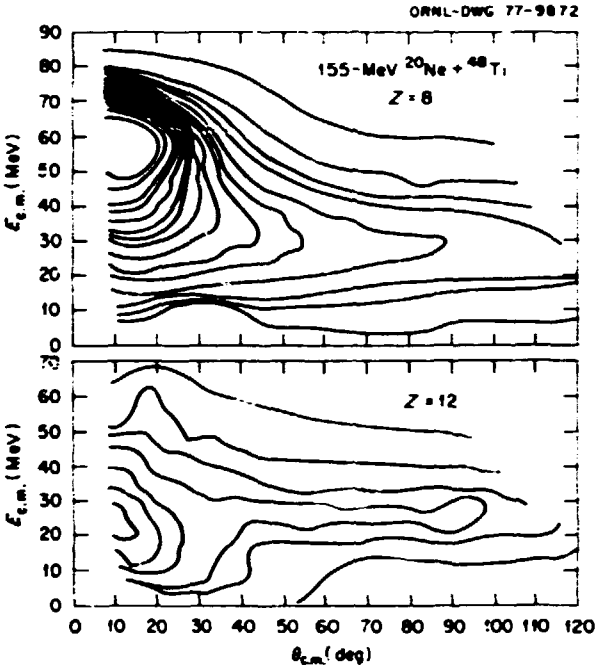

Fig. 2.14. Relative yields for $Z = 8$ and $Z = 12$ plotted as a contour map in the c.m. energy and angle plane.

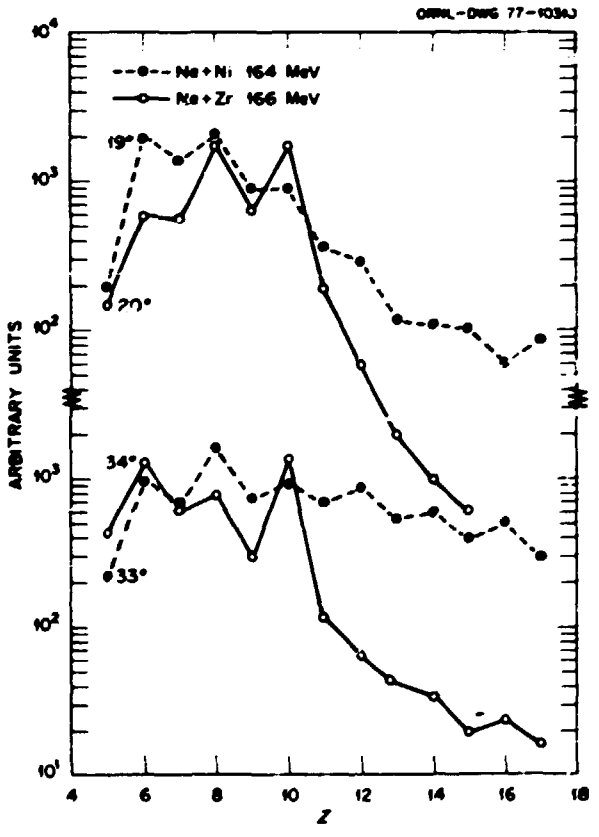

Fig. 2.15. Arbitrarily normalized Z distributions for Ne + Ni and Ne + Zr. Comparison is made for the most nearly identical lab angles between the two systems.

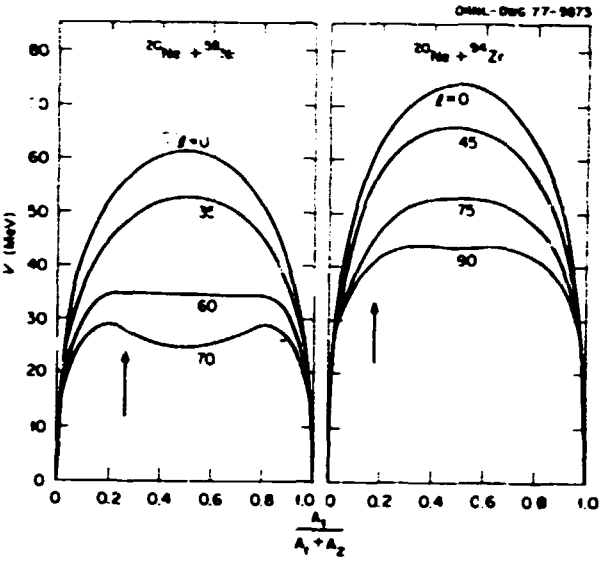

Fig. 2.16. Potential energy curves for various angular-momentum states for Ne + Ni and Ne + Zr.

reactions is approximately 75 to 91. Figure 2.16 shows the potential energy as a function of l and of mass asymmetry. The injection points for our reactions are indicated by arrows. As one can see, the surfaces differ for the two systems at the larger l values. The driving forces are such that the Ne + Zr system is likely to exhibit a preference for stripping, while the Ne + Ni system may exhibit a preference for pickup. The range of l values contributing in this nickel reaction is about 56 to 72. Other factors that have not been taken into account may play equally important roles in the transfer process and drive the reaction more toward transfer of particles away from the projectile.

1. Chemistry Division.
2. Tokyo Metropolitan University, Tokyo, Japan.
3. *Phys. Div. Annu. Prog. Rep. Dec. 31, 1975*, ORNL-5137, pp.26-32.

PRODUCTION OF $^{245,244}Cf$ IN REACTIONS[1] OF ^{239}Pu WITH ^{12}C, ^{16}O, ^{20}Ne, AND ^{14}N

R. L. Hahn[2] F. Hubert[3]
K. S. Toth P. F. Dittner[2]

In our continuing study of the mechanisms of deep inelastic or multinucleon transfer reactions in the heavy elements, we have used recoil techniques in irradiations of ^{239}Pu with beams of ^{12}C, ^{16}O, ^{20}Ne, and ^{14}N to produce ^{245}Cf and ^{244}Cf. Because of the large Coulomb barriers for charged-particle emission and

because Γ_n/Γ_f decreases rapidly with increasing Z in this region of the periodic table, one would expect that the production of californium nuclides from plutonium involves little or no contribution from the transfer from projectile to target of clusters containing more than four protons. Thus, these reactions may offer a way of selecting a particular transfer reaction path for investigation.

Our data strongly support this notion. Furthermore, they indicate that the same type of mechanism occurs in the transfer reactions induced by ^{12}C, ^{16}O, and ^{20}Ne, namely, a two-step process, such as (1) the transfer of a beryllium-like cluster from projectile (HI) to target, $^{239}Pu + HI \rightarrow {}^{247}Cf^{*} + (HI\text{-}Be)$; and (2) the evaporation of neutrons, in competition with fission, from the excited intermediate nucleus, $^{247}Cf^{*} \rightarrow {}^{247-x}Cf + xn$. In particular, the experimental excitation functions obtained with ^{12}C, ^{16}O, and ^{20}Ne have similar maximum values, about 10 μb, and have the same energy dependence when plotted as a function of the excitation energy of $^{247}Cf^{*}$. Some 20 to 40 MeV of excitation energy are deposited in the intermediate nucleus as a result of the transfer. The average kinetic energies measured for the californium recoils are also in general agreement with the predictions of a model that describes the details of the first step of the transfer process. Preliminary analysis of the data obtained with ^{14}N indicates that the recoil energies are consistent with the proposed transfer mechanism, but that the cross sections obtained are much smaller than those obtained with alpha-particle cluster projectile, such as ^{12}C, ^{16}O, and ^{20}Ne.

---

1. This account will appear in the *Chem. Div. Annu. Prog. Rep. Mar. 31, 1977*, ORNL-5297 (to be published).
2. Chemistry Division.
3. Centre d'Études Nucléaires, Bordeaux-Gradignan, France.

NONSTATISTICAL EFFECTS IN THE DECAY OF THE COMPOUND NUCLEUS ^{170}Yb

D. G. Sarantites[1] *R. A. Dayras*
J. H. Barker[2] M. L. Halbert
L. Westerberg[3] D. C. Hensley

We have produced highly excited ^{170}Yb compound nuclei in a variety of heavy-ion reactions with ORIC. Their de-excitation by emission of light particles and gamma rays has been under study. Previous reports[4,5] describe the gamma-ray multiplicity measurements for bombardments of ^{150}Nd with ^{20}Ne at four bombarding energies corresponding to ^{170}Yb excitation from 93 to 132 MeV. The results showed good agreement with the expectations for statistical decay of the compound nucleus.

The earlier work has been augmented in several ways, as indicated below in Table 2.4:

Table 2.4 Bombardment conditions for experiments leading to ^{170}Yb compound nuclei

Beam	Target	Beam energy (MeV)	^{170}Yb excitation (MeV)	Anti-Compton	Particle detector angle (°)		
					n	p,α (in plane)	p,α (in plane)
^{4}He	^{166}Er	67.6	64.2	X			
		80.2	76.6	X			
		95.3	91.3	X			
^{12}C	^{158}Gd	94.4	94.4				
		125.0	*106.2*				
		142.2	121.7	X			
		152.3	131.3		21, 82	90	55, 135, 135
		153.0	131.8				
		164.9	142.9	X			
^{20}Ne	^{150}Nd	97.5	63.2	X			
		113.7	77.7	X			
		128.8	92.7				
		145.2	107.1				
		164.6	*123.3*				
		173.2	132.2		15, 90		45
		175.2	134.3	134.3			
^{40}Ar	^{130}Te	158.8	56.5				

1. Two additional $^{20}Ne + ^{150}Nd$ bombardments were made at lower energies. As before, the first three moments of the multiplicity distribution were determined for several reaction channels.
2. Cross bombardments were made with three other systems leading to the same compound nucleus at approximately the same excitation energies to obtain gamma-ray multiplicity information.
3. Particle-gamma coincidence measurements were made with both ^{20}Ne and ^{12}C, forming ^{170}Yb at 132 MeV excitation. In these runs, spectra of neutrons, charged particles, and gamma rays were obtained simultaneously with the multiplicity information.
4. The evaporation-residue, symmetric-fission, and total-reaction cross sections for 175-MeV $^{20}Ne + ^{150}Nd$ were measured by means of Z-identifying telescopes without detection of gamma rays, as described in the next section of this report.

The method used for the experiments included in steps 1 and 2 above was similar to the earlier one.[4-6] In brief, spectra from a Ge(Li) detector at 90° were recorded in coincidence with yes/no signals from nine 2- by 3-in. NaI detectors distributed over one hemisphere. Nineteen 8K spectra were produced on-line in the disk memory of the computer. Ten of them were sorted according to whether the Ge(Li) pulse was accompanied by 0, 1, 2, ..., 9 NaI pulses; the other nine are the spectra in one-fold coincidence with each NaI counter. In some of these experiments the Ge(Li) counter was placed inside an NaI annulus that was operated in anticoincidence to reject Compton-scattered events.

For the particle gamma-ray coincidence experiments (item 3), large-area (200 to 300 mm^2) silicon detectors were placed close to the target to detect charged particles. Large plastic scintillators (25 or 30 cm in diameter) 80 or 100 cm from the target were used to produce time-of-flight neutron spectra, using the cyclotron rf as a time reference. The digitized linear signals from the silicon detectors, TAC outputs, and two of the NaI counters were recorded event by event on magnetic tape along with the coincident Ge(Li) pulse height and a bit pattern showing which, if any, of the NaI detectors had fired. The same 19 Ge(Li) spectra were produced on-line.

The principal results from the ($^4He,xn$), ($^{20}Ne,xn$), and ($^{40}Ar,xn$) experiments are shown in Fig. 2.17. The data are grouped according to excitation energy in the compound nucleus. The quantity $\langle M \rangle_x$ is the average number of gamma rays in the cascade that populates the ground state for the xn exit channel. For the ^{20}Ne and ^{40}Ar bombardments, the number of gamma rays increases strongly as fewer neutrons are emitted, in agreement with what is expected if the neutrons are statistically evaporated. For large x in the ($^4He,xn$) reactions the values of $\langle M \rangle_x$ are similar to those for the ^{20}Ne compartments, but for small x the multiplicity is much reduced. In fact, fewer gamma rays are emitted for $x \sim 2$ than for $x \gtrsim 6$. This result is consistent with the well-known behavior[7] of ($^4He,xn$) reactions above about 25 MeV: high-energy particles are emitted far more frequently than the statistical model allows, and the excitation functions for small x have tails that extend to very high energy. The cross-section data in Fig. 2.17 show this tailing effect: although the ($^4He,xn$) yield for large x matches that for ($^{20}Ne,xn$), there is a very large excess yield for small x.

The deviations from statistical behavior have been successfully accounted for in many ^4He reactions by emission of one particle before equilibrium has been established.[7] The full lines in Fig. 2.17 show that calculations based on this model[8] reproduce the cross sections quite well,

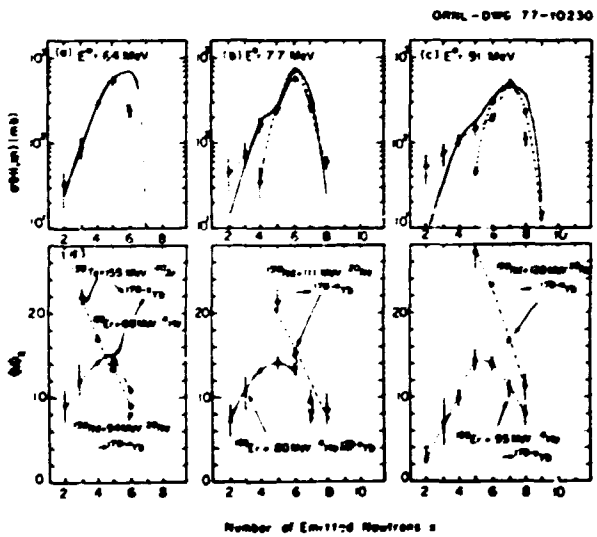

Fig. 2.17. Cross sections, σ, and average gamma multiplicities, $\langle M \rangle_x$, for $^{166}Er(^4He,xn)$, $^{150}Nd(^{20}Ne,xn)$, and $^{130}Te(^{40}Ar,xn)$ as a function of the number of neutrons emitted, x. The compound-nucleus excitation energies shown are those for the ^4He bombardments; they are about 2 to 3 MeV higher in each case for the ^{20}Ne data and 7 MeV lower for the ^{40}Ar data. The full lines for σ are calculations from the geometry-dependent hybrid model (ref. 8), including preequilibrium emission of the first neutron. The dashed and dotted lines are meant only to connect the data points.

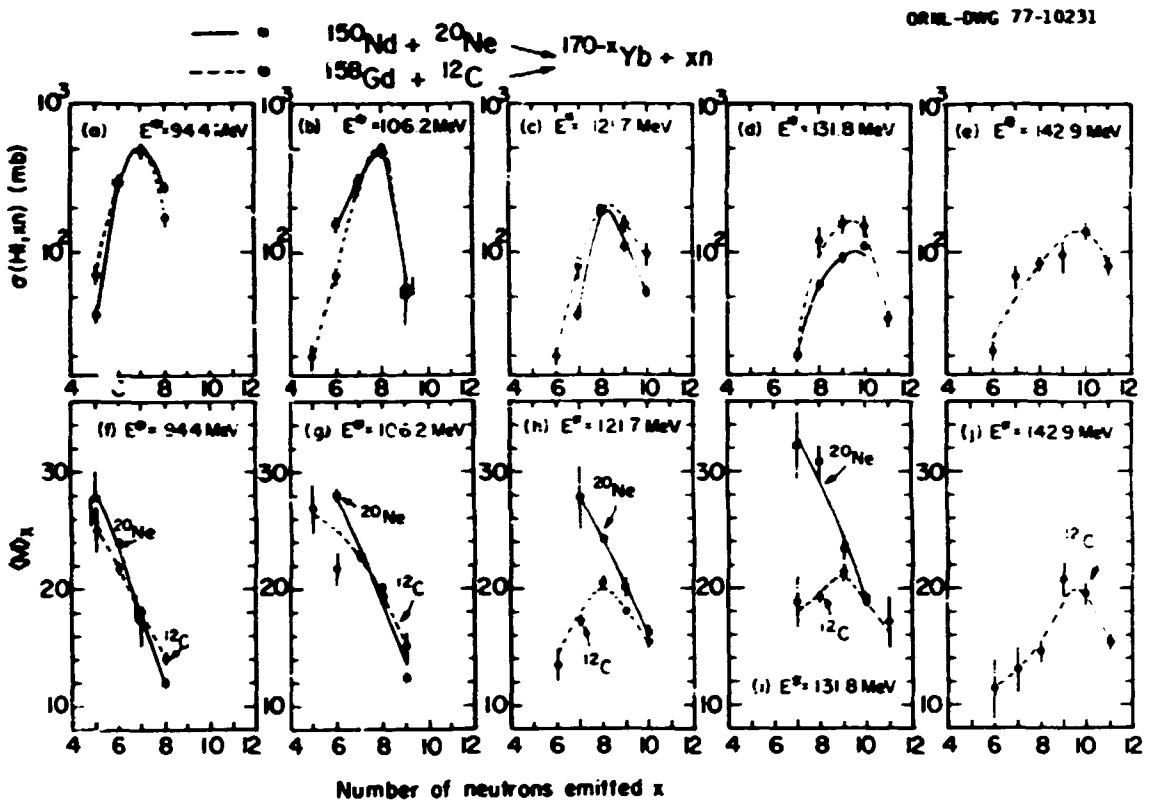

Fig. 2.18. Cross sections, σ, and average gamma multiplicities, $\langle M \rangle_x$, for ^{158}Gd(^{12}C,xn) and ^{150}Nd(^{20}Ne,xn) at five excitation energies of the compound nucleus ^{170}Yb, as a function of x. The ^{20}Ne results are interpolated from data at nearby energies (ref. 5). The lines drawn through the points have no theoretical significance.

except for the smallest values of x at the two higher beam energies. This deviation can be accounted for by emission of a second preequilibrium neutron.

The (^{12}C,xn) results are compared with (^{20}Ne,xn) results in Fig. 2.18. There is a remarkable transition in $\langle M \rangle_x$ vs x for ^{12}C from near-statistical behavior at the lowest excitation energy to very nonstatistical behavior at the highest energy, a condition reminiscent of the preequilibrium results for ^{4}He.

Particle gamma-ray coincidence data for both ^{12}C and ^{20}Ne beams were taken at 132-MeV excitation energy. Some of the alpha spectra are shown in Fig. 2.19. In the ^{12}C data, there is a marked trend toward higher alpha energy with decreasing x, another indication of preequilibrium emission. The effect with ^{20}Ne at the same excitation energy is much smaller, although there is some evidence for it in the $7n\alpha$ channel. [In this connection, we note from Fig. 2.18 that the (^{20}Ne,$7n$) multiplicity for 132-MeV excitation is somewhat lower than expected from the slope of the ^{20}Ne data at lower energies. Perhaps a deviation

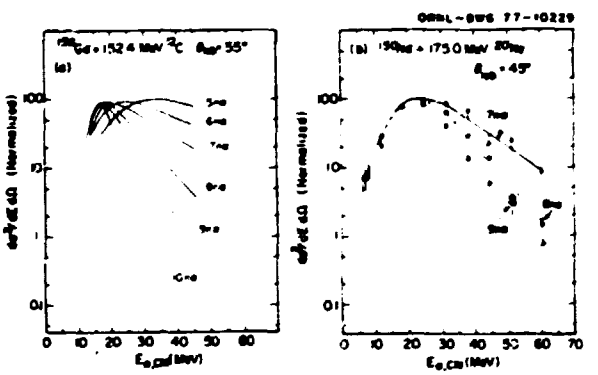

Fig. 2.19. Spectra of alpha particles in coincidence with gamma rays identifying the various reaction channels.

from statistical behavior is beginning here for ^{20}Ne also. The velocity of the ^{20}Ne particles in this case is just slightly below that of the ^{12}C at its lowest bombardment energy.]

In summary, the results indicate that, except possibly at the highest energy, the ^{40}Ar and ^{40}Ne bombardments produce compound nuclei that

de-excite statistically according to the expectations for a fully equilibrated system. The ^{4}He-induced reactions show dramatically the influence of preequilibrium emission of one or more particles. The ^{12}C bombardments display a transition from near equilibrium at the lowest beam energy to strong nonequilibrium effects at the highest energy.

1. ORAU summer research participant, 1976; permanent affiliation: Washington University, St. Louis, Mo.
2. St. Louis University, St. Louis, Mo.
3. Washington University, St. Louis, Mo.
4. *Phys. Div. Annu. Prog. Rep. Dec. 31, 1975*, ORNL-5137, p. 38.
5. D. G. Sarantites et al., *Phys. Rev. C* 14, 2138 (1976).
6. L. Westerberg et al., submitted to *Nuclear Instruments and Methods*.
7. M. Blann, *Ann. Rev. Nucl. Sci.* 25, 123 (1975).
8. M. Blann, *Overlaid ALICE—A Statistical Model Computer Code Including Fission and Preequilibrium Models*, ERDA Report COO-3493-29 (1976), unpublished.

FUSION OF ^{20}Ne AND ^{150}Nd AT 175 MeV

M. L. Halbert R. L. Ferguson[1]
R. A. Dayras F. Plasil
D. G. Sarantites[2]

Measurements[3] of gamma-ray yields from bombardments of ^{150}Nd by ^{20}Ne showed that at 128 MeV the xn and $xn\alpha$ product yields accounted completely for the fusion cross section predicted by the Bass model,[4] but that at 165 and 172 MeV, only about half of the predicted fusion cross section appeared in these channels. There were indications from the gamma-ray work that other evaporation channels were significant at the higher energies. Also, it seemed that fission might be playing a significant role because it is known to account for over 7% of the fusion cross section at 144 MeV and is expected to increase with energy.[5]

Measurements of the evaporation residues and symmetric-fission products were made at 175.3 MeV by means of three heavy-ion ΔE-E telescopes in the 24-in. chamber at angles from 3.5 to 100°. At the same time, data were obtained on elastic scattering. The target was an ^{150}Nd foil rolled to a thickness of 0.5 mg/cm^2.

The results are shown in Table 2.5 and in Fig. 2.20. The fusion cross section, equal to the sum of the evaporation and fission processes, is in good agreement with the Bass-model[4] prediction or the similar Glas-Mosel model[6] prediction with equivalent parameters. Thus the cross section missing from the xn and $xn\alpha$ gamma yields is due to

Table 2.5. Cross sections for ^{20}Ne + ^{150}Nd at 175.3 MeV

	σ (mb)
$\sigma(xn) + \sigma(xn\alpha)$[a]	594 ± 89
Evaporation residues	1150 ± 90
Fission	290 ± 35
Fusion	1440 ± 105
Bass model[b]	1398
Total reaction[c]	2630 ± 20[d]

[a]From gamma-ray yield at 172.4 MeV (ref. 3).
[b]Using parameters (r_0 = 1.07 fm, d = 1.35 fm, a = 17.0 MeV (ref. 4).
[c]From quarter-point recipe, $\theta_{1/4}$ = 30.4 ± 0.2° laboratory (ref. 7).
[d]Error due to uncertainty in $\theta_{1/4}$.

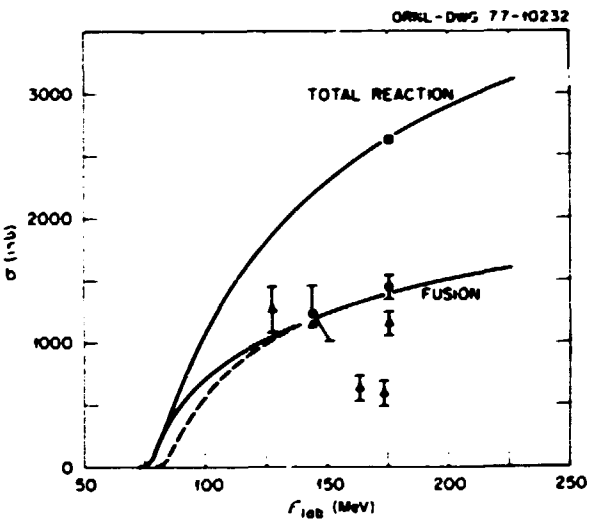

Fig. 2.20. Measured (points) and calculated (curves) cross sections for ^{20}Ne on ^{150}Nd. The $\sigma(xn) + \sigma(xn\alpha)$ from gamma measurements (ref. 3), Δ; evaporation residues, ▲; fusion, ●; total reactions, ■. The full points at 144 MeV are from ref. 5; the full points at 175 MeV are from the present work. The full curves are from ref. 6, the lower one (fusion) using parameters based on the Bass model (r_{0B} = 1.07 fm, V_{0m} = 62.1 MeV), while the upper one (reaction cross section) was forced to pass through the measured value by choosing r_{0B} = 1.53 fm and V_B = 68.34 MeV. The dashed line is the Bass-model prediction (ref. 4) for r_0 = 1.07, d = 1.35, a = 17.0

the opening of other evaporation channels and the appreciable fission cross section (20% of σ_{fusion}).

The removal of flux from the elastic channel provided the estimate of the total reaction cross section by means of the quarter-point recipe.[7-9] The interaction distance R implied by the resulting cross section is 12.28 fm if evaluated from the asymptotic form[10]

$$\sigma_{reaction} = \pi R^2 (1 - V_B(R)/E_{c.m.}) ;$$

$V_B(R)$ was taken to be the Coulomb potential of two touching spheres (70.34 MeV) plus a nuclear potential of −2 MeV.[11] This result is insensitive to the choice of the nuclear potential and corresponds to $r_0 = 1.53 \pm 0.01$ fm, the uncertainty being given by a ±2-MeV uncertainty in $V_B(R)$. This value of r_0 is larger than the usual one (about 1.4 fm) obtained from directly measured reaction cross sections close to the barrier.[12,13] However, it is consistent with results from similar analyses of the ^{20}Ne-induced reaction data reported above and of the detailed elastic data obtained at this laboratory for ^{12}C, ^{16}O, and ^{20}Ne on ^{208}Pb at 8 and 12 MeV/nucleon;[14] and for ^{16}O on ^{28}Si, ^{59}Co, and ^{60}Ni at 142 MeV.[15]

---

1. Chemistry Division.
2. Washington University, St. Louis, Mo.
3. D. G. Sarantites et al., *Phys. Rev. C* 14, 2138 (1976).
4. R. Bass, *Phys. Lett.* 47B, 139 (1973).
5. A. M. Zebelman et al., *Phys. Rev. C* 10, 200 (1974).
6. D. Glas and V. Mosel, *Nucl. Phys.* A237, 429 (1974).
7. J. S. Blair, *Phys. Rev.* 95, 1218 (1954).
8. W. E. Frahn, *Ann. Phys. (N.Y.)* 72, 524 (1972).
9. The formulas are found in J. R. Birkelund et al., *Phys. Rev. C* 13, 133 (1976).
10. C. Y. Wong, *Phys. Rev. Lett.* 31, 766 (1973).
11. G. R. Satchler, *Reactions between Complex Nuclei*, ed. R. L. Robinson et al., North-Holland, Amsterdam, 1974, p. 171.
12. H. H. Gutbrod, W. G. Winn, and M. Blann, *Nucl. Phys.* A213, 267 (1973).
13. L. C. Vaz and J. M. Alexander, *Phys. Rev. C* 10, 464 (1973).
14. J. B. Ball et al., *Nucl. Phys.* A252, 208 (1975).
15. G. R. Satchler et al., to be published in *Nuclear Physics*.

FUSION OF LIGHT NUCLEI

The ^{14}N + ^{12}C System and the Liquid-Drop Limit

J. Gomez del Campo
R. A. Dayras
P. H. Stelson
R. G. Stokstad
C. Oliver[1]
M. Zisman[1]

The experimental program on the fusion of light nuclei has concentrated on studying the fusion cross section for one system, ^{14}N + ^{12}C, over a wide range of bombarding energy. Previous measurements[2] covered the range $E = 43$ to 178 MeV, using ^{14}N beams from ORIC. The measured fusion cross sections (σ_{fus}) were consistent with the entrance channel model of Glas and Mosel,[3] and at the highest energy (178 MeV) the deduced critical angular momentum for ^{26}Al was equal to the predicted liquid-drop limit.[4] In order to establish whether the compound nucleus could be formed with angular momentum larger than this limit, measurements at $E = 248$ and 158 MeV were made using the LBL 88-in. cyclotron. Energy spectra and angular distribution were measured for reaction products with $2 \leq Z \leq 13$, using solid-state counter telescopes. The energy spectra of the reaction products with $Z = 5$ to 9 exhibit two components at forward angles. As discussed in ref. 2, the lower energy component corresponds to evaporation residues and the higher energy component to direct-reaction products. The features of the energy spectra taken at 248 MeV were qualitatively similar to those observed at lower energies and therefore could be analyzed in the manner described in ref. 2.

At sufficiently high bombarding energies, there can be a nonnegligible probability for the compound nucleus to evaporate five alpha particles or four alpha particles plus several nucleons, leaving a lithium or a beryllium nucleus as the residue. Because it was not possible to identify the evaporation-residue component in the lithium and beryllium spectra, we have used the evaporation code LILITA[5] to estimate the fraction of the fusion cross section which would appear as residues with $Z = 3$ or 4. These values are 4 and 13% at 158 and 248 MeV respectively. This procedure also enables an estimate of the ^{8}Be and ^{9}B residues which, because of their particle-unstable ground states, cannot be identified by ordinary experimental techniques. Confidence in this method of estimating the undetected residues is based on the successful prediction of relative intensities for different residual elements over a wide range of bombarding energies, using a single set of parameters.[2] Figure 2.21 shows the measured and predicted relative intensities of the evaporation residues at $E = 158$ and 248 MeV respectively.

The deduced values of σ_{fus} at $E = 158$ MeV (including the 4% estimated increase for residues with Z less than or equal to 4) is 987 ± 80 mb. At $E = 248$ MeV, this value is 717 ± 85 mb, including the 13% estimated increase for residues with Z less than or equal to 4. The value of σ_{fus} at 248 MeV represents a decrease of 219 mb below the cross section expected by an entrance-channel model[3] for the fusion process.

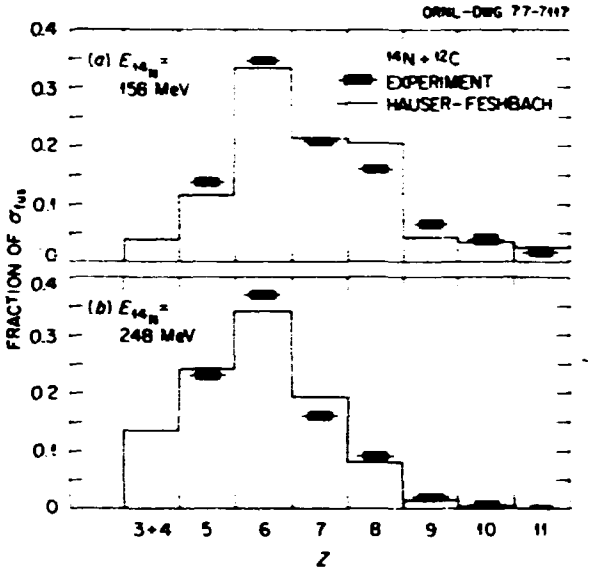

Fig. 2.21. Angle-integrated yields for evaporation residues with $Z = 5$ to 11, expressed as a fraction of σ_{fus}. The histograms are the predictions of the code LILITA.

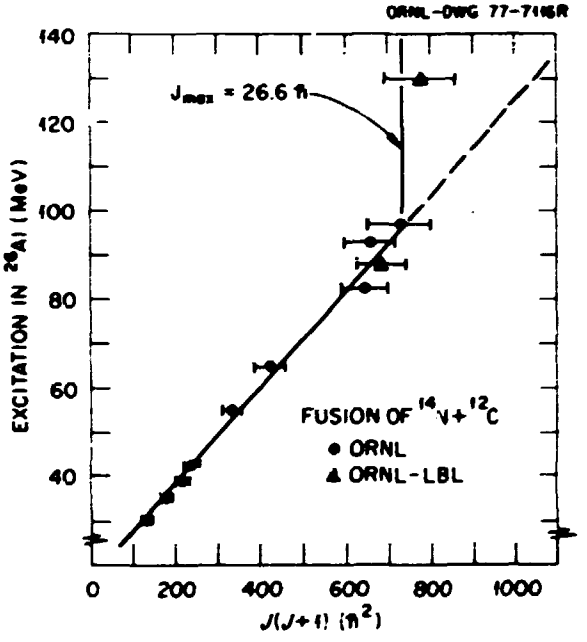

Fig. 2.22. Values of the critical angular momentum, J, plotted as $J(J+1)$ vs excitation energy in ^{26}Al. The dashed line is a fit to all data points except that at 130-MeV excitation.

However, the deduced critical angular momentun of 27.5 + 1.7 ħ is in agreement with the prediction of the rotating liquid-drop limit.[4] This fact suggests that we have observed the absolute maximum angular momentum which the ^{26}Al compound nucleus can sustain. Our results for the critical angular momentum deduced from σ_{fus} are presented in Fig. 2.22, where the round points correspond to the ORIC measurements[2] and the triangles to the results obtained at the LBL 88-in. cyclotron. The solid line at $J(J+1) = 734\ \hbar^2$ corresponds to the predicted liquid-drop limit,[4] $J_{max} = 26.6\ \hbar$.

1. Lawrence Berkeley Laboratory, Berkeley, Calif.
2. R. G. Stokstad et al., *Phys. Rev. Lett.* 36, 1529 (1976). The results present in Fig. 2.22 for $145 \leq E_{lab} \leq 178$ have been revised upward by small amounts corresponding to the estimated $Z = 3$ and $Z = 4$ residues. Also, new measurements are included for E_{lab} = 37.5 and 53 MeV.
3. D. Glas and V. Mosel, *Nucl. Phys.* A237, 429 (1974).
4. S. Cohen, F. Plasil, and W. J. Swiatecki, *Ann. Phys. (N. Y.)* 82, 557 (1974).
5. J. Gomez del Campo, computer code LILITA (unpublished).

THE $^{16}O + ^{10}B$ SYSTEM

Limitation on the Fusion Cross Sections, Entrance Channel or Compound Nucleus

J. Gomez del Campo
J. A. Biggerstaff
R. A. Dayras
A. H. Snell[1]
P. H. Stelson
R. G. Stokstad

The fusion cross section for $^{10}B + ^{16}O$ has been measured with ^{16}O beams at energies of 42, 46.5, 50.9, and 93.5 MeV in an attempt to determine whether the limitation on σ_{fus} arises from entrance-channel (EC) dynamics or with the compound nucleus (CN). This can be determined in principle by comparing the ratio[2] of σ_{fus} for $^{14}N + ^{12}C$ to $^{16}O + ^{10}B$ at the same excitation energy, E_x, in ^{26}Al. Table 2.6 shows the ratio $R = \sigma_{fus}(^{14}N + ^{12}C)/\sigma_{fus}(^{16}O + ^{10}B)$, where R_{CN} and R_{EC} correspond to the ratios expected for a limitation originating with the compound nucleus and in the entrance channel respectively. R_{EC} has been calculated using the Glas-Mosel[3] prediction for σ_{fus} which fits the $^{14}N + ^{12}C$ data. The last column in Table 2.6 shows the experimental ratio, R_{exp}, obtained from our previous $^{14}N + ^{12}C$ measurements[2] and the present $^{16}O + ^{10}B$ data. As can be seen from Table 2.6, the experimental ratios for $E_x = 35.67$ to 39.12 are in complete agreement with the entrance-channel limitation. At the highest excitation energy (55.5 MeV), however, the value of σ_{fus} for $^{16}O + ^{10}B$ is 22% larger than the one predicted by the entrance-channel model. Uncertainties in the absolute target thickness cannot account for this difference because

Table 2.6. Ratio of $\sigma_{fus}(^{14}N + ^{12}C)$ to $\sigma_{fus}(^{16}O + ^{10}B)$ at an excitation energy E_x (MeV) in ^{26}Al

E_x	R_{CN}	R_{EC}	R_{exp}
35.67	0.75	0.94	1.0
37.37	0.76	0.99	0.99
39.12	0.78	0.98	0.99
55.5	0.85	1.0	0.78

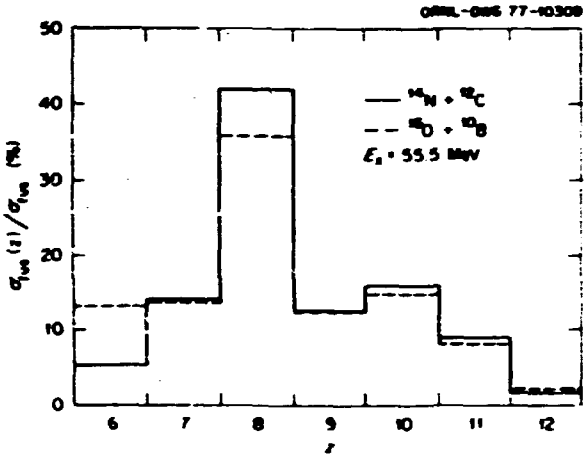

Fig. 2.23. Angle-integrated yields for evaporation residues with $Z = 6$ to 12, expressed as a fraction of σ_{fus}, at an excitation energy in ^{26}Al of 55.5 MeV. The solid histogram corresponds to the residues from $^{14}N + ^{12}C$ (ref. 2), and the dashed line corresponds to the present data for $^{10}B + ^{16}O$.

the same target was used for the four $^{16}O + ^{10}B$ measurements). The presence of ^{12}C and ^{16}O contaminants, however, might affect the results of the highest energy, because almost 60% of σ_{fus} comes from residues with Z less than or equal to 8. Because the discrepancy at the highest energy would establish a significant departure from the systematics in this mass region, additional measurements with other ^{10}B targets are in progress.

Figure 2.23 shows the comparison between the yields of evaporation residues obtained for $^{14}N + ^{12}C$ (solid line) and $^{16}O + ^{10}B$ (dashed line) at $E_x = 55.56$ MeV. The major discrepancy between the two systems occurs for residues with Z less than or equal to 8, whereas for heavier residues the decay of the compound nucleus appears independent of its mode of formation.

1. Consultant with the Physics Division.

2. R. G. Stokstad et al., *Phys. Rev. Lett.* 36, 1529 (1976). The results present in Fig. 2.22 for $145 \leq E_{lab} \leq 178$ have been revised upward by small amounts corresponding to the estimated $Z = 3$ and $Z = 4$ residues. Also, new measurements are included for $E_{lab} = 37.5$ and 53 MeV.

3. D. Glas and V. Mosel, *Nucl. Phys.* A237, 429 (1974).

YRAST LEVELS IN ^{27}Al SUGGESTED BY RESONANCE STRUCTURE IN THE $^{12}C(^{15}N,\alpha)$ REACTION

J. Gomez del Campo
J. L. C. Ford, Jr.
R. L. Robinson
M. E. Ortiz[1]
A. Dacal[1]
E. Andrade[1]

Resonances have been observed in the excitation functions for a number of heavy-ion reactions, although most notably in the exit channels of $^{12}C + ^{12}C$ and $^{12}C + ^{16}O$.[2,3] We have also observed many strong resonances in the $^{12}C(^{15}N,\alpha)^{23}Na$ reaction, which may be due to the strong population of nonoverlapping states near the yrast line in the compound nucleus ^{27}Al.

A total of 30 excitation functions were measured in 200-keV intervals with 80-keV resolution for bombarding energies between 21.4 and 39.0 MeV at a laboratory angle of 7° by means of the split-pole spectrograph at the EN tandem accelerator. Excitation functions for an additional 11 states from 9.5 to 12.2 MeV in ^{23}Na were measured over a more limited range of bombarding energies. These measurements, which cover a wide interval of incident and excitation energies, then yield a very large sample (containing over 3000 cross-section values) for comparison with the statistical model.

Typical measured excitation functions are indicated by the solid lines in Fig. 2.24. Despite the rapid fluctuations observed in the data, which are expected from the statistical model to be strongest at a forward angle such as 7° (lab), a second underlying structure is nevertheless apparent. A measurement of the coherence width by the conventional peak-counting method[4] yields a width, Γ_f, of 158 keV at an excitation energy of 32 MeV in ^{27}Al, a value in reasonable agreement with systematics for this mass region.[5]

In order to emphasize the underlying resonant structure, a running average of the data was performed using an averaging interval, Δ, equal to three times the coherence width. The averaged cross sections are given by dashed curves in Fig. 2.24. In this figure, correlated resonances can be observed at various incident energies for the different particle groups. For example, correlations occur at 10.7 MeV (c.m.) between the 0.0-, 0.44-, and 3.67-MeV states and at 15.1 MeV between the 3.67-, 6.58-, 7.98-, and

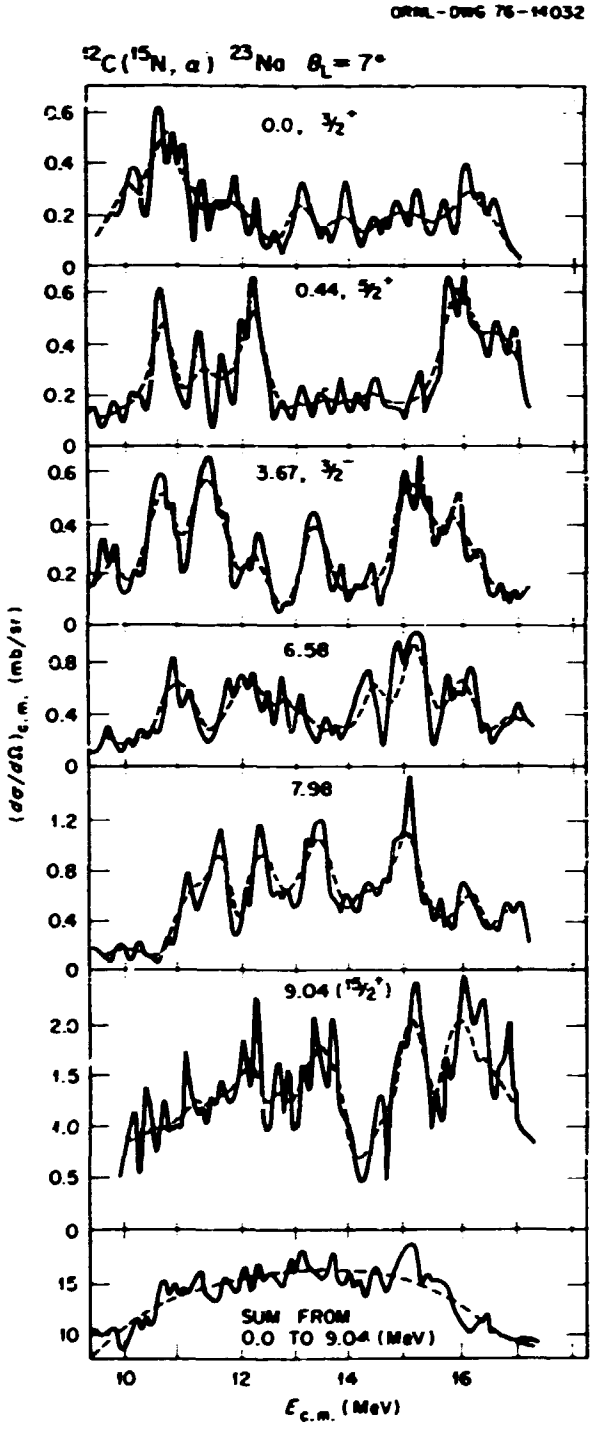

Fig. 2.24. Typical measured excitation functions for the $^{12}C(^{15}N,\alpha)$ reaction, indicated by solid lines. Dashed curves result from averaging over an interval equal to three coherence widths.

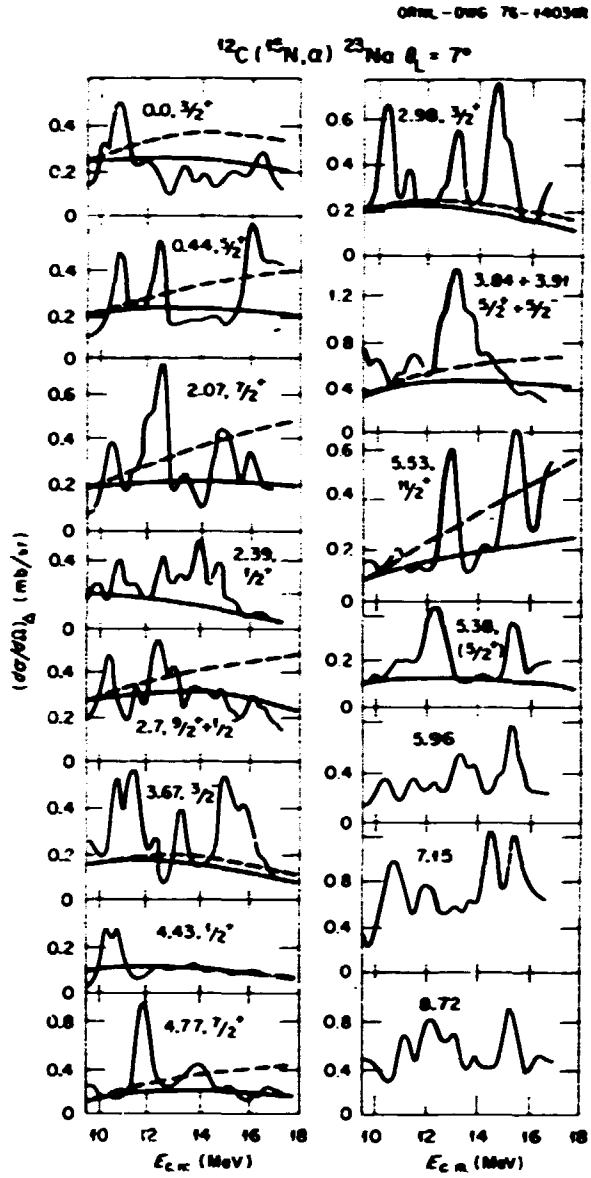

Fig. 2.25. Excitation functions for the $^{12}C(^{15}N,\alpha)$ reaction averaged over an interval, Δ, equal to three times the coherence width. The results of H-F calculations without angular-momentum cutoff (dashed curves) and with cutoff (solid curves) are indicated for states of known or probable spins.

9.04-MeV states. The bottom curve of the figure shows that the resonances disappear when the cross sections for a large number (31) of states are summed.

The energy-averaged cross sections, such as those shown in Fig. 2.25, then contain 216 peaks whose widths, areas, and centroids were analyzed after a smooth background passing through the minima of the structure was subtracted. The average width was 0.44 ± 0.1 MeV. The resonant energies of apparently correlated states were averaged to obtain values for the average resonant energy, $\bar{E}$, and the standard deviation, ΔE, which was typically 0.1

MeV. Figure 2.25(*a*) displays the number of such alpha-particle groups as histograms whose positions and widths correspond to $\bar{E} \pm \Delta E$. The observed correlations, large widths, about $3\Gamma_f$, and large deviations from the average cross sections seen in the data are not easily explained by the statistical model alone.

The solid and dashed lines drawn through the averaged excitation functions displayed in Fig. 2.25 are the results of Hauser-Feshbach (H-F) calculations with and without the effects of angular momentum cutoff. The parameters used were the same as for the previous analysis of this reaction.[6] The values for the angular momentum cutoff, J_C, were obtained by fitting H-F calculations to regions of the excitation functions of known spin states where the correlated structure was absent. Such regions occur, for example, above 12 MeV (c.m.) for the 0.0- and 4.43-MeV states, above 13 MeV for the 4.77-MeV level, and between 13 and 15 MeV for the 0.44-MeV state. The J_C values determined by the procedure are given by $E_x = (8.7)^{-1} J_C(J_C + 1) + 16.25$ MeV for excitation energies, E_x, in ^{27}Al between 27.3 and 34.5 MeV; for this energy range, J_C is greater than or equal to $^{21}/_2$. In general, the H-F calculations give reasonable fits to nonresonant regions of the excitation functions or pass through the minima in the resonant structure, thus adequately accounting for the portion of the observed cross sections due to statistical fluctuations.

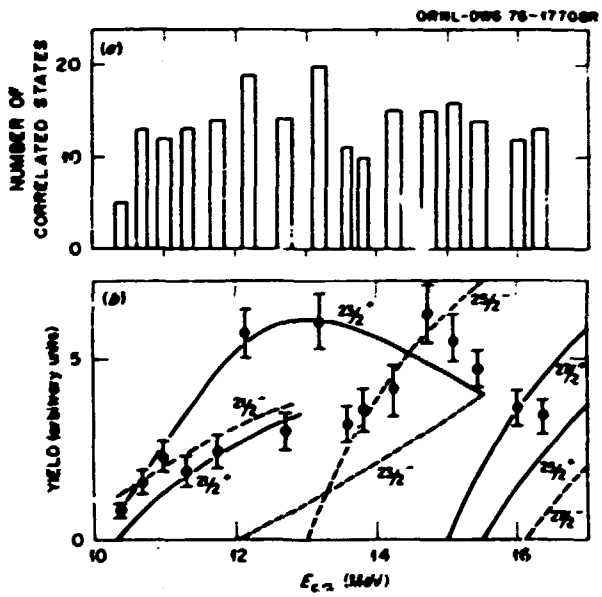

Fig. 2.26. (*a*) Histogram indicating the number of correlated states observed as a function of the incident energy (c.m.); (*b*) sum of the yields, or resonance strengths, for the correlated resonances of (*a*). Solid and dashed lines are calculated theoretical resonance cross sections with the spins and parities indicated.

Angular-momentum considerations may account for the origin of the resonant structure. In the present experiment, we are in the vicinity or approaching the members of the yrast line at high excitation energies in ^{27}Al. Therefore, the values of the angular-momentum cutoff required to fit the nonresonant structure may represent the spins for which the condition Γ/D very much greater than 1 necessary for the statistical model is no longer valid. However, a narrow range of spin values contributes to the observed resonant structure. Spins less than J_C will be included in the H-F calculations, and the contribution of levels with these angular-momentum values will be in the general background underlying the resonances. If the total angular momentum is greater than $^{27}/_2$, then the transmission coefficients are vanishingly small. Consequently, only values between $^{21}/_2$ and $^{27}/_2$ can produce resonances, because these levels are close to the yrast line and have widths comparable to or less than the level spacing.

The resonance strengths may be used to yield compound nuclear spins, as was demonstrated by analyses of (α,p) reactions.[7,8] The points in the lower portion of Fig. 2.26 are the resonant areas summed over all correlated peaks as a function of the c.m. energy. The solid and dashed curves correspond to calculations with a single-level formula for different compound spin and parity values. The particle widths in the entrance and exit channels have been replaced by the appropriate optical-model transmission coefficients. However, it is necessary to normalize the set of calculated curves to the data at one point. Only normalizing the curve for $^{23}/_2^+$ to the second resonance at 10.7 MeV provides the satisfactory fit to all the data seen in Fig. 2.26(*b*). Note that the curve for each J value terminates at the excitation energy calculated from the equation for E_x as a function of J_C, because overlapping resonances for higher energies are once more to be expected. If the resonances at incident energies of 10.4 and 16.0 MeV (c.m.) are interpreted as due to $^{23}/_2^+$ and $^{27}/_2^+$ levels, then the excitation energies of these states are close to those predicted by an extrapolation of the ground-state band. Thus the curves suggest a value for the spin of the level in ^{27}Al corresponding to each observed resonance.

In conclusion, a large number of correlated resonances with intermediate widths were observed in the ^{12}C(^{15}N,α) excitation functions, as well as in

more rapid statistical fluctuations. Hauser-Feshbach calculations appear to reproduce the statistical portion of the cross sections. The resonant strengths of their energy dependence suggest that the resonances result from the excitation of high-spin states in ^{27}Al.

1. Instituto de Fisica, Universidad Nacional Autonoma de Mexico, Mexico.

2. D. A. Bromley, *Proceedings of the Second International Conference on Clustering Phenomena in Nuclei*, College Park, Md., Apr. 21-25, 1975, p. 465.

3. H. Feshbach, *J. Phys. (Paris)* C5 Suppl 11, 5 (1976).

4. J. Gomez del Campo et al., *Nucl. Phys.* A262, 125 (1976).

5. D. Shapira, R. G. Stokstad, and D. A. Bromley, *Phys. Rev. C* 10, 1063 (1974).

6. D. E. Gustafson et al., *Phys. Rev. C* 13, 691 (1976).

7. E. Sheldon et al., *Proceedings of the International Conference on Statistical Properties of Nuclei*, ed. J. B. Garg, Plenum, New York, 1971, p. 121.

8. W. A. Schier et al., *Nucl. Phys.* A254, 80 (1975).

MEASUREMENTS OF THE COHERENCE WIDTHS Γ IN ^{27}Al BY THE ^{12}C(^{15}N,α) REACTION

J. Gomez del Campo — M. E. Ortiz[1]
J. L. C. Ford, Jr. — A. Dacal[1]
R. L. Robinson — E. Andrade[1]

In a previous study[2] of the coherence widths Γ in ^{28}Si, it has been shown that the dependence of Γ vs the excitation energy of the compound system provides a way to extract the moment of inertia and spin-cutoff parameters of the nucleus in the framework of the statistical model. As part of a systematic study of this effect, we have measured the coherence widths in ^{27}Al, using the ^{12}C(^{15}N,α) reaction. A total of 30 excitation functions were measured for the bombarding energy range from 21.4 to 39 MeV in 200-keV intervals and for excitation energies in ^{23}Na from 0.0 to 9.04 MeV. An additional ten excitation functions from 9.15 to 12 MeV for a reduced bombarding energy range were also measured. The targets were ^{12}C foils (10 μg/cm^2 thick) and were bombarded with ^{15}N ions extracted from the EN tandem accelerator to give an overall energy resolution of 80 keV. The alpha particles were detected using a 60-cm-long gas proportional counter placed at the focal plane of an Enge magnetic spectrograph.

Figure 2.27 shows 14 of the measured excitation functions. The Γ values were extracted by the usual peak-counting technique, but the autocorrelation functions did not yield reliable Γ values due to the presence of strong intermediate structure of about

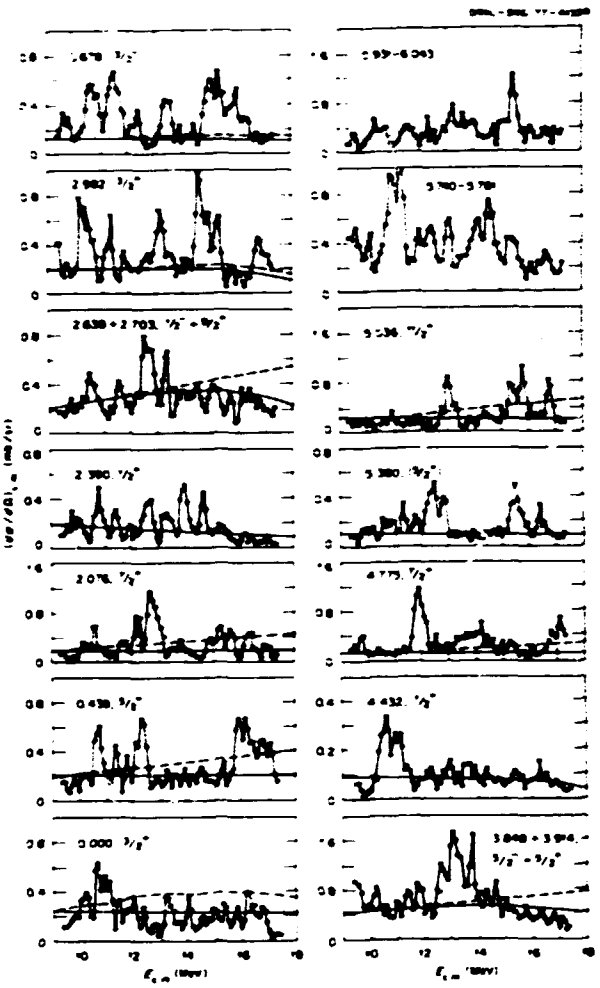

Fig. 2.27. Excitation functions for states in ^{23}Na measured by the ^{12}C(^{15}N,α) reaction at a laboratory angle of 7°.

400 keV, as reported elsewhere.[3] Figure 2.28 shows the coherence widths extracted from the data of Fig. 2.27, and the dashed lines represent the various theoretical predictions, using the values of $I/\hbar^2$ indicated in the figure. As can be seen, a value of 5.3 can be clearly preferred for $I/\hbar^2$. This value is consistent with that previously obtained for ^{28}Si.[2] The values for the level density parameters for ^{27}Al used in calculating the Γ values in Fig. 2.28 were a = 3.56 MeV^{-1} and Δ = 1.18 MeV.

The H-F calculations used to estimate the number of open channels employed in the calculation of Γ used the same set of parameters as in ref. 4 (the entrance-channel optical potential was taken from ref. 5). In order to account for the nonstatistical portion of the cross sections, an angular momentum cutoff was used[3] according to the relation $E_x = (8.7)^{-1}$

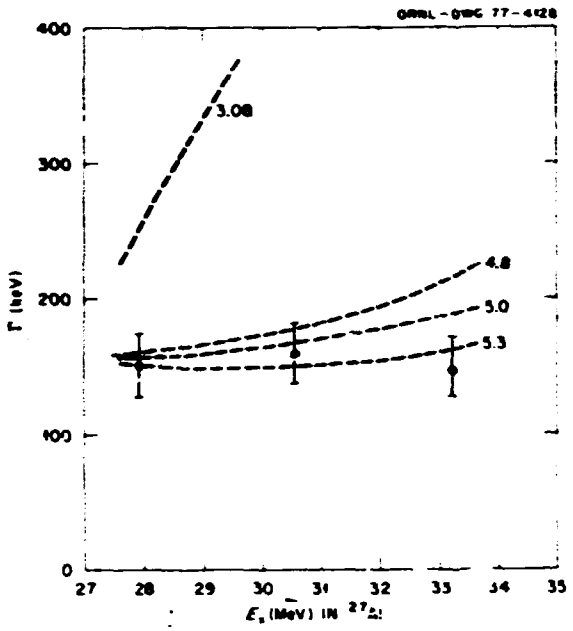

Fig. 2.28. Plot of Γ (coherence width) vs the excitation energy in ^{27}Al. Data points correspond to the measured widths from the excitation functions of Fig. 2.27. The dashed lines are theoretical calculations for values of $I/\hbar^2$ from 3.08 to 5.3.

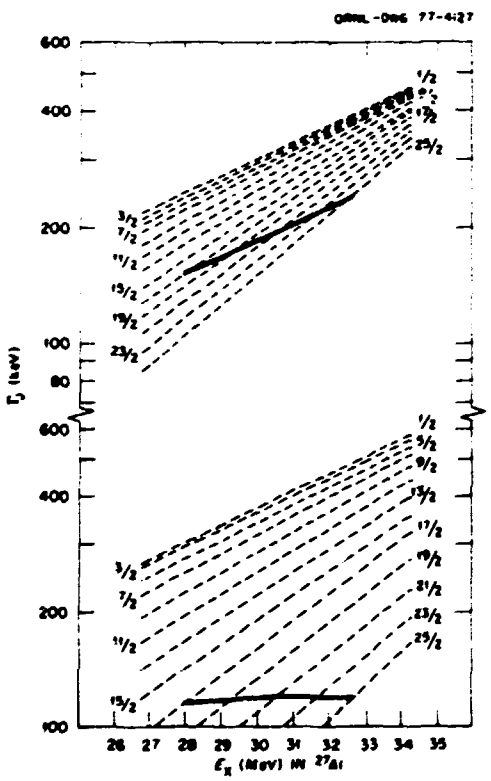

Fig. 2.29. Partial widths Γ_γ vs E_x calculated with the H-F denominator from the program HELGA. Curves at the top are for $I/\hbar^2 = 4.08$ and those at the bottom are for $I/\hbar^2 = 5.3$.

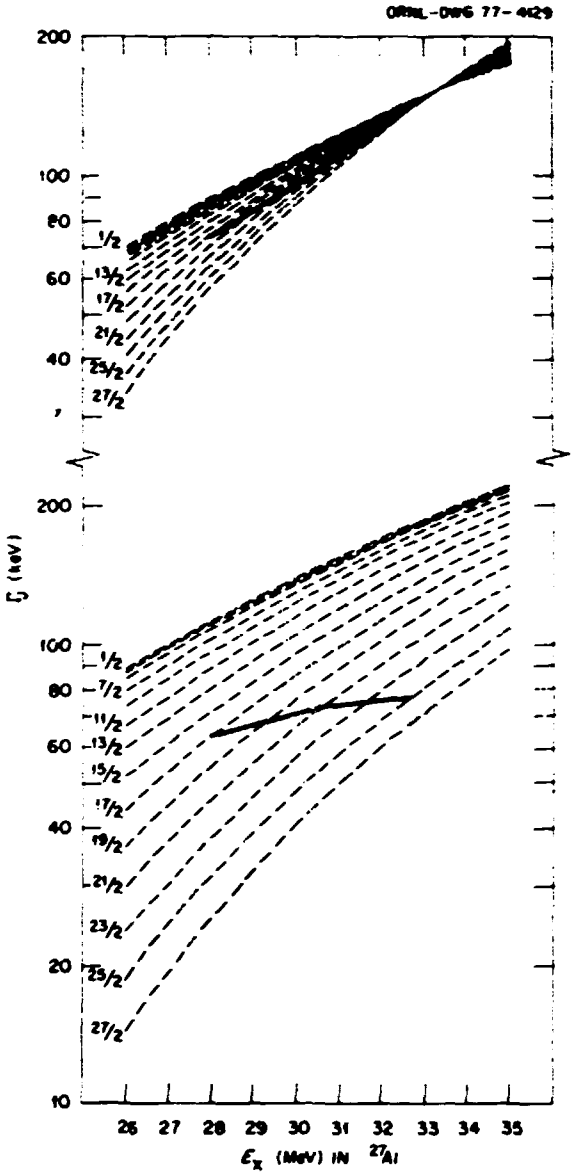

Fig. 2.30. Results similar to those of Fig. 2.29 except that the denominator has been replaced by the approximation of Eberhard et al. (ref. 6).

$J_C(J_C + 1) + 16.25$ MeV for excitation energies between 27.3 and 34.5 MeV.

It was pointed out in ref. 2 that the slope of Γ vs E_x depends only on $I/\hbar^2$ and not on the level density parameters a and Δ. However, the authors did not investigate possible effects due to varying the H-F denominator (the number of open channels). In the present study, we have calculated the H-F denominator, using the approximation suggested by Eberhard et al.[6] Figures 2.29 and 2.30 show the effect due to changes in the H-F denominator on the partial

widths Γ_J. Figure 2.29 shows the results of the calculations, using the H-F denominator as computed by code HELGA.[7] The dashed lines correspond to the different Γ_J values calculated for the indicated J values. The set of curves on the bottom of the figure is calculated with $I/\hbar^2 = 4.8$. The solid lines shown in the figure connect the Γ_J values for which σ_J (the partial H-F cross section) has its maximum value at a given excitation energy. The parameters a and Δ are the same as for Fig. 2.28. Similar results are shown in Fig. 2.30, except in this case the H-F denominator has been calculated using the Eberhard approximation.[6] The values for a, Δ, and $I/\hbar^2$ are identical to those used for Fig. 2.29. Even though there is a change of about a factor of 2 in the magnitude of the curves between Figs. 2.29 and 2.30, the slope of the solid lines is but slightly changed. This result then confirms our previous observation that the most sensitive parameter affecting the slope of the Γ vs E_x curve is the moment of inertia, $I/\hbar^2$.

1. Instituto de Fisica, Universidad de Mexico. Mexico.
2. J. Gomez del Campo et al., *Nucl. Phys.* A262, 125 (1976).
3. See this report, J. Gomez del Campo et al., "Yrast Levels in ^{23}Al Suggested by Resonance Structure in the ^{12}C(^{15}N,α) Reaction."
4. D. E. Gustafson et al., *Phys. Rev. C* 13, 691 (1976).
5. D. L. Hanson et al., *Phys. Rev. C* 9, 929 (1974).
6. K. A. Eberhard et al., *Nucl. Phys.* A125, 673 (1969).
7. S. K. Penny, "Computer Code HELGA" (unpublished).

HIGH-SPIN STATE STUDY[1] OF ^{23}Na

S. T. Thornton[2] L. C. Dennis[2]
D. E. Gustafson[2] T. C. Schweizer[2]
K. R. Cordell[2] J. L. C. Ford, Jr.

Angular distributions of the ^{12}C(^{15}N,α)^{23}Na reaction have been repeated with improved resolution for four bombarding energies between 36.4 and 38.8 MeV with the Enge split-pole magnetic spectrograph on the EN tandem accelerator. The improved resolution of 60 keV enabled us to separate doublets at 2.64 to 2.70 MeV, 3.85 to 3.91 MeV, and 6.04 to 6.11 MeV. Each doublet contains one member of the $K^\pi = {}^1/_2^-$ rotational band. This band appeared to be enhanced in earlier data.[3] States with excitation energies up to 12 MeV in ^{23}Na were populated in the new data, and a new statistical compound-nucleus calculation has been performed with the code HELGA for comparison with the energy-averaged $\sigma(\theta)$ values of both the previous and the new data.

Careful consideration has been given to critical angular momentum in the compound nucleus and to the level density parameters. For the range of bombarding energies used, a J_C of ${}^{27}/_2$ is consistent with the grazing angular momentum in the entrance channel and with a more sophisticated analysis based on relative experimental and HELGA-predicted cross sections.

The suggestions of high-spin state assignments were performed for three rotational bands ($K^\pi = {}^3/_2^+$,

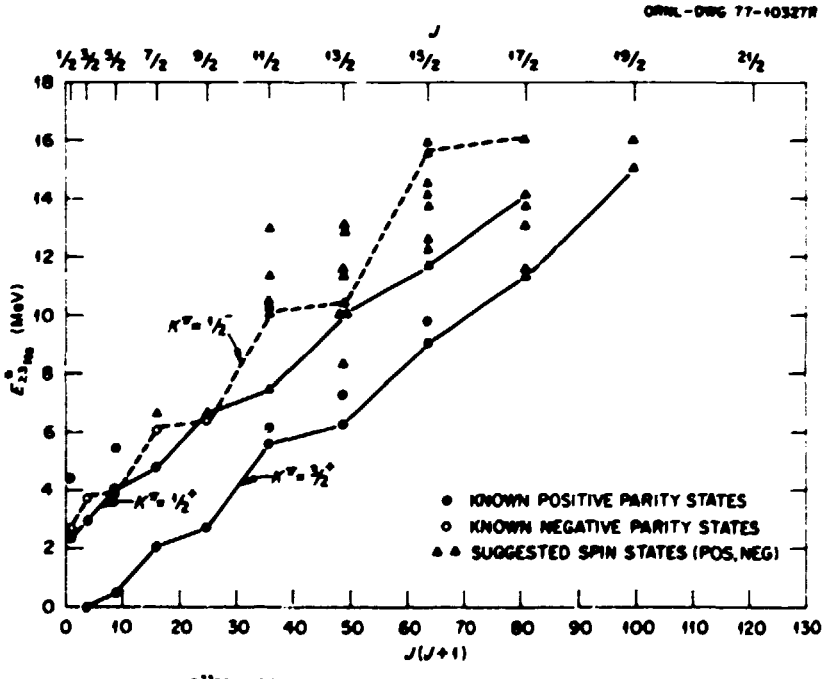

Fig. 2.31. Known rotational bands of ^{23}Na with known and proposed spins. The moment-of-inertia parameter, $\hbar^2/2I$, is similar for the ${}^3/_2^+$ and ${}^1/_2^+$ bands but is slightly larger for the ${}^1/_2^-$ band.

$^1/_2^+$, and $^1/_2^-$), as well as for many other states, and are shown in Fig. 2.31. The positive-parity band spin assignments were aided greatly by the shell-model calculations of Wildenthal.[4] Spin suggestions through $^{19}/_2^+$ for the $^3/_2^+$ band and through $^{17}/_2^+$ for the $^1/_2^+$ band were made.

The negative-parity states data have not been previously reported. The $K^\pi = {}^1/_2^-$ band is extremely interesting because it may be interpreted in terms of strong coupling through the Nilsson model or as weak coupling by a $p_{1/2}$ hole coupled to the ^{24}Mg ground-state band. Both concepts have been used to correctly explain the excitation energies of the band members. We have suggested members up through $^{17}/_2^-$ for this band. From the work of Watt et al.,[5] there are reasons to believe the ^{24}Mg ground-state band may terminate with the 8^+ member, which couples with the proton hole to create the $^{17}/_2^-$ state in ^{25}Na.

The three rotational bands of ^{23}Na appear to have slightly different moment-of-inertia parameters and deformations. Generally, the levels of ^{23}Na seem well described by the shell and Nilsson models.

---

1. Supported in part by the National Science Foundation.
2. University of Virginia, Charlottesville.
3. D. E. Gustafson et al., *Phys. Rev. C* 13, 691 (1976).
4. B. H. Wildenthal, private communication.
5. A. Watt, D. Kelvin, and R. R. Whitehead, *Phys. Lett.* 63B, 385 (1976).

COHERENCE-WIDTH MEASUREMENTS OF THE COMPOUND NUCLEI ^{26}Al AND ^{25}Mg[1]

K. R. Cordell[2] P. G. Lookadoo[2]
S. T. Thornton[2] T. C. Schweizer[2]
L. C. Dennis[2] J. Gomez del Campo
J. L. C. Ford, Jr.

Excitation functions have been measured for 20 excited states or unresolved multiplets of ^{22}Na populated by the ^{12}C(^{14}N,α)^{22}Na reaction at a laboratory angle of 7° and for bombarding energies from 22.0 to 39.2 MeV in approximately 200-keV steps. The ^{14}N beams were extracted from the EN tandem accelerator, and the alpha particles were momentum-analyzed with the Enge split-pole magnetic spectrograph.

By carefully determining level density parameters and by using various optical-model potential sets, we were able to correctly predict our alpha cross sections, as well as previously measured ^{12}C(^{14}N,α)^{24}Mg and ^{12}C(^{14}N,^{6}Li)^{20}Ne data,[3] with the H-F code HELGA. We used the same parameters to predict cross sections consistent with our previous analyses[4-6] for the same exit reaction channels but with a different entrance channel, ^{16}O + ^{10}B.

Volant et al.[3] have reported that the ^{12}C(^{14}N,^{6}Li)^{20}Ne reaction data are quite sensitive to a critical angular momentum cufoff, J_C, below about 40 MeV, whereas the d channel is not sensitive. We found that the sensitivity to J_C of the absolute cross sections for the alpha channel depends a great deal on the optical-model parameters used in the entrance channel. However, by examining relative cross sections, as suggested by Klapdor et al.,[7] the same J_C is found for all optical-model potentials in the entrance channel. We used the latter method to determine $J_C = 10\,\hbar$ and 12 $\hbar$ for excitation energies of 29 and 32 MeV, respectively, in ^{26}Al. These values are consistent with other published values.

In addition to the H-F analysis, a fluctuation analysis of the excitation functions was also done. The coherence width (Γ) was extracted by the peak counting method and was compared with theoretical predictions of Γ calculated from the partial cross sections $\sigma(J)$ and the level density parameters of ^{26}Al. Figure 2.32 shows the comparison. The value of $c(= I/\hbar^2)$ that best fit the data is 5.65 MeV^{-1}, and the extracted r_0 (assuming a rigid-body value) is 1.54 fm. This value is slightly higher than the 1.46-fm value obtained in similar analyses[8,9] for ^{28}Si and ^{27}Al. However, the nonstatistical behavior observed at low bombarding energies may contribute to a large damping of the fluctuations in the energy regions corresponding to the first two data points in Fig. 2.32. Correcting the coherence width for this effect

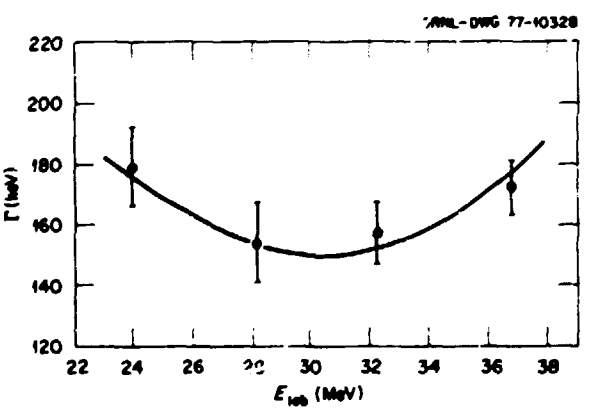

Fig. 2.32. Theoretical calculations for ^{26}Al, using level density parameter a = 3.54 MeV and moment-of-inertia ($I/\hbar^2$ MeV^{-1}) 5.64. The spin cutoff parameter σ^2 is related to the moment of inertia by $\sigma^2 = I/\hbar^2\,T$, where T is the nuclear temperature.

favors a lower value of r_0, improving the agreement with the value of r_0 for other nuclei in the *s-d* shell.

A similar study of the coherence widths of ^{25}Mg was performed by studying the ^{12}C(^{13}C,α)^{21}Ne reaction. Excitation functions were measured at 7°(laboratory) for bombarding energies from 18 to 32 MeV in 200-keV steps for states in ^{21}Ne up to an excitation energy of 9 MeV. A resolution of 45 keV enabled us to resolve some 40 states. Critical angular momentum effects were considered. The experimental and theoretical coherence widths were compared as done previously for ^{28}Si, ^{27}Al, and ^{26}Al.

Energy-averaged $\sigma(\theta)$ values have also been obtained in order to make high-spin state suggestions. Calculations with HELGA indicate quite varying shapes of $\sigma(\theta)$ for different spins. Comparison with shell-model calculations was used to locate the suggested member of rotational bands in ^{21}Ne.

---

1. Supported in part by the National Science Foundation.
2. University of Virginia, Charlottesville.
3. C. Volant et al., *Nucl. Phys.* **A238**, 120 (1975).
4. J. L. C. Ford, Jr., et al., *Nucl. Phys.* **A226**, 189 (1974).
5. J. Gomez del Campo et al., *Phys. Rev. C* **9**, 1258 (1974).
6. J. L. C. Ford, Jr., et al., *Z. Phys.* **269**, 147 (1974).
7. H. V. Klapdor, H. Reiss, and G. Rosner, *Nucl. Phys.* **A262**, 157 (1976).
8. J. Gomez del Campo et al., *Nucl. Phys.* **A262**, 125 (1976).
9. See this report, J. Gomez del Campo et al., "Yrast Levels in ^{27}Al Suggested by Resonance Structure in the ^{12}C(^{15}N,α) Reaction."

HEAVY-ION NEUTRON YIELDS

J. K. Bair P. D. Miller
J. Gomez del Campo P. H. Stelson

Final data are now available for the total neutron yields resulting from the bombardment of thin targets of ^{12}C, ^{13}C, ^{16}O, and ^{18}O by ^{12}C, ^{13}C, ^{16}O, and ^{18}O. These measurements are made at energies over the barrier region and cover five or six decades of yield. Accuracy is about 5%. A paper is being prepared based on these results.

RESONANCE STRUCTURE IN THE TOTAL NEUTRON YIELD FOR THE ^{12}C + ^{12}C SYSTEM

J. K. Bair P. D. Miller
J. Gomez del Campo P. H. Stelson

As part of a program of searching for nonstatistical resonances for heavy-ion systems, where the mass numbers of the target and projectile are greater than or equal to 20, the total neutron yield for the ^{12}C + ^{12}C system has been measured. The yield curve Y was measured for E_{lab} = 7 to 40 MeV in 200-keV steps.[1] Figure 2.33 displays a portion of the yield from $E_{c.m.}$ = 5 to 13 MeV. A statistical analysis of the data from $E_{c.m.}$ = 5 to 10 MeV has been performed[2] using a running average Δ = 2 MeV (about 20 Γ, where Γ is the coherence width). The number of effective channels (N) was calculated using the STATIS code,[3] and a comparison of the theoretical probability distribution P_N vs the experimental one indicates the presence of strong nonstatistical components. The smooth (solid) curve Y_{BGD} on Fig. 2.33 follows the energy dependence of the H-F cross section for single neutron emission for $E_{c.m.} < 10$ MeV and has been normalized to the data in such a way that $Y \geq Y_{BGD}$.

Figure 2.34 shows the result of substracting the Y_{BGD} curve from the measured yield; as can be seen, a strong resonant behavior is present. The vertical arrows drawn on the figure correspond to the resonance energies previously observed for α, p, n, and ^{8}Be channels. The resonances at $E_{c.m.}$ = 5.6, 5.9, and 6.3 MeV correspond to the well-known sub-Coulomb resonances.[4] However, we also observe at 6.6 and 7.15 MeV strong resonances previously unreported. The arrows labeled α for $E_{c.m.}$ larger than 7.5 MeV agree within 100 keV with our present measurement.[5] A total of eight resonances of those

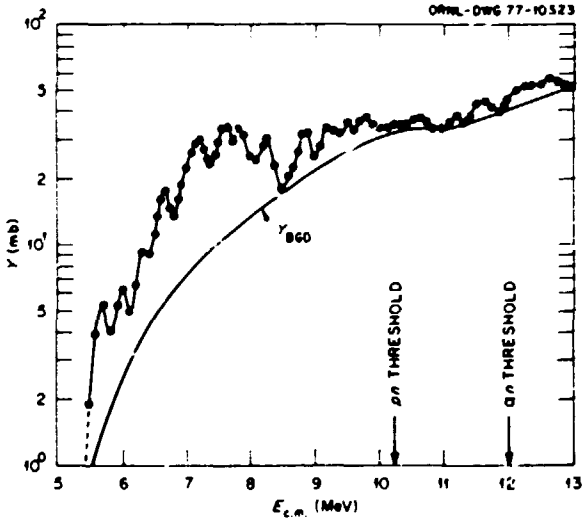

Fig. 2.33. Yield Y (mb) for the ^{12}C + ^{12}C system plotted vs the center-of-mass energy (MeV). The solid line Y_{BGD} is discussed in the text.

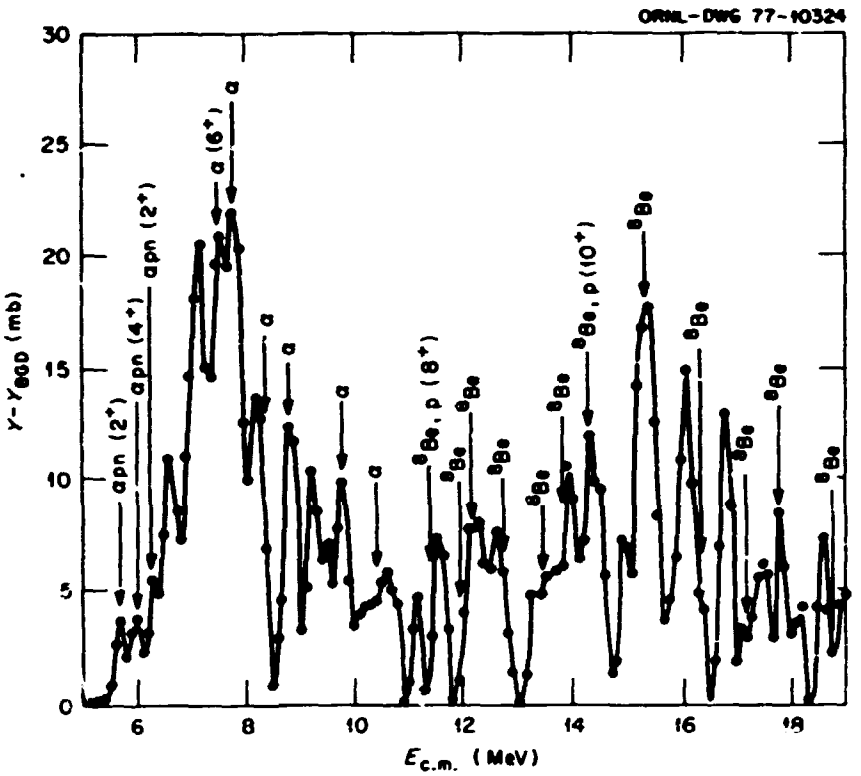

Fig. 2.34. $Y - Y_{BGD}$(mb) for the $^{12}C + ^{12}C$ system. The arrows indicate the resonance energy measured in previous work for the charged-particle channels p, α, and ^8Be.

reported[6] for the ^8Be channel are also in good agreement with the resonances seen in the present work. This is also the case for the $^{12}C(^{12}C,p)$ resonances[7] at 11.3 and 14.7 MeV.

The abundant resonance structure observed in the present measurement and the clear correlation with previous α, p, and ^8Be measurements represent a challenge to current theoretical models for heavy-ion resonance reactions.[4,8]

1. The yield Y is defined as $Y = \sigma_n \cdot \nu$, where σ_n is the total neutron cross section and ν is the average number of emitted neutrons per neutron-producing event.

2. R. A. Dayras et al., *Nucl. Phys.* A265, 153 (1976).
3. R. G. Stokstad, "Computer Code STATIS" (unpublished).
4. D. A. Bromley, *Clustering Phenomena in Nuclei*, vol. II, p. 465, ed. D. A. Goldberg, J. B. Morrison, and S. J. Wallace, ERDA Technical Information Center, Springfield, Va., 1976.
5. K. A. Erg et al., *Phys. Rev. Lett.* 37, 670 (1976).
6. N. R. Fletcher et al., *Phys. Rev. C* 13, 1173 (1976).
7. E. R. Cosman et al., *Phys. Rev. Lett.* 35, 265 (1975).
8. H. Feshbach, *J. Phys. (Paris), Colloq. 37*, C5, 177 (1976).

OBSERVED DIFFERENCES IN ^{200}Po COMPOUND NUCLEI PRODUCED BY ^{40}Ar AND ^{84}Kr PROJECTILES[1]

R. L. Hahn[2] Y. LeBeyec[3]
K. S. Toth M. W. Guidry[4]

As part of our program to study compound nuclei produced in reactions with very heavy ions, we have produced ^{200}Po compound nuclei with beams of ^{40}Ar and ^{84}Kr. The experiments were done at the Super-HILAC, Lawrence Berkeley Laboratory, with a gas-jet system used to collect and assay the alpha-radioactive polonium isotopes. Our data for the reactions $^{40}Ar(^{160}Dy,xn)^{200-x}Po$ have been discussed previously.[5,6]

Recently, we obtained data for the reactions $^{84}Kr(^{116}Cd,xn)^{200-x}Po$. These results, along with the earlier data for ^{40}Ar, are plotted in Fig. 2.35 as excitation functions. It is seen for a given (heavy-ion, xn) reaction that the cross sections for krypton-induced reactions are smaller than those obtained with argon, and the peaks of the krypton excitation functions are shifted to higher excitation energies

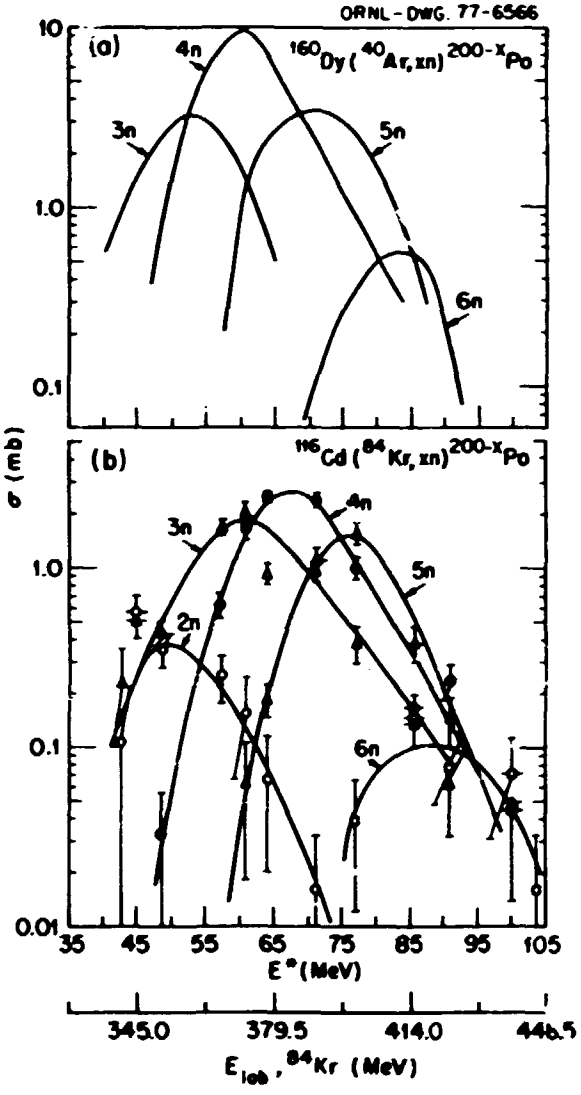

Fig. 2.35. Excitation functions for polonium nuclides produced in the reactions $^{40}Ar + {}^{160}Dy$ and $^{84}Kr + {}^{116}Cd$. The curves of part (*a*) are from ref. 5, while part (*b*) shows data for the krypton reactions as a function of excitation energy, E^*, and of ^{84}Kr bombarding energy.

with respect to the argon curves. These observations are qualitatively consistent with our earlier results for erbium compound nuclei produced with argon and krypton beams[7] and indicate that the decay of compound nuclei produced by such heavy beams does depend on the specific mode of formation.

1. An account of this work is also included in the *Chem. Div. Annu. Prog. Rep. Mar. 31, 1977*, ORNL-5297 (to be published).
2. Chemistry Division.
3. Institut de Physique Nucleaire, Orsay, France.
4. Lawrence Berkeley Laboratory, Berkeley, Calif.

5. *Chem. Div. Annu. Prog. Rep., Nov. 1, 1975*, ORNL-5111, p. 70.
6. Y. LeBeyec et al., *Phys. Rev. C* **14**, 1038 (1976).
7. H. Gauvin et al., *Phys. Rev. C* **10**, 722 (1974).

STUDY OF EVAPORATION RESIDUE PRODUCTS FROM ^{86}Kr BOMBARDMENTS OF ^{65}Cu, ^{90}Zr, AND ^{109}Ag

M. Blann[1] P. D. Goldstone[2]
H. C. Britt[2] H. H. Gutbrod[4]
B. H. Erkkila[3] F. Plasil
R. L. Ferguson[3] R. H. Stokes[2]

We have continued our study[5] of heavy-ion fusion reactions at the LBL Super-HILAC by measuring both cross sections and mass and charge distributions of evaporation residue products in ^{86}Kr bombardments of ^{65}Cu, ^{90}Zr, and ^{109}Ag. In interpreting the results of these experiments, we have utilized a nuclear de-excitation calculation that includes fission competition.[6]

Our earlier results on evaporation residue cross sections from the $^{40}Ar + {}^{109}Ag$ reaction were in good agreement with theoretical calculations[7] and encouraged us to make similar comparisons using krypton ions. With a 1.5-m time-of-flight apparatus, we have obtained evaporation residue cross sections at three bombarding energies for $^{86}Kr + {}^{65}Cu$, at two energies for $^{86}Kr + {}^{90}Zr$, and at one energy for $^{86}Kr + {}^{109}Ag$.[7] The data for $^{86}Kr + {}^{65}Cu$ are shown in Fig. 2.36. The experimental points are bracketed by two options of the theoretical calculation, and the agreement is satisfactory.

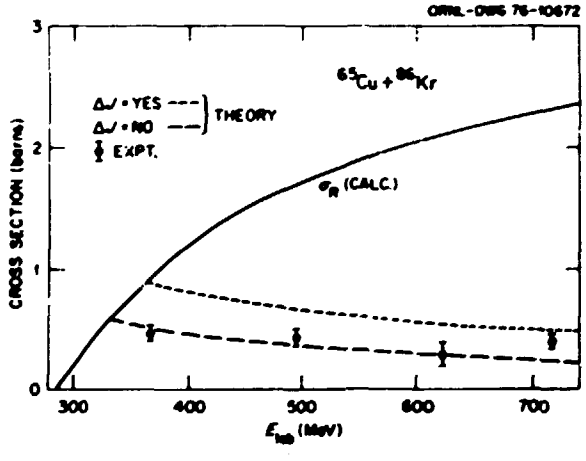

Fig. 2.36. Cross section for evaporation residue products as a function of laboratory bombarding energy for $^{86}Kr + {}^{65}Cu$. Dashed curves represent theoretical calculations. ΔJ = NO indicates that particles do not remove angular momentum. σ_R is the total reaction cross section calculated with an optical model.

The $^{108}Ag + ^{86}Kr$ experiment was carried out at a bombarding energy of 720 MeV. The evaporation residue cross section was found to be 28 ± 8 mb. This is considerably lower than the theoretical prediction of 135 mb, which was obtained without the adjustment of any parameters. When the level density parameters were varied, however, the calculated evaporation residue cross section was found to be very sensitive to the ratio of the level density parameter for fission, a_f, to the level density parameter for particle emission, a_ν. For example, for $a_f/a_\nu = 1.0$, $\sigma_{ER} = 135$ mb; for $a_f/a_\nu = 1.05$, $\sigma_{ER} = 31$ mb; and for $a_f/a_\nu = 1.1$, $\sigma_{ER} = 0.4$ mb. Because $a_f/a_\nu = 1.1$ is not an unreasonable value, the experimental value of 28 mb is not in sharp disagreement with theory. On the other hand, since the calculated value of σ_{ER} is so sensitive to the value of a_f/a_ν and since the exact value of a_f/a_ν is not known for each specific case, the calculations may be of limited value in predicting evaporation residue cross sections. However, this appears to be the case only for such systems as $^{86}Kr + ^{108}Ag$, in which the fission barrier at zero angular momentum, B_f^0, is relatively low (11.7 MeV). In cases in which B_f^0 is relatively high (e.g., $B_f^0 = 33.7$ MeV for $^{86}Kr + ^{65}Cu$), σ_{ER} calculations are not too sensitive to the value of a_f/a_ν. For example, in the case of 506-MeV ^{86}Kr bombardments of ^{65}Cu, calculated σ_{ER} values are 353 mb with $a_f/a_\nu = 1.0$ and 289 mb with $a_f/a_\nu = 1.1$. Therefore, provided B_f^0 is considerably greater than the lowest particle-binding energy, the calculations may be used to make predictions of evaporation residue cross sections because these are fairly insensitive to the choice of a_f/a_ν.

For 716- and 366-MeV $^{86}Kr + ^{65}Cu$, we have determined mass and charge distributions of evaporation residue products, using the time-of-flight apparatus and a ΔE-E telescope. The mass distribution from the 716-MeV experiment is given in Fig. 2.37 by the points. The histogram indicates the result of a theoretical calculation[8] of the type mentioned above. Except for the shift in scales, which is due to inadequate calibration of the time-of-flight apparatus, the agreement is excellent. The measured charge distribution was found to be broader than that calculated, but the broadening could be accounted for by the relatively poor resolution of the ΔE counter used. In subsequent runs, both the time-of-flight calibration and the ΔE detector resolution have been improved, and our experiments at the Super-HILAC are continuing.

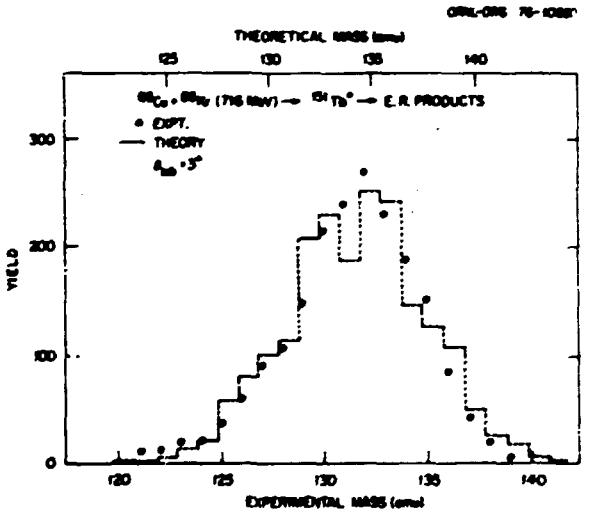

Fig. 2.37. Calculated and experimental mass distributions of evaporation residue products from 716-MeV ^{86}Kr bombardments of ^{65}Cu. The absolute experimental mass scale is subject to some uncertainty.

1. University of Rochester, Rochester, N.Y.
2. Los Alamos Scientific Laboratory, Los Alamos, N.M.
3. Chemistry Division.
4. Gesellschaft für Schwerionenforschung, Darmstadt, Germany.

5. Due to the collaborative nature of this experiment, a similar report appears in the *Chem. Div. Annu. Prog. Rep. Mar. 31, 1977*, ORNL-5297 (to be published).

6. M. Blann and F. Plasil, *ALICE: A Nuclear Evaporation Code*, AEC Report COO-3494-10 (1973).
7. H. C. Britt et al., *Phys. Rev. C* 13, 1483 (1976).
8. H. C. Britt et al., *Proceedings of the Symposium on Macroscopic Features of Heavy-Ion Collisions*, vol. II, ERDA Report ANL PHY-76-2 (1976).

LIFETIMES OF GROUND-BAND STATE IN ^{192}Pt AND ^{194}Pt AND CONSIDERATIONS OF THE ROTATION-ALIGNMENT MODEL

N. R. Johnson — D. G. Sarantites[3]
P. P. Hubert[1] — J. Urbon[3]
E. Eichler[2] — S. W. Yates[4]
Thomas Lindblad[5]

Recently we have begun lifetime measurements[6] on members of the ground bands in ^{192}Pt and ^{194}Pt. There are two primary reasons for these measurements. First, we are interested in understanding some of the strong irregularities observed[7-9] in the rotational-like band structure of the even $^{188-194}Pt$ isotopes. A pronounced compression of the energy spacing between the 10^+ and 12^+ states is observed, and the level spacing pattern above spin 12^+ in ^{190}Pt

and ^{192}Pt resembles that of the low-spin states. Furthermore, a $B(E2; 12^+ \rightarrow 10^+)$ value of $(0.33 \pm 0.06)e^2b^2$ has been deduced from the measured[9] half-life of the 12^+ level in ^{192}Pt; this value is only about 50% of the rotational limit based on an average of the ^{192}Pt $B(E2; 2^+ \rightarrow 0^+)$ measurements. The above observations have been interpreted[7,9] within the rotation-alignment (RA) model,[10,11] and the anomalies are reproduced if an oblate deformation is assumed for the nucleus together with alignment of two $i_{13/2}$ neutrons. A measurement of the lifetimes of the states up to 12^+ should add some clarity to the picture. A second reason for this study involves a discrepancy of more than a factor of 2 between the previously measured[12] half-life value of the 4^+ state in ^{192}Pt and that predicted by either the RA or the pure rotational models.

Lifetime measurements were carried out by the Doppler-shift recoil-distance method. The states were Coulomb-excited by a beam of 149-MeV ^{40}Ar ions from the ORIC. The target was a 3.1-mg/cm^2 metallic platinum foil enriched to 57% in ^{192}Pt and to 26% in ^{194}Pt. When the ^{40}Ar backscattered ions were detected in coincidence with an annular silicon detector, the average recoil velocity imparted to the platinum ions was $v/c = 0.0249 \pm 0.0004$. Details of the experimental method and data analysis techniques are described by Johnson et al.[13] and by Sturm and Guidry.[14]

Due to the low Coulomb excitation cross section with ^{40}Ar ions, we were able to get good data for only three states in ^{192}Pt and only two states in ^{194}Pt. A summary of the results and comparisons with previous measurements are given in Table 2.7.

As pointed out in a recent paper,[15] both the RA and pure rotational models give essentially the same predictions, which are in excellent agreement with our experimental values for the states obtained here.

Table 2.7. Half-life and $B(E2)$ values for ^{192}Pt and ^{194}Pt

	Transition	E_γ (keV)	$T_{1/2}$ (psec)		α_T[a]	$B(E2), e^2b^2$
			Previous work	Present work		
^{192}Pt	$2 \rightarrow 0$	316.49	35.3 ± 2.8[b] 33.6 ± 4.5[c] 45.1 ± 0.5[d] 42.8 ± 1.5[e] 39.3 ± 2.2[f]	48.5 ± 2.5	0.0831	0.34 ± 0.02
	$4 \rightarrow 2$	468.06	11.8 ± 2.1[b]	4.2 ± 0.2	0.0287	0.58 ± 0.03
	$6 \rightarrow 4$	580.80		1.8 ± 0.7	0.0172	0.47 ± 0.18
^{194}Pt	$2 \rightarrow 0$	328.50	37.7 ± 1.8[f] 50.5 ± 2.2[g] 41.8 ± 1.0[h] 41.8 ± 0.5[d] 34.7 ± 3.5[i] 41.8 ± 2.9[j]	45.0 ± 2.4	0.0746	0.31 ± 0.02
	$4 \rightarrow 2$	482.65	4.4 ± 0.7[f]	3.7 ± 0.2	0.0267	0.57 ± 0.03

[a]Total internal conversion coefficients have been reduced by 2% to account for possible deviations from theory found in this region by Stelson and Raman. *Sources:* R. S. Hager and E. C. Seltzer, *Nucl. Data A* 4, 397 (1968); O. Dragoun, Z. Plajner, and F. Schmutzler, *Nucl. Data A* 9, 119 (1971); and P. H. Stelson and S. Raman, private communication, 1976.

[b]Value from Schwarzschild determined by delayed-coincidence method (ref. 12).

[c]Value from Beraud et al. determined by centroid-shift method. *Source:* R. Beraud et al., *Phys. Rev. C* 1, 303 (1970).

[d]Calculated from (α, α') Coulomb excitation $B(E2)$ values of Ronningen et al. *Source:* R. M. Ronningen et al., *Bulletin of the American Physical Society*, in press.

[e]Value from Smith and Simms determined by centroid-shift method. *Source:* G. J. Smith and P. C. Simms, *Nucl. Phys.* A202, 409 (1973).

[f]Calculated from the Coulomb excitation $B(E2)$ value of Milner et al. *Source:* W. T. Milner et al., *Nucl. Phys.* A177, 1 (1971).

[g]Recoil-distance measurement by Nord. *Source:* R. H. Nord, Thesis, University of Wisconsin, 1971, unpublished.

[h]Calculated from $(^{16}O, ^{16}O')$ and (p,p') Coulomb excitation $B(E2)$ values of Glenn et al. *Source:* J. E. Glenn et al., *Phys. Rev.* 188, 1905 (1969).

[i]Value from Berkes et al. determined by centroid-shift method. *Source:* I. Berkes et al., *Phys. Rev. C* 6, 1098 (1972).

[j]Calculated from inelastic alpha-particle-scattering work of Baker et al. *Source:* F. T. Baker et al., *Phys. Rev. Lett.* 37, 193 (1976).

We plan further measurements following Coulomb excitation with still heavier projectiles in the hope of exciting the 10^+ state and providing a more rigorous test of the RA model. This is based on the suggestion by Piiparinen et al.[8] that the $(\pi h_{11/2})^2_{10}$ configuration is the main component in the wave function of the 10^+ state, while the $I \geq 12^+$ states are primarily described by the $\nu i_{13/2}$ configuration. Calculations[9] in the RA model indicate that if this is the case, then the $B(E2)$: $10^+ \rightarrow 8^+$) as well as the $B(E2)$; $12^+ \rightarrow 10^+$) will be reduced considerably so that the lifetime of the 10^+ state would be about 1 psec.

1. On leave from University of Bordeaux, France.
2. Deceased.
3. Washington University, St. Louis, Mo.
4. University of Kentucky, Lexington.
5. Research Institute for Physics, Stockholm, Sweden.
6. An account of this work appears in the *Chem. Div. Annu. Prog. Rep. Mar. 31, 1977*, ORNL-5297 (to be published).
7. L. Funke et al., *Phys. Lett.* **55B**, 436 (1975).
8. M. Piiparinen et al., *Phys. Rev. Lett.* **34**, 1110 (1975).
9. S. A. Hjorth et al., *Nucl. Phys.* **A262**, 328 (1976).
10. F. S. Stephens and R. S. Simon, *Nucl. Phys.* **A183**, 257 (1972).
11. F. S. Stephens et al., *Nucl. Phys.* **A222**, 235 (1974).
12. A. Schwarzschild, *Phys. Rev.* **141**, 1206 (1966).
13. N. R. Johnson et al., *Phys. Rev. C* **12**, 1927 (1975).
14. R. J. Sturm and M. W. Guidry, *Nucl. Instrum. Methods* **138**, 345 (1976).
15. N. R. Johnson et al., *Phys. Rev. C* **15**, 1325 (1977).

PROPERTIES OF ^{164}Er IN THE BAND-CROSSING REGION

N. R. Johnson	I. Y. Lee[4]
E. Eichler[1]	D. Cline[4]
S. W. Yates[2]	R. S. Simon[4]
R. M. Ronningen[3]	P. A. Butler[4]
R. D. Hichwa[3]	P. Colombani[4]
J. H. Hamilton[3]	M. W. Guidry[4]
L. L. Riedinger[4]	F. S. Stephens[4]
A. C. Kahler[4]	R. M. Diamond[4]

Erbium-164 belongs to the class of nuclei termed "backbenders," so named because of the abrupt increase in the moment of inertia at about spin 14^+ in the ground-state rotational band. In an extensive experimental investigation[6] of the high-spin states in this nucleus completed recently, we have made some significant new findings.

Normally, the behavior of backbending nuclei is established from the gamma-ray cascade down through the yrast sequence following a compound-nucleus reaction. However, during the past year in a collaborative effort carried out at the Berkeley Super-HILAC, we showed for the first time that it is possible to excite the ground band of ^{164}Er through the backbend and up to the 18^+ level in the yrast sequence by the Coulomb excitation mechanism.[7] In addition, we saw good evidence for excitation of the 16^+ and 18^+ members of the ground-state band.

In order to get information on higher spin states in ^{164}Er, and hopefully to find the 14^+ member of the excited band, we carried out extensive gamma-gamma coincidence measurements at the ORIC, utilizing the reaction ^{150}Nd(^{18}O,4$n\gamma$)^{164}Er. These experiments were quite successful, as the deduced level scheme of Fig. 2.38 illustrates. Above the band-crossing point, we now have several states in both the yrast sequence and the ground band. Additionally, we obtained the necessary gamma-ray branching ratio from the 16^+ state, which makes it possible to calculate the important interaction matrix element between the two bands. This matrix element is 54 keV, a small value that is completely compatible with interpreting the backbending here in terms of the rotation-alignment model.[8]

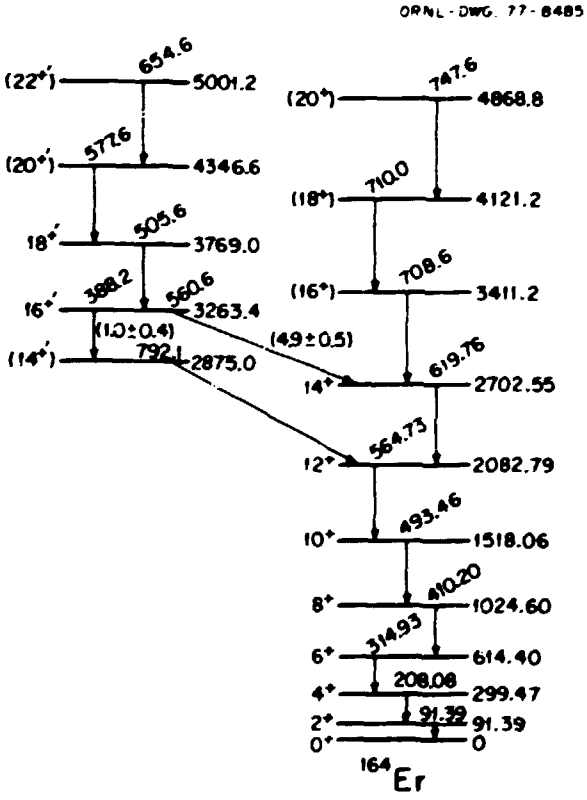

Fig. 2.38. Level scheme of ^{164}Er deduced from both Coulomb excitation and compound-nucleus reaction experiments. The intensities of the 560.6- and [illegible]-keV transitions are shown in parentheses.

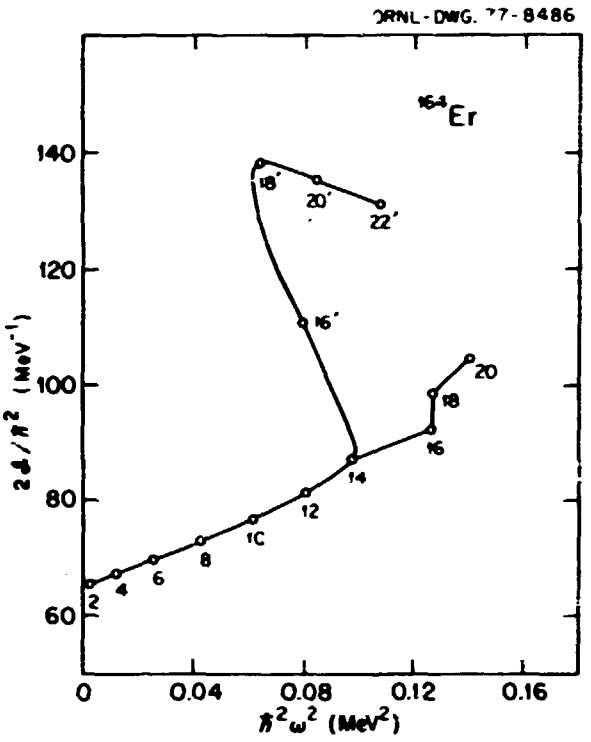

Fig. 2.39. Conventional plot of $2\mathcal{I}/\hbar^2$ vs $(\hbar\omega)^2$ for ^{164}Er to illustrate the backbending effect.

A conventional backbending plot of these data is shown in Fig. 2.39. Note that, at the 16$^+$ state of the ground band, there is a discontinuity, which may indicate the intersection of this band with a second excited band.

---

1. Deceased.
2. University of Kentucky, Lexington.
3. Vanderbilt University, Nashville, Tenn.
4. University of Tennessee, Knoxville.
5. Lawrence Berkeley Laboratory, Berkeley, Calif.
6. An account of this work appears in the *Chem. Div. Annu. Prog. Rep. Mar. 31, 1977*, ORNL-5297 (to be published).
7. I. Y. Lee et al., *Phys. Rev. Lett.* 37, 420 (1976).
8. F. S. Stephens and R. S. Simon, *Nucl. Phys.* A183, 257 (1972).

LIFETIMES OF GROUND-BAND STATES IN ^{150}Nd

S. W. Yates[1] L. L. Riedinger[2]
N. R. Johnson A. C. Kahler[2]

Recent measurements of reduced transition probabilities of high-spin states in strongly deformed nuclei have shown that these nuclei are well understood in terms of the rotational model.[3] However, pronounced deviations from the rotational description have been observed for $B(E2)$ values of ground-band states in transitional nuclei and are often interpreted as due to band-mixing between the ground band and low-lying beta-vibrational and gamma-vibrational bands. The observed increase in $B(E2)$ for such nuclei has been taken[4] to be of the form

$$B(E2; I \rightarrow I-2) = B_0(E2; I \rightarrow I-2) \times \left[1 + \frac{\alpha}{2}\left[I(I+1) + (I-2)(I-1)\right]\right]^2,$$

where $B_0(E2)$ is the unmixed rigid rotor value and α is a mixing (or stretching) parameter. Although previous work has accounted for deviations in terms of the single parameter α, it may well be that other explanations such as fourth-order cranking, centrifugal stretching, and Coriolis antipairing can also account for nonrotational behavior.

In a further study of the problem with these nuclei just at the boundary of the strongly deformed region, the ground-state rotational band of ^{150}Nd has been investigated by using the Doppler-shift recoil-distance technique. Recoil-distance measurements are preferred, since no other method is believed to be of comparable accuracy in the half-life range under study. In addition, this method involves fewer assumptions than are employed in other measurements such as multiple Coulomb excitation yields.

An isotopically enriched 2.8-mg cm^2 ^{150}Nd foil was bombarded with 149-MeV ^{40}Ar^{9+} ions from the ORIC. Following Coulomb excitation of the target nuclei, the backscattered ^{40}Ar ions were detected in an annular surface-barrier detector. Spectra of gamma rays in coincidence with the backscattered ions were taken at several target-stopper separations. A plot of the ratio of the unshifted gamma-ray intensity divided by the total gamma-ray intensity as a function of the target-stopper separation is shown in Fig. 2.40, and the resulting half-lives and $B(E2)$ values are summarized in Table 2.8. The details of the method of data analysis are given elsewhere (see refs. 5 and 6). While the 10$^+$ rotational state is clearly excited in the Coulomb excitation process, an unfortunate degeneracy between its gamma ray and another gamma ray from a known vibrational level prevents our obtaining a half-life value for this state.

It is clear from the $B(E2)$ ratios in Table 2.8 that there is enhancement in the transition strength as one goes to higher spin. The enhancements are very similar to those found in the case of ^{152}Sm (ref. 7). An

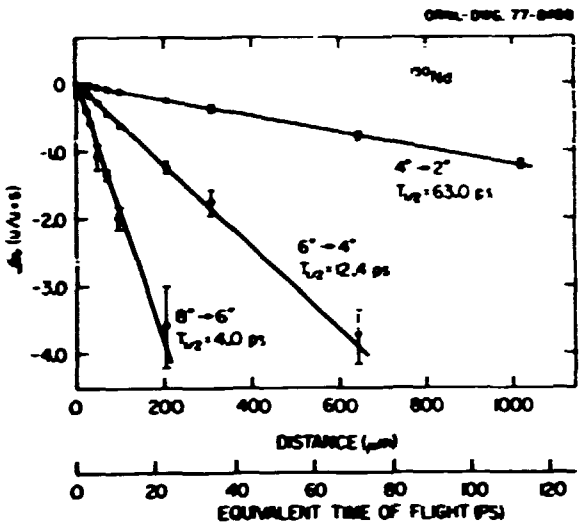

Fig. 2.40. Plot of the ratio of the unshifted gamma-ray intensity to the unshifted plus shifted intensity as a function of the target-stopper separation for three of the transitions in ^{150}Nd.

Table 2.8. Summary of half-life and $B(E2)$ data for ^{150}Nd

Transition	E_γ (keV)	T_1 (psec)	$B(E2)$, e^2b^2	$\frac{B(E2)_{exp}}{B(E2)_{theory}}$
$2^+ \rightarrow 0^+$	130.3	1440 ± 70	0.56 ± 0.03	(1.00)[a]
$4^+ \rightarrow 2^+$	251.2	63.0 ± 3.2	0.82 ± 0.04	1.03 ± 0.05
$6^+ \rightarrow 4^+$	339.0	12.4 ± 1.1	0.98 ± 0.09	1.13 ± 0.09
$8^+ \rightarrow 6^+$	409.3	4.0 ± 0.4	1.21 ± 0.12	1.33 ± 0.13

[a]All ratios are normalized to this ratio as unity.

informative method of comparing these experimental results with the single parameter prescription is by a plot as shown in Fig. 2.41. A plot of this type should yield a straight line, the slope of which is α and the intercept, $B_0(E2)$. A weighted least-squares fit to the data indicates a constant value for $\alpha = (1.9 \pm 0.4) \times 10^{-3}$ and $B_0(E2) = 0.542 \pm 0.008$. Note that this value is nearly identical to values of the mixing parameter determined for the other $N = 90$ isotones, ^{152}Sm and ^{154}Gd, which indicates only small changes in the nuclear structure with increasing proton number in this region.

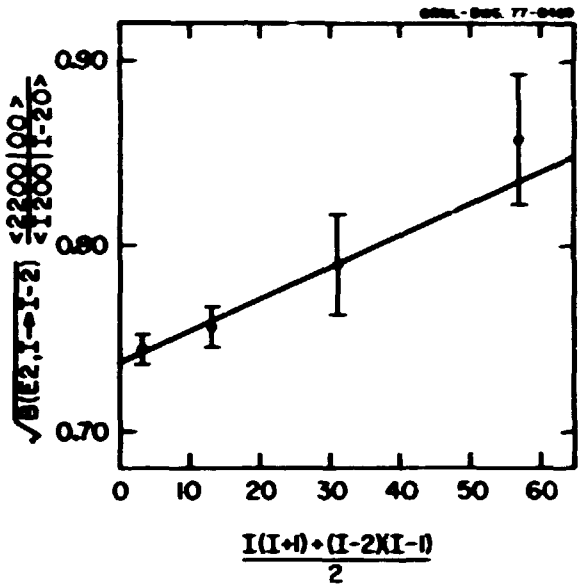

Fig. 2.41. Plot of

$$\sqrt{B(E2; I \rightarrow I-2)} \; \frac{\langle 2020|00\rangle}{\langle I020|I-20\rangle} \text{ vs } \frac{1}{2}[I(I+1)+(I-2)(I-1)]$$

for ^{150}Nd. The part in bracket notation is a ratio of Clebsch-Gordon coefficients.

BANDS IN ODD-A THALLIUM ISOTOPES

A. C. Kahler[1] N. R. Johnson[3]
L. L. Riedinger[2] R. L. Robinson

In the past year, experiments at the ORIC on ^{191,193}Tl have been completed. In addition, work on ^{189}Tl has been initiated at the Berkeley 88-in. cyclotron, using an (^{28}Si,4$n\gamma$) reaction. A primary purpose of these measurements is to follow the systematic trends of odd-A proton bands in this transitional region immediately below lead. This region is quite interesting in that it displays a variety of nuclear shapes and coupling schemes.

The $h_{9/2}$ and $i_{13/2}$ bands observed in thallium nuclei can be viewed as rather strongly coupled particles on slightly oblate mercury cores. Both of these Nilsson orbitals intrude across the $Z = 82$ shell model gap into the low-energy level schemes of thallium nuclei. By studying the spacings in these bands, we hope to learn much about the details of the couplings of these particles to their respective cores.

The yrast structure in the odd-A thallium nuclei is the $h_{9/2}$ band. The systematics of this band in the thallium nuclei are shown in Fig. 2.42. The work on ^{195,197}Tl has been performed in a Stockholm-Jülich collaboration[4] and the ^{191,193}Tl results are from our experiments. In each case, the $\frac{21}{2}^-$ member

1. University of Kentucky, Lexington.
2. University of Tennessee, Knoxville.
3. An account of this work is also included in *Chem. Div. Annu. Prog. Rep. Mar. 31, 1977*, ORNL-5297 (to be published).
4. R. M. Diamond et al., *Nucl. Phys.* A184, 481 (1972).
5. N. R. Johnson et al. *Phys. Rev.* C 12, 1927 (1975).
6. R. J. Sturm and M. W. Guidry, *Nucl. Instrum. Methods* 138, 345 (1976).
7. N. Rud et al., *Nucl. Phys.* A191, 545 (1972).

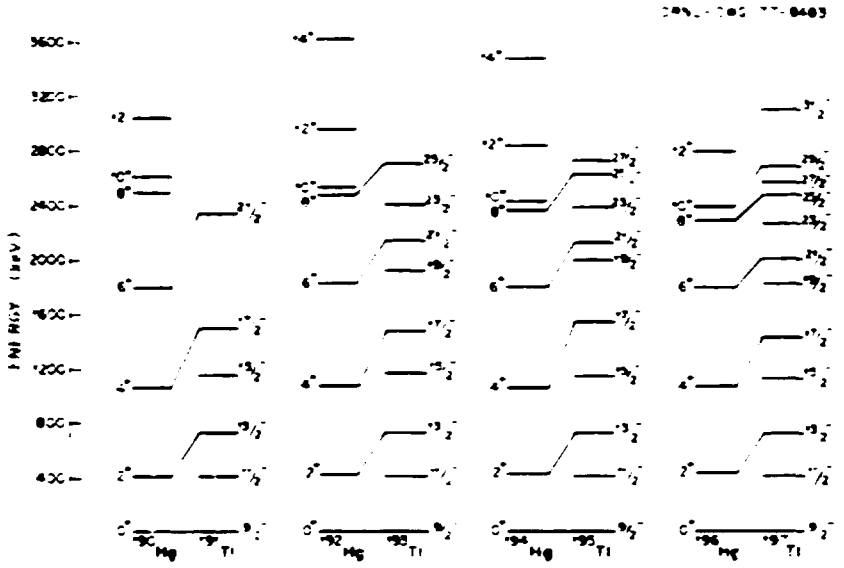

Fig. 2.42. Systematics trend of the $h_{9/2}$ band in thallium nuclei. The A = 195,197 results come from ref. 1; the A = 191,193 results are from the present experiments. Very qualitative comparisons are made with the even-A mercury cores.

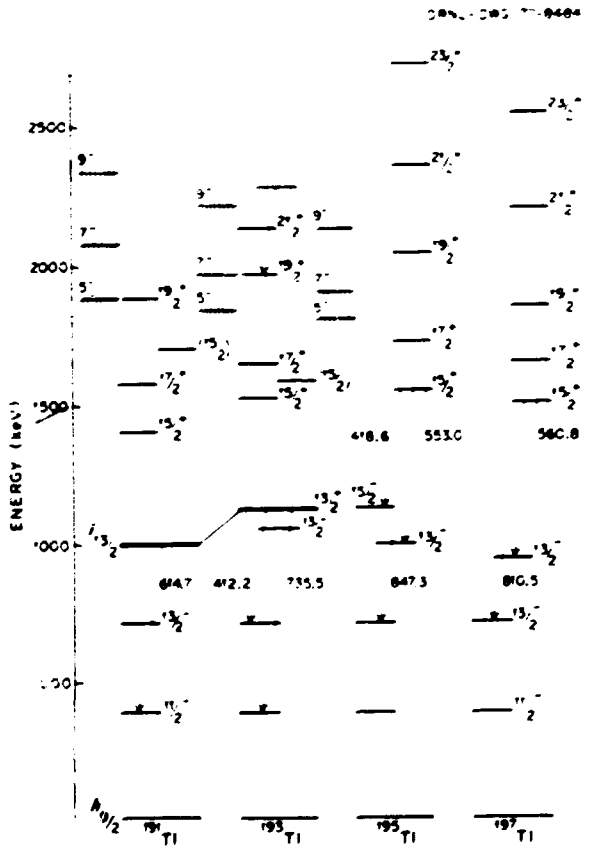

Fig. 2.43. Trend of positive-parity states in thallium nuclei. The A = 195,197 results come from ref. 1; the A = 191,193 results are from the present experiments. The positions of the 5⁻ band in ^{190,192,194}Hg are shown as hatched lines.

of the band breaks the trend established by the lower members. Furthermore, compressed levels are observed at higher spins in ^{195,197}Tl. The cause of this change in the $h_{9/2}$ band is not really understood. Lieder et al.[5] have proposed that the higher-spin states reflect the $10^- - 8^-$ compression in this core, as illustrated in Fig. 2.42. Work is continuing on the theoretical explanation of these changes in the $h_{9/2}$ band.

Positive-parity bands are also observed in these thallium nuclei, as shown in Fig. 2.43. However, it seems that we observe a vastly different structure in ^{191,193}Tl than that seen in ^{195,197}Tl. Our in-beam work, our UNISOR measurements on ^{193}Pb decay, and the earlier work of Newton et al.[6] lead to the placement of an $i_{13/2}$ band in ^{193}Tl. We observe in ^{191}Tl a similar band at a slightly lower energy. This band is evidently not the same as that observed in ^{195,197}Tl; the latter begins with $^{15}{}_2{}^+$ level and is explained[5] as a three-quasi-particle structure. The rapidly falling $i_{13/2}$ band evidently absorbs reaction strength in ^{191,193}Tl, although we have candidates for an analogous $^{15}{}_2{}^+$ state in these nuclei.

---

1. Graduate student, University of Tennessee, Knoxville.
2. Consultant, University of Tennessee, Knoxville.
3. Chemistry Division.
4. R. M. Lieder et al., p. 112 in *Stockholm Annu. Rep., 1975*.
5. R. M. Lieder, International Conference on Collectivity of Medium and Heavy Nuclei, Tokyo, September 1976.
6. J. O. Newton, F. S. Stephens, and R. M. Diamond, *Nucl. Phys.* **A236**, 225 (1974).

HIGH-SPIN STATES IN ^{185}Au

A. C. Kahler[1] R. L. Robinson
L. L. Riedinger[2] E. F. Zganjar[4]
N. R. Johnson[3] A. Visvanathan[4]

As part of our continuing study of high-spin states in odd-A transitional nuclei, levels in ^{185}Au have been observed following the ^{169}Tm(^{20}Ne, $4n\gamma$) reactions at ORIC. We have accumulated γ-γ-t, γ-rf, and angular distribution data, using both thin and thick targets. These data have enabled us to identify two decoupled bands (Fig. 2.44).

The lower-lying band is believed to be built on the $[541]_{1/2}$: $h_{9/2}$ proton orbital. In the heavier odd-A gold isotopes, this orbital is rapidly approaching the ground state. In fact, the ^{185}Au ground state of $^{3}/_{2}^{-}$ is thought to be part of the $[541]_{1/2}$ band structure. It lies anomalously low in energy, as do the $^{9}/_{2}^{-}$, $^{13}/_{2}^{-}$, $^{17}/_{2}^{-}$, ... levels, because of the large decoupling parameter for this orbital. At this point, a low-energy highly converted $^{9}/_{2}^{-} \rightarrow {}^{5}/_{2}^{-}$ quadrupole transition has been unobserved, and all energies are given with respect to the $^{9}/_{2}^{-}$ level.

The second decoupled band is tentatively identified as the $[660]_{1/2}$ $i_{13/2}$ proton. The band head is seen only weakly in the present measurements but is more strongly populated in the decay of a high-spin ^{185}Hg isomer, as observed in UNISOR measurements (described also in this report). As in the $h_{9/2}$ band, the proposed $^{13}/_{2}^{+}$, $^{17}/_{2}^{+}$, $^{21}/_{2}^{+}$, ... levels are evidently depressed in energy relative to the $^{15}/_{2}^{+}$, $^{19}/_{2}^{+}$, ... levels. Electron measurements are in progress to confirm or deny the $E1$ character of the 424-keV dipole gamma ray. The only other high-j particle on which a band could be built is the $[505]_{11/2}$: $h_{11/2}$ proton. However, this high-Ω orbital should not give rise to a decoupled band. Additionally, if this band resulted from the $h_{11/2}$ proton, the 1031.4-keV level would be $^{15}/_{2}^{-}$, but

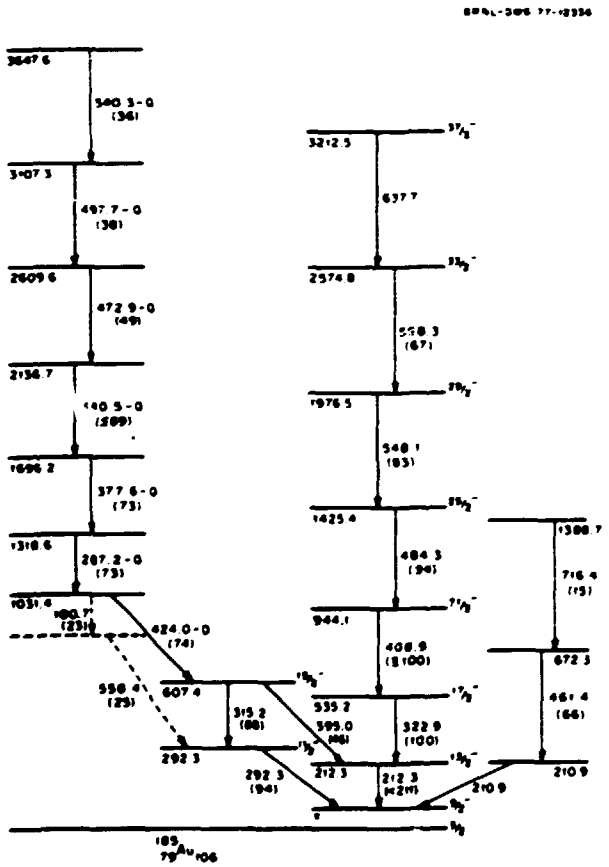

Fig. 2.44. Band structure of ^{185}Au. Gamma-ray intensities observed in the (^{20}Ne,$4n\gamma$) reaction are given in parentheses below the transition energies in keV. The low-energy $^{9}/_{2}^{-} \rightarrow {}^{5}/_{2}^{-}$ transition has not been observed.

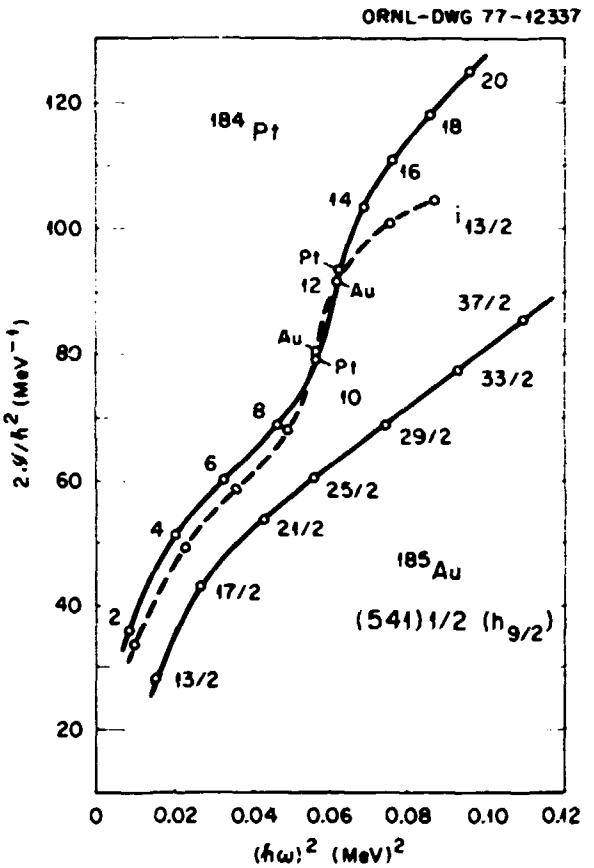

Fig. 2.45. Plot of essentially the moment of inertia vs the square of the rotational frequency for the core, ^{184}Pt, and for the ^{185}Au proton bands, $h_{9/2}$ and probably $i_{13/2}$.

the angular distribution data for the .24-keV gamma ray would not support the required $\Delta I = 0$ nature of this transition.

Assuming the correctness of the $[660]_{1/2}$ assignment, ^{185}Au presents an excellent opportunity to study the cause of backbending in this transition region. The downsloping nature of both $[541]_{1/2}$ and $[660]_{1/2}$ orbitals as a function of deformation guarantees that both particles have the same deforming effect on the ^{184}Pt core. As shown in Fig. 2.45, the $h_{9/2}$ band does not backbend, while the proposed $i_{13/2}$ proton band closely follows the ^{184}Pt core in its slight backbending. This contrasting behavior presents the first conclusive proof that the Coriolis alignment of $h_{9/2}$ protons is responsible for backbending in the light, prolate platinum and osmium nuclei. The $i_{13/2}$ proton orbit evidently contributes little to backbending because of its elevated energy relative to the Fermi surface. There are $i_{13/2}$ neutron orbits near the Fermi surface, but our results demonstrate that they do not play a crucial role here, contrary to the conclusions of Beshai et al.[5]

1. Graduate student, University of Tennessee, Knoxville.
2. Consultant, University of Tennessee, Knoxville.
3. Chemistry Division.
4. Louisiana State University, Baton Rouge.
5. S. Beshai et al., *Z. Phys.* A277, 351 (1976).

ODE TO AN UNIDENTIFIED ISOTOPE

R. B. Piercey[1] A. V. Ramayya[1]
J. H. Hamilton[1] R. L. Robinson
R. M. Ronningen[1] H. J. Kim

"My heart aches and a drowsy
numbness pains my sense,
as though of hemlock I had drunk"[2]
While in-beam gamma rays
have fallen like the rains,
one group unidentified
has brought on us a blue funk.

In studying ^{74}Se produced by bombarding ^{60}Ni with 46-MeV ^{16}O ions at the ORNL tandem accelerator, a group of unidentified gamma rays were observed. From γ-γ coincidence studies, 13 transitions could be assigned to energy levels at 187, 383, 656, 813, 878, 1161, 1474, 1646, and 2054 keV and four to tentative levels at 70, 356, 1184, and 2534 keV, as shown in Fig. 2.46. They are not seen in any radioactive decays studied after the run nor in other studies to our knowledge.

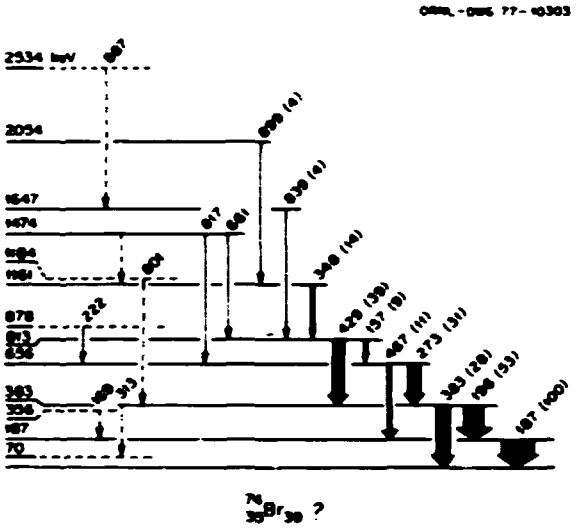

Fig. 2.46. Experimental level scheme attributed to ^{74}Br.

From calculations of the cross section with the program ALICE, which generally reproduces the experimental cross section in the mass region, we find that we are missing most of the predicted cross section that leads to ^{74}Br in our in-beam study. We see in-beam some weak transitions that feed the 1$^-$, 28-min isomer of ^{74}Br.

In the radioactive decay, however, we see more strongly the decay of the 4$^-$, 42-min isomer of ^{74}Br. Thus, we know we are populating states that feed the high-spin isomer. If we assign the above unknown group to ^{74}Br, the experimental cross sections are in general agreement with the calculations. Nothing is known about high-spin levels in ^{74}Br at present. We believe these new transitions are from high-spin states that feed the 4$^-$ level in ^{74}Br. Much less likely, but possible, is that these transitions involve decays into the spin $^7/_2$ isomers of ^{71,73}Se.

1. Vanderbilt University, Nashville, Tenn.
2. John Keats, "Ode to a Nightingale."

IN-BEAM GAMMA-RAY SPECTROSCOPY OF ^{72}Ge

A. C. Rester[1] A. V. Ramayya[2]
A. P. de Lima[2,3] H. Kawakami[2,4]
J. H. Hamilton[2] R. M. Ronningen[2]
R. L. Robinson H. J. Kim

The levels of ^{72}Ge have been investigated to higher spin via the ^{68}Zn(^{6}Li,pn)^{72}Ge reaction at a beam

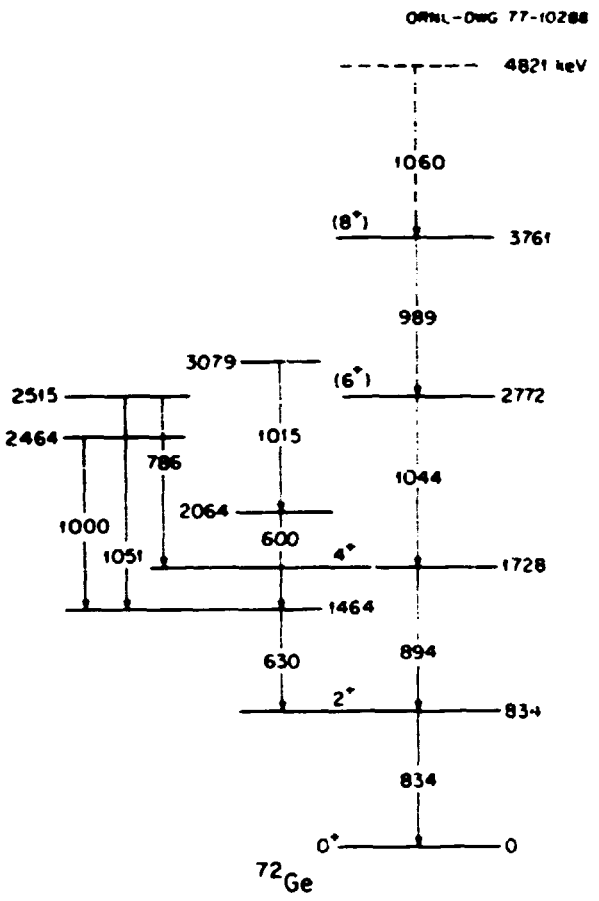

Fig. 2.47. Levels in ^{72}Ge.

energy of 26 MeV. Gamma-gamma coincidence and angular distribution measurements were carried out. From the γ-γ coincidence studies, two and possibly three new levels are established in the yrast cascade as shown in Fig. 2.47. Analysis of the angular distribution data to obtain the spins is in progress. All the levels below 2550 keV have been seen in the decay of ^{72}As to ^{72}Ge.[5]

More of the feeding goes by the main yrast cascade in ^{72}Ge. Also, the transition from the 8$^+$ to the 6$^+$ level is lower in energy than the 6 to 4 transition which may indicate that this 8$^+$ level is a two-particle state with a $(g_{9/2})^2$ configuration as suggested in our ^{68}Ge work[6] rather than a continuation of the ground-state band.

1. Tennessee Technological University, Cookeville.
2. Vanderbilt University, Nashville, Tenn.
3. On fellowship sponsored by the Portuguese government.
4. On leave from the Institute for Nuclear Study, Tokyo.
5. K. R. Alvar, *Nucl. Data Sheets* 11, 121 (1974).
6. See this report, A. P. de Lima et al., "Multiple Band Structure in ^{68}Ge and the $g_{9/2}$ Orbital."

MULTIPLE BAND STRUCTURE IN ^{68}Ge AND THE $G_{9/2}$ ORBITAL

A. P. de Lima[1,2] R. M. Ronningen[2]
J. H. Hamilton[2] H. Kawakami[2,4]
R. L. Robinson R. B. Piercey[2]
A. V. Ramayya[2] H. J. Kim
B. van Nooijen[2,3] W. K. Tuttle
L. K. Peker[5]

Even- and odd-parity bands have been observed in nuclei in the $A = 70$ region with rotational-like level spacings.[6,7] As part of a systematic program to investigate the structure of nuclei in this region, we have studied levels in ^{68}Ge to high spin. In-beam gamma-ray spectroscopy (including angular distribution), γ-γ coincidence, and lifetime measurements were made via the ^{58}Ni(^{12}C,2p)^{68}Ge reaction with a beam energy of 39 MeV. The yrast cascade to 12$^+$ was reported at the Caen Conference.[8] Here we report a more complete analysis of the coincidence and angular distribution data that yields a surprising new richness of band structures not previously identified in this region.

Figure 2.48 presents our results. The first striking new result is the discovery of three 8$^+$ levels with definite bands built on two of these levels. The A_2 and A_4 coefficients for the 1141.3-, 1353.6-, and 1670.0-keV transitions are 0.324(24), −0.117(29); 0.356(16), −0.120(17); and 0.31(3), −0.11(3) respectively. These and the direction correlation from oriented states (DCO) γ-γ correlation results favor 8$^+$ assignments for the three levels these transitions depopulate. Other spins assigned to the bands built on these levels are supported but not always proven by the data and so are somewhat tentative. The fascinating behavior of the moments of inertia, $\mathcal{J}$, with spin of these even parity states is shown in Fig. 2.49.

The 5366.8-keV level is easily interpreted as the continuation of the ground-state band. If one looks at the mean lifetimes of the other two 8$^+$ states, one finds that both are retarded when compared with the 6-4 transition. Thus the lifetimes and the changes in $\mathcal{J}$ at 8$^+$ for these two bands indicate they have significant changes in structure. In weakly deformed nuclei where the Fermi energy is close to the $\Omega = {}^1/_2$, large $j(i_{13/2}, h_{11/2}, g_{9/2})$ levels, strong Coriolis coupling is expected to give rise to aligned ($I = I_0, I_0, 2 \ldots$) bands based on $(j)^2$ two-particle configurations and to partly aligned rotational bands based on negative-parity two-particle configurations ($i_{13/2}$; $f_{5/2}$, $p_{3/2}$), ($h_{11/2}$; $d_{5/2}$, $g_{7/2}$), or ($g_{9/2}$; $f_{5/2}$, $p_{3/2}$), $I = 5^-, 7^-, 9^-; 6^-, 8^-$, 10^-. Such bands have been seen in Pt; in Hg nuclei with $\nu(i_{13/2})$; in Ba, Ce, and Nd with $\pi(h_{11/2})$; and in

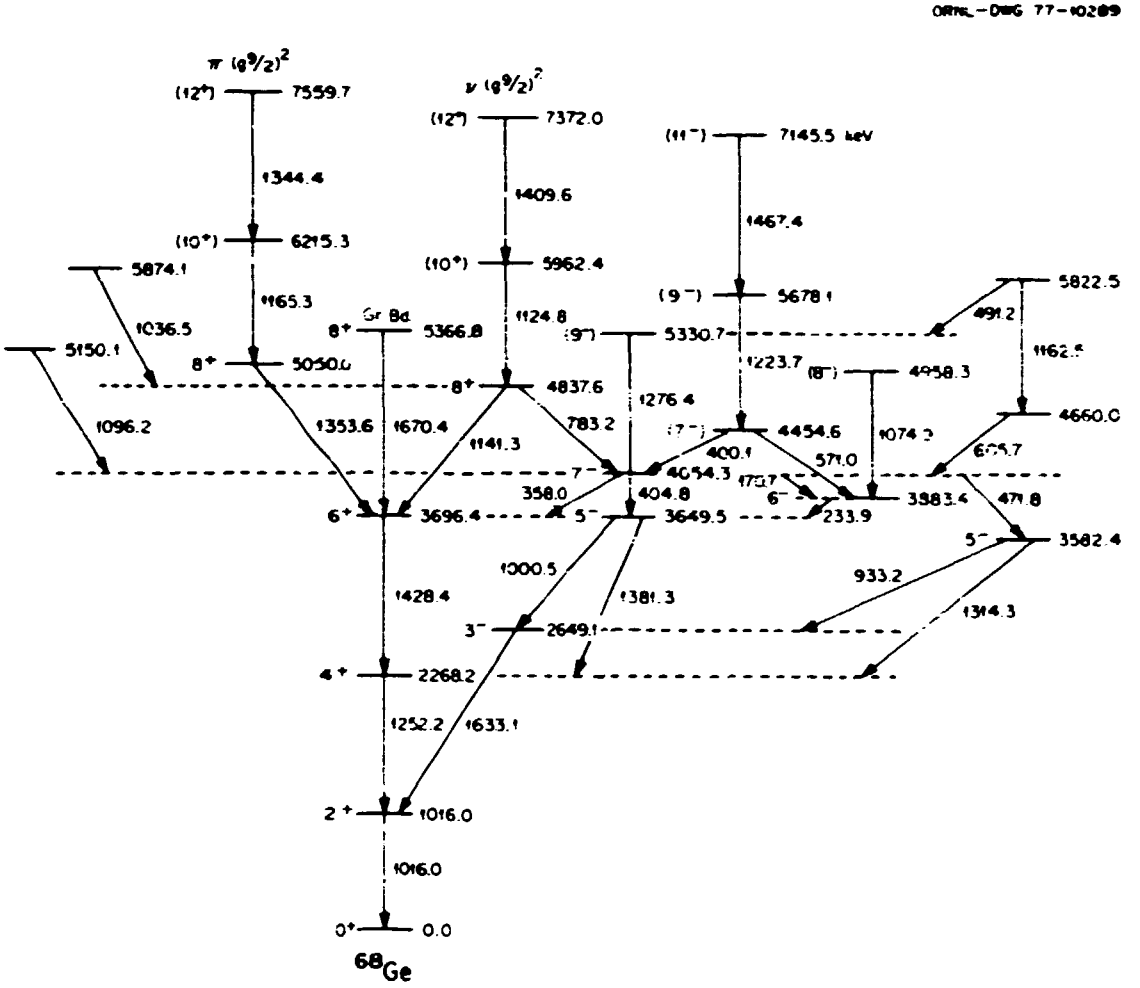

Fig. 2.48. Levels in ^{68}Ge.

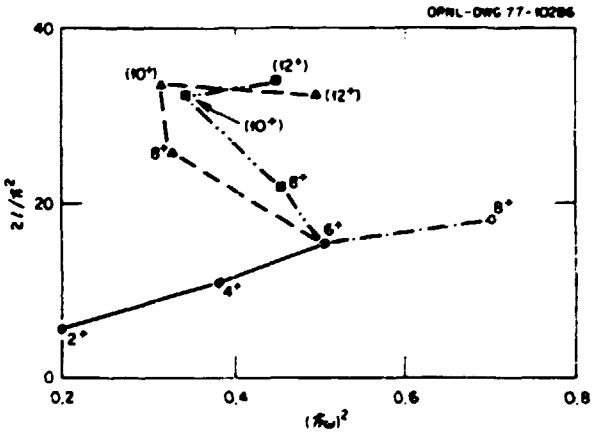

Fig. 2.49. Plot of the moment of inertia vs rotational energy for three cascades in ^{68}Ge.

Ru, Pd, and Cd with $\nu(h_{11/2})$ configurations. In these nuclei with N much greater than Z, the condition for a strong Coriolis coupling exists only for proton or for neutron configurations but not for both, and so only proton or neutron bands are observed. In the $A = 70$ region, however, where both N and $Z = 30$ to 38, one could have both proton and neutron bands based on these $g_{9/2}$ orbitals. The two observed rotational bands built on the two 8$^+$ levels in ^{68}Ge can be considered the first evidence for both proton $\pi(g_{9/2})^2$ and neutron $\nu(g_{9/2})^2$ bands. Further support of this idea is found in the negative-parity states, where we can expect negative-parity bands based on proton ($g_{9/2}$; $f_{5/2}$, $p_{3/2}$) and neutron ($g_{9/2}$; $f_{5/2}$, $p_{3/2}$) configurations. Indeed, there are several negative-parity

bands seen in ^{66}Ge which have the expected properties.

1. On fellowship, sponsored by the Portuguese government
2. Vanderbilt University, Nashville, Tenn.
3. On leave from Delft Technological University, Netherlands
4. On leave from Institute for Nuclear Study, Tokyo, Japan
5. Free University of Amsterdam, Netherlands
6. J. H. Hamilton et al., *Phys. Rev. Lett.* 32, 239 (1974); 36, 304 (1976).
7. K. B. Piercey et al., *Phys. Rev. Lett.* 37, 496 (1976).
8. A. P. de Lima et al., p. 52 in *Proceedings European Conference on Nuclear Physics with Heavy Ions, Sept. 6-10, 1976*, ed. B. Fernandez et al., Caen, France, 1976.

EVIDENCE FOR BAND STRUCTURE AND POSSIBLE TRIAXIAL DEFORMATION IN ^{65}Ga

H. Kawakami[1,2] A. V. Ramayya[2]
A. P. de Lima[2,3] R. L. Robinson
J. H. Hamilton[2] H. J. Kim
R. M. Rominger[2] L. K. Peker[4]

Rotational-aligned bands are well established in heavy odd-A nuclei. In the region of weak deformation for heavy nuclei, evidence for triaxial shapes has been extracted from such bands; for examples, see refs. 5 and 6. Bands with moderate deformation built on the $g_{9/2}$ orbital in odd-A nuclei in the mass-70 region are now observed; for examples, see refs. 7 and 8. As reported elsewhere,[9] evidence for the importance of the $g_{9/2}$ orbital is seen also in even-A nuclei in this region. Additional information on high-spin states in odd-A nuclei is needed to test the rotational-aligned coupling model[10] and the possible existence of triaxial shapes in the $A = 70$ region.

The levels in ^{65}Ga have been investigated by in-beam gamma-ray spectroscopy through γ-γ coincidence and gamma-ray angular distribution measurements. The reaction ^{58}Ni(^{12}C,αp)^{65}Ga at a projectile energy of 39 MeV was used. The primary levels observed are shown in Fig. 2.50, where they are grouped into cascade bands. One sees evidence for bands built on the $f_{5/2}$ and $g_{9/2}$ proton orbitals. Note the unusual spin sequence for the negative-parity band of $^{5}/_{2}^{-}$, $^{9}/_{2}^{-}$, $^{7}/_{2}^{-}$, $^{13}/_{2}^{-}$, and $^{11}/_{2}^{-}$. For the positive-parity $g_{9/2}$ band, there is also evidence for such staggering. These staggered-spin cascades suggest that ^{65}Ga may have triaxial deformation and, since $E(^{15}/_{2}^{-} \rightarrow {}^{13}/_{2}^{-}) > E(^{17}/_{2}^{-} \rightarrow {}^{13}/_{2}^{-})$, suggest that gamma is less than 30°.

The other very interesting feature of these levels is the $^{21}/_{2}^{+}$ level at 4333 keV. The low energy, 310.6 keV, of the $^{21}/_{2}^{+} \rightarrow {}^{17}/_{2}^{+}$ transition clearly indicates a change in the level structure from the band built on

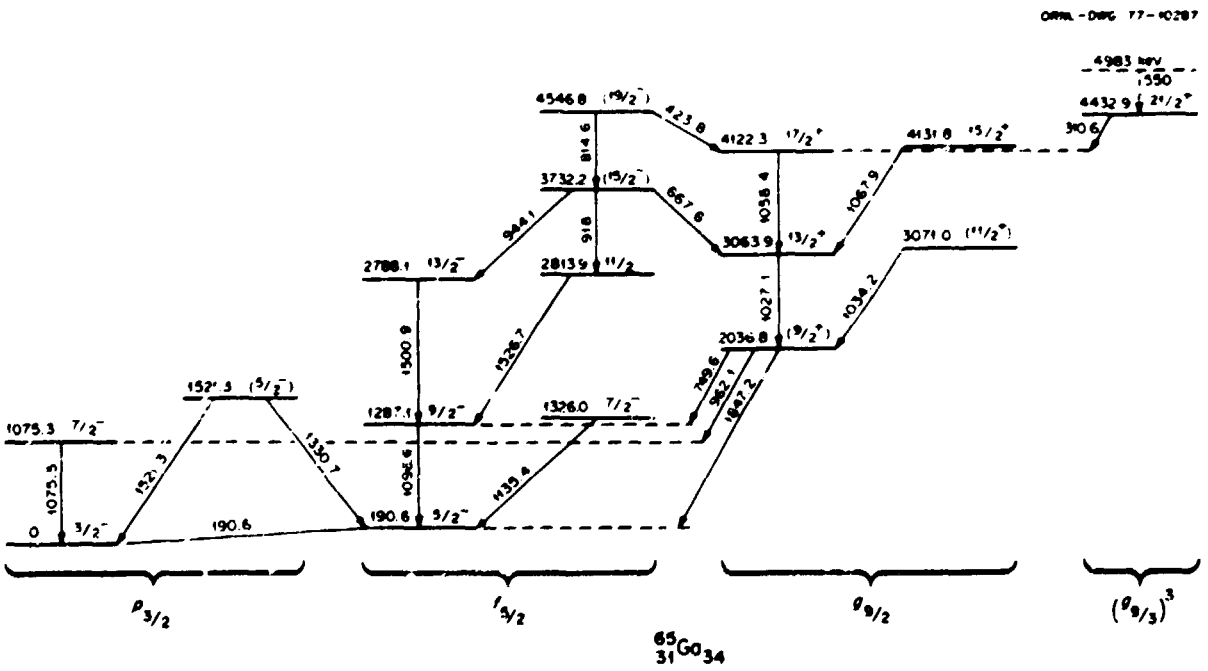

Fig. 2.50. Levels in ^{65}Ga.

the $g_{9/2}$ state at 2037 keV. Nearby even-mass nuclei have 8^+ states in the range of 4.5 to 5 MeV; these have been interpreted as $(g_{9/2})^2$ configurations.[9] Since the lowest spin of a $(g_{9/2})^3$ configuration is $\frac{21}{2}^+$, we suggest that the level at 4333 keV may be such a three-particle configuration.

---

1 On leave from the Institute for Nuclear Study, Tokyo, Japan
2 Vanderbilt University, Nashville, Tenn
3 On fellowship, sponsored by the Portuguese government
4 Free University of Amsterdam, Netherlands
5 J. Meyer ter Vehn et al., *Phys. Rev. Lett.* **32**, 1383 (1974)
6 E. F. Zganjar et al., *Phys. Lett.* **58B**, 159 (1975)
7 B. Herskind et al., *Phys. Lett.* **61B**, 33 (1976)
8 G. F. Neal et al., *Nucl. Phys.* **A280**, 161 (1977)
9 See this report, A. P. de Lima et al., "Multiple Band Structure in ^{66}Ge and the $g_{9/2}$ Orbital."
10 F. S. Stephens, *Rev. Mod. Phys.* **47**, 43 (1975)

HIGH-SPIN STATES IN ^{64}Zn

J. C. Wells, Jr.[1] H. J. Kim
Linda Fugate[1] W. T. Milner
R. O. Sayer[2] G. J. Smith
R. L. Robinson R. M. Ronningen[3]

As part of a program to systematically study higher-spin states of even-mass nuclei in the range $A \approx 70$, we have investigated the gamma rays of ^{64}Zn resulting from the heavy-ion reactions ^{51}V(^{16}O,$p2n$) with $E_{^{16}O} = 36$ to 46 MeV and ^{59}Co(^{7}Li,$2n$) with $E_{^7Li} = 18$ MeV. Measurements were made of excitation functions, gamma-ray singles and γ-γ coincidence spectra, and Doppler broadening for gamma-ray lines. We have constructed an energy-level scheme and deduced spins and parities, gamma-ray branching ratios, and gamma-ray radiative admixtures. The energy-level scheme is shown in Fig. 2.51. Preliminary results have been reported previously.[4,5]

We have determined lifetimes of a number of the gamma rays from ^{64}Zn by analysis of the Doppler-broadened line shapes from spectra obtained at 0° to the beam direction. We also obtained lifetime measurements by the Doppler-shift recoil-distance method, in which the reaction products recoiled into a vacuum and were stopped by a movable plunger set at distances of 56 to 1270 μm from the target. Our lifetime results are given in Table 2.9. We find good agreement with the results of Charvet et al.[6] and Bruandet et al.[7]

The 4236.7-, 2736.1-, and 1799.2-keV levels may be the 6^+, 4^+, and 2^+ members of a second band. Second 2^+ and 4^+ levels are found in ^{62}Zn and ^{66}Zn,[8,9] but a second 6^+ level is not reported.

If the levels at 2999.0, 3924.5, and 4980.8 keV are in fact 3^-, 5^-, and 7^-, we see a striking similarity to the 3^-, 5^-, and 7^- levels in ^{66,68}Zn and ^{68,70}Ge.[9-12] However, in

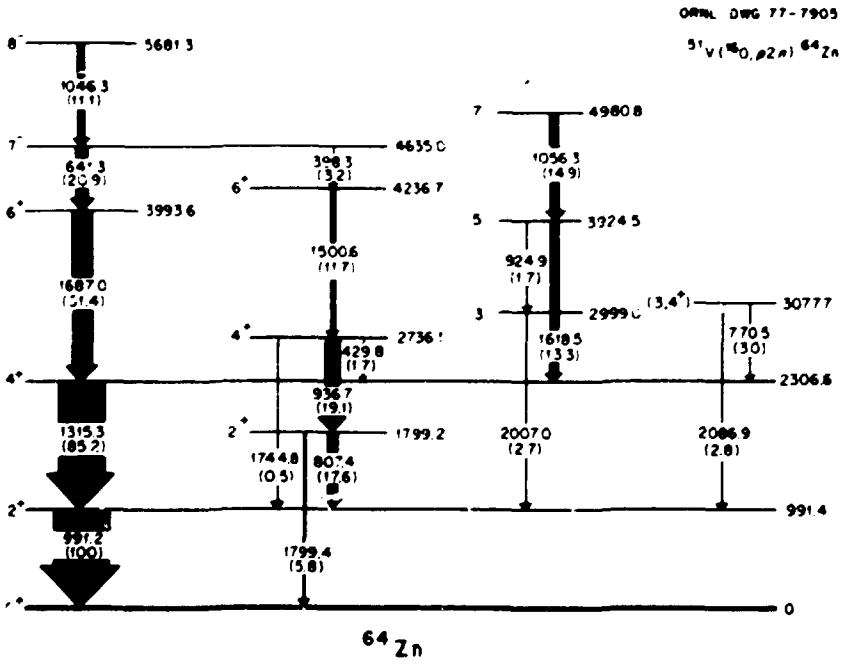

Fig. 2.51. Levels and transitions of ^{64}Zn.

Table 2.9 Composite mean lifetimes of gamma rays from ^{64}Zn obtained from the shape of the Doppler-broadened gamma-ray peaks and from the recoil-distance measurements

Level (keV)	E_γ (keV)	This work, τ (psec)	Other works, τ (psec)
1799.2	807.4	3 ± 2	2.6 ± 0.7[a]
	1799.3	3 ± 2	2.6 ± 0.7[a]
2306.6	1315.1	1.4 ± 0.8	0.63 ± 0.12[a]
2736.2	429.8	5 ± 3	
	936.7	2.5 ± 1.0	3.0 ± 1.0[a]
2999.0	2007.0	0.11 ± 0.05	
3077.7	770.5	1.4 ± 0.4	2.0 ± 1.2[a]
	2086.9	1.5 ± 0.5	2.5 ± 1.1[a]
3925.3	924.9	<2.5	
3993.6	1687.0	0.22 ± 0.05	
4236.7	1500.6	1.8 ± 0.3	
4635.0	398.3	152 ± 14	
	641.3	143 ± 8	130 ± 15[b]
4980.8	1056.6	1.9 ± 0.6	
5681.3	1046.3	1.4 ± 0.3	

[a] Ref. 6
[b] Ref. 7

each of these is reported a 6$^+$ level between the 5$^-$ and 7$^-$ levels. We do not find a 6$^+$ level in ^{64}Zn.

Note the long lifetime (145 psec) of the 7$^-$ 4635.0-keV level. This level is de-excited by two $E1$ transitions, each of which is retarded by 5×10^4. A possible explanation is that this state consists of a totally aligned $g_{9/2}$ quasi-particle and an $f_{5/2}$ quasi-particle.

1. Tennessee Technological University, Cookeville.
2. UCC-ND Computer Sciences Division.
3. Vanderbilt University, Nashville, Tenn.
4. R. O. Sayer et al., p. 146 in *Proceedings of the International Conference on Reactions between Complex Nuclei, Nashville, Tennessee, 1974*, ed. R. L. Robinson et al., North-Holland, Amsterdam, 1974.
5. Linda Fugate et al., *Bull. Am. Phys. Soc.* **22**, 565 (1977).
6. A. Charvet et al., *Phys. Rev. C* **13**, 2237 (1976).
7. J. F. Bruandet et al., *J. Phys. (Paris) Lett.* **37**, L-63 (1976).
8. J. F. Bruandet et al., *Z. Phys.* **A279**, 69 (1976).
9. J. F. Bruandet et al., *Phys. Rev. C* **12**, 1739 (1975).
10. J. F. Bruandet et al., *Phys. Rev. C* **14**, 103 (1976).
11. E. Nolte et al., *Z. Phys.* **268**, 267 (1974).
12. R. L. Robinson et al., to be published in *Physical Review*.

^{200}Po AND ^{200}Bi DECAY

R. W. Lide[1] L. L. Riedinger[1]
C. R. Bingham[1] J. A. Vrba[1]

The alpha decay of ^{200}Po has been the subject of many experimental studies,[2] but to our knowledge, no reliable information exists concerning the electron capture decay of this nucleus to levels in ^{200}Bi. While the decay of ^{200}Bi has been reported previously,[3] a thorough spectroscopic study with extensive γ-γ coincidence data and conversion electron data is still lacking. Because ^{200}Po decays to the odd-odd nucleus ^{200}Bi, theoretical interpretation of the levels may be difficult. The low-lying states in ^{200}Bi are formed by a combination of both odd proton and odd neutron in the shell above $N = 82$, and thus there will be several ways to form positive-parity states, and, in particular, 1$^+$ states, which can be fed by a spin-allowed, isospin-allowed transition. Hence, we expect the decay scheme for ^{200}Po to be somewhat complex. It will perhaps be possible to locate a number of 1$^+$ states in ^{200}Bi and then to speculate about their structure. The ground state of ^{200}Bi is a known 7$^+$ state[4] probably resulting from the $(\nu f_{5/2} \pi h_{9/2})$ configuration. By exciting the proton from the $h_{9/2}$ orbit to the $f_{7/2}$ orbit, a 1$^+$ state should be produced at low excitation energy having a large beta decay feeding from ^{200}Po. The rapid decay of such a state to the (7$^+$) ground state would require at least three transitions and, unless intermediate spin states intercede, would be prohibited.

The ^{200}Bi nuclei decay to ^{200}Pb, a closed-shell nucleus. We have an interest in locating the collective bands in such nuclei to compare their level spacings with the predictions of a vibrational model such as the interacting boson model (IBA).[5] The interpretation of excited bands such as the expected 5$^-$, 7$^-$, 9$^-$, ... bands in terms of particle-core decoupling by the Coriolis force will also be pursued. The IBA model predicts a 3$^-$ state at an energy below the 5$^-$, 7$^-$, 9$^-$, ... bands, such as those seen earlier in ^{190}Hg. It would be of interest to search for such a 3$^-$ state and thus give additional credibility to the phonon model. Perhaps a closed-shell nucleus such as ^{200}Pb would be a suitable nucleus to search for such an octupole vibrational state.

During a UNISOR run with an ^{14}N beam and a natural iridium target we obtained gamma-ray multiscale data and γ-γ coincidence data on the mass-200 sources. Analysis of the multiscale data has revealed approximately 30 transitions with a half-life near 11 min, the half-life previously reported for the alpha decay of ^{200}Po. To our knowledge, none of the observed gamma-ray transitions have been previously reported. Particularly strong lines were observed at transition energies near 147, 204, 328, 430, 434, 618, 671, 797, and 849 keV. Coincidence spectra have been obtained for every transition. The decay scheme resulting from the analysis of the coincidence data is shown in Fig. 2.52. The two

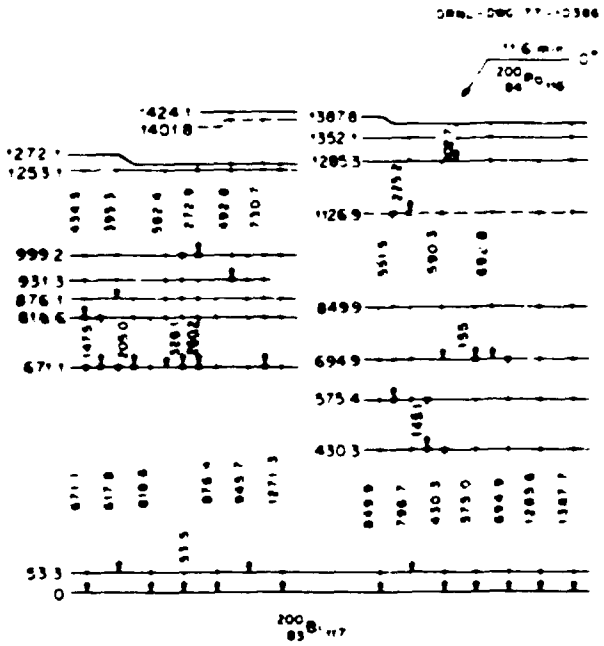

Fig. 2.52 Preliminary scheme of levels in ^{200}Bi populated by the electron capture decay of ^{200}Po. The relationship of the currently observed levels to the previously known 7$^-$ state in bismuth is not known

strongest transitions at 618 and 671 keV originate from a single level at 671 keV. By detailed balance of the population and depopulation of this state by gamma-ray transitions, we conclude that the 671-keV state is directly fed with a log ft of 5.7 (which means that it is a spin-allowed, isospin-allowed transition) and is hence a 1$^-$ state. Conversion electron data are needed to determine the multipolarity of the observed transitions and hence to shed light on the spins of the observed states in ^{200}Bi. Since the ground state is a known 7$^-$ state, we should point out that the lowest level shown in Fig. 2.52 is not the ground state but is probably a new unstudied low-spin isomer of ^{200}Bi. Also, some of the decay structures on the right part of the figure may not actually end on the level shown but on some other level.

We have some evidence that the lowest level shown in Fig. 2.52 is a low-spin isomer which decays directly by electron capture. By comparing the intensities of gamma rays in lead with those of previous studies where bismuth was made directly,[2] it is observed that the present sources populate high-spin states in lead much less strongly. For example, the ratio of 7$^-$ to 5$^-$ intensity to the 2$^+ \rightarrow$ 0$^+$ ground-state intensity is 0.06 for the present study and about 0.44 from the directly produced bismuth sources.[3] While our data were taken for only a limited time (≈20 min), we estimate that the half-life of the 7$^-$ ground state is 35 min. We suspect that the two low levels seen in Fig. 2.52 are low-spin couplings of the $(\pi f_{5/2}{}^{-1} h_{9/2})$ configuration, of which the 7$^-$ ground state is a member.

New data are needed to determine internal-conversion coefficients, to search for low-energy isomeric transitions, and to measure the half-life of the new isomer.

1 University of Tennessee, Knoxville

2 See, for example, A. Siivola, *Nucl. Phys.* **A101**, 129 (1967).

3 See, for example, M. Pautrat et al., *Nucl. Phys.* **A201**, 469 (1973).

4 S. Axensten, C. M. Johansson, and I. Lindgren, *Ark. Fys.* 15, 465 (1959).

5 A. Arima and F. Iachello, *Phys. Lett.* **57B**, 39 (1975).

^{199,201}Po DECAY

R. Stone[1] W. R. Western[2]
C. R. Bingham[1] R. A. Braga[2]
L. L. Riedinger[1] J. L. Wood[2]
R. W. Fink[2]

The purpose of the present study is to observe the trend of the single proton states immediately above the $Z = 82$ gap and the collective bands built on these single-particle states. In gold and thallium the shape of the core is apparently quite crucial in determining the detailed ordering of levels in these bands. Since bismuth is on the other side of a shell closure, the $h_{11/2}$ state will be a hole in a possibly deformed polonium core, and the $h_{9/2}$ structure should be a particle weakly coupled to a spherical lead core.

Gamma-ray multiscale and γ-γ coincidence data were obtained for mass-199 and -201 sources produced in the UNISOR facility. Preliminary analysis of the mass-199 and -201 multiscale data show several discrepancies with an earlier study.[3] In the case of ^{199}Po, the two strongest transitions following the decay of a high-spin isomer at 500 and 1002 keV appear to have half-lives of 4.1 ± 0.2 min, which is consistent with the previously reported half-life of 4.2 ± 0.3 min and is also consistent with their relative intensities. However, the previously reported transition at 274 keV was not strongly observed; it cannot be due to decay of the same isomer as that producing the 500- and 1002-keV transitions. Other fairly strong transitions with half-lives consistent with the high-spin isomer were located at 146, 362, 601, 845, and 1110 keV. The 362-keV transition was previously assigned to the low-spin isomer, but the

remainder of these and about five weaker transitions were not reported. Our preliminary analysis also reveals a very strong transition at 1034 keV with a half-life of 5.4 ± 0.3 min, which is consistent with the half-life of the low-spin isomer in ^{199}Po reported previously.[3] However, nine other transitions reported previously as following the decay of the low-spin isomer were not present in the present spectra, although judging by the 1034-keV transition, they should be easily measured. We conclude that either the other transitions were not due to the decay of a ^{199}Po isomer or that the 1034-keV transition is due to the high-spin isomer. The somewhat different half-life for the strong 1002- and 1034-keV transitions favors the first of these possibilities. A thorough analysis of the γ-γ coincidence data will perhaps shed new light on these discrepancies. We still wish to measure the conversion electron coefficients in order to determine multipolarities and possible spins. Interpretation of the level scheme in terms of particle core coupling, including Coriolis mixing, will be attempted.

1. University of Tennessee, Knoxville
2. Georgia Institute of Technology, Atlanta
3. A. Korman et al., *Acta Phys. Pol. B* 7, 141 (1976).

PARTICLE AND HOLE STRUCTURES IN ^{193,195,197}Tl

L. L. Riedinger[1] G. D. O'Kelley[2]
L. L. Collins[1] J. L. Wood[3]
C. R. Bingham[1] M. S. Rapaport[1]
R. W. Fink[1]

During the past year, extensive measurements have been performed on the decay of 45-min ^{197}Pb to thallium through the use of the UNISOR facility, and previously initiated ^{193,195}Pb experiments have been completed. The A = 197 measurements have been crucial in elucidating the trends suggested by the lighter nuclei. The $i_{13/2}$ isomer in ^{197}Pb populates 23 levels which cascade into the $h_{9/2}$ state in thallium and 12 other levels which feed the $h_{11/2}$ level. In addition, its 19% isomeric branch to the low-spin ground state of ^{197}Pb results in the observation of 22 low-spin levels in thallium, many more than those seen in the A = 193 and 195 cases.

In all these isotopes, the difference between the particle and hole states is striking. In ^{197}Tl, 12 levels, all at least 616 keV above the $h_{11/2}$ excitation, feed only the $h_{11/2}$ state. The absence of band structure is indicative of the fact that the $h_{11/2}$ level is actually a hole state coupled to the rather spherical ^{198}Pb core (E_{2^+} = 1063 keV). Some of these 12 levels undoubtedly result from the weak coupling of the $h_{11/2}$ hole to the 2$^+$ of ^{198}Pb, but others may be due to couplings of other hole states to higher lying states in ^{198}Pb. The fact that these 12 high-spin levels evidently do not decay to the high-spin states built in the $h_{9/2}$ particle excitation is indicative of this great difference in the cores for particle and hole states.

The core for the $h_{9/2}$ level is a slightly oblate mercury core, and consequently a quasi-rotational band results. The non-yrast members of this structure are quite sensitive to core triaxiality. Figure 2.53 displays the trend of these $h_{9/2}$ levels in ^{193,195,197}Tl and a comparison with a Meyer-ter-Vehn triaxial rotor calculation. The second $\frac{9}{2}^-$ is readily explained as the coupling of the $h_{9/2}$ particle with the second (triaxial) 2$^+$ state of the core. Candidates for the $\frac{7}{2}^-$ band (opposite coupling of $h_{9/2}$ and second 2$^+$) exist close to the predicted values for γ = 38°. Another band of levels is seen at least partially in all three nuclei. The calculation of Fig. 2.53 used a large value of λ, the Fermi-surface parameter, to bring the $K = \frac{1}{2}^-$ component of the $h_{9/2}$ structure low enough in energy. A preferred explanation may be that this band results somewhat from the $f_{7/2}$ shell model state, a conclusion verified by a Nilsson calculation for the proper ϵ_2 and ϵ_4 values.

1. University of Tennessee, Knoxville.
2. Chemistry Division.
3. Georgia Institute of Technology, Atlanta.

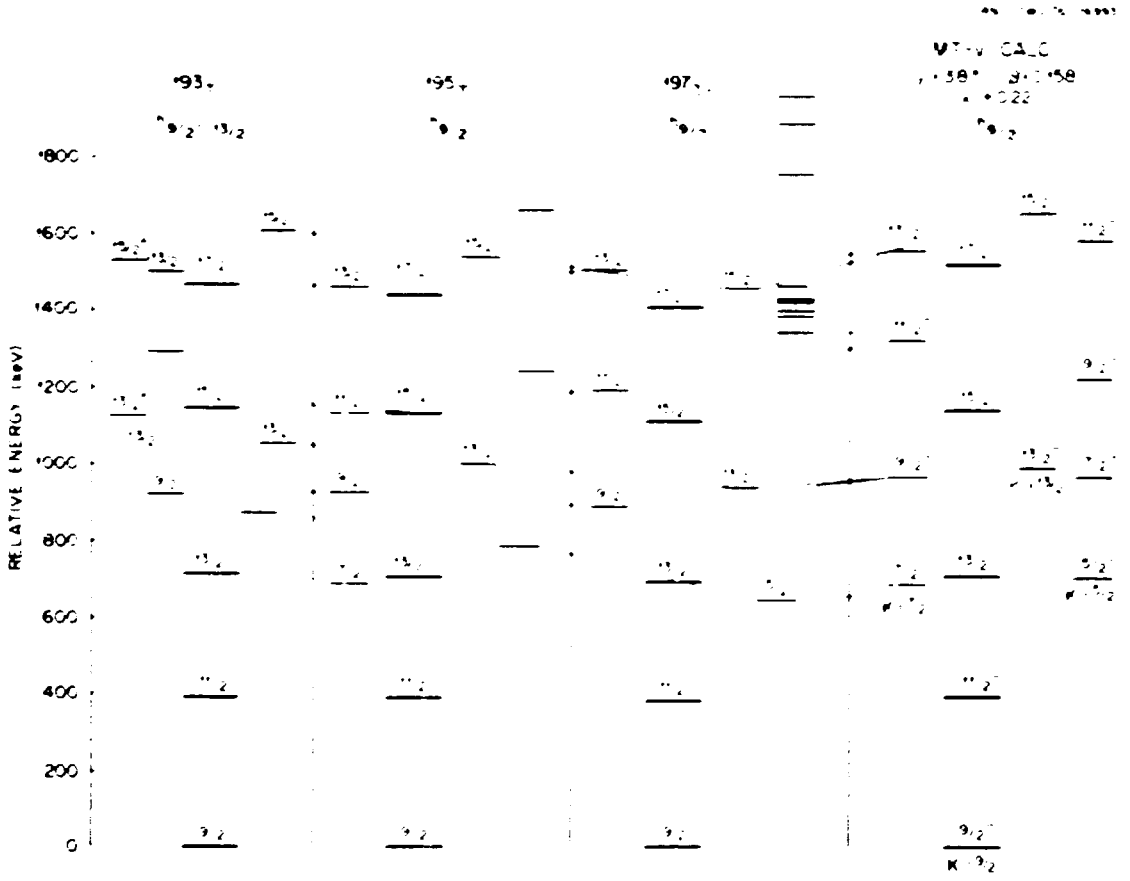

Fig. 2.53. Trend of levels built on the $h_{9/2}$ proton state in ^{193,195,197}Tl and comparison to a Meyer-ter-Vehn triaxial rotor calculation for $\gamma = 38°$.

LEVELS IN ODD-ODD ^{196}Tl

J. A. Vrba[1] C. R. Bingham
L. L. Riedinger E. L. Robinson[2]
B. O. Hannah[3]

In the past few years, much effort at UNISOR has been expended in studying the behavior of single-proton and -neutron states in the Au-Hg-Tl region. Much has been learned about the positions of these shell-model states, and now is the time to look into the couplings of these various orbitals to form states in odd-odd gold and thallium nuclei. Theorists are becoming interested in rotational bands in these nuclei at high spins, but a knowledge of the low-energy low-spin states will be necessary for the interpretation of (HI,xn) data on high-spin states. We have studied the decay of 37-min ^{196}Pb at the UNISOR facility; gamma-ray data (singles and coincidence) and conversion-electron data were accumulated as the activity was produced by Ref(^{18}O,xn) and (^{16}O,pxn) reactions. The 4.5-min ^{196}Bi activity was also observed, but most of our effort to date has been spent on analyzing the Pb → Tl results. Approximately 49 transitions have been placed in a decay scheme containing 16 levels. The most recent previous work[1] on this activity led to the assignment of the lowest seven states.

Our results on levels in ^{196}Tl are compared in Fig. 2.54 with levels seen in adjacent thallium nuclei. The results on the A = 192 and 194 cases come from other UNISOR measurements by the same group, whereas the A = 198 and 200 experiments were performed by Jung[4] and by Doebler et al.[5] respectively. In spite of the complexity of the individual decay schemes, one can definitely notice systematic trends. In assigning certain proton and neutron couplings to these levels, one must consider the neighboring odd-A nuclei. In ^{195}Tl, the lowest-lying proton states are the $s_{1/2}$ (ground state), $d_{3/2}$, and $h_{9/2}$. The lowest neutron states in ^{195}Hg are the $p_{1/2}$ (ground state), $p_{3/2}$, and $f_{5/2}$,

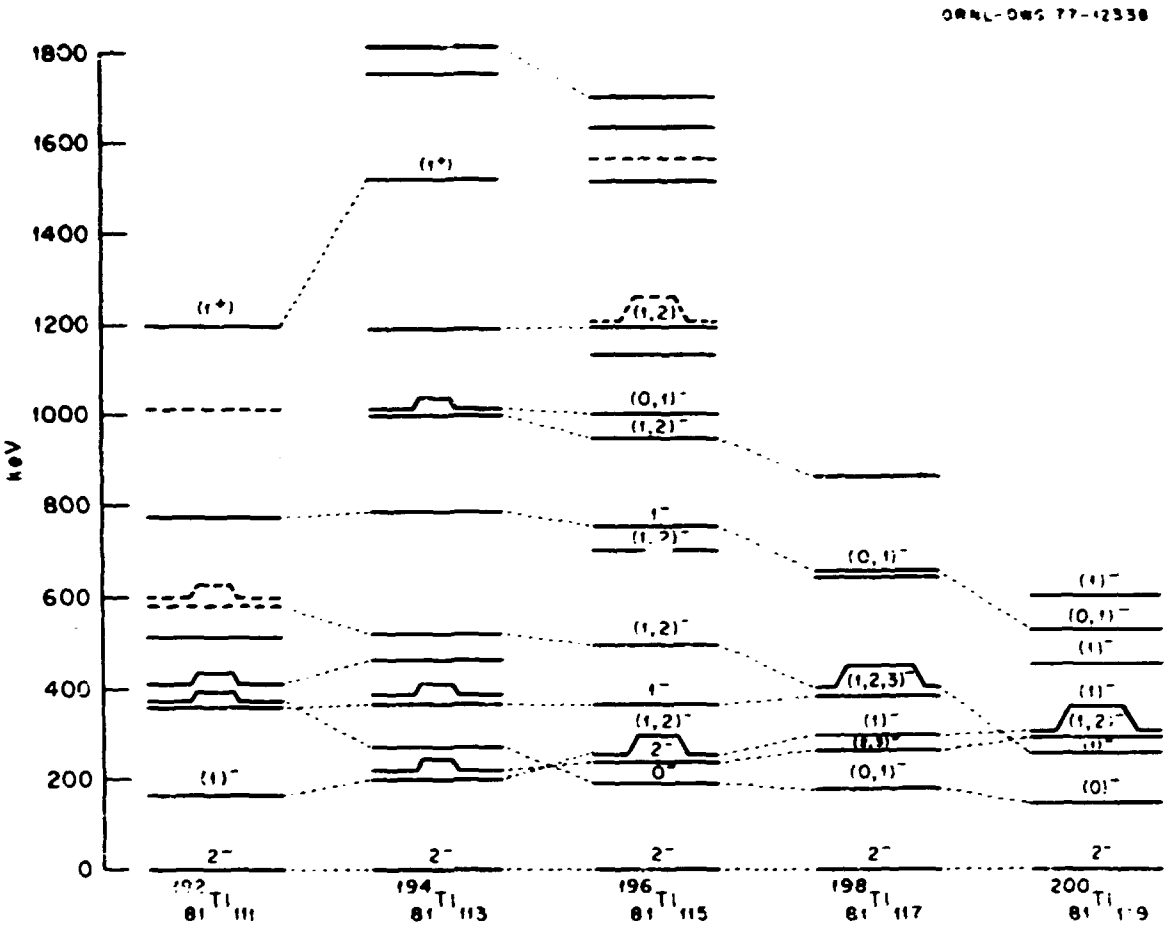

Fig. 2.54. Trends of levels in odd-odd thallium nuclei. The A = 192, 194, 196 results come from UNISOR measurements, while the A = 198 and 200 results come from refs. 4 and 5 respectively.

The 2^- ground state of the even-A thallium isotopes likely results from the (p,n) coupling of $(s_{1/2},p_{3/2})$. The 1^- state resulting from the other coupling of these orbitals is probably the fourth excited level at 366 keV in ^{196}Tl, since, in the other even-A thallium nuclei, it maintains a rather constant energy relative to the ground state. The low-lying 0^- state rises with decreasing neutron number and seems to be associated with the $(s_{1/2},p_{1/2})$ configuration, since the $p_{1/2}$ proton orbital similarly increases relative to the $p_{3/2}$ state in odd-A thallium nuclei. The rising fifth excited state at 494 keV in ^{196}Tl may be the 1^- coupling of these states. A 1^- level in ^{196}Tl at 775 keV seems also to be associated with levels rising with decreasing neutron number, as is the state at 953 keV. These are possibly different couplings of the $(d_{3/2},p_{1/2})$ configuration, in view of the trend of the $p_{1/2}$ state in odd-A thallium nuclei. A possible 1^+ state is seen in ^{192,194}Tl and has been tentatively assigned to the $(h_{11/2},h_{9/2})$ coupling. A search of our data for high-energy $E1^+$ transitions has been unsuccessful so far, indicating that this 1^+ level has probably moved to a higher energy in ^{196}Tl and thus receives little population in the decay of the parent. Work is continuing on interpretation of these levels and trends.

---

1. University of Tennessee, Knoxville.
2. University of Alabama, Birmingham.

3. J. Svedberg and B. Jung, *Ark. Fys.* 19, 441 (1961).
4. B. Jung, *Nucl. Phys.* 10, 440 (1959).
5. R. E. Doebler, W. C. McHarris, and W. H. Kelly, *Phys. Rev. C* 2, 2422 (1970).

POSITRON MEASUREMENTS

J. L. Weil B. D. Kern[1]

Positron measurements on mass-separated sources from the UNISOR facility have been made on the A = 186, 187, and 188 chains (starting with thallium) produced by $^{180}W + ^{14}N$. Lifetime and endpoint energy determinations have been made for the A = 186 chain on-line, for the A = 187 chain both on-line and off-line, and for the A = 188 chain off-line with the inclusion of β^+-γ coincidence spectra. High-energy positrons of approximately 6 MeV energy have been observed in the decay of ^{186}Tl, in agreement with mass-table predictions. The study of these chains is being continued. Analysis of similar data on the A = 190, 191, and 193 chains is in progress.

1 Department of Physics, University of Kentucky, Lexington

FURTHER STUDY OF ^{186}Tl ALPHA DECAY

M. A. Ijaz[1] H. K. Carter[2]
C. R. Bingham[3] E. L. Robinson[4]
K. S. Toth

In the previous annual progress report,[5] it was stated that 28-sec ^{186}Tl had an alpha branching ratio of $(6 \pm 2) \times 10^{-4}$ and an alpha decay energy of 5.641 ± 0.010 MeV. The nuclide had been produced in a $^{180}W(^{14}N,10n)$ reaction, and, following mass separation at the UNISOR facility, its decay properties were investigated with alpha-particle and gamma- and x-ray detectors. The presence of ^{186}Tl was established by the gamma-ray measurements, its electron-capture decay to ^{186}Hg being well characterized.[6] In addition to the ^{186}Hg alpha group,[7] the alpha-particle spectra contained a doublet with about 12 keV separating the components. The higher-energy portion, 5.653 MeV, was known[8] to be 48-sec ^{185}Hg. Its alpha decay branch is more than 300 times greater than that of ^{186}Hg; its appearance in the A = 186 spectra was apparently due to a small amount of cross contamination as a result of an excursion of the mass separator. The lower-energy part of the doublet seemed to decay with a half-life somewhat shorter than 48 sec and was assigned to ^{185}Tl.

A ^{180}W target (enriched to 92.6%) recently became available to us. Because of the confusing structure of the doublet peak, we decided to repeat the experiment by producing ^{186}Tl in the $^{180}W(^{14}N,8n)$ reaction. This production mode was expected to improve the yield of ^{186}Tl with respect to neighboring products involving charged-particle evaporation from the compound system. Indeed, we found in the new gamma-ray measurements that the ^{186}Tl yield had increased by a factor of 3 from the previous experiment, while that of ^{185}Hg had remained the same. From the previously mentioned alpha branch, we should have observed 70 alpha-particle counts due to ^{186}Tl in the first 30 sec of counting. Instead, only seven counts were seen around the energy region of the doublet. Therefore, the 5.641-MeV peak cannot be due to ^{186}Tl alpha decay. While the nature of the doublet originally observed at about 5.65 MeV is not understood at this time, it would appear to be connected with the decay of ^{185}Hg. [In the present experiment, the marked decrease of the number of counts in that energy region is explained in terms of the improvement of the $(^{14}N,xn)$ vs $(^{14}N,pxn)$ yields.]

Scattered counts clustered around 5.76 MeV were observed to decrease in number with a half-life of >20 sec. The energy is close to the value of 5.765 MeV assigned to ^{186}Tl by Bourgeois et al., whose unpublished data are listed in a recent compilation.[9] If this assignment is correct, then the alpha branching ratio of ^{186}Tl is about a factor of 10 less than the value of 6×10^{-4} reported earlier.[5]

1 Virginia Polytechnic Institute and State University, Blacksburg.
2. University of Tennessee, Knoxville.
3. UNISOR, Oak Ridge, Tenn.
4. University of Alabama at Birmingham.

5. K. S. Toth et al., *Phys. Div. Annu. Prog. Rep. Dec. 31, 1975*, ORNL-5137, p. 20.
6. J. H. Hamilton et al., *Phys. Rev. Lett.* 35, 562 (1975).
7. P. G. Hansen et al., *Nucl. Phys. A* 148, 249 (1970).
8. H. Gauvin et al., *Ann. Phys.* 9(5), 241 (1975).

DECAY OF ^{184}Hg TO ^{184}Au

W. G. Nettles[1] J. H. Hamilton[1]
R. Beraud[1] A. V. Ramayya[1]
J. D. Cole[1] E. H. Spejewski[2]
K. S. R. Sastry[3]

The levels in ^{184}Au have been investigated by electron and gamma multiscale and electron-gamma-time and gamma-gamma-time coincidence studies of the decay of ^{184}Hg mass separated on-line at UNISOR. The ^{184}Hg mass chain was entered at mercury and thallium in bombarding ^{180}W with ^{14}N. No previous levels have been assigned in ^{184}Au. We have established eight definite levels and two tentative levels, as shown in Fig. 2.55.

The lifetimes of several levels were extracted from the e-gamma-t and gamma-gamma-t data. By pulling gates on the 156.2- and 236.2-keV transitions and building the time spectra, we established that the 156.2-keV transition follows the one at 236.2-keV. The 156.0-keV-level half-life is 36 ± 6 nsec (Fig. 2.56), which is consistent with an $E2$ transition. For four of the next five levels, $T_{1/2} \leq 2$ nsec to indicate dipole depopulation.

Faessler and his collaborators are following up their work on even-even nuclei[4] in this region to calculate the properties of the odd-odd nuclei.[5] The levels in ^{184}Au provide a sensitive test in comparison to gold nuclei with $A \geq 194$ because the large change in neutron number brings in different orbitals. Further information on spins and parities in ^{184}Au is needed to test their calculations.

1 Vanderbilt University, Nashville, Tenn.
2 UNISOR, Oak Ridge, Tenn.
3 University of Massachusetts, Amherst.
4 H. Toki et al., *Nucl. Phys.* A279, 1 (1977).
5 A. Faessler, private communication, April 1977.

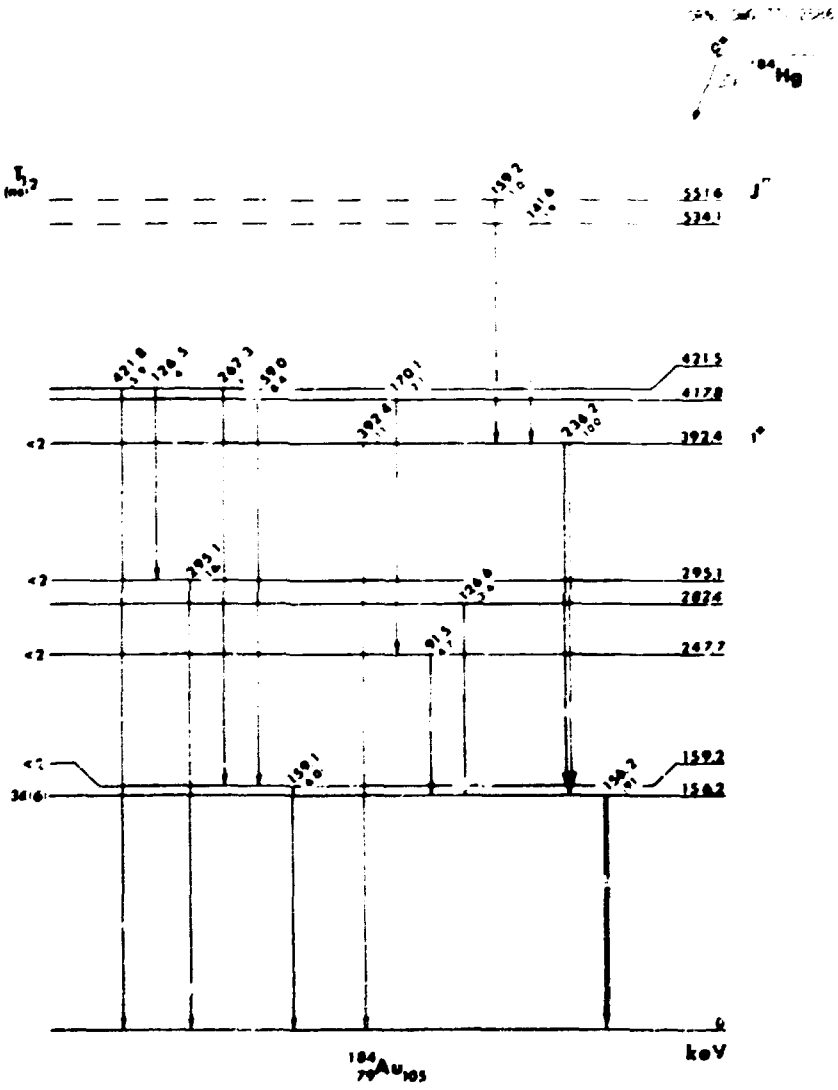

Fig. 2.55. Levels in ^{184}Au populated in the decay of ^{184}Hg.

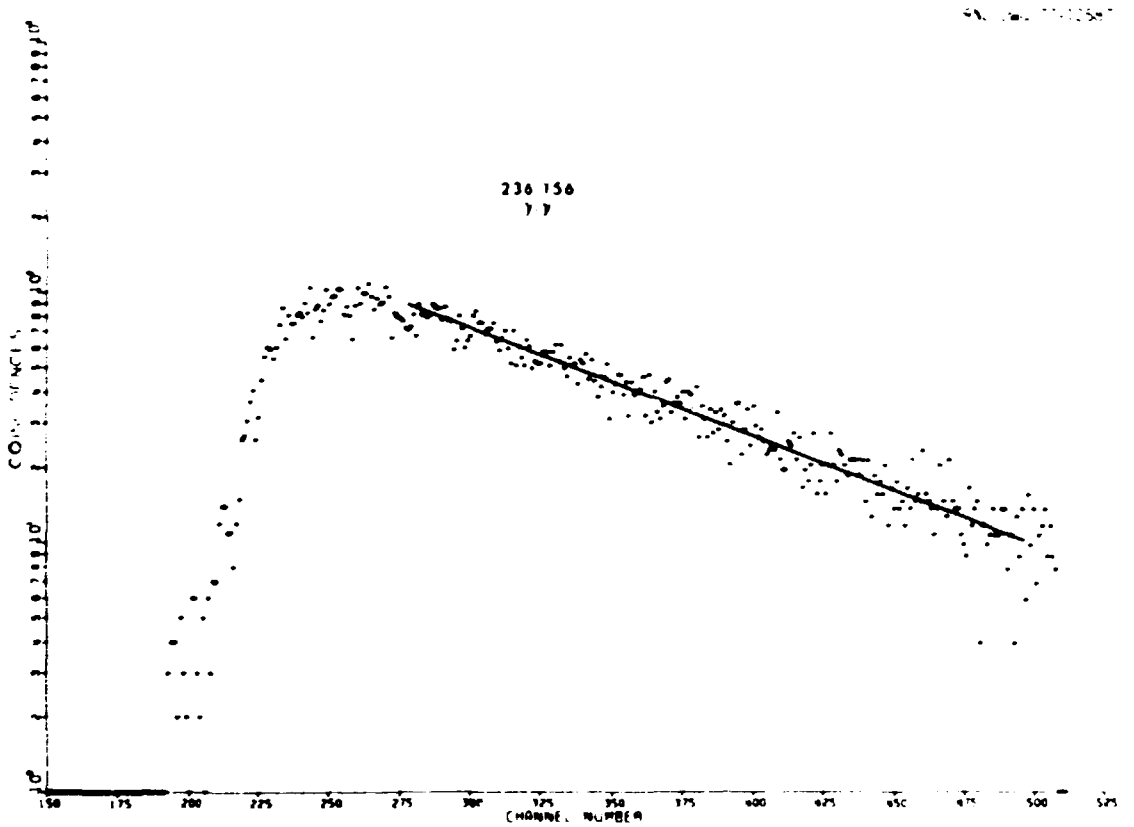

Fig. 2.56. Gamma-gamma time spectrum starting with the 236-keV gamma ray.

BEHAVIOR OF THE EXCITED DEFORMED BAND AND SEARCH FOR SHAPE ISOMERISM IN ^{184}Hg

J. D. Cole[1] K. S. Toth
J. H. Hamilton[1] E. L. Robinson[4]
A. V. Ramayya[1] K. S. R. Sastry[5]
W. G. Nettles[1] J. Lin[1]
H. Kawakami[1] F. T. Avignone[5]
E. H. Spejewski[1] W. H. Brantley[5]
M. A. Ijaz[1] P. V. G. Rao[6]

In a recent letter,[10] we reported the coexistence and crossing of two bands of states, one built on a near spherical and one on a deformed shape in both ^{186,188}Hg. Recent theoretical calculations[11-13] predict that the deformed band will continue to drop in ^{184}Hg. The large change in the radii of ^{187,185}Hg as compared with ^{187}Hg (ref. 14) is presently explained by these calculations.[11-13] A continued drop in energy of the deformed band predicted for ^{184}Hg must occur if this explanation is correct. Equally important, Kolb and Wong[11] have pointed out that the ground-state properties in this transitional region depend sensitively on the single-particle spectra, and this is why earlier calculations[15,16] have incorrectly predicted permanent large deformations in ^{184}Hg and ^{186}Hg. Conversely, Kolb and Wong[11] emphasize that these mercury nuclei provide a good probe of the single-particle spectrum in the deformed region. Dickmann and Dietrich[11] predict that the 0^+ deformed band heads in ^{186,188}Hg should be shape isomers. They predict that the $E2$ decay of 0^+ deformed band heads to the first excited 2^+ states, considered to be a mixture of near spherical and deformed states, will be hindered so that these 0^+ states will be shape isomers with roughly 10 to 20 nsec mean lives in ^{186,184}Hg.

To test these theoretical ideas, we identified (at the UNISOR facility) the new isotope ^{188}Tl, which was produced by bombarding an isotopically enriched target of ^{180}W with ^{14}N ions of 177 MeV. Multiscale alpha, gamma, and conversion-electron singles, and e-gamma and gamma-gamma coincidences were carried out on-line for the 184 mass chain. There is

beta decay to the 8⁺ yrast level, but the dominant decay is to the first 2⁺ level. The 8 → 6, 6 → 4, 4 → 2, and 2 → 0 transitions, alpha, and electron spectra all have 11 ± 1 sec half-lives within limits of error. Thus, either the high- and low-spin isomers of ^{184}Tl have similar half-lives or there is unobserved isomeric feeding between them. Our e-gamma coincidence and singles data established a 0⁺ level at 375 keV, in good agreement with the energy predicted from fitting the 10⁺, 8⁺, and 6⁺ energies[7] to a rotational energy formula. The band structure of ^{184}Hg is compared with the heavier mercury nuclei in Fig. 2.57.

The energy extracted for the deformed 2⁺ state from the rotational formula on the basis of other band members is very near the nearly constant energy of the 2⁺ spherical states in ^{186}⁻^{190}Hg (Fig. 2.57). These two 2⁺ states are strongly mixed in the theoretical calculations[11,13] so that one could be pushed up and the other down. Such mixings[11,13] can explain the observed branching ratios from both 4⁺ states. In summary, the energies of these new 0⁺ and 2⁺ members of the deformed band are in very good agreement with the theoretical calculations[11,13] and substantiate the predicted drop in deformed-band-head energy in ^{184}Hg. The systematic behavior of the near-spherical and deformed bands shown in Fig. 2.57 confirm the more recent theoretical calculations[11,13], including the details of the energy spacings and branching ratios.[13]

Other than the yrast cascade and the 0⁺, 2⁺, and tentative 4⁺ levels discussed above, only one other level is established by coincidence data at 983 keV. The 983-keV level decays predominantly to the 0⁺ 375-keV level, with the (2 → 0) / (2 → 2) gamma-ray branching ratio nearly equal to 1.3. (An impurity line prevents a precise determination.) The 608.3-keV transition is the strongest line in the gate on the *K* line of the 375.2-keV transition, and no such high-energy decays to the 0⁺ band heads were observed in the ^{186,188}Tl decays.[10] The 983-keV level is in the energy range expected for a two-phonon-type 2⁺ state. However, because it strongly decays to the excited 0⁺ state, it is interesting to speculate that this could be a 2⁺ beta- or gamma-type vibrational state built on the deformed band. Because both lower 2⁺ states have strong deformed components, decays to these levels would also be expected.

Now look at the predicted shape isomerism[11] of the 0⁺ band heads. Figure 2.58 is a plot of the delayed coincidences between the *K* electrons of the 375-keV *E0* transitions and gamma rays (primarily 511 annihilation radiation and 608-keV gamma rays,

Fig. 2.57. Systematics of the deformed and near-spherical bands in light-mass mercury isotopes. Source: J. D. Cole et al., "Behavior of the Excited Deformed Band and Search for Shape Isomerism in ^{184}Hg," *Phys. Rev. Lett.* 37, 1185 (1976). Used by permission of the American Physical Society.

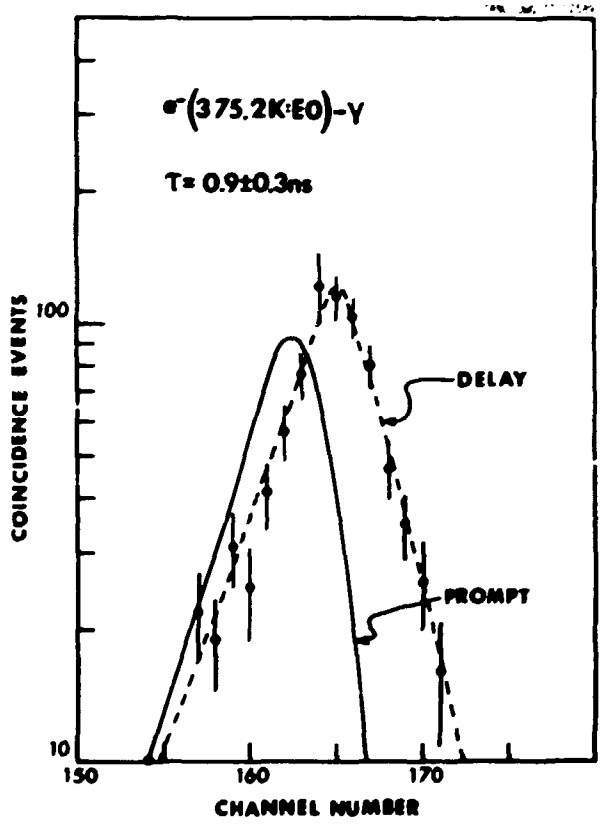

Fig. 2.58. Delayed coincidences of *K* electrons of the 375-keV *E0* transition with gamma rays. The prompt curve is also shown. Source: J. D. Cole et al., "Behavior of the Excited Deformed Band and Search for Shape Isomerism in ^{184}Hg," *Phys. Rev. Lett.* 37, 1185 (1976). Used by permission of the American Physical Society.

with x rays excluded). The centroid-shift method yielded a mean life of 0.9 ± 0.3 nsec, which is an order of magnitude shorter than predicted. The prediction, however, was based on the $E2$ strength, which is probably negligible for the 8-keV transition in ^{186}Hg. Our data show the importance of the neglected $E0$ mode in ^{186}Hg, where the deformed and near-spherical states are weakly mixed, according to Kolb and Wong.[13] In any prediction of lifetimes of shape isomers, this mode must be considered. There is still the question of hindrance of the $E0$ mode. Unfortunately, there are no accurate measurements of 0^+ state lifetimes in this region. For essentially no decay via an 8-keV transition, we extract from τ a monopole matrix element $\rho = 0.07^{+}_{-}$. This ρ is a factor of 5 smaller than those observed from 0^+ beta-type vibrational states in deformed rare-earth nuclei. While these beta vibrational states are in a different region, the differences in ρ are suggestive that retardation for a shape isomer has occurred as expected. The monopole strength in a coexistence model must be calculated before predictions of shape isomerism really can be tested. Indeed, these 0^+ states provide sensitive tests of future calculations.

---

1. Vanderbilt University, Nashville, Tenn.
2. UNISOR, Oak Ridge, Tenn.
3. Virginia Polytechnic Institute and State University, Blacksburg.
4. University of Alabama at Birmingham.
5. University of Massachusetts, Amherst.
6. Tennessee Technological University, Cookeville.
7. University of South Carolina, Columbia.
8. Furman University, Greenville, S.C.
9. Emory University, Atlanta, Ga.
10. J. H. Hamilton et al., *Phys. Rev. Lett.* **35**, 562 (1975).
11. F. Dickman and K. Dietrich, *Z. Phys.* **271**, 417 (1974).
12. S. Frauendorf and V. V. Pashkevich, *Phys. Lett.* **55B**, 365 (1975).
13. D. Kolb and C. Y. Wong, *Nucl. Phys.* **A245**, 205 (1975).
14. J. Bonn, G. Hubert, H. Kluge, and E. W. Otten, *Phys. Lett.* **38B**, 308 (1972).
15. A. Faessler et al., *Phys. Lett.* **39B**, 579 (1972).
16. M. Cailliau et al., *Phys. Lett.* **46B**, 11 (1973).
17. N. Rud et al., *Phys. Rev. Lett.* **31**, 1421 (1973).

ALPHA-DECAY PROPERTIES OF THE NEW ISOTOPES ^{184}Tl AND ^{185}Tl, AND SEARCH FOR THE ALPHA EMITTERS ^{182}Tl AND ^{183}Tl

K. S. Toth[1] J. Lin[1]
M. A. Ijaz[1] E. L. Robinson[4]
C. R. Bingham[2] H. K. Carter[5]

^{184}Tl and ^{185}Tl

A preliminary search for the alpha-decay properties of the unknown isotopes ^{184}Tl and ^{185}Tl was reported previously. The attempt was made by bombarding ^{nat}W with 180-MeV ^{14}N ions. While this incident energy is the maximum ^{14}N^{5+} beam attainable at the ORIC, it is below the expected maxima of the (^{14}N, 11n) and (^{14}N, 12n) excitation functions. The alpha spectra of the mass-separated sources showed the presence of small amounts of ^{186}Hg and ^{185}Hg at A = 185 and 184 respectively. Extremely weak new alpha groups were also seen at these mass numbers, but their nuclidic assignments could not be established.

Therefore, the indications were that the production of these nuclei would necessitate the use of a ^{186}W target. This isotope comprises only 0.13% of natural tungsten. It is available enriched to 92.6%, but only in the form of WO$_3$. The cost of manufacturing a self-supporting metallic foil for use in the UNISOR-integrated target-ion source was prohibitive. The powdered oxide was therefore used as follows. It was first pressed into a graphite felt cloth and then bombarded with an electron beam. The heating converted the oxide to the metal, which then bonded to the graphite and, in this manner, could be used in the ion source.

As before, the target was irradiated with ^{14}N ions. After separation, products with a given mass number were extracted from the focal plane of the separator to a tape transport system. Following a suitable collection interval, the radioactive sample was automatically moved to a counting station where alpha-particle and gamma- and x-ray measurements could be made simultaneously. The absolute efficiencies of the three detectors used were determined by calibrating them with standard sources of known strengths.

The alpha spectra measured at A = 185 and 184 are shown in Fig. 2.59. An alpha group, 5975 ± 5 keV with a half-life of 1.7 ± 0.2 sec, was assigned to ^{185}Tl. At A = 184, two alpha groups, 6162 ± 5 and 5988 ± 5 keV, were found to decay with the same 10 ± 2 sec half-life and were assigned to ^{184}Tl. Several weak alpha-particle peaks (labeled by question marks) are unassigned because their half-lives could not be determined.

In the A = 184 gamma-ray spectra, the $8^+ \rightarrow 6^+$, $6^+ \rightarrow 4^+$, $4^+ \rightarrow 2^+$, and $2^+ \rightarrow 0^+$ ^{184}Hg transitions (earlier observed in an in-beam investigation[14]) were found to decay with a half-life of 11 ± 2 sec, in agreement with those measured for the ^{184}Tl alpha groups. The $2^+ \rightarrow 0^+$ 367-keV ^{184}Hg transition encompasses essentially all of the ^{184}Tl electron-capture-β^+ decay strength. From its intensity and by summing the intensities of the 5.99- and 6.16-MeV alpha peaks, we deduce the ^{184}Tl alpha-decay branch to be (2.1 ± 0.7) × 10^{-2}. The

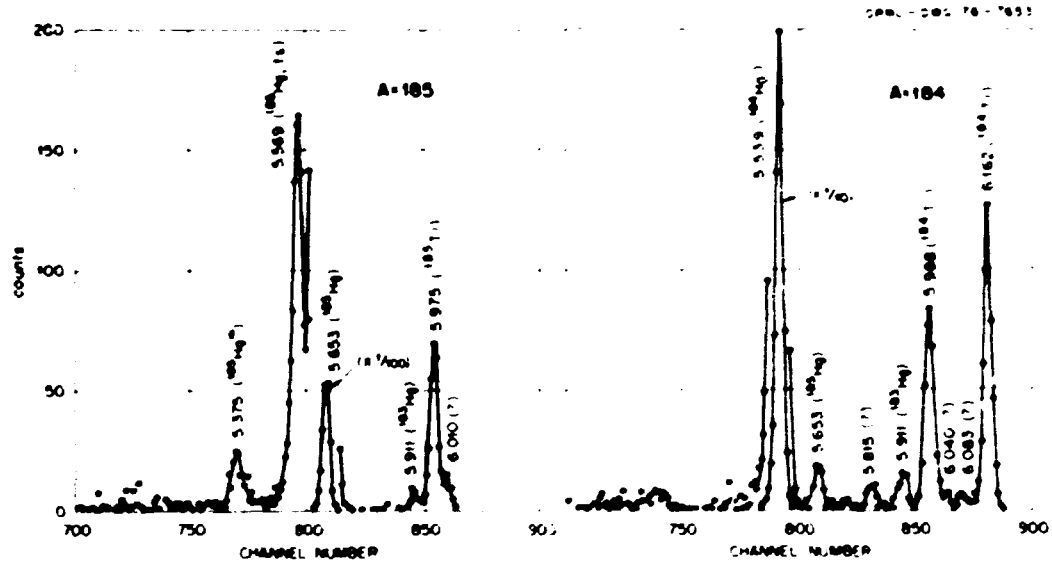

Fig. 2.59. Alpha-particle spectra measured in ^{14}N bombardments of ^{180}W for masses of 185 and 184. Energies shown above the various peaks are in units of MeV. The 5.97-MeV alpha-group seen at $A = 185$ is assigned to the new isotope ^{185}Tl. At $A = 184$ two alpha-groups, 5.99 and 6.16 MeV, are assigned to the new ^{184}Tl isotope because they decay with the same half-life. Several weak alpha-groups labeled by question marks are unassigned.

electron-capture β^+ decay scheme of ^{185}Tl is not well understood at this time, and no attempt was made to deduce its branching ratio.

The identification of the new isotope ^{184}Tl has provided the basis for the study of its electron-capture β^+ decay scheme; this parallel investigation[7] has found the 0^+ band head of a strongly deformed rotational band to lie at 375 keV. This represents a steady drop in the excitation energy of the band head as one goes from ^{186}Hg to ^{184}Hg, which is in agreement with theoretical predictions.[9]

The discovery of ^{185}Tl now permits the investigation of its electron-capture β^+ decay. Establishment of a ground-state rotational band in ^{185}Hg would provide direct evidence that this nucleus is deformed in its ground state. Such a deformation is the generally accepted explanation of the sudden increase[10] in the charge radius at ^{185}Hg, but this explanation has not been verified.

Search for ^{182}Tl and ^{183}Tl

From the known alpha-decay properties of $^{184,185}Tl$, one would predict that $^{182,183}Tl$ should have large alpha branches. Thus, despite the fact that the beam energy would once again be below the peaks of the $(^{14}N, 11n)$ and $(^{14}N, 12n)$ excitation functions, the hope was that this could be compensated for by the increase in the branching ratios.

The half-lives of these isotopes are expected to be less than 1 sec, while the transit time of the UNISOR collection tape system is about 0.5 sec. Therefore the following technique was developed. A Si(Au) alpha detector was placed so that the source could be moved from the deposition point in front of the detector in 50 msec. The time of arrival of each alpha event and the digitized pulse height were stored in list-mode fashion on magnetic tape. The data could then be used to build alpha-particle spectra as a function of time or time spectra for a given alpha group.

Approximately 8 hr of bombardment time was utilized to collect data at each mass number. A small amount of ^{182}Hg and ^{183}Hg alpha activity was observed; no new alpha groups were seen. We conclude that the production cross sections for ^{182}Tl and ^{183}Tl are extremely low and/or their half-lives are short as compared with the holdup time in the separator ion source.

---

1. Virginia Polytechnic Institute and State University, Blacksburg.
2. University of Tennessee, Knoxville.
3. Tennessee Technological University, Cookeville.
4. University of Alabama at Birmingham.
5. UNISOR, Oak Ridge, Tenn.
6. K. S. Toth et al., "On-Line Mass Separator Studies of Thallium and Mercury Alpha Emitters with $A \geq 186$," *Phys. Div. Annu. Prog. Rep. Dec. 31, 1975*, (1976), p. 20.

7. N. Rud et al., *Phys. Rev. Lett.* 31, 1421 (1973).
8. J. D. Cole et al., *Phys. Rev. Lett.* 37, 1185 (1976).
9. S. Frauendorf and V. V. Pashkevich, *Phys. Lett.* 55B, 365 (1975).
10. T. Bengtsson et al., *Phys. Lett.* 38B, 383 (1972).

DECAY OF HOLMIUM ISOTOPES TO LEVELS IN DYSPROSIUM NUCLEI NEAR THE $N = 82$ CLOSED SHELL

K. S. Toth M. A. Ijaz
C. R. Bingham P. Singh
H. K. Carter D. Sousa

This report deals with an extension of what has been a systematic study of low-lying states in nuclei near the $N = 82$ closed shell. One assumes that these states can thus be described in terms of the single-particle model. Our earlier work had stopped at terbium ($Z = 65$); we are now in the process of looking at dysprosium nuclei ($Z = 66$). Earlier,[1] the decay of ^{151}Dy[2] ($N = 81$) was investigated, and the excitation energies of the $\nu s_{1/2}$, $\nu d_{3/2}$, and $\nu h_{11/2}$ single-neutron states in ^{151}Dy were determined. The main motivation of the present study is the investigation of levels in ^{153}Dy, a nucleus that has 83 neutrons, so that its states should be describable by neutron orbitals beyond the $N = 82$ shell. Levels in ^{153}Dy have recently[3] been studied by the in-beam technique; our investigation was intended to complement these data via the decay of ^{153}Ho. This isotope had not been observed previously. We felt that the decay of ^{153}Ho (looked at only briefly by Bowman et al.[4]) should also be studied before launching into a search for ^{152}Ho.

Holmium isotopes were produced by bombarding ^{144}Sm with ^{11}B ions to form the compound system ^{155}Ho. Two bombarding energies were selected on the basis of statistical model calculations, that is, 60 and 75 MeV to peak on the ^{144}Sm(^{11}B,4n) and ^{144}Sm(^{11}B,5n) excitation functions.

The technique involves the use of a gas-jet system where products recoiling out of the thin target are stopped in helium gas. The products are then transported through a 10-m capillary to a shielded area for gamma-ray measurements. The recoils are collected on a tape attached to an automated system. The radioactive recoils are collected for a preset time and then moved in front of Ge(Li) detectors, where counting begins while a new source of activity is collected. Coincidence and singles gamma-ray measurements are made simultaneously.

^{153}Ho

At the 60-MeV bombarding energy, a 527.1-keV gamma ray was observed. Because of its half-life and because it was not seen at 75 MeV, we believe that it represents the electron-capture decay of 36-sec ^{153}Ho, the (^{11}C,3n) product. Until now, only its alpha-decay properties have been studied.[5] From those studies it is known that this 36-sec activity represents a high-spin species due to the $h_{11/2}$ proton orbital. The fact that only one gamma ray has been identified at this time is consistent with the decay properties of the high-spin isomer in ^{151}Tb, the isotone of ^{153}Ho. In that instance, a 796.0-keV gamma ray represents[2] essentially all of the beta-decay strength. This gamma ray follows an allowed (log ft = 4.2) beta transition corresponding to a change of an $h_{11/2}$ proton orbital in ^{151}Tb to an $h_{9/2}$ neutron state located at 796.0 keV in ^{151}Gd. Therefore, we propose that the new gamma ray observed in the present study establishes the location of the $h_{9/2}$ neutron state in ^{153}Dy to be at 527.1 keV.

^{150}Ho

As in the previous work[4] on ^{150}Ho decay, four strong gamma rays (394.2, 551.1, 653.4, and 803.4 keV) were observed in coincidence with one another. With the exception of the 394.2-keV gamma ray, these transition energies agree with those measured earlier.[4] The half-life of ^{150}Ho, however, was determined to be 30 ± 2 sec rather than about 20 sec as reported by Bowman et al.

The four transitions are placed in a ^{150}Dy level scheme, as shown in Fig. 2.60. The scheme is based primarily on analogies with neighboring even-even nuclei, particularly ^{148}Gd, the isotone of ^{150}Dy. The level scheme[6] of ^{148}Gd as populated in the decay of the ^{148}Tb high-spin isomer is also included in Fig. 2.60. Again, four strong transitions are seen in coincidence. In this instance, there are several in-beam studies that corroborate the ^{148}Gd level scheme. The proposal is that high-spin isomers in odd-odd nuclei in this mass region result from coupling an $h_{11/2}$ proton to an $f_{7/2}$ neutron, giving rise to a 9$^-$ spin. The isomer decays primarily to an 8$^-$ state in the even-even daughter via an allowed beta transition, the 8$^-$ state arising from the coupling $h_{9/2}$ and $f_{7/2}$ neutrons. The ^{150}Dy cascade is such that the upper three gamma rays are about 85% of the $2^+ \rightarrow 0^+$ transition intensity. In ^{148}Gd the number is more like 95%, with the less intense cascade through the negative parity states

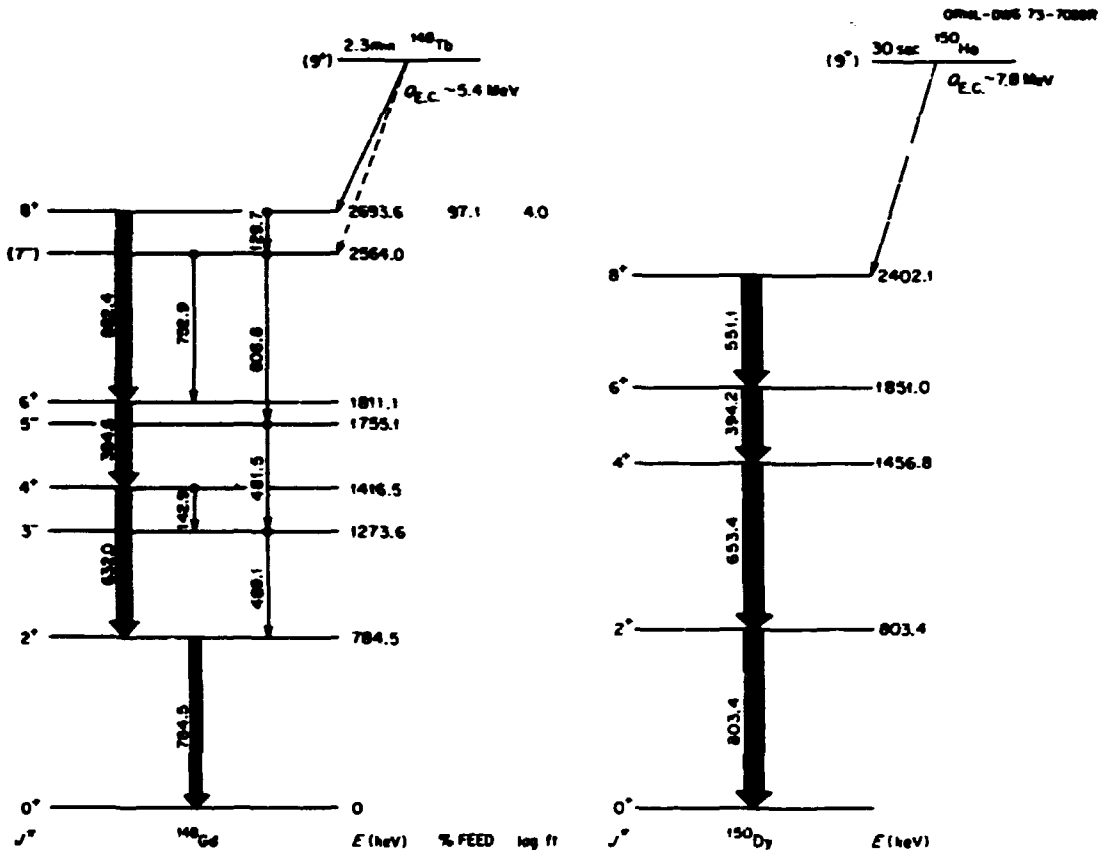

Fig. 2.60. Levels in ^{148}Gd and ^{150}Dy as populated in the decay of the high-spin isomers in ^{148}Tb and ^{150}Ho respectively.

making up the difference. In the ^{150}Ho case, another state(s) in ^{150}Dy is apparently being populated whose de-exciting transitions we have been unable to observe so far.

^{149}Ho

At the 75-MeV incident energy, a gamma ray was observed with an energy of 1090.8 keV and a half-life of about 20 sec. We assign it to the new isotope ^{149}Ho because it is in coincidence with dysprosium K x rays, and its excitation function is similar to those of gamma rays following the decay of ^{149}Dy and ^{149}Tb. In the in-beam study,[6] the most intense gamma ray observed had an energy of 1073 keV and represented the de-excitation of the first excited state to the ground state in ^{149}Dy. A weak gamma ray of that energy was seen in the present study; its half-life, however, could not be determined because of poor counting statistics.

Figure 2.61 shows the systematics of neutron orbitals beyond $N = 82$ for even-Z isotones with 83 neutrons, as extended to ^{149}Dy. According to ref. 6, the $i_{13/2}$ state located at 997 keV in ^{147}Gd has moved up to 1073 keV. Our proposal is that the new isotope represents the $h_{11/2}$ high-spin isomer in ^{149}Ho. The decay of the analogous state in ^{147}Tb populates[10] three levels in ^{147}Gd (see Fig. 2.61) as follows: (1) 1397 keV, $h_{9/2}$ neutron state, 85%; (2) 1798 keV, a fragment of the same orbital, 14%; and (3) 997 keV, $i_{13/2}$ neutron state, 1%. Therefore, we suggest that the 1090-keV transition de-excites the main $h_{9/2}$ neutron state, which has moved down in energy from 1397 to 1090 keV, as one goes from ^{147}Gd to ^{149}Dy. At this time, the other ^{149}Dy $^9/_2^-$ level (at 1798 keV in ^{147}Gd) has not been identified. We also hope to find the $d_{5/2}$ proton state in ^{149}Ho that should populate the $p_{3/2}$ and $f_{5/2}$ neutron states. This low-spin species in ^{147}Tb

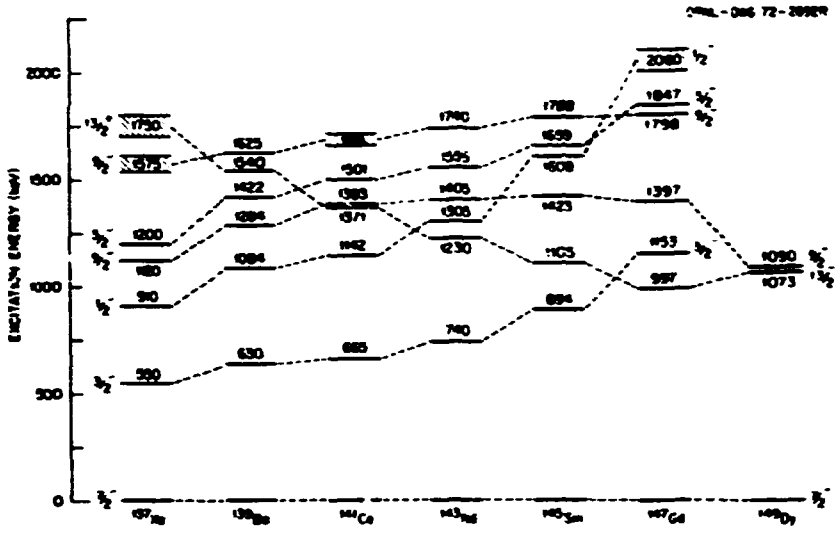

Fig. 2.61. Systematics of single-neutron states in even-Z $N = 83$ isotones. The 1090 $h_{9/2}$ neutron state in ^{149}Dy is populated in the decay of the new isotope, ^{149}Ho.

is known[10] to decay to these ^{147}Gd states located at 1153 and 1847 keV respectively (see Fig. 2.61).

---

1. University of Tennessee, Knoxville.
2. UNISOR, Oak Ridge, Tenn.
3. Virginia Polytechnic Institute and State University, Blacksburg.
4. Eastern Kentucky University, Richmond.
5. K. S. Toth et al., "Excitation Energies of the $h_{11/2}$ and $d_{3/2}$ Neutron States in ^{145}Gd and ^{147}Dy," *Phys. Div. Annu. Prog. Rep. Dec. 31, 1974*, ORNL-5025, p. 51.
6. A. M. Stefanini, P. Kleinheinz and M. R. Maier, *Phys. Lett.* **62B**, 405 (1976).
7. W. W. Bowman, D. R. Haenni, and T. T. Sugihara, Progress Report 1972, Cyclotron Institute, Texas A & M University, p. 30, unpublished.
8. K. S. Toth et al., *Phys. Rev. C* 2, 1480 (1970).
9. K. S. Toth et al., *Phys. Rev. C* 11, 1370 (1975).
10. E. Newman et al., *Phys. Rev. C* 9, 674 (1974).

LIFETIME OF THE FIRST EXCITED 0^+ STATE IN ^{116}Sn

E. P. de Lima[1] A. P de Lima[1]
H. Kawakami[1] W. Dunn[1]
A. V. Ramayya[1] J. H. Hamilton[1]
H. K. Carter[2]

The first excited 0^+ state in ^{116}Sn is only 464 keV above the first 2^+ state at 1293 keV. Studies of the anomolously low 0^+ state in ^{72}Se have led to a picture of the coexistence of near-spherical and deformed shapes,[3,4] with the excited 0^+ state the band head of a deformed band.

We have carried out studies of the lifetime of the 1757-keV 0^+ level in ^{116}Sn to gain further insight into the structure of this level and test for the possible existence of shape coexistence in ^{116}Sn.

The measurement was carried out with two fast plastic scintillators and the UNISOR-Tennelec data acquisition system. The data were stored in the gamma-gamma-time mode. The levels in ^{116}Sn were populated from the decay of 54-min ^{116m}In produced in the Oak Ridge Research Reactor (ORR). Gates were set on Compton edges of transitions into the level of interest and the 1273-keV $2^+ \rightarrow 0^+$ transition to the ground state. The data were analyzed by the best-fit method, and a half-life of 150 ± 50 psec was found for the 0^+ level. Unfortunately, the $E0$ matrix element is unknown. A theoretical calculation has been done for ^{119}Sn. If we use that result, we find the lifetime is essentially that of the $E2$ transition; because the $E2$ conversion coefficient is so small, it is for the $E2$ gamma ray. In Weisskopf single-particle units, there is an enhancement of 5.1. If we use the single-particle formulas[3,4] as used for ^{72,74}Se, where enhancements of 36 ± 7 and 14 ± 2 were found for the $0^{+\prime} \rightarrow 2^+$ transitions, there is essentially no enhancement. Thus, there is less collective strength to the first 2^+ level than in the selenium cases. Recently, a group at the Free University in Amsterdam[5] found a rotational-like band built on this 0^+ state. The 2^+ member, however, is far from the first excited 2^+ level, so these states may not be mixed as found in ^{72}Se, and the $0^{+\prime} \rightarrow 2^+$ transition may not be enhanced as in the

selenium nuclei. The ^{116}Sn case may be closer to a true-shape isomer.

1. Vanderbilt University, Nashville, Tenn.
2. UNISOR, Oak Ridge, Tenn.
3. J. Hamilton, *Phys. Rev. Lett.* 32, 239 (1974).
4. V. Ramayya et al., *Phys. Rev. C* 12, 1360 (1975).
5. L. Peker, private communication, May 1977.

UNISOR DEVELOPMENT

R. L. Mlekodaj[1] J. H. Hamilton[2]
E. H. Spejewski[1] R. A. Braga[3]
A. V. Ramayya[2] E. F. Zganjar[4]
K. S. R. Sastry[3] A. Visvanathan[4]
H. K. Carter[1] E. L. Robinson[1]
F. T. Avignone[4] R. W. Fink[5]

Ion Sources and Targets

The on-line surface-ionization ion source underwent extensive off-line testing. Major design changes led to a source with improved operating characteristics. Several versions of this source are now being used. An all-graphite source is being used for the alkali elements that are easy to surface ionize. This graphite source has yielded very high efficiencies in on-line runs with rubidium and cesium products. The elements more difficult to surface ionize are run in a source with a tantalum body and either a tungsten or rhenium ionizing tip. The operation with stable rare-earth elements is now routine, and on-line tests for rare earths have been planned. These sources are operated with about 1 mg/cm^2 wolfram windows, which have shown excellent stability at ion-source temperatures (≤2600°C) and under heavy-ion bombardment.

A new high-temperature plasma source has been designed and constructed. The high temperature of this source is achieved by an eightfold reduction in the volume, as compared with our Nielsen-type source, while maintaining the same power input. The temperature of the discharge area of this source is estimated to be 2000°C. Efficiencies of 13% have been achieved for stable xenon separations. On-line runs for volatile elements such as mercury have given efficiencies comparable to our Nielsen source, but efficiencies for less volatile elements like lead and bismuth are greatly improved. This new source has also yielded short-lived gold isotopes, which have not been observed coming out of the Nielsen source. This source will also be tested for use with rare-earth products.

Targets of ^{180}W have been fashioned by direct conversion of WO_3 to tungsten by electron-beam heating while supported in the graphite felt matrix. Nearly quantitative conversion has resulted in requiring only a few milligrams of the very expensive ^{180}W (92.6% enriched) to produce these targets. These targets have shown excellent long-term durability in our Nielsen source, but they are gradually destroyed if used in the new high-temperature source.

Experiments with powder targets have been carried out for elements whose melting points are too low to be used directly as targets. Both CeO_2 and ZnO have been tried as powders supported in the graphite felt matrix. The tests indicated that these types of targets will be of limited value because of the evaporation or sublimation of the oxides under the bombardment of the cyclotron beam. This type of target may find limited application under special circumstances when other forms of the target are not possible and when the cyclotron beam current can be limited to the extent necessary to prevent evaporation of the target material.

One problem area for the UNISOR mass separator has been that the target area is at high potential and the incident cyclotron beam is stopped in the ion source, making it difficult to continuously monitor the beam on target. To relieve this situation, a new beam monitor system that allows the cyclotron beam to be continuously monitored has been developed. This monitor is based on secondary electron emission as the beam passes through a thin foil just before striking the target. The secondary electrons emitted from the foil are collected in a positively biased section. This electron current information is then transmitted to ground potential by use of a fiber optical system.

Tape Transport and Data Acquisition Development

Improvements have been made to the tape transport system and data acquisition that will enable new experiments to be carried out at UNISOR, improve the quality of data, and reduce the lower limit of half-life that can be studied. First, changes have been made to the tape transport control system and driving motors, reducing the transport time to the first detector station to 0.2 sec. To reduce the losses incurred in acquiring spectrum multiscale data, additional memory has been added. A total of 32,768 channels of data storage is now available to be used for singles, spectrum multiscaling, or coincidence monitoring. A turbomolecular pumping system has

been installed, replacing the only remaining diffusion pump on the tape transport that enables the use of high-quality cooled-electron detectors.

A scanning Gerholm-lens spectrometer[8] has been installed on the tape transport and has been tested off-line. A special wide-pass baffle and cooled Si(Li) detector were developed to provide an electron spectrometer with an absolute efficiency of greater than 2% and with a transmission-independent energy resolution. The resulting electron spectra are free from gamma-ray interferences and summing peaks. A Ge(Li) detector can view the source position, thus enabling high-quality electron-gamma-ray coincidence data.

A mini-orange spectrometer has also been constructed for the tape transport system. This permanent magnet system allows electrons to be focused onto a cooled Si(Li) detector while filtering out most of the photons.

A digital clock has been interfaced to the computer-based data acquisition system. The 16-bit digital output has a time resolution from 1 μsec to 1 sec and is designed so that the time of each event can be stored in the computer. Typical usage has been to store the digitized energy pulse height and digitized time of arrival of the pulse in list-mode fashion on magnetic tape. The list data can then be used to construct energy spectra as a function of time (very short time spectra multiscaling) or time spectra for a particular energy window. A technique[9] for determining state lifetimes in the millisecond-to-second range has been adapted by using this clock and writing special software for our system. We are in the final testing stages of this technique.

A simple new tape transport has been designed, constructed, and tested off-line for use on the 30° separator beam lines. The new tape transport is essentially a vacuum tube through which the tape passes with tape seals[10] maintaining the vacuum in the chamber. This design allows the feed, take-up reels, and the tape capstan mechanism to be in air, thus greatly simplifying the design over our present tape system. Gamma-ray data will be taken by depositing the separator beam on the tape in the vacuum chamber. After the appropriate time, the tape drive is pulsed by the computer, which moves the source out of the vacuum to a position in front of the detectors. For measurements requiring the source to remain in vacuum, a chamber can be attached in order to position detectors in the vacuum chamber. While the new system will not be able to move the tape as fast as the old one, the new system should be more versatile in all other aspects while being about an order of magnitude cheaper to build.

---

1. UNISOR, Oak Ridge, Tenn.
2. Vanderbilt University, Nashville, Tenn.
3. University of Massachusetts, Amherst.
4. University of South Carolina, Columbia.
5. Georgia Institute of Technology, Atlanta.
6. Louisiana State University, Baton Rouge.
7. University of Alabama at Birmingham.

8. F. T. Avignone III, J. E. Pinkerton, and J. H. Treeblood, *Nucl. Instrum. Methods* 107, 453 (1973).
9. J. Glatz and K. F. G. Lobner, *Nucl. Instrum. Methods* 44, 237 (1971).
10. H. K. Carter and R. L. Mlekodaj, *Nucl. Instrum. Methods* 128, 611 (1975).

DECAY-IN-FLIGHT MEASUREMENTS OF ALPHA ACTIVITY

T. J. Cleary K. S. Toth
F. E. Gross S. Bart[1]
D. C. Hensley E. V. Hungerford[1]
C. R. Bingham[2]

The heavy-ion beams available at the ORIC make possible the investigation of half-lives in the 1-nsec to 1-μsec range by the observation of charged-particle decays-in-flight. The basic features of this technique are illustrated in Fig. 2.62. The nuclear recoils produced in reactions induced by heavy ions incident on a suitable target are scattered forward into a solid angle centered about the primary beam. A detector is positioned downstream from the target to look for decay activity from the recoils. A trajectory detector designed especially for this purpose is shown in Fig. 2.63. It consists of three detection elements placed inside a gas-filled chamber. A thin window permits the nuclear particles to enter the chamber. In the first stage of the system (see Fig. 2.62), a position-sensitive wire is used to determine the position of the decay particle at the entrance to the detector. An ionization-chamber region then provides a ΔE signal. Finally, a position-sensitive solid-state detector is used to obtain an E signal and to ascertain the position of the particle at the rear of the detector.

The ΔE-E signals provide mass identification of the particle, while the two position signals permit reconstruction of the flight path of the decay particle. Finally, timing signals from the front stage of the detector and the cyclotron rf are used to generate a time-to-amplitude converter (TAC) spectrum. From this information, it should be possible to derive the half-life for the decay and a precise energy determina-

tion of the decay by removal of the Doppler-broadening effects associated with the decay-in-flight.

In order to test the trajectory detector, measurements were made using the $^{208}Pb(^{14}N,5n)$ reaction at 88 MeV to produce the alpha-radioactive nuclide ^{217}Ac. The data are being analyzed to extract alpha-decay energy and half-life information and to compare these results with previous measurements[3] on the same isotope. In addition to searching for new alpha emitters, the technique is also suitable for use in investigating new delayed-proton and fission-isomer activities. Another use of the detector is for the study of the emission of long-range alpha-particle groups and the resulting provision of structure information concerning nuclei far from stability (see, e.g., the recent work of Nomura[4] on ^{216}Ra).

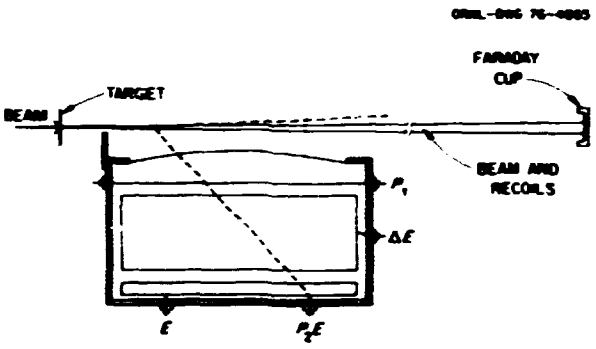

Fig. 2.62. Schematic diagram of decay-in-flight technique for measuring half-life activities.

1. University of Houston, Houston, Tex.
2. University of Tennessee, Knoxville.
3. T. Nomura et al., *Phys. Lett.* 40B, 543 (1972).
4. T. Nomura et al., *Phys. Lett.* 58B, 273 (1975).

LIGHT-ION NUCLEAR RESEARCH

Radiation-induced effects in solids have been studied with alpha-particle and deuteron beams from ORIC. Although occupying only a small part of the total beam time, such measurements are prompted by problems of enormous practical significance in the development of new energy sources.

Basic research with light-ion beams was carried out at ORIC, at ORNL with the EN tandem accelerator, at the Indiana University Cyclotron Facility (IUCF), and at KVI Groningen, Netherlands, with the isochronous cyclotron. A description of the (p,n) time-of-flight facility at IUCF is included. Many *E2* and *E4* matrix elements have been determined in rare-earth nuclei through the use of Coulomb-excitation studies with alpha beams. A measurement of the magnetic moment of the neutron was completed at the Institut Laue-Langevin, Grenoble, France. The

Fig. 2.63. Picture of trajector detector. The three stages of the detector system are attached to the chamber lid shown on the left, with the chamber itself shown on the right.

measurement is nearly 100 times more precise than the previous one.

RADIATION-ENHANCED CREEP MEASUREMENTS

T. C. Reiley[1] R. L. Auble
P. Jung[1] M. G. Duncan[2]

A creep machine has been developed to study the effects of radiation damage on the creep rate of reactor structural alloys, developmental alloys, and pure metals, using a 60-MeV ^{4}He beam from ORIC to simulate the effects of high-energy neutron bombardment. During 1976, two experiments were conducted. The first experiment was designed to study the ORIC beam properties and utilized a small mockup of the creep apparatus. Numerous OPTIC calculations were generated prior to the run, and beam scanning was performed to test their accuracy. It was found that the predicted beam profiles and transmission were reasonably well reproduced, although the predicted quadrupole currents were as much as 20% too high. In the second experiment, the completed creep machine was installed, and all systems were tested. Most of the equipment was found to operate satisfactorily, notably the sample temperature controller provided about 0.005°C control accuracy and 200-msec recovery from major (100%) beam transients. The data acquisition system using the CAMAC interface at ORIC and software provided by D. C. Hensley worked quite well. However, a number of problems were uncovered, and many corrections and improvements have been made as a result of this test run.

1. Metals and Ceramics Division.
2. Consultant.

THICK-TARGET NEUTRON YIELDS FROM d + Be AND d + Li AT E_d = 40 MeV

M. J. Saltmarsh C. B. Fulmer
C. A. Ludemann R. C. Styles[1]

Neutron sources based on the d + Be or d + Li reactions can provide a good simulation of the neutron spectrum to be expected at the first wall of a D-T fusion reactor and are therefore useful for fusion-related radiation-damage studies. In order to better characterize the existing ORIC d + Be source[2] and to provide data for the proposed d + Li sources,[3,4] we have measured the thick-target neutron yields by both time-of-flight (lithium and beryllium) and foil-activation (beryllium) techniques in the angular range of 0 to 90°. The results were used to develop a dosimetry technique suitable for this type of source.

Figure 2.64 shows some of the time-of-flight (TOF) data from d + Be taken at two different flight paths, 0.75 and 3 m. The overall normalization uncertainty is estimated to be ±15%. Total neutron yields (E_n greater than 2 MeV) as a function of scattering angle are shown in Fig. 2.65, the experimental points being derived from the TOF data and from activation measurements using Ni, Co, and Nb foils. The normalization uncertainties for these four sets of data are estimated to be ±15% (TOF, nickel) and ±10% (cobalt, niobium). The solid line represents the weighted average of all the data. Time-of-flight data taken using a lithium target were very similar to the d + Be data.[2]

The yield measurements outlined above were all made in good geometry, while irradiations made with the d + Be neutron source require the samples and dosimetry foils to be placed very close to the beryllium target in order to maximize the neutron flux. The basis of our dosimetry technique is to assume

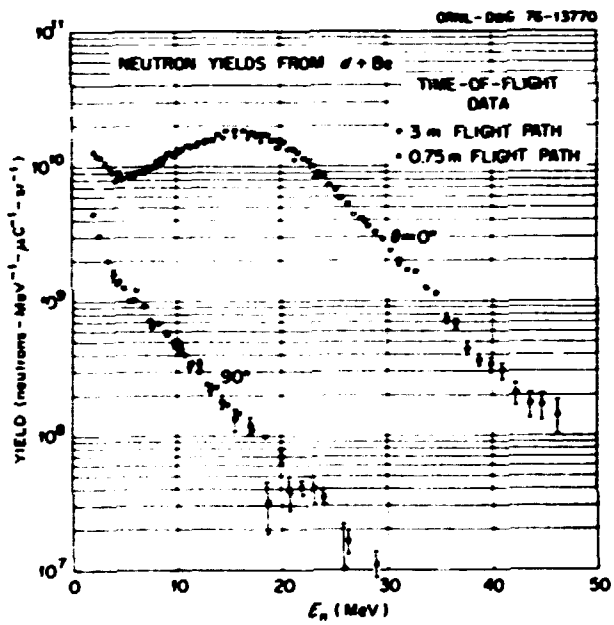

Fig. 2.64. Time-of-flight data from 40-MeV deuterons on a thick beryllium target, showing representative error bars. The 0.75-m data (open circles) have been normalized to the 3-m data in the energy range 7.5 MeV < E_n < 12.5 MeV. The system resolution (3-m data) varies from about 200 keV at E_n = 5 MeV to about 6 MeV at E_n = 40 MeV.

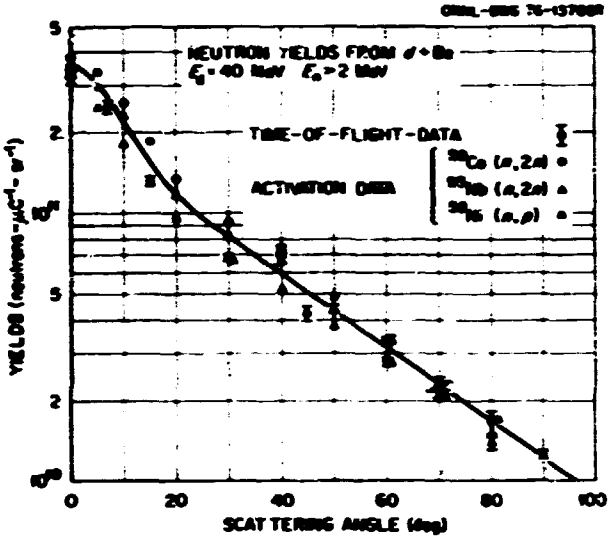

Fig. 2.65. Experimental values of neutron yield obtained in the present work for 40-MeV deuterons on thick beryllium targets.

that the shape of the neutron spectrum at a given point on the sample can be represented by the shape seen in good geometry at some effective scattering angle, θ_{eff}. This angle is derived from the ratio of the 810-keV gamma activities from the $^{58}Ni(n,p)$ and $^{59}Co(n,2n)$ reactions, while the total neutron yield is derived from the absolute value of one or the other of these activities. This sequence of measurements is illustrated in Fig. 2.66. The nickel and cobalt dosimetry foils are in the form of 2.5-cm-diam disks from which 1.5-mm-diam samples are punched in the pattern indicated at the top of Fig. 2.66. The point of maximum activity (i.e., the center of the neutron beam spot) is found by inspection, and the activity of each sample is plotted as a function of the distance r from this point, as shown in the upper part of Fig. 2.66. From these curves, the spectrum shape parameter, θ_{eff}, and the neutron fluence are derived as a function of r, as shown in the lower part of Fig. 2.66.

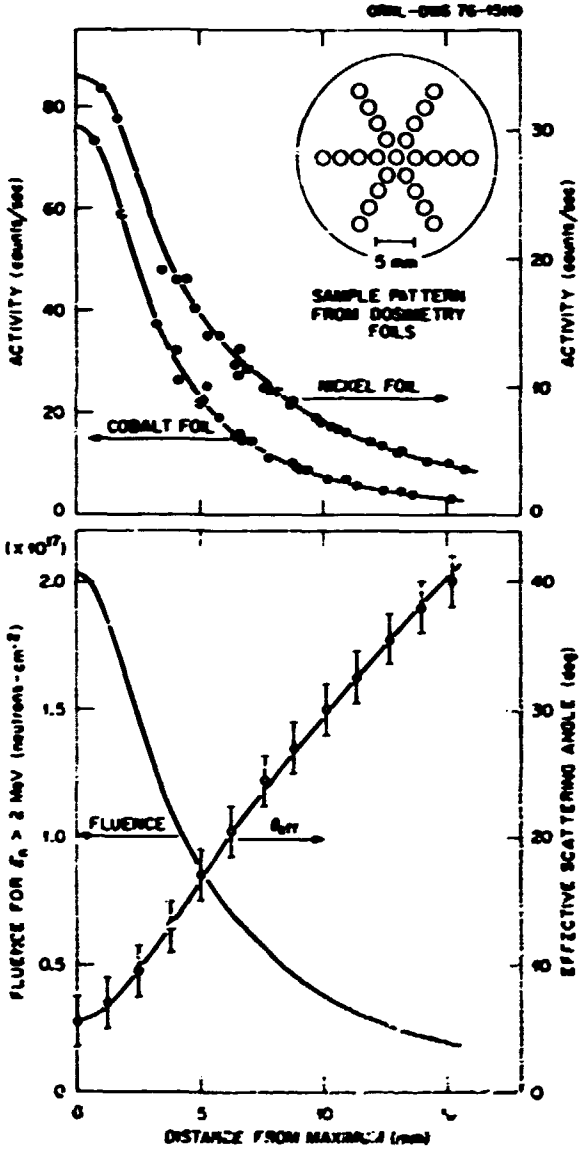

Fig. 2.66. Dosimetry method used for d + Be neutron source. The upper graphs show the distribution of ^{59}Co activity for the cobalt and nickel dosimetry foils. The lower plots show the spatial dependence of θ_{eff} and neutron yield inferred from these measurements.

1. Oak Ridge Associated Universities undergraduate research trainee from Berry College; present affiliation, University of Georgia, Athens.

2. M. J. Saltmarsh et al., *Characteristics of an Intense Neutron Source Based on the d + Be Reaction*, ORNL/TM-5696 (1976). This report has also been submitted to *Nuclear Instruments and Methods*.

3. M. J. Saltmarsh and R. E. Worsham, *INGRID—An Intense Neutron Generator for Radiation-Induced Damage Studies in the CTR Materials Program*, ORNL/TM-5233 (1976).

4. P. Grand, *Accelerator-Based Neutron Generator*, BNL-20159 (1975).

DAMAGE PRODUCTION BY d + Be NEUTRONS

J. B. Roberto[1] R. R. Coltman, Jr.[1]
C. E. Klabunde[1] M. J. Saltmarsh
J. M. Williams[1] C. B. Fulmer

The damage produced by high-energy (about 14-MeV) neutrons is of considerable experimental and theoretical interest due to the potentially deleterious

effects of such neutrons on fusion-reactor first-wall materials. Knowledge of point-defect generation rates for these neutrons is central to an understanding of fusion-neutron damage processes.

We have estimated defect production rates in Cu, Nb, and Pt induced by d + Be neutrons from the ORIC source[2] by measuring the changes in electrical resistivity at 4.2° K during n ..tron irradiation.[3] The results, shown in Fig. 2.67, indicate that the damage produced was proportional to neutron fluence over the range of the experiments.

A comparison was made of the damage produced by d + Be neutrons to that produced by fission neutrons. The experimental and theoretical ratios for these two neutron spectra show satisfactory agreement for all materials studied, as is shown in Table 2.10. Isochronal annealing studies were also made on the irradiated samples from 10 to 400° K and were compared with data from samples irradiated in thermal and fission neutron spectra.[4] The platinum results (Fig. 2.68) showed the greatest dependence of the damage recovery curve upon the neutron spectrum. The differences suggest substantial configurational differences in the primary damage state resulting from d-Be neutrons and fission neutrons in platinum, indicating the formation of more stable cascade structures at the higher neutron energies. However, the agreement between the experimental and theoretical ratios for total damage production summarized in Table 2.10 shows that the damage

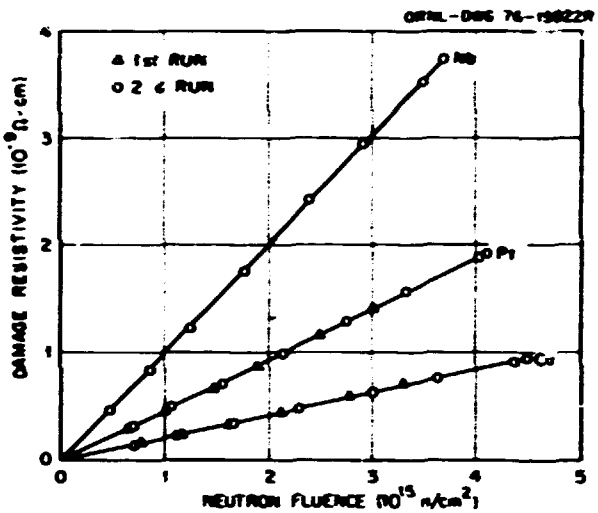

Fig. 2.67. Measured changes in resistivity at 4.2° K as a function of neutron fluence for Cu, Nb, and Pt irradiated with the d-Be neutron source.

production at 4.2° K scales with damage energy. Thus the increased cascade stability in platinum appears not to be due to increased recombination of nascent close pairs during the damage process. Instead, for the higher-energy neutrons, a relatively higher proportion of interstitials is produced in clusters or in close enough proximity to cluster after a few jumps.

Table 2.10. Ratio of damage production per neutron, (d + Be)/fission

Sample	Experiment	Theory
Copper	3.3 ± 0.7	2.9 ± 0.4
Niobium	2.6 ± 0.5	2.8 ± 0.4
Platinum	2.7 ± 0.5	3.7 ± 0.5

1. Solid State Division.
2. M. J. Saltmarsh et al., *Characteristics of an Intense Neutron Source Based on the d + Be Reaction*, ORNL TM-5696 (1976). This report has also been submitted to *Nuclear Instruments and Methods*.
3. J. B. Roberto et al., "Damage Production by High-Energy d-Be Neutrons in Cu, Nb, and Pt at 4.2 K," to be published in *Applied Physics Letters*.
4. J. B. Roberto et al., "Isochronal Recovery of High-Energy d-Be Neutron Damage in Cu, Nb, and Pt from 8-400 K," submitted to the *Journal of Nuclear Materials*.

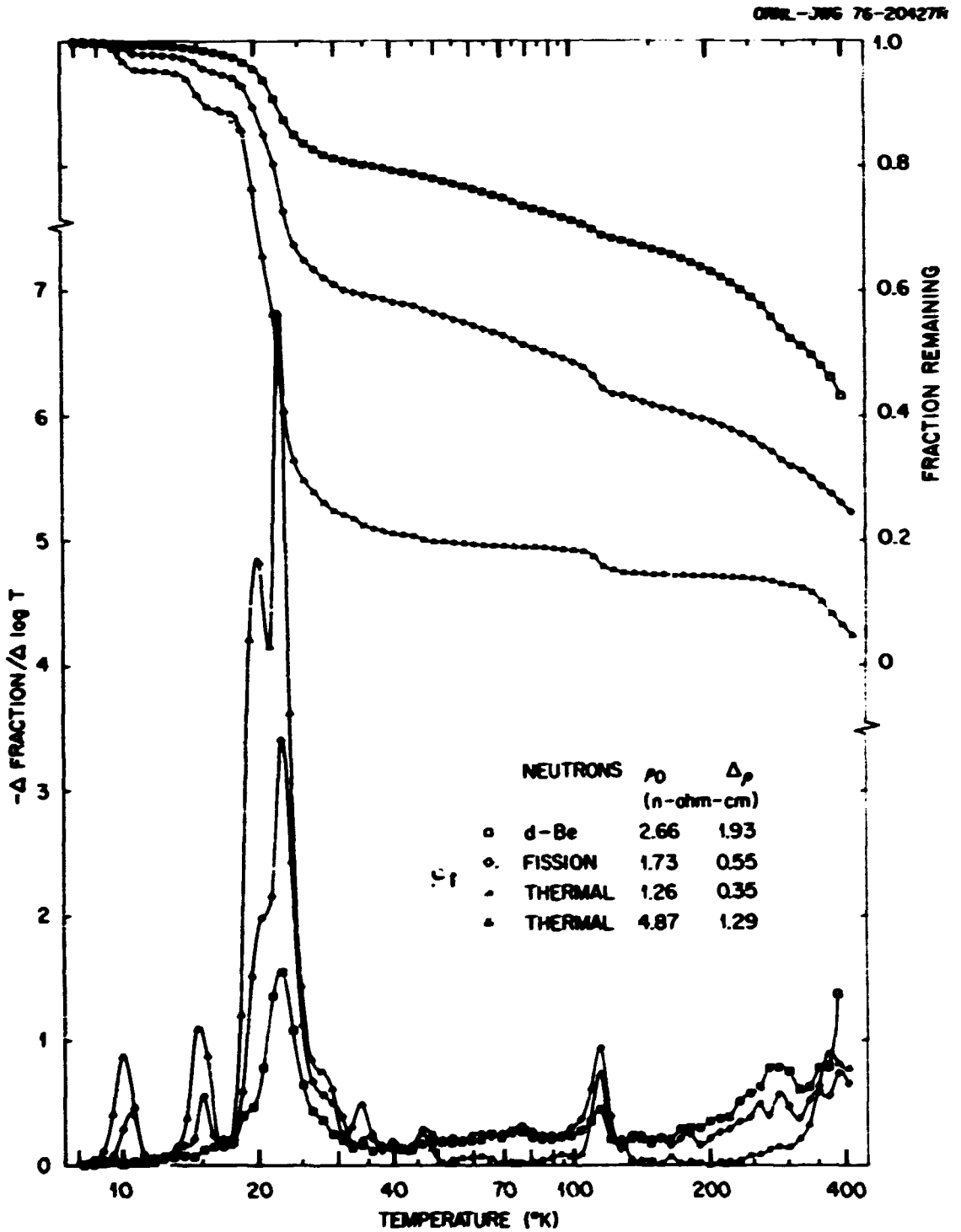

Fig. 2.68. Isochronal recovery curves of electrical resistivity for d-Be, fission, and thermal-neutron-induced damage in platinum.

(^{3}He,t) REACTIONS ON SELF-CONJUGATE TARGETS

C. D. Goodman F. E. Bertrand
R. L. Auble D. C. Kocher

We have measured, with high resolution, triton spectra from ^{16}O(^{3}He,t)^{16}F, ^{12}C(^{3}He,t)^{12}N, and ^{28}Si(^{3}He,t)^{28}P to follow up our earlier discovery of an isolated peak in the ^{16}O(^{3}He,t)^{16}F spectrum.[1] Because the oxygen target was a quartz flake, we also measured the spectrum from a silicon target to be able to subtract the background from the oxygen spectrum, and we measured the spectrum from carbon to be able to use the resolved $0^+ - 1^+$, $0^+ - 2^+$, and $0^+ - 2^-$ transitions as calibrations.

The spectrum from the oxygen target is simple, having only two strong peaks, the one discovered earlier and one corresponding to the 0.42-MeV level of ^{16}F. Other levels of ^{16}F are only weakly excited. Viewed with the good resolution of the present experiment, the high-excitation peak appears to be due to a level at 6.7 MeV in ^{16}F with a satellite at 6.9 MeV. Its angular distribution peaks at a laboratory angle of 13°, while the angular distribution for the 0.4-MeV state peaks at a laboratory angle of about 5°.

Because ^{16}O is both a self-conjugate and a closed-shell nucleus, no isospin-flip or spin-flip isospin-flip (also known as $M1$ or Gamow-Teller) transitions are possible. The low-lying particle-hole strength should, therefore, be associated with $(p)^{-1}(s,d)^1$ negative-parity states. The excitation of these states should be via $L = 1$ and $L = 3$. The data suggest that nearly all of the $L = 1$ strength lies in the 0.4-MeV state, and nearly all of the $L = 3$ strength lies in the 6.7-MeV state.

For the carbon target, we expect to see particle-hole states within the p shell, and indeed both the 1^+ ground state and the 2^+ first excited state are strongly excited. As we noted in the discussion of (p,n) reactions in another contribution to this annual report, the transition ^{12}C ground state $-$ ^{12}N ground state is the analog of an $M1$ transition. At higher excitation, there are broad bumps that do not resolve into individual levels and look qualitatively similar to the (p,n) spectra reported above. This strength is probably due to particle-hole states involving a particle in the s-d shell and possibly in the f shell. The only clearly resolved peak belonging to that configuration is the 2^- state at 1.2 MeV.

The spectrum from the silicon target is quite complicated and shows many resolved levels. The $M1$ analog state, at 2.1 MeV in ^{28}P, is strongly excited as it is in (p,n). If one smears the resolution, one obtains a spectrum that looks qualitatively similar to the ^{28}Si$(p,n)^{28}$P spectrum. The (^{3}He,t) data are being analyzed.

---

1. *Phys. Div. Annu. Prog. Rep. Dec. 31, 1975*, ORNL-5137, p. 69.

^{74,76}Ge(p,t) REACTION STUDIES

A. C. Rester[1] J. B. Ball
R. L. Auble

It has been suggested[2] that the rather unusual properties of the anomalously low-lying 0.690-MeV 0^+ excited state in ^{72}Ge might be explained on the basis of a coupling of pairing and quadrupole vibrational modes. We have attempted to test this proposition with two-nucleon transfer reactions on the germanium isotopes. On the basis of the pairing-phonon vibrational explanation, one would expect that, in (p,t) transitions to the ^{74}Ge 0^+ states, almost all of the $L = 0$ strength would go to the ground state, whereas in (p,t) transitions to the ^{72}Ge 0^+ states, a considerable amount of the $L = 0$ strength would go to the 0.690-MeV excited state and, as a result of anharmonicities, to higher-lying 0^+ states as well.[3]

Just this picture is observed in experiment (Fig. 2.69). Greater than 98% of the total ^{76}Ge(p,t) $L = 0$ strength goes to the ground-state transition, whereas in ^{74}Ge(p,t), the $L = 0$ strength is fractionated, with 72% going to the ground state, 19% to the 0.690-MeV state, 5% to the 3.155-MeV state, and 4% to the 4.180-MeV state transitions. Within the 15% error limits on our cross-section measurements, the total strength of all $L = 0$ transitions to each nucleus is the same.

A rather surprising feature of the present results is that within each nucleus, there are families of states whose angular distributions have the same shapes which are very well reproduced by the single-step distorted-wave Born-approximation (DWBA) calculations as well as families whose angular distribution shapes are not at all fitted by the DWBA. The latter type are predominant in ^{72}Ge, whereas the former are predominant in ^{74}Ge. Evidently, a structural-phase transition is taking place between ^{72}Ge and ^{74}Ge. Preliminary results of a theoretical investigation[4] of the nuclear structure in this region suggest that the addition of two neutrons to ^{72}Ge may cause the nuclear shape to change from oblate to asymmetric. The effect such a picture would have on the

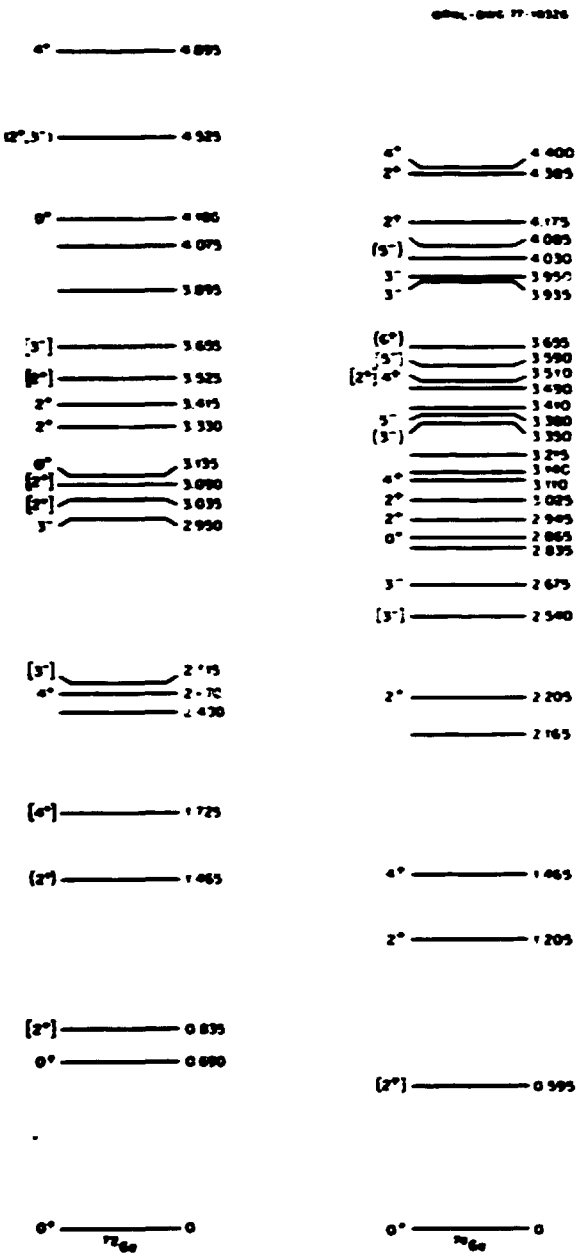

Fig. 2.89. Energy levels populated in ^{70,72}Ge(p,p') at $E_p = 35A$ MeV. The energy-level uncertainties are ±5 keV. Spins in brackets are tentatively assigned on the basis of similarities of angular distributions to those of levels with known $J\pi$. Spins not in brackets were assigned on the basis of good agreement with DWBA calculations.

pairing vibrational interpretation of the 0⁺ state structure is not yet clear.

1. Tennessee Technological University, Cookeville.
2. J. Hadermann and A. C. Rester, *Nucl. Phys.* A231, 120 (1974).
3. B. Sorensen, *Nucl. Phys.* A 34, 1 (1969).
4. K. Kumar and A. C. Rester, private communication.

^{58}Ni(p,p') REACTION AT 60 MeV: STUDY OF THE ANALYZING POWER FOR INELASTIC EXCITATION OF THE GIANT-RESONANCE REGION OF THE NUCLEAR CONTINUUM AND OF LOW-LYING BOUND STATES[1]

D. C. Kocher E. E. Gross
F. E. Bertrand E. Newman[2]

The analyzing power of the giant-resonance region of the nuclear continuum and of low-lying bound states for incident 60-MeV polarized protons from the ORIC has been investigated in the ^{58}Ni(p,p') reaction. The measurements are compared with collective-model DWBA calculations employing a spin-orbit transition potential of the full-Thomas form and optical-model parameters which give a good description of the analyzing power for proton elastic scattering from ^{58}Ni at 60 MeV. The predicted analyzing powers for the giant quadrupole ($E2$) resonance at $E_x = 16.5$ MeV and for low-lying bound states with $J^\pi = 2^+, 3^-$, and 4^+ are in qualitative agreement with the measurements for $\theta_{lab} = 15$ to 60°. However, a systematic discrepancy is observed for the quadrupole resonance, where the measurements for $\theta_{lab} = 15$ to 30° are considerably more negative than in the calculations. A similar but less pronounced effect is observed for the strongly excited 2^+ and 3^- bound states. Improved fits to the analyzing power for the quadrupole resonance are obtained by reducing the spin-orbit diffuseness parameter or by including an attractive imaginary spin-orbit potential. Analysis of the cross section for a weaker resonance at $E_x = 13.5$ MeV indicates an $E2$ assignment. The analyzing power for the unstructured nuclear continuum above the giant resonance is $A_y \approx -0.05 \pm 0.01$ at most angles between 15 and 40°.

1. Abstract of paper published in *Phys. Rev. C* 14, 1392 (1976).
2. Chemical Technology Division.

DIRECT EVIDENCE FOR A NEW GIANT RESONANCE AT 80 $A^{-1/3}$ MeV IN THE LEAD REGION[1]

F. E. Bertrand H. P. Morsch[2]
T. Ishimatsu[2] K. van der Borg[2]
M. N. Harakeh[2] A. van der Woude[2]

The giant-resonance regions of ^{208}Pb, ^{209}Pb, ^{197}Au, and ^{209}Bi have been studied using inelastic scattering

of 120-MeV alpha particles from the KVI cyclotron. The scattered particles were detected in semiconductor-counter telescopes, yielding an energy resolution of about 100 keV (FWHM). Figure 2.70 shows giant-resonance spectra from all four targets. Although the spectra are dominated by the now well-established[1] giant quadrupole resonance located at 63 $A^{-1/3}$, each spectrum provides evidence for a second peak located at about 80 $A^{-1/3}$. Figure 2.71 shows the

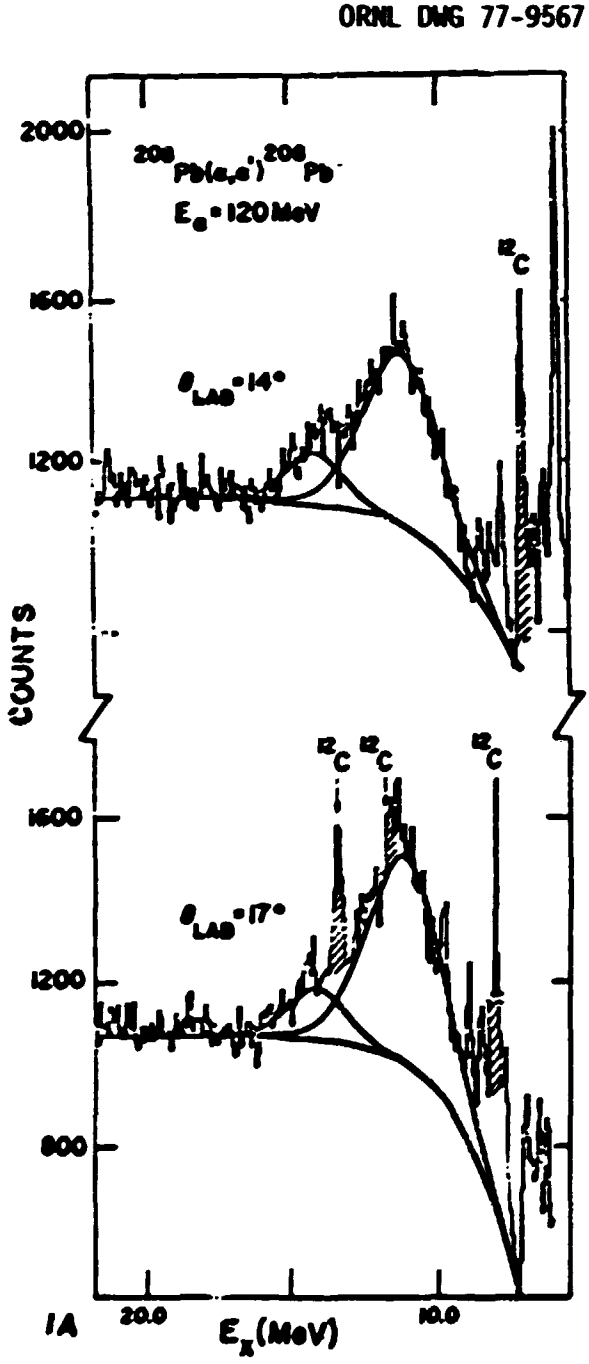

Fig. 2.70. Spectra of ^{208}Pb taken at 14 and 17°. The two Gaussian peaks and the assumed underlying continuum that were fitted to the data are indicated.

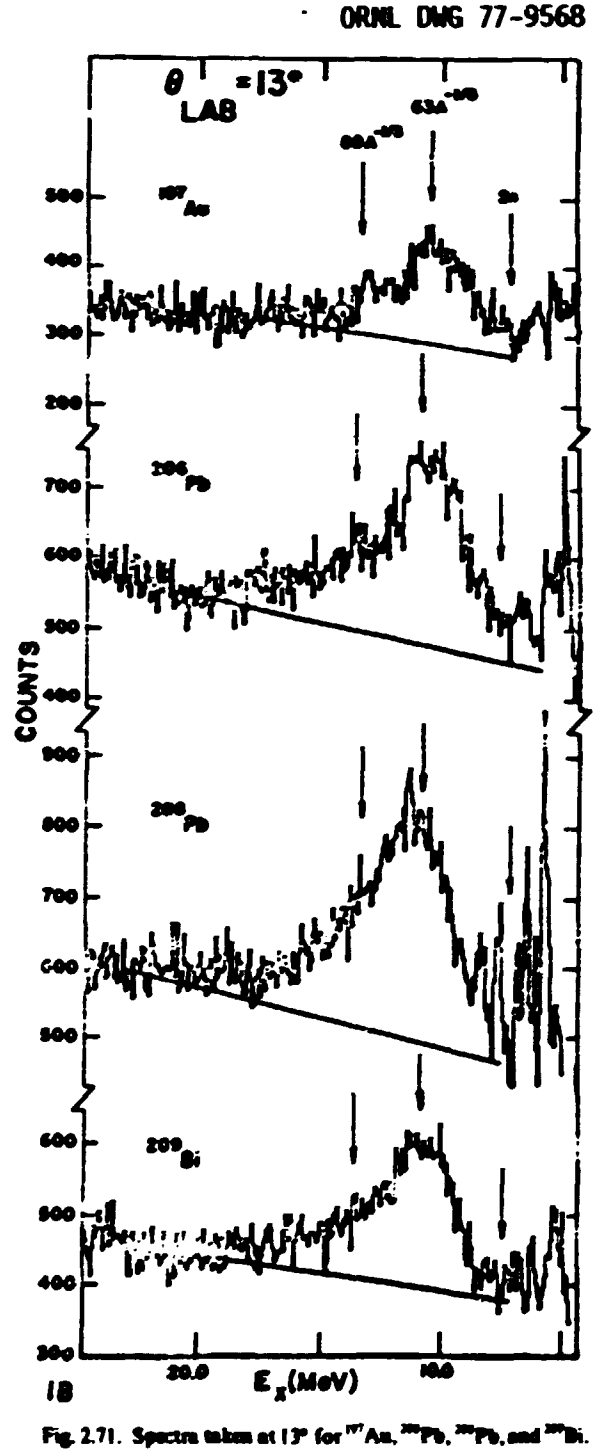

Fig. 2.71. Spectra taken at 13° for ^{197}Au, ^{206}Pb, ^{208}Pb, and ^{209}Bi. The neutron separation energy and the excitation corresponding to 63 $A^{-1/3}$ MeV are indicated by arrows. The straight line is only to guide the eye.

decomposition of a ^{208}Pb spectrum into the two giant-resonance components.

Angular distributions for the 10.9-MeV resonance ($63\ A^{-1/3}$) in ^{208}Pb are in excellent agreement with calculated $L = 2$ angular distributions normalized to exhaust about 100% of the $T = 0$, $E2$ energy-weighted sum rule (EWSR). The angular distribution for the 13.9-MeV resonance is equally well described by $L = 0$, 2, or 4 calculations which correspond to 100, 50, or 17% exhaustion of the corresponding $E0$, $E2$, and $E4$ EWSR respectively.

1. Summary of work published in *Phys. Rev. Lett.* 38, 676 (1977).
2. Kernfysisch Versneller Instituut, Groningen, Netherlands.
3. F. E. Bertrand, *Annu. Rev. Nucl. Sci.* 26, 457 (1976).

HIGH-RESOLUTION STUDY OF THE GIANT-RESONANCE REGION IN ^{28}Si BY INELASTIC ALPHA-PARTICLE SCATTERING

F. E. Bertrand M. N. Harakeh[1]
K. van der Borg[1] S. Y. van der Werf[1]
A. van der Woude[1]

For nuclei with mass number greater than about 40, the giant quadrupole resonance (GQR) is observed as a single broad peak.[2] However, for lighter nuclei some evidence had been obtained[3,4] for considerable fragmentation of the GQR strength. We have studied the ^{28}Si giant-resonance region, utilizing a high-resolution alpha-scattering experiment.[5]

The data were obtained using the 120-MeV alpha-particle beam from the KVI cyclotron. The scattered alpha particles were detected with semiconductor detectors, yielding about 90 keV (FWHM) energy resolution. Figure 2.72 shows inelastic alpha spectra at several angles from ^{28}Si. Because isovector states (e.g., giant dipole resonance) will not be excited by the ^{28}Si(α,α') reaction, only $T = 0$ states appear in the alpha spectra.

Considerable structure is observed in the giant-resonance region of ^{28}Si. The angular distributions for the various peaks have been compared with collective-model DWBA calculations. While most of the observed structure is found to be $E2$, some peaks are better described by $L = 3$ and, in one case, $L = 0$ calculations. The sum of the $E2$ cross sections in the 15.5- to 23-MeV region of ^{28}Si exhausts $27 \pm 6\%$ of the $T = 0$, $E2$ energy-weighted sum rule.

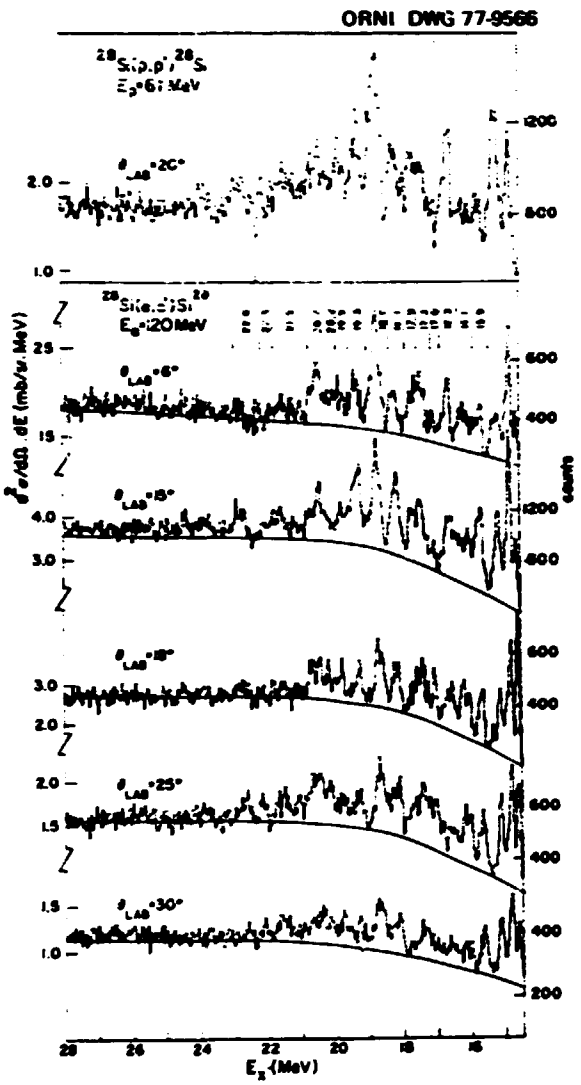

Fig. 2.72. Spectra of inelastic alpha-particle scattering on ^{28}Si. The assumed continuum underlying the resonance peaks is indicated for each angle by a solid line. Energy bins are shown which define the spectral region integrated over to obtain cross sections for the various peaks.

1. Kernfysisch Versneller Instituut, Groningen, Netherlands.
2. F. E. Bertrand, *Annu. Rev. Nucl. Sci.* 26, 457 (1976).
3. M. N. Harakeh et al., *Nucl. Phys. A* 265, 189 (1976).
4. F. E. Bertrand et al., *Phys. Div. Annu. Prog. Rep. Dec. 31, 1975*, ORNL-5137, p. 63.
5. Summary of work to be published in *Physics Letters*.

SEARCH FOR GIANT RESONANCES WITH (p,n) REACTIONS

C. D. Goodman J. Knudson[1]
F. E. Bertrand T. Witten[1]
R. Madey[1] J. Rapaport[2]
B. Anderson[1] D. Bainum[2]
A. Baldwin[1] M. B. Greenfield[3]
C. C. Foster[4]

Neutron spectra from $^{12}C(p,n)^{12}N$ and $^{28}Si(p,n)^{28}P$ are each dominated by a prominent sharp peak (see Fig. 2.73), which in each case is the analog of the giant $M1$ resonance in the target nucleus. The $M1$ resonances are the 15.1-MeV $T=1, 1^+$ state in ^{12}C and the 11.4-MeV $T=1, 1^+$ state in ^{28}Si.

The relationship between the $M1$ character of these levels and the excitation of their analogs in (p,n) reactions provides an example of how certain aspects of nuclear structure become manifest in different modes of excitation. The so-called $M1$ giant resonances in self-conjugate nuclei have been predicted theoretically[5] and observed experimentally[6] through electromagnetic interactions. It has also been pointed out that the largest part of the $M1$ operator operating on a $T=0$ nucleus is essentially equivalent to an isovector spin-flip.[7] Thus the giant $M1$ resonance is connected to the ground state by an isospin-flip, spin-flip. The $M1$ state is the $T_z=0$ member of a $T=1, 1^+$ isospin triplet.

That the analog of the $M1$ state is excited strongly in the (p,n) reaction can be understood qualitatively through recognizing that it is also a particle-hole state in which the particle and the hole are opposite in spin and isospin but have the same orbital angular momentum. Formally, it is excited by the interaction operator $(\sigma\cdot\sigma)(\tau_-\tau)$, where the subscripted operators refer to the nucleons in the nucleus, and the non-subscripted operators refer to the projectile. The spin operator is σ, and the isospin operator is τ. The spin-flip transitions are the only ones that can take place without change of orbital angular momentum or principal quantum number in a $T=0$ nucleus, because $(\tau_-\tau)$ by itself operating on a $T=0$ nuclear wave function gives zero. Furthermore, we have already noted that spin-flip ($M1$) strength is concentrated,[5] so all the $L=0$ strength is concentrated in a sharp peak.

The other features of the spectra can be characterized as two broad peaks at higher excitation. Because these do not appear to have the same shape at different angles, we can infer that neither peak should be characterized as a concentration of a particular multipole strength.

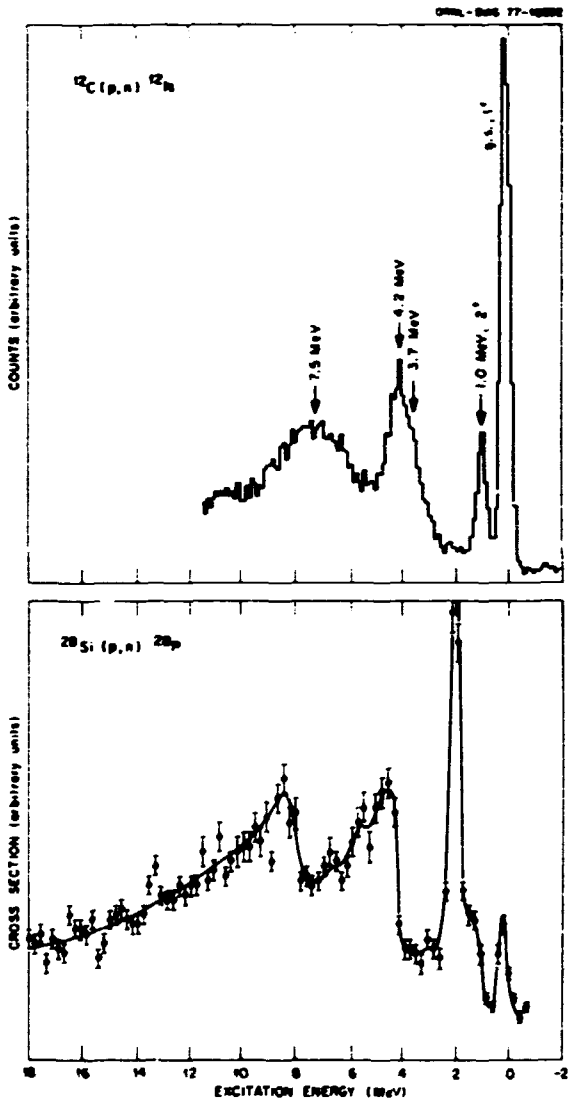

Fig. 2.73. Energy spectra for $^{12}C(p,n)^{12}N$ and $^{28}Si(p,n)^{28}P$ at $\theta(\text{lab}) = 12°$. The prominent sharp peak in each spectrum is the analog of the giant $M1$ resonance.

The experiment was originally undertaken to project out the $T=1$ components of collective multipole resonances.[8,9] The spectra do not clearly show evidence of concentrated multipole strength other than the $M1$. In particular, the analog of the giant dipole resonance is not evident. The conclusion to be drawn is probably that the (p,n) reaction does not couple strongly to that mode of excitation, because the $E1$ resonance is believed to be isovector and should have an analog.

The broad bumps in the spectra could be clusters of higher multipole particle-hole strength of the type described by Moffa and Walker.[10]

The data were obtained by time-of-flight measurements at the IUCF, using 61.9-MeV protons. The experiment is in progress, and data on other targets are expected soon.

1. Kent State University, Kent, Ohio.
2. Ohio University, Athens.
3. Florida Agricultural and Mechanical University, Tallahassee.
4. Indiana University, Bloomington.
5. D. Kurath, *Phys. Rev.* 130, 1525 (1963).
6. L. W. Fagg, *Rev. Mod. Phys.* 47, 683 (1975), and references therein.
7. G. Morpurgo, *Phys. Rev.* 110, 721 (1958).
8. F. E. Bertrand, *Ann. Rev. Nucl. Sci.* 26, 457 (1976).
9. G. R. Satchler, *Nucl. Phys.* A195, 1 (1972).
10. P. J. Moffa and G. E. Walker, *Nucl. Phys.* A222, 140 (1974).

NEUTRON TIME-OF-FLIGHT EXPERIMENTS AT THE INDIANA UNIVERSITY CYCLOTRON FACILITY

C. D. Goodman[1] C. Goulding[2]
C. C. Foster[1] J. Rapaport[3]
M. Greenfield[2] D. Bainum[1]

We are engaged in an ORNL-IUCF collaborative program with participants from other universities to study medium-energy (p,n) reactions. A beam-swinger system, originally built for use at ORIC, has been moved to IUCF, and its geometry has been modified to accommodate the higher proton energies of IUCF.

The magnet system provides variation of the angle of incidence of the proton beam on the target continuously over a range of 26°. Thus the flight path remains fixed in measuring angular distributions.

We have developed a highly efficient time-compensated neutron detector.[4] The scintillator volume is almost 20 times as great as that of the detectors used to obtain the data on $^{12}C(p,n)^{12}N$ and $^{28}Si(p,n)^{28}P$ described above, and the observed overall time resolution is slightly better.

The detector employs a scintillator 15 × 15 × 100 cm viewed at one end by a single phototube. Time compensation is accomplished by tilting the axis with respect to the flight path so that the sum of neutron and photon transit times is approximately independent of the position of the scintillation. Compensation for the variation in rise time of the light pulses over the long scintillator is accomplished with extrapolated zero timing.

This detector is equivalent to a 100% efficient detector with the cross-sectional area of its small (15 × 15 cm) face. It will enable us to perform experiments that were not feasible with the smaller detectors.

1. Indiana University, Bloomington.
2. Florida Agriculture and Mechanics University, Tallahassee.
3. Ohio University, Athens.
4. C. D. Goodman et al., submitted to *Nuclear Instruments and Methods*.

COULOMB EXCITATION OF 2^+ AND 3^- STATES IN ^{192}Pt AND ^{194}Pt

R. M. Ronningen[1] J. H. Hamilton[1]
R. B. Piercey[1] S. Raman
A. V. Ramayya[1] P. H. Stelson
W. K. Dagenhart

Transitional nuclei and recently platinum isotopes have become the subjects of much experimentation. The high-spin level spacings in $^{190-194}$Pt have been mapped out by heavy-ion reactions[2-4] with the rotation-alignment model[5] invoked to explain[2-4,6] the anomalous level behaviors. Also, Coulomb nuclear interferences in the excitation of ^{194}Pt have been studied[7] to yield relative phases as well as magnitudes of transition-matrix elements connecting the ground states and the first two $J^\pi = 2^+$ states.

In this work we have obtained precise values of $B(E2; 0^+ \rightarrow 2_1^+)$ for both ^{192}Pt and ^{194}Pt by employing the magnetic-spectrographic analysis of ^{3}He ions, scattered after Coulomb excitation from thin targets of high purity.

The Coulomb excitation of ^{192,194}Pt, by 14.9-MeV ^{4}He ions from the ORNL tandem Van de Graaff accelerator, was studied using an Enge split-pole spectrograph and a 60-cm gas-flow proportional counter. Our targets were about 30-μg/cm^2 separated material of greater than 99% isotopic purity deposited on 65-μg/cm^2 carbon-foil backings.

Experimental ratios of inelastic-to-elastic scattering differential cross sections were compared with ratios calculated with the aid of both semiclassical (de Boer-Winther) and quantal (AROSA) Coulomb-excitation codes.

Our study indicates smaller $B(E2)$ values to the 2^+ states than do most previous measurements for both ^{192,194}Pt. Such data should be of interest not only to experimentalists needing precise values to interpret their experiments, but also to theorists as well.

A report of our experiment and results has been prepared and accepted for publication.

1. Vanderbilt University, Nashville, Tenn.
2. L. Funke et al., *Phys. Lett.* 55B, 436 (1975).
3. J. C. Cunnane et al., *Phys. Rev. C* 13, 2197 (1976).
4. S. S. Hjorth et al., *Nucl. Phys.* A262, 328 (1976).
5. F. S. Stephens and R. S. Simon, *Nucl. Phys.* A183, 257 (1972).
6. N. R. Johnson et al., submitted to *Physical Review*.
7. F. Todd Baker et al., *Phys. Rev. Lett.* 37, 193 (1976).

COULOMB EXCITATION OF ^{166,168,170}Er WITH ^{4}He IONS

F. K. McGowan R. L. Robinson
W. T. Milner P. H. Stelson

The reaction on ^{166,168,170}Er induced by ^{4}He ions selectively excites 2^+ and 3^- states by direct $E2$ and $E3$ Coulomb excitation. We present results from gamma-ray spectroscopy with 14-MeV ^{4}He ions on isotopically enriched targets of ^{166}Er, ^{168}Er, and ^{170}Er. Gamma-ray spectra were observed at $\theta_\gamma = 0$, 55, and 90° with respect to the beam direction with a 30-cm^3 Ge(Li) detector located 7 cm from the target. For the conditions of the experiment, the use of first-order treatment of the excitation process is adequate for the analysis of thick-target gamma-ray yields. The experimental results for the reduced transition probabilities, $B(E\lambda, 0 \rightarrow J = \lambda)$, are summarized in Table 2.11. The K,J^π assignments were deduced primarily from our gamma (θ) measurements, ratios of reduced-transition probabilities, and other nuclear-spectroscopy studies that have been summarized.[1-3]

1. A. Bayra, *Nucl. Data Sheets* 14, 471 (1975).
2. L. R. Greenwood, *Nucl. Data Sheets* 11, 385 (1974).
3. M. R. Schmorak and R. L. Auble, *Nucl. Data Sheets* 15, 371 (1975).

$E2$ AND $E4$ REDUCED-MATRIX ELEMENTS OF ^{154,156,158,160}Gd AND ^{176,178,180}Hf

R. M. Ronningen[1] W. Lourens[5]
J. H. Hamilton[1] L. L. Riedinger[6]
L. Varnell[2] F. K. McGowan
J. Lange[3] P. H. Stelson
A. V. Ramayya[1] R. L. Robinson
G. Garcia-Bermudez[4] J. L. C. Ford, Jr.

In the last few years, a variety of experimental studies of even-mass nuclei in the Sm-Os region have been carried out to test the theoretical predictions of hexadecapole deformations.[7-13] The hexadecapole deformation with β_4 greater than 0 is expected[7-13] to maximize in the region $146 < A < 160$, pass through zero for $160 < A < 170$, and become maximum-negative around $178 < A < 190$. Since 1971, we have been involved in measurements to test the region of maximum-positive deformation and the region when

Table 2.11. Experimental results for $B(E\lambda, 0 \rightarrow J = \lambda)^a$

Nucleus	Level (keV)	K,J^π	$E\lambda$	$B(E\lambda, 0 \rightarrow J)$ ($e^2 \cdot b^\lambda$)	$B(E\lambda)$ $B(E\lambda)_{sp}$[b]
^{166}Er	786	$2,2^+$	$E2$	0.140 ± 0.008	5.2
	1159	$?,2^+$	$E2$	0.0042 ± 0.0006	0.15
	1514	$2,3^-$	$E3$	0.061 ± 0.010	5.3
	1528	$?,2^+$	$E2$	0.018 ± 0.002	0.66
	1719	$?,3^-$	$E3$	0.032 ± 0.005	2.8
^{168}Er	821	$2,2^+$	$E2$	0.131 ± 0.008	4.7
	1431	$0,3^-$	$E3$	0.043 ± 0.006	3.6
	1633	$2,3^-$	$E3$	0.060 ± 0.012	5.1
^{170}Er	934	$2,2^+$	$E2$	0.102 ± 0.006	3.6
	960	$0,2^+$	$E2$	0.0079 ± 0.0009	0.28
	1332	$?,2^+$	$E2$	0.0074 ± 0.0011	0.27
	1371	$?,2^+$	$E2$	0.0032 ± 0.0005	0.11
		or			
		$?,3^-$	$E3$	0.020 ± 0.003	1.6

[a] For those cases where the K,J^π assignments of the states are not known from other nuclear-spectroscopy studies, the $B(E\lambda, 0 \rightarrow J = \lambda)$ are given for both assignments $J = 2^+$ and $J = 3^-$.

[b] $B(E\lambda)_{sp} = [(2\lambda + 1)\, 4\pi]/[3^\lambda + 3)^2\, (0.12A^{1/3})^{2\lambda}\, e^2 b^\lambda$ for $J_i = 0$, $J_f = \lambda$.

the values were predicted to go negative.[14] We summarize here the findings for the M_{04} matrix elements for several gadolinium and hafnium nuclei.

The Coulomb excitation studies were carried out with alpha particles well below the Coulomb barrier by requiring the target and projectile nuclear surfaces to be separated by about 7 F. Experiments were carried out at 150° and in some cases at 90°. The experimental ratios of the different cross sections for inelastic-to-elastic scattering were compared with ratios calculated with the aid of the quantum mechanical Coulomb excitation code AROSA. Corrections were applied for the 6⁺ ground; for 0, 2, and $4K^{\pi} = 0^{+}$ and 2^{+} levels; and for stretching. Our results are given in Table 2.12, along with other values which have been obtained concurrently by other groups. In Fig. 2.74, the systematics of all the β_4 measurements in the 150 to 190 region are presented.

The important new results found in our work concern the hafnium nuclei. There are two values of the $E4$ matrix element which will reproduce the 4^{+} cross section—one with a positive and one with a negative sign. The positive-sign values for gadolinium are in good agreement with theory and other measurements which chose this sign. In hafnium, however, the positive sign leads to a β_4 that systematically does not agree with the theoretical prediction, although the errors are large on each individual value. On the other hand, the negative values yield much larger negative β_4 values than predicted by theory. Thus, for either sign there is disagreement with a rotational interpretation of the experimental data as a hexadecapole deformation. The negative M_{04} matrix elements would yield a shape for ^{180}Hf like that of a tin can. In a subsequent Coulomb-nuclear interference experiment,[15] we have found that indeed the large negative solution of the $E4$ matrix element reported here is correct.

---

1. Vanderbilt University, Nashville, Tenn.
2. Jet Propulsion Laboratory, Pasadena, Calif.
3. Ruhr-Universität, Bochum, Germany.
4. Fellow, Consejo Nacional de Investigaciones Scientificas y Tecnicas; currently with Atomic Energy Commission, Buenos Aires, Argentina.
5. Delft Technological University, Netherlands.
6. University of Tennessee, Knoxville.
7. S. G. Nilsson et al., *Nucl. Phys.* A131, 1 (1969).
8. U. Götz et al., *Nucl. Phys.* A192, 1 (1972).
9. P. Möller, *Nucl. Phys.* A142, 1 (1970).
10. H. Flocard, P. Quentin, and D. Vautherin, *Phys. Lett.* 46B, 304 (1973).
11. Bozena Nerlo-Pomorska, "Electric Multipole Moments of Atomic Nuclei," Report 1538, Institute of Nuclear Research, Warsaw, Poland (1974).
12. Bozena Nerlo-Pomorska, private communication.
13. J. A. Gareev, S. P. Ivanova, and V. V. Pashkevich, *Yad. Fiz.* 11, 1200 (1970); translated in *Sov. J. Nucl. Phys.* 11, 667 (1970).
14. L. Varnell et al., *Bull. Am. Phys. Soc.* 17, 899 (1972).
15. R. M. Ronningen et al., to be published.

Table 2.12. Experimental values of $E2$ and $E4$ matrix elements

Nucleus	E_{2^+} (keV)	θ_{lab} (deg)	E_α (MeV)	$\langle 0^+ \|M(E2)\| 2^+ \rangle$ [eb]			$\langle 0^+ \|M(E4)\| 4^+ \rangle$ [eb²]		
				This work	Other measurements	Reference	This work	Other measurements	Reference
^{156}Gd	123	150	11.5	1.963(20)	1.950(11)	*a*		0.64($\frac{6}{7}$)	*a*
^{156}Gd	89.0	150	11.5	2.146(14)					
		150	12.0	2.128(12)					
		150	12.5	2.137(12)					
				Av 2.136(7)	2.142(20)	*a*	0.42(8)	0.41($\frac{12}{19}$)	*a*
^{158}Gd	79.5	150	12.0	2.230(12)	2.233(11)	*b*	0.34($\frac{20}{22}$)	0.40(9)	*b*
					2.23(3)	*c*		0.34(11)	*c*
					2.244(18)	*d*		0.39(13)	*d*
^{160}Gd	75.1	90	15.0	2.269(14)	2.283(14)	*b*	0.35($\frac{9}{7}$)	0.28($\frac{8}{9}$)	*b*
					2.29(2)	*c*		0.36(10)	*c*
^{176}Hf	88.4	150	13.5	2.278(12)					
			14.0	2.290(20)					
				Av 2.281(10)			0.26(12) or −0.76(15)		
^{178}Hf	93.1	150	14.0	2.204(12)			0.23($\frac{11}{20}$) or −0.67(20)		
^{180}Hf	93.3	150	13.5	2.176(12)			0.23($\frac{15}{21}$) or −0.66(20)		
		150	14.0	2.176(20)			0.18($\frac{15}{20}$) or −0.62(25)		
				Av 2.176(10)			Av 0.21($\frac{11}{16}$) or −0.65(16)		

[a] H. J. Wollersheim and Th. W. Elze, *Nucl. Phys.* A278, 87 (1977).
[b] A. H. Shaw and J. S. Greenberg, *Phys. Rev. C* 10, 263 (1974).
[c] K. A. Erb et al., *Phys. Rev. Lett.* 29, 1010 (1972).
[d] H. J. Wollersheim et al., *Phys. Lett.* 48B, 323 (1974); H. J. Wollersheim, W. Wilcke, and Th. W. Elze, *Phys. Rev. C* 11, 2008 (1975).

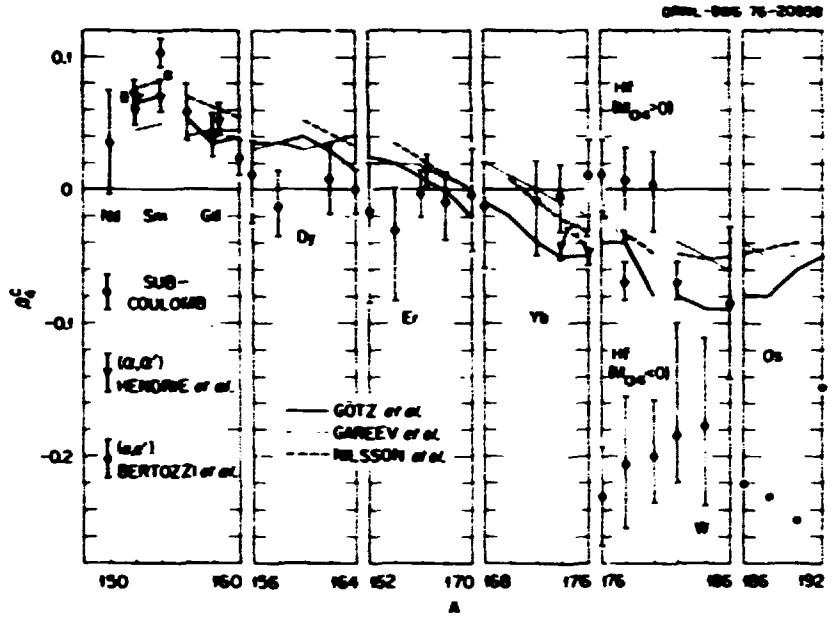

Fig. 2.74. Values of $\beta\xi$ are compared with the theoretical calculations of Nilsson et al. in ref. 7, Götz et al. in ref. 8, and Gareev et al. in ref. 13.

COULOMB EXCITATION MEASUREMENTS OF REDUCED *E2* AND *E4* TRANSITION MATRIX ELEMENTS IN ^{156,158}Dy, ^{162,164}Er, AND ^{168}Yb

R. M. Ronningen[1] H. Kawakami[1,2]
R. B. Piercey[1] B. van Nooijen[1,3]
J. H. Hamilton[1] R. S. Grantham[1,4]
C. F. Maguire[1] W. K. Dagenhart
A. V. Ramayya[1] L. L. Riedinger[5]

Proton-rich Dy, Er, and Yb nuclei off the stability line have been the subject of much investigation in seeking an understanding of the phenomena of "backbending," that is, abrupt changes in the moment of inertia with increase in spin. Nuclei in this region have been studied by *xn* reactions, and more recently, through the stable isotopes via Coulomb excitation produced with beams up to xenon. Crucial to both the extraction of experimental excitation probabilities for high-spin states as well as to the basis for theoretical calculations is a precise knowledge of the *E2* and *E4* reduced-transition matrix elements to the 2^+ and 4^+ members of the ground band. Also, current theoretical calculations[6-13] of ground-state deformations have shown that even a small hexadecapole component in the nuclear shape can have important effects on nuclear properties. These effects include asymmetries, prolate-oblate ground-state shape transition regions, and stability against beta decay, alpha decay, and spontaneous fission.

To provide accurate knowledge of the *E2* and *E4* matrix elements as needed in the analysis of experimental heavy-ion studies and theoretical calculations, we carried out measurements of these matrix elements for the five very low natural abundance (less than or equal to 0.14%, except ^{164}Er, which is 1.6%) isotopes ^{156,158}Dy, ^{162,164}Er, and ^{168}Yb. High-purity (99%) targets were prepared in the Oak Ridge Sector Isotope Separator. The measurements and analysis were carried out as in our galodinium and hafnium studies.[14] Our results are presented in Table 2.13. Our M_{04} values are in agreement, within errors, with the theoretical predictions.[6-13]

1. Vanderbilt University, Nashville, Tenn.
2. On leave from University of Tokyo, Japan.
3. On leave from Delft Technical University, Delft, Netherlands.
4. Oak Ridge Associated Universities Summer Fellow.

Table 2.13. Values of M_{02}, M_{04}, β_2^c, β_4^c, and $B(E2)$ extracted from the present work (Other, less accurate measurements of $B(E2)$ values are given for comparison. The $|M_{02}|$ values are from the average values.)

Nucleus	E_{2^+} (keV)	$\lvert M_{02}\rvert$ eb	$\lvert M_{04}\rvert$ eb^2	β_2^c	β_4^c	This work $B(E2)$ e^2b^2	θ (deg)	Other studies $B(E2)$ e^2b^2
^{156}Dy	138	1.929(7)	$0.21^{+0.16}_{-0.20}$	$0.287^{+0.011}_{-0.014}$	$0.01^{+0.05}_{-0.06}$	3.72(3)	150	3.79(30)
								3.74(23)
								3.74(30)
^{158}Dy	99	2.161(9)	$0.16^{+0.10}_{-0.15}$	$0.323^{+0.007}_{-0.010}$	$-0.01^{+0.03}_{-0.02}$	4.67(4)	150	4.67(40)
								4.56(27)
								4.73(23)
								4.41(25)
								4.76(24)
^{162}Er	101	2.238(7)	$0.16^{+0.14}_{-0.26}$	$0.320^{+0.009}_{-0.017}$	$-0.02^{+0.04}_{-0.07}$	5.06(4)	150	4.89(25)
						4.96(6)	90	5.82(50)
						5.01(3)	Av	
^{164}Er	91	2.341(9)	$0.12^{+0.12}_{-0.13}$	$0.335^{+0.006}_{-0.009}$	$-0.03(3)$	5.48(5)	150	5.20(35)
						5.47(5)	90	5.63(23)
						5.48(4)	Av	
								5.78(32)
^{168}Yb	88	2.402(8)	$0.19^{+0.14}_{-0.19}$	$0.325^{+0.009}_{-0.012}$	$-0.01(^{0.03}_{-0.05})$	5.81(5)	150	5.43(25)
						5.72(6)	90	5.68(95)
						5.77(4)	Av	

5. University of Tennessee, Knoxville.
6. S. G. Nilsson et al., *Nucl. Phys.* A131, 1 (1969).
7. U. Götz et al., *Nucl. Phys.* A192, 1 (1972).
8. P. Möller, *Nucl. Phys.* A142, 1 (1970).
9. H. Flocard, P. Quentin, and D. Vautherin, *Phys. Lett.* 46B, 304 (1973).
10. Bozena Nerlo-Pomorska, *Nucl. Phys.* A259, 481 (1976).
11. Bozena Nerlo-Pomorska, "Electric Multipole Moments of Atomic Nuclei," Report 1538, Institute of Nuclear Research, Warsaw, Poland (1974).
12. Bozena Nerlo-Pomorska, private communication.
13. F. A. Gareev, S. P. Ivanova, and V. V. Pashkevich, *Yad. Fiz.* 11, 1200 (1970); translated in *Sov. J. Nucl. Phys.* 11, 667 (1970).
14. R. M. Ronningen et al., to be published

NUCLEAR TRANSITION PROBABILITY, $B(E2)$, FOR $0^+_{g.s.} \rightarrow 2^+_{first}$ TRANSITIONS

S. Raman C. W. Nestor, Jr.[1]
W. T. Milner P. H. Stelson

A widely used compilation of experimental results for the reduced electric quadrupole transition probability [$B(E2)\uparrow$] between the 0^+ ground state and the first 2^+ state in even-even nuclei was published in 1965.[2] This compilation contained 476 measured $B(E2)$ values from 133 references, leading to adopted $B(E2)$ values for 155 nuclei. We have updated this compilation with coverage of literature up to April 1977. The present compilation contains 1400 entries from 550 references, leading to adopted $B(E2)$ values for 250 nuclei. Preliminary summary drawings (Fig. 2.75) are shown here.

We note that (1) many nuclei have now been studied by more than one technique, (2) the $B(E2)$ values have greatly improved accuracies, especially through inelastic scattering measurements, (3) $B(E2)$ values are now known for a large number of unstable nuclei, mainly via lifetime measurements, usually recoil distance technique or Doppler shift attenuation method, and (4) there are definite indications that (above $A = 150$) the Hager and Seltzer theoretical $E2$ conversion coefficients are systematically about 2% higher than those derived from $B(E2)$ values and $T_{1/2}$ measurements.

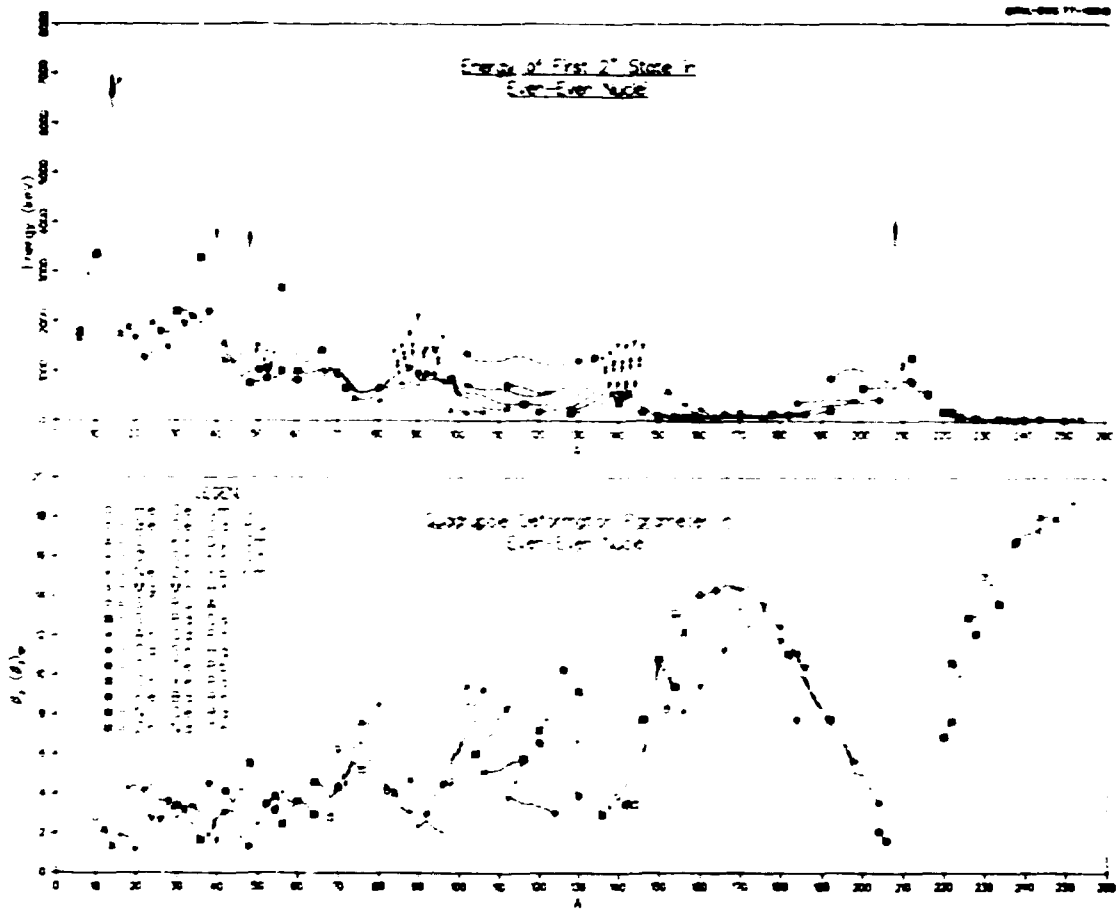

Fig. 2.75. Preliminary summary drawings from a $B(E2)$ compilation.

The present compilation is expected to appear in *Atomic Data and Nuclear Data Tables* by the end of 1977.

1. UCC-ND Computer Sciences Division.

2. P. H. Stelson and L. Grodzins, *Nucl. Data Sect. A* 1, 21 (1965).

NEUTRON YIELDS FROM (α,n) REACTIONS

J. K. Bair J. Gomez del Campo

When the neutron yield from a $^{239}PuO_2$ source, calculated from thin-target (α,n) cross-section data[1,2] and the alpha-particle dE/dx values,[3] was compared with the precision experimental value,[4] the calculated value appeared to be low by about one-third. This discrepancy was surprising but not impossible in view of the stated ±23% error in the cross section and the ±5 to 10% uncertainty in the energy-loss values. Our interest in this discrepancy, together with recent engineering interest in infinitely thick-target (α,n) yields, has prompted the present series of measurements.

The $^{18}O(\alpha,n)$ cross section has been remeasured using an anodized tantalum target containing 50.5 $\mu g\ cm^2$ (±6%) of oxygen. This new value is 1.35 times the value given by Bair and Willard.[1] Because both the ^{17}O and ^{18}O cross sections of Bair and Haas are based on the ^{18}O value of Bair and Willard, the ^{17}O and the ^{18}O cross sections of both references should be multiplied by 1.35 and have a new error assigned of about ±8%.

Total neutron-yield measurements have been made on infinitely thick targets of SnO_2 and $^{28}SiO_2$. The SnO_2 results, calculated using the new cross-section values, are now 9% low compared with the experimental SnO_2 data. The calculated value for

$^{28}SiO_2$ is about 1.5% high. The calculated $^{238}PuO_2$ yield is less accurate than the precision source measurement, because the cross-section data used in the calculation end some 0.4 MeV below the energy of ^{239}Pu alpha particles. If one uses the SnO_2 thick-target data to make this extrapolation, one finds that the calculated value is about 8 to 10% low.

The general agreement between the measured infinitely thick-target yields and those calculated from the thin-target cross section is considered satisfactory in view of the ±8% error on the cross-section data and the 5 or 10% error on the alpha-particle energy-loss values.

The (α,n) yield has also been measured for infinitely thick natural isotopic targets of Si, B, and Mg. The bombarding alpha-particle energy ranges from 3 or 4 MeV to a maximum of 9 MeV.

1. J. K. Bair and H. B. Willard, *Phys. Rev.* 128, 299 (1962).
2. J. K. Bair and F. X. Haas, *Phys. Rev. C* 7, 1356 (1973).
3. L. C. Northcliffe and R. F. Schilling, *Nucl. Data Tables* 7, 233 (1970).
4. J. K. Bair and H. M. Butler, *Nucl. Technol.* 19, 202 (1973).

PRECISION MEASUREMENT OF THE MAGNETIC MOMENT OF THE NEUTRON

W. B. Dress N. F. Ramsey[1]
P. D. Miller G. L. Greene[2]
J. M. Pendlebury[3]

We have completed a precision measurement of the magnetic dipole moment (MDM) of the neutron at the High Flux Reactor, Institute Laue-Langevin, Grenoble, France. This experiment employed a novel method of nuclear magnetic resonance in flowing water in order to monitor the magnetic environment of the neutrons as they passed through our spectrometer. The neutron magnetic resonance spectrometer, designed and built at ORNL for a series of measurements designed to search for the electric dipole moment of the neutron, was modified for the MDM experiment after the last electric dipole measurement.[4]

Figure 2.76 shows the spectrometer as modified for flowing water (omitted from this figure are details of the neutron polarization and detection). The protons in H_2O were polarized by passage through a baffled chamber immersed in a 14-kG field. They then passed either through an outer tube (when used as a monitor) or through the middle tube (normally the neutron beam tube) when comparisons between middle and outer tubes were being made.

Each of the three tubes passes through two rf coils separated by 60 cm (see Fig. 2.77). These coils introduce spin-flips of the Ramsey type in the polarized protons and neutrons. A typical proton resonance is shown in Fig. 2.78, where the frequency of the rf power in the two coils was changed in order to vary the spin-flip transition probability.

The MDM measurement consisted of first calibrating the outer, or monitor, tube by comparing the resonant frequency of the protons in the middle and outer tubes; then the middle tube was emptied, and neutrons were allowed to pass through. The resonant frequency of the neutrons was compared with the proton frequency in the outer tube. The result,

$$\rho = (\nu_n^{mid}/\nu_p^{mid}) \times (\nu_p^{out}/\nu_p^{mid}) ,$$

is the product of the ratios of the four experimentally measured frequencies. The subscripts n and p refer to neutrons and protons respectively; "mid" and "out" refer to the middle and outer tubes. The calibration (comparison of proton frequencies) was remeasured after each run.

The apparatus was rotated by 180° in order to cancel small effects, such as the Doppler shift due to motion toward and away from the rf coils; any constant phase shifts due to geometry or electrical circuit differences; and the Millman shift, which is produced by fringing effects upon entering and leaving the rf regions. The most serious effect, the Bloch-Siegert shift due to the presence of a contrarotating magnetic field (the other half of our applied oscillating rf field), was determined by varying the rf power and extrapolating to zero.

The preliminary result, as yet uncorrected for temperature effects on the diamagnetism of dissolved oxygen in the water (an effect of a few parts in 10^5), is

$$\mu_n/\mu_p = 0.68497969\ (19) ,$$

where 19 is the uncertainty in the last two digits. Corrections have been made for the geometry of the H_2O sample, the presence of the H_2O near the neutron beam, and the shielding of the protons in H_2O. This number is nearly 100 times more precise than the previous measurement.[5] Simple symmetry theory without any symmetry breaking gives a prediction of exactly two-thirds for $|\mu n/\mu p|$.

1. Harvard University, Cambridge, Mass.
2. Graduate student from Harvard University, Cambridge, Mass.
3. University of Sussex, Brighton, United Kingdom.
4. W. B. Dress et al., *Phys. Rev. D* 15, 9 (1977).
5. V. W. Cohen, N. K. Corngold, and N. F. Ramsey, *Phys. Rev.* 104, 283 (1956).

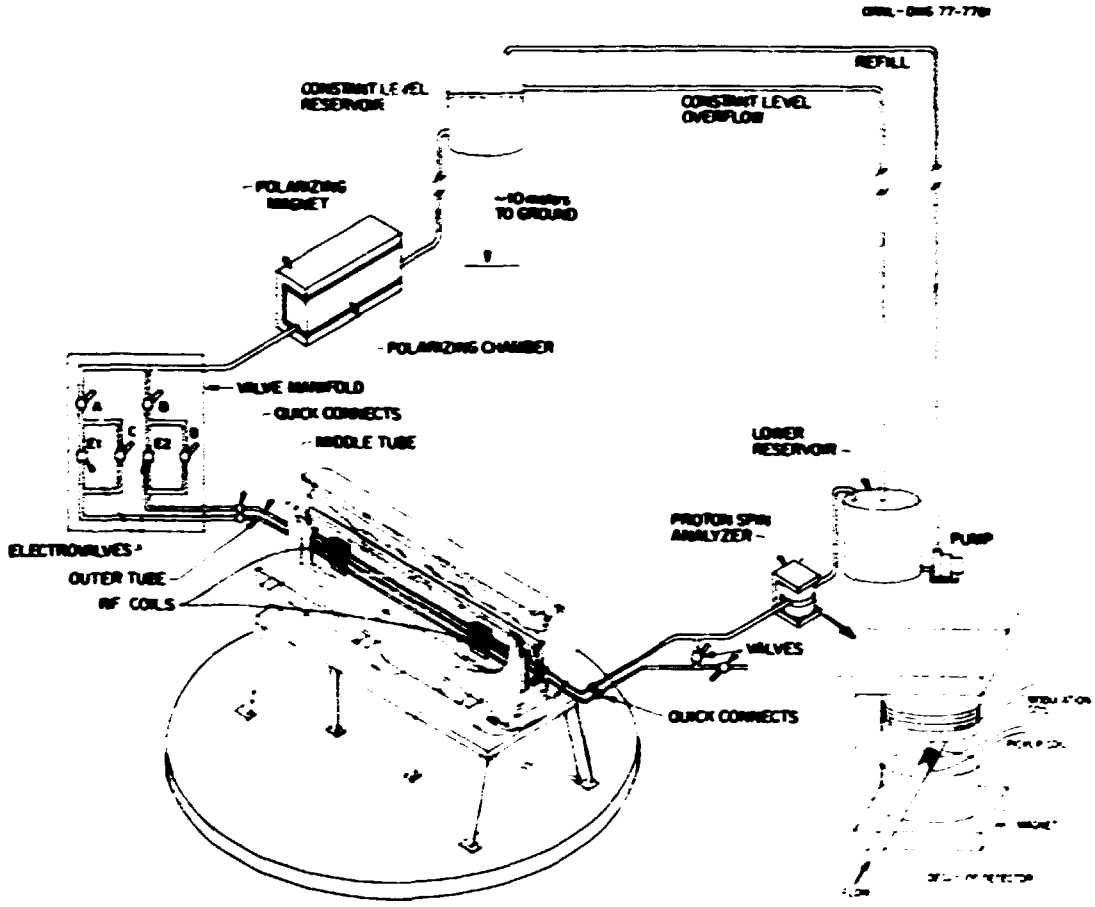

Fig. 2.76. Pictorial representation of the experiment showing the H_2O (proton) circuit. For clarity, the details of the neutron polarization and detection have been suppressed.

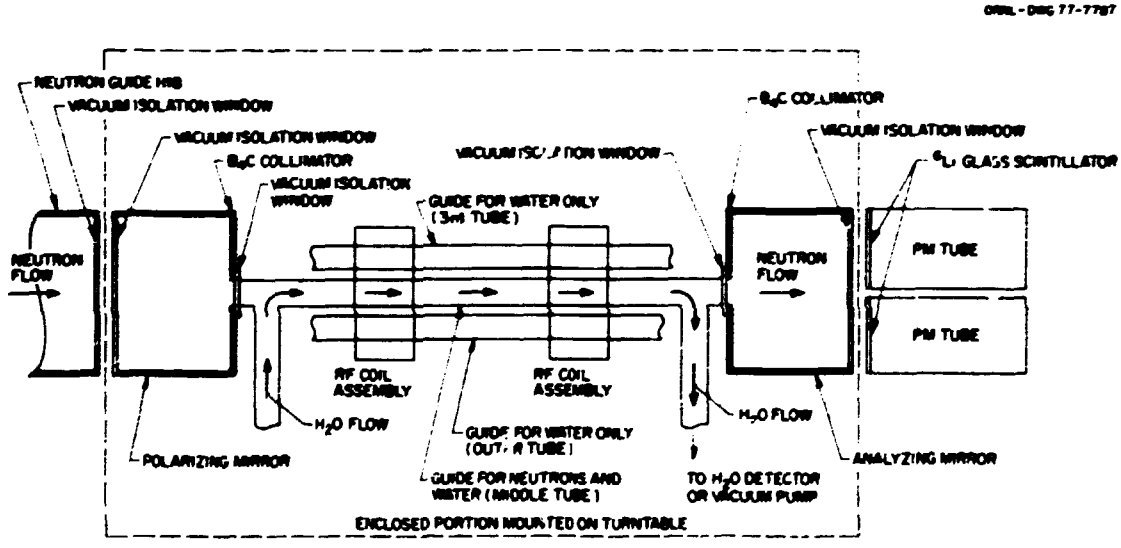

Fig. 2.77. Schematic view of both neutron and proton flows. For neutron measurements, the middle tube was emptied of water.

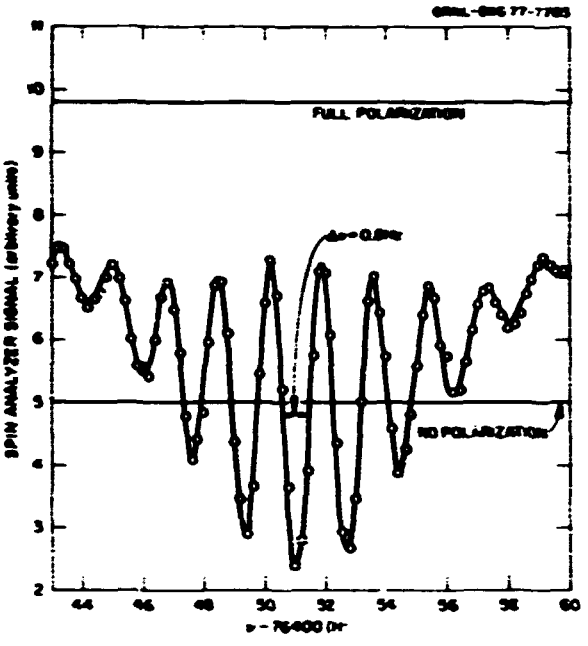

Fig. 2.78. Typical proton resonance. Plotted is the signal from a phase-detection circuit measuring the signal strength in the pick-up coil as a function of the frequency in the rf coils.

NEW RESULTS FROM STUDIES ON RADIOACTIVE HALOS

S. Raman
R. V. Gentry[1]
C. J. Sparks, Jr.[2]
M. O. Krause[1]
W. H. Christie[3]
E. Ricci[3]
H. L. Yakel[2]
C. A. Gossett[4]
W. T. Milner
J. B. Bates[5]

Despite the pessimism generated by calculations showing that the formation of superheavy elements during most of the *r*-process is quite difficult, several intensive searches have been undertaken in the past for these elements. A recent letter[6] presented evidence for the existence of several superheavy elements. This discovery was based on proton excitation of x-ray spectra from monazite inclusions extracted from Madagascar mica in which the inclusions had generated giant halo discolorations. A more sensitive x-ray fluorescence experiment was carried out subsequently at the Stanford Synchrotron Radiation Project. No evidence was found[7] in the x-ray spectra for the existence of superheavy elements in these inclusions. For example, in Fig. 2.79, we have compared the x-ray spectra from sample 19-D

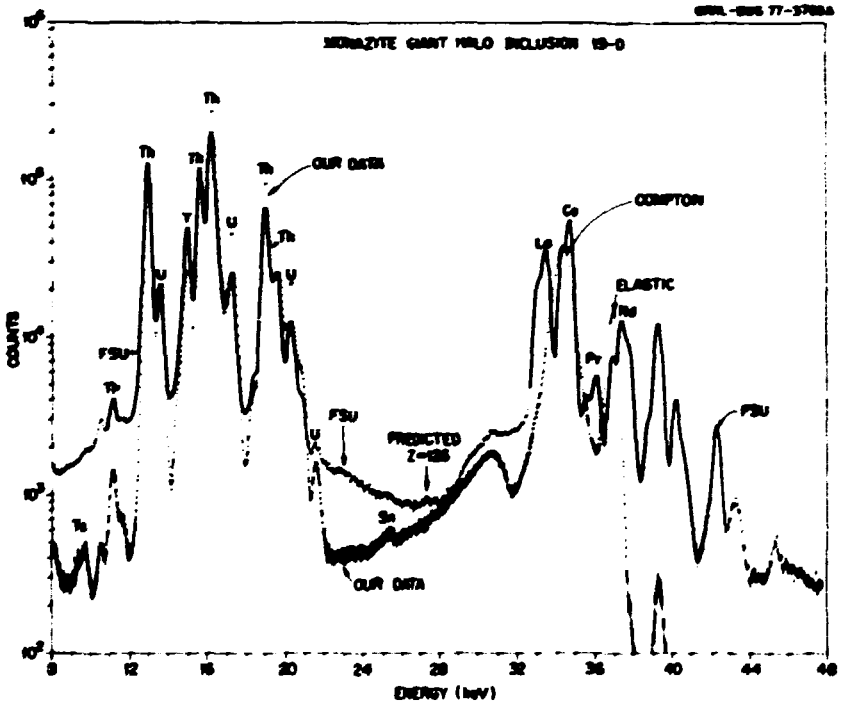

Fig. 2.79. Comparison of our data with those obtained at Florida State University.

excited either by 5.9-MeV protons (Florida State University data) or by 37.5-keV photons (our data). Any x-ray peak attributable to superheavy elements should be enhanced about 50 times in our data compared with the Florida State University data.

Data from the Stanford experiment and earlier ion-microprobe mass-spectrometry experiments carried out at Oak Ridge have, however, provided unexpected new results. These results are from several opaque amorphous inclusions, accompanied by both regular and giant halos, extracted from the same piece of Madagascar mica which has been a rich source of transparent crystalline monazite inclusions. In the x-ray fluorescence results, the amorphous inclusions show a depletion of lead (Fig. 2.80) by a factor of 7. The ion-microprobe results are even more striking (Fig. 2.81). While the spectra from monazite inclusions show ^{208}Pb and ^{206}Pb peaks arising from the decay of ^{238}U and ^{232}Th, respectively, those from the opaque inclusions show only the ^{208}Pb peak. The ^{206}Pb peak is diminished by a factor of 20 compared with the monazite inclusion. These observations raise some interesting geological and cosmological questions. Finally, new measurements (infrared and Raman spectroscopy) are under way at Oak Ridge to test the hypothesis[8] that the giant halos are produced by knock-on protons due to the interaction of alpha particles with water presumed to be present in or near the inclusions.

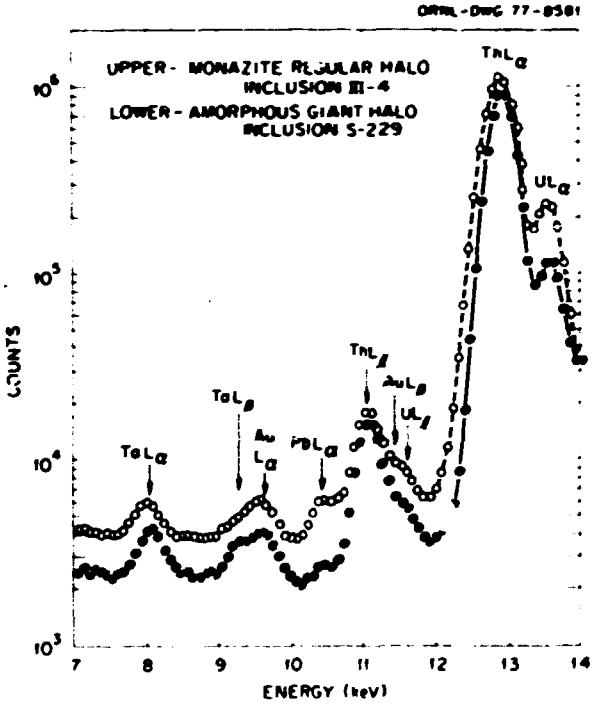

Fig. 2.80. Selected portions of spectra excited by synchrotron radiation.

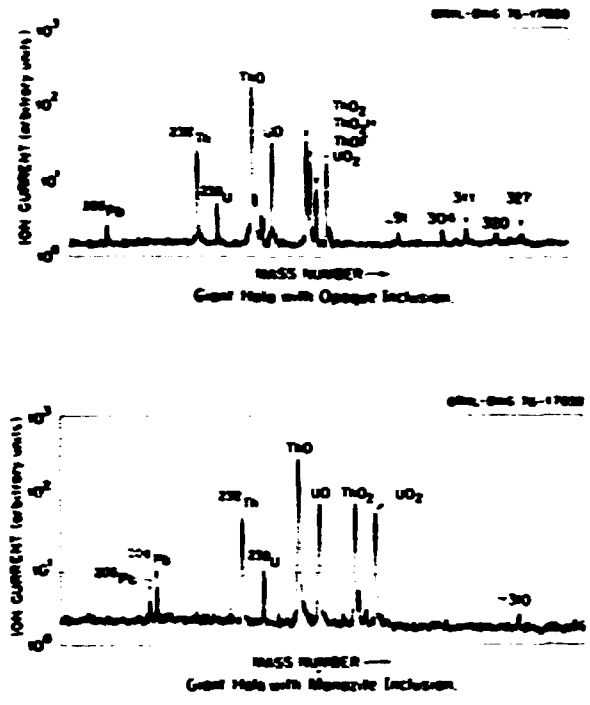

Fig. 2.81. Data obtained with an ion-microprobe mass spectrometer. The peaks above $A = 290$ are due to molecular ions.

---

1. Chemistry Division.
2. Metals and Ceramics Division.
3. Analytical Chemistry Division.
4. Great Lakes Colleges Association, DePauw University, Greencastle, Ind.
5. Solid State Division.
6. R. V. Gentry et al., *Phys. Rev. Lett.* 37, 11 (1976).
7. C. J. Sparks, Jr., et al., *Phys. Rev. Lett.* 38, 205 (1977).
8. U. von Wimmersperg and J. P. F. Sellschop, *Phys. Rev. Lett.* 38, 886 (1977).

NEUTRON PHYSICS

INTRODUCTION

During this report period, the nuclide ^{209}Pb was studied in great detail at an excitation energy of 7.37 to about 8.0 MeV via all possible neutron techniques available at ORELA. The excellent energy resolution (less than 1 keV) of ORELA is needed to interpret both neutron measurements and previous photoneutron measurements. In order to determine the spins, parities, and neutron widths of the excited states in this energy region, a detailed multilevel

analysis was made on high-resolution total cross-section data and elastic angular distribution data. These assignments are needed to permit gamma-ray radiative strengths (also measured at ORELA) to be assigned to the appropriate multipole, that is, $E1$ or $M1$. The combined experiments have succeeded in locating about 50% of the $M1$ strength expected for this nuclide, with a sizable fraction of it at an excitation energy of 7.5 MeV. Four states at 7.5 MeV with spins at 1^+ have a factor of 4 to 5 larger gamma and neutron widths than the average of other 1^+ states and constitute a "doorway" in both the neutron and photon channels.

Information was also obtained on the $E2$ strength for ^{208}Pb, possible doorway states in the s-, p-, and d-wave neutron channels, and for p- and d-wave neutron strength functions for the three permissible J values. Additional work is required to investigate the region above an excitation energy of 8.0 MeV to locate definitely the remainder of the $M1$ strength and to search for higher-energy doorway states.

Another discovery of the period was the identification of three $T = {}^3/_2$ analog states from high-resolution total cross-section measurements on ^{24}Mg. This is the first time that a $T_>$ state had been reported from neutron measurements. The strengths of these states give information on the isospin impurities of the states and the average mixing-matrix element.

A program to measure and analyze the differential elastic-scattering cross section at several angles at both the 80- and 200-m flight stations was initiated. The measurement of the shape of resonances at appropriate angles is a very sensitive method of determining l values of resonances, as was shown for ^{207}Pb and ^{24}Mg. This technique supplements the procedure we have used previously of assigning J's and l's to the resonances from a careful analysis of total cross-section data alone, such as the analysis done for ^{40}Ca presented in this report.

Another new program was developed during the period to enable predictions to be made of radiative widths for medium-weight nuclides. This work resulted from investigations of the $3p$ resonance near $A = 100$ in neutron and proton strength functions. Using the codes developed, available level densities, and a simple parameterization of the gamma-ray strength function, an excellent fit is obtained to the average radiative widths for s-wave resonances for $75 < A < 130$. The resulting prediction of the radiative widths of p-wave resonances for A about 90 requires significant valency capture to obtain agreement with experiment.

New developments in the capture cross-section program were improvements in electronics, permitting reliable measurements to be made up to 2 MeV (2 μsec after the gamma flash), and a thin-wall gas sample holder for rare-gas samples.

After several years of effort, two experiments relating to neutron standard cross sections were concluded with gratifying results. The results of a cooperative experiment at Harwell on the (n,p) scattering angular distribution at 27.3 MeV is considered to have an uncertainty of approximately less than 2%. Direct measurements of the ^{6}Li(n,α) cross section have been analyzed to give a value of 3.34 b at 244 keV with an uncertainty of about 3%, in excellent agreement with the value obtained from R-matrix calculations fitting the ORELA total cross-section data.

Active programs have continued for the measurement of fission, capture, and total cross sections. The fission measurements are on the actinides such as ^{243}Cm and ^{245}Cm. In order to measure the fission cross section of ^{241}Am, a new fission chamber with an innovation to reduce the effects of alpha pileup is being developed. The capture measurements were concerned with nuclides such as ^{208}Pb and ^{209}Bi, of interest in nucleosynthesis; ^{232}Th and ^{91}Zr, of interest in reactor design; and nuclides of interest to basic nuclear physics. The total cross-section measurements were on nuclides such as ^{7}Li, of interest in fusion; ^{237}Np, of interest in subthreshold fission; and the isotopes of zinc.

Many papers have been published on the results of ORELA measurements; they are listed under "Publications" in this report. In this section, only topics of most current interest have been selected for presentation.

POSITIVE IDENTIFICATION OF $J^\pi = 1^+$ ($M1$ RADIATING) LEVELS IN ^{208}Pb

D. J. Horen J. A. Harvey
N. W. Hill[1]

From high-resolution neutron transmission and elastic scattering measurements on ^{207}Pb, we have been able to make the first definitive assignment of $J^\pi = 1^+$ to levels in ^{208}Pb. By combining our results with the ^{207}Pb(n,γ) data from Allen and Macklin,[2] we can make the first positive assignment of $M1$ strength in ^{208}Pb. The search for such strength has been the subject of numerous works published during the past

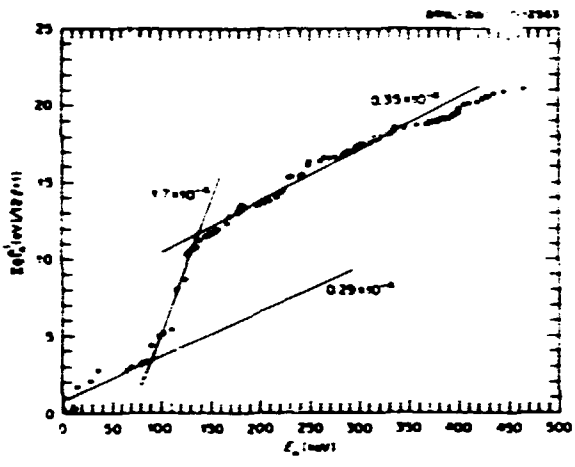

Fig. 2.82. Plot of $\Sigma\, g\Gamma_n^l/(2I+1)$ vs neutron energy. The slope corresponds to the p-wave strength function. A radius of 8.042 fm was used in calculating the reduced neutron widths.

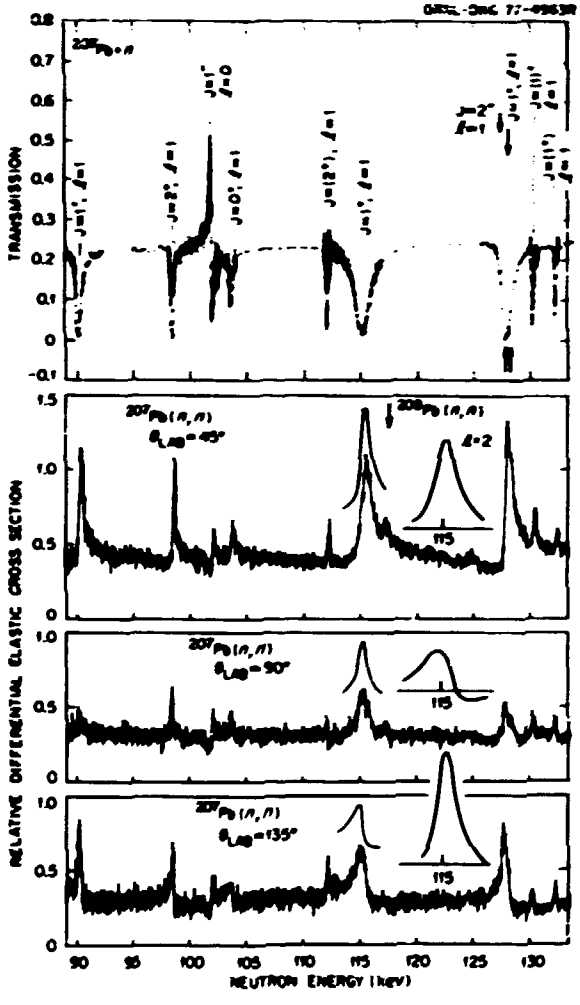

Fig. 2.83. Neutron transmission and differential elastic scattering spectra for ^{207}Pb. The differential cross sections are given in relative units. The calculated cross sections for the 115.7-keV (resonance plus interference only) resonance (assuming $l = 1$ or 2) normalized to the same relative scale as the experimental data at 45° are also shown for comparison. The potential phase shifts were taken as $\phi_0 = -40.1°$ and $\phi_1 = -1.3°$.

ten years. Much confusion has been generated due to the inability of the experimental methods employed to allow the assignment of unambiguous parity to levels deduced to have $J = 1$.

In our work,[1] a significant change in the p-wave strength function ("doorway state") was observed to occur at $E_n \approx 120$ keV (i.e., 7.49 MeV in ^{208}Pb) (see Fig. 2.82). The primary resonances responsible for this change were determined from the transmission data to have $J = 1$. The parities have been determined uniquely from the observed changes in shape of the resonance cross sections [i.e., $\sigma(E,\theta)$] with angle (see Fig. 2.83).

Additional work is required to locate definitively the remainder of the $M1$ strength in ^{208}Pb and to resolve inconsistencies in reported works on this subject before a comparison with theoretical predictions will become meaningful.

---

1. Instrumentation and Controls Division.
2. B. J. Allen and R. L. Macklin, *Proceedings of the Third Neutron Cross Section and Technology Conference*, Knoxville, Tenn., CONF-710301 (March 1971), p. 764.
3. D. J. Horen, J. A. Harvey, and N. W. Hill, *Bull. Am. Phys. Soc.* 22, 543 (1977); paper submitted to *Physical Review Letters*.

PHOTON AND d-WAVE NEUTRON $J^\pi = 1^-$ CORRELATED DOORWAY STATE IN ^{208}Pb

D. J. Horen J. A. Harvey

In a study of the ^{207}Pb + n reaction, we have shown that a number of $J^\pi = 1^-$ resonances are formed by an admixture of $(s+d)$-wave neutrons.[1] The fact that the reduced neutron width for the d-wave component of the 256.43-keV resonance represents an appreciable fraction of the Wigner limit has led us to examine the possibility that this resonance might be associated with a doorway state in the ^{207}Pb + n reaction. In Fig. 2.84, we plot the reduced neutron widths for the s- and d-wave components of observed $J^\pi = 1^-$ resonances. Here the reduced width is defined as $\Gamma_n^l/\sqrt{E_n}v_l$, where Γ_n^l is the observed neutron width, E_n is the neutron energy in eV, and v_l is the penetration factor for neutrons with orbital angular momentum l. Also shown in Fig. 2.84 are the ground-state radiative widths determined from measurements of the ^{207}Pb(n,γ) and ^{208}Pb(γ,n) reactions.[2-5]

Note that strength in the s-wave channel is concentrated in the vicinity of 450 keV, while, as mentioned above, the d-wave strength is mainly contained in the 256.43-keV resonance. The photon channel also shows an enhancement of strength in the vicinity of 256 keV. Lane has pointed out that the $\nu 4s$-$\nu 3p^{-1}$ and $\nu 3d$-$\nu 3p^{-1}$ $1p$-$1h$ states do not participate completely in the giant $E1$ resonance, and part of the

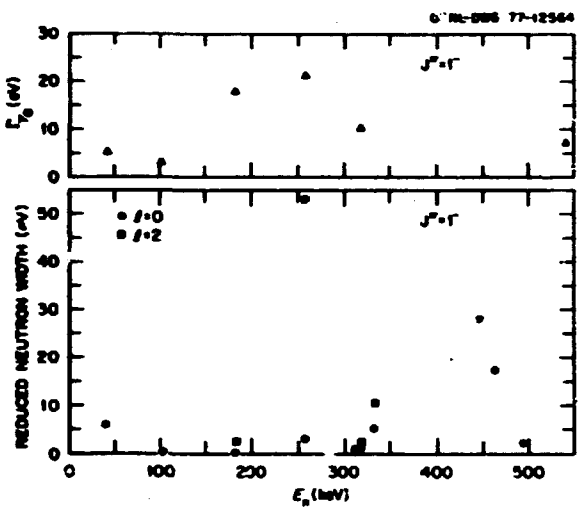

Fig. 2.84. Plots of ground-state radiative widths and reduced neutron widths vs neutron energy for $J^\pi = 1^-$ resonances in ^{207}Pb + n.

dipole strength from these configurations is located in the region of 3 to 7.6 MeV in ^{208}Pb.[6]

We suggest that there is a correlated doorway state (i.e., in the $E1$ photon and d-wave neutron channels) in the vicinity of 776 keV which is associated with a fragment of the $\nu 3d$-$\nu 3p^{-1}$ configuration. Whether there is a correlation in the photon channel with the doorway state near 450 keV in the s-wave channel remains to be investigated.[7]

---

1. D. J. Horen, J. A. Harvey and N. W. Hill, to be published in *Physics Letters*.
2. S. Raman, M. Mizumoto, and R. L. Macklin, (private communication).
3. C. D. Bowman et al., *Phys. Rev. Lett.* 25, 1302 (1970).
4. L. C. Hacke and K. G. McNeill, *Can. J. Phys.* 53, 1422 (1975).
5. R. E. Toohey and H. E. Jackson, *Phys. Rev. C*6, 1440 (1972).
6. A. M. Lane, *Ann. Phys.* 63, 171 (1971).
7. This doorway state has been pointed out by F. T. Seibel, E. G. Bilpuch, and H. W. Newson, *Ann. Phys.* 69, 451 (1972).

FIRST MEASUREMENT OF SEPARATED NEUTRON *p*-WAVE STRENGTH FUNCTIONS FOR NON-ZERO SPIN TARGETS

D. J. Horen J. A. Harvey
N. W. Hill[1]

In the case of neutron scattering on targets with non-zero spin ($I \neq 0$), the channel spin can assume two values, that is, $s = I \pm 1/2$. Because ^{207}Pb has $I = 1/2$, neutrons which carry in one unit of angular momentum can form levels in the ^{208}Pb compound system with $J = 0^-$, 1^-, and 2^-. Levels having $J = 0^-$ can be formed only by neutrons which have their intrinsic spin opposite to the direction of their angular momentum (i.e., $p_{1/2}$), while those having $J = 2^-$ must be formed with neutrons in a $p_{3/2}$ state. Hence, measurements of the neutron widths of resonances having $J = 0^-$ or 2^- yield information on the $p_{1/2}$ and $p_{3/2}$ neutron strength functions respectively.

If the compound-nucleus theory is applicable, the spin-spin interaction is negligible, and the strength function depends solely on l and J, then the strength function for forming $J^\pi = 1^-$ resonances should be equal to the sum of the strength functions for forming $J^\pi = 0^-$ and 2^- resonances.

From analyses of our transmission and scattering data on ^{207}Pb, we have been able to make definitive or probable assignments of about 24 resonances each having $J^\pi = 0^-$ or 2^- and approximately 40 resonances with $J^\pi = 1^-$ in the neutron energy interval 3 to 400 keV. The p-wave strength functions for each J value are shown in Fig. 2.85. From the shapes of the curves of $\Sigma\Gamma_n^l(J)$ vs E_n above the "doorway state" (i.e., E_n greater than 150 keV), we find $S^1(0^-) = 4.1 \times 10^{-4}$,

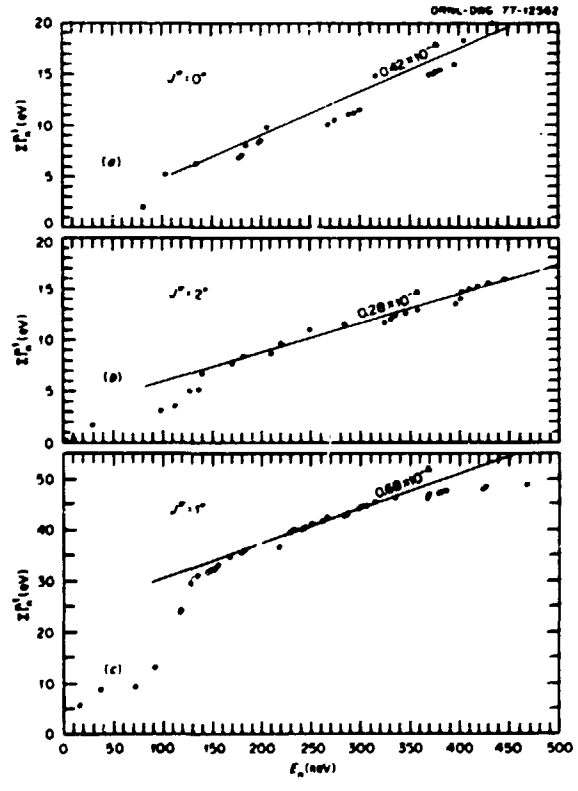

Fig. 2.85. Plot of $\Sigma\Gamma_n^l$ vs neutron energy for p-wave resonances with (a) $J = 0^-$, (b) $J = 2^-$, and (c) $J = 1^-$.

$S^1(2^+) = 2.8 \times 10^{-5}$, and $S^1(1^+) = 6.7 \times 10^{-5}$. These results are consistent with the assumption presented previously and represent the first measurement of *p*-wave neutron strength functions for each of the three compound states (i.e., three different *J*) that can be formed in the scattering of neutrons on targets with non-zero spin.

These measurements were made possible by the high resolution achievable at ORELA.

1. Instrumentation and Controls Division.

NEUTRON CAPTURE BY ^{208}Pb AND ^{209}Bi

R. L. Macklin J. Halperin[1]
R. R. Winters[2]

For these closed 126 neutron-shell nuclei, the binding energy of an additional neutron is exceptionally low (3.9 and 4.6 MeV respectively). Correspondingly, the average capture cross sections are very low and are best measured with good experimental resolution to individual resonances. Both nuclei are on the *s*-process path of stellar nucleosynthesis in the terminal loop. Two weak capturing resonances near stellar interior temperatures (about 30 keV) were discovered in ^{208}Pb + *n* (at 43.29 and 47.26 keV) well below the previously known 70- and 78-keV resonances. Large radiative widths (about 2 eV) were also found for a group of six resonances (721 to 826 keV) also seen in transmission and assigned spins of $^5/_2$. The spins are half way to the ground-state $^9/_2$ of ^{209}Pb, allowing an extra 2 MeV or so for the primary gamma ray via quadrupole radiation. In ^{209}Bi + *n*, the level density is enough greater than for ^{208}Pb + *n* that average capture in the energy range 30 to 900 keV, where some individual levels were missed, could still be measured. Individual resonance parameters were fitted to the capture data from 2.6 to 30 keV as well as to those resonances reported in transmission from 30 to 70 keV. The ^{209}Bi(n,γ) work has been reported in the *Physical Review*[3] and the ^{208}Pb(n,γ) work in the *Astrophysical Journal*.[4]

1. Chemistry Division.
2. Denison University, Granville, Ohio.
3. R. Macklin and J. Halperin, "Resonance Neutron Capture by ^{209}Bi," *Phys. Rev. C* 14, 1359 (1976).
4. R. L. Macklin, J. Halperin, and R. R. Winters, "Neutron Capture by ^{208}Pb at Stellar Temperatures," to be published in *Astrophysical Journal*.

^{232}Th(n,γ) Cross Section

Below a neutron energy of a few keV, the resonance parameters for thorium have been well determined in earlier work. At much higher energies of primary importance in some breeder and converter nuclear reactor cycles, the earlier data are rather widely scattered. Our measurements from 2.6 to 800 keV support the earlier results below 4 keV and support recent results reported since 1972 in lying significantly below current evaluations (by about 30% from 100 to 400 keV in the case of our data and ENDF/B-IV). The effect of inelastic scattering to the 49-keV level shows up strongly as competition with capture above the inelastic threshold. Intermediate structure was not found, but the cross-section fluctuations (in the 0.25-keV steps up to 100 keV) were measured.

FINE STRUCTURE *F* A NEW *M*1 GIANT RESONANCE AND THE TAIL OF THE ISOSCALAR *E*2 GIANT RESONANCE IN ^{208}Pb

S. Raman G. L. Morgan[2]
M. Mizumoto[1] J. Halperin[3]
R. L. Macklin G. T. Chapman[2]
G. G. Slaughter R. R. Winters[4]

In a simple shell-model picture, two 1^+ states are expected in ^{208}Pb at about 7 MeV, resulting from the one-particle, one-hole ($1p$-$1h$) configurations $\nu(i^{-1}_{13/2}, i_{11/2})$ and $\pi(h^{-1}_{11/2}, h_{9/2})$. These states are expected to nearly exhaust a transition strength of about 36 μ_0^2. The inclusion of $2p$-$2h$ configurations results in the splitting of these states into many components.

We have identified 18 *M*1 transitions in ^{208}Pb and have measured their ground-state radiative widths in a study of the ^{207}Pb(n,γ) reaction combined with the results from recent transmission and elastic-scattering measurements.[5] In the excitation region between 7.37 and 8.23 MeV, about 50% of the expected total *M*1 strength in ^{208}Pb has been located. Recent (γ,n) polarization measurements[6] have located an additional about 30% *M*1 strength in the unbound region (see Fig. 2.86).

Primary *E*2 transitions are extremely rare in (n,γ) reactions. In ^{208}Pb, we have also obtained the ground-state radiative widths of 25 *E*2 transitions from 2^+ resonances (see Fig. 2.87). They represent 0.5% of the total energy-weighted isoscalar sum-rule strength, the expected strength in the Lorentzian tail

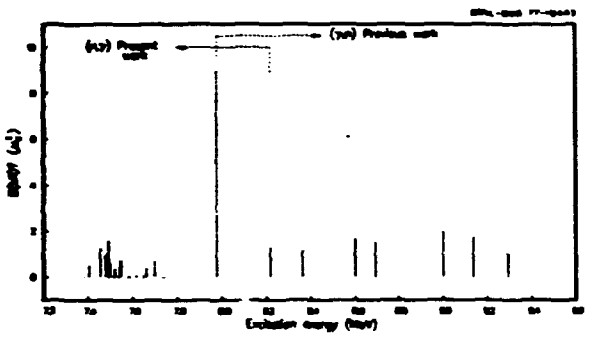

Fig. 2.86. Summary of $M1$ strengths in the unbound region of ^{208}Pb. Previous work refers to the findings of Laszewski, Holt, and Jackson (ref. 6).

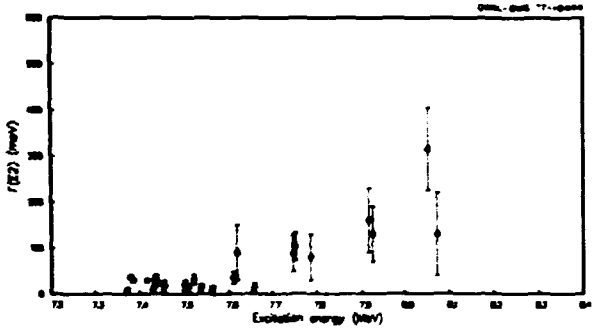

Fig. 2.87. Summary of $E2$ strengths in the unbound region of ^{208}Pb.

assuming that a giant $E2$ resonance 3 MeV wide at 10.9 MeV is about 3%.

---

1. Japan Atomic Energy Research Institute, Tokai-mura, Japan.
2. Neutron Physics Division.
3. Chemistry Division.
4. Denison University, Granville, Ohio.
5. D. J. Horen, J. A. Harvey, and N. W. Hill, to be published in *Physical Review Letters*.
6. R. M. Laszewski, R. J. Holt, and H. E. Jackson, *Phys. Rev. Lett.* 38, 813 (1977).

PARITY OF THE $J = 1$, 7.060-MeV LEVEL IN ^{208}Pb

D. J. Horen F. P. Calprice[1]
D. Mueller[1] D. Kouzes[1]

The 7.061-MeV level in ^{208}Pb has been tentatively assigned by Freedman et al.[2] as having a value of $J^{\pi} = 1^{+}$. Because this level has a ground-state radiative width of about 23 eV, such an assignment would exhaust a significant fraction of the expected $M1$ strength in ^{208}Pb. In fact, the sum of reported $M1$ strength in ^{208}Pb by researchers at ORNL[3-4] and at Argonne[5-7] and by Freedman et al.[2] exceeds that predicted in theoretical calculations. For this reason, it was considered desirable to perform experiments that might verify levels which have been tentatively assigned as 1^{+} and have large Γ_{γ_0}.

The Princeton University AVF cyclotron and QDDD spectrograph were utilized to measure the ^{207}Pb(d,p) reaction. An experimental resolution of about 10.5 keV was achieved. Preliminary angular distributions for forming levels at 7.060 and 7.080 MeV are shown in Fig. 2.88. Among others, Freedman et al.[2] have assigned the 7.080-MeV level as having $J^{\pi} = 1^{-}$. From Fig. 2.88, it can be seen that the 7.060- and 7.080-MeV levels have almost identical stripping patterns and, hence, most likely the same parity. This would imply negative parity for the 7.060-MeV level, thus removing it from being associated with $M1$ strength in ^{208}Pb. However, final conclusions on this point must await the results of final analysis and DWBA calculations.

---

1. Princeton University, Princeton, N. J.
2. S. J. Freedman et al., *Phys. Rev. Lett.* 37, 1606 (1976).
3. D. J. Horen, J. A. Harvey, and N. W. Hill, *Bull. Am. Phys. Soc.* 22, 543 (1977).
4. S. Raman et al., *Bull. Am. Phys. Soc.* 22, 542 (1977).
5. R. E. Toohey and H. E. Hackson, *Phys. Rev. C* 6, 1406 (1972).
6. R. J. Holt and H. E. Jackson, *Phys. Rev. Lett.* 36, 244 (1976).
7. R. M. Lazewski, R. J. Holt, and H. E. Jackson, *Phys. Rev. Lett.* 38, 813 (1977).

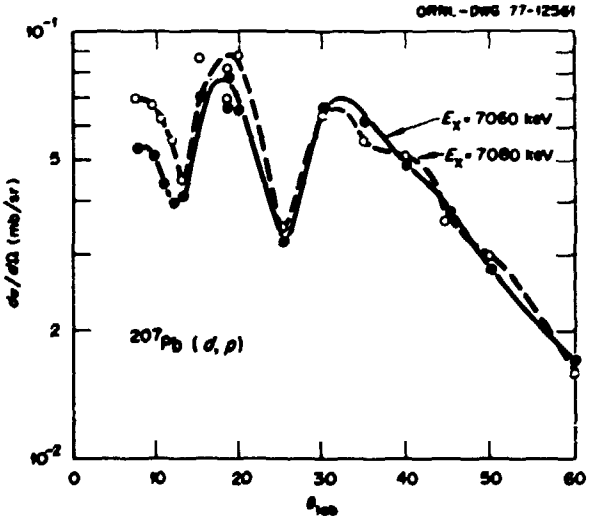

Fig. 2.88. Preliminary angular distributions for forming the 7.060- and 7.080-MeV levels in ^{208}Pb.

RESONANCES IN $^{207}Pb + n$ OBSERVED IN TRANSMISSION AND ELASTIC-SCATTERING MEASUREMENTS

D. J. Horen J. A. Harvey
N. W. Hill[1]

The analyses of high-resolution neutron transmission and elastic-scattering data on ^{207}Pb have been completed in the energy interval 3 to 500 keV. Approximately 120 resonances have been analyzed and definite or probable J^π values assigned. In this energy interval, only two s-wave resonances with $J^\pi = 0^-$ have been observed. The main neutron s-wave strength is located in the vicinity of $E_n = 450$ keV and supports the suggestion of a common "doorway state" in the lead isotopes as proposed by Farrell et al.[2]

Because the probability of missing $J = 1$, s-wave resonances in these measurements is rather small, the ratio of the number of observed $J^\pi = 1^+$ to $J^\pi = 1^-$ resonances (i.e., about 4:1) would imply that either there are a number of missed $J^\pi = 1^-$ resonances which are formed by neutrons with $l = 2$, or that the expression for the level density, $\rho(E,J)$, has a parity-dependent term in this energy interval. It should be noted that we have tentatively assigned three resonances with $J^\pi = (1^-)$ and $l = 2$. Also, there are a number of levels reported to have $J^\pi = 1^-$ in the bound-state region of ^{208}Pb, but only one as yet with $J^\pi = (1^+)$, and this latter assignment is tentative.

These results are being prepared for publication.

1. Instrumentation and Controls Division.
2. J. A. Farrell et al., *Phys. Lett.* 17, 286 (1965).

ABSOLUTE MEASUREMENT OF THE $^6Li(n,\alpha)$ CROSS SECTION IN THE REGION OF THE 244-keV RESONANCE

C. Renner[1] N. W. Hill[2]
J. A. Harvey K. Rush[2]

For nearly 30 years, the $^6Li(n,\alpha)$ cross section has been used as a standard for neutron cross-section measurements below about 500 keV. The $^6Li(n,\alpha)$ cross section was selected as a standard cross section because it varies as $1/v$ below about 10 keV and because of its relatively large cross section, the large Q value of the reaction, and the availability of ^6Li detectors (notably ^6Li glass scintillators). About three years ago, after 25 years of effort involving dozens of independent measurements of the $^6Li(n,\alpha)$ cross section at many different laboratories using different techniques[3] [which produced values at the peak of the 244-keV resonance differing by about 40% (from 2.7 to 3.7 b)], it was hoped that the peak value of 3.0 b from direct (n,α) measurements was known to about 5%. However, using a multichannel multilevel R-matrix analysis of total cross-section data, Hale[4] obtained a value of 3.5 b for this (n,α) peak cross section; when he also included $(t + \alpha)$ elastic scattering, Hale obtained a value of 3.4 b, obviously in disagreement with the directly measured (n,α) value.

In 1975, a program was begun at ORELA to measure the $^6Li(n,\alpha)$ cross section, using a neutron beam filtered through 8 or 12 in. of Armco iron, which produces several monoenergetic groups of neutrons about 2 keV wide). Signal-to-background ratios of greater than about 1000:1 can readily be achieved using this technique; at the same time, problems arising from the gamma flash are eliminated. Of particular interest are the neutron groups at 82, 128, 137, 168, 184, 219, 244, 274, and 311 keV.

The $^6Li(n,\alpha)T$ events were detected either by a 1-mm-thick, 25.4-mm-diam piece of ^6Li glass scintillator or by a 12.7-mm-thick, 111-mm-diam piece of ^6Li glass scintillator. The 12.7-mm lithium glass was mounted in a transmission configuration and was used as the neutron monitor. The ^6Li content of the 1-mm piece of ^6Li glass was determined from the $1/v$ slope of the total cross section measured from about 0.05 to 100 eV. The ^6Li content of the 12.7-mm piece was obtained from σ_T measurements ranging from about 10 to 1000 eV. Both pieces of ^6Li glass were scanned with a narrow neutron beam and the scanning showed that the ^6Li content was uniform to slightly less than 1%. Pulse-height distributions with both detectors were measured for about 20 neutron groups, and backgrounds were measured for most groups. Although the efficiency for a neutron interacting in the ^6Li glass detector is quite low, the probability of observing the (n,α) events which have taken place in the ^6Li glass scintillator is very high (about 99%) and it can be determined accurately. Monte Carlo calculations must be made in order to correct for the scattering of the silicon, oxygen, and lithium in the lithium glass and for the silicon and oxygen in the quartz light pipe and phototube glass. This correction amounts to 10% at 244 keV with a 3-mm quartz light pipe and 20% at 311 keV. In order to check these correction factors, we made a

comparison between the counting rates of the 1- and the 12.7-mm ^{6}Li glass after a normalization to the same flux and multiple-scattering corrections were applied. Although the corrections involved were very large for the 12.7-mm glass (30% at 244 keV and 50% at 310 keV), we obtained good agreement (about 4%) between the counting rates of both detectors at the two energies. From this we can estimate an accuracy of about 1% for the correction factor for the 1-mm lithium glass. Another experiment is in progress in order to check these correction factors more accurately. Using a program written by W. E. Kinney, Monte Carlo calculations for the lithium glass detectors were made.

The neutron flux was measured with an NE-110 detector either 7.5 or 2.0 cm thick. The pulse-height distributions for the same ~20 neutron groups and backgrounds were measured for both NE-110 detectors. For the 7.5-cm-thick NE-110 flux monitor, the efficiency for a neutron interaction in the detector is very high (about 99% at 220 keV) and can be determined accurately vs neutron energy, but the probability of producing enough light to produce a measurable pulse is only 90 ± 1% and drops sharply below about 150 keV. For the 2-cm-thick NE-110 monitor, the efficiency for a neutron interaction is lower (about 70% at about 244 keV), and it can also be determined accurately vs neutron energy, but the probability of detecting the event is higher for the lower-energy neutron groups. To determine the overall detection efficiencies of these two monitors, detailed comparisons were made with calculated responses, using Monte Carlo techniques. In order to make this calculation, the light response of the NE-110 for protons was measured relative to the electron pulse-height response for gammas from an ^{22}Na source. A 6-mm-thick NE-110 was chosen for this measurement. The number of photo electrons emitted by the photocathode per unit energy of the protons was measured. Because this number was very low, a Poisson distribution was applied in the calculation to take into account the poor statistics at low energies. A Gaussian distribution was also applied to take into account the overall resolution of the detector. Monte Carlo calculations for the NE-110 detectors for the experimental conditions used in this experiment were made using a program written by G. L. Morgan.

The value obtained for the (n,α) cross section at 244 keV was 3.34 b, with an uncertainty of about 3%. Some experiments are still in progress in order to better estimate this uncertainty. This value is in excellent agreement with the *R*-matrix calculations made by Hale[5] for the recent ENDF/B-V. It also agrees with the recent value of 3.15 ± 0.15 b reported by Lamaze[6] and of 3.306 b reported by Gayther.[7]

1. Visitor from Instituto de Energia Atomica, Brazil.
2. Instrumentation and Controls Division.
3. D. I. Garber and R. R. Kinsey, *Neutron Cross Sections*, BNL-325,3d ed., vol. II (January 1976).
4. G. M. Hale, "*R*-Matrix Analysis of the Light Element Standards," *Proceedings of a Conference on Neutron Cross Sections and Technology*, vol. 1, 302 (1975).
5. G. M. Hale, "*R*-Matrix Analysis of the ^{7}Li System," *International Specialists Symposium on Neutron Standards and Applications*, National Bureau of Standards, March 1977.
6. G. P. Lamaze et al., *Proceedings of the International Conference on the Interactions of Neutrons with Nuclei*, vol. 2, 1341 (1976).
7. D. G. Gayther, *A Measurement of the ^{6}Li(n,α) Cross Section*, AERE-R 8556, Atomic Energy Research Establishment, Harwell, England (1977).

EMPIRICAL PREDICTIONS OF RADIATIVE WIDTHS FOR $75 < A < 130$

C. H. Johnson

There are frequent needs to extrapolate from known total radiative widths to unknown widths for nuclei or excitation energies that can be measured only with difficulty, if at all. For example, radiative widths are needed for predicting neutron capture. The usual assumption is the Axel-Brink hypothesis that every final state for gamma-ray emission has built upon it the same electric giant dipole resonance as does the ground state. This useful approximation should not be accepted too literally. In particular, we can hardly expect the extrapolated Lorenzian tail from the giant dipole to give accurate predictions because only about 1% of the dipole sum resides in the neutron-separation energy. In that regard, the important quantity is $\sigma_g\Gamma_g^2/E_g^4$, where E_g is the dipole-resonant energy, Γ_g is the width, and σ_g is the peak cross section. In Fig. 2.89, the data points are observed[1] values of this quantity. But the use of these values in the statistical theory along with level densities from the back-shifted Fermi gas model[2] leads to total radiative widths often in poor agreement with those observed. In particular, the values near $A = 100$ are predicted too large by a factor of 3.

The empirical curve in Fig. 2.39 leads to radiative widths for *s*-wave neutron resonances agreeing to ±25% with two-thirds of the observed values. This curve corresponds to two standard expressions in

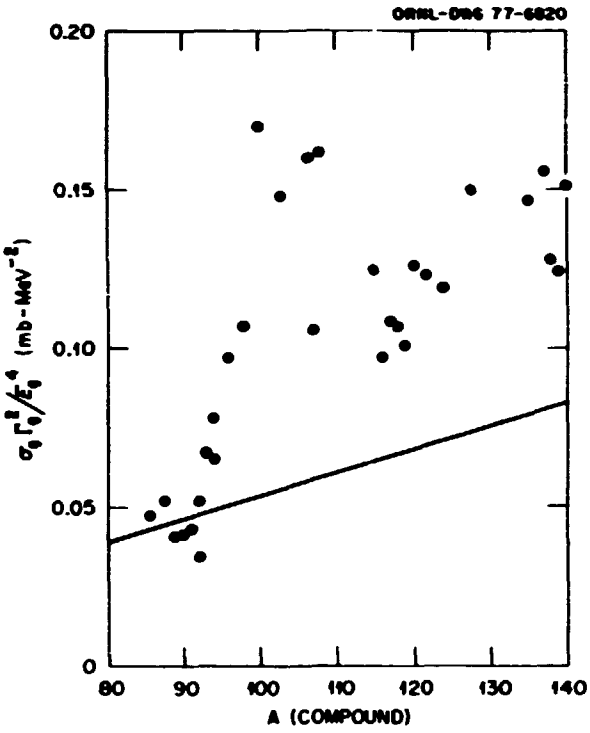

Fig. 2.89. Parameter from the electric giant dipole for predicting radiative widths. The points are from the observed dipole, but the curve is required to give average fits to observed radiative widths.

addition to an empirical one. The standard expressions give the observed dipole energy and the sum rule:

$$E_g = 76\ A^{1/3}\text{MeV}\ ,$$

$$\sigma_g\Gamma_g = 38\ NZ\ A\ \text{MeV-mb}\ .$$

The additional empirical expression for this mass region is

$$\Gamma_g = 100\ A\ \ NZ\ \text{MeV}\ .$$

Other parameterizations could be used, but the important point is that the normalization and A dependence for the Lorenzian tail must first be examined in conjunction with the assumed level density function and known radiative widths before predicting unknown widths. (Calculations were done here using a subroutine of the computer program HELGA.[4])

1. B. L. Bermanm, *At. Data Nucl. Data Tables* 15, 319 (1975).
2. W. Dilg et al., *Nucl. Phys.* A217, 269 (1973).
3. *Resonance Parameters*, compiled by S. F. Mughabghab and D. I. Garber, BNL-325, 3d ed., vol. I, National Technical Information Service, Springfield, Virginia, 1973.
4. S. K. Penny, private communication.

PROTON AND NEUTRON 3*p* RESONANCE NEAR $A = 100$

C. H. Johnson A. Galonsky[1]

Although the neutron p-wave-size resonance in the strength functions near mass 100 has been studied experimentally and theoretically over a period of almost 20 years, the shape of this resonance is still not well established. Early measurements[2] showed a double peak with maxima near $A = 92$ and 108. The presence of two maxima was first attributed[2,3] to the spin-orbit potential, but later calculations[4,5] showed that the normal spin-orbit coupling has a negligible effect on the resonant shape. Buck and Perey[6] attributed the splitting to quadrupole vibrations and found, using known deformation parameters, that the size resonance should fall sharply on the high-mass side ($A = 95$ to 105) and have a broad structural shoulder near $A = 110$. Improved later data[6] agreed fairly well with these calculations.

However, in 1974, Camarda[7] made precision neutron transmission measurements for elements in this mass region and found the p-wave strength function to have a smooth A dependence and no splitting. Perhaps Camarda's data do not include enough elements to show the expected vibrational structure; nevertheless, it seems that his strength for ^{101}Rh is larger than would be expected for that deformable nucleus.

More recently, Boldeman et al.[8,9] analyzed resonant neutron capture data obtained at ORELA for isotopes of zirconium and molybdenum and found a resonance much narrower than Camarda's. Qualitatively, their results agree with the vibrational predictions on the high-mass side but not on the low-mass side.

The point of the present analysis is that supplementary data on strength functions can be obtained from the proton total-reaction cross sections, essentially the (p,n) cross sections, for protons incident below the Coulomb barrier. The neutron and proton projectiles each have their merits. A virtue for protons is that the $3p$ state is quasibound by the Coulomb potential. Thus, a giant p-wave resonance may be seen as a function of proton energy for a given target with a given deformation parameter. Such resonances were found from precision (p,n) cross

sections for isotopes of tin and were published during the present period.[9]

Earlier (p,n) data from the laboratory[11,12] did not cover large enough energy regions to reveal the resonant peak. However, given the accurate data on tin, we can now predict the resonance energies fairly reliably from those observed for the tin isotopes. Thus, if a conventional optical model is valid, these older data should be described by only minor adjustments in the imaginary or absorptive potential. On the other hand, if vibrational effects are important, the model parameters for tin may not be valid near $A = 105$.

Using the optical-model search routine GENOA,[13] we analyzed the observed (p,n) cross sections for 2.5- to 5.5-MeV protons on nuclei from $A = 89$ to 130. We corrected for gamma-ray competition with neutron emission, using the Hauser-Feshbach program HELGA.[10,14] Each excitation function was fit by adjusting the absorptive surface diffuseness a_D and well depth W_D. The results are that all of these nuclei require nearly the same diffuseness (a_D nearly equal to 0.4 F), but the absorptive well depths must be greatly increased near $A = 105$ in order to give the rather flat or energy-independent strength functions. The fitted well depths are shown by solid points in Fig. 2.90. Previously determined[10] values for the tin isotopes are designated by "x." The curve is drawn visually.

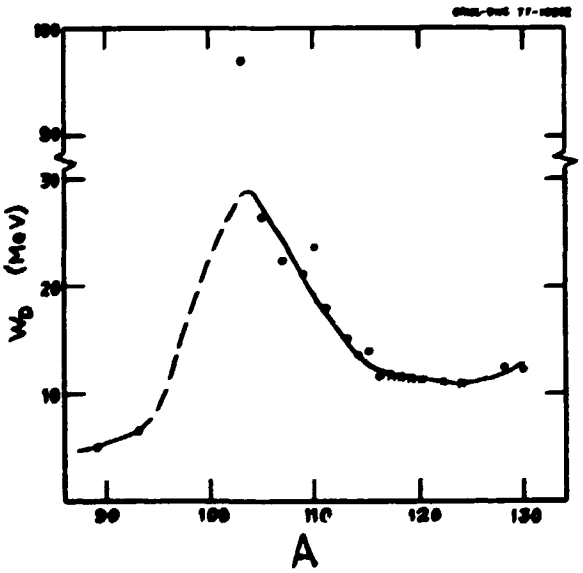

Fig. 2.90. Imaginary well depths to fit strength functions for protons incident below the Coulomb barrier. The solid points are from the present analysis; x's are from ref. 9. The curve is drawn visually.

It is probable that these data could be described by introducing some sort of A-dependence in one or more of the several optical-model parameters, but it is clear that a simple model with the usual small A dependences in all parameters cannot fit the data. This is evidence that an analogous variation occurs for neutrons.

1. Michigan State University, East Lansing.
2. L. W. Weston et al., *Ann. Phys.* **10**, 477 (1960).
3. H. Fiedeldey and W. E. Frahn, *Ann. Phys.* **19**, 128 (1962).
4. T. K. Krueger and B. Margolis, *Nucl. Phys.* **28**, 587 (1961).
5. B. Buck and F. Perey, *Phys. Rev. Lett.* **8**, 444 (1962).
6. H. W. Newson in *Nuclear Structure Studies with Neutrons*, ed. M. Nève de Mévergnies, P. Van Assche, and J. Verview, North-Holland, Amsterdam, 1966, p. 195.
7. H. S. Camarda, *Phys. Rev. C* **9**, 28 (1974).
8. J. W. Boldeman et al., *Nucl. Phys.* **A269**, 31 (1976).
9. A. R. de L. Musgrove et al., *Nucl. Phys.* **A270**, 108 (1970).
10. C. H. Johnson et al., *Phys. Rev. C* **15**, 196 (1977).
11. C. H. Johnson, A. Galonsky, and C. N. Inskeep, *Phys. Div. Annu. Prog. Rep. Mar. 25, 1960*, ORNL-2910, p. 25.
12. C. H. Johnson and R. L. Kernell, *Phys. Div. Annu. Prog. Rep. Dec. 31, 1965*, ORNL-3924, p. 86.
13. F. G. Perey, private communication.
14. S. K. Penney, private communication.

THE 292.4-eV NEUTRON RESONANCE PARAMETERS OF ZIRCONIUM-91

R. L. Macklin J. Halperin[1]
J. A. Harvey N. W. Hill[2]

The lowest strong s-wave neutron resonance in zirconium has a major influence on the magnitude of, and change in, neutron absorption as a function of zirconium thickness. Yet the experimental determination of the radiative capture width of this resonance remained uncertain to at least ±20%. Zirconium is used for reactor fuel clad and for some structural components. We have analyzed both neutron capture and transmission data taken at the ORELA neutron time-of-flight facility for the 292.4-eV resonance parameters. The spin assignment $J = 2^+$ is supported. We find that the neutron width $\Gamma_n = 866 \pm 11$ MeV and the radiative width $\Gamma_\gamma = 86.8 \pm 2.2$ MeV indicate less neutron capture than do parameters derived from earlier studies. This lower capture, however, is more compatible with integral measurements and a lead slowing-down spectrometer measurement.

1. Chemistry Division.
2. Instrumentation and Controls Division.

keV CAPTURE CROSS SECTIONS

B. J. Allen[1] M. Mizumoto[6]
J. W. Boldeman[1] A. R. Musgrove[1]
G. T. Chapman M. S. Pandey[7]
D. Drake C. Perey
E. D. Earle[3] F. G. J. Perey
J. B. Garg[4] R. B. Perez
J. Halperin[5] S. Raman
W. J. Kenney[1] G. de Saussure
R. L. Macklin R. R. Spencer
J. Malanify[2] H. Weigmann[8]
R. R. Winters[9]

Many ORELA measurements have been reported (see "Publications" in this report) during 1976 and the first half of 1977. The target isotopes included are listed here:

^{91,92,94}Zr; ^{46,47,48,49,50}Ti; ^{24,25,26}Mg; ^{165}Ho; ^{203,205}Tl; ^{209}Bi; ^{63,65}Cu; ^{54,56}Fe; ^{42,43,44}Ca; ^{92,94,95,96,97,98,100}Mo; ^{59}Co; ^{50,52,53,54}Cr; ^{88}Sr; ^{89}Y; ^{134,136,137}Ba; ^{142,143,144,145,146,148}Nd

Most of this work involved extracting single-level parameters, and the results were studied for evidence of valence neutron capture. New measurements during the reporting period were made on the following:

^{23}Na; ^{31}P; ^{nat}Cd; ^{nat}Mg; ^{206,207,208}Pb; ^{207}Pb($n,2\gamma$); ^{207}Pb(n,γ_0); ^{209}Bi; ^{59,60,61,62,64}Ni; ^{191,193}Ir; ^{175}Lu; ^{100,101,102,104}Ru; ^{28}Si(n,γ_0)

1. Australian Atomic Energy Commission, Lucas Heights, Australia.
2. Los Alamos Scientific Laboratory, Los Alamos, N. M.
3. Chalk River Nuclear Laboratories, Chalk River, Ontario, Canada.
4. State University of New York at Albany.
5. Chemistry Division.
6. Japan Atomic Energy Research Institute, Tokai-mura, Japan.
7. College of William and Mary, Williamsburg, Va.
8. Bureau Central de Mesures d'Nucleaires, Geel, Belgium.
9. Denison University, Granville, Ohio.

STATISTICAL ENHANCEMENT OF *p*-WAVE NEUTRON CAPTURE FOR $A \sim 90$

C. H. Johnson

Measurements[1-5] at ORELA of average total radiative widths Γ_γ from neutron capture on nuclei near $A \sim 90$, namely, isotopes of Y, Sr, Zr, and Mo, have shown that $\Gamma_{\gamma p}$ for *p*-wave neutron resonances is usually somewhat larger than $\Gamma_{\gamma s}$ for *s*-wave resonances. Qualitatively, this is expected because the low-lying final states in this mass region are mostly of even parity; these can be reached by *E*1 transitions from the odd-parity *p*-wave resonant levels. Because the neutron and gamma-ray widths show correlations, we know[1-5] that valency capture occurs, and we might expect the valency theory to account quantitatively for the excess *p*-wave capture. However, Musgrove et al.[1-5] calculated that the valency part is generally less than observed.

Using the program HELGA,[6] the known levels from the *Nuclear Data Sheets*, the back-shifted Fermi gas model for the continuum, and empirical gamma-ray strength functions from this mass region,[7] we have calculated the *p*-wave enhancement expected from the statistical model under the assumption that the *E*1:*M*1 strength ratio is 7:1. In Fig. 2.91, the predicted differences, $\Gamma\gamma p - \Gamma\gamma s$, are shown by solid bars. The figure shows that the sums of the statistical and valency predictions agree well with the observed enhancements. Thus, there is no

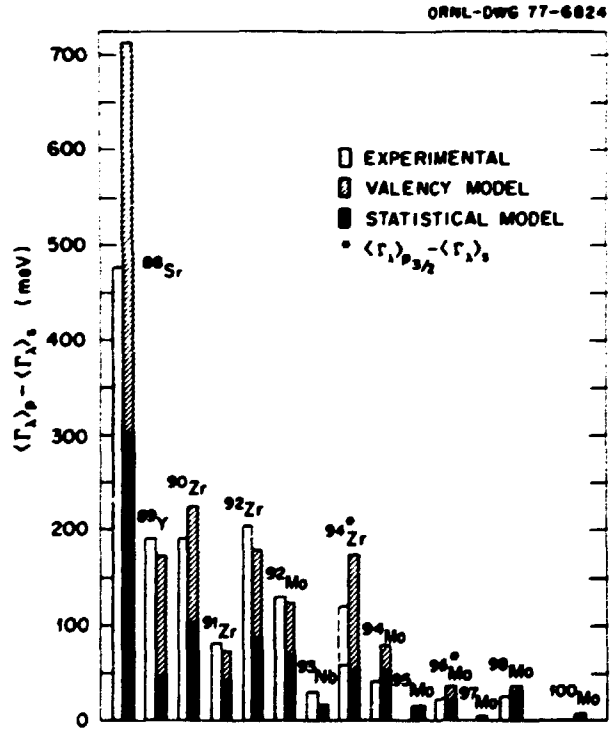

Fig. 2.91. Differences between average total radiative widths for *p*-wave and *s*-wave neutron resonances ($\Gamma_{\gamma p} \equiv \langle\Gamma_\lambda\rangle_p$ and $\Gamma_{\gamma s} \equiv \langle\Gamma_\lambda\rangle_s$). The statistical calculations are from the present work; the valency calculations and experimental values are from refs. 1-5.

need to invoke other nonstatistical effects such as doorway states.

1. A. R. Musgrove et al., *Nucl. Phys.* A270, 108 (1996).
2. J. W. Boldeman et al., *Nucl. Phys.* A206, 1 (1975).
3. J. W. Boldeman et al., *Nucl. Phys.* A269, 397 (1976).
4. J. W. Boldeman et al., to be published in *Nuclear Physics*.
5. A. R. Musgrove et al., to be published in *Nuclear Physics*.
6. S. K. Penney, private communication.
7. See this report, C. H. Johnson, "Empirical Predictions of Radiative Widths for $75 < A < 130$."

ISOSPIN IMPURITIES IN ISOBARIC ANALOG STATES IN $^{24}Mg + n$

H. Weigmann[1] R. L. Macklin
J. A. Harvey

Within 2 MeV above the neutron separation energy of ^{25}Mg, there are three $T = 3/2$ levels: the isobaric analog states of the ground state ($J = 5/2$) and the first two excited states ($J = 3/2^+$ and $1/2^+$) of ^{25}Na. These three analog states have been observed previously from charged-particle reactions and photonuclear measurements; however, they had not been observed in neutron-induced reactions. In fact, a $T > 1$ state has never been identified from neutron measurements. A measurement of the neutron widths of these states gives information on the isospin impurities in either the initial or final state.

We have made high-resolution ($\Delta E/E < 0.1\%$) transmission measurements on a sample of natural magnesium, using the 200-m flight path at ORELA, and capture cross-section measurements, using enriched samples of the magnesium isotopes. The data have been analyzed to obtain the neutron widths and the radiation widths of about 25 resonances in $^{24}Mg + n$. The neutron resonances at 475.4, 555.4, and 1567 keV are the three $T = 3/2$ analog states of special interest. The first two resonances are d-wave resonances (corresponding to states with $J = 3/2$ and $5/2$) and have reduced neutron widths about 50 times smaller than the average width for $T = 1/2$ d-wave resonances, indicating an isospin impurity of about 2%. However, the resonance at 1567 keV is a large s-wave, $T = 3/2$ resonance which has a reduced neutron width about 18% that of the average of three $T = 1/2$ s-wave resonances observed at lower neutron energies. This corresponds to an average-mixing matrix element of from 90 to 150 keV.

A detailed paper on this work has recently been published.[2]

1. Visiting scientist from Bureau Central de Mesures d'Nucleaires, Geel, Belgium.

2. H. Weigmann, R. L. Macklin, and J. A. Harvey, *Phys. Rev.* C 14, 1328 (1976).

STRENGTH FUNCTIONS FOR p-WAVE NEUTRON RESONANCES IN ^{40}Ca

J. L. Fowler C. H. Johnson

There have been extensive measurements and compilations of s-wave strength functions, the average reduced width of resonances divided by the average level spacing, as obtained from low-energy neutron cross sections. However, information on p-wave strength functions is rather sparse and somewhat contradictory. The neutron energy resolution available from ORELA enables us to resolve resonances at higher energies where p-wave resonances are prominent. In the case of ^{40}Ca neutron scattering, we have assigned l values for resonances up to 1 MeV neutron energy by observing the interference between resonant and potential scattering.[1]

The computer program with which we analyze individual resonances not only gives the potential-scattering phase shifts, but also the natural widths and energies of the resonances. In extracting the reduced neutron widths from the measured natural widths, we use penetration factors calculated for a radius of interaction of 5.70 F, which corresponds to 10% depth of a Woods-Saxon potential of radius 4 F and diffuseness of 0.77 F.

Figure 2.92 shows plots of the sum of the reduced widths from 50 keV to an energy, E, as a function of E for $J = 1/2^-$ and $J = 3/2^-$ resonances. The slopes of the lines through the data give the strength functions, except for small corrections for missed levels. Because our experimental resolution ΔE in the MeV varies with energy as $\Delta E = (\sqrt{0.235 + 0.71E})E \times 10^{-3}$ (ref. 2) and the penetration factor for p-wave neutrons varies as about $E^{3/2}$ in the energy region 0.1 to 1.0 MeV, the fraction of missed levels should be almost independent of energy. Our cross-section data indicate this is approximately true. The peaks we neglected to analyze (about 1/2 b) correspond to a reduced width for $p_{1/2}$ resonances of about 30 eV, and this value is constant within a factor of 2 from 50 keV to 1.0 MeV.

A comparison of our p-wave resonance assignments with assignments deduced from a neutron-capture experiment[3] in the region 50 to 350 keV suggests that we missed about 50% of narrow $p_{1/2}$ resonances and somewhat fewer $p_{3/2}$ resonances. Porter-Thomas plots of our reduced widths are consistent with our missing $p_{1/2}$ levels with reduced widths of less than 30 eV and with these missed levels

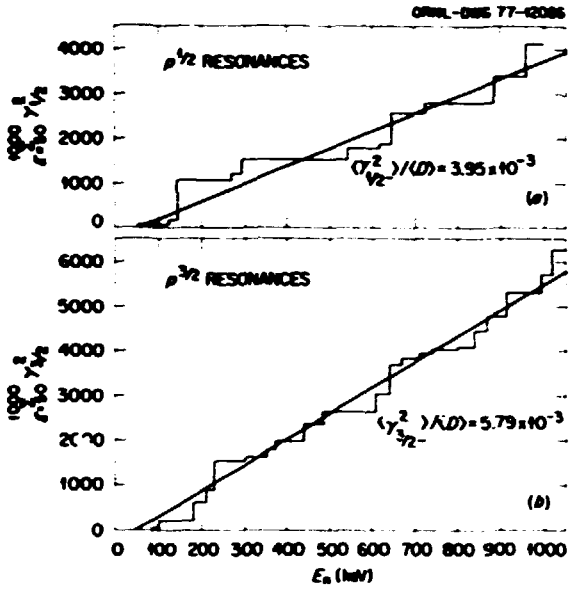

Fig. 2.92. Strength function for p-wave resonances in ^{56}Ca neutron scattering. (a) $p^{1/2}$ resonances. (b) $p^{3/2}$ resonances.

representing half of the total number of levels. Nevertheless, the correction to the strength function for these missed levels is small. For $p_{1/2}$ resonances, the correction amounts to a 9.5% addition to the strength function obtained from Fig. 2.92; in the case of $p_{3/2}$ resonances, the correction amounts to a 2.0% addition.

The final values for the strength functions in dimensionless units are

$$\langle\gamma^2_{1/2}\rangle/\langle D\rangle = (4.3 \pm 0.5) \times 10^{-3} ,$$

$$\langle\gamma^2_{3/2}\rangle/\langle D\rangle = 5.9 \pm 0.6) \times 10^{-3} ,$$

with the more usual definition of p-wave reduced widths,

$$\Gamma^1_n = \Gamma_n \sqrt{\frac{1\ \text{eV}}{E\ (\text{eV})}}\ \frac{1+\rho^2}{\rho^2} ,$$

where $\rho = kR_0$, with $R_0 = 1.4\,A^{1/3}$ F, the $p_{1/2}$ strength function is $(1.4 \pm 0.14) \times 10^{-5}$, and the $p_{3/2}$ strength function is $(1.8 \pm 0.2) \times 10^{-5}$.

1. C. H. Johnson and J. L. Fowler, *Bull. Am. Phys. Soc.* 18, 1401, (1973).
2. J. L. Fowler, C. H. Hohnson, and N. W. Hill, p. 525 in *Proceedings of the International Conference on Nuclear Physics*, Munich, Germany, August–September 1973.
3. A. R. Musgrove et al., *Nucl. Phys.* A259, 365 (1976).

MEASUREMENT OF THE NEUTRON TOTAL CROSS SECTION OF SODIUM

D. C. Larson[1] J. A. Harvey
N. W. Hill[2]

Sensitivity-analyses studies for the upper axial shield of the Clinch River Breeder Reactor indicated that 40% of the integrated tissue-dose sensitivity to the sodium-neutron total cross section comes from the interference minimum of the 300-keV resonance. Due to the large quantities of liquid sodium coolant present in this reactor, this "window" below this resonance takes on new significance, because a small change in the cross section produces a large change in the transmission. Also, recent thick-sample measurements on this minimum by Brown et al.[3] showed a significant discrepancy with earlier data of Cierjacks et al.[4] Furthermore, no high-resolution data were available at lower energies, leading to large uncertainties estimates in the ENDF/B-IV evaluation.[5]

We have made high-resolution transmission measurements on an 8.1-cm ($i.e.$, N = 4.90 b/atom) sample of pure sodium from 32 keV to 37 MeV, using 5-nsec electron bursts. The transmitted beam was detected by an NE-110 proton-recoil detector located at the 200-m flight path.

Figure 2.93 shows a comparison of our data (averaged by ten channels) with the ENDF/B-IV evaluation from 190 to 310 keV, the region of most serious disagreement. We observed eight resonances in this region, four of which had not been seen in previous transmission measurements. The data have been fitted very well with a program including resonance-resonance interference. Resonance

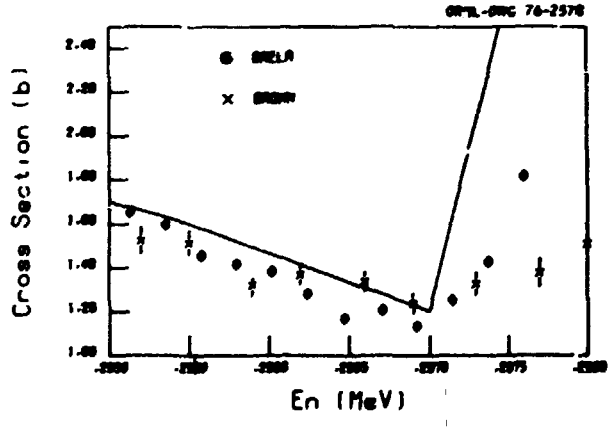

Fig. 2.93. Comparison of data (averaged by 10 channels) with the ENDF/B-IV evaluation from 190 to 310 keV.

energies are 201.2, 214, 236.8*, 239.5*, 298.1, 299.4*, and 305.2* keV, where the asterisk labels the new resonances. The minimum at 296.8 keV is about 10% lower than ENDF/B-IV values and results in a factor of about 2 more leakage than had previously been calculated. A detailed listing of the cross sections with errors and graphs is given in the work of Larson, Harvey, and Hill.[6]

1. Neutron Physics Division.
2. Instrumentation and Controls Division.
3. P. H. Brown et al., *Trans. Am. Nucl. Soc.* 21, 505 (1975).
4. S. Cierjacks et al., *High-Resolution Total Neutron Cross Sections between 0.5 to 30 MeV*, Karlsruhe report KFK-1000 (June 1968).
5. N. C. Paik and T. A. Pitterle, *Evaluation of Sodium-23 Neutron Data for the ENDF/B Version III File, Appendix A*, WARD-3045T4B-2, Westinghouse Advanced Reactors Division (April 1972), and *ENDF/B-IV*, MAT 1156, National Neutron Cross-Section Center, Brookhaven National Laboratory, Upton, N.Y. (1974).
6. D. C. Larson, J. A. Harvey, and N. W. Hill, *Measurement of the Neutron Total Cross Section of Sodium from 32 keV to 37 MeV*, ORNL TM-5614 (October 1976).

NEUTRON TOTAL CROSS SECTION OF ^{249}Cf

J. A. Harvey N. W. Hill[2]
R. W. Benjamin[1] S. Raman

In June 1975, transmission measurements were made on two samples of ^{249}Bk (330-day half-life) shortly after chemical separation so that they contained only 2% ^{249}Cf. Eighteen months later, when the composition was about 30% ^{249}Bk and about 70% ^{249}Cf, transmission measurements were again made on the same two samples. Neutrons were detected using an 11.0-cm-diam, 1.3-cm-thick ^{6}Li glass scintillator located at a 17.8-m flight path. Some measurements were made with samples cooled with liquid nitrogen, and some were made with samples at room temperature. The measurements covered the energy range from 0.005 to about 1000 eV with an energy resolution of about 0.3%.

Of the 24 resonances observed up to 20 eV, 16 are due to ^{249}Bk still present in the sample. The largest resonance in ^{249}Cf is the known one at 0.70 eV. The present data will be analyzed in conjunction with the earlier ^{249}Bk total cross-section data and the ORELA fission cross-section data of ^{249}Cf measured by Dabbs et al.[3] to determine the parameters of the resonances. Because it is not possible to make a direct capture cross-section measurement on this nuclide, the capture cross section must be determined from the resonance parameters or from the difference of the total and fission cross-section data, since the scattering is small. The work is part of a cooperative program between the Oak Ridge National Laboratory and Savannah River Laboratory.

1. Savannah River Laboratory, Aiken, S.C.
2. Instrumentation and Controls Division.
3. J. W. T. Dabbs et al., *Phys. Div. Annu. Prog. Rep. Dec. 31, 1973*, ORNL-4937, p. 181.

FISSION CROSS-SECTION MEASUREMENTS ON SMALL ULTRAPURE CURIUM SAMPLES

J. W. T. Dabbs N. W. Hill
C. E. Bemis, Jr. S. Raman

Measurements on ^{243}Cm began in December 1975.[1] These runs were completed in mid-July 1976 and included the new ^{6}LiF–NE-110 neutron flux monitor.[2] The results of the ^{243}Cm measurements were sufficiently encouraging that a decision was made to repeat the ^{245}Cm measurements, using the new lower background collimator system and the ^{6}Li beam monitor in these measurements as well, because they were clearly superior to the previous measurements. Accordingly, a remeasurement of ^{245}Cm began in October 1976 and was completed in April 1977. The long-running times are occasioned both by the small quantities of material and low count rates and by the unavailability of full-power pulses from the accelerator at all times. Following the ^{245}Cm measurements, a sequence of background runs was made using different thicknesses of ^{238}U and natural copper filters for blacking out "neutrons" of energies corresponding to particular resonances in the filter material. These runs were completed in June 1977, and analysis of the data began at that time. A number of new resonances were observed in the fission cross section of ^{243}Cm. The ^{243}Cm data will be completed first because there are no remaining problems, except with the ^{6}Li beam monitor response.

The ^{245}Cm data will require a very careful background analysis in order to incorporate the substantial body of data taken prior to the change to the ^{6}LiF–NE-110 beam monitor installation, which was accompanied by an improved collimator system. These data are sufficiently valuable to justify the effort to retrieve them.

1. J. W. T. Dabbs et al., *Phys. Div. Annu. Prog. Rep. Dec. 31, 1975*, ORNL-5137, p. 3.

2. See this report, C. Renner et al., "Absolute Measurement of the $^6Li(n,\alpha)$ Cross Section in the Region of the 244-keV Resonance."

FISSION CROSS-SECTION MEASUREMENTS ON ^{241}Am

J. W. T. Dabbs H. Weigmann
H. W. Sang[1]

A program for measurement of the fission cross section of ^{241}Am has been started. Because of the small subthreshold fission cross sections expected with this nuclide, a large-area chamber containing several milligrams of ^{241}Am appeared desirable. This has led to the design of a fission ionization chamber with parallel plates in which a separator constructed of hexagonal-shaped cells of phenolic plastic has been introduced. The ratio of the dimension of each cell to the plate spacing is approximately 3:1. In this way, the length of particle tracks for particles moving approximately parallel to the plates is restricted to the width of each cell. It is thus expected that the maximum alpha-particle pulses will be held to values small compared with the majority of minimum fission-fragment pulses.

A computer simulation of the expected behavior of such a chamber, based on Monte Carlo calculations of multiple-pulse pileup,[2] indicates that it should be possible to utilize alpha-particle rates as great as 10^8 events/sec in each section of the chamber; this would be accompanied by a loss of some 20% of the fission events caused by impingement of fission fragments on the cell walls after a short path length.

A test chamber has been constructed. This chamber will undergo tests during the summer of 1977; if these tests are successful and performance as good as that indicated in the computer simulation is obtained, additional ^{241}Am plates for this chamber will be fabricated and a measurement of this cross section carried out with it. Serious discrepancies exist in presently available data, but funding restrictions have dictated a cautious approach.

1. Summer graduate research participant from the Massachusetts Institute of Technology, Cambridge, Mass.

2. J. W. T. Dabbs, *Phys. Div. Annu. Prog. Rep. Dec. 31, 1975*, ORNL-5137, p. 4.

ANGULAR MOMENTUM DETERMINATION OF RESONANCES IN $^{24}Mg + n$ BY ELASTIC NEUTRON SCATTERING

D. J. Horen J. A. Harvey
N. W. Hill[1]

The angular momentum values of 15 resonances in $^{24}Mg + n$ have been determined by elastic neutron scattering. These measurements were performed at the 200-m flight path at ORELA. The change in shape of the differential cross section [i.e., $\sigma_{LA}(E,\theta)$] vs angle has been observed for most of these resonances. Assignments of $l = 2$ for five resonances could be made on the basis of their distinct interference pattern in the 90° cross-section data.

These results have been published[2] and complement the neutron transmission data obtained by Weigmann et al.[3]

1. Instrumentation and Controls Division.

2. D. J. Horen, J. A. Harvey, and N. W. Hill, *Phys. Rev. C* 15, 1168 (1977).

3. H. Weigmann, R. L. Macklin, and J. A. Harvey, *Phys. Rev. C* 14, 1328 (1976).

NUCLEAR STRUCTURE OF ODD-A ISOTOPES STUDIED VIA (n,γ) REACTION

S. Raman G. G. Slaughter
R. F. Carlton[1] M. R. Meder[2]

The tin isotopes are well suited to a study of nuclear structure within the framework of the nuclear shell model, because the magic number of protons ($Z = 50$) minimizes the need for considering n,p pairing interactions in theoretical calculations, and because the large number of stable isotopes makes it possible to study systematic trends in both experimental and shell-model features. The experimental data presently available concerning the energy levels in the odd-A tin isotopes are not as extensive as one might expect on the basis of their theoretical importance. Thermal-neutron capture studies have not been widely used due to the extremely small capture cross sections for the heavier even-A tin isotopes. Most experimental studies (especially nucleon transfer studies) are beset with the problem of interference from isotopic impurities. This usually necessitates an extensive study of all tin isotopes before conclusive

results may be obtained. Resonance neutron capture offers a powerful technique for studying tin isotopes, because interference from unwanted isotopes can be greatly suppressed through the combination of enriched targets and selection of resonances known to be in the nucleus under study. We have, therefore, undertaken a systematic study of the level structure of six odd tin isotopes between $A = 116$ and $A = 125$. Results obtained for ^{121}Sn, ^{123}Sn, and ^{125}Sn have been already published.[3] Analyses of results for ^{115}Sn, ^{117}Sn, and ^{119}Sn have been completed.

In a parallel effort, we have also calculated spectroscopic information (level energies, electromagnetic moments, and transition rates) for the odd-mass tin isotopes. Our basic model of the odd-mass nucleus pictures it as being formed by coupling the motion of the odd neutron quasi-particle to the states of the neighboring even-mass core, where the core is assumed to exhibit quadrupole vibrations. The effects on energies and electromagnetic properties arising from exchange between two quasi-particle excitations in the core and the odd quasi-particle are taken into account through perturbation theory.

A paper summarizing systematic trends in tin isotopes based on measurements and calculations is being prepared for publication.

---

1. Middle Tennessee State University, Murfreesboro.
2. Georgia State University, Atlanta.
3. R. F. Carlton, S. Raman, and G. G. Slaughter, *Phys. Rev. C* 14, 1439 (1976); *Phys. Rev. C* 15, 883 (1977).

ANGULAR DISTRIBUTION OF NEUTRON-PROTON SCATTERING AT 27.3 MeV

J. L. Fowler[1] M. Hussain[3]
J. A. Cookson[2] C. A. Uttley[2]
R. B. Schwartz[4]

Although the nucleon-nucleon interaction is basic to nuclear physics, for three decades of this nuclear age the *n-p* differential cross section for forward scattering of neutrons at about 30 MeV has been lacking. Bryan and Binstock,[5] among others, have pointed out that, to determine the singlet *p*-wave phase shift for *n-p* scattering, one needs good forward-angle differential cross sections between 25 and 50 MeV.

Figure 2.94 shows a schematic layout of the experiment we set up at the Atomic Energy Research Establishment Laboratory in Harwell, England,[6,7] to measure the differential scattering of neutrons from protons at 27.3 MeV. Ten-MeV deuterons from the Harwell tandem generator bombarded tritium gas in a 10-cm-long cell. The resulting T(d,n)^{4}He neutrons scatter from a 3-cm-diam by 3-cm-long plastic scintillator and are detected by a 10-cm-diam by 2.54-cm-thick NE-102A plastic scintillator. The signal due to the pulse from the detection of the neutron in the large scintillator gave the start signal for a time-of-flight measurement of the neutrons, and the delayed pulse from the proton recoil in the scattering scintillator gave the stop signal. A neutron monitor used a similar technique to identify scattered neutrons from the T(d,n)^{4}He reaction.

Figure 2.95 shows the neutron time-of-flight spectra when the neutron detector is at 17° to the primary neutron beam direction. Increasing time-of-flight is toward lower channels, so the gamma peak appears in the upper channels. The constant time-independent background of 17 counts/channel under the gamma peak extends under the peak due to scattered 27.3-MeV neutrons. Directly below these 27.3-MeV neutron peaks is a small (about 4%) peak we have identified as arising from inelastic scattering of neutrons from ^{12}C. The inelastically scattered neutrons gave the start pulse in the large scintillator, and the 4.43-MeV de-excitation gamma ray gave the delayed stop pulse in the scattering scintillator. At angles between 26.6 and 45.0°, the ^{12}C(n,$n'\gamma$) peaks were under the T(d,n) neutron peaks, but at 50.8° the inelastic peak is above the *n-p* scattering peak in energy, and it is 0.5% of the *n-p* peak. We find the energy position of the ^{12}C(n,$n'\gamma$) peak relative to that of the *n-p* peak shifts with angle as expected from kinematics. Furthermore, using pulse-shape discrimination, we have demonstrated that the small inelastic peak is associated with a gamma-ray pulse in the scattering scintillator. To correct for the ^{12}C(n,$n'\gamma$) neutrons under the *n-p* peak, we have used the measured ^{12}C(n,$n'\gamma$) cross section to extrapolate the ^{12}C(n,$n'\gamma$) under the *n-p* scattering peaks. At 21.6-MeV neutron or proton energies, these cross sections are similar.

Because the energy of the *n-p* scattered neutrons varies rapidly with angle, we have to know how the efficiency of the large detector varies with energy. Cookson et al.[8] describe the reaction chamber we used to obtain the absolute efficiency of the neutron detector by use of the associated particle method. The deuteron beam produces the D(d,n)^{3}He reaction or the T(d,n)^{4}He reaction in the chamber, and a collimated beam of ^{3}He or ^{4}He particles is detected with a ΔE counter at 45, 65, or 80° to the incident beam direction. We measure the time of flight of the neutrons in delayed coincidence with the ^{3}He or ^{4}He

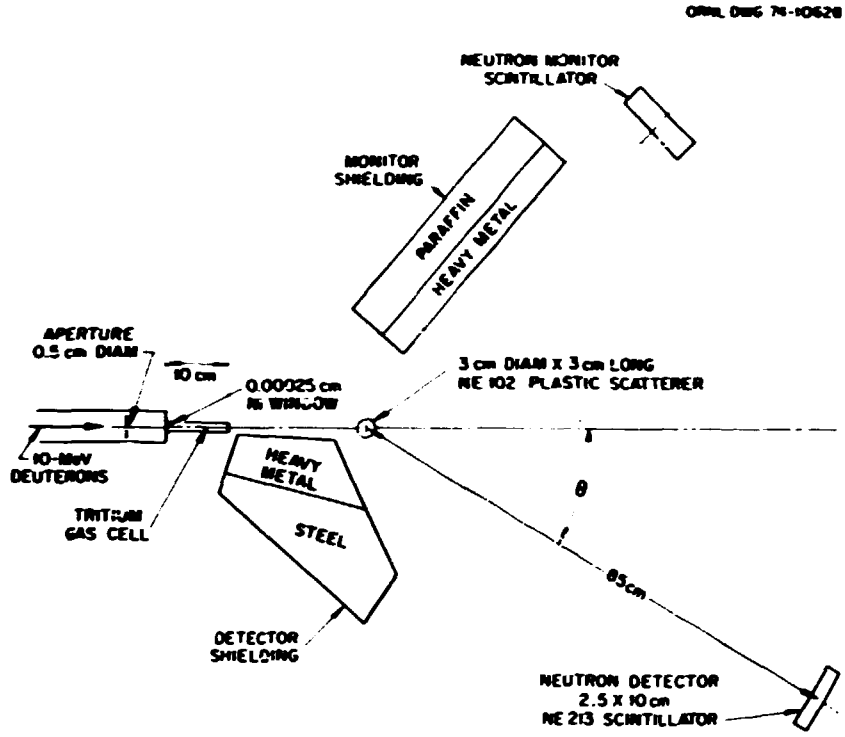

Fig. 2.94. Experimental layout for angular distribution measurements by detecting scattered neutrons.

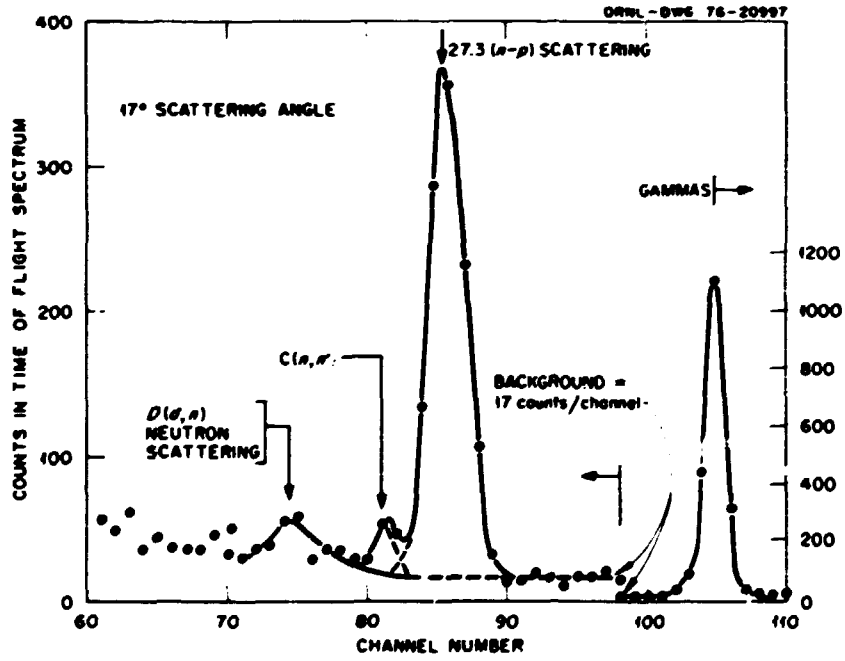

Fig. 2.95. Time-of-flight spectrum of scattered events at a laboratory angle of 17°.

particles. Except for small corrections, the efficiency is simply the counts in the neutron spectra divided by the ^{3}He or ^{4}He counts. Figure 2.96 gives our measurements of the absolute efficiency of the large neutron detector as a function of neutron energy. The solid line is a calculated efficiency curve from a Monte Carlo code of Stanton with modifications by McNaughton.[9] We used the actual data points, however, to calibrate our detecting system.

Figure 2.97 gives our relative cross sections for *n-p* scattering together with relative cross sections of Burrows[10] for backward scattering of neutrons. Notice the suppressed zero. The errors for our forward scattering data do not include an uncertainty for our efficiency measurements, which from Fig. 2.96 we estimate to be about ±1.4%. The data agree best with the phase shift analysis of Hopkins and Breit.[11]

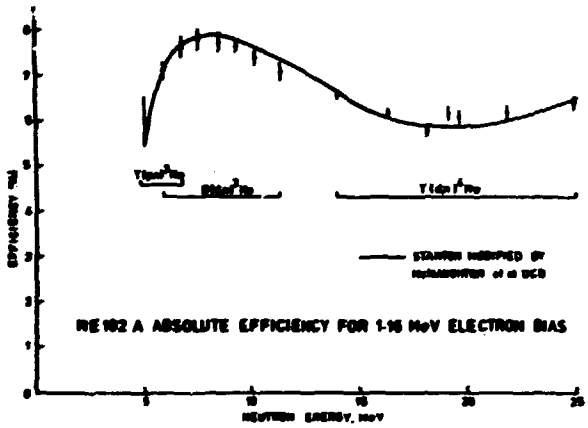

Fig. 2.96. Absolute efficiency of a 10-cm-diam. by 2.54-cm-thick NE-102A plastic scintillator for a bias of 1.16-MeV electron energy (4-MeV neutron bias).

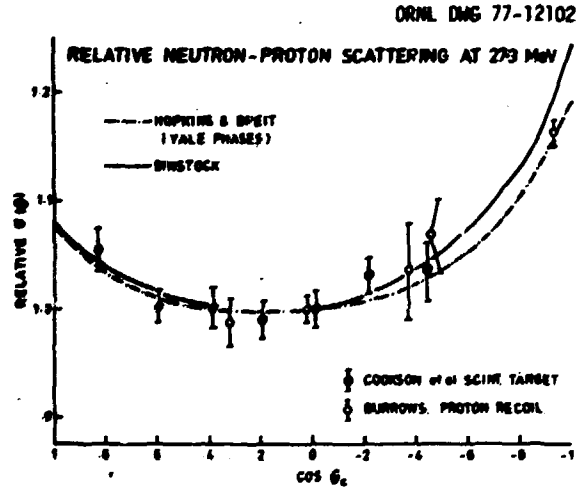

Fig. 2.97. Relative neutron-proton scattering at 27.3 MeV.

1. On assignment to AERE Harwell, United Kingdom, from ORNL.
2. AERE Harwell, United Kingdom.
3. At AERE Harwell, United Kingdom, on leave from the University of Dacca, Bangladesh.
4. On assignment to AERE Harwell, United Kingdom, from the National Bureau of Standards, Washington, D.C.
5. R. Bryan and J. Binstock, *Phys. Rev.* 8D, 1397 (1973).
6. J. L. Fowler et al., *Bull. Am. Phys. Soc.* 22, 53 (1977).
7. J. A. Cookson et al., *Soviet Conference on Neutron Physics, Kiev, April 1, '977*, pp. 18-22.
8. J. A. Cookson et al., p. 66 in *Proceedings of the Conference on Nuclear Cross Sections and Technology*, vol. 1, ed. R. A. Schrack and C. D. Bowman, NBS-425.
9. M. W. McNaughton et al., *Nucl. Instrum. Methods* 116, 25 (1974).
10. T. W. Burrows, *Phys Rev. C* 7, 1306 (1973).
11. J. C. Hopkins and G. Breit, *Nucl. Data Tables* A9, 137 (1971).

ANALYSIS OF RESPONSE OF ^{6}LiF-NE-110 BEAM MONITOR

J. W. T. Dabbs R. L. Macklin
L. M. Petrie[1]

A Monte Carlo analysis of the response of the new beam monitor to neutrons of various energies has been undertaken as a result of a preliminary analysis, which appeared to indicate that substantial variations in the response of this detector may occur as a function of energy. This analysis is not yet complete, but the first results indicate that a complete analysis over the entire energy range will be required to give satisfactory results in the curium measurements described elsewhere in this report. Accordingly, this work is in progress.

1. UCC-ND Computer Sciences Division.

MESON PHYSICS

Experiments in elastic and inelastic scattering are being conducted at the Los Alamos Meson Physics Facility (LAMPF) by a group including scientists from ORNL, the Los Alamos Scientific Laboratory, the University of South Carolina, and the Virginia Polytechnic Institute and State University. The ORNL researchers have participated in all phases of these projects.

π^+-NUCLEUS ELASTIC SCATTERING AT LOW ENERGIES

F. E. Bertrand
T. P. Cleary
E. E. Gross
N. W. Hill[1]
C. A. Ludemann
R. L. Burman[2]
R. P. Redwine[2]
M. Moinester[3]
C. W. Darden[4]
R. D. Edge[4]
D. Malbrough[4]
T. Marks[4]
B. M. Preedom[4]
M. Blecher[5]
K. Gotow[5]
D. Jenkins[5]
F. Milder[5]

Elastic scattering is the simplest form of pion-nucleus interaction. High-precision angular distribution measurements will permit the testing of the large number of theoretical calculations of this interaction and will provide information necessary for the analysis of more complicated interactions, such as inelastic pion scattering. We have initiated a study of pion-nucleus elastic scattering which, when completed, will provide data at several incident energies between 10 and 100 MeV on five target nuclei.

Data have been taken for ^{12}C, ^{16}O, ^{40}Ca, ^{90}Zr, and ^{208}Pb, using 50- and 40-MeV incident π^+ projectiles. In addition, data were obtained on ^{12}C, using 30-MeV π^+ projectiles. The measurements were made using ΔE vs E counter telescopes constructed of plastic scintillators. Ten counter telescopes were used simultaneously, and data were obtained at 18 angles between 25 and 160°.

Figure 2.98 shows preliminary angular distributions for 50-MeV π^+ projectiles on the several targets studied. Absolute uncertainty for the final data should range from 3 to 7%. Phase shift and optical-model analyses of the data are now in progress.

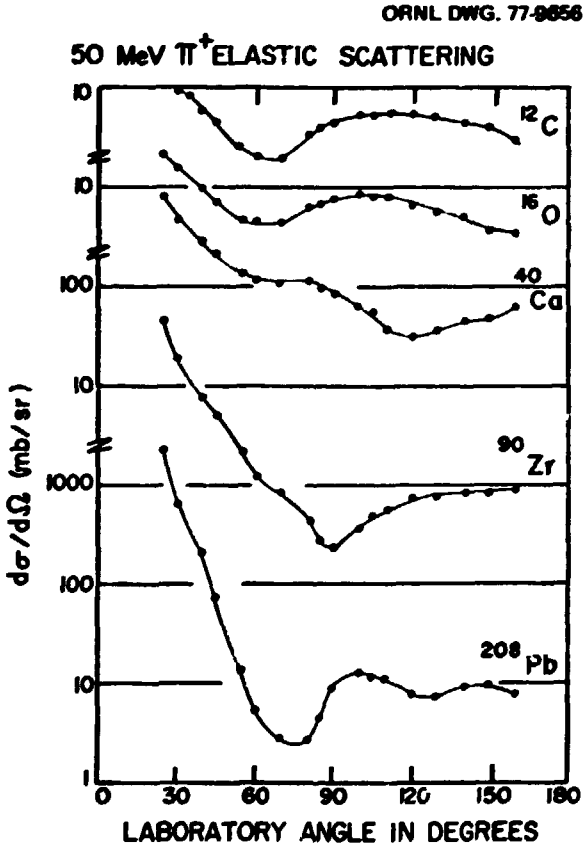

Fig. 2.98. Preliminary angular distributions for 50-MeV π^+ on ^{12}C, ^{16}O, ^{40}Ca, ^{90}Zr, and ^{208}Pb. The curves are drawn to guide the eye.

1. Instrumentation and Controls Division.
2. Los Alamos Scientific Laboratory, Los Alamos, N.M.
3. On leave at Los Alamos Scientific Laboratory from the University of Tel Aviv, Tel Aviv, Israel. Consultant to ORNL Physics Division, June 1976–March 1977.
4. University of South Carolina, Columbia.
5. Virginia Polytechnic Institute and State University, Blacksburg.

INELASTIC SCATTERING OF 50-MeV π^+

F. E. Bertrand
R. L. Burman[1]
R. D. Edge[2]
M. Blecher[3]
T. P. Cleary
R. P. Redwine[1]
D. Malbrough[2]
K. Gotow[3]
E. E. Gross
M. Moinester[4]
T. Marks[2]
D. Jenkins[3]
C. A. Ludemann
C. W. Darden[2]
B. M. Preedom[2]
F. Milder[3]

We have initiated a systematic study of pion-nucleus inelastic scattering for pion energies below approximately 100 MeV. These studies should provide information on the pion-nucleus reaction mechanism and may provide nuclear-structure information for states not strongly excited by other projectiles.

The measurements will be made using the bicentennial spectrometer, a magnetic spectrometer designed specifically for these experiments (Fig. 2.99). The spectrometer is a broad-range device in that about 25% in momentum is covered for one field setting. Maximum solid angle is approximately 8 msr. Scattered pions are detected using helical wire chambers and plastic scintillators placed in the focal plane.

The spectrometer has been used in one run, and the performance was found to be generally satisfactory. The energy resolution at 0° scattering angle was about 350 keV (FWHM), approximately the design

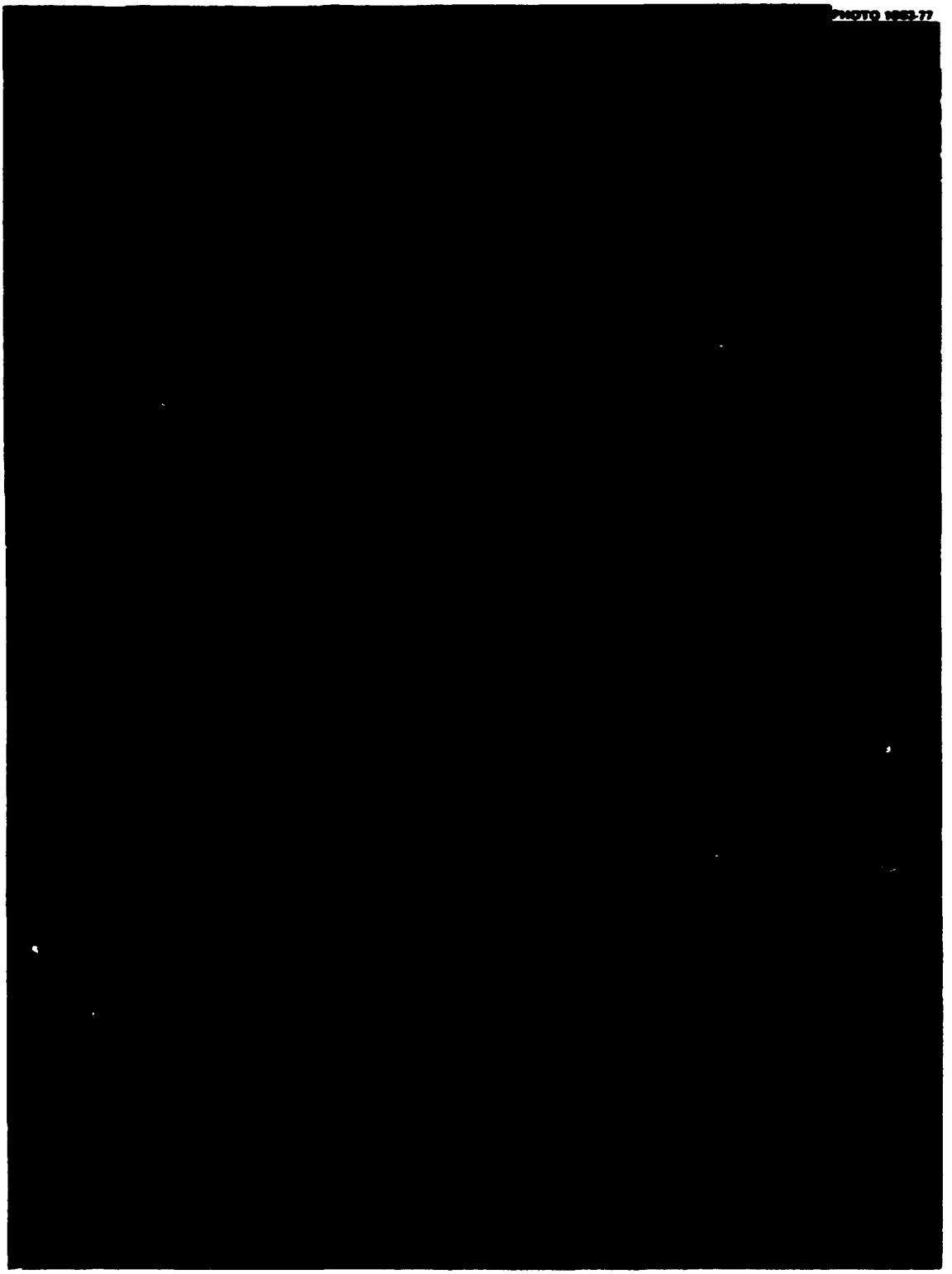

Fig. 2.99. Biconcentral spectrometer.

limit. However, the resolution broadened to about 700 keV (FWHM) when the spectrometer was moved from 0°. The source of this discrepancy is under investigation.

Data were taken at two angles, 40 and 80°, on ^{16}O, ^{40}Ca, ^{58}Ni, and ^{208}Pb during the spectrograph development run. Figure 2.100 shows a spectrum of ^{40}Ca at 80°. In addition to the elastic peak, two other peaks at about 3.7 and 6.6 MeV of excitation are prominently observed. There is also some evidence for another peak at about 11 MeV. The observed 3.7- and 6.6-MeV peaks coincide in energy with well-known levels. The statistical accuracy of the data is insufficient to permit analysis of the high-excitation regions of the spectra.

Based on the spectra presently available, which show reasonably large cross sections (0.5 to 1 mb/sr) for excitation of low-lying states, additional runs are planned for early 1978 in which angular distributions will be obtained.

1. Los Alamos Scientific Laboratory, Los Alamos, N.M.
2. University of South Carolina, Columbia.
3. Virginia Polytechnic Institute and State University, Blacksburg.
4. On leave at Los Alamos Scientific Laboratory from the University of Tel Aviv, Tel Aviv, Israel. Consultant to ORNL Physics Division, June 1976–March 1977.

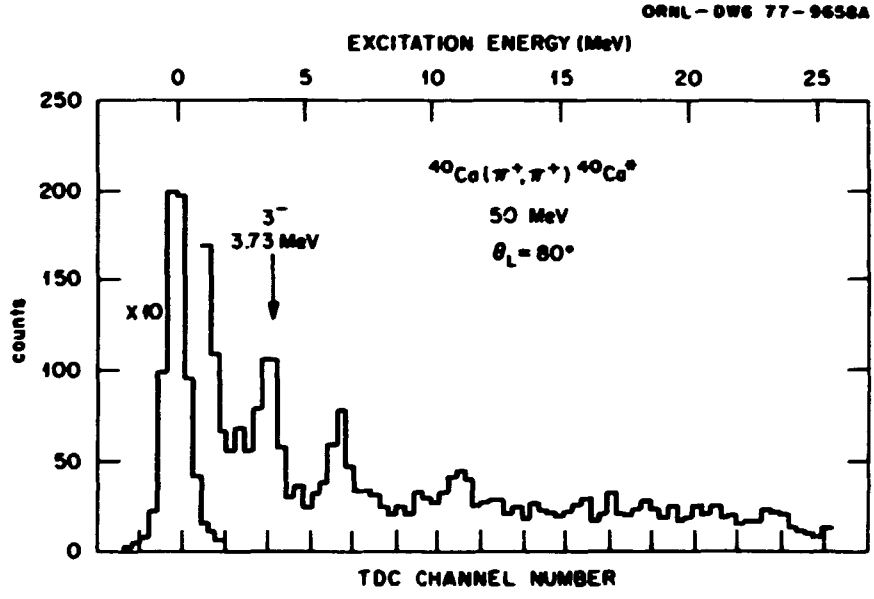

Fig. 2.100. Spectrum from the $^{40}Ca(\pi^+,\pi^+)$ reaction at 80° for $E_{\pi^+} = 50$ MeV.

3. Theoretical Nuclear Physics

INTRODUCTION

The emphasis of the research in nuclear theory continued to be in the area of descriptions of heavy-ion collisions, in support of a similar emphasis in the experimental program. The heavy-ion theory program at ORNL is characterized by both depth and breadth. Three different, but complementary, approaches are taken to the study of the results of collisions of heavy ions. The three approaches are time-dependent Hartree-Fock (TDHF) theory, nuclear hydrodynamics, and classical microscopic scattering.

For the TDHF and nuclear hydrodynamics calculations, numerical integration techniques are used. The computer time required for these procedures depends critically on the dimensionality and mesh size used. Thus, in both cases, codes to do two-dimensional and three-dimensional calculations have been made. The faster 2-D codes have been applied in idealized cases to assess the physical content of the methods; with respect to the 3-D codes, our effort has concentrated on developing techniques to make them efficient enough to make more realistic calculations feasible. As this report is in preparation, a series of full 3-D calculations in both the TDHF and nuclear hydrodynamics models is being formulated.

These detailed calculations have been complemented by some more traditional liquid-drop model calculations in which we have studied surface diffuseness effects and the effects of the rupture of finite-radius necks. Also, some study continues of the microscopic foundations of nuclear hydrodynamics. Efforts continue in nuclear reaction theory. A phenomenological optical potential has been developed which accurately reproduces coupled-channel effects in heavy-ion Coulomb excitation. Folding models have been used to calculate optical potentials starting from realistic interactions.

TIME-DEPENDENT HARTREE-FOCK CALCULATIONS FOR AXIALLY SYMMETRIC SYSTEMS

S. E. Koonin[1] H. Feldmeier[2]
K. T. R. Davies S. J. Krieger[3]
V. Maruhn-Rezwani J. W. Negele[4]

Time-dependent Hartree-Fock (TDHF) calculations for the collision of two nuclei have been performed in the two-dimensional axial-frame approximation.[5,6] In this model it is assumed that the nuclear system remains axially symmetric about the line joining the two colliding nuclei. This line then rotates in real three-dimensional space with an angular frequency ω:

$$\omega = d\theta/dt = L/I \quad , \tag{1}$$

where L is the angular momentum of the system and I is its moment of inertia.

Since last year a number of new features have been incorporated into our axially symmetric TDHF program. Five of these features are discussed below.

Separation of Neutron and Proton States—Calculations with the Full Skyrme Force

We now allow for the isospin degree of freedom, so the neutron and proton wave functions are no longer identical. To avoid treating neutrons and protons separately, we previously used an effective charge,[5,6]

an approximation which is valid only for light systems.

A second change has been to extend our theory to treat the nonlocal parts of the complete Skyrme force.[7] The two-body part of the Skyrme force, without the spin-orbit contribution, is of the form

$$v_{12} = t_0(1 + x_0P_\sigma)\delta(\mathbf{r}_1 - \mathbf{r}_2) + \tfrac{1}{2}t_1[\delta(\mathbf{r}_1 - \mathbf{r}_2)p^2 + p^2\delta(\mathbf{r}_1 - \mathbf{r}_2)] + t_2\mathbf{p}\delta(\mathbf{r}_1 - \mathbf{r}_2)\mathbf{p} \quad (2a)$$

where P_σ is the spin-exchange operator and $\mathbf{p} \equiv \frac{1}{2i}(\nabla_1 - \nabla_2)$.

The force also contains a three-body term,

$$v_{123} = t_3\delta(\mathbf{r}_1 - \mathbf{r}_2)\delta(\mathbf{r}_2 - \mathbf{r}_3) \quad . \quad (2b)$$

The parameters t_0, x_0, t_1, t_2, and t_3 have been determined by fitting the binding energy and density of infinite nuclear matter and also the binding energy and radius of ^{16}O.[7] In our previous studies,[5,6] we used a simplified version of the Skyrme force in which $t_1 = t_2 = 0$. It is thought that this simplified force is too naive and restrictive, especially for heavy systems.

Mass-Asymmetrical Collisions

Our codes have been generalized to treat systems which are not reflection-symmetric about the midplane of the collision axis.

Self-Consistent Phase Theory

In our previous studies,[5,6] the moment of inertia in Eq. (1) was computed using the rigid, clutching model, in which it is assumed that the moment of inertia is that of two point masses when the two ions are separated and is the rigid body value when the two ions "clutch," or interpenetrate one another. This approximation has been removed by the development of a fully self-consistent phase theory for the calculation of the moment of inertia.[8] In this theory both the centrifugal force and the average effect of the Coriolis force are included.

In the usual axially symmetric TDHF theory, one deals with the single-particle wave functions

$$\psi_i(\rho, z)\exp(im\phi), \quad i = 1, 2, \ldots, A \quad ,$$

where ψ_i is complex and ρ, z, and ϕ refer to cylindrical coordinates. In the phase theory this wave function is replaced by the more general form

$$\psi_i(\rho, z)\exp\{i[m\phi + g(\rho, z)\cos\phi]\}, \quad i = 1, 2, \ldots, A. \quad (3)$$

where g is a *real* function of ρ and z. One then takes variations with respect to the ψ_i's and g, which yields TDHF equations for the ψ_i's and an inhomogeneous partial differential equation for g.[8] The latter can be easily solved by the Peaceman-Rachford method.[9] This method results in TDHF calculations that are only about 5% slower for light nuclei than those using the rigid, clutching model. This percentage decreases as we go to heavier systems.

Self-Consistent Initial Wave Functions

In order to avoid energy and density oscillations at the beginning of the calculation, it is important at $t = 0$ to use correct self-consistent single-particle wave functions for each of the two colliding ions. The force used for calculating the static wave functions should be exactly the same as that used in the TDHF calculation. A code has been developed to calculate static HF wave functions for the full Skyrme force given by Eq. (2).

Charge and Mass Distributions

A true TDHF wave function ψ is a Slater determinant at all times. Initially the determinant may be written as an antisymmetrized product of two nonoverlapping determinants describing the separated ions. Thus, at $t = 0$ the wave function is an eigenfunction of the operators $\hat{N}_R$ and $\hat{N}_L$, which count the number of nucleons to the right ($z > z_d$) and to the left ($z < z_d$) of the dividing plane z_d for the reaction. Of course, $\hat{N}_R + \hat{N}_L = \hat{N}$, the total number operator. After the reaction, the wave function is no longer an eigenfunction of the separate operators $\hat{N}_R$ and $\hat{N}_L$ but rather only of $\hat{N}$. That is, at any later time, t, the wave function will, in general, be a wave packet containing states with a diverse number of particles in the right- or left-hand space. Asymptotically, the distribution in particle number is time independent and we may, therefore, calculate the probability, $P(A_R)$, that the final state contains A_R particles in the right-hand space (and $A_L = A - A_R$ particles in the left-hand space). We have written a code to calculate the quantity:

$$P(A_R) = \frac{A!}{A_L!A_R!}\int_{-\infty}^{z_d} dz_1 dz_2 \ldots dz_{A_L} \times \int_{z_d}^{\infty} dz_{A_L+1} \ldots dz_A |\psi|^2 \quad . \quad (4)$$

where for simplicity of notation all other integration variables other than z have been suppressed. We also calculate for a given number of particles on the right-hand side, A_R, the separate probabilities for finding Z_R protons and N_R neutrons on the right-hand side (with $Z_R + N_R = A_R$). The calculated charge and mass distributions can be directly compared with the experimental results.

Considerable effort has also been devoted in the last year to various methods for speeding up the computer codes to make them more efficient. Other features which we plan to include in our future calculations are pairing effects and spin-orbit forces. We now present some results of our calculations.

In Fig. 3.1 the energy loss and scattering angle are plotted as a function of the angular momentum L for TDHF calculations of $^{16}O + {}^{16}O$ and $^{40}Ca + {}^{40}Ca$, using the rigid, clutching model.[9] The deep minimum observed in each reaction for the deflection function occurs at an L value which corresponds to an orbiting trajectory. As the angular momentum is increased beyond the orbiting value, the attraction of the nuclear potential is almost counterbalanced by the centrifugal and Coulomb repulsion. For L above grazing (≈45 for $^{16}O + {}^{16}O$; ≈100 for $^{40}Ca + {}^{40}Ca$) the trajectories are nearly pure Coulomb. Plots of the energy loss and deflection-function curves for the self-consistent phase theory are dramatically different from the curves shown in Fig. 3.1. In the phase theory there is much more energy loss, particularly for low L, and the orbiting L is shifted to a considerably smaller value.

The scattering behavior for the reaction $^{14}N + {}^{12}C$ is shown in Fig. 3.2, which displays the asymptotic laboratory energy of the more energetic reaction product as a function of the final laboratory scattering angle, for various L values.[9] Comparable experimental curves were extracted from the fragment energy distributions at a given angle by determining the mean energy of the direct inelastic component.[10] There is, of course, one experimental curve for each outgoing mass, each of which is included in the TDHF final state. The intrinsic mass spread is further broadened by the evaporation of light particles from the excited, inelastically scattered fragment. The direct inelastic cross section near 10° in the laboratory system is associated with only the upper branch in Fig. 3.2 ($L \approx 30.5$ to $L \approx 28.5$), since the reactions pertaining to the other branches have lost more energy and are assumed to have fused. The agreement with experiment for the upper branch is excellent.

Finally, in Fig. 3.3 we show a density profile for the reaction $^{16}O + {}^{40}Ca$ at a laboratory energy of 224 MeV and an angular momentum of 15. This calculation was made using the full Skyrme force, Eq. (2), with separate neutron and proton states, and using the self-consistent phase theory. The two ions approach each other with little distortion until they coalesce at $t \approx 0.15$. The compound system undergoes a series of shape oscillations until $t \approx 0.375$, when a

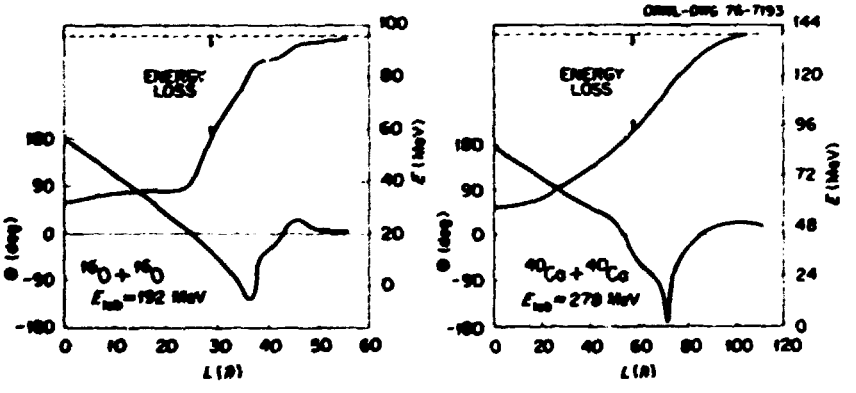

Fig. 3.1. Deflection and energy-loss functions for representative $^{16}O + {}^{16}O$ and $^{40}Ca + {}^{40}Ca$ reactions. The dotted line represents elastic scattering.

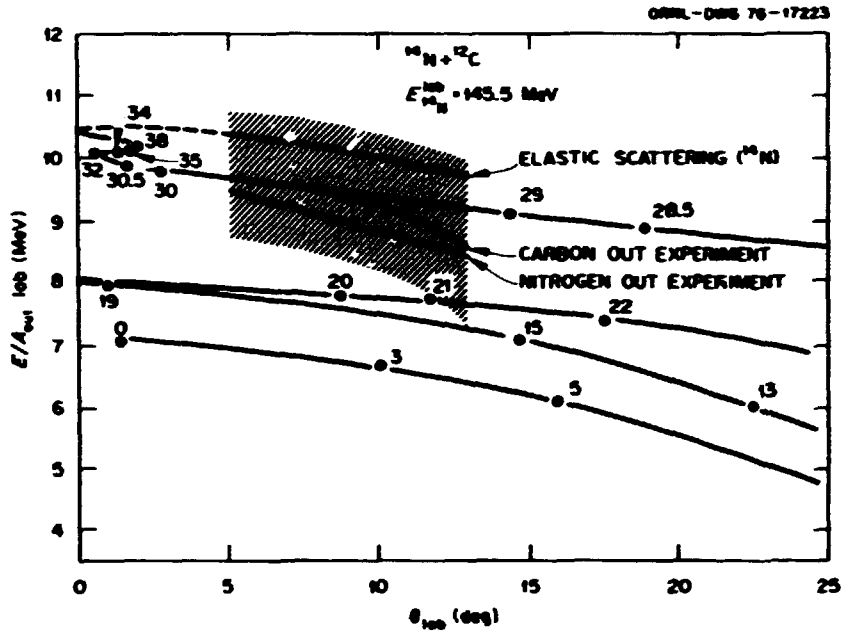

Fig. 3.2. Outgoing energy per particle as a function of the laboratory scattering angle at a bombarding energy of 145.5 MeV for the $^{14}N + ^{12}C$ reaction. The numbers on each curve indicate the TDHF angular momenta. The experimental curve (dashed lines) is for direct inelastic reaction products of various masses and should be compared with the upper part of the theoretical curve. The shaded area corresponds to the width of the energy distribution of the direct inelastic ^{12}C fragment yield.

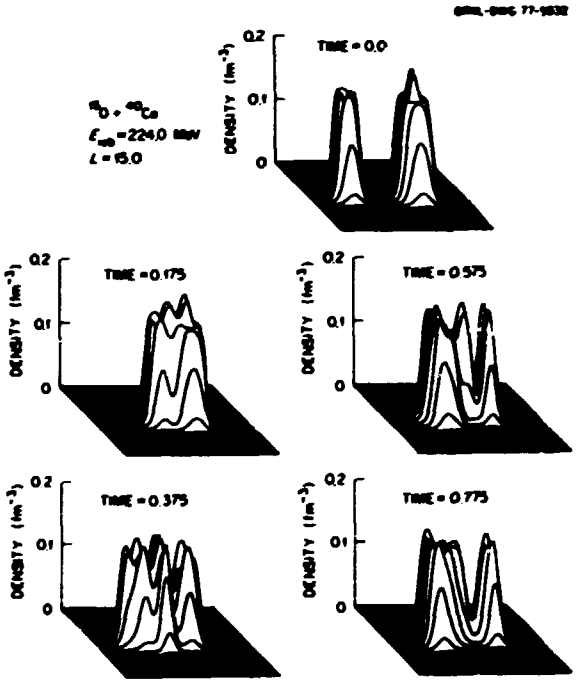

Fig. 3.3. Density profile for an $^{16}O + ^{40}Ca$ reaction, at E_{lab} = 224 MeV, L = 15. The density in units of fm^{-3} is plotted vertically above the (ρ, z) plane. The times are in units of 10^{-21} sec.

pronounced neck starts to form. However, due to the delicate balance of nuclear, Coulomb, and centrifugal forces, the system does not undergo scission until $t \approx 0.775$, after which the two ions separate.

1. Niels Bohr Institute, Copenhagen, Denmark.
2. Technische Hochschule, Darmstadt, Germany.
3. University of Illinois at Chicago Circle.
4. Massachusetts Institute of Technology, Cambridge.
5. S. E. Koonin et al., *Phys. Rev. C* 15, 1359 (1977).
6. V. Maruhn-Rezwani, K. T. R. Davies, and S. E. Koonin, *Phys. Lett.* 67B, 134 (1977).
7. D. Vautherin and D. M. Brink, *Phys. Rev. C* 5, 626 (1972).
8. H. Feldmeier, to be published as an ORNL report.
9. R. Varga, *Matrix Iterative Analysis*, Prentice-Hall, Englewood Cliffs, N. J., 1962, p. 209.
10. R. G. Stokstad et al., *Phys. Rev. Lett.* 36, 1529 (1976); and private communication.

TDHF DESCRIPTION OF THE $^{14}N + ^{12}C$ REACTION

J. A. Maruhn R. Y. Cusson[1]

The previously developed computer code for the calculation of heavy-ion reactions in a three-dimensional TDHF description has been applied to a study of the $^{14}N + ^{12}C$ reaction at 8 MeV per nucleon.

where a comparison of results with the measurements of Stokstad et al.[2] is possible.

The behavior of the nuclei according to these calculations may be understood to a large extent in analogy to that of waterdrops colliding, as studied experimentally in ref. 3. At quite large impact parameters, outside the range of the nuclear forces, there is only Coulomb interaction, and the scattering angle is small and positive, as shown in Fig. 3.4. At smaller impact parameters the influence of the nuclear forces is felt, which opposes the Coulomb repulsion, so that the scattering angle, after reaching a maximum, the "grazing angle," goes down sharply and turns toward negative values.

Still going toward decreasing values of the impact parameter, we then see a relatively narrow area of very large scattering angles, which correspond to a long period of joint rotation of the interacting nuclei, in this case allowing for almost one full revolution.

At still smaller impact parameters, however, and extending to central collisions, the interaction time and the net scattering angle decrease again.

In fact, for central collisions a very rapid reseparation of the fragments is observed, analogous to the "vibrational instability" known from waterdrop experiments.[3] However, the masses of the two fragments are exchanged in the process, which leads to the assumption that they actually "pass through" each other. This assumption cannot be made definite in quantum mechanics, though, because nucleon exchange and "passing through" are indistinguishable processes. The time dependence of the density for a small impact parameter is depicted in Fig. 3.5.

The main data obtained from a TDHF calculation are thus the final scattering angles for each angular momentum and also the final energies. Their dependence on angular momentum is shown in Fig. 3.6.

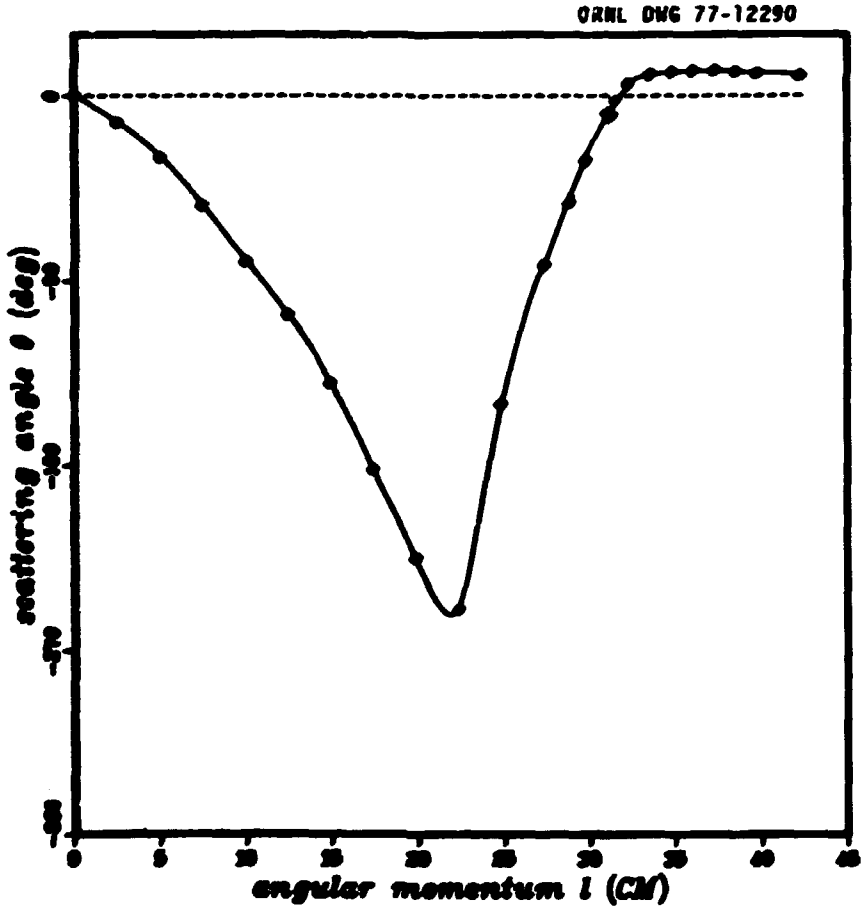

Fig. 3.4. Deflection function $\theta = \theta(l)$ for $^{14}N + ^{12}C$ at 8 MeV/A.

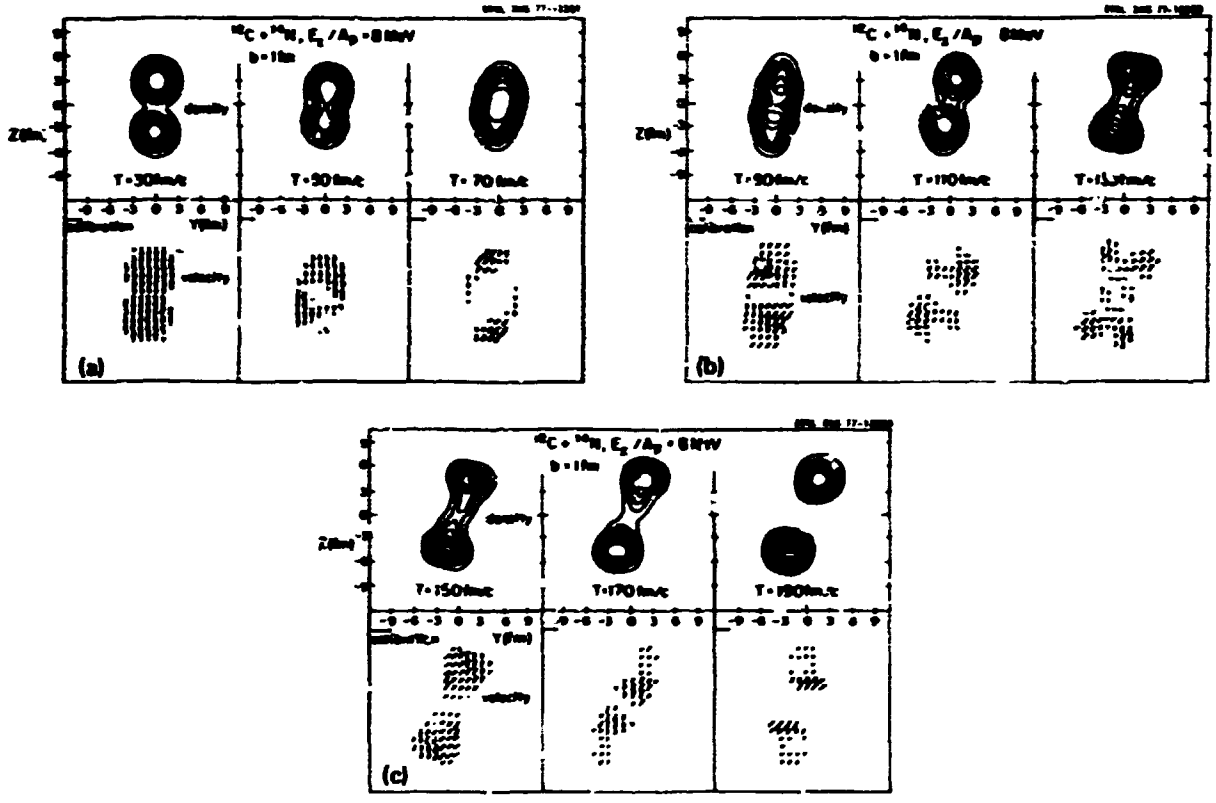

Fig. 3.5. Time dependence of density and velocity field in the scattering plane for an impact parameter of 1 fm.

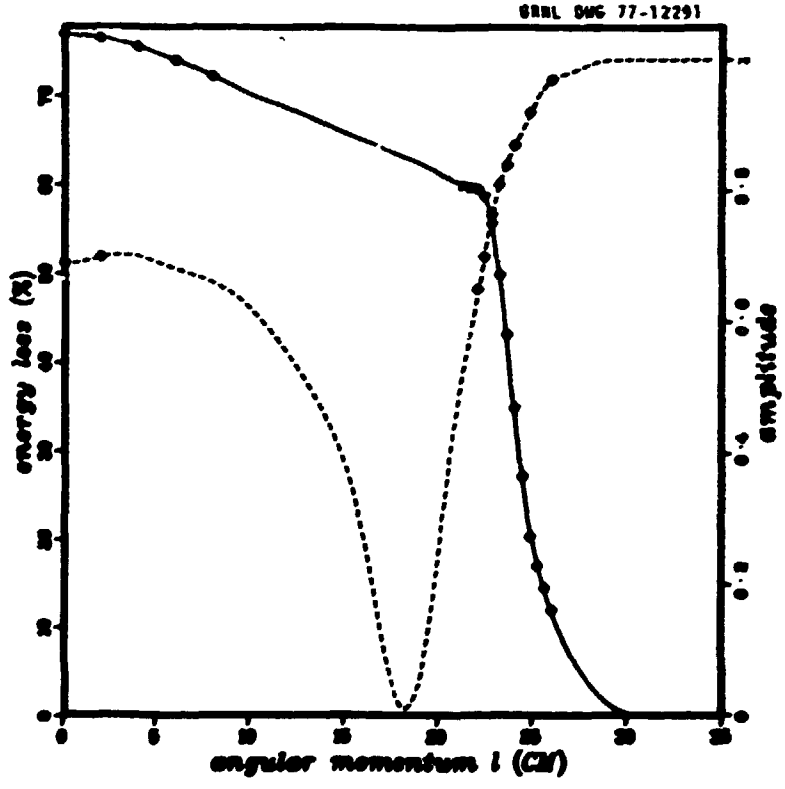

Fig. 3.6. Dependence of kinetic energy loss (in percent of initial kinetic energy) and amplitude for staying in the direct inelastic channel (dashed line) as a function of angular momentum.

These two quantities are sufficient to determine the scattering cross section completely within the framework of classical mechanics. The results obtained in this way, however, strongly disagree with experimental data. It thus appears that there are serious shortcomings in the simple pure TDHF model. Closest examination of the problem reveals some features of TDHF that may be responsible:

1. The TDHF wave function, being constrained to a single Slater determinant, does not describe population of several outgoing channels with a fractional transmission coefficient for each. In this case, for example, there is no amplitude for complete fusion, although fusion is known experimentally to be the dominating process.
2. Like every shell model wave function, the TDHF wave function does not describe a free-wave packet for its center-of-mass motion; instead, the center of mass is bound in the average potential. Thus the center of mass remains localized even asymptotically, and essentially only classical scattering can be obtained.

In order to circumvent these difficulties, it was decided to add considerations that were extraneous to TDHF as such but were assumed to supply reasonable physical behavior where it is lacking in the pure TDHF theory.

The first problem can be surmounted by noting that the TDHF solutions represent highly excited compound systems during the collision. However, in TDHF no evaporation takes place. Knowing the excitation energy E^* as a function of time, we can utilize a statistical model to compute the probability for evaporation, $\exp(-\Gamma_\nu h)$, at a given time. The probability for evaporating at least one particle during the collision will then be given as

$$1 - C_l^2 = \exp\left\{-\frac{1}{\hbar}\int \Gamma[E^*(t)]\, dt\right\}$$

for each angular momentum l. Since it may be assumed that the loss of more than 8 MeV of excitation will lead to fusion of the compound system and that evaporation will be the dominant process of deexcitation, we may to some approximation identify the probability C_l^2 for no evaporation with that for staying in the direct inelastic channel and not fusing. The C_l^2 thus acts as transmission coefficients in the scattering problem.

To remedy the second problem, we take recourse to semiclassical scattering theory, which allows us to compute the scattering phase shift δ_l from the classical deflection function $\theta(l)$ as[4]

$$\delta_l \cong \tfrac{1}{2}\int_{l+\frac{1}{2}}^{\infty} \theta(l)\, dl \ .$$

In addition, to obtain a quantum-mechanical treatment we have to allow interference of the different final states. This can be done by smearing final states with an energy-dependent weight function $g(E) \propto \exp[\alpha(E - E_l)^2]$, where E_l is the final energy for angular momentum l as obtained from TDHF.

With these modifications the differential cross section for direct inelastic scattering may be obtained from the scattering amplitude

$$f(\theta, E) = \frac{i}{2}\sum_l \frac{(2l+1)}{k} g(E) C_l \exp(2i\delta_l) P_l(\cos\theta) \ .$$

All the quantities entering this equation are now computable from the TDHF results. The amplitude C_l (Fig. 3.6) is 1 at very large angular momenta and then decreases, reaching a miminum for those values of l with long orbiting, as discussed above. For small angular momenta it rises again, but because of the high excitation energies encountered, there is still a considerable probability for fusion in spite of the short collision time.

Finally, the direct inelastic cross section is compared with experimental data (Fig. 3.7). It shows the same average exponential decay as for the experimental cross section, but with an oscillation superimposed. This oscillation probably will be damped if the distribution of final states in angular momentum, as well as in energy, is considered.

Knowledge of the transmission coefficients C_l^2 also enables us to compute the fusion cross section:

$$\sigma_{fus} = \frac{\pi}{k^2}\sum_l (2l+1)(1 - C_l^2) \ .$$

With the data shown in Figs. 3.4 and 3.6 the result was 850 mb, compared with the experimental value of 900 ± 100 mb.

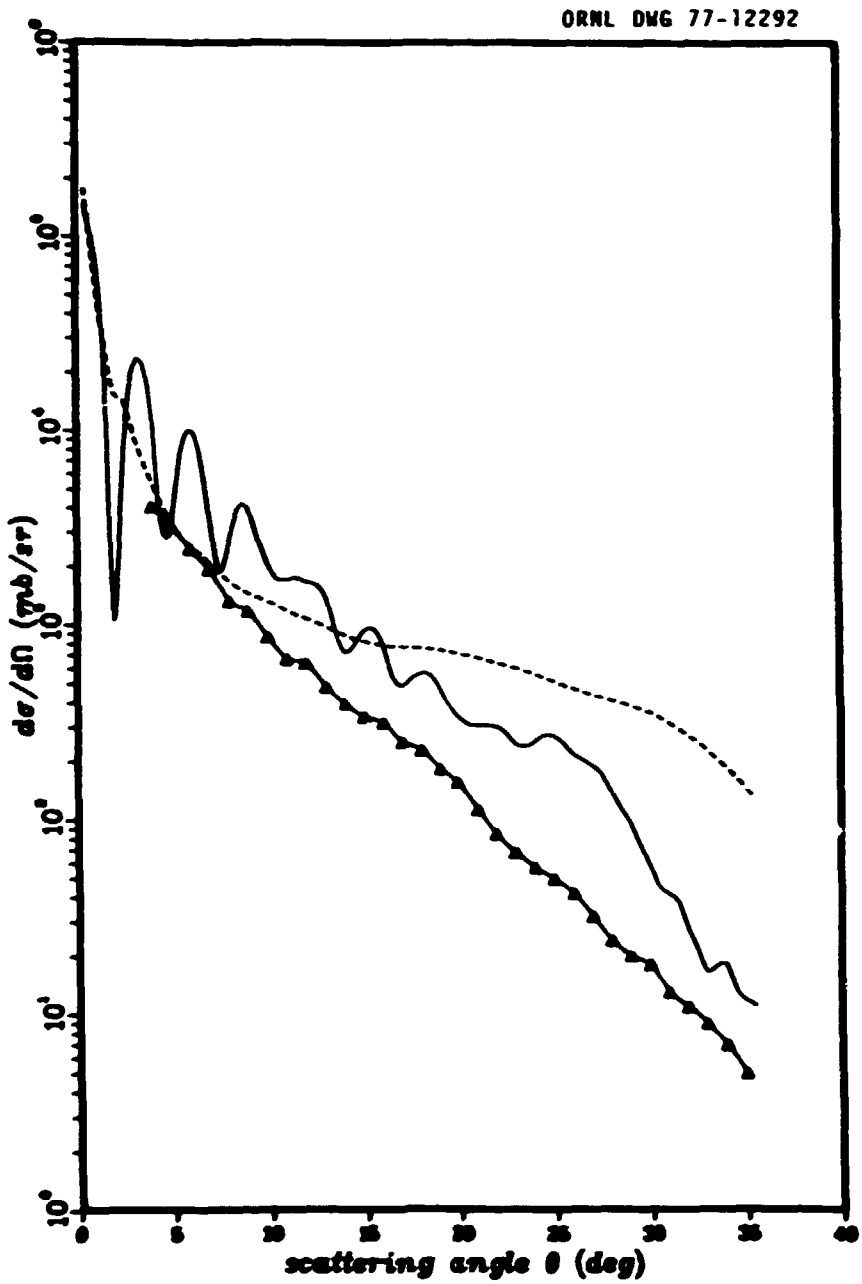

Fig. 3.7. Differential cross section for direct inelastic scattering of $^{14}N + ^{12}C$ at 8 MeV/A. Triangles: experimental data. Solid line: theoretical result. Dashed line: contribution to be expected theoretically from vibrational instability at small angular momenta; because of the low outgoing energies it cannot easily be distinguished from fusion residues experimentally.

We acknowledge stimulating discussions with H. W. Meldner.

1. Consultant to ORNL from Duke University, Durham, N.C.

2. R. G. Stokstad, J. Gomez del Campo, J. A. Biggerstaff, A. H. Snell, and P. Stelson, *Phys. Rev. Lett.* 36, 1529 (1976); and R. G. Stokstad, private communication.

3. J. R. Adams, N. R. Lindblad, and C. D. Hendricks, *J. Appl. Phys.* 39, 5173 (1968).

4. K. W. Ford and J. A. Wheeler, *Ann. Phys.* 7, 259 (1959).

NUCLEAR HYDRODYNAMICS IN TWO AND THREE DIMENSIONS

Henry Tang[1] C. Y. Wong

In order to simulate the dynamics of heavy-ion collisions in the hydrodynamical model, we solve numerically the complete set of hydrodynamical equations for the collision of two cylinders or two spheres of nuclear matter,[2] using the Boris-Book algorithm of flux-corrected transport and the time-step splitting method.[3] The two-dimensional result is useful in assessing the accuracy of the method and in paving the way for three-dimensional calculations which are required in order to compare with experimental results.

Apart from the features due to nuclear interactions, the nuclear fluid is ascribed to be viscous, compressible, and thermally conducting. The separation of the nuclear interaction into a short-range density-dependent part and a long-range Yukawa part allows the use of an equation of state to represent the properties of the nuclear fluid.

We shall show some typical results we have obtained. In our plots the density contours are graded in steps of 0.025 fm^{-3}, and the current vector at a point is displayed as an arrow which originates from the point in question and has a length proportional to the magnitude.

Figure 3.8 shows the dynamics for the two-dimensional case of a collision of two "nuclei" (cylinders) with radii 2.5 fm at an energy E (per projectile nucleon with the target at rest) of 20 MeV. The impact parameter B for this case is 0 fm. The shear viscosity coefficient η and the compressional viscosity coefficient ζ are set equal to 10^{-4} MeV/($fm^2 \cdot c$) and the thermal conductivity κ is set equal to 10^{-4} c/fm^2.

In our equation of state for nuclear matter, we used an incompressibility of 143 MeV, which corresponds to a critical kinetic energy of 7.9 MeV per nucleon above which the speed of sound is exceeded. Thus, in our case with the collision of 20 MeV per nucleon, the density in the central region increases rapidly from 0.15 fm^{-3} to 0.25 fm^{-3}. This high density drops down slightly to about 0.20 fm^{-3} at $t \approx 35$ fm/c, at which time the current field becomes nearly isotropical. The dynamics do not appear to alter significantly for the next 100 fm/c. There is at the early stage a rapid flow in a direction perpendicular to the collision axis, to be followed by a nearly isotropical current distribution at the later stage. The large velocities at the surface, upon exceeding a certain limit, provide the necessary escape velocities for nucleons. One therefore expects emission of nucleons first in a direction perpendicular to the collision axis, to be followed by an isotropic emission at a later stage.

In Fig. 3.9, we show the same collision at an impact parameter of 4 fm. With such an impact parameter, the resultant central density is not as high as in the head-on case. At $t = 20.25$ fm/c, after the central density attains a single peak, there develops an attempt to split the density into two parts. However, for such a small system, the attractive nucleon-nucleon interaction is able to bring the system together without splitting at a later stage. The system appears to be fused at 160 fm/c.

Results in Fig. 3.8 and 3.9 were obtained with small values of viscosity coefficients and thermal conductivity. Now, if one uses the shear viscosity coefficient determined by Davies et al.,[4] that is, $\eta = 5.7$ MeV/($fm^2 \cdot c$), and uses $\zeta = 0.01$ MeV/($fm^2 \cdot c$) and $\kappa = 0.1$ MeV/fm^2, one finds that for the same head-on collision at 20 MeV the maximum density achieved is only 0.20 fm^{-3}, as compared with the 0.25 fm^{-3} for the previous case with small dissipative constants. Furthermore, after a maximal compression is achieved, the maximum density later drops down to 0.10 fm^{-3}. The density, however, maintains a radial expansion. Such an expansion is possible in spite of the low densities, since the temperature is now high enough to generate sufficient pressure for the expansion.

Using algorithms similar to those used in the two-dimensional calculations, a three-dimensional code has also been written which allows for shear, compressional viscosity, and thermal conductivity. We show in Fig. 3.10 a collision of ^{16}O with ^{16}O at 320 MeV laboratory energy and an impact parameter of 4 fm. The viscosity parameters are chosen to be $\eta = \zeta = 10^{-4}$ MeV/($fm^2 \cdot c$) and $\kappa = 10^{-4}$ MeV/fm^2. We are plotting the density contour only along a cut about the symmetry plane. As is observed, the central

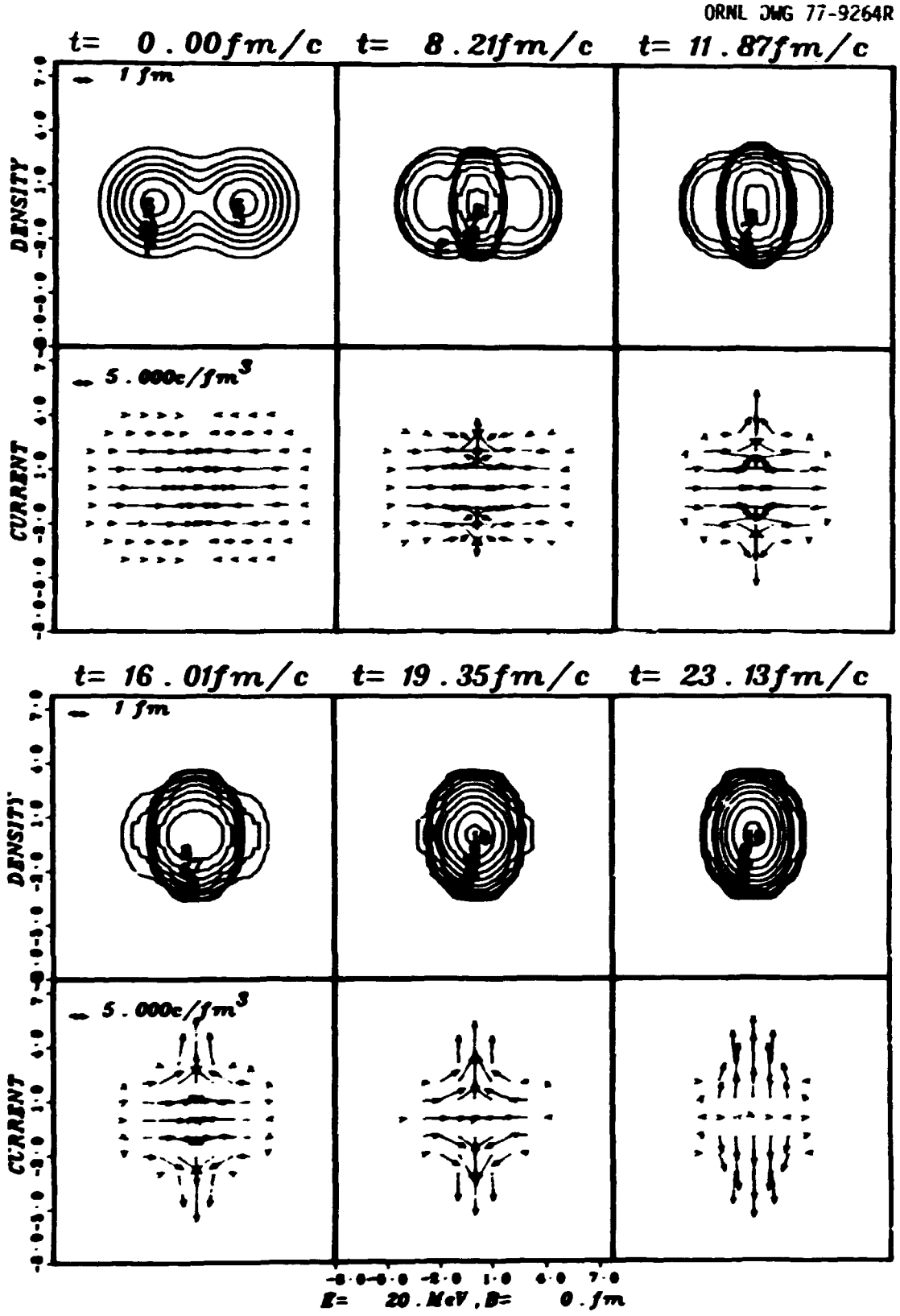

Fig. 38. Dynamics for the two-dimensional case with an impact parameter of 0 fm.

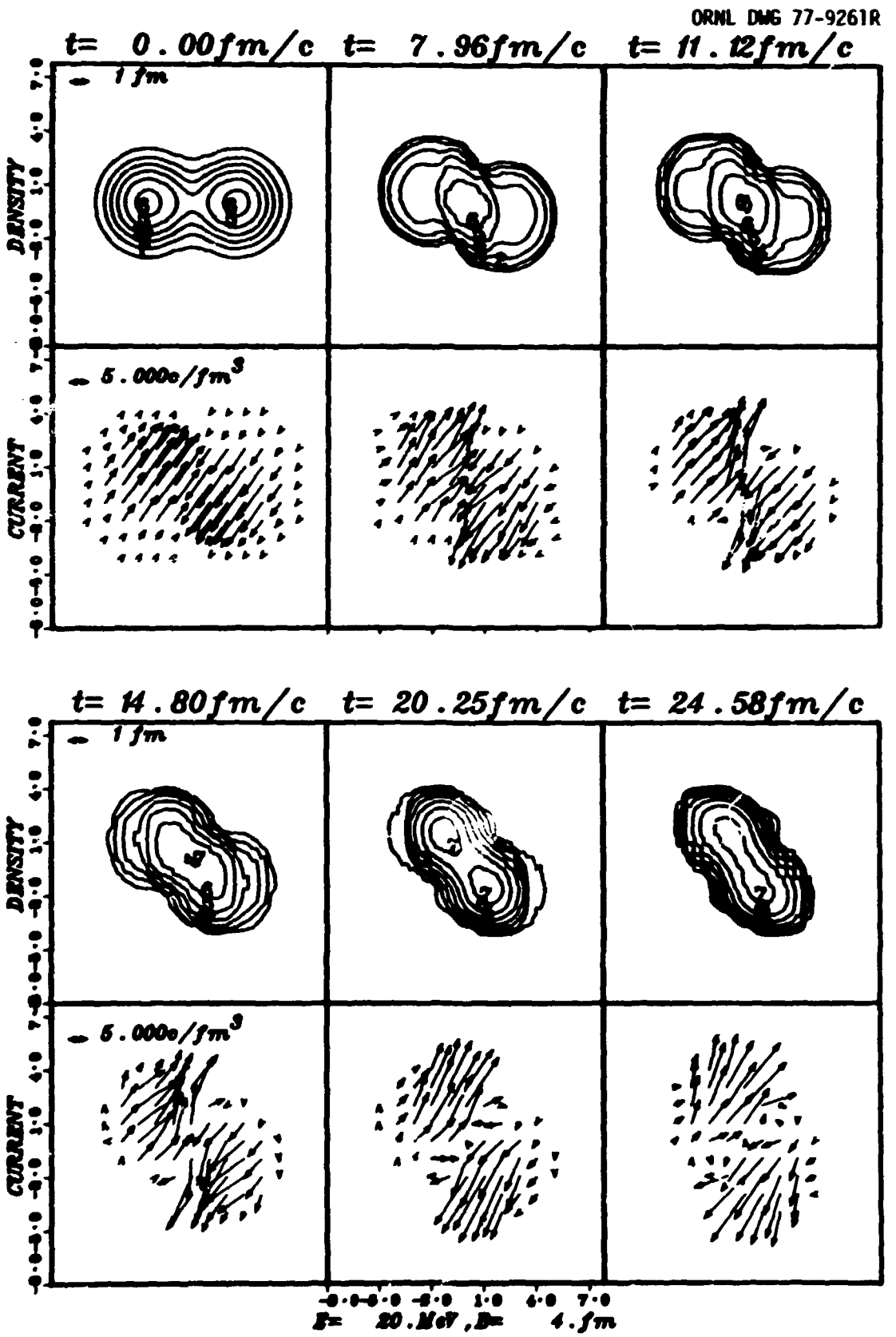

Fig. 3.9. Dynamics for the two-dimensional case with an impact parameter of 4 fm.

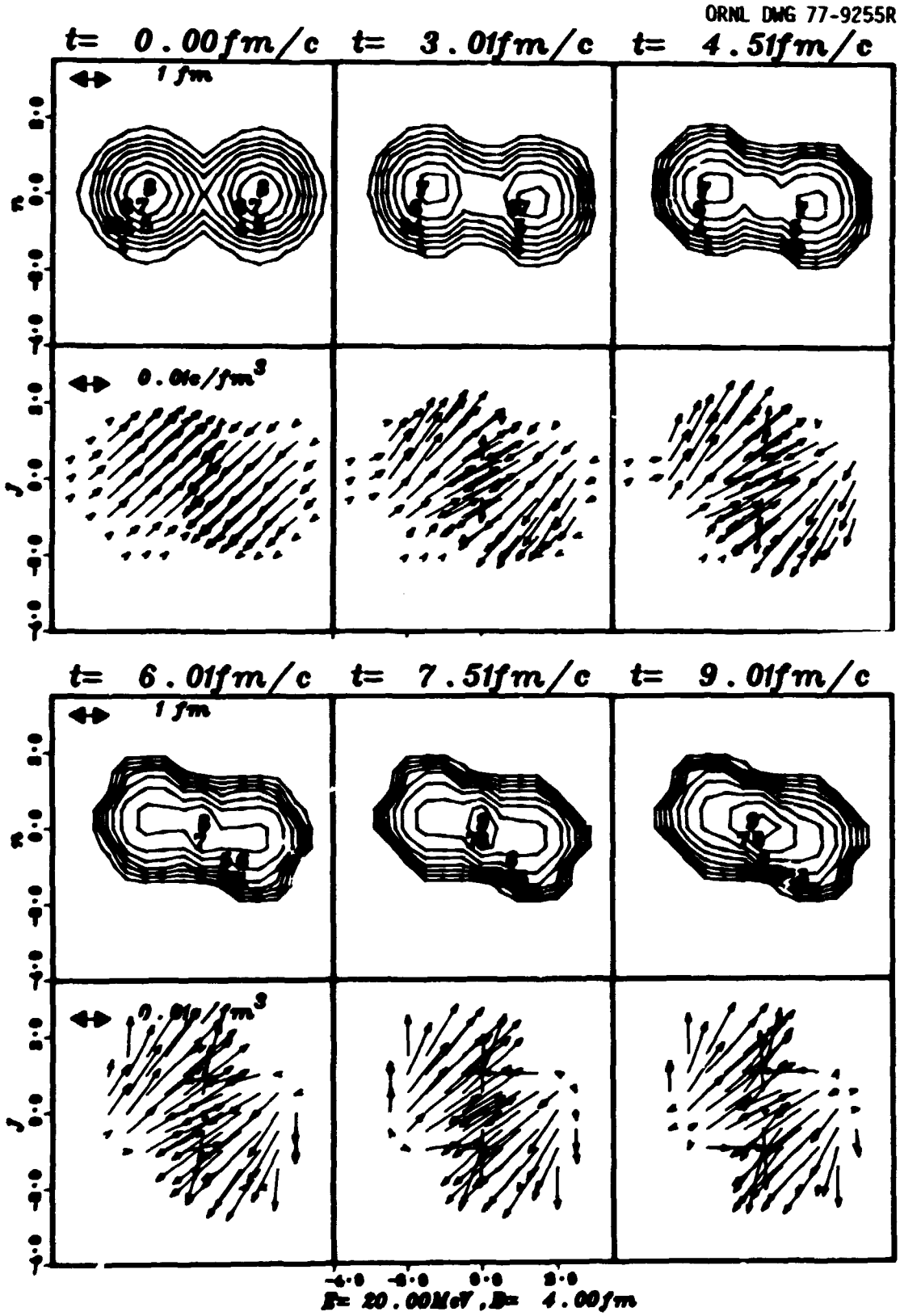

Fig. 3.10. Dynamics for the three-dimensional case with an impact parameter of 4 fm.

density rapidly merges to force a high-density core region which is followed by a rotation of the whole region.

1. Yale University, New Haven, Conn.
2. H. Tang and C. Y. Wong, *Bull. Am. Phys. Soc.* 22, 645 (1977).
3. J. P. Boris et al., *J. Comp. Phys.* 11, 38(1973); 18, 248 (1975); and 20, 397 (1976).
4. K. T. R. Davies et al., submitted to *Physical Review*.

FLUID-DYNAMICAL MODEL IN THREE DIMENSIONS

J. A. Maruhn T. A. Welton

In the past year, significant progress was made in the development of an efficient, fully three-dimensional code for solution of the hydrodynamic equations.[1] Extensive tests have been done with the code representing the macroscopic fluid variables on a spatial mesh of $32 \times 32 \times 17$ points, which for representing an $^{16}O + {}^{16}O$ collision allows a physical distance between mesh points of 0.6 fm. It was found in the one-dimensional test calculations that because of the short range (0.5 fm) of the Yukawa potential involved, the mesh point separation should be below this value to yield a reasonable accuracy in consistency checks—for example, energy conservation. The value 0.6 fm certainly does not fulfill that requirement, so one can only assume the results are at best suggestive.

The typical behavior of the results is shown in Figs. 3.11 and 3.12, which exhibit the time dependence of the density for head-on collisions at two different energies. Apparently the overall behavior is reasonable—that is, fusion and settling down to a compound system occurring at the low energy and flattening to a disklike shape at the high energy. There are shockfronts separating the compressed overlap zone from the inflowing matter.

In detail, however, there are serious problems which make these results unacceptable. The shapes have a marked tendency to exhibit four diamond-like configurations, even in the equilibrium state, which is unrealistic. Also, there is an energy loss during the collision comparable in magnitude to the initial kinetic energy. (This energy can be accounted for by properly heating up the shock zone, but since the shocks are too narrow this cannot be done satisfactorily.)

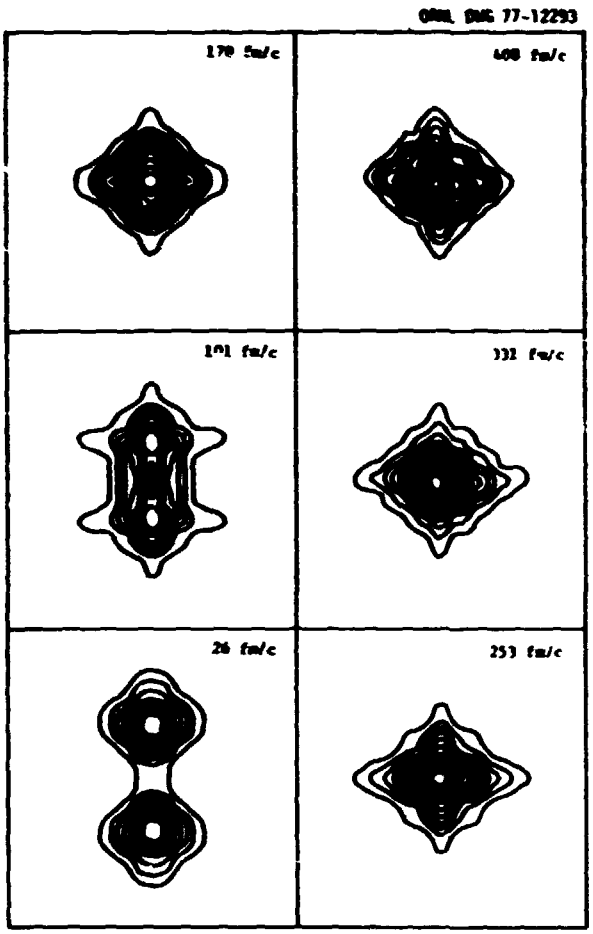

Fig. 3.11. Head-on collision of $^{16}O + {}^{16}O$ at 1.2 MeV/A in the c.m. system.

Since it thus appears obvious that a finer numerical mesh is called for, what is the raison d'être of this first three-dimensional code? Why not code for a higher accuracy from the start? Although the mesh sizes we used were unrealistic, there were several reasons for starting with this unrealistic case:

1. It is a relatively simple code, which uses about the maximum number of mesh points that can be dealt with in the computer core memory without using a swapping space on disk.
2. It made possible many numerical tests at a reasonable expense. A number of properties of the underlying algorithm could be tested without need for high physical accuracy.
3. It provided a first glimpse at the behavior to be expected of the physical system.

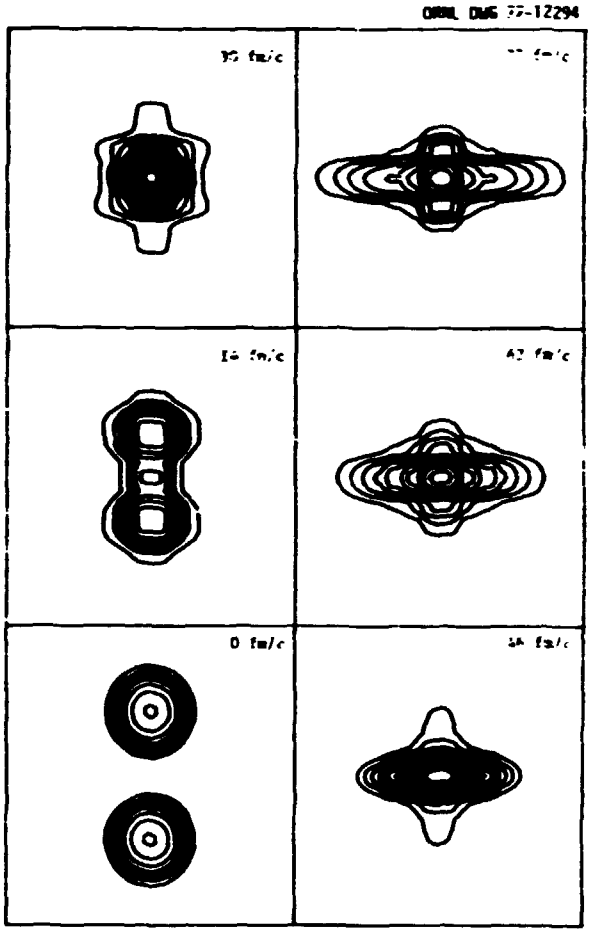

Fig. 3.12. Head-on collision of $^{16}O + ^{16}O$ at 19 MeV/A in the c.m. system.

4. It gave computing time estimates which can be extrapolated to the higher-accuracy code. The time of 3 sec per time step seemed quite encouraging as to the feasibility of the latter.

5. Since it is a thoroughly tested code, large parts of it can be transcribed simply into the bigger code now being developed. However, the new code will utilize disk swapping extensively and thus needs much more organization. First timing measurements for the refined calculation put it at 20 sec per time step, which with 100 to 200 time steps needed per collision, would keep it well within the realm of the possible.

1. J. A. Maruhn, T. A. Welton, and C. Y. Wong, *Phys. Div. Annu. Prog. Rep. Dec. 31, 1975*, ORNL-5137, pp. 134–35.

MANIFESTATIONS OF THE QUANTUM STRESS TENSOR

C. Y. Wong

Previously, starting from the time-dependent Schrödinger equation, we introduced a quantum stress tensor to exhibit the correspondence principle explicitly.[1] We have now investigated how such a quantum stress tensor manifests itself in providing peculiar nonclassical effects. We find that for a fermion system in a relatively smooth potential, the quantum stress tensor is related to the density n by

$$p_n = \left[\frac{\hbar^2}{12m}\nabla^2 n + \frac{\hbar^2}{5m}\left(\frac{6\pi^2}{g}\right)^{2/3} n^{5/3}\right]\delta_n .$$

The second term in the squared bracket is the usual pressure for a degenerate Fermi gas with degeneracy order g, while the first term, which appears to be novel, is proportional to the second spatial derivative of the density. This particular spatial dependence of the quantum stress tensor is found to give rise to density oscillations of finite and infinite fermion systems. The wavelength of the oscillation is inversely proportional to the square root of the incompressibility.

In another investigation we examine the form of the quantum stress tensor in a special case of the RPA approximation when the strength of the collective motion is concentrated in one particular state. In this case the time dependence of the spatial wave function can be properly described in terms of a displacement and a phase factor common to all single-particle states.[2] The quantum stress tensor is found to be proportional to the first spatial derivative of the displacement vector. The equation of motion becomes the Lamé equation which describes the propagation of elastic waves, a characterization first observed by Bertsch.[2]

1. C. Y. Wong, *J. Math. Phys.* 17, 1008 (1976).
2. G. F. Bertsch, *Ann. Phys.* 86, 138 (1974); *Nucl. Phys.* A249, 253 (1975).

DIFFUSE-SURFACE CORRECTIONS

K. T. R. Davies J. R. Nix[1]

We have calculated several quantities of physical interest for an arbitrarily shaped diffuse-surface

nuclear density distribution.[2] The surface is made diffuse by folding a short-range function over a uniform sharp-surface distribution of appropriate shape; that is, the density is described by

$$\rho(\mathbf{r}_1) = \rho_0 \int_s d^3r_2 g(|\mathbf{r}_1 - \mathbf{r}_2|) \ , \tag{1}$$

where the integration is over the sharp-surface shape. Most of our methods apply to arbitrary folding functions g, but for definiteness we have specialized most of our results to the Yukawa shape,

$$g(|\mathbf{r}_1 - \mathbf{r}_2|) = \frac{1}{4\pi a^2} \frac{\exp(-|\mathbf{r}_1 - \mathbf{r}_2|/a)}{|\mathbf{r}_1 - \mathbf{r}_2|/a} \ . \tag{2}$$

The quantities calculated include the moment of inertia about an arbitrary axis, generalized multipole moments, Coulomb and nuclear potentials, and Coulomb and nuclear energies.

Many of our results[2] are of practical importance in the theory of nuclear fission and heavy-ion reactions. In nuclei, the distance over which the density changes from 10 to 90% of its central value is approximately 2.4 fm. This distance is comparable to the nuclear radius for very light nuclei and is roughly 30% of the radius for very heavy nuclei. Thus, diffuse-surface corrections can be substantial, especially for very light nuclei. For example, we find that for light nuclei the diffuse nuclear surface increases the moment of inertia by about 50%, which increases the critical angular momentum at which compound-nucleus formation is no longer possible. Also, the diffuseness corrections to the Coulomb energy contain a term that is proportional to the surface area, which increases somewhat the effective surface energy of nuclei.

Recently, we have also derived expressions for the diffuse-surface corrections to the two central moments for reflection-symmetric shapes[3]

$$r = 2\langle z \rangle \ , \tag{3}$$

$$\sigma = 2\langle (z - \langle z \rangle)^2 \rangle^{1/2} \ , \tag{4}$$

where the angular brackets denote an average over the half-volume to the right of the midplane of the shape. These moments are coordinates for the two most important symmetric degrees of freedom encountered in dynamical calculations of fission and heavy-ion reactions. The coordinate r gives the distance between the centers of mass of the two halves of the system, and σ is a measure of the elongation of each half about its center of mass. We estimate that in very light nuclei the diffuse-surface corrections to r and σ are roughly 20 and 40% respectively.

---

1. Los Alamos Scientific Laboratory, Los Alamos, N.M.

2. K. T. R. Davies and J. R. Nix, *Phys. Rev. C* 14, 1977 (1976).

3. K. T. R. Davies, A. J. Sierk, and J. R. Nix, *Phys. Rev. C* 13, 2385 (1976).

RUPTURE OF THE NECK IN NUCLEAR FISSION

K. T. R. Davies J. R. Nix[2]
R. A. Managan[1] A. J. Sierk

We have completed new fission studies which take into account the rupture of the neck at a nonzero radius. These dynamical calculations are performed using classical equations of motion.[3,4] The collective potential energy is calculated by means of a modified liquid-drop model, in which the nuclear energy is obtained from a double-volume integral of a Yukawa effective two-body potential.[5,6] This interaction takes into account the finite range of the nuclear potential, which is very important for describing neck formation in fission or two nearly touching nuclei in a heavy-ion reaction. The collective kinetic energy is calculated for incompressible, nearly irrotational flow by use of the Werner-Wheeler method.[3,7] The transfer of energy from collective motion into internal motion is included by means of the Rayleigh dissipation function, which is calculated for two types of dissipation: (1) ordinary two-body viscosity which arises from individual two-body collisions, and (2) one-body viscosity which occurs because of nucleons colliding with a moving potential wall. Here we shall report the results of studies involving mainly two-body viscosity.

In previous dynamical calculations of fission,[3,4] scission was defined as occurring at a configuration for which the radius of the neck vanishes. However, scission should in fact occur before the nucleus reaches this limiting configuration because of the delicate balance between the Coulomb and nuclear forces during the dynamical descent from the fission saddle point. For large necks the attractive nuclear force is larger than the repulsive Coulomb force, and the nucleus is stable against neck rupture. Eventually the repulsive Coulomb force becomes larger in

magnitude than the attractive nuclear force. The neck then ruptures at a nonzero radius, as illustrated in Fig. 3.13.

We calculate the Coulomb and nuclear interaction energies for a shape like that shown in Fig. 3.13. These energies can be easily evaluated[6,7] as functions of the separation parameter s between the two portions of the system. The total interaction force is then given by

$$F = \lim_{s \to 0} \left[\frac{-\partial E(s)}{\partial s} \right] , \tag{5}$$

where

$$E(s) = E_N(s) + E_C(s) , \tag{6}$$

the sum of the nuclear and Coulomb interaction energies. Note that we have mentally sliced the system into two portions at its minimum neck radius and have calculated the force required to separate these portions while keeping their shapes fixed. Scission is defined as that configuration where F vanishes.

For either one- or two-body dissipation, we find that the neck radius at rupture is about 2 fm for actinide nuclei. This relatively large neck-rupture radius increases somewhat the translational kinetic energy of the fission fragments at infinity as compared with that calculated for a zero-neck-radius scission configuration. The calculated fission-fragment kinetic energy is shown in Fig. 3.14 as a function of $Z^2/A^{1/3}$ for various values of the two-body viscosity coefficient μ. The dashed curves give the contributions to the kinetic energy acquired prior to neck rupture, which are somewhat smaller than the corresponding values for a zero-neck-radius scission given in ref. 3. Nevertheless, the more compact shapes

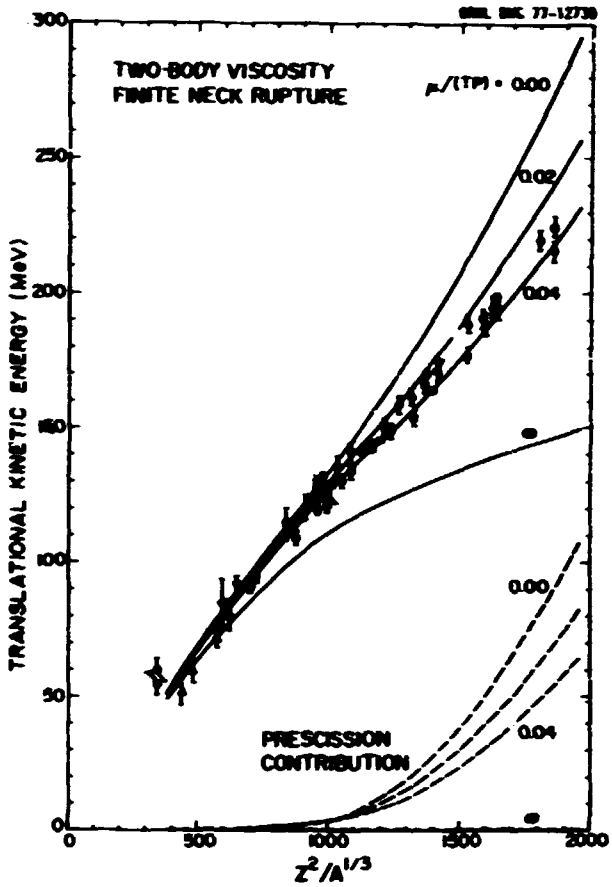

Fig. 3.14. Comparison of experimental most-probable fission-fragment kinetic energies with results calculated for different values of the two-body viscosity coefficient μ (solid curves). The dashed curves give the calculated translational kinetic energies acquired prior to neck rupture. The experimental data are for the fission of nuclei at high excitation energies, where the most probable mass division is into two equal fragments. The open symbols represent values for equal mass divisions only, and the solid symbols represent values averaged over all mass divisions. The experimental data are exactly the same as those in Fig. 12 of ref. 3, where references to the appropriate experimental papers can be found.

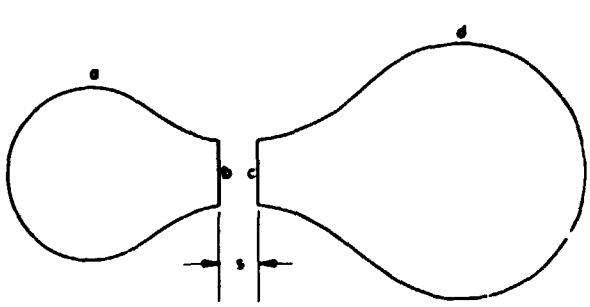

Fig. 3.13. Illustration of the neck-rupture degree of freedom. The nucleus is sliced into two portions at its minimum neck radius. In evaluating the interfragment forces, we take the limit of $s \to 0$.

at neck rupture lead to final kinetic energies that are always larger than those calculated for a zero-neck-radius scission. Therefore, to reproduce the same experimental data with the present calculations requires a larger two-body viscosity than with the earlier calculations.

In particular, it can be seen from Fig. 3.14 that the value

$$\mu = 0.03 \pm 0.01 \text{ terapoise}$$
$$= 19 \pm 6 \times 10^{-24} \text{ MeV·sec/fm}^3$$

accounts for most of the experimental data to within their uncertainties. As in ref. 3, we place greater weight on the experimental data for lighter actinide nuclei than on that for very heavy nuclei. The present value of μ is twice as large as that obtained in ref. 3 and is about 60% of the value required to critically damp quadrupole oscillations of heavy actinide nuclei. This large change in the value of μ arising solely from incorporating a finite neck rupture indicates the sensitivity of the results to the precise details of the model.

---

1. Rice University, Houston, Tex.
2. Los Alamos Scientific Laboratory, Los Alamos, N.M.

3. K. T. R. Davies, A. J. Sierk, and J. R. Nix, *Phys. Rev.* C 13, 2385 (1976).
4. J. R. Nix, *Nucl. Phys.* A130, 241 (1969).
5. J. R. Nix and A. J. Sierk, *Phys. Scr.* 10A, 94 (1974).
6. K. T. R. Davies and J. R. Nix, *Phys. Rev.* C 14, 1977 (1976).
7. K. T. R. Davies and A. J. Sierk, *J. Comp. Phys.* 18, 311 (1975).

ROTATING TOROIDAL NUCLEI

C. Y. Wong

The equilibrium shape of a nucleus under rotation has been the subject of many investigations. From the survey of Cohen, Plasil, and Swiatecki,[1] we know how, in the liquid-drop model, the equilibrium shapes vary with the angular momentum and the fissility parameter. As of yet, much of the discussion of a rotating nucleus is limited to shapes with the topology of a sphere. However, for very rapidly rotating systems, the moment of inertia can be readily increased if the mass is distributed in the form of a torus. Equilibrium or quasi-equilibrium toroidal systems become possible.[2] Indeed, many rapidly rotating and gravitating toroidal objects have been observed.[3] It is therefore of interest to investigate the stability of rotating toroidal nuclei.

In the discussion of rotating toroidal nuclei in equilibrium, we shall restrict ourselves to cases where the fluid elements of the nucleus are in a uniform rotation about the symmetry axis with a common angular velocity and where the meridian of the toroid is restricted to be circular. Such a problem lends itself to a simple treatment in toroidal coordinates in terms of which analytic expressions for various relevant quantities are already known.[4]

The toroidal threshold, above which rotating toroidal nuclei can be in equilibrium, is shown in Fig. 3.15 as a solid curve in the x-y plane. Here x is the

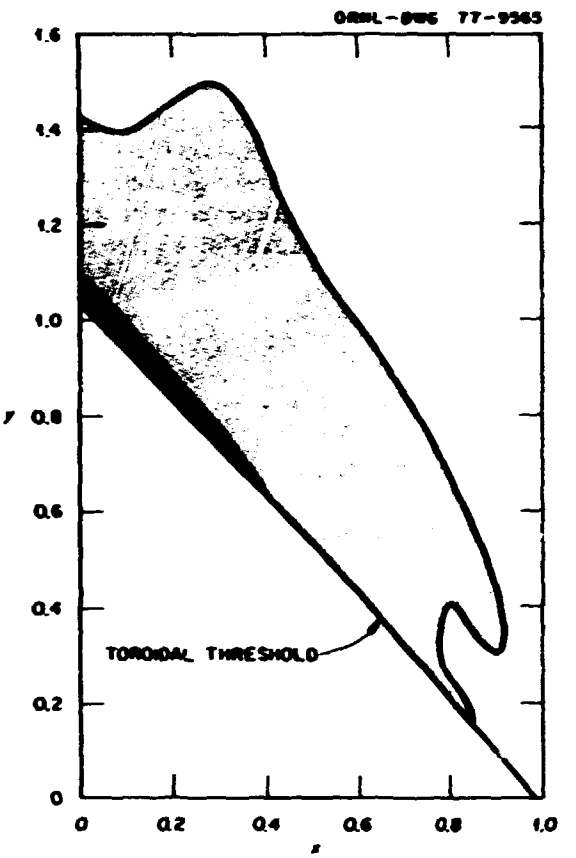

Fig. 3.15. Toroidal threshold and regions stable against sausage distortions in the x-y plane, where x is the fissility and y the rotational parameter. The solid curve is the toroidal threshold above which toroidal figures of equilibrium are possible. The shaded region is the stable region when the nucleus still undergoes uniform rotation after a sausage distortion, while the dotted region is the stable region if an axially nonuniform flow follows a sausage distortion.

fissility parameter defined in the usual way, and y is the rotational parameter defined by[1]

$$y = E_r^{(0)}/E_s^{(0)},$$

where $E_r^{(0)}$ and $E_s^{(0)}$ are, respectively, the rotational energy and the surface energy if the nucleus is in the spherical shape. One observes that the threshold curve can be approximated by the straight line $x + y \cong 1$.

The toroidal equilibrium we have obtained is stable against axisymmetric distortions of the nucleus. However, in our previous analysis of the stability of a nonrotating toroidal nucleus, the axially asymmetric sausage instability was found to be the most important instability. For a rotating toroidal nucleus,

a rigorous treatment of stability against sausage distortions would require a complete hydrodynamical analysis, since the perturbation of the shape will in general be associated with a nonuniform perturbation of the flow. We shall defer such a dynamical treatment until a later date and content ourselves with simple cases where the flow patterns are assumed known.

In the presence of dissipation, viscous forces can transfer the necessary angular momentum point by point and can dissipate the necessary energies to convert a nonuniform rotation into a uniform rotation, after a certain lapse of time. How rapid such a conversion can take place is completely unknown. For the case when uniform rotation follows rapidly from an axially asymmetric hydrodynamical flow, one can determine the region of stability for the toroidal nuclei. They are shown as the hatched region in Fig. 3.15. The region of stability is very small indeed. However, in the opposite extreme of axially asymmetric flow under axially asymmetric distortions, one can follow Dyson[5] to assume that the flow speed adjusts itself to maintain a constant flow rate across the meridians, when the circumference of the meridian varies in an asymmetrical way. Under such an assumption, the region of stability is much expanded and is shown as the dotted region in Fig. 3.15. In terms of the units of angular momentum for nuclei along the beta stability line, the stable toroidal region is shown as the dotted region in Fig. 3.16. It

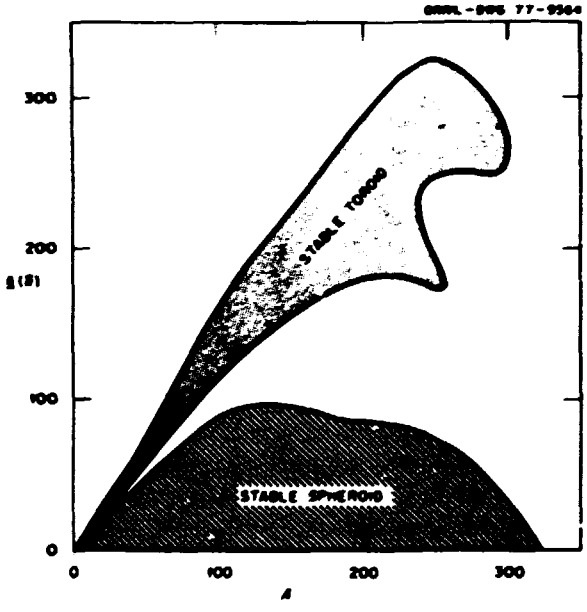

Fig. 3.16. Region of stable toroid under the assumption of nonuniform flow in a sausage distortion represented in the angular momentum (I) and mass (A) plane for nuclei along the β-stability line.

appears that, under Dyson's assumption, rotating toroids are stable against sausage deformation with angular momentum as large as $I \approx 300$ ħ, and these nuclei once formed, will de-excite with the emission of a sequence of gamma rays whose energies are characterized by the large moment of inertia of the toroid. Such de-excitations will bring the nuclei to the toroidal thresholds at which a change of topology will occur. Since the rotational parameters at the toroidal threshold are greater than those of Cohen, Plasil, and Swiatecki's limits for the fission barrier to vanish, these nuclei will undergo fission. The fission event is, however, delayed by the emission of the sequence of gamma rays and may provide a signature for the detection of the intermediate states of rotating toroidal nuclei.

1. S. Cohen, F. Plasil, and W. J. Swiatecki, *Ann. Phys. (N.Y.)* 82, 557 (1974).
2. C. Y. Wong, *Astrophys. J.* 190, 675 (1974).
3. J. Tieys, "Ring Galaxies," Ph.D. thesis, Columbia University, 1973; V. C. Rubin and W. K. Ford, *Astrophys. J.* 159, 379 (1970).
4. C. Y. Wong, *Ann. Phys.* 77, 279 (1973).
5. F. W. Dyson, *Philos. Trans. R. Soc. London* 184, 43 (1892).

CLASSICAL MANY-BODY CALCULATIONS OF FAST HEAVY-ION COLLISIONS

J. P. Bondorf[1] S. Garpman[1]
H. T. Feldmeier[2] E. C. Halbert

Here we report on "SIMON," a simple simulation method for describing heavy-ion collisions. It is a classical many-body method and is most suitable for beam energies of several hundred MeV per nucleon. Such high-energy collisions are of great interest because they may lead to new phenomena—for example, to nuclear-matter densities several times that of ground-state matter. However, for beam energies ≥100 MeV per nucleon, present-day many-body *quantum mechanical* treatments are likely to be inadequate. This is so because of the restrictions (e.g., Hartree-Fock determinantal form) that are imposed on the wave functions in order to make quantum mechanical calculations feasible. This probable inadequacy explains, in part, why classical and quasi-classical approaches are being tried.

Without going into detail we remark that our SIMON method is intermediate in character between two more familiar classical many-body approaches—the equations-of-motion approach[4] and the intranuclear cascade approach.[5] It is somewhat closer to the intranuclear cascade approach, for it

calculates the motion of all the individual nucleons by using nucleon-nucleon cross sections rather than nucleon-nucleon potentials.

At present, our SIMON code incorporates very crude physical assumptions—for example, we use nonrelativistic mechanics; we neglect nuclear binding, Coulomb effects, and internal kinetic energy of the initial nuclei; and we allow only elastic isotropic nucleon-nucleon scattering, with the cross section $\sigma = 25$ mb independent of energy, charge, and density. For beam energies of 200 to 400 MeV per nucleon, the 25-mb cross section is roughly realistic. Some other classical methods are now considerably superior to SIMON in incorporating realistic features. For example, equations-of-motion methods use nucleon-nucleon potentials and so incorporate some binding effects, and some intranuclear cascade methods incorporate not only detailed energy-dependent differential nucleon-nucleon cross sections but also pion production and pion absorption. It is possible to improve the present SIMON code by including the realistic features now in intranuclear cascade codes. Such an effort might be well worthwhile, because the basic scheme of SIMON seems to allow more rapid and economical computation than do the basic schemes of the other classical methods.

Since our SIMON scheme is a classical many-body method, most of the numerical results which we report are averaged in two ways—over appropriate portions of phase space and over many simulated nuclear collisions. Figures 3.17 through 3.20 show some results from application of SIMON to head-on $^{238}U + {}^{238}U$ collisions, and to $^{20}Ne + {}^{238}U$ collisions at all impact parameters.[4]

In Fig. 3.17 we illustrate how a head-on-colliding U + U system changes shape with time and eventually disintegrates. The results in this figure have not been averaged over finite volumes, and furthermore they were obtained from only one simulated collision. Consequently, Fig. 3.17 shows microscopic fluctuations and microscopic asymmetries in contrast to the macroscopic cylindrical symmetry and macroscopic forward-backward symmetry of a head-on U + U collision.

Figure 3.18 shows calculated central densities vs time during a head-on U + U collision. The SIMON results in this figure were averaged within small cylindrical volumes and over nine or ten simulated U + U collisions. The figure shows results obtained from three alternative "scattering mechanisms":

1. Hard-sphere scattering. The nucleons are modeled as spheres of diameter $D = \sqrt{\sigma/\pi} \approx 0.9$ fm (so that $\sigma = 25.4$ mb). Here, if two approaching nuclei have impact parameter $b \leq 0.9$ fm, they scatter as soon as their separation decreases to 0.9 fm. The scattering angle is calculated by using billiard-ball mechanics.
2. RIHC (repulsive impact scattering with hard cores). Here, if two approaching nucleons have impact parameter $b \leq \sqrt{\sigma/\pi}$, they scatter as soon as their separation decreases to b or to 0.5 fm—whichever happens sooner. In either case the scattering angle Ω (in the nucleon-nucleon c.m. system) is chosen randomly, assuming uniform distribution over the hemisphere corresponding to repulsive scattering.
3. 4π impact scattering. This is the same as (2), with two exceptions. The hard core is absent (so that all scatterings occur at impact-parameter distance), and Ω is distributed uniformly over 4π.

Mechanism (1) allows internucleon distances ≤ 0.9 fm; mechanism (2), ≤ 0.5 fm; and mechanism (3), 0 fm. These differences obviously affect the density achieved during nucleus-nucleus collision. As Fig. 3.18 shows, the calculated ratio of maximum particle density to the precollision nuclear density is ≈ 2 or 3, depending on the nucleon-nucleon scattering mechanism used.

Figure 3.19 illustrates further results from head-on U + U collisions; it shows RIHC results for density all along the collision axis. During the collision, the RIHC density rises to a maximum ≈ 2.5 times normal; the central dense region (i.e., the region in which the density exceeds the precollision nuclear density) is significantly smaller than the overlap region of two noninteracting nuclei; and there is no evidence for either a sharp shock front or a sharp overlap front.

Figure 3.20 shows double-differential cross sections, $d^2\sigma/(dE\,d\Omega)$ vs E, for protons emitted from bombardment of ^{238}U by ^{20}Ne at 250 MeV per nucleon (lab). The experimentally observed results[5] are plotted as triangles. The heavy-line histogram shows results from a hard-sphere SIMON calculation. The other two histograms show results from two other recent detailed calculations[6] a fluid-dynamic calculation and an intranuclear cascade calculation. None of the three detailed calculations give results that fit the measured data well at all angles and energies; but all three detailed calculations show some features in qualitative agreement with the measured data, and the hard-sphere SIMON results are not outclassed by results from either of the other

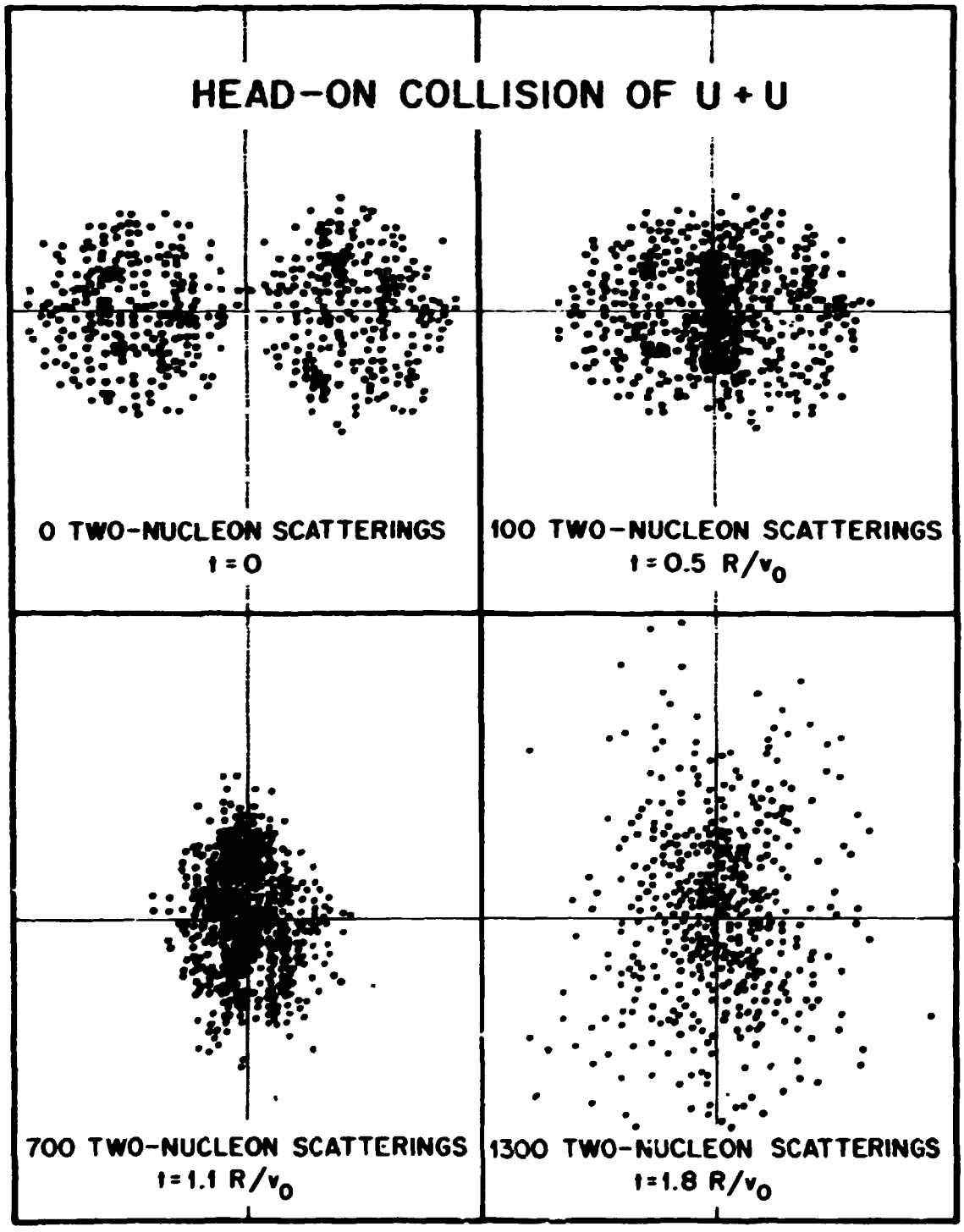

Fig. 3.17. Projections, on a plane through the collision axis, of the positions of individual nucleons during a head-on collision of two ^{238}U nuclei. Each projection plot is labeled with the number of already-occurred nucleon-nucleon scatterings, and also the time t in units of R/v_0. (Here R is the ^{238}U radius, and $2v_0$ is the relative speed of the two initial nuclei.)

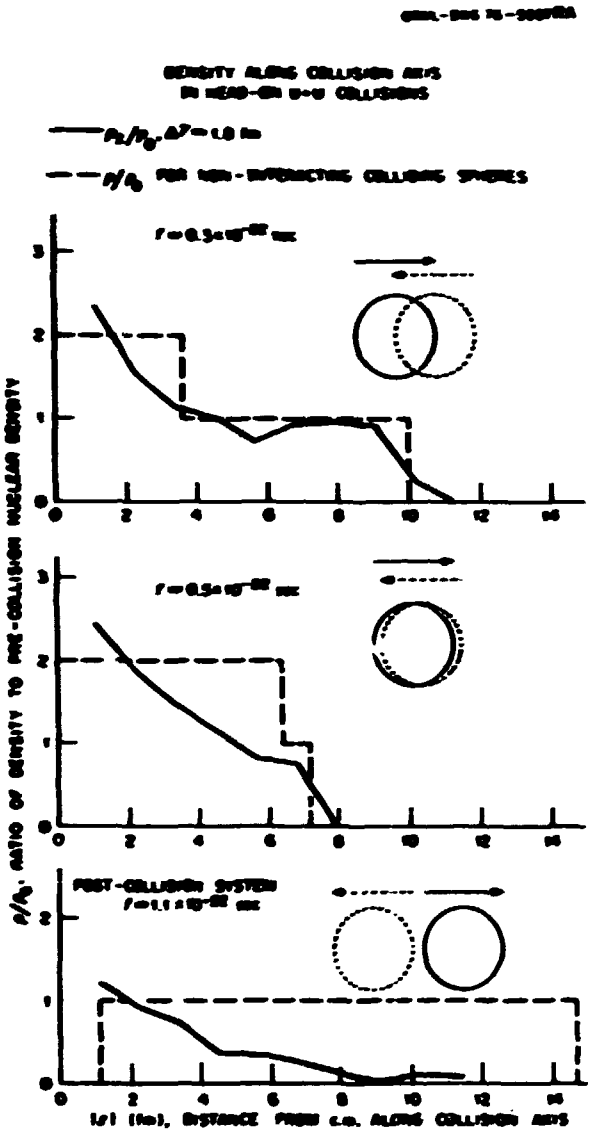

Fig. 3.18. Time-dependent densities near the colliding system's c.m. for three different choices of the nucleon-nucleon scattering mechanism. Each curve is a 9- or 10-collision average of volume-averaged densities. In each case, the volume was a disk, cylindrically symmetric around the z axis, with mean $z = 0$, z thickness 1.1 fm, and outer radius 2.8 fm. At time t_1 two noninteracting colliding spheres would first touch; at t they would completely overlap; and at t_2 they would have just finished passing through each other.

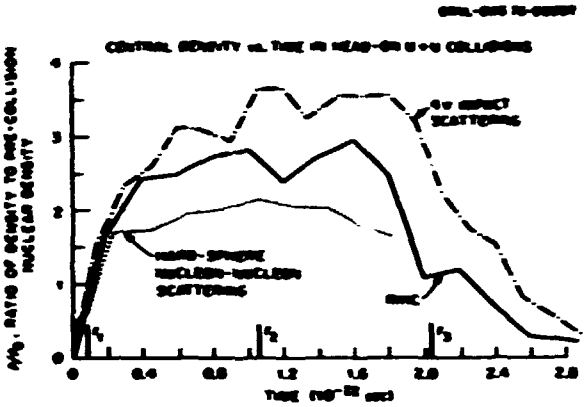

Fig. 3.19. Densities calculated along the collision axis z, at different times during collision. At each time, the circle diagrams and long-dashed lines describe two colliding noninteracting spheres of density ρ_0. All other results are densities calculated by using the RHIC interaction, then averaging within finite volume elements, and then further averaging over 10 collisions differing only in their random numbers. We first calculated $\rho \pm (\Delta r)$, for which the volume elements were small cylinders, symmetric around the collision axis z, each of radius Δr, z span 1.13 fm, and mean $z = |z|$ as plotted. To get $\rho \pm (\Delta r)$, we made a further average over two similar cylinders at $z = +|z|$ and $-|z|$.

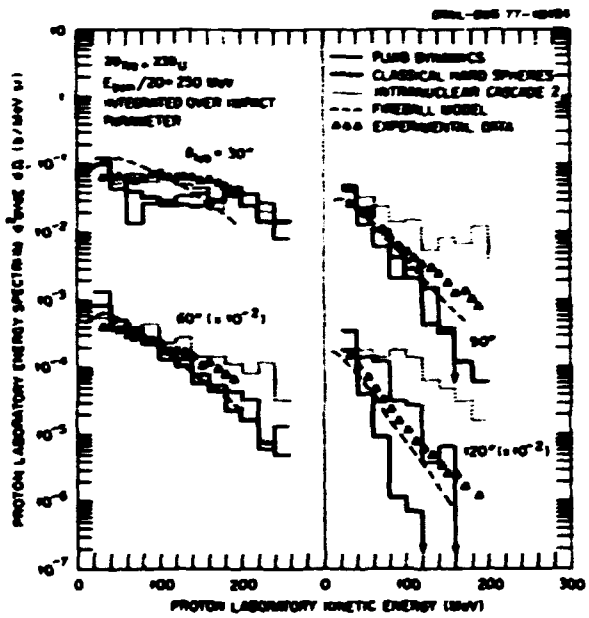

Fig. 3.20. Calculated and experimental proton energy spectra. Angular bins of 10° width are used for the calculated histograms. The experimental results and the fireball-model results are from ref. 6.

two detailed calculations. The dashed curve in Fig. 3.20 shows results calculated from an extremely simple, nondetailed geometric-thermodynamic "fireball" model.[6] We call it nondetailed because, unlike the three methods represented by histograms, it does not purport to calculate time-and-position-dependent details, such as matter density during the nuclear collision. Instead, it makes simple geometrical assumptions about the number of nucleons suffering interaction during the heavy-ion collision, and then it assumes an isotropic Maxwell-Boltzmann distribution for those nucleons considered to have interacted. Despite its simplicity, the fireball model gives results which fit the measured data in Fig. 3.20 better than do any of the histograms resulting from detailed calculations. Work is in progress now to analyze and understand the discrepancies among these Ne + U results.

---

1. Niels Bohr Institute, Copenhagen, Denmark.
2. Guest assignee from Technische Hochschule Darmstadt, Germany, under NATO Fellowship.
3. NORDITA, Copenhagen, Denmark.
4. A. R. Bodmer and C. N. Panos, *Phys. Rev. C* 15, 1342 (197—).
5. R. K. Smith and M. Danos, p. 89 in *Proc. Int. Workshop on Gross Properties of Nuclei and Nuclear Excitations I, Hirschegg, Kleinwalsertal, Austria, 1976*, Technische Hochschule Darmstadt Report No. AED-CONF 77-017-000, 197— (unpublished).
6. G. D. Westfall et al., *Phys. Rev. Lett.* 37, 1202 (1976).
7. A. A. Amsden et al., to be published in *Physical Review Letters*.

NUCLEAR REACTION THEORY: A DYNAMIC POLARIZATION POTENTIAL FOR COULOMB EXCITATION EFFECTS ON HEAVY-ION SCATTERING

W. G. Love T. Terasawa
G. R. Satchler

Recent measurements on heavy-ion elastic scattering have confirmed very large deviations from the simple Fresnel diffraction pattern due to Coulomb excitation. We have derived a second-order polarization potential which is able to reproduce these effects and which, consequently, does not require the costly solution of coupled equations. This does not make use of an adiabatic approximation; indeed, the imaginary part of the potential is dominant and the real part is negligible. Quadrupole excitation of low-lying states is by far the most important contribution to the imaginary potential, and each of these excitations is proportional to $B(E2)$. The radial dependence is basically $1/r^4$ but with a correction factor for the slowing down of the ions due to their mutual Coulomb repulsion. The latter shortens the range of the potential somewhat. There are no adjustable parameters, and the accuracy of the predicted potential was tested by comparison with "exact" coupled-channel calculations. An example of an application to actual data[7] is shown in Fig. 3.21. The polarization potential U_p was added to a conventional Woods-Saxon potential U_0 whose

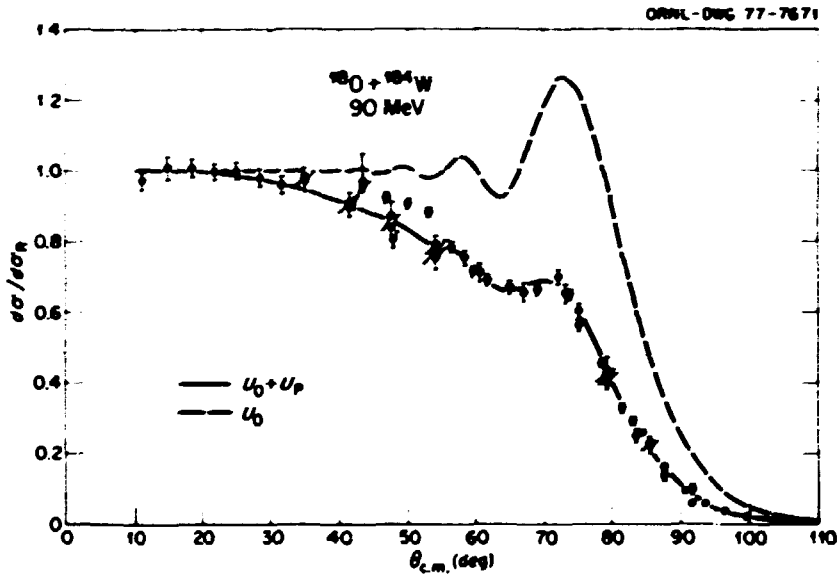

Fig. 3.21. Fit to the measured cross sections for $^{18}O + ^{184}W$, using the polarization potential U_p plus a Woods-Saxon potential U_0.

real depth was fixed but whose radius, diffuseness, and imaginary strength were adjusted for optimum fit to the data. The deviation from Rutherford scattering at the forward angles is due to absorption by the long-ranged polarization potential. The dashed curve shows the Fresnel-like pattern due to U_0 alone.

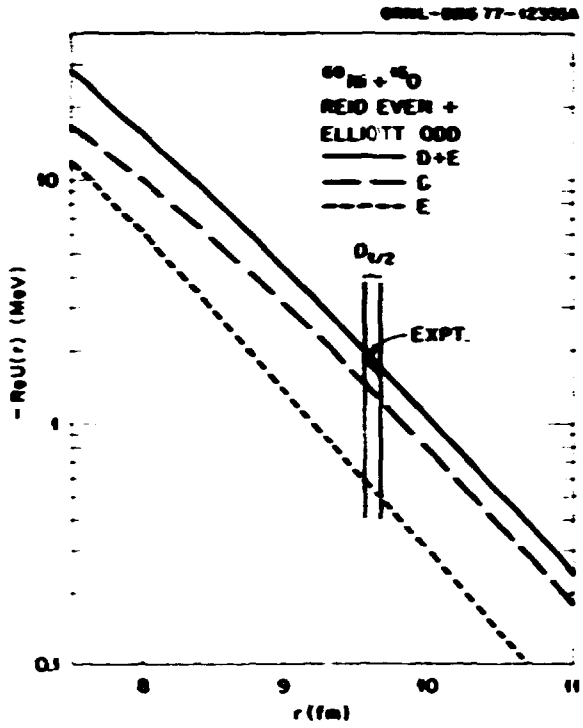

Fig. 3.22. Calculated potential for $^{16}O + ^{60}Ni$ near the strong absorption radius $D_{5/2}$; D = direct, E = exchange.

---

1. Summer research participant from the University of Georgia, Athens.
2. Guest scientist from the University of Tokyo, Tokyo, Japan.
3. G. [illegible] et al., *Phys. Rev. Lett.* 38, 354 (1977); J. R. Comfort, private communication (1978).

MICROSCOPIC DESCRIPTION OF SCATTERING

W. G. Love L. D. Rickertsen
G. R. Satchler

"Microscopic" means a description using nucleon-nucleon forces and detailed nuclear wave functions rather than phenomenological optical potentials and collective models. In practice it means simple folding models in which an effective nucleon-nucleon interaction is folded into the nuclear densities (or transition densities for inelastic scattering), together with some treatment of nucleon exchange. The first aim is to test "realistic" effective interactions against experiment in cases where the densities are known reasonably well. Further, we wish to see whether such interactions are equally effective for light and heavy ions, since these probe different regions of the nuclei. If the interactions satisfy these tests, we have a model with some predictive power; alternatively it can then be used to test model wave functions.

Two such (real) interactions have been obtained. The first, which was derived[1] from G-matrix elements based on the Reid potential, accurately reproduces[2] empirical heavy-ion potentials as well as giving good fits to (p,n), (p,p'), and (n,n') data.[3] The second interaction, also based[4] on the Reid potential, is a density-dependent G-matrix. Each is represented by a sum of three local Yukawa terms. Their $S = T = 0$ parts give very similar results, despite the strong density dependence of the second force.

The real parts of the optical potentials for many heavy-ion systems have been calculated, and[5] these generally agree to within about 10% with the areas determined empirically (in the region of the strong absorption radii to which the scattering is sensitive). Figure 3.22 shows an example[4] for $^{16}O + ^{60}Ni$. These results are being reviewed. Preliminary results[6] for heavy-ion inelastic scattering are also encouraging for those cases in which some independent information about the transition densities are available for example, from electron scattering (see also contributions in the experimental section of this report).

The same interactions give optical potentials for neutron and proton elastic scattering which are in satisfactory agreement with experiment, although they tend to have mean square radii that are slightly too small. Such deficiencies could be due to higher-order effects which have been neglected, such as virtual excitation of collective surface modes and coupling to pickup channels.[7] The initial applications of these interactions to inelastic scattering have been made to transitions such as the excitation of the lowest 3⁻ states in ^{40}Ca and ^{208}Pb for which good RPA transition densities are available. The results are very good. Initial attempts to explore other parts of the forces [e.g., by application to (p,n) reactions[8]] are also encouraging.

One important application of these techniques is to the analysis of light-ion excitation of giant

resonances in nuclei.[1] The new interactions will be used together with improved wave functions that have become available.

1. Summer research participant from the University of Georgia, Athens.

2. Present address: Science Applications, Inc., Oak Ridge, Tenn.

3. G. Bertsch et al., to be published.

4. G. R. Satchler and W. G. Love, *Phys. Lett.* **65B**, 415 (1976), and to be published.

5. W. G. Love, *Phys. Rev. C* **15**, 1261 (1977), and to be published.

6. V. Espen and B. Day, *Phys. Lett.* **63B**, 25 (1976), and private communication.

7. I. D. Rukerthen et al., *Proc. Symp. Macroscopic Features Heavy Ion Collisions*, Argonne National Laboratory Report ANL PHY-76 2, 1976; G. R. Satchler, to be published in *Nucl. Phys.*

8. R. S. Mackintosh and A. M. Kobos, *Phys. Lett.* **62B**, 127 (1976).

9. E. C. Halbert et al., *Nucl. Phys. A* **245**, 189 (1975).

PROTON DENSITY DISTRIBUTIONS IN LIGHT NUCLEI

R. L. Becker J. A. Smith[1]

Recent inclusion of meson-exchange contributions to high-momentum-transfer, elastic, electron scattering from nuclei has strongly reduced the discrepancy between calculated and experimental charge form factors.[2] However, the exchange calculations depend on the assumed nuclear forces, nuclear structure theory, and meson theory; therefore, conventional single-nucleon charge and body densities inferred from experiment are now model dependent. Uncertainties in experimental data and lack of data beyond a maximum momentum transfer lead to uncertainties in the inferred densities. If these uncertainties are small enough, a consistency check can be made between the density assumed in the meson-exchange calculation and the output density band.

We have investigated the uncertainties in the quasi-experimental body densities in ^{4}He obtained by subtracting meson-exchange contributions based on the Reid and Hamada-Johnston interactions. A strikingly large uncertainty in the central body density was obtained; shapes ranging from a large central depression to a peak were allowed. By considering the interference between meson-exchange and single-nucleon amplitudes, we concluded that data between $q_{max} \approx 4.5$ fm^{-1} and $1.5q_{max}$ might considerably improve the test of consistency of the nuclear force models employed. Similar analyses of electron scattering from other light nuclei are in progress.

1. Present address: Department of Astronomy, Yale University, New Haven, Conn.

2. W. M. Kloet and J. A. Tjon, *Phys. Lett.* **49B**, 419 (1974).

3. M. Gari, H. Hyuga, and J. Zabolitzky, *Nucl. Phys.* **A271**, 365 (1976).

4. Nuclear Data Project

R. L. Auble[1] J. Halperin[1] S. J. Ball[2]
J. R. Beene B. Harmatz S. H. Dockery[2]
F. E. Bertrand[1] M. J. Martin R. L. Haese[2]
Y. A. Ellis M. R. Schmorak F. W. Hurley[2]
W. B. Ewbank K. S. Toth[1] M. R. McGinnis[2]
M. L. Halbert[1] M. P. Webb[1] J. T. Miller[2]

INTRODUCTION

The Nuclear Data Project (NDP) is the primary U.S. center for collecting, evaluating, storing, and disseminating nuclear structure information for the basic research community. The computer files of evaluated nuclear structure data also serve as basic support for many applied programs which require a documented authoritative base of radioactive decay or other nuclear structure information.

The project staff at Oak Ridge National Laboratory (ORNL) operates as a comprehensive integrated data evaluation center which includes features of a technical documentation center, a scientific research group for data evaluation, and a center for preparation of special publications. In addition to these self-contained activities, NDP provides technical leadership and guidance for national and international networks for nuclear structure data evaluation.

TECHNICAL DOCUMENTATION CENTER

In support of its data evaluation work, the NDP maintains a complete multiply indexed bibliography to nuclear structure references (NSR). The bibliography is computer based and serves as an international resource for scientific and technical research workers. References can be retrieved selectively by nucleus, reaction, or any other quantity mentioned in the keyword abstract.

During 1976, over 5000 references to new nuclear structure measurements and calculations were indexed and added to the NSR master file. New entries are sorted by topic and published three times each year in "Recent References" issues of *Nuclear Data Sheets*.

A magnetic tape version of the complete master NSR file (about 50,000 indexed entries, 1960-1976, in ORNL's ADSEP format) was sent to the Kurchatov Institute (U.S.S.R.) as part of the U.S. participation in an international exchange of nuclear structure information. The tape was successfully processed in Moscow, and a dialogue is being established to develop a format for routine exchange of indexed bibliographic information. A tape containing keyword abstracts for results reported at three recent Russian conferences was received from the U.S.S.R. These references (also in ADSEP format) are being merged into the NSR file.

Relevant new entries to the NSR file are distributed every month to each mass-chain evaluator. This regular service is being provided for 21 *A*-chain data evaluators. Three additional groups receive regular notification of new literature relevant to special data compilations (atomic

masses, nuclear moments, photonucleur reactions).

Most requests for information received by NDP are at least partly satisfied by a search through the NSR file for references on a particular topic. The development and support of Oak Ridge Computerized Hierarchical Information System (ORCHIS) at ORNL provide convenient, inexpensive, and powerful search capabilities for ADSEP data bases. For long computer printouts, NDP has begun using the microfilm printer that recently became available. Although the device currently has a severely restricted character set, most information in the NSR file is understandable.

1. Part-time assignment to Nuclear Data Project.
2. Technical support staff.
3. Scientific support staff.

SCIENTIFIC DATA CENTER

The evaluated nuclear structure data file (ENSDF) summarizes the experimental knowledge about each nucleus, each reaction, and each decay scheme. The ENSDF is a valuable source of established data for use in calculations, systematic studies of nuclear properties, and preparing standard collections of accepted data.

The file of evaluated nuclear structure data has grown by about 20% during the last 18 months by inclusion of additional evaluations from *Nuclear Data Sheets*. Nuclear level information on over 1700 nuclei are now summarized by ENSDF. Data from 1400 decay schemes are included, as well as structure information from over 2000 nuclear reactions. The ENSDF coverage of the periodic table is illustrated for "adopted levels" and "decay schemes" by the graphs in Fig. 4.1.

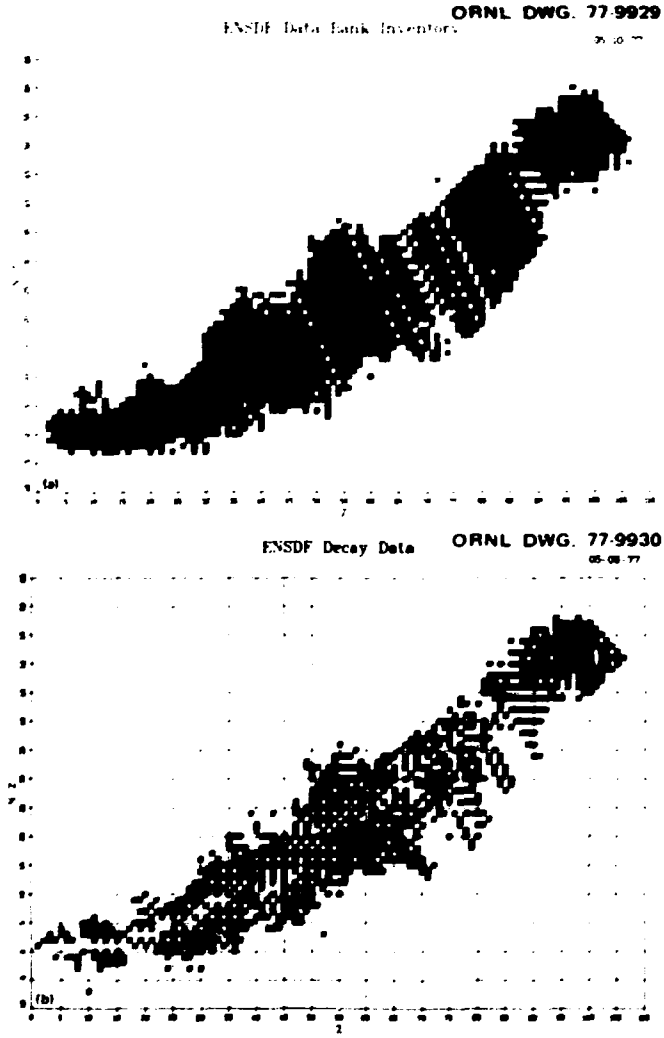

Fig. 4.1. Evaluated nuclear structure data file status, May 1977. (*a*) Nuclei included in ENSDF; (*b*) decay schemes included in ENSDF (by parent).

Complete magnetic tape copies of the permanent master file ENSDF are prepared at six-month intervals for distribution by the National Nuclear Data Center (NNDC) at Brookhaven. Copies have also been sent directly to network groups in the United Kingdom and West Germany, together with programs for maintaining the ENSDF system in an IBM computer environment. A tape containing only decay-scheme data has been sent to Idaho National Engineering Laboratory (INEL) (to be used in preparing input for ENDF/B) and to Grenoble, France (for use in a similar radioactivity file). Data checking performed by each user provides information for further improvement in ENSDF quality and consistency.

A number of requests for nuclear structure data have been filled from ENSDF by retrieving a desired selection of data, then using one or more of the NDP supporting programs to prepare tables or displays in a format that is easily understood by the user, such as the radioactivity files described in an accompanying abstract.

SCIENTIFIC DATA EVALUATION GROUP

The NDP data evaluation group consists of scientists who are skilled in understanding and interpreting experimental results from radioactivity or nuclear reactions. The principal activity of this group is to review and update the ENSDF as new experimental results appear. The scientists of the NDP evaluation group also provide a pool of experienced talent which can focus on specific problems as required by other Energy Research and Development Administration (ERDA) programs.

The NDP data evaluation group prepared revised versions of 49 mass chains during the past 18 months and assisted with five additional mass chains published in *Nuclear Data Sheets* in collaboration with Nuclear Information Research Associates sponsored by the National Science Foundation. This was accomplished in addition to the increased work load caused by national and international collaboration in nuclear structure data evaluation (see "Nuclear Data Networks") and full- or part-time work with NDP.

A natural consequence of a systematic review of experimental data is the recognition of systematic trends or inconsistent results. The NDP has continued the policy of reporting such observations at scientific meetings as well as in the *Nuclear Data Sheets*.

Many NDP staff members are involved in research work in addition to their evaluation responsibilities. These activities are not mentioned here, but are described in other sections of the Physics Division report.

PUBLICATIONS: *NUCLEAR DATA SHEETS*

The NDP publications group uses the master files of bibliographic and numeric data to prepare camera-ready copy for *Nuclear Data Sheets*. The computer programs which perform these tasks have been designed to take advantage of hardware and software maintained by the Computer Sciences Division in support of extensive information center activities at ORNL. During the past 18 months, the NDP prepared 12 *A*-chain issues and 5 issues of "Recent References" for publication in *Nuclear Data Sheets*. The *A*-chain issues contain complete revisions of *Nuclear Data Sheets* for 62 mass values.

Data for each mass chain were prepared in computer-readable ENSDF format; data sheets and drawings were assembled automatically from the ENSDF data sets; and the data sets have been filed onto the permanent master file of evaluated data.

A new section has been added to "Recent References" which contains an index to unpublished work that has been included in the NSR file during a four-month period.

Publication of the 1974–1976 reaction list for charged-particle reactions concludes the activities of the Charged-Particle Cross-Section Center at Oak Ridge. The Reaction Index section of "Recent References" indexes much of the same literature in slightly less detail. The NNDC at Brookhaven has assumed responsibility for investigating additional indexing required by users of charged-particle bibliographies.

NUCLEAR DATA NETWORKS

With the establishment of national and international networks of data evaluators, NDP has assumed the additional responsibility of providing technical leadership for the networks. The NDP must direct a share of its resources toward helping the other groups prepare high-quality data evaluations that can be merged into ENSDF. The NDP data evaluation group has a reduced evaluation responsibility (about 100 *A*-chains rather than about 200), which can be maintained on the four-year cycle requested by ERDA.

1. Three training sessions for new data evaluators have been organized and conducted. These meetings introduced each new data evaluator to the structure of the data file, services available from NDP, and techniques used at NDP to choose adopted values from among various measurements. These sessions were attended by new data evaluators from Oak Ridge, Brookhaven, Idaho Falls, Daresbury (United Kingdom), and Karlsruhe (West Germany).
2. The NDP hosted a meeting of the U.S. Nuclear Data Network, at which the operations of the network were further defined. Representatives attended from all six U.S. network locations, as well as from ERDA and National Academy of Sciences (NAS).
3. Complete copies of all data included in ENSDF were generated in July 1976 and January 1977 for distribution to the network. Programs to maintain ENSDF in an IBM environment were also sent to the network evaluators in the United Kingdom and West Germany.
4. A tape containing several physics programs used by NDP in data evaluation was sent to U.S. network groups at NNDC and INEL for use by their new evaluators.
5. A complete indexed reference tape was sent to the Kurchatov Institute for use in the U.S.S.R. data evaluation effort. A tape containing indexed references to three Soviet conferences was received from Moscow in a similar format. The tape exchange is a step toward defining an acceptable format for exhange of bibliographic information.
6. Documentation of programs used by NDP for physics calculations was prepared for distribution to the networks. These programs have been developed by NDP and are used routinely to extend and to check ENSDF data sets. (Examples include log-ft calculation, internal-conversion-coefficient interpolation, and least-squares level calculation.)
7. A review procedure for new A-chain evaluations has been drafted for study by the network. The NDP is committed to review the first mass chain from each new evaluation group, but an independent review panel will help to distribute this work load among qualified non-NDP reviewers as well.
8. At the request of the international network, NDP has drafted a list of suggested procedures for data evaluation. Agreement on certain standard procedures can simplify the review process and will assure some uniformity throughout ENSDF. The NDP has also prepared a critique of an automated "data evaluation" procedure suggested by the U.S.S.R. data evaluators.
9. At the June 1977 meeting of the American Nuclear Society (ANS), NDP initiated and organized a special session to describe several sources of technical information for nuclear scientists and engineers. The special session was jointly sponsored by three ANS divisions.

COMPUTER FILE OF DECAY RADIATIONS FOR APPLIED USERS

M. J. Martin R. L. Haese
D. C. Kocher[1] R. L. Auble
W. B. Ewbank

In response to requests from users of radioactivity data, the Nuclear Data Project has included in ENSDF an extensive collection of decay scheme information. For this collection of about 400 nuclides, the nuclear decay information contained in ENSDF has been supplemented (by the addition of K, L, etc., internal conversion coefficients, average beta-energies, and K, L, etc., electron-capture branching ratios) so that a complete computer file of nuclear radiations plus x-ray and Auger-electron radiations can be produced by the NDP program MEDLIST. New decay schemes prepared for ENSDF will routinely include this information where available. For many of the data sets included in this collection, additional evaluation has been performed so as to include the results of new research published since the most recent complete mass-chain evaluation.

The following is a list of requests; it should be noted that they contain considerable overlap.

1. NCRP (220 decay schemes)—prepared over a period of several years by NDP for the National Council on Radiation Protection (NCRP). A MEDLIST output will be included as an appendix in an NCRP report.[2] A preliminary version of the data on 194 of these nuclides has already been published.[3]

2. ESD/NRC (240 decay schemes)—prepared for the Nuclear Regulatory Commission (NRC) by the ORNL Environmental Sciences Division (ESD)[4] using the ENSDF formats and systems designed by NDP. Most of these radionuclides occur in the routine release of effluents from nuclear reactors. Data for many of the nuclei in this group were taken from the NCRP file; others were prepared by extending decay sets in ENSDF which were based on data in the *Nuclear Data Sheets*. In some cases, newer results were evaluated by ESD and later merged with ENSDF.

3. CTD (up to 1030 decay schemes)—being prepared for use by the Waste Management Analysis Section of ORNL's Chemical Technology Division (CTD). ENSDF data will be used to generate as many of these decay schemes as have been experimentally established. For other nuclei, the ENSDF data are being further supplemented by calculated values or other estimates of half-lives and decay energies.

4. ALSDECAY (85 decay schemes)—assembled from ENSDF for analysis of cooling problems encountered in the irradiation of stainless steel.

---

1. Environmental Sciences Division.
2. *A Manual of Radioactivity Measurements Procedures*, NCRP report, to be published.
3. *Nuclear Decay Data for Selected Radionuclides*, M. J. Martin, ed., ORNL-5114 (March 1976).
4. *Nuclear Decay Data for Radionuclides Occurring in Routine Releases from Nuclear Power Reactors*, D. C. Kocher, ed., ORNL/NUREG/TM-102, to be published.

ALPHA-DECAY RATES FOR EVEN-EVEN NUCLEI IN THE $204 \leq A \leq 256$ REGION

Y. A. Ellis K. S. Toth

As part of data-compiling activities, alpha-decay rates are systematically examined and reviewed for nuclei which undergo that particular mode of decay. Transition rates are considered within the spin-independent formalism developed by Preston.[1] In his equations, the nuclear potential, V, is taken to be simply a rectangular well; that is, V is constant for distances (r) less than R and equal to $2Ze^2/r$ for r greater than R. The atomic number, Z, and the radius, R, used in the calculation are those of the daughter nuclei.

In alpha-decay theory, transitions that proceed between the ground states of even-even nuclei are assumed to be unhindered so that their theoretical rates are taken to be identical to experimental values. These experimental transition rates and alpha-decay energies are therefore used to determine R and V. For all other alpha-decay transitions, R values are chosen from neighboring even-even nuclei and are used together with experimental alpha-decay energies to calculate theoretical rates. These rates are then compared with experimental rates to determine hindrance factors. In many instances, hindrance factors can be useful in spin and parity assignments.

A convenient way to study the systematics of alpha-decay rates is to examine the trends with both neutron and atomic numbers of the r_0 parameter as defined in the usual manner; that is, $R = (r_0 A^{1/3})10^{-13}$ cm. As part of reviewing the mass chains (A = 214, 218, 222, 226, 230, 234, 238, 242), we evaluated and chose the best available alpha-decay data for even-even nuclei in the region above lead. Figure 4.2 shows the deduced r_0 parameters as a function of neutron number for isotopes ranging from polonium (Z = 84) to fermium (Z = 100). Well-known shell effects can be clearly observed. The parameters drop precipitously as the N = 126 closed shell is approached. A similar but less pronounced effect can be noted as a result of the N = 152 subshell. The effect of the proton closed shell at Z = 82 can also be seen; namely, the r_0 parameters decrease as one goes from radium (Z = 88) to polonium (Z = 84).

In the neutron region between about 130 and 150, the curves for each element vary rather smoothly. Therefore, it is possible to obtain reasonably accurate r_0 values by extrapolation, as indicated in Fig. 4.2 for two elements, curium and californium. These extrapolated values can be used to estimate undetermined alpha-decay branching ratios. Two nuclides were selected as examples, ^{238}Cm and ^{242}Cf. In Fig. 4.3, we have plotted alpha-decay branches as a function of r_0 for the two isotopes. Cross-hatched areas indicate the range of ratios consistent with the extrapolations from Fig. 4.2. For ^{238}Cm, one deduces an alpha-branch of (4^{+2}_{-1})%. The only value available in the literature[2] is given as about 1%. We feel that our errors on the r_0 parameter are extreme ones; therefore, the alpha-decay branch of ^{238}Cm is larger than 1%. In the case of ^{242}Cf, no branch has

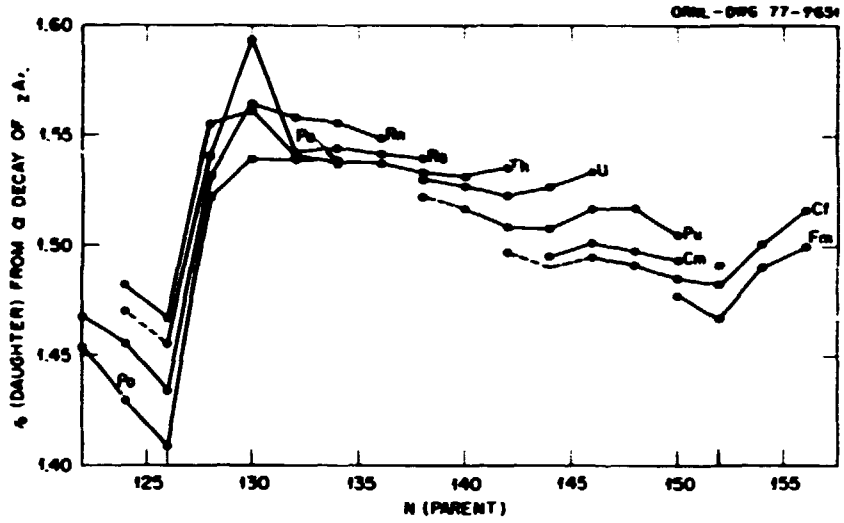

Fig. 4.2. Plot of r_0 parameters for even-even nuclei in the mass region above lead as a function of neutron number.

been reported.[1] We estimate its alpha-decay branching to be $(52^{+20}_{-14})\%$.

We plan to extend this survey into the region below lead and then to systematically deduce estimates for unknown alpha-decay branching ratios.

1. M. A. Preston, *Phys. Rev.* 71, 865 (1947).
2. G. H. Higgins, Thesis, University of California (1952). UCRL-1796 (1952).
3. R. J. Silva et al., *Phys. Rev.* C 2, 1948 (1970).

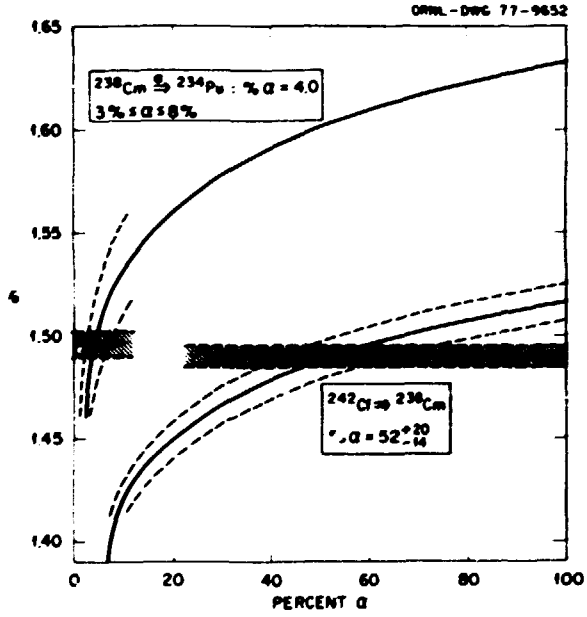

Fig. 4.3. Alpha-decay branching ratios plotted as a function of r_0 parameters for ^{242}Cf and ^{238}Cm. Cross-hatched areas indicate the possible range of alpha branches consistent with extrapolated values of r_0 for the two nuclides (see Fig. 4.2).

5. Magnetic Fusion Energy Applied Physics Research

BLISTERING OF STAINLESS STEEL BY ENERGY-DISPERSED HELIUM BEAMS

J. A. Ray C. F. Barnett

Blistering of stainless steel by an energy-dispersed (0- to 40-keV) neutral beam has been studied. The energy-dispersed beam was formed by passing a 40-keV He^+ beam through an accelerator-type structure gas cell in which a decelerating potential was placed across the electrodes. By knowing the electron capture and stripping cross sections of He^+ and He^0 in helium gas, the computed He^0 energy distribution was a maximum at low energies (100 eV) and decreased approximately 10%, reaching a sharp cutoff at 40 keV. Figure 5.1 shows two electron-microscope photographs for two stainless steel specimens bombarded by a monoenergetic, 40-keV He^+ beam and an energy-dispersed helium beam of 0 to 40 keV to a dose of 1.9×10^{18} and 2.6×10^{18} p/cm^2 respectively. The damage or density of surface blisters was less but clearly present for the energy-dispersed beam. However, on a second run, no blistering from an energy-dispersed beam was found. Electron microscopic examination revealed evidence of surface oxidation.

This discrepancy has been traced to errors in the calculated distribution function. Measurements of the neutral distribution revealed a peak in the distribution at the higher energies, with the lower energies being depleted by the defocusing action of the decelerating electrodes. Increasing the neutralizing cell pressure to 8×10^{-3} torr partially fills in the low-energy distribution. Work is now under way to correct the defocusing property of the neutralizing cell.

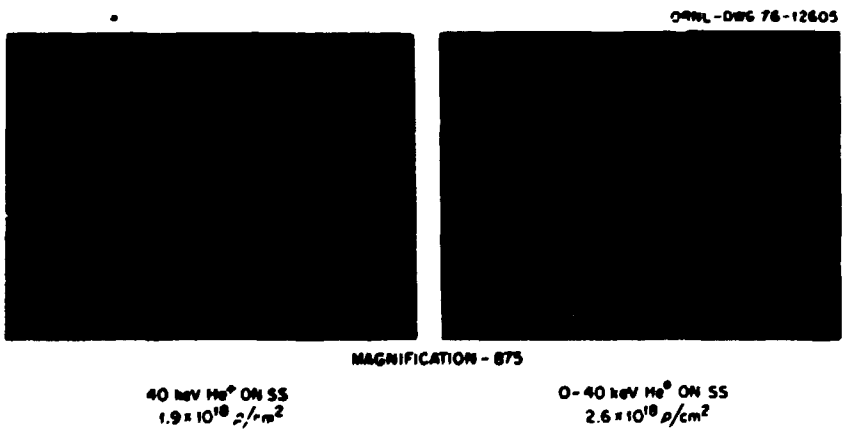

Fig. 5.1. Electron-microscope photographs of two stainless steel specimens bombarded by monoenergetic and energy-dispersed helium beams.

CONTROLLED FUSION ATOMIC DATA CENTER

C. F. Barnett M. I. Wilker
S. W. Hawthorne G. S. McNeilly

The compilation *Atomic Data for Controlled Fusion Research* has been distributed to the fusion research community. Because parts of the compilation are now two years old, data revisions are being made with emphasis on those atomic collisions involving impurities found in high-temperature plasmas. Evaluated cross-section compilations are in progress for charge exchange and electron excitation and ionization collisions for multicharged ions. To make the data more compatible with the needs of plasma modeling, a program has been completed to convert the cross-section data to reaction rates and analytical expressions for the case of beam-Maxwellian distributions.

In cooperation with the Atomic Transition Probabilities Data Center at the National Bureau of Standards, the bimonthly publication of the *Atomic Data for Fusion* bulletin has continued. From an initial mailing of 57, the number has grown to 400. The bulletin has proven to be a very effective means of transferring recently acquired data to the fusion community several months before the data appear in laboratory records or open literature.

Searching, evaluating, and entering bibliographical data into the computer file have continued. Work is proceeding to evaluate critically the completeness of the file. After references that had been omitted have been added to the file, an index bibliography for specific collisional processes will be published.

During 1976, talks were continued with the International Atomic Energy Agency to determine the role the agency would undertake in their new program to provide the international fusion community with atomic data pertinent to fusion research. Their initial effort will be confined to the publication of a comprehensive bibliography compiled from inputs from the United States, the United Kingdom, the Federal Republic of Germany, the U.S.S.R., France, and Japan.

SUBMILLIMETER LASER PLASMA DIAGNOSTICS

D. P. Hutchinson K. L. Vander Sluis
P. A. Staats

During the past year, developments have continued of a high-power submillimeter laser system to measure the ion temperature in thermonuclear plasmas via coherent Thomson scattering. Based on a feasibility study performed in 1975,[1] the Thomson scattering experiment requires a submillimeter source with the following parameters: (1) a wavelength between 300 and 600 μm, (2) a power level of less than or equal to 1 MW, (3) a line width at FWHM of less than or equal to 30 MHz, and (4) a pulse length of 200 to 300 nsec. The detector for the scattered signal will be a heterodyne receiver with a noise-equivalent power of 10^{-18} W/Hz, a bandwidth of 1 GHz or greater, and a cw submillimeter laser for use as a local oscillator. Therefore, we are developing both cw and pulsed lasers for the Thomson scattering experiment; the CH_3F laser has been improved, and, in addition, both a cw and a pulsed submillimeter laser based on the 447-μm CH_3I line have been developed for use in this measurement. The cw CH_3I laser, optically pumped by the P(18) 10.6-μm CO_2 line, exhibited better power conversion efficiency and amplitude stability than did the CH_3F operating in the same laser cavity. The amplitude stability is greater, because the CH_3I molecule is pumped by a CO_2 laser operating at line center, as opposed to the CH_3F molecule, which must be pumped approximately 20 MHz off line center, thus allowing greater drift and frequency jitter.

A new pulsed far-infrared oscillator based on an unstable resonator geometry has been operated using CH_3I (447 μm), CH_3F (496 μm), and D_2O (385 and 361 μm). Average power output varied from approximately 12 kW with CH_3I to 125 kW with D_2O. A schematic diagram of the oscillator is shown in Fig. 5.2. The performance of the oscillator has been characterized by the quantum conversion efficiency, which, by definition, is 100% when one-half of the CO_2 pump photons are converted to submillimeter photons. The quantum conversion efficiency is plotted in Fig. 5.3 as a function of the output-coupler reflectivity for D_2O lasing gas. Two curves are shown: a 1- and a 2.5-m cavity length. For the two cavities used, the measured quantum efficiency or output power of the 1-m cavity was approximately a factor of 2 greater than that of the 2.5-m cavity. Maximum efficiency was obtained using a 37% reflectivity for the output coupler. The improvement in conversion efficiency when the oscillator length was decreased from 2.5 m to 1 m is due to the more efficient trapping and absorption of the CO_2 pump beam. We are continuing work on this resonator to determine the mode quality and spectral purity of the output pulses.

Two different CO_2 lasers were used in these investigations. One was a 10-J grating-tuned TEA

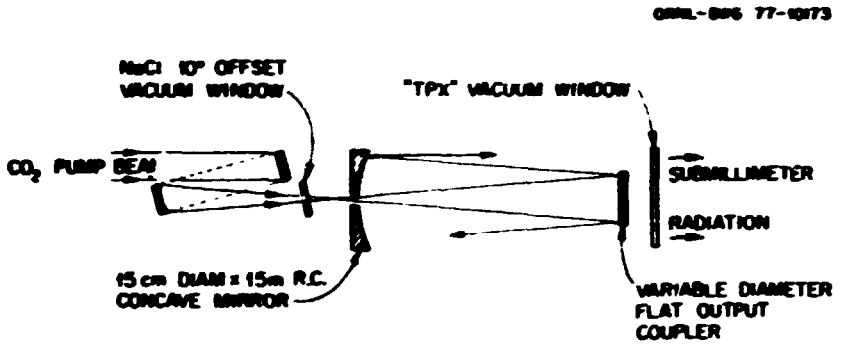

Fig. 5.2. Schematic diagram of the optically pumped submillimeter unstable resonator oscillator.

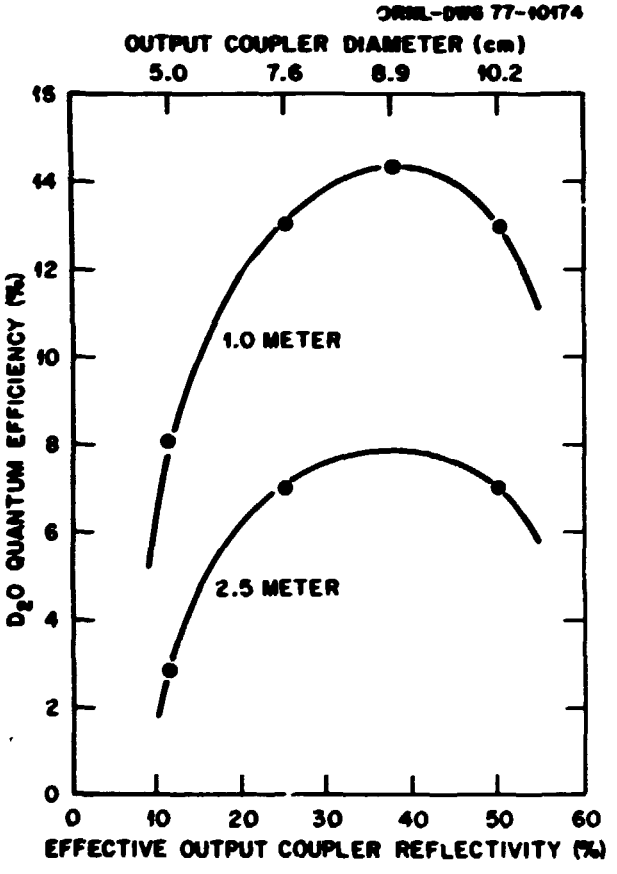

Fig. 5.3. Quantum efficiency of the oscillator vs output coupler reflectivity for two cavity lengths.

CO_2 laser, which typically produced 7.3 J on the P(22) 9-μm line used to pump D_2O, 8.5 J on the P(20) 9-μm line used to pump CH_3F, and 7.8 J on the P(18) 10-μm line used to pump CH_3I. The other laser relied on the injection of a cw signal tuned to the desired wavelength to pull the TEA CO_2 laser to oscillation on the proper transition. This injection-tuned laser produced approximately 4 J on each of the pump lines. The significant difference between these two lasers is the CO_2 line width. Pulses from the two lasers were observed by a 1-nsec-response photon drag detector and were recorded on a transient recorder. When the frequency was computer-analyzed by a fast Fourier transform routine, the frequency spectrum of the grating-tuned laser contained considerable energy beyond 500 MHz from the line center. The spectrum of the injection-tuned laser was confined to a bandwidth of 50 MHz.

The unstable resonator was developed to serve as the oscillator in a 1-MW oscillator-amplifier system for the ion temperature measurement. A schematic diagram of the proposed system is shown in Fig. 5.4. The oscillator will be excited by a 15-J TEA CO_2 laser, and the amplifier will be driven by a 150-J TEA CO_2 laser. The wavelength tuning of the CO_2 laser will be achieved by an injection tuning technique developed last year. The submillimeter amplifier utilizes parabolic beam-expanding optics that produce a large volume necessary to absorb the 150-J pump pulse. At the same time, the amplifier has a short length to inhibit superradiance: the overall length of the amplifier is 1 m, with a diameter of 0.64 m. This geometry yields an active volume of 230 liters. The construction of the amplifier stage has recently been completed, and the system is undergoing initial tests to determine the conversion efficiency, spectral purity, and transverse-gain profile.

The detector for the Thomson scattering diagnostic test will be a heterodyne receiver using a cw submillimeter laser as a local oscillator. The front end of the receiver consists of a mixer mount for a Schottky diode and an injection system for the local oscillator. The scattered signal with a bandwidth of 1 GHz will be stored by a Teletronix transient digitizer system, and the spectrum will be analyzed by a fast Fourier transform program in the PDP-11 computer,

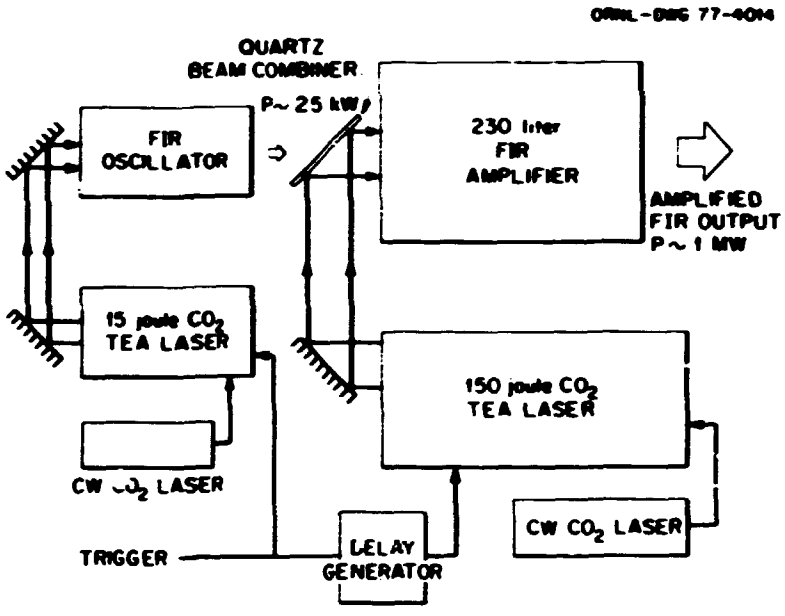

Fig. 5.4. Schematic diagram of the oscillator-amplifier system.

which forms part of the digitizer package. When this analysis device was used to determine the spectra of the two CO_2 pump lasers described above, the results confirmed that the device has the frequency capabilities necessary to analyze the Thomson scattered spectrum.

Based on our work with CH_3I, a high-power (40 mW) cw submillimeter laser has been built to serve as a local oscillator for both the ion Thomson scattering receiver and a narrow-band synchrotron emission detector.

Studies have been undertaken during the past year to develop a fast-scanning Fourier transform spectrometer to measure the broadband synchrotron emission from high-temperature plasmas and a method of measuring the current density profile in a Tokamak discharge by Faraday rotation.

1. D. P. Hutchinson and K. L. Vander Sluis, *Proposed Spatial Ion Temperature Measurements with an FIR Laser*, ORNL TM-5071 (November 1975).

ELECTRON TRANSFER BETWEEN HELIUM-LIKE IONS AND HELIUM

D. H. Crandall

Single- and double-electron transfer cross sections have been measured for B^{3+}, C^{4+}, N^{5+}, and O^{6+} in collision with helium at velocities between 0.5 and 1.2×10^8 cm/sec. The single-electron capture cross sections peak near 15×10^{-16} cm^2 for each case except C^{4+}, where single capture is anomalously low. The double-capture cross sections are about 3×10^{-16} cm^2 except for B^{3+}, where the highest observed value is 1.5×10^{-16} cm^2. These measurements for B^{3+} and C^{4+} compare well with existing experiments and theory, except for the C^{4+} single capture. Within the narrow range tested, C^{4+} and B^{3+} cross sections exhibit variation with velocity, but N^{5+} and O^{6+} cross sections remain constant.

CHARGE-TRANSFER COLLISIONS OF MULTICHARGED IONS WITH ATOMIC HYDROGEN: MEASUREMENTS WITH THE TANDEM VAN DE GRAAFF

H. J. Kim R. A. Phaneuf
F. W. Meyer P. H. Stelson

Utilizing energetic silicon-ion beams from the tandem Van de Graaff accelerator and a thermally dissociated atomic hydrogen target, we measured the electron capture cross sections, $\sigma_{q,q-1}$, for ^{28}Si ions on a hydrogen target. Molecular hydrogen was thermally dissociated by direct ohmic heating of a gas target cell.[1] The incident ion charge ranged from q = 2 to 7, and the incident energy ranged from E = 1.4 to 5.7 MeV. This energy range is equivalent to 50 to 200

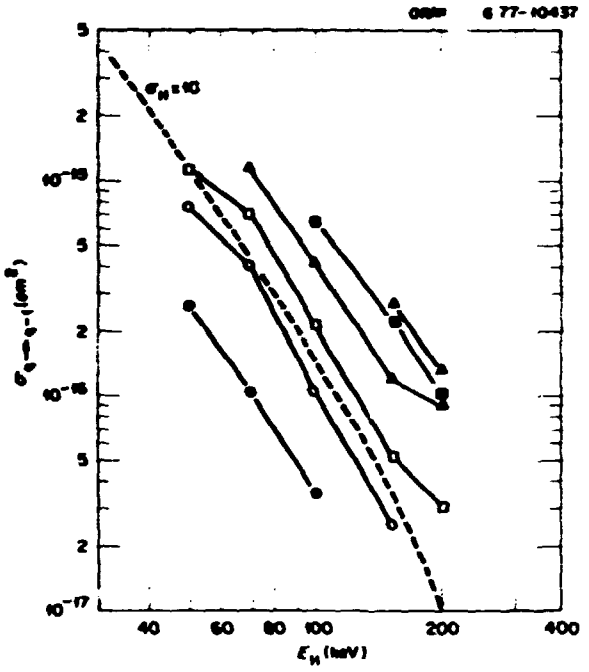

Fig. 5.5. Single-electron-capture cross sections for silicon multicharged ions in atomic hydrogen. *For comparison,* the capture cross section for protons in atomic hydrogen is also shown by the dashed curve. Solid circle, $q = 2$ (incident charge state); open circle, $q = 3$; open square, $q = 4$; open triangle, $q = 5$; closed square, $q = 6$; closed triangle, $q = 7$.

keV hydrogen energy E_H (or incident energy per nucleon) and encompasses the Tokamak Fusion Test Reactor injection energy, $E_H = 60$ keV. The measured cross sections are shown in Fig. 5.5. Also shown for comparison are proton + H cross sections, σ_H.

Cross sections $\sigma_{q,q-1}$ decrease rapidly and monotonically with energy in a manner similar to σ_H, although the values are much greater. At a given incident energy, the cross section increases with incident charge, q, for all energies: a simple expression $\sigma_{q,q-1} \propto q^{m(E)}$ with $2 < \alpha < 2.5$ represents the data well.

In order to cross-check our previous $\sigma_{q,q-1}$ values for fast Fe^{q+} + H measured by using an indirectly heated target,[2] we remeasured a number of Fe^{q+} cross sections with the present target. For reasons as yet unknown, presently measured values are significantly smaller.

1. G. W. McClure, *Phys. Rev.* 148, 47 (1966).
2. J. E. Bayfield, *Rev. Sci. Instrum.* 40, 869 (1969).

STARK MEASUREMENTS OF ELECTRIC FIELDS IN ORMAK

K. L. Vander Sluis P. M. Bakshi[1]

Previous analysis of line profile measurements of the Balmer alpha, beta, gamma, and delta radiation of hydrogen in ORMAK involved data-averaging by a computer. In order to eliminate these computer routines as an influencing factor, several sets of data were analyzed directly from the Biomation recording with individual treatment. There were two weaknesses in the computer routines: first, the averaging process, which tended to mask obvious noise; and second, the sampling method, which ignored a slight variation in wavelength dispersion as a periodic function of time.

The Biomation recorded approximately 100 samples of the line intensity in 100 msec. Each data point represented a 10-μsec average of the photomultiplier current. In this time interval, the rotating plate will change the wavelength by 0.032 Å. This is $^1/_{20}$ of the band pass of the slit of the spectrometer, which, for the 40-μ slit used, is 0.65 K. This technique provided a distinguishing feature to separate qualitatively real wavelength variations from random time events. Examination of the raw Biomation data shows many single events which have a rise and decay time of over a few channels, typically three to five. A plasma current variation of this time characteristic cannot represent a wavelength character because the slit function of the spectrometer covers 20 channels. However, it is possible that the probability of observing a signal at that wavelength is low, and one is observing fluctuation in the signal level. In either case, the process of averaging over 11 channels erases this time feature and yields a broadened signal which is difficult to distinguish from the real 20-channel wavelength information.

This analysis provides evidence of why variations of the order of 0.25 Å in the positions of real peaks occur. It also confirms that the signals are too close to the noise level to provide meaningful measurements of weak satellites. Finally, the major features of the profiles correspond to the basic Balmer emissions and to known impurity spectra.

1. Consultant, Boston College, Brighton, Mass.

CHARGE-TRANSFER COLLISIONS OF MULTICHARGED IONS WITH ATOMIC AND MOLECULAR HYDROGEN: MEASUREMENTS WITH LOW-ENERGY ACCELERATORS

R. A. Phaneuf F. W. Meyer
D. H. Crandall

The study of electron transfer in collisions between multiply charged ions and atomic hydrogen is fundamental to the understanding of charge-transfer mechanisms, due to the relatively small number of electrons comprising the ion-atom system. In addition, such studies are of practical interest because of potential applications in various areas of technology, such as the neutral-beam injection heating of fusion plasmas.

Experiments to measure charge-transfer cross sections for multiply charged ions of helium, carbon, nitrogen, and oxygen incident on atomic and molecular hydrogen gas targets were initiated in June 1976, utilizing the 600-kV accelerator located in the Fusion Energy Division.[1,2]

Charge- and mass-analyzed beams of up to triply ionized C, N, and O, as well as $^4He^+$ and $^3He^{2+}$, were produced in a simple hot-filament electron-impact ion source and accelerated through voltages ranging from 10 to 600 kV. Charge states greater than 3+ were produced by stripping fast 2+ and 3+ ions on thin Formvar foils or, in a few cases, on residual gas. The desired charge state was selected by electrostatic deflection and passed through a tungsten oven in which hydrogen could be thermally dissociated. The primary and charge-transfer components in the emergent beam were separated by a second stage of electrostatic deflection and were counted using a channel electron multiplier.

The directly heated tungsten-hydrogen oven is essentially the same as that previously used and described by McClure.[3] The degree of dissociation of hydrogen was determined by monitoring the variation with oven temperature of double-electron capture by 20-keV protons with H_2 and argon target gases in the oven.[4,5] For a heating current of 130 A, which resulted in an estimated oven temperature of 2350°K, the dissociation fraction was determined to be 95%. The target thicknesses were determined by normalizing to well-known cross sections for single-electron capture by 20-keV protons incident on hydrogen and H_2 targets.

Results of the electron-capture cross-section measurements for oxygen ions incident on both atomic and molecular hydrogen targets are presented in Fig. 5.6. The results for both incident nitrogen and carbon ions are qualitatively similar. At the lower velocities, where the relative particle motion is comparable to that of the outer atomic electrons (v about 2×10^8 cm sec), the collision cross sections are determined by the detailed behavior of the potential curves of the quasi-molecule formed during the collision, which can differ considerably from system to system. At these low velocities, no general trends are apparent in the data. The capture cross sections for C^{q+}, N^{q+}, and O^{q+} ions incident on H_2 are in good agreement with the measurements of Crandall et al.[6] over the range of velocities where the measurements overlap ($5 \times 10^7 < v < 1 \times 10^8$ cm sec).

At higher velocities (v less than about 2×10^8 cm sec), however, momentum transfer becomes the dominant mechanism for charge transfer. In this velocity region, the cross sections for C^{q+}, N^{q+}, and O^{q+} projectiles for q less than 2 are similar in magnitude, fall off similarly with velocity, and scale approximately as q^2, as predicted by the Born approximation. At the highest velocities, the cross sections for electron capture from H_2 targets are

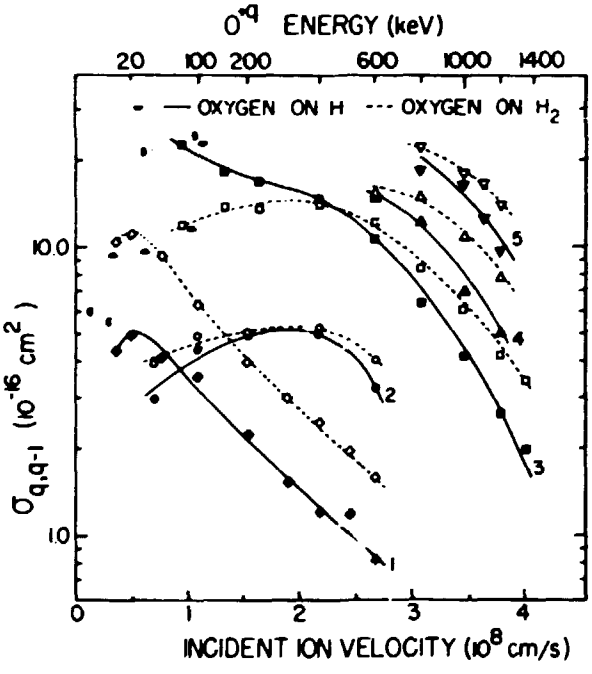

Fig. 5.6. Experimental electron-capture cross sections for $O^{q+} + H \rightarrow O^{(q-1)+} + H^+$ (solid points and curves), and for $O^{q+} + H_2 \rightarrow O^{(q-1)+} + H_2^+$ (open points and dashed curves). The solid curves are labeled by the incident ionic charge "q". Diamonds, $q = 1$; circles, $q = 2$; squares, $q = 3$; triangles, $q = 4$; inverted triangles, $q = 5$.

roughly double those for atomic-hydrogen targets in all cases. Recent classical Monte Carlo calculations[7-9] of cross sections for electron capture at these higher velocities by multiply charged C, N, O, and He ions in atomic hydrogen are in good quantitative agreement with the present data.

In the case of He^{2+} ions incident on molecular hydrogen, our measurements of σ_{21} and σ_{20} agree well with previous measurements.[10-13] For atomic hydrogen, the present data are in excellent agreement with the measurements of Shah and Gilbody,[10] and with those of Fite et al.[14] as renormalized by Shah and Gilbody,[10] but disagree substantially with those of Bayfield and Khayrallah.[11] For collisions of He^{+} ions with atomic hydrogen, the present σ_{10} cross sections are believed to be the first reported experimental values for total electron capture.

In addition, the ORNL Penning ionization gage (PIG) heavy-ion facility was utilized for charge-exchange cross-section measurements of lithium-like and helium-like ions of B, C, N, O, and F with atomic and molecular hydrogen targets at lower velocities (v less than or equal to 1×10^8 cm/sec). The molecular-hydrogen measurements are in excellent agreement with experimental results of Crandall et al.,[6] and the atomic-hydrogen cross sections are in fair agreement with absorbing-sphere Landau-Zener calculations of Olson and Salop.[15] These atomic-hydrogen measurements, however, disagree with experimental results of Bayfield et al.[16] Additional experiments with Bayfield[17] and Gardner[17] employing their apparatus and the ORNL PIG ion source are in progress.

1. R. A. Phaneuf and R. H. McKnight, *Bull. Am. Phys. Soc.* 21, 1266 (1976).
2. F. W. Meyer, R. A. Phaneuf, and R. H. McKnight, *Topical Conference on Atomic Processes in High-Temperature Plasmas*, Knoxville, Tenn., 1977.
3. G. W. McClure, *Phys. Rev.* 148, 47 (1966).
4. J. E. Bayfield, *Rev. Sci. Instrum.* 40, 869 (1969).
5. G. J. Lockwood, H. F. Helbig, and E. Everhart, *J. Chem. Phys.* 41, 3820 (1964).
6. D. H. Crandall, D. C. Kocher, and M. L. Mallory, *Phys. Rev. A* 15, 61 (1977).
7. R. E. Olson and A. Salop, accepted for publication by *Physical Review A*.
8. R. E. Olson et al., submitted to *Physical Review A*.
9. R. A. Phaneuf et al., letter submitted to *Journal of Physics B*.
10. M. B. Shah and H. B. Gilbody, *J. Phys. B* 7, 630 (1974).
11. J. E. Bayfield and G. A. Khayrallah, *Phys. Rev. A* 11, 920 (1974); *Phys. Rev. A* 12, 869 (1975).
12. L. I. Pivovar, M. T. Novikov, and V. M. Tubaev, *Sov. Phys.-JETP* 15, 1035 (1962).
13. R. A. Baragiola and I. B. Nemirovsky, *Nucl. Instrum. Methods* 110, 511 (1973).
14. W. L. Fite, A. C. H. Smith, and R. F. Stebbings, *Proc. R. Soc. London, Ser. A* 268, 527 (1962).
15. R. E. Olson and A. Salop, *Phys. Rev. A* 14, 579 (1976).
16. J. E. Bayfield et al., *Abstracts of the Fifth International Conference on Atomic Physics*, Berkeley, Calif., 1976.
17. Participants from the University of Pittsburgh, Pittsburgh, Pa.

ELECTRON COLLISIONS WITH MULTICHARGED IONS

D. H. Crandall P. O. Taylor[1]
R. A. Phaneuf D. C. Gregory[1]
G. H. Dunn[1]

Electron-impact ionization and excitation of multicharged ions of C, N, and O were measured using ions from the ORNL PIG ion source[2] crossed by an electron beam, as illustrated in Fig. 5.7. These experiments are in cooperation with the Joint Institute for Laboratory Astrophysics (JILA), Boulder, Colorado. The measurements extend our understanding of basic atomic-collision processes and have application for interpreting plasma-light emission and for modeling behavior of the high-temperature plasmas of astrophysics and fusion.

The measured absolute cross section for excitation of the C^{5+} ($2s$-$2p$) resonance transition shown in Fig. 5.8 is the first excitation measurement of a multiply charged ion. The Gaunt-factor curve shown is a semiempirical estimate obtained by generalizing the behavior of known excitation cross sections for neutral atoms.[3] Such estimates have been used in plasma models and are of questionable accuracy, as illustrated by the present case. However, the theoretical Coulomb-Born and two-state close-coupling calculations[4] are in excellent agreement with the experiment—the best agreement ever obtained by two-state approximations for near-threshold excitation of a positive ion. The measurements will be extended to excitation of N^{4+} ($2s$-$2p$) and possibly to some ions of other isoelectronic sequences to provide further tests of theory.

Electron-impact ionization cross sections have been measured for C^{3+}, N^{3+}, N^{4+}, and O^{3+} for energies between threshold and 500 eV. Figure 5.9 shows results for C^{3+} and comparisons with other work. The Lotz[5,6] semiempirical cross-section estimates are similar to the Gaunt factor for excitation and have been most widely used in plasma modeling. Present data support other evidence[7] that the exchange classical impact parameter (ECIP) theory due to

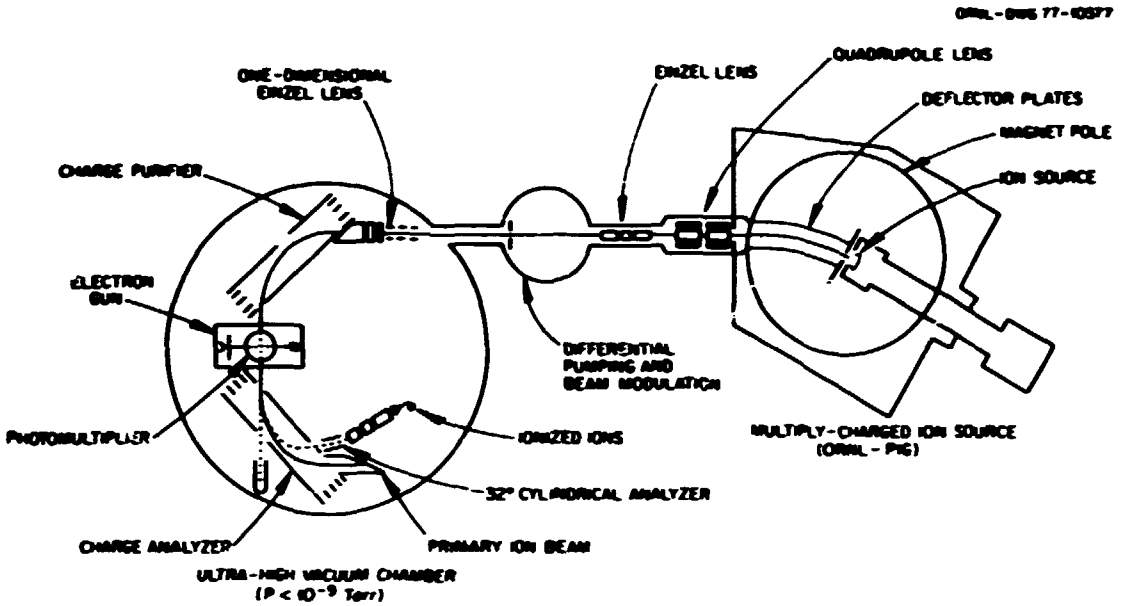

Fig. 5.7. Schematic diagram of the apparatus for electron-impact excitation and ionization experiments.

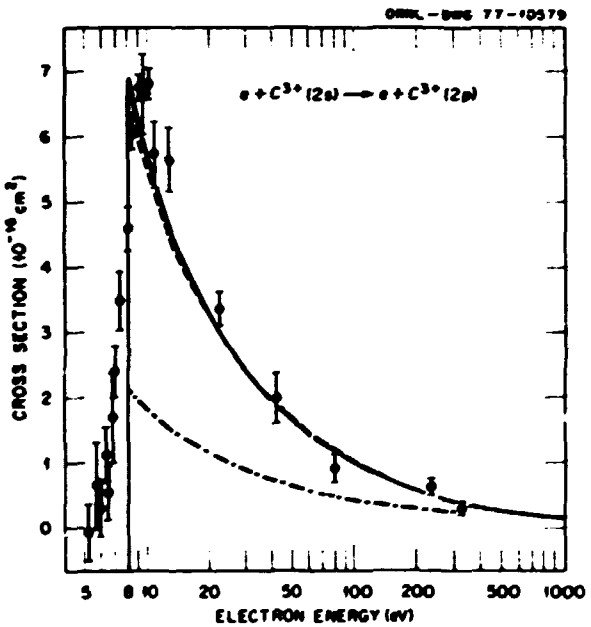

Fig. 5.8. The excitation of C^{3+} ($2s$-$2p$) by electron impact. Data points are present measurements; dotted curve is the Gaunt-factor semiempirical estimate (ref. 3); solid curve is Coulomb-Born calculation; dashed curve is the two-state close-coupling calculation (ref. 4).

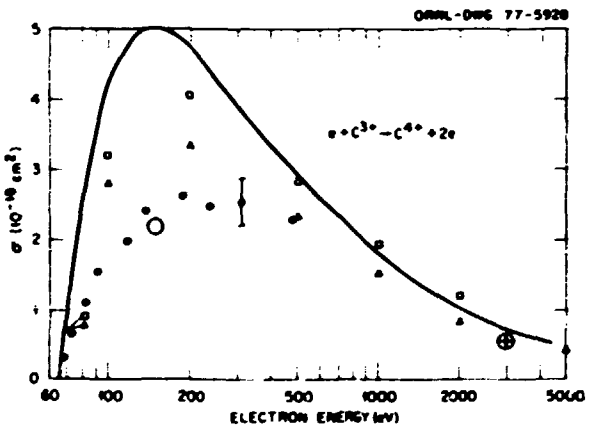

Fig. 5.9. Electron-impact ionization of C^{3+}. Solid points show present data; solid curve shows classical binary encounter approximation (A. Salop, submitted to *Physical Review A*); open squares show Lotz semiempirical estimate (ref. 5); open triangles show exchange classical impact parameter calculation (W. D. Barfield, conference on *Atomic Processes in High-Temperature Plasmas*, Knoxville, Tenn., February 1977); open circle shows experimental cross section deduced for reaction rate in plasma (ref. 8); open circle with cross shows cross section deduced from plasma reaction rate [E. D. Donnets, *IEEE Trans. Nucl. Sci.* NS-23(2), 897 (1976)].

Burgess provides the most reliable calculated values. The results deduced from ionization rates in a θ-pinch plasma[7] are in good agreement with the present data for the C^{+} case, but for N^{4+} the plasma measurements were a factor of 2 lower than our data.

Our ionization measurements will be extended to a few more ions and to higher energies during 1978. The existing results for both ionization and excitation cross-section measurements will be presented at the International Conference on Electron and Atomic Collisions in Paris, July 1977, and are being prepared for publication.

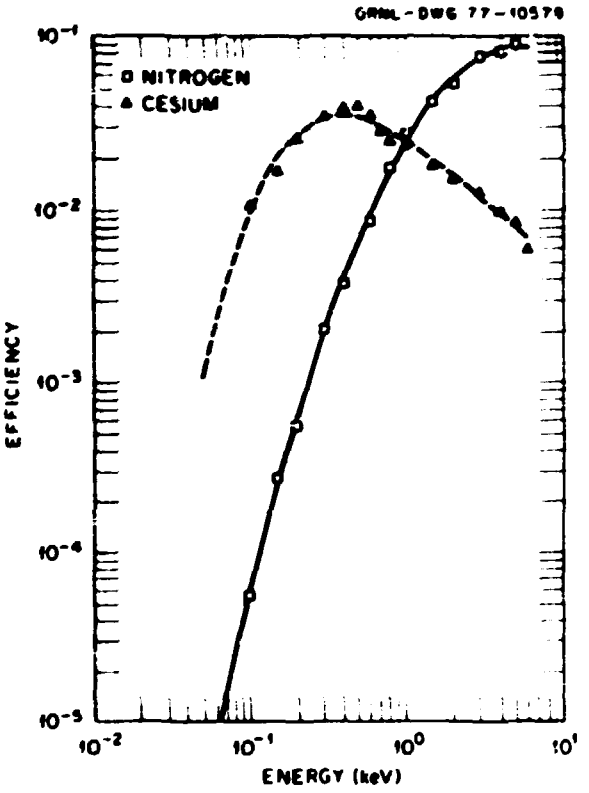

Fig. 5.10. Efficiency of a cesium heat-pipe vapor cell to convert low-energy hydrogen atoms to H^-. Shown for comparison is the efficiency of a conventional N_2 gas cell to convert hydrogen atoms to H^-.

1. Participants from the Joint Institute for Laboratory Astrophysics, Boulder, Colorado.
2. M. J. Mallory and D. H. Crandall, *IEEE Trans. Nucl. Sci.* NS-23(2), 1069 (1976).
3. M. J. Seaton, *Atomic and Molecular Processes*, ed. D. R. Bates, Academic Press, New York, 1962, p. 414.
4. The close coupling calculations are being carried out by R. J. W. Henry and J. N. Gau at Louisiana State University and separately by W. D. Robb at Los Alamos Scientific Laboratory. The Coulomb-Born (with exchange calculation) is by J. B. Mann of Los Alamos. All of these results and present data were reported at the conference on *Atomic Processes in High-Temperature Plasmas*, Knoxville, Tenn., February 1977, sponsored by ERDA-DMFE and the ORNL Controlled Fusion Atomic Data Center.
5. W. Lotz, *Astrophys. J. suppl.* 14, 207 (1967).
6. W. Lotz, *Z. Phys.* 206, 241 (1968).
7. A. Burgess et al., to be published in *Monthly Notices of the Royal Astronomical Society*.
8. H. J. Kunze, *Phys. Rev. A* 3, 937 (1971).

NEUTRAL-PARTICLE SPECTROMETERS

J. A. Kay D. A. Brisson[1]
C. F. Barnett

A parallel-plate ion energy analyzer and a Wien-type ion velocity filter analyzer using an N_2 gas cell to strip energetic hydrogen atoms have been fabricated, calibrated, and placed in operation on the ELMO Bumpy Torus (EBT) plasma to determine the plasma ion temperature. Measurements made by the EBT group have confirmed previously measured ion temperatures, indicating that previous measurements were not distorted by the presence of impurity neutrals escaping the plasma.

Using heat pipe techniques, we fabricated a cesium oven and calibrated it to convert hydrogen atoms to H^-. Figure 5.10 shows the spectrometer efficiency as a function of hydrogen energy. Also shown for comparison is the efficiency of a conventional nitrogen conversion cell in which H^+ was converted to H^-. At an energy of 100 eV, the cesium conversion cell is 2^1 orders of magnitude more efficient than the nitrogen cell. The spectrometer has been placed in operation on EBT and has increased the reliability of the data for low-energy neutrals.

1. ORAU Research Participant, North Carolina State University, Raleigh.

6. Atomic and Molecular Physics

Accelerator-Based Research

INTRODUCTION

P. D. Miller C. D. Moak

The following research areas are being actively pursued, in most cases with beams of particles from the EN tandem accelerator: Ion Stripping in Gases and Solids; Ionic States inside Solids, Inner-Shell and Outer-Shell Excitation of Multiply Charged Ions; Radiative and Nonradiative Electron Capture by Multiply Charged Ions; Beam Foil Spectroscopy and Target Atom Radiation; Auger and Autoionization Processes; Stopping Powers of Heavy Ions in Gases, Solids, and in Crystal Channels; Coulomb Excitation and Molecular Orbital Promotion of Atomic States of Heavy Atoms; Electron Ejection from Solids; and Quasi-molecular X-Ray Studies.

Results in these areas have already made impacts in the related fields of fundamental atomic structure, ion penetration in matter, radiation damage in solids, ion-induced x rays for chemical analysis, accelerator technology, and thermonuclear studies. Highly stripped heavy ions affect the performance of thermonuclear plasmas. These particles, if present as impurities in controlled thermonuclear reactor (CTR) devices, can produce serious power losses through radiative and nonradiative electron capture. A better understanding of these loss processes may be helpful in the choice of materials that will be exposed to plasmas. Stopping powers and range measurements are useful in understanding neutron radiation damage for fission and fusion technology, as well as in having a basic understanding of fundamental mechanisms of ion-stopping power and of solid-state physics.

In 1962, the discovery of multicomponent heavy-ion beams with the EN tandem accelerator led to the routine use of heavy ions for solid-state physics research and to a program of stopping-power measurements; both these areas are still being pursued. Early use of bromine and iodine ions as simulated fission fragments led to studies of fission detectors, crystal channeling, and charge states of stripped ions, in addition to ordinary stopping phenomena.

Table 6.1 summarizes the activities on the EN tandem Van de Graaff accelerator for the past year. Some of the results of group I have been published.[1] Other work by this group has shown that, when ion and target Z are matched, the target atoms are able to fill K-shell holes carried by the ion with high probability. This effect is so prominent that the charge-state distribution of chlorine ions passing through a KCl target is almost one-half charge less than is the case with carbon or aluminum targets. This direct transfer of electrons from inner shell to inner shell of identical particles is a subject under intensive study in several laboratories. Group VII in Table 6.1 has also been concerned with the direct transfer of electrons from the target K shell to K-shell vacancies in the incident projectile. These studies were made by measuring K x-ray yields from ^{22}Ti, ^{29}Cu, and ^{32}Ge bombarded by 52-MeV $^{14}Si^{q+}$. When vacancies were present in the silicon ($q = 13^+$, 14^+), large contributions due to electron transfer were observed, which increased by a factor of about 10 as Z_2 approached Z_1. These results and a quantitatively satisfactory comparison to a new theory of electron capture[2] with no adjustable parameters have been accepted for publication in *Physical Review A*.

Group II in Table 6.1 has developed a new method for the measurement of charge-state distributions of stripped ions; a system for doing the measurements has been built and has proved to be a better way to evaluate the performance of gas-stripper equipment designed for tandem accelerators. The method consists of using a gas cell fitted with exit apertures which exactly conform to the acceptance cone angle of the assumed accelerator-tube optic system, followed by a magnetic quadrupole which selectively focuses the entire cone of ions of one

Table 6.1. Summary of current atomic physics activities and recent accomplishments on the EN tandem Van de Graaff

Personnel group	Activity and recent results	Significance
I. C. D. Moak, P. D. Miller, J. Gomez del Campo, S. Datz,[a] P. Dittner[a]	Investigation of higher order Z_1 effects and effects of screening by bound projectile K electrons on the electronic stopping of channeled ions. Recent results: • Stopping of frozen charge states of ions C^{q+}, N^{q+}, O^{q+}, and F^{q+} in the Au [111] planar channel is very closely proportional to q^2. • Stopping of bare nuclei with $Z_1 = 1-9$ and velocities corresponding to 2.0 and 3.5 MeV/amu in the Au [111] planar channel is not proportional to Z_1^2 and is not in agreement with proposed theories leading to additive Z_1^3 and Z_1^4 corrections to the stopping power formula.	Important for the quantitative understanding of the slowing down of charged particles such as a. fission fragments in reactors, b. recoil ions in CTR reactions, c. beam particles in targets for nuclear or atomic physics experiments.
II. G. D. Alton, C. M. Jones, C. D. Moak, P. D. Miller, L. B. Bridwell,[b] Q. C. Kessel,[c] H. Scott,[d] B. W. Wehring[e]	Studies of absolute yields of highly stripped heavy ions from beams traversing gas and foil strippers. Cl, Fe, and I ions have been studied with N_2, Ar, Kr, and Xe gas strippers and in some cases compared to C foils. Particular emphasis on the small-angle angular distributions.	Results of these studies will be used for the design of an optimum stripper for the terminal of the HHIRF 25-MV tandem. In some cases multiple electron-loss cross sections are derived.
III. H. J. Kim, F. W. Meyer, R. N. Phaneuf, P. H. Stelson, J. E. Bayfield,[f] P. Koch,[g] L. Gardner,[h] I. A. Sellin,[i] R. S. Thoe,[j] J. P. Forester,[j] H. C. Hayden[c]	Measurements of charge transfer cross sections for protons and highly ionized Fe ions incident on atomic hydrogen, H_2, and Ar.	The results for Fe ions are of direct interest to MFE because of the presence of highly stripped Fe impurity ions in CTR plasmas. The proton results are important in distinguishing asymptotic fundamental theories and are important for the neutral beam injection problem for MFE.
IV. C. D. Moak, J. A. Biggerstaff, B. R. Appleton,[k] T. S. Noggle,[k] C. W. White,[k] G. Clark[l]	Investigation of surface and volume contributions to radiative electron capture by fast heavy ions, using crystalline channeling.	In crystal channels, ions can move in an almost pure electron medium of very high density, by eliminating nuclear stopping, close impact collisions do not obscure the longer range radiative capture effects. The channel simulates a stream of electrons passing the ion at velocities of interest to the MFE program.
V. P. M. Griffin, I. A. Sellin,[i] D. J. Pegg,[i] R. S. Thoe,[i] S. B. Elston,[i] J. P. Forester,[j] C. R. Vane,[j] R. S. Peterson, H. C. Hayden, J. J. Wright,[m] K.-O. Groeneveld,[n] S. R. Schumann,[n] S. Bashkin,[o] K. W. Jones,[p] T. H. Kruse,[q] D. J. Pisano,[p] R. Laubert[r]	Measurements of lifetimes and spectra of ultraviolet and soft x-ray emitting states of heavy ions which have been highly ionized and excited by passage through foils or gases. Recent results are the measurement of many lifetimes of $\Delta n = 0$ transitions within the L shell of highly ionized Si, S, and Cl and within the M shell of Fe.	Because many of these same ions occur as impurity constituents in plasmas, the results are of direct interest to the MFE program, and to astrophysics.
VI. B. R. Appleton,[k] T. S. Noggle,[k]	Measurements of radiation damage in Al by Al ions, as evidenced	These studies are fundamental to an understand-

BLANK PAGE

		a stream of electrons passing the ion at velocities of interest to the MFE program.
V. P. M. Griffin, I. A. Sellin,[i] D. J. Pegg,[i] R. S. Thoe,[i] S. B. Elston,[i] J. P. Forester,[j] C. R. Vane,[j] R. S. Peterson, H. C. Hayden, J. J. Wright,[m] K.-O. Groeneveld,[n] S. R. Schumann,[n] S. Bashkin,[o] K. W. Jones,[p] T. H. Kruse,[q] D. J. Pisano,[p] R. Laubert[r]	Measurements of lifetimes and spectra of ultraviolet and soft x-ray emitting states of heavy ions which have been highly ionized and excited by passage through foils or gases. Recent results are the measurement of many lifetimes of $\Delta n = 0$ transitions within the L shell of highly ionized Si, S, and Cl and within the M shell of Fe.	Because many of these ions occur as impurity constituents in plasmas, the results are of direct interest to the MFE program, and to astrophysics.
VI. B. R. Appleton,[k] T. S. Noggle,[k] C. W. White[k]	Measurements of radiation damage in Al by Al ions, as evidenced by the dependence of Al resistivity on accumulated dose.	These studies are fundamental to an understanding of radiation damage by recoiling atoms of the material itself.
VII. P. D. Miller, G. Basbas,[s] J. L. Duggan,[s] F. D. McDaniel,[s] J. D. Gressett,[t] D. Johnson,[t] B. D. Payne,[t] G. Pepper,[t] R. Rice,[t] A. D. Toten,[t] J. Ricomi,[t] R. P. Chaturvedi,[u] R. M. Wheeler,[u] F. Elliot,[v] K. A. Kuenhold,[v] J. McCoy,[v] A. R. Zander,[w] L. A. Rayburn,[x] J. Lin,[y] S. J. Cipolla,[z] G. Lapicki[m]	Measurements of x-ray production cross sections for a variety of heavy ions. Recent results include: • cross sections for production of K x rays from targets $Z_2 = 20-50$, L x rays from targets of $Z_2 = 56-83$, M x rays from targets of $Z_2 = 78-83$ for incident ions of $Z_1 = 5-9$, as a function of bombarding energy. • Incident charge-state dependence of K x-ray production cross sections for Si on Sc, Ti, Cu, and Ge have been measured.	a. These systematic studies have led to the development of consistent theoretical corrections to the simple plane wave Born approximation. b. A quantitative theory of target K-electron capture by projectiles with K vacancies has been developed which is in agreement with these experiments.

[a]Chemistry Division.
[b]Murray State University, Murray, Ky.
[c]University of Connecticut, Storrs.
[d]Cornell University, Ithaca, N.Y.
[e]University of Illinois, Urbana-Champaign.
[f]University of Pittsburgh, Pittsburgh, Penn.
[g]Yale University, New Haven, Conn.
[h]Yale University, thesis student, New Haven, Conn.
[i]University of Tennessee, Knoxville.
[j]University of Tennessee, thesis student, Knoxville.
[k]Solid State Division.
[l]Solid State Division on assignment from Mineral Research Laboratory, CSIRO, Sydney, New South Wales, Australia.
[m]University of New Hampshire, Durham.
[n]Institute für Kernphysik der Universität, D-6 Frankfurt/M. 90, Germany.
[o]University of Arizona, Tucson.
[p]Brookhaven National Laboratory, Upton, N.Y.
[q]Rutgers University, New Brunswick, N.J.
[r]New York University, New York.
[s]North Texas State University, Denton.
[t]North Texas State University, thesis student, Denton.
[u]State University of New York, Cortland.
[v]Tulsa University, Tulsa, Okla.
[w]East Texas State University, Commerce.
[x]University of Texas, Arlington.
[y]Tennessee Technological University, Cookeville.
[z]Creighton University, Omaha, Nebr.

BLANK PAGE

charge state at a time into an electrostatic analyzer where quantitative measurements of yield per unit input current of that charge state can be made. The new system performs the integration of an entire angular distribution out to the correct solid angle, charge by charge, eliminating the computer errors which accumulate when very narrow angular distributions are integrated numerically. The price is that, in principle, only one charge at a time can be measured. In practice, it has been found that, for the smaller charge states, the scattering is so nearly forward that several charges can be measured on each run. Using the tandem Van de Graaff accelerator, group III in Table 6.1 has measured electron capture cross sections for Fe^{q+} $(6 < q < 14)$ over the energy range $30 < E_H < 290$ in atomic and molecular hydrogen and argon. The charge-state dependence ranges from $q^{1.5}$ at low values of q and E to $q^{3.0}$ for higher values of q and E. An empirical scaling formula has been found to relate the Fe^{q+} + H cross sections to those of H^+ + H.

The unique constraints imposed on the interactions of energetic heavy ions with target atoms as a result of the channeling effect have been utilized by the members of group IV in Table 6.1 for investigating the phenomenon of radiative electron capture for totally stripped oxygen ions. Along with the cross-section measurements, group IV members have measured the numbers of ions which capture electrons specifically at the two surfaces of the crystal specimen; they have found that the two surfaces give differing amounts of surface capture, and sputter-ion cleaning does not seem to affect this difference. The cause of the difference is not known at this time.

The activities of group V in Table 6.1 are summarized in the next section. The activity of group VI, consisting entirely of personnel from the Solid State Division, is summarized in Table 6.1.

1. S. Datz et al., *Phys. Rev. Lett.* 38, 1145 (1977).
2. G. Lapicki and W. Losonsky, *Phys. Rev. A* 15, 896 (1977).

ATOMIC STRUCTURE AND COLLISION EXPERIMENTS

P. M. Griffin — H. C. Hayden[3]
D. J. Pegg[1] — R. S. Peterson[1]
I. A. Sellin[1] — S. R. Schumann[2]
S. B. Elston[1] — R. S. Thoe[1]
J. P. Forester[1] — C. R. Vane[1]
K.-O. Groeneveld[2] — J. J. Wright[4]

Our principal research activity concerns the atomic structure and collision phenomena of highly stripped ions in the range $Z = 10$ to 35. The primary objective of our research is the study of atomic structure of highly ionized heavy ions and their modes of formation and destruction in collisions. The decay of excited states of these ions by radiative and by electron-emission processes is the phenomenon we study in carrying out these experiments. Our major tools are the various heavy-ion accelerators at Oak Ridge National Laboratory (ORNL) and Brookhaven National Laboratory (BNL); x-ray, soft x-ray, and extreme-ultraviolet spectrometers; electron spectrometers; and a variety of peripheral equipment associated with these devices. Our main experimental activities of the past 18 months are summarized in the succeeding paragraphs.

Lifetimes and Spectra Using Beam-Foil Excitation

We have concentrated our efforts in this area on multiply charged heavy ions of simple structure, that is, ions with only a few active electrons. Most of the transitions studied are in-shell ($\Delta n = 0$) electric-dipole processes, a large number of which are the principal resonance transitions of highly stripped ions. The beam-foil excitation method has been employed to measure both wavelengths (transition energies) and lifetimes (transition rates) by a time-of-flight technique. From a combination of both of these quantities, the f value, a measure of the strength of a transition, can be obtained, which is of great value to spectroscopic diagnostics in high-temperature plasmas and astrophysics.

This f value also serves as a convenient "bridge" between experiment and theory in atomic structure. Our f value results are compared with relativistic calculations which often involve intermediate coupling due to the substantial magnitude of the spin-orbit interaction in these highly ionized systems. One of the purposes of our work is to confirm these recent calculations in an attempt to extrapolate the f-value regularities along isoelectronic sequences (f vs $1/Z$) that have already been established in the non-relativistic region of lower Z ions.

In this report period we have studied $\Delta n = 0$ transitions[5-10] in highly ionized Si, S, Cl, Fe, Cu, and Br. In the elements Si, S, and Cl, we studied intrashell L-shell transitions for ions isoelectronic with lithium through fluorine. These measurements were made using MeV/amu ion beams from the ORNL tandem Van de Graaff accelerator. Similar in-shell transitions were studied in the M shells of the elements Fe, Cu, and Br. Specifically, we limited this work to sodium-like and magnesium-like structures such as Fe^{15+} and Fe^{14+}. The work[10] on sodium-like copper

and bromine was performed on the BNL MP tandem Van de Graaff accelerator due to the energy limitations of the ORNL EN tandem. The work on Br^{24+}, which required a beam energy of 151 MeV, represents lifetime measurements on the most highly stripped member of the sodium isoelectronic group ever studied to date. These higher energy experiments were performed by two of us in collaboration with B. M. Johnson and K. W. Jones of Brookhaven National Laboratory, J. L. Cecchi of Princeton University, and T. H. Kruse of Rutgers University. Typical examples of some of our results are shown in Figs. 6.1 and 6.2 and in Table 6.2

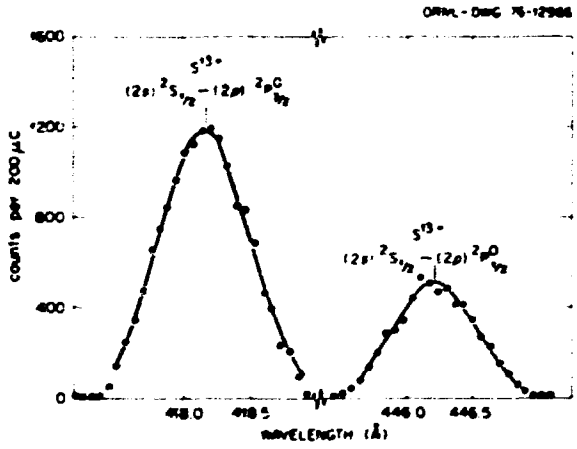

Fig. 6.1. Spectral scan showing the doublet splitting of the resonance lines of lithium-like sulphur (S^{13+}). The wavelength scale is "as observed," in which there is a Doppler shift of approximately 0.46 Å.

In an experiment involving the "neon target spectrum" produced by impingement of foil-transmitted highly stripped heavy projectile ions, it

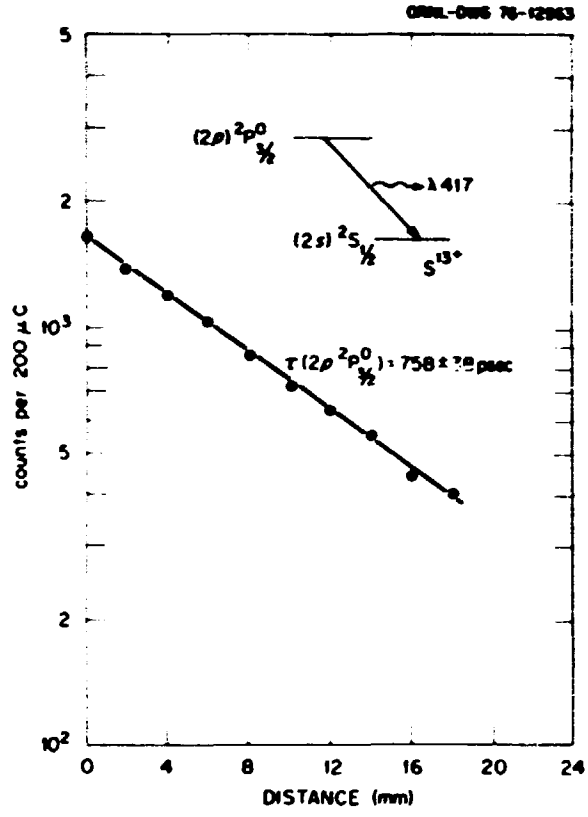

Fig. 6.2. Typical decay curve from the $(1s^2 2p)^2 P^0_{3/2}$ level of lithium-like sulphur (S^{13+}).

Table 6.2. Lifetimes and oscillator strengths of levels in some highly ionized sulfur ions

Ion	Wavelength	Transition	Lifetime of upper level (10^{-12} sec)		Oscillator strength	
			This work	Theory	This work	Theory
S^{13+}	417.69	$(1s^2 2s)^2 S_{1/2} - (1s^2 2p)^2 P^o_{3/2}$	767 ± 39	817.[a] 817.[b]	0.068	0.064,[a] 0.064[b]
S^{13+}	445.72	$(1s^2 2s)^2 S_{1/2} - (1s^2 2p)^2 P^o_{1/2}$	918 ± 92	993.[a] 993.[b]	0.032	0.030,[a] 0.030[b]
S^{12+}	256.69	$(1s^2 2s^2)^1 S_0 - (1s^2 2s 2p)^1 P^o_1$	157 ± 16	131.[a] 126.[b]	0.189	0.227,[a] 0.235[b]
S^{12+}	301.04	$(1s^2 2s 2p)^1 P^o_1 - (1s^2 2p^2)^1 S_0$	79 ± 15	75.[a] 81.[b]	0.057	0.060,[a] 0.056[b]
S^{12+}	308.95	$(1s^2 2s 2p)^3 P^o_2 - (1s^2 2p^2)^3 P_2$	168 ± 9	210.[b]	0.085	0.068[b]
S^{12+}	280.42	$(1s^2 2s 2p)^1 P^o_1 - (1s^2 2p^2)^1 D_2$	689 ± 35	559.[a] 346.[b]	0.091	0.112,[a] 0.181[b]
S^{11+}	218.23,221.44	$(1s^2 2s^2 2p)^2 P^o_{3/2} - (1s^2 2s 2p^2)^3 P_{3/2,5/2}$	81 ± 8	53.[a] 46.,[b] 48.[c]		
S^{11+}	243.09	$(1s^2 2s 2p^2)^4 P_{5/2} - (1s^2 2p^3)^4 S^o_{3/2}$	90 ± 9	54.[a] 49.[b]		
S^{11+}	288.39,299.64	$(1s^2 2s^2 2p)^2 P^o_{1/2,3/2} - (1s^2 2s 2p^2)^2 D_{3/2,5/2}$	410 ± 41	383.[a] 344.,[b] 385.[c]		
S^{10+}	291.27	$(1s^2 2s 2p^2)^3 D_{3/2} - (1s^2 2p^3)^3 D_{5/2}$	190 ± 19	146.[a]		
S^{10+}	188.69	$(1s^2 2s^2 2p^2)^3 P_1 - (1s^2 2s 2p^3)^3 S^o_1$	35 ± 4	23.[a] 21.,[b] 22.[c]		
S^{10+}	190.46	$(1s^2 2s^2 2p^2)^1 D_2 - (1s^2 2s 2p^3)^1 P^o_1$	39 ± 4	29.[a] 32.[c]		
S^{10+}	216.00	$(1s^2 2s^2 2p^2)^1 D_2 - (1s^2 2s 2p^3)^1 D^o_2$	73 ± 7	47.[a] 41.,[b] 77.[c]		
S^{10+}	267.10	$(1s^2 2s^2 2p^2)^3 P_2 - (1s^2 2s 2p^3)^3 P^o_1$	150 ± 15	136.[a] 114.,[b] 133.[c]		
S^{10+}	295.59	$(1s^2 2s 2p^3)^1 D^o_2 - (1s^2 2p^4)^1 D_2$	70 ± 7	72.[a] 67.[b]		
S^{9+}	180.77	$(1s^2 2s^2 2p^2)^2 D^o_{3/2} - (1s^2 2s 2p^3)^2 P_{3/2}$	23 ± 2	20.[a] 19.[c]		

[a] U. I. Safronova, A. N. Ivanova, and V. N. Kharitonova, *Theor. Exp. Chem. (USSR)* 5, 209 (1969).
[b] M. Cohen and A. Dalgarno, *Proc. R. Soc. London, Ser. A* 280, 258 (1964).
[c] O. Stanojev, *Nucl. Instrum. Methods* 110, 193 (1973).

was found that the cross section for production and excitation of Ne^{q+} L x rays, belonging to charge states $q = 2$ to 5 and falling in the energy range of 25 to 180 eV, was great enough that a grazing incidence grating spectrometer could be used for their dispersion and detection. This gave rise to line widths less than or equal to 0.007 eV which were due entirely to instrumental broadening because of the relatively low recoil velocities of the emitters, which in turn led to negligible Doppler broadening.[11]

Electron Spectroscopy and Collision Studies of Core-Excited States of the Alkali Metals

Our previous spectroscopic observations[12] have made possible a study of the mechanisms responsible for populating core-excited states in alkali ion-atom collisions at impact energies in the 10- to 50-keV range.

Autoionization electron spectra from low-energy collisions of Li^+ ions with gaseous helium targets are of considerable current importance for several reasons. First, the $(Li,He)^+$ system is the simplest asymmetric collision system involving atomically structured particles in which core excitation occurs, and is thus potentially amenable to an ab initio theoretical treatment. Second, core-excited states are copiously produced in these collisions, predominantly through the quasi-molecular promotion mechanism proposed by Fano and Lichten.[13] Third, core-excited states of light atoms and ions decay almost exclusively through autoionization rather than by radiative modes; hence, observation of the ejected electrons is superior to detection of radiation as a means of probing the excitation mechanism. Fourth, because only one final state is possible for the autoionization decay of singly core-excited states in lithium, interpretation of the spectra in terms of populated states is relatively straightforward.

Current models[14] of the molecular-orbital promotion mechanism are almost exclusively independent electron models; that is, the molecular states are treated essentially as products of one-electron orbitals, with electron-electron interactions included only to the extent that they cause a screening of the nuclear charges. We have obtained and reported[15] preliminary results which appear to be at variance with these simple models; an example of the pertinent spectra appears in Fig. 6.3. Shown are the spectra of electrons ejected from neutralized lithium projectiles after single collisions at 10 and 50 keV with helium target atoms. Of particular interest is the behavior as a function of impact energy of the two lines attributed

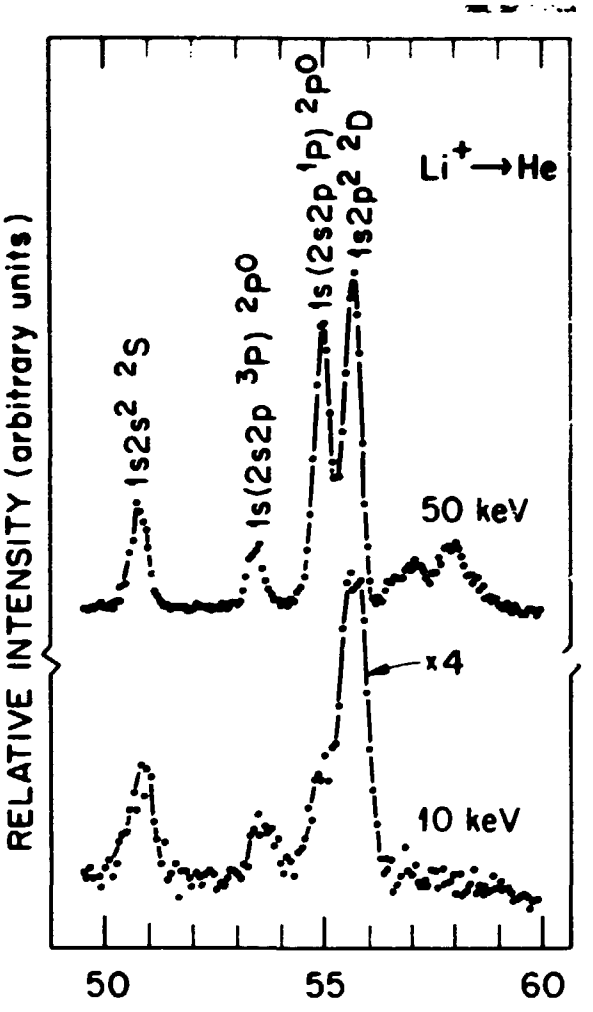

Fig. 6.3. Spectra of electrons ejected by neutralized lithium projectiles after single collisions with a helium gas target, for impact energies of 10 and 50 keV. The 10-keV spectrum has been magnified by a factor of 4. Electron energies are given in the rest frame of the projectile, and line assignments are those given by Pegg et al. (ref. 12).

to autoionization decay of $1s(2s2p^1P)^2P^0$ and $1s(2s2p^1P)^2P^0$ core-excited states of neutral lithium. Because these states have the same electronic configuration and differ only in the coupling of the $n = 2$ electrons, independent-electron models do not explicitly distinguish between them, but instead predict a constant ratio for their relative line intensities. Accordingly, a study of excitation cross sections of these and other states is expected to provide important clues to the many-electron aspect of quasi-molecular promotion mechanisms. Similar work is in progress to study excitation of other alkalis in collision with various gas targets.

Low-Energy Ne^{q+} + Ne Collisions Involving *K*-Vacancy Production

In an experiment on the Penning Ion-Source Facility and at New York University, *K*-vacancy production (signatured by the emission of x rays) has been studied at various projectile energies in the collision system $^{A}Ne^{q+} + {}^{B}Ne$ ($A, B = 20$ or 22; $q = 1 - 5$). One of the principal purposes of this experiment was to study the influence of the number of $2p$ vacancies carried into the collision by the projectile. Our results indicate that *K* x-ray production cross sections for this system scale appreciably more strongly than n^6 (n = number of initial $2p$ vacancies), the result predicted by Briggs and Macek[16] for symmetric collisions. Eichler and Wille,[17] however, have shown recently that the Ne^{q+} + Ne system cannot be considered as being symmetric for large q, and our results would seem to confirm this.

Another objective of this work was to test the mass-dependence (isotope) effect, using both ^{20}Ne and ^{22}Ne as either projectile or target in experiments. This hypothesis is fundamental in the theory of *K*-vacancy production as given by Briggs and Macek.[16] A basic approximation employed in the theory assumes that *K*-vacancy production in symmetric collisions between different isotopes of the same element would be approximately the same in collisions at the same relative velocity (the "equal velocity rule").

The most significant result of our mass-dependence studies is that, at sufficiently high relative velocities, the previously mentioned "equal velocity rule" holds very well. For velocities near threshold (where *K*-vacancy yield varies nearly vertically with beam energy), isotope effects as large as 40% have been observed. This large isotope effect (40% yield difference for a 10% mass difference) can be understood in terms of the molecular-collision model of Barat, Fano, and Lichten[18] at small collision velocities. The mass-dependence experiment was done at New York University in collaboration with R. Laubert and F. K. Chen and provided the first precise test of the theoretical predictions, using *K* x-ray production as a measurement of the *K*-vacancy production.[19]

Electron Capture by keV Energy Multiply Charged Ions in H, H_2, He, and Ar Targets

Another application of the ORNL Penning Ion-Source Facility involved the measurement of electron transfer at keV beam energies. Projectiles used in this work were B^{q+} ($q = 2-4$), C^{q+} ($q = 2-4$), N^{q+} ($q = 2-5$), and O^{q+} ($q = 2-5$). Targets were atomic and molecular hydrogen and helium and argon. The work was a collaborative effort with members of the Yale University collisions group (J. E. Bayfield, L. D Gardner, and P. M. Koch), which supplied the atomic hydrogen target. The essential results can be found in the paper by Bayfield et al.[20]

In another collaboration with this same group, we studied electron transfer at MeV beam energies for the fundamental collision system $H^+ + H$. These studies are of considerable significance because they relate to one of the most basic problems of scattering theory, the three-body problem. Preliminary results of this work are given in the paper by Gardner et al.[21] At this time, analysis of the data is still under way. Because the electron transfer cross sections at these energies are so small, the experiment is very sensitive to even small concentrations of contaminants in the target, and these impurities will set the limit of precision attained in this work.

---

1. University of Tennessee, Knoxville.
2. Institut fur Kernphysik der Universitat Frankfurt, Frankfurt M, West Germany.
3. University of Connecticut, Storrs.
4. University of New Hampshire, Durham.
5. D. J. Pisano et al., submitted to *Physical Review A*.
6. D. J. Pegg et al., *Phys. Lett. A* 58, 349 (1976).
7. D. J. Pegg et al., *Phys. Rev. A* 14, 1036 (1976).
8. D. J. Pegg et al., to be published in *Astrophysics Journal*, 214, 331 (1977).
9. D. J. Pegg et al., *Phys. Rev. A* 15, 1958 (1977).
10. D. J. Pegg et al., submitted to *Physical Review Letters*.
11. I. A. Sellin, to be published in the *Proceedings of the Fourth Conference on the Application of Small Accelerators, North Texa State University, October 25–27, 1976*.
12. D. J. Pegg et al., *Phys. Rev. A* 12, 1330 (1975).
13. U. Fano and W. Lichten, *Phys. Rev. Lett.* 14, 627 (1965).
14. See, for example, K. Taulbjerg and J. S. Briggs, *J. Phys. B* 8, 1895 (1975); J. Eichler et al., *Phys. Rev. A* 14, 707 (1976), and references quoted therein.
15. S. B. Elston et al., *Bull. Am. Phys. Soc.* 22, 655 (1977); S. Schumann et al., *Proceedings of the Tenth International Conference on the Physics of Electronic and Atomic Collisions*, to be published.
16. J. S. Briggs and J. H. Macek, *J. Phys. B.* 5, 579 (1972).
17. J. Eichler and U. Wille, *Phys. Rev. Lett.* 33, 56 (1974).
18. M. Barat and W. Lichten, *Phys. Rev. A* 6, 211 (1972).
19. R. S. Peterson et al., *Phys. Rev. Lett.* 37, 984 (1976).
20. J. E. Bayfield et al., p. 126 in *Proceedings of the Fifth International Conference on Atomic Physics*, ed. R. Marrus, M. H. Prior, and H. A. Shugart, University of California, Berkeley, 1976.
21. L. D. Gardner et al., *Bull. Am. Phys. Soc.* 21, 1265 (1976).

Atomic and Molecular Physics Other than Accelerator-Based Research

ELECTRON SPECTROSCOPY

INTRODUCTION

T. A. Carlson P. Agron[1]
W. B. Dress G. L. Nyberg[2]
F. A. Grimm[3]

The program on electron spectroscopy has been directed toward the development of x-ray and ultraviolet photoelectron spectroscopy as tools for the study of surfaces. An important breakthrough in our program occurred in February 1977 when an ultraviolet lamp, which has been designed to yield polarized He (21.22-eV) radiation, was successfully integrated into our spectrometer. A detailed description of this lamp appears in a separate section of this report. Data have been obtained on oriented crystals of copper and nickel, both in clean condition and after exposure to gases to effect monolayer adsorption. These studies are being carried out as a function of surface orientation and direction of polarization. From these studies, one hopes to deduce the nature of the chemical bonding of the molecule to the surface and the orientation of the molecule relative to the surface. The information derived from ultraviolet studies can be coupled with that obtained from Auger and core-shell photoelectron spectroscopy to provide a powerful tool for characterizing molecular behavior on surfaces, which is of important interest to heterogeneous catalysis. For this purpose, a cooperative program with the catalysis group in chemistry has been initiated.

In addition to performing photoelectron spectroscopy studies, we have also been involved in photon-induced Auger spectroscopy. (A summary of this work also appears below.) The advantages of photon-induced Auger spectroscopy as opposed to electron impact are that the spectra have much better peak-to-background ratios and are less susceptible to charging and radiation damage. In addition, photoelectron data can be taken simultaneously, which is of particular interest in evaluating the basic nature of chemical shifts in the two different electron spectroscopies. Concomitant to the experimental program, an attempt is being made to support the program with theoretical calculations. Computations have been carried out on the effect of chemical shifts in Mg/MgO systems and in gaseous H_2S for both the photoelectron and Auger processes. Calculations on angular distribution have also been initiated in collaboration with Burke Ritchie.[4]

1 Chemistry Division
2 La Trobe University, Bundoora, Victoria, Australia
3 Consultant to ORNL from University of Tennessee, Knoxville
4 University of Alabama, Tuscaloosa

K-LL AUGER PROCESSES IN THIRD-ROW ELEMENTS

T. A. Carlson G. L. Nyberg
W. B. Dress

The third-row elements, which in the periodic table begin with neon ($Z = 10$) and conclude with argon ($Z = 18$), form an important group with which to examine the basic nature of the Auger process because they are the lightest elements for which an Auger process can take place involving only filled core shells. Auger transitions are fairly well described by the L-S coupling scheme, and there appear for all practical purposes only five lines in the spectrum:

(1,2) $1s\text{-}2p2p[K\text{-}L_{II}L_{III}(^1D), K\text{-}L_{II}L_{II}(^1S)]$;

(3,4) $1s\text{-}2p2s[K\text{-}L_1L_{II,III}(^1P), K\text{-}L_1L_{II}(^1P)]$;

(5) $1s\text{-}2s2s[K\text{-}L_1L_1(^1S)]$.

The ^1P states associated with the $1s\text{-}2p2p$ transition are not allowed in LS coupling, and the ^1P states associated with the $1s\text{-}2s2p$ transition are insufficiently split in energy that they appear as one line.

The *K-LL* Auger processes of the third-row elements are of particular interest because they are highly sensitive to electron correlation effects; and though involving only core atomic-like orbitals, they may be strongly affected by the chemical environment, because the valence shell is directly above the L shell.

In our report, we have concentrated our attention on Mg, Al, and Si metals and their respective oxides, although we have carried out preliminary studies on a variety of other solids containing third-row elements. To gain a comprehensive picture of the problem, we have compared our results with literature values for both theory and experiment for elements from $Z = 10$ to 20. The principal phenomena

of interest fall into four topics: energy, intensity, chemical shifts, and satellite structure.

Energy

Figure 6.4 shows a typical *K-LL* spectrum of aluminum. The spectra are obtained with a double-focusing electron spectrometer, using the aid of a position-sensitive detector.[3] The metal is polycrystalline and is cleaned in situ with an argon ion gun. The Auger electron spectra are taken under UHV conditions. The initial *K* vacancies are created by photoionization, using Al K_α x rays for magnesium and Ag *L* x rays for *Z* greater than 12. In addition to the normal *K-LL* Auger lines, Fig. 6.4 shows additional structure due to plasmon losses, both bulk and surface. It may also be noted that the Auger peaks broaden for transitions involving the L_1 shell due to Coster-Kroning transitions that occur with 2*s* vacancies.

In Table 6.3 are listed the Auger energies of Mg, Al, and Si metals. Results previously obtained on magnesium[3] and aluminum[4] show that agreement with our data is good. The relative energy spacings between the different Auger lines also agree fairly well between magnesium metal and the atomic state of magnesium. In comparing experimental results with theoretical calculations of Shirley,[4] one finds that, except for the $K\text{-}L_2L_3(^1S)$ transition, the energy separations are larger for experimental values. The discrepancy lies partly in the fact that relaxation energy in Shirley's calculation has only been treated approximately (static relaxation) and partly through the neglect of electron correlation.

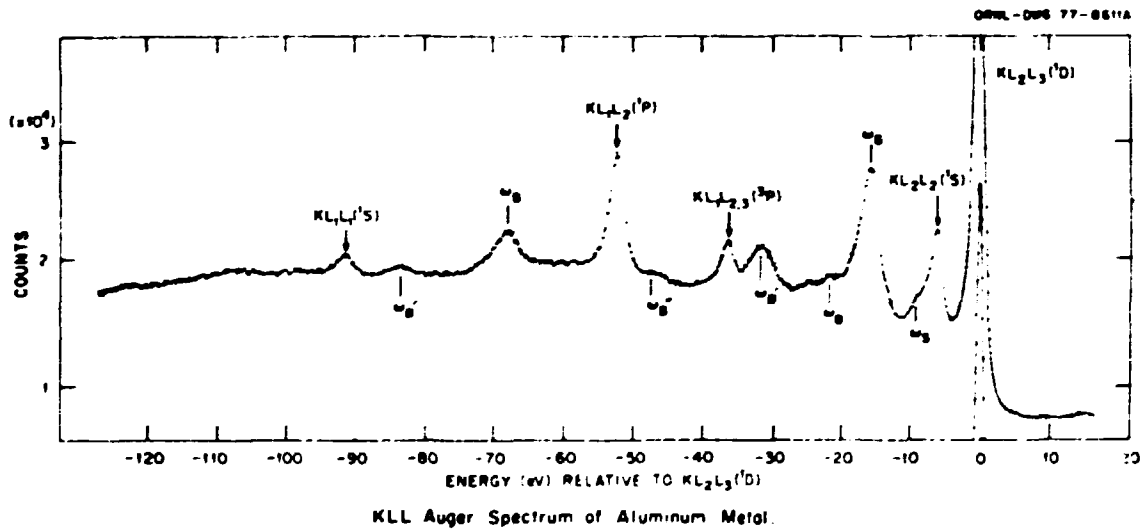

Fig. 6.4. Aluminum *K-LL* Auger spectrum. The *K-LL* Auger lines are labeled as to the particular configuration. The peaks labeled ω_s and ω_B are the surface and bulk plasmon loss peaks, and as such are always lower in energy than the parent line. ω indicates a second plasmon loss, etc.

Table 6.3. *K-LL* Auger energies for magnesium, aluminum, and silicon metals (eV)

Transition	Magnesium	Magnesium (theory)[a]	Aluminum	Aluminum (theory)[a]	Silicon	Silicon (theory)[a]
$KL_2L_3\ ^1D$	0 (1185.10)	0 (1174)	0 (1393.44)	0 (1383)	0 (1616.48)	0 (1607)
$L_2L_2\ ^1S$	5.25	6	6.01	7	6.93	8
$L_1L_2\ ^1P$	31.52	29	36.24	35	41.09	39
$L_1L_2\ ^3P$	45.53	43	52.03	51	58.48	57
$L_1L_2\ ^1S$	79.41	73	90.89	87	102.89	96

[a] D. A. Shirley, *Phys. Rev. A* 7, 1520 (1973).

Intensity

The relative intensities of the *K-LL* Auger lines for light elements have been of concern for many years, because, although the relatively simple *L-S* coupling scheme could be applied, the comparison between theory and experiment has been much poorer than for heavier elements. The reason for this lies in the importance of electron correlation. The inclusion of *S*-state configuration interaction greatly improved the situation, but not until Kelley[4] applied his many-body perturbation theory in the case of neon was there good agreement between theory and experiment.

In Fig. 6.5 is plotted the intensity of the $K\text{-}L_1L_2(^1P)$ line relative to the most intense Auger line as a function of Z and chemical state. Similar plots are available for the other lines. Theoretical calculations with only limited configuration interaction are shown by a dotted line. The behavior of free atoms is indicated by a dot-dash line. It is evident that both electron correlation and the nature of the chemical state play crucial roles in the transition probabilities of *K-LL* Auger processes for the third-row elements.

Chemical Shifts

Figure 6.6 shows a portion of the *K-LL* Auger spectra of a highly oxidized surface of aluminum, together with the photoelectron spectra arising from x-ray photoemission in the 2*s* and 2*p* shells of aluminum. Fortuitously, both the Auger and photoelectron spectra occur in the same energy range and can be easily compared. Three doublets occur due to the presence of both the aluminum metal and aluminum oxide. It is to be noted that the chemical

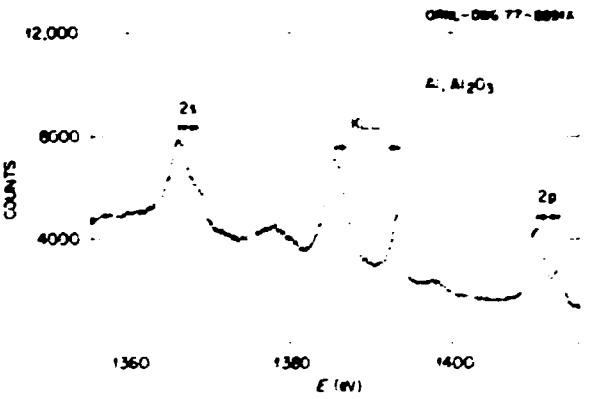

Fig. 6.6. Portion of a spectrum taken with oxidized aluminum. The central large peak is due to an Auger transition in the oxide, while the peak to the right is the corresponding transition in the metal; the difference in energy between these two lines is the *chemical shift*. The doublet on the right is due to photoejection from the 2*p* shell of aluminum, the left-hand member showing the effect of the oxide. The same is true for the doublet on the left, which is due to photoejection from the 2*s* shell.

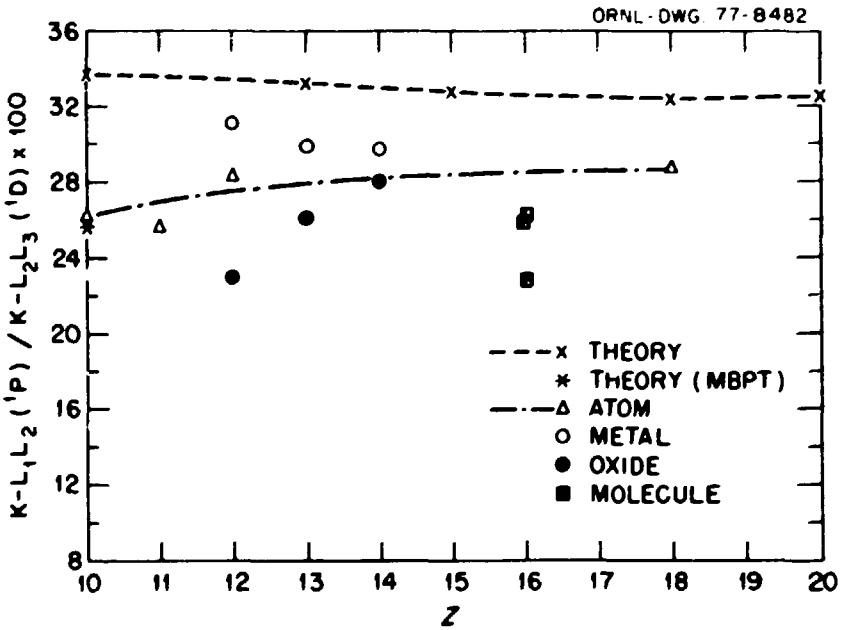

Fig. 6.5. Intensity of the $K\text{-}L_1L_2(^1P)$ Auger line relative to the most intense *K-LL* Auger line as a function of Z and chemical state. Limited configuration-interaction calculations are shown by the dashed line, and free-atom behavior is indicated by the dot-dash line.

shift in the case of the Auger process is considerably larger than in the case of photoionization. This difference has been related to the difference in relaxation energies between the two processes, and it can be shown that the change in chemical shifts observed in Auger processes as compared with photoionization, $\Delta\alpha$, is relative to the extra-atomic relaxation created by a single hole $\Delta\alpha \cong 2\Delta R^{+}$, where R^{+} is the extra-atomic relaxation energy.

Table 6.4 lists various chemical shifts for metal and metal oxide systems. It is to be noted that in each case the Auger process yields a much larger chemical shift than the corresponding photoelectron shift. From the above expression, it would appear that the extra-atomic relaxation energy for the metal–metal oxide pairing is fairly constant between Mg, Al, and Si. It is also interesting to note that the chemical shift for the *K* shell is slightly larger than for the *L* shell, and the shift for the 2*p* orbital is greater than that of the 2*s* orbital. The shifts for the various Auger lines for a given metal–metal oxide pair are fairly constant, although the 1*s*-2*p*2*p* transition may contain the largest shift. It is also noteworthy to point out that when correction is made for extra-atomic relaxation energy in the case of magnesium, the photoelectron chemical shift is negative, suggesting that in the frozen-orbital approximation it may be more difficult to remove a core electron from the magnesium metal than from magnesium oxide.

Table 6.4 Chemical shifts for metal–metal oxides (eV)

Auger	Magnesium	Aluminum	Silicon
KLL ^1D	5.2	7.4	7.9 9.8
KLL ^1S			
KLL ^3P	5.2	7.0	
KLL ^1P	5.1	6.9	7.3 9.3
KLL ^1S	4.7	7.1	
Photoelectron			
K	1.5	3.0	2.6 4.9
L	1.0	2.5	
L	1.2	2.8	3.0 5.0

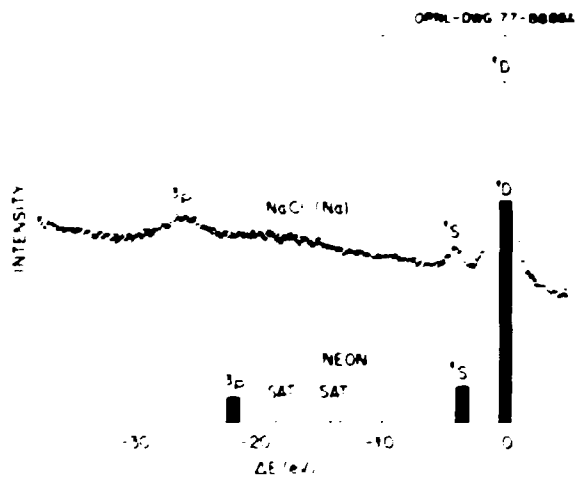

Fig. 6.7. Comparison of the Auger spectrum of sodium in NaCl (data curve) with the neon Auger spectrum (vertical bars).

Satellite Structure

Satellite structure in an Auger process may occur as the result of extra excitation in the original formation of the core vacancy. Auger processes taking place in such excited atoms will give lines at slightly different energies (usually lower) than the normal diagram lines. In addition, excitation such as electron shake-up can also occur in the Auger process itself, yielding satellite structure. Figures 6.7–6.9 show comparison of a portion of an Auger spectra for Na^{+}, K^{+}, and Rb^{+}, together with the spectrum of the rare gas that is adjacent to the alkali metal ion in the periodic table. In gases a multitude of satellite lines are found in Auger spectra, but as seen in the NaCl spectra, these lines are not readily observable, partly because of poorer peak-to-background ratios in solids and partly because the satellite lines in solids may be broadened due to a multiplicity of states. However, in the case of potassium, Fahlman[7] discovered a number of years ago the presence of a very intense satellite structure. A similar structure has been seen by us in K_2HPO_4. Although there are a number of satellite lines in argon, these lines do not

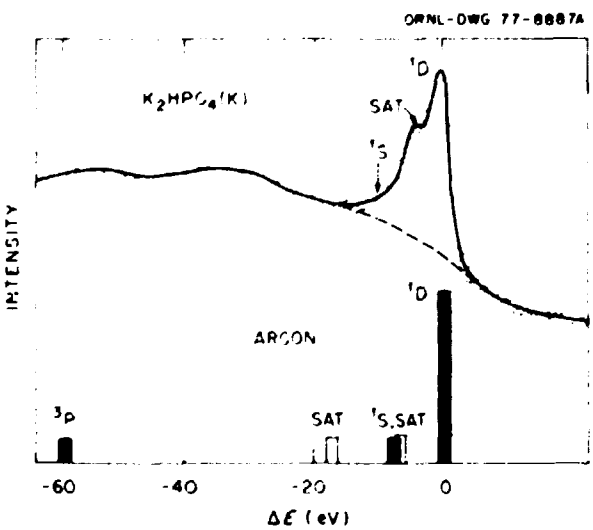

Fig. 6.8. Comparison of the Auger spectrum of potassium in K_2HPO_4 (dash curve) with the argon Auger spectrum (vertical bars).

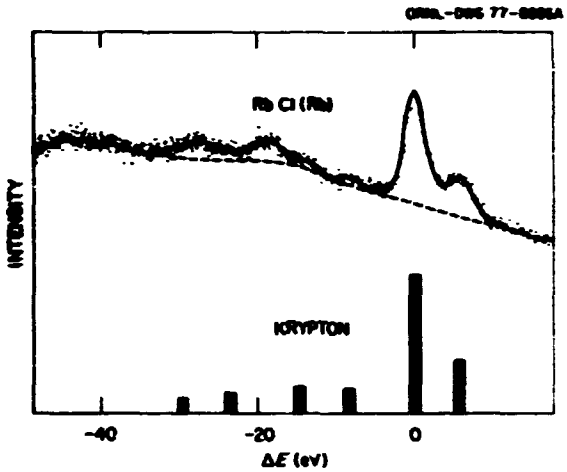

Fig. 6.9. Comparison of the Auger spectrum of rubidium in RbCl (data curve) with the krypton Auger spectrum (vertical bars).

have the intensity of those found with potassium. We extended the search to Rb ($Z = 37$), but for practical reasons looked at the *L-MM* Auger spectrum rather than the *K-LL*. The observed spectrum is similar to that seen with krypton. The *L-MM* lines have not been assigned according to diagram and satellite structure. However, unlike the potassium spectra, rubidium shows no strong structure not seen in the corresponding rare gas, krypton, and the results on potassium remain a curious aonormality.

1. La Trobe University, Bundoore, Victoria, Australia.
2. For a description of the latest version of our electron spectrometer see *Phys. Div. Annu. Prog. Rep. Dec. 31, 1975*, ORNL-5137, p. 157.
3. L. Ley et al., *Phys. Rev. B* 11, 600 (1975).
4. G. Dufour et al., *Phys. Scr.* 13, 370 (1976).
5. D. A. Shirley, *Phys. Rev. A* 7, 1520 (1973).
6. H. P. Kelley, *Phys. Rev. A* 11, 556 (1975).
7. C. D. Wagner, *Faraday Discuss. Chem. Soc.* 60, 291 (1975).
8. A. Fahlman et al., *Z. Phys.* 192, 482 (1966).

POLARIZED HeI RADIATION FOR SURFACE STUDIES

W. B. Dress F. H. Ward[1]
T. A. Carlson G. L. Nyberg[2]

A polarized-radiation source has been designed and built for use in our surface-studies program. The lamp, based on the work of Horton et al.,[3] is windowless and employs triple-differential pumping for compatibility with the ultrahigh-vacuum source chamber. The light from the discharge in helium is polarized by a triple reflection from a series of gold mirrors, producing a plane polarized beam of HeI radiation (21.22-eV) with a polarization of 80%. The plane of polarization can be rotated through more than 180° without breaking vacuum.

We have thus far used the lamp to study single crystals of copper and nickel as well as adsorbed CO and benzene thiol (a model heteromolecule encountered in coal catalysis work). In these studies, the crystal surface—usually the 110 or 111 face—was cleaned by ion bombardment, and spectra as a function of angle and polarization were taken. The clean crystal was then exposed to a few L (1 L = 1 Langmuir = 10^{-6} torr·sec) of adsorbate such as CO, and the same series of measurements were repeated. Comparison between the clean crystal and the crystal plus adsorbate, combined with a knowledge of the spectrum of the molecule in a gaseous state, allows one to determine which orbitals in the adsorbate molecule are responsible for the bonding to the crystal. Similarly, the change in the 3*d* band structure (the structure lying a few electron volts below the Fermi energy) reflects those crystal orbitals involved in the bonding; thus, a knowledge of specific bonding sites on the crystal may be inferred. These studies have a bearing on the fundamental problem of catalysis.

The information obtained by varying the polarization direction and the direction of the ejected electron with respect to the crystal normal will, when coupled with a good theory of angular emission of photoelectrons, provide information about the chemisorption bond geometry and the angular variations of the molecular orbitals involved in the bond. Figure 6.10 shows a preliminary study on a clean copper crystal. Spectra are shown as a function of angle and polarization direction. The differences between the various spectra indicate both the geometrical structure of the crystal (its Fermi surface, more precisely) and its orientation in our source chamber. The dramatic changes produced by varying the polarization direction show the increased resolution obtainable with polarized radiation (the result using unpolarized light would be a sum of the spectra with the different polarizations).

During the coming year, we plan to explore the most interesting possibilities given to us by this lamp, such as bond direction, molecular orientation, energy

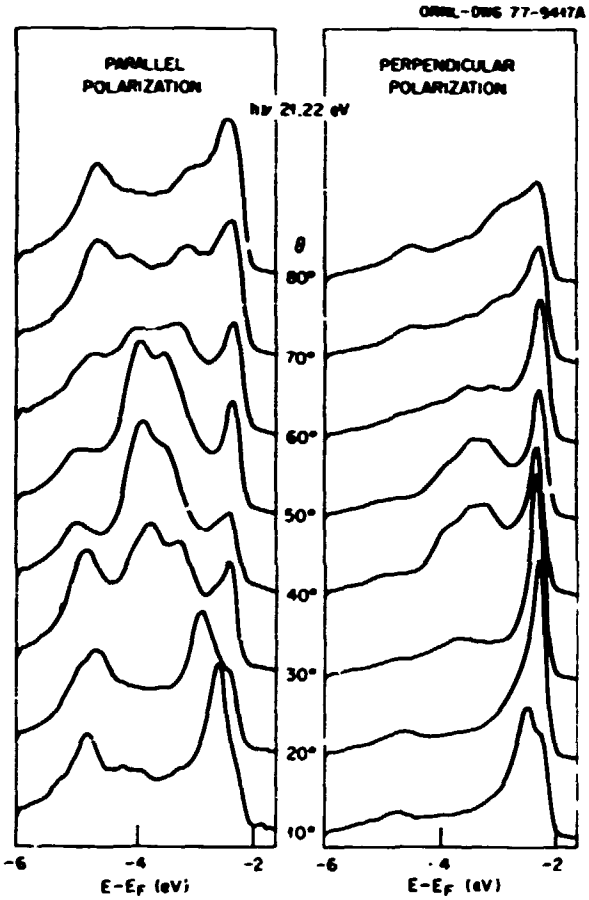

Fig. 6.10. Angular study of the 110 face of copper. The two sets of curves are taken with parallel polarization (the electric vector in the plane of incidence defined by the crystal normal and the direction of the incident radiation) and perpendicular polarization (the electric vector perpendicular to the plane of incidence). The angle θ is the polar angle between the ejected electron and the crystal normal. The angle between the photon beam and the ejected electrons was 90° for these measurements.

shifts due to adsorption, and possibly even some surface reactions.

1. Plant and Equipment Division.
2. La Trobe University, Bundoore, Victoria, Australia.
3. V. G. Horton et al., *Appl. Opt.* 8, 667 (1969).

HOLOGRAPHIC OPTIC ELEMENT RESEARCH

J. J. Cowan

This project was initiated last year with support from the Exploratory Studies Program. The objective was to study means of making blazed, aberration-corrected diffraction gratings by a new process utilizing optical guided waves. In the past several months, research has been carried out to meet this objective; in addition, other related results have been obtained, some of which are summarized below.

Holographic Gratings: Planar and Aberration-Corrected Concave Types

Experiments have been conducted to produce diffraction gratings holographically. The method consists of coating glass blanks with a positive-type photoresist, exposing with intersecting argon ion laser beams (488 nm) that have been spatially filtered and expanded, and then developing. Exposed portions of the photoresist are dissolved, leaving a sinusoidal relief pattern, and the glass blank may then be used as a transmission grating. When the blank is coated with a layer of aluminum, a reflection grating results. Plane and concave glass blanks have been utilized. Using the former, one makes an ordinary planar reflection grating; using the latter, one can make a special type of reflection concave grating that is corrected for coma and astigmatism and is more efficient than the ruled type. A concave reflection grating corrected for astigmatism was made that showed a measured efficiency almost twice that of a ruled grating for the spectral region of the argon ion laser wavelengths. Several types of photoresist have been studied to test their usefulness as holographic recording materials. These include, in addition to the positive Shipley AZ 1350B used above, Kodak KPR negative resist, Horizons Research negative Aquarist and Solvarist, and NRC photopolymer.

Blazed and High-Line Density Holographic Gratings Produced by Use of Optical Guided Waves

A method of producing asymmetric (blazed) groove profiles and high-line densities on holographic gratings by use of optical guided waves has been developed. A layer (400 nm) of photoresist ($n = 1.64$), acting as both a recording medium and a wave guide, was spin coated onto one face of an equilateral glass prism ($n = 1.5$) that had been coated with a thin (35-nm) coupling silver layer. The prism was illuminated with a collimated beam of light (488 nm) from an argon laser. Part of this beam excited a guided mode (TM_2, 463.3 nm) within the photoresist, and part was reflected internally within the prism, passing through the photoresist as an ordinary wave (297.6 nm). Interference of these waves produced, upon development, an asymmetric groove profile (blaze angle = 22.2°, period $d = 748$ nm) that had a

decided on-to-off blaze intensity ratio (almost 2:1 for this case). If two incident beams were used, each of which excited a surface mode (TM_1) but in opposite directions, a small grating period (d = 163.5 nm or 6112 lines/mm) would be achieved. With a denser prism and excitation of the plasmon (TM_0) mode, a period smaller than half the wavelength in the medium can be obtained (over 6720 lines/mm). The high energy densities realizable with guided waves permit a considerable reduction in the usual exposure times for photoresist, thus allowing the use of the shorter wavelength weak laser lines for recording.

Holographic Zone Plates

Initial experiments have been attempted to produce holographic zone plates. This is done by allowing two coherent beams of light, one of which is a plane wave and the other a spherically diverging wave, to interfere on a photoresist-coated glass plate. A zone plate was made in this fashion, using a collimated beam of light and another beam diverging from a pinhole spatial filter after having passed through a 5× microscope objective lens. The zone plate prepared this way demonstrated excellent focusing properties with visible light, and the zone structure, when examined by microscope, showed the proper concentric regularity. The next step in this development will be to process the zone plate and coat it in such a way that one has concentric metal zones on a glass substrate. When this technique is perfected, a similar structure can be prepared on a substrate transparent to x rays, such as carbon. If one uses a thin carbon film coated on a glass plate for a substrate, the carbon film can be separated and will be self-supporting. Once zone plates are prepared in this fashion, tests will be run with soft x rays, using our grazing incidence monochromator to determine their efficiencies and resolution.

USE OF GROUP THEORY IN THE INTERPRETATION OF INFRARED AND RAMAN SPECTRA

E. Silberman[1] H. W. Morgan

Application of the mathematical theory of groups to the symmetry of molecules is a powerful method which permits the prediction, classification, and qualitative description of many molecular properties. In the particular case of vibrational molecular spectroscopy, applications of group theory lead to simple methods for the prediction of the number of bands to be found in the infrared and Raman spectra, their shape and polarization, and the qualitative description of the normal modes with which they are associated. A summary has been prepared which contains the tables necessary for the application of group theory to vibrational spectroscopy and instructions on how to use them for molecular gases, liquids, and solutions. A brief introduction to the concepts, definitions, nomenclature, and formulas is also included.

1. Fisk University, Nashville, Tenn.

7. High-Energy Physics

H. O. Cohn
G. T. Condo[1]
W. M. Bugg[1]
E. L. Hart[1]
H. R. Brashear[2]
T. H. Handler[3]

INTRODUCTION

High-energy research at Oak Ridge National Laboratory (ORNL) is geared toward experiments that study the interaction and production of elementary particles in a bubble chamber. Because the maximum measurable momentum of a track in a bubble chamber is limited by the track length, magnetic field strength, and distortion, it is desirable to augment bubble-chamber measurements with external position-sensitive particle detectors. If one also wishes to obtain information on neutral particles, it is necessary to add efficient shower detectors. At ORNL, we have participated in a number of experiments to implement these goals. Such experiments have been approved to be run at Fermi National Accelerator Laboratory (FNAL), Stanford Linear Accelerator Center (SLAC), and Argonne National Laboratory (ANL).

EXPERIMENTS AT 147 GeV/c

Further results were obtained in the experiments at 147 GeV c in the FNAL hybrid spectrometer. In a study of ρ^0 inclusive production, it was found that the average number of ρ^0 per inclusive $\pi^- p$ interaction is 0.35 ± 0.06, which is almost unchanged from the value found for interactions as low as 15 GeV c.

The two-prong inelastic events were found to be 80% due to diffractive dissociation of beam or target particle in equal amounts. Four constraint-class analyses of $\pi^- p \rightarrow \pi^- p \pi^+ \pi^-$ were possible. The 3π mass spectrum displayed A_1, A_2, and A_3 peaks. Also, evidence for charged-cluster emission in 147 GeV c $\pi^- p$ collisions was found. Runs with positive incident particles (π^+ and p) were made, and for part of the data a lead-glass shower detector was tested. In this detector, a spatial resolution of about 3.5 mm for determining the position of electronic showers in the energy range of 30 to 100 GeV c is possible. These experiments involve a collaboration with about 12 institutions.

π^+-DEUTERON INTERACTION

In collaboration with Florida State University (FSU), 3114 events of the reaction $\pi^+ d \rightarrow \pi^+ \pi^- pp_s$ at 15 GeV c, where p_s is a nonparticipating spectator, were studied in the SLAC 82-in. bubble chamber. A longitudinal phase space (LPS) analysis was performed to separate the various t-channel exchange mechanisms, such as π or Pomeron exchange. The validity of the LPS method was tested for pion exchange by generating events using the one-pion-exchange model modified by absorption (OPEA). The model and the data agreed extremely well. The principal features of the data include the ρ^0, f^0, Δ^{++}, and N^{*+}s. The LPS analysis also reveals the g^0, but a slight modification of the standard LPS selection criteria enhances the g^0, as expected by OPEA model calculations.

$\pi^- p$ INTERACTIONS AT 8 GeV/c

About 150,000 events have been measured at ORNL for this experiment. Our collaborators [Massachusetts Institute of Technology (MIT) and Tahoku University] have measured equal amounts of data. The data are being readied for analysis in the form of data summary tapes.

Our principal goal from the $\pi^- p$ experiment is to examine the one-constraint channels, $\pi^- p \rightarrow$

$n\pi^+\pi^+\pi^-\pi^-$ and $\pi^- p \to np\pi^+\pi^-\pi^0$, for evidence of associated $A_2(1320)\,\Delta(1238)$ production. Because all three charge states of the A_2 are available in a single experiment, such an observation should provide an interesting check on the hypothesis of charge independence for resonance production. Because of the large size of the experiment, it is anticipated that the collaborators will also undertake projects where large statistics are mandatory. This would include, for example, a phase-shift analysis of single-pion production in the reactions $\pi^- p \to \pi^+\pi^- n$.

HYBRID 40-IN. π^+-d EXPERIMENT AT SLAC

This experiment has been approved by SLAC to be run in collaboration with Duke University and Florida State University. The unusual feature will be a very large (2.85 by 1.2 m and 65 cm thick) lead-glass shower detector.

The purpose of this experiment is to make a definitive study of $\pi^+ d$ reactions for which more than a single π^0 is produced. Aside from an analysis of the reactions such as $\pi^+ n \to p\pi^+\pi^0$, $p\pi^+\eta^0$, $p\pi^+\omega^0$, $p\eta^+\eta^0$, etc., it should also be possible to isolate the nondeuteron breakup reactions such as $\pi^+ D \to \pi^+\pi^0 D$ and $\pi^+\pi^+\pi^-\pi^0 D$, which have generally been elusive because of the large elastic and/or diffractive backgrounds and the low-constraint nature of the events. Another strong impetus for doing this experiment is the possibility of obtaining a reasonable sample of $\pi^+ D \to P_s p\pi^+\pi^+\pi^0$ events, which could prove decisive in indicating the dynamic nature of the A_1.

---

1. Consultant with ORNL from the University of Tennessee, Knoxville.
2. Instrumentation and Controls Division.
3. Guest assignee to ORNL from the University of Tennessee, Knoxville.

8. Publications

Prepared by Wilma L. Stair

The following listing of publications includes those articles by Physics Division staff members and associates *which have appeared in print from January 1976 through April 1977.* Some few articles published in 1975, not previously reported in the Division's Annual Report, are also included. Articles pending publication as of May 1, 1977, are listed immediately following this section.

BOOK, JOURNAL, AND PROCEEDINGS ARTICLES

Allen, B. J., A. R. de L. Musgrove, J. W. Boldeman, M. J. Kenny, and R. L. Macklin, "Resonance Neutron Capture in ^{56}Fe," *Nucl. Phys.* A269, 408–28 (1976).

Alton, G. D., "Preliminary Evaluation of a Modified Hortig-Geometry Negative-Ion Source Using a Negative-Ion Source Test Facility," *IEEE Trans. Nucl. Sci.* (Proceedings of the International Conference on Heavy Ion Sources, Gatlinburg, Tenn., October 1975) NS-23(2), 1113–17 (1976).

Alvarez, I., C. Cisneros, C. F. Barnett, and J. A. Ray, "Electron Capture and Stripping Cross Sections for Tl and K Ions and Atoms," *Phys. Rev. A* 13, 1728–33 (1976).

Alvarez, I., C. Cisneros, C. F. Barnett, and J. A. Ray, "Negative-Ion Formation from Dissociative Collisions of H_2^+, H_3^+, and HD_2^+ in H_2, He, and Xe," *Phys. Rev. A* 14, 602–7 (1976).

Andersen, J. U., L. Kochbach, E. Laegsgaard, M. Lund, and C. D. Moak, "Angular Dependence of Probability for Proton-Induced Cu *K*-Shell Ionization at Large Scattering Angles," *J. Phys. B* 9, 3247–62 (1976).

Andersen, J. U., F. Laegsgaard, M. Lund, and C. D. Moak, "Z_1 Scaling for Impact-Parameter Dependence of Inner-Shell Ionization by Heavy Ions," *Nucl. Instrum. Methods* (Proceedings of the Sixth International Conference on Atomic Collisions in Solids, Amsterdam, Netherlands, September 1975) 132, 507–16 (1976).

Appleton, B. R., J. A. Biggerstaff, T. S. Noggle, R. M. Ritchie, S. Datz, C. D. Moak, and H. Verbeek, "Radiative Electron Capture by Highly Stripped Ions in Single Crystal Channels," *Nucl. Instrum. Methods* (Proceedings of the Sixth International Conference on Atomic Collisions in Solids, Amsterdam, Netherlands, September 1975) 132, 521–22 (1976).

Auble, R. L., "Nuclear Data Sheets for $A = 69$," *Nucl. Data Sheets* 17, 193–224 (February 1976).

Auble, R. L., "Nuclear Data Sheets for $A = 50$," *Nucl. Data Sheets* 19, 291–336 (November 1976).

Auble, R. L., "Nuclear Data Sheets for $A = 57$," *Nucl. Data Sheets* 20, 327–71 (March 1977).

Auble, R. L., "Nuclear Data Sheets for $A = 56$," *Nucl. Data Sheets* 20, 253–326 (March 1977).

Auble, R. L., H. R. Hiddleston, and C. P. Browne, "Nuclear Data Sheets for $A = 131$," *Nucl. Data Sheets* 17, 573–615 (April 1976).

Auble, R. L., R. R. Todd, L. E. Samuelson, W. H. Kelly, and W. C. McHarris, "Nuclear Data Sheets for $A = 102$," *Nucl. Data Sheets* 19, 1–32 (September 1976).

Bagieu, G., A. J. Cole, R. de Swiniarski, C. B. Fulmer, D. H. Koang, and G. Mariolopoulos, "Optical Model Analysis of 41-MeV Alpha Particles Scattering from ^{28,29,30}Si and ^{27}Al and Nuclear Matter Distribution," pp. 83–84 in *Proceedings, Radial Shape of Nuclei Conference, Cracow, Poland, June 1976*, ed. M. Guenin, European Physical Society, 1976.

Bapu, P., R. Endorf, B. Meadows, M. M. Nussbaum, H. O. Cohn, W. M. Bugg, G. T. Condo, and E. L. Hart, "Photoproduction of ρ^0 and ρ^- Mesons at 3 GeV," *Phys. Rev. D* 15, 26–35 (1977).

Burdin, T. T., J. G. Pronko, R. E. McDonald, A. R. Pietti, and J. B. McGrory, "Gamma-Ray Spectroscopy of Low-Lying States in ^{56}Cr," *Phys. Rev. C* 14, 1782–88 (1976).

Burnett, C. F. (invited paper), "Atomic Physics in the Controlled Thermonuclear Research Program," p. 846 in *Physics of Electronic and Atomic Collisions* (Proceedings of the International Collision Conference, Seattle, Wash., July 1975), ed. J. S. Risley and R. Geballe, University of Washington Press, 1976.

Burnett, C. F. (invited paper), "Role of Impurities in Magnetically Confined High Temperature Plasmas," pp. 375–90 in *Atomic Physics 5* (Proceedings of the Fifth International Conference on Atomic Physics, Berkeley, Calif., July 1976), ed. R. Marrus, M. Prior, and H. Shugart, Plenum, New York, 1977.

Bayfield, J. E., P. M. Koch, L. D. Gardner, I. A. Sellin, D. J. Pegg, R. S. Peterson, and D. J. Crandall, "An Experimental Survey of Electron Transfer in keV Collisions in Multiply Charged Ions with Atomic Hydrogen," p. 126 in *Atomic Physics 5* (Proceedings of the Fifth International Conference on Atomic Physics, Berkeley, Calif., July 1976), ed. R. Marrus, M. Prior, and H. Shugart, Plenum, New York, 1977.

Bemis, C. E., Jr., R. L. Ferguson, F. Plasil, R. J. Silva, Frances Pleasonton, and R. L. Hahn, "Fragment-Mass and Kinetic-Energy Distributions from the Spontaneous Fission of ^{252}No," *Phys. Rev. C* 15, 705–12 (1977).

Bendjaballah, N., J. Dalmunay, T. Nomura, and H. J. Kim, "Possible Shape Transition in the Yrast Band of ^{56}Fe," *Phys. Rev. Lett.* 36, 1536–39 (1976).

Berlanger, M., F. Hanappe, C. Ngo, J. Peter, F. Plasil, and B. Tamain, "Deep Inelastic Collisions between 280-MeV ^{63}Cu Ions and ^{93}Nb Nuclei," *Nucl. Phys.* A276, 347–53 (1977).

Bertrand, F. E., "Excitation of Giant Multipole Resonances through Inelastic Scattering," *Annu. Rev. Nucl. Sci.* 26, 457 (1976).

Bertrand, F. E., "Excitation of Giant Resonances via Inelastic Hadron Scattering," vol. I of *Proceedings, Symposium on Highly Excited States in Nuclei Jülich, West Germany, September 1975*, ed. A. Faessler, C. Mayer-Boricke, and P. Turek, KFA report, 1975.

Bertrand, F. E., and R. L. Auble, "Nuclear Data Sheets for $A = 76$," *Nucl. Data Sheets* 19, 507–55 (December 1976).

Bertrand, F. E., and D. C. Kocher, "Excitation of Giant Resonances in ^{208}Pb and ^{197}Au via Proton Inelastic Scattering," *Phys. Rev. C* 13, 2241–46 (1976).

Bingham, C. R., L. L. Riedinger, F. E. Turner, B. D. Kern, J. L. Weil, K. J. Hofstetter, J. Lin, E. F. Zganjar, A. V. Ramayya, J. H. Hamilton, J. L. Wood, G. M. Gowdy, R. W. Fink, E. H. Spejewski, W. D. Schmidt-Ott, R. L. Mlekodaj, H. K. Carter, and K. S. R. Sastry, "Decay of Mass-Separated ^{192}Tl and ^{190}Hg," *Phys. Rev. C* 14, 1586–1600 (1976).

Boldeman, J. W., B. J. Allen, A. R. de L. Musgrove, and R. L. Macklin, "keV Neutron Capture in ^{91}Zr," Australian Atomic Energy Commission Research Establishment Report, AAEC/E367 (1976).

Boldeman, J. W., B. J. Allen, A. R. de L. Musgrove, and R. L. Macklin, "Valence Neutron Capture in ^{88}Sr," *Nucl. Phys.* A269, 397–407 (1976).

Boldeman, J. W., A. R. de L. Musgrove, B. J. Allen, J. A. Harvey, and R. L. Macklin, "The Neutron Total and Capture Cross Sections of ^{92,96}Zr," *Nucl. Phys.* A269, 31–45 (1976).

Bondorf, J. P., H. T. Feldmeier, S. Garpman, and E. C. Halbert, "Classical Microscopic Description of U + U Collisions," *Phys. Lett.* 65B, 217–20 (1976).

Bondorf, J. P., P. J. Siemens, H. Feldmeier, S. Garpman, and E. C. Halbert, "Classical Microscopic Description of Fast Heavy-Ion Collisions," pp. 483–90 in vol. II of *Proceedings, Symposium on Macroscopic Features of Heavy-Ion Collisions, Argonne, Illinois, April 1976*, Contributed Papers, ANL/PHY-76-2, 1976.

Bondorf, J. P., P. J. Siemens, S. Garpman, and E. C. Halbert, "Classical Microscopic Calculation of Fast Heavy-Ion Collisions," *Z. Phys.* A279, 385–94 (1976).

Brady, F. P., N. S. P. King, M. W. McNaughton, and G. R. Satchler, "Excitation of Analogs of Giant Dipole States via ^{27}Al(n,p)^{27}Mg," *Phys. Rev. Lett.* 36, 15-17 (1976).

Bridwell, L. B., J. A. Biggerstaff, G. D. Alton, C. M. Jones, P. D. Miller, Q. Kessel, and B. W. Wehring, "Multiple Electron Loss Cross Sections for 60-MeV I^{+10} in Single Collisions with Xenon," pp. 657-64 in vol. II of *Beam Foil Spectroscopy* (Proceedings of the Conference, Gatlinburg, Tenn., September 1975), ed. I. A. Sellin and D. J. Pegg, Plenum, New York, 1976.

Britt, H. C., B. H. Erkkila, P. D. Goldstone, R. H. Stokes, F. Plasil, R. L. Ferguson, and H. H. Gutbrod, "Evaporation Residue Cross Sections from ^{86}Kr Bombardment of ^{63}Cu, ^{90}Zr, and ^{107}Ag," pp. 491-98 in vol. II of *Proceedings, Symposium on Macroscopic Features of Heavy-Ion Collisions, Argonne, Illinois, April 1976*, ANL PHY-76-2, 1976.

Britt, H. C., B. H. Erkkila, R. H. Stokes, H. H. Gutbrod, F. Plasil, R. L. Ferguson, and M. Blann, "Argon- and Krypton-Induced Reactions at Energies of 4-7 MeV amu," *Phys. Rev. C* 13, 1483-95 (1976).

Brown, B. A., A. Arima, and J. B. McGrory, "*E2* Core-Polarization Charge for Nuclei Near ^{16}O and ^{40}Ca," *Nucl. Phys.* A277, 77-108 (1977).

Butler, H. M., C. B. Fulmer, and K. M. Wallace, "Neutron Shielding of Cyclotron Targets," *Health Phys.* 31, 62-66 (1976).

Carlson, G. H., W. L. Talbert, Jr., and S. Raman, "Nuclear Data Sheets for $A = 118$," *Nucl. Data Sheets* 17, 1-37 (January 1976).

Carlson, T. A., "Satellite Structure in the Photoelectron Spectra of Transition Metal Compounds Ionized in the K Shell of the Metal Ion," *Faraday Discuss. Chem. Soc.* (Proceedings of the Faraday Society Discussion on Electron Spectroscopy of Solids and Surfaces, Vancouver, B.C., July 1975) 60, 30-36 (1975).

Carlson, T. A. (invited paper), "Multiple Excitation in Free Molecules," pp. 343-53 in *Photoionization and Other Probes of Many-Electron Interactions* (Proceedings of the NATO Advanced Study Institute, Carry-Le-Rouet, France, August-September 1975), ed. F. J. Wuilleumier, Plenum, New York, 1976.

Carlson, T. A., book review of *Photoelectron Spectroscopy* (J. H. D. Eland, 239 pp., Halsted, 1974), *Am. Sci.* 63, 460 (1975).

Carlson, T. A., book review of *Methods of Surface Analysis* (ed. A. W. Czanderna, 481 pp., Elsevier, Amsterdam, Netherlands, 1975), *Anal. Chem.* 48, 859A (1976).

Carlson, T. A., W. B. Dress, F. A. Grimm, and J. S. Haggerty, "Study of Satellite Structure Found in the Photoelectron Spectra of Gaseous Alkenes," *J. Electron Spectrosc.* 10, 147-54 (1977).

Carlton, R. F., S. Raman, J. A. Harvey, and G. G. Slaughter, "Neutron Transmission and Capture Gamma-Ray Measurements of ^{120}Sn + n," *Phys. Rev. C* 14, 1439-50 (1976).

Carlton, R. F., S. Raman, and G. G. Slaughter, "Neutron Capture Gamma-Ray Studies of Levels in ^{121}Sn and ^{123}Sn," *Phys. Rev. C* 15, 883-93 (1977).

Carter, H. K., E. H. Spejewski, R. L. Mlekodaj, A. G. Schmidt, F. T. Avignone, C. R. Bingham, R. A. Braga, J. D. Cole, A. V. Ramayya, E. L. Robinson, K. S. R. Sastry, and E. F. Zganjar, "The UNISOR ISOL Data Acquisition System," *Nucl. Instrum. Methods* 139, 349-53 (1976).

Chrien, R. E., G. W. Cole, G. G. Slaughter, and J. A. Harvey, "Failure of Bohr's Compound Nucleus Hypothesis for the ^{97}Mo(n,α)^{94}Mo Reaction," *Phys. Rev. C* 13, 578-84 (1976).

Cisneros, Carmen, I. Alvarez, C. F. Barnett, and J. A. Ray, "Differential Scattering and Total Cross Sections of Hydrogen and Deuterium Atoms in Nitrogen," *Phys. Rev. A* 14, 84-87 (1976).

Cisneros, Carmen I. Alvarez, C. F. Barnett, and J. A. Ray, "Angular Distributions and Total Cross Sections for D$^-$ Formation from Interaction of D$^+$ and D^0 with Cesium," *Phys. Rev. A* 14, 76-83 (1976).

Cisneros, Carmen, I. Alvarez, C. F. Barnett, J. A. Ray, and A. Russek, "Angular Distributions and Total Cross Sections for D$^-$ Formation from Interaction of D$^+$ with Cesium," *Phys. Rev. A* 14, 88-99 (1976).

Cole, J. D., J. H. Hamilton, A. V. Ramayya, W. G. Nettles, H. Kawakami, E. H. Spejewski, M. A. Ijaz, K. S. Toth, E. L. Robinson, K. S. R. Sastry, J. Lin, F. T. Avignone, W. H. Brantley, and P. V. G. Rao, "Behavior of the Excited Deformed Band and Search for Shape Isomerism in ^{194}Hg," *Phys. Rev. Lett.* 37, 1185 97 (1976).

Condo, G. T., W. M. Bugg, E. L. Hart, H. O. Cohn, and R. D. McCulloch, "Nuclear Absorption of Slow Antiprotons," pp. 11 16 in vol. II, chap. VI, *Proceedings, Fourth International Symposium on Nuclear-Antinuclear Interaction, Syracuse, New York, May 1975*, 1975.

Crandall, D. H., "Charge Exchange of Multi-Charged Ions of C, N, and O in H$_2$," pp. 190 91 in *Electronic and Atomic Collisions* (Proceedings of the Nineteenth International Conference, Seattle, Wash., July 1975), ed. J. S. Risley and R. Geballe, University of Washington Press, Seattle, 1975.

Crandall, D. H., M. L. Mallory, and D. C. Kocher, "Charge Exchange between Multi-Charged Ions of C, N, and O and Molecular Hydrogen," *Phys. Rev. A* 15, 61 69 (1977).

Crandall, D. H., R. E. Olson, E. J. Shipsey, and J. C. Browne, "Single and Double Charge Transfer in C^{+4}-He Collisions," *Phys. Rev. Lett.* 36, 858 60 (1976

Crandall, D. H., J. A. Ray, and Carmen Cisneros, "Channeltron Efficiency for Counting of H$^-$ and H at Low Energy," *Rev. Sci. Instrum.* 46, 562 64 (1975).

Cusson, R. Y., R. Hilko, and D. Kolb, "Realistic Heavy-Ion Adiabatic Potentials," *Nucl. Phys.* A270, 437 70 (1976).

Cusson, R. Y., and J. Maruhn, "Dynamics of ^{12}C + ^{12}C in a Realistic T.D.H.F. Model," *Phys. Lett.* 62B, 134 38 (1976).

Cusson, R. Y., R. K. Smith, and J. A. Maruhn, "Time-Dependent Hartree-Fock Calculation of the ^{16}O + ^{16}O Reaction in Three Dimensions," *Phys. Rev. Lett.* 36, 1166 69 (1976).

Cusson, R. Y., H. P. Trivedi, H. W. Meldner, M. S. Weiss, and R. E. Wright, "Self-Consistent K-Matrix-Model Calculation for Finite and Superheavy Nuclei," *Phys. Rev. C* 14, 1615 29 (1976).

Davies, K. T. R., S. E. Koonin, J. R. Nix, and A. J. Sierk, "Macroscopic and Microscopic Approaches to Nuclear Dissipation," p. 8 in *Proceedings, International Workshop III on Gross Properties of Nuclei and Nuclear Excitations, Hirschegg, Austria, January 1975*, Technische Hochschule Darmstadt Report No. AED CONF-75 009 000, 1975.

Davies, K. T. R., and J. R. Nix, "Calculation of Moments, Potentials, and Energies for an Arbitrarily Shaped Diffuse-Surface Nuclear Density Distribution," *Phys. Rev. C* 14, 1977 94 (1976).

Davies, K. T. R., A. J. Sierk, and J. R. Nix, "Effect of Viscosity on the Dynamics of Fission," *Phys. Rev. C* 13, 2385 2403 (1976).

Dayras, R. A., R. G. Stokstad, Z. E. Switkowski, and R. M. Wieland, "Gamma-Ray Yields from ^{12}C + ^{12}C Reactions near and below the Coulomb Barrier," *Nucl. Phys.* A265, 153 88 (1976).

deLange, J. C., R. Kamermans, R. D. Vis, A. van Poelgeest, H. Verheul, and W. B. Ewbank, "The Level Structure of ^{97}Tc," *Nucl. Phys.* A258, 141 51 (1976).

deLima, A. P., J. H. Hamilton, A. V. Ramayya, B. van Nooijen, R. M. Ronningen, H. Kawakami, R. B. Piercey, R. L. Robinson, H. J. Kim, W. K. Tuttle, and L. K. Peker, "Anomalous Behavior of Yrast States in ^{68}Ge," p. 84 in *Proceedings, European Conference on Nuclear Physics with Heavy Ions, Caen, France, September 1976*, ed. B. Fernandez et al., European Physical Society, 1976.

deLima, A. P., B. van Nooijen, R. M. Ronningen, H. Kawakami, J. H. Hamilton, A. V. Ramayya, R. B. Piercey, R. L. Robinson, H. J. Kim, and W. K. Tuttle, "High Spin States and Possible Band Crossings in ^{68}Ge," *Proceedings, International Conference on Selected Topics in Nuclear Structure, Dubna, U.S.S.R., June 1976*, Joint Institute for Nuclear Research, 1976.

de Swiniarski, R., G. Bagieu, M. Bedjidiam, C. B. Fulmer, J. Y. Grossiord, M. Massaad, J. R. Pizzi, and M. Gusakow, "Inelastic Scattering of 30-MeV Polarized Protons from ^{90,91}Zr and ^{92}Mo," pp. 35 36 in *Proceedings, Fourth International Symposium on Polarization Phenomena in Nuclear Reactions, Zurich, Switzerland, August 1975*, ed. W. Grüebler and V. Konig, Birkhauser Verlag, Basel, 1976.

de Swiniarski, R., G. Bagieu, M. Massaad, Dinh-Lien Pham, M. Bedjidian, J. Y. Grossiord, M. Gusakow, J. R. Pizzi, and C. B. Fulmer, "Macroscopic and Microscopic Model Analysis of Inelastic Scattering of 30-MeV Polarized Protons from ^{96,98}Zr and ^{92}Mo," *Phys. Lett.* **61B**, 37-40 (1976).

Dress, W. B., Jr., "Observation of Two Photons in n-p Capture," pp. 203-10 in *High-Energy Physics and Nuclear Structure* (Proceedings of the Conference, Santa Fe, N.M., June 1975), ed. D. E. Nagle, A. S. Goldhaber, C. K. Hargrave, R. L. Burman, and B. G. Storms, AIP Conf. Proc. No. 26, AIP, New York, 1975.

Dress, W. B., P. D. Miller, J. M. Pendlebury, P. Perrin, and N. F. Ramsey, "Search for an Electric Dipole Moment of the Neutron," *Phys. Rev. D* **15**, 9-21 (1977).

Ellis, Y. A., "Nuclear Data Sheets for A = 216," *Nucl. Data Sheets* **17**, 329-39 (March 1976).

Ellis, Y. A., "Nuclear Data Sheets for A = 220," *Nucl. Data Sheets* **17**, 341-50 (March 1976).

Ellis, Y. A., "Nuclear Data Sheets for A = 224," *Nucl. Data Sheets* **17**, 331-66 (March 1976).

Ellis, Y. A., "Nuclear Data Sheets for A = 243," *Nucl. Data Sheets* **19**, 103-41 (September 1976).

Ellis, Y. A., "Nuclear Data Sheets for A = 245," *Nucl. Data Sheets* **19**, 143-79 (September 1976).

Ellis, Y. A., "Nuclear Data Sheets for A = 247," *Nucl. Data Sheets* **19**, 181-202 (September 1976).

Ellis, Y. A., "Nuclear Data Sheets for A = 230," *Nucl. Data Sheets* **20**, 139-63 (February 1977).

Ewbank, W. B., R. L. Haese, F. W. Hurley, and M. R. McGinnis, "Recent References (December 16, 1975, through April 15, 1976)," *Nucl. Data Sheets* **19**, 203-90 (October 1976).

Ewbank, W. B., R. L. Haese, F. W. Hurley, and M. R. McGinnis, "Recent References (April 16-August 15, 1976)," *Nucl. Data Sheets* **20**, 1-72 (January 1977).

Ewbank, W. B., R. L. Haese, F. W. Hurley, and M. R. McGinnis, "Recent References (August 16-December 15, 1975)," *Nucl. Data Sheets* **18**, 1-85 (May 1976).

Ewbank, W. B., R. L. Haese, F. W. Hurley, and M. R. McGinnis, "Recent References (August 16-December 15, 1976)," *Nuclear Data Sheets* **20**, 429-549 (April 1977).

Fong, D., M. Heller, A. Shapiro, M. Widgoff, F. Bruyant, D. Bogert, M. Johnson, R. Burnstein, C. Fu, D. Petersen, M. Robertson, H. Rubin, R. Sard, A. Snyder, J. Tortora, D. Alyea, C-Y. Chien, P. Lucas, A. Pevsner, R. Zdanis, J. Brau, J. Grunhaus, E. S. Hafen, R. I. Hulsizer, U. Karshon, V. Kistiakowsky, A. Levy, A. Napier, I. A. Pless, P. C. Trepagnier, J. Wolfson, R. K. Yamamoto, H. Cohn, T. C. Ou, R. Plano, T. Watts, E. Brucker, E. Koller, P. Stamer, S. Taylor, W. Bugg, G. Condo, T. Handler, E. Hart, H. Kraybill, D. Ljung, T. Ludlam, and H. D. Taft, "Evidence for Charged Cluster Emission in 147-GeV c π p Collisions," *Phys. Lett.* **61B**, 99-102 (1976).

Fong, D., M. Heller, A. Shapiro, M. Widgoff, F. Bruyant, D. Bogert, M. Johnson, R. Burnstein, C. Fu, D. Petersen, M. Robertson, H. Rubin, R. Sard, A. Snyder, J. Tortora, D. Alyea, C-Y Chien, P. Lucas, A. Pevsner, R. Zdanis, J. Brau, J. Grunhaus, E. Hafen, R. Hulsizer, U. Karshon, V. Kistiakowsky, A. Levy, A. Napier, I. Pless, P. Trapagnier, R. Yamamoto, H. Cohn, T. C. Ou, R. Plano, T. Watts, E. Brucker, E. Koller, P. Stamer, S. Taylor, W. Bugg, G. Condo, T. Handler, E. Hart, H. Kraybill, D. Ljung, T. Ludlam, and H. Taft, "Inelastic Two-Prong Events in 147-GeV c π p Collisions," *Nucl. Phys.* **B104**, 32-51 (1976).

Fong, D., M. Heller, A. M. Shapiro, M. Widgoff, F. Bruyant, D. Bogert, M. Johnson, R. Burnstein, C. Fu, D. Petersen, M. Robertson, H. Rubin, R. Sard, A. Snyder, J. Tortora, E. D. Alyea, Jr., C. Y. Chien, P. Lucas, A. Pevsner, R. Zdanis, J. E. Brau, J. Grunhaus, E. S. Hafen, R. I. Hulsizer, U. Karshon, V. Kistiakowsky, A. Levy, P. C. Trepagnier, J. Wolfson, R. K. Yamamoto, H. O. Cohn, T. C. Ou, R. J. Plano, T. L. Watts, B. Brucker, E. Koller, P. Stamer, S. Taylor, W. M. Bugg, G. Condo, T. Handler, E. Hart, H. Kraybill, D. Ljung, T. Ludlam, and H. D. Taft, "Average Charged Multiplicity in $\pi^- + p \rightarrow \pi_{ch} + X$ at 147-GeV/c and Comparison with Other Reactions," *Phys. Rev. Lett.* **37**, 736-39 (1976).

Forester, J. P., R. S. Peterson, P. M. Griffin, D. J. Pegg, H. H. Haselton, K. H. Liao, I. A. Sellin, J. R. Mowat, and R. S. Thoe, "Autoionizing States in Highly Ionized Oxygen, Fluorine, and Silicon," pp. 451-59 in vol. I of *Beam Foil Spectroscopy* (Proceedings of the Conference, Gatlinburg, Tenn., September 1975), ed. I. A. Sellin and D. J. Pegg, Plenum, New York, 1976.

Fowler, J. L., "Neutrons and Energy," p. 611 in *Proceedings, International Conference on the Interaction of Neutrons with Nuclei, Lowell, Massachusetts, July 1976*, ed. Eric Sheldon et al., CONF-760715-P1, 1976.

Fowler, J. L., and W. W. Havens, Jr., "Nuclear Cross Sections for Nuclear Energy," *Phys. Today*, pp. 42–50, August 1976.

Friedland, E., M. Goldschmidt, C. A. Widener, J. L. C. Ford, Jr., and S. T. Thornton, "Spectroscopic Investigation of the ^{144}Sm(^{3}He,α)^{143}Sm Reaction," *Nucl. Phys.* A256, 93 (1976).

Fulmer, C. B., D. C. Hensley, J. C. Hafele, C. C. Foster, N. M. O'Fallon, W. Eidson, and S. A. Gronemeyer, "Back Angle ^{3}He and Alpha-Particle Elastic Scattering from ^{27}Al," *Phys. Rev. C* 13, 937–43 (1976).

Gizon, J., A. Gizon, and D. J. Horen, "Possible Coexistence of Prolate and Oblate Shapes in ^{132}Ba," p. 48 in vol. I of *Proceedings, International Symposium on Highly Excited States in Nuclei, Jülich, West Germany, September 1975*, ed. A. Faessler, C. Meyer-Boricke, and P. Turek, JUL-CONF 16, 1975.

Gomez del Campo, J., M. E. Ortiz, A. Dacal, J. L. C. Ford, Jr., R. L. Robinson, P. H. Stelson, and S. T. Thornton, "Study of the Coherence Widths Γ in ^{28}Si Measured by the ^{12}C(^{18}O,α) Reaction," *Nucl. Phys.* A262, 125–36 (1976).

Goodman, C. D., W. R. Wharton, and D. C. Hensley, "The Reaction ^{14}C(^{7}Li,^{7}He)^{14}N and the Distribution of Gamow-Teller Strength," *Phys. Lett.* 64B, 417–20 (1976).

Gowdy, G. M., A. C. Zenoulis, J. L. Wood, K. R. Baker, R. W. Fink, J. L. Weil, B. D. Kern, H. J. Hofstetter, E. H. Spejewski, R. L. Mlekodaj, H. K. Carter, W. D. Schmidt-Ott, J. Lin, C. R. Bingham, L. L. Riedinger, E. F. Zganjar, K. S. R. Sastry, A. V. Ramayya, and J. H. Hamilton, "On-Line Mass Separator Investigation of New Isotope 2.9-sec ^{116}I," *Phys. Rev. C* 13, 1601–08 (1976).

Griffin, J. J., and C. Y. Wong, "Vibrational Instability: A Possible Test of Nuclear Hydrodynamics," pp. 366–80 in *Proceedings, Fourteenth International Winter Meeting on Nuclear Physics, Bormio, Italy, January 1976*, Institute of Nuclear Physics, Milan, Italy, 1976.

Griffin, P. M., D. J. Pegg, I. A. Sellin, K. W. Jones, D. Pisano, T. H. Kruse, and S. Bashkin, "Extreme Ultraviolet Spectra of Highly Stripped Si Ions," pp. 321–29 in vol. 1 of *Beam Foil Spectroscopy* (Proceedings of the Conference, Gatlinburg, Tenn., September 1975), ed. I. A. Sellin and D. J. Pegg, Plenum, New York, 1976.

Gross, E. E., "Calibration of an Analyzing Magnet Using an Alpha Source and Heavy-Ion Beams," *Nucl. Instrum. Methods* 135, 401–02 (1976).

Gustafson, D. E., J. Gomez del Campo, R. L. Robinson, P. H. Stelson, P. D. Miller, and J. K. Bair, "High-Spin States of ^{28}Mg Populated in the ^{12}C(^{18}O,α) Reaction," *Nucl. Phys.* A262, 96–112 (1976).

Gustafson, D. E., S. T. Thornton, T. C. Schweizer, J. L. C. Ford, Jr., P. D. Miller, R. L. Robinson, and P. H. Stelson, "High-Spin States of the $K^{\pi} = \frac{1}{2}^{-}$ and $\frac{1}{2}^{+}$ Bands of ^{23}Na," *Phys. Rev. C* 13, 691–98 (1976).

Halbert, M. L., R. G. Stokstad, F. Plasil, F. E. Obenshain, D. C. Hensley, A. H. Snell, R. L. Ferguson, and F. Pleasonton, "Strongly Damped Collisions of 164- and 173-MeV ^{20}Ne on Ni," pp. 601–08 in vol. II of *Proceedings, Symposium on Macroscopic Features of Heavy-Ion Collisions, Argonne, Illinois, April 1976*, ANL, PHY-76-2, 1976.

Halbert, M. L., P. O. Tjøm, I. Espe, G. B. Hagemann, B. Herskind, M. Neiman, and H. Oeschler, "High-Spin States in ^{74}Se," *Nucl. Phys.* A259, 496–512 (1976).

Hamilton, J. H., K. R. Baker, C. R. Bingham, E. L. Bosworth, H. K. Carter, J. D. Cole, R. W. Fink, G. Garcia Bermudez, G. M. Gowdy, K. J. Hofstetter, M. A. Ijaz, A. C. Kahler, B. D. Kern, W. Lourens, B. Martin, R. L. Mlekodaj, A. V. Ramayya, L. L. Riedinger, W. D. Schmidt-Ott, E. H. Spejewski, B. N. Subba Rao, E. L. Robinson, K. S. Toth, F. Turner, J. L. Weil, J. L. Wood, A. Xenoulis, and E. F. Zganjar, "New Isotope ^{193}Pb and the Structure of ^{191}Tl; Shape Coexistence in ^{185}Hg and in ^{187}Au; and a New Ion Source: Recent UNISOR Research," *Izv. Akad. Nauk SSSR, Ser. Fiz.* 40, 2–21 (1976).

Hamilton, J. H., H. L. Crowell, R. L. Robinson, A. V. Ramayya, W. E. Collins, R. M. Ronningen, V. Maruhn-Rezwani, J. Maruhn, N. C. Singhal, H. J. Kim, R. O. Sayer, T. Magee, and L. C. Whitlock, "Lifetime Measurements to Test the Coexistence of Spherical and Deformed Shapes in ^{72}Se," *Phys. Rev. Lett.* 36, 340–42 (1976).

Harakeh, M. N., K. van der Borg, T. Ishimatsu, H. P. Morsch, A. van der Woude, and F. E. Bertrand, "Direct Evidence for a New Giant Resonance at 80 $A^{-1/3}$ MeV in the Lead Region," *Phys. Rev. Lett.* **38**, 676–79 (1977).

Harmatz, B., "Nuclear Data Sheets for A = 167," *Nucl. Data Sheets* **17**, 143–92 (January 1976).

Harmatz, B., "Nuclear Data Sheets for A = 151," *Nucl. Data Sheets* **19**, 33–102 (September 1976).

Harmatz, B., "Nuclear Data Sheets for A = 197," *Nucl. Data Sheets* **20**, 73–117 (February 1977).

Harmatz, B., and J. R. Shepard, "Nuclear Data Sheets for A = 148," *Nucl. Data Sheets* **20**, 373–427 (March 1977).

Harvey, J. A., "Neutron Resonances: Neutron Reaction Mechanisms and Nuclear Structure," pp. 143–67 in *Proceedings, International Conference on the Interaction of Neutrons with Nuclei, Lowell, Massachusetts, July 1976*, ed. Eric Sheldon et al., CONF-760715-P1, 1976.

Hillis, D. L., E. E. Gross, D. C. Hensley, L. D. Rickertsen, C. R. Bingham, A. Scott, and F. T. Baker, "Multi-Step Processes in the Inelastic Scattering of 70.4-MeV ^{12}C from ^{144}Nd," *Phys. Rev. Lett.* **36**, 304–6 (1976).

Horen, D. J., "Nuclear Data Sheets for A = 228," *Nucl. Data Sheets* **17**, 367–90 (1976).

Horen, D. J., "Status of Decay Schemes," Environmental Protection Agency Report 670/4-75-006, U.S. Government Printing Office, Washington, D.C., pp. 4–6, June 1975.

Horen, D. J., and B. Harmatz, "Nuclear Data Sheets for A = 176," *Nucl. Data Sheets* **19**, 383–444 (November 1976).

Horen, D. J., J. A. Harvey, and N. W. Hill, "Angular Momentum Determination of Resonances in ^{24}Mg + n by Elastic Neutron Scattering," *Phys. Rev. C* **15**, 1168–70 (1977).

Howard, F. T., "Cyclotrons 1975," pp. 640–43 in *Proceedings, Seventh International Conference on Cyclotrons and Their Applications, Zurich, Switzerland, August 1975*, ed. W. Joho, Birkhauser Verlag, Basel, 1975.

Hudson, E. D., R. S. Lord, L. L. Riedinger, J. A. Martin, J. K. Bair, L. N. Howell, F. Irwin, J. W. Johnson, G. S. McNeilly, and S. W. Mosko, "Magnet Model Studies for Separated-Sector Heavy-Ion Cyclotrons," pp. 197–200 in *Proceedings, Seventh International Conference on Cyclotrons and Their Applications, Zurich, Switzerland, August 1975*, ed. W. Joho, Birkhauser Verlag, Basel, 1975.

Hudson, E. D., M. L. Mallory, and R. S. Lord, "Production of Positive Ion Beams from Solids," *IEEE Trans. Nucl. Sci.* (Proceedings of the International Conference on Heavy-Ion Sources, Gatlinburg, Tenn., October 1975), NS-23(2), 1065–68 (1976).

Hudson, E. D., J. A. Martin, M. L. Mallory, F. E. McDaniel, and F. Irwin, "Magnetic Field Trimming Studies for a Separated-Sector Cyclotron," pp. 201–4 in *Proceedings, Seventh International Conference on Cyclotrons and Their Applications, Zurich, Switzerland, August 1975*, ed. W. Joho, Birkhauser Verlag, Basel, 1975.

Hudson, E. D., G. A. Palmer, C. L. Haley, and M. L. Mallory, "Cyclotron Heavy-Ion Beam Intensity Enhancement by Using an Easily Ionized Support Gas in the Ion Source," *Nucl. Instrum. Methods* (letter) **141**, 381–82 (1977).

Huray, P. G., T. J. Kirthlink, F. E. Obenshain, J. O. Thomson, and Cheng May Tung, "^{197}Au Isomer Shift Studies of Charge Density Perturbations in Au-Based Alloys," *Phys. Rev. B* **14**, 4776–81 (1976).

Hutchinson, D. P., and K. L. Vander Sluis, "Injection Tuning of a Pulsed TEA CO$_2$ Laser," *Appl. Opt.* **16**, 293–94 (1977).

Ijaz, M. A., J. Lin, E. L. Robinson, and K. S. Toth, "Alpha Decay of ^{177}Tl," *Phys. Rev. C* **14**, 264–66 (1976).

Johnson, C. H., "A Ring Lens for Producing Uniform Density Ion Beams," pp. 38–41 in *Experimental Methods for Charged-Particle Irradiations* (Proceedings of the Symposium, Gatlinburg, Tenn., September 1975), ed. David Kramer, ERDA CONF-750947, 1975.

Johnson, C. H., J. K. Bair, and C. M. Jones, "Thresholds for ^{116}Sn(p,n) and ^{117}Sn(p,n)," *Phys. Rev. C* **15**, 915–20 (1977).

Johnson, C. H., J. K. Bair, C. M. Jones, S. K. Penny, and D. W. Smith, "*P*-Wave Size Resonances Observed by the (p,n) Reaction for 2.6- and 7-MeV Protons Incident on Isotopes of Sr," *Phys. Rev. C* 15, 196 216 (1977).

Jones, C. M. (invited paper), "Large Tandem Accelerators," *IEEE Trans. Nucl. Sci.* (Proceedings of the International Conference on Heavy-Ion Sources, Gatlinburg, Tenn., October 1975), NS-23(2), 913 17 (1976).

Kern, B. D., J. L. Weil, J. H. Hamilton, A. V. Ramayya, C. R. Bingham, L. L. Riedinger, E. F. Zganjar, J. L. Wood, G. M. Gowdy, R. W. Fink, E. H. Spejewski, H. K. Carter, R. L. Mlekodaj, and J. Lin, "Mass Differences of Proton-Rich Atoms Near $A = 116$ and $A = 190$," pp. 81 87 in vol. 5 of *Atomic Masses and Fundamental Constants*, ed. J. H. Sanders and A. H. Wapstra, Plenum, New York, 1976

Kim, H. J., "Nuclear Data Sheets for $A = 59$," *Nucl. Data Sheets* 17, 485 517 (April 1976).

Kim, H. J., R. L. Robinson, W. K. Tuttle III, R. Ronningen, R. O. Sayer, and J. C. Wells, Jr., "^{55}Cr High-Spin States," p. 90 in *Proceedings, European Conference on Nuclear Physics with Heavy Ions, Caen, France, September 1976*, ed. B. Fernandez et al., European Physical Society, 1976.

Kocher, D. C., "Nuclear Data Sheets for $A = 120$," *Nucl. Data Sheets* 17, 39 95 (January 1976).

Kocher, D. C., "Nuclear Data Sheets for $A = 74$," *Nucl. Data Sheets* 17, 519 72 (April 1976).

Kocher, D. C., "Nuclear Data Sheets for $A = 55$," *Nucl. Data Sheets* 18, 463 551 (August 1976).

Kocher, D. C., and R. L. Auble, "Nuclear Data Sheets for $A = 58$," *Nucl. Data Sheets* 19, 445 506 (December 1976).

Kocher, D. C., F. E. Bertrand, E. E. Gross, and E. Newman, "^{60}Ni(p,p') Reaction at 60 MeV: A Study of the Analyzing Power for Inelastic Excitation of the Giant Resonance Region of the Nuclear Continuum and of Low-Lying Bound States," *Phys. Rev. C* 14, 1392 1411 (1976).

Koonin, S. E., K. T. R. Davies, V. Maruhn-Rezwani, H. Feldmeier, S. J. Krieger, and J. W. Negele, "Time-Dependent Hartree-Fock Calculations for ^{16}O + ^{16}O + ^{40}Ca Reactions," *Phys. Rev.* 15, 1359 74 (1977).

Koonin, S. E., V. Maruhn-Rezwani, K. T. R. Davies, H. Feldmeier, S. J. Krieger, and J. W. Negele, "Time-Dependent Hartree-Fock Calculations of Heavy-Ion Collisions," pp. 637–43 in vol. II of *Proceedings, Symposium on Macroscopic Features of Heavy-Ion Collisions, Argonne, Illinois, April 1976*, Contributed Papers, ANL/PHY-76-2, 1976.

Koonin, S., V. Maruhn-Rezwani, K. T. R. Davies, H. Feldmeier, S. J. Krieger, and J. W. Negele, "Microscopic Calculation of Energy Loss in Heavy-Ion Collisions," p. 145 in *Proceedings, European Conference on Nuclear Physics with Heavy Ions, Caen, France, September 1976*, ed. B. Fernandez et al., European Physical Society, 1976.

Kuenhold, K. A., J. L. Duggan, F. D. McDaniel, A. D. Ray, A. Zander, and P. D. Miller (invited paper), "Production of *L* X Rays by 9.5- to 41.8-MeV Fluorine Ions Incident on Six Elements from Pr to Bi," *Proceedings, Fourth Conference on Application of Small Accelerators, Denton, Texas, October 1976*, pp. 334 37, IEEE Conf. Record Publication No. 76CH1175-9 NTS, 1977.

Larson, J. D., and C. M. Jones, "Phase Space Acceptance and Emittance in Beam Transport with Application to Tandem Accelerators," *Nucl. Instrum. Methods* 140, 489 504 (1977).

Laubert, R., R. S. Peterson, J. P. Forester, K. H. Liao, P. M. Griffin, H. Hayden, S. B. Elston, D. J. Pegg, R. S. Thoe, and I. A. Sellin, "Differences in the Production of Noncharacteristic Radiation in Gaseous and Solid Targets," *Phys. Rev. Lett.* 36, 1574 75 (1976).

LeBeyec, Y., R. L. Hahn, K. S. Toth, and R. Eppley, "Reactions of ^{40}Ar with ^{160}Dy, ^{164}Dy, and ^{174}Yb," *Phys. Rev. C* 14, 1038 47 (1976).

Lewis, M. B., F. K. McGowan, C. H. Johnson, and M. J. Saltmarsh, "The Oak Ridge CN Van de Graaff Facility for Heavy-Ion Radiation Damage Studies," pp. 15 37 in *Experimental Methods for Charged-Particle Irradiations* (Proceedings of the Symposium, Gatlinburg, Tenn., September 1975), ed. David Kramer, ERDA CONF-750947, 1975.

Lord, R. S., E. D. Hudson, G. S. McNeilly, R. O. Sayer, J. B. Ball, M. L. Mallory, S. W. Mosko, R. M. Beckers, K. N. Fischer, J. A. Martin, and J. D. Rylander, "The Oak Ridge Isochronous Cyclotron as an Energy Booster for a 25-MV Tandem," pp. 622-25 in *Proceedings, Seventh International Conference on Cyclotrons and Their Applications, Zurich, Switzerland, August 1975*, ed. W. Joho, Birkhauser Verlag, Basel, 1975.

Love, W. G., "Microscopic Description of Sn(p,n) Reactions," *Phys. Rev. C* 15, 1261-63 (1977).

Love, W. G., and G. R. Satchler, "A New Interaction for Heavy-Ion Scattering," p. 6 in *Proceedings, European Conference on Nuclear Physics with Heavy Ions, Caen, France, September 1976*, ed. B. Fernandez et al., European Physical Society, 1976.

Lowry, M., J. S. Schweitzer, R. Dayras, and R. G. Stokstad, "Cross Sections for ^{8}Li Production in the Reactions ^{10}B + ^{16}O and ^{12}C + ^{14}N," *Nucl. Phys.* A259, 122-28 (1976).

Macdonald, J. R., M. O. Brown, S. J. Dzuchlewski, L. M. Winters, R. Laubert, I. A. Seilin, and J. R. Mowat, "Charge Dependence of K X-Ray Production in Nearly Symmetric Collisions of Highly Ionized S and Cl Ions in Gases," *Phys. Rev. A* 14, 1997-2009 (1976).

Macklin, R. L., "Neutron Capture Cross Sections of ^{93}Nb from 2.6 to 700 keV," *Nucl. Sci. Eng.* 59, 12-20 (1976).

Macklin, R. L., "The ^{165}Ho(n,γ) Standard Cross Section from 3 to 450 keV," *Nucl. Sci. Eng.* 59, 231-36 (1976).

Macklin, R. L., "Electrostatic Energy Storage," *Nature* 262, 171 (1976).

Macklin R. L., and J. Halperin, "Resonance Neutron Capture by ^{209}Bi," *Phys. Rev. C* 14, 1389-91 (1976).

Macklin, R. L., J. A. Harvey, J. Halperin, and N. W. Hill, "The 292.4-eV Neutron Resonance Parameters of ^{91}Zr," *Nucl. Sci. Eng.* 62, 174 (1977).

Macklin, R. L., and R. R. Winters, "Stellar Neutron Capture in the Thallium Isotopes," *Astrophys. J.* 208, 812 (1976).

Mallory, M. L., and D. H. Crandall, "A Penning Multiply Charged Heavy-Ion Source Test Facility," *IEEE Trans. Nucl. Sci.* NS-23(2), 1069-72 (1976).

Mallory, M. L., K. N. Fischer, and E. D. Hudson, "Isochronous Cyclotron Harmonic Beam Space Charge Effect," *Nucl. Instrum. Methods* 135, 29-38 (1976).

Mallory, M. L., E. D. Hudson, and J. W. Hale, "Increased Cyclotron Beam Intensity Using a Harmonic Beam Interceptor," *Nucl. Instrum. Methods* 137, 379-80 (1976).

Mallory, M. L., and G. S. McNeilly, "A Method for the Acceleration of Radioactive Nuclei," *Nucl. Instrum. Methods* 138, 421-24 (1976).

Martin, J. A., "Accelerators for Heavy Ions," pp. 574-83 in *Proceedings, Seventh International Conference on Cyclotrons and Their Applications, Zurich, Switzerland, August 1975*, ed. W. Joho, Birkhauser Verlag, Basel, 1975.

Martin, J. A., "VIIth International Conference on Cyclotrons and Their Applications," *Part. Accel.* (News & Views) 7, 58-59 (1975).

Martin, M. J., and P. H. Stelson, "Nuclear Data Sheets for A = 184," *Nucl. Data Sheets* 21, 1-89 (May 1977).

Maruhn, J. A., and R. Y. Cusson, "Time-Dependent Hartree-Fock Calculation of ^{12}C + ^{12}C with a Realistic Potential," *Nucl. Phys.* A270, 471-88 (1976).

Maruhn, J. A., R. Y. Cusson, and R. K. Smith, "Time-Dependent Hartree-Fock Calculation for Non-Head-on Collisions of ^{16}O + ^{16}O," pp. 671-79 in vol. II of *Proceedings, Symposium on Macroscopic Features of Heavy-Ion Collisions, Argonne, Illinois, April 1976*, Contributed Papers, ANL PHY-76-2, 1976.

Maruhn, J. A., and W. Greiner, "Collective Effects on Mass Asymmetry in Fission," *Phys. Rev. C* 13, 2404-12 (1976).

Maruhn, J. A., T. A. Welton, and C. Y. Wong, "Remarks on the Numerical Solution of Poisson's Equation for Isolated Charge Distribution," *J. Comput. Phys.* 20, 326-35 (1976).

McDaniel, F. D., J. L. Duggan, P. D. Miller, and G. D. Alton, "*K*-Shell Ionization of Elements Ca to Zn for 0.5- to 2.5-MeV/amu ^{14}N Ion Bombardment," *Phys. Rev. A* 15, 846–55 (1977).

McGowan, F. K., and W. T. Milner, "Reaction List for Charged-Particle-Induced Nuclear Reactions $Z = 1$ to $Z = 98$ (H to CF)—October 1974 to December 1975," *At. Data Nucl. Data Tables* 18, 1–136 (1976).

McNeilly, G. S., E. D. Hudson, R. S. Lord, M. L. Mallory, J. E. Mann, J. B. Ball, and J. A. Martin, "Design Study for the Conversion of the Oak Ridge Isochronous Cyclotron from an Energy Constant of $K = 90$ to $K = 300$," pp. 626–29 in *Proceedings, Seventh International Conference on Cyclotrons and Their Applications, Zurich, Switzerland, August 1975*, ed. W. Joho, Birkhauser Verlag, Basel, 1975.

Mlekodaj, R. L., E. H. Spejewski, H. K. Carter, and A. G. Schmidt, "The UNISOR Integrated Target-Ion Source," *Nucl. Instrum. Methods* 139, 299–303 (1976).

Moak, C. D. (invited paper), "Stripping in Foils and Gases," *IEEE Trans. Nucl. Sci.* (Proceedings of the International Conference on Heavy-Ion Sources, Gatlinburg, Tenn., October 1975, NS-23(2), 1126–32 (1976).

Moak, C. D., B. R. Appleton, J. A. Biggerstaff, M. D. Brown, S. Datz, T. S. Noggle, and H. Verbeek, "The Velocity Dependence of the Stopping Power of Channeled Iodine Ions from 0.6 to 60 MeV," *Nucl. Instrum. Methods* (Proceedings of the Sixth International Conference on Atomic Collisions in Solids, Amsterdam, Netherlands, September 1975), 132, 95–98 (1976).

Monigold, G., F. D. McDaniel, J. L. Duggan, R. Mehta, R. Rice, and P. D. Miller (invited paper), "*K*-Shell X-Ray Production Cross Sections of Selected Elements Al to Ni for 4.0- to 38.0-MeV ^{10}B Ions," *Proceedings, Fourth Conference on Application of Small Accelerators, Denton, Texas, October 1976*, pp. 70–74 in IEEE Conf. Record Publication No. 76CH1175-9, NTS, 1977.

Mosko, S. W., D. D. Bates, R. R. Bigelow, E. K. Cottongim, E. P. Pipes, and K. Sueker, "A 120-kA Pulsed dc Power System with Computerized Thyristor Triggering," pp. 465–69 in *Proceedings, Sixth Symposium on Engineering Problems of Fusion Research, San Diego, California, November 1975*, IEEE Pub. No. 75CH1097-5-NPS, 1976.

Mosko, S. W., E. D. Hudson, R. S. Lord, M. L. Mallory, J. E. Mann, J. A. Martin, G. S. McNeilly, J. B. Ball, K. N. Fischer, L. L. Riedinger, and R. L. Robinson, "A Separated-Sector Cyclotron Post-Accelerator for the Oak Ridge Heavy-Ion Laboratory," pp. 600–603 in *Proceedings, Seventh International Conference on Cyclotrons and Their Applications, Zurich, Switzerland, August 1975*, ed. W. Joho, Birkhauser Verlag, Basel, 1975.

Musgrove, A. R. de L., B. J. Allen, J. W. Boldeman, D. M. H. Chan, and R. L. Macklin, "Resonant Neutron Capture in ^{40}Ca," *Nucl. Phys.* A259, 365–77 (1976).

Musgrove, A. R. de L., B. J. Allen, J. W. Boldeman, D. M. H. Chan, and R. L. Macklin, "Odd-Even Effects in Radiative Neutron Capture by ^{42}Ca, ^{43}Ca, and ^{44}Ca," *Nucl. Phys.* A279, 317–32 (1977).

Musgrove, A. R. de L., B. J. Allen, J. W. Boldeman, and R. L. Macklin, "keV Neutron Capture Cross Sections of ^{134}Ba and ^{136}Ba," *Nucl. Phys.* A256, 173–88 (1976).

Musgrove, A. R. de L., B. J. Allen, J. W. Boldeman, and R. L. Macklin, "Average Neutron Resonance Parameters and Radiative Capture Cross Sections for the Isotopes of Molybdenum," *Nucl. Phys.* A270, 108–40 (1976).

Namenson, A. I., A. Stolovy, and J. A. Harvey, "Neutron Resonances in ^{185}Re and ^{187}Re," *Nucl. Phys.* A266, 83–108 (1976).

Obenshain, F. E., J. C. Williams, and L. W. Houk, "Hyperfine Interactions at ^{61}Ni in Ionic Nickel Compounds," *J. Inorg. Nucl. Chem.* 38, 19–21 (1976).

Oeschler, H., G. Hagemann, M. L. Halbert, and B. Herskind, "Heavy-Ion-Induced Transfer Reactions on ^{148}Nd," *Nucl. Phys.* A266, 262 (1976).

Pancholi, S. C., and M. J. Martin, "Nuclear Data Sheets for $A = 138$," *Nucl. Data Sheets* 18, 167–222 (June 1976).

Pandey, M. S., J. B. Garg, and J. A. Harvey, "Neutron Total Cross Sections and Resonance Parameters of ^{63}Cu and ^{65}Cu-I," *Phys. Rev. C* 15, 600–14 (1977).

Pandey, M. S., J. B. Garg, R. L. Macklin, and J. Halperin, "High-Resolution Neutron Capture Cross Sections in ^{63}Cu and ^{65}Cu–II," *Phys. Rev. C* 15, 615–29 (1977).

Peebles, P. Z., M. Parvarandeh, and C. M. Jones, "Shunt Impedance of Spiral-Loaded Resonant RF Cavities," *Part. Accel.* 6, 201–9 (1975).

Pegg, D. J. (invited paper), "Autoionizing States in the Alkalis," pp. 419–35 in vol. I of *Beam Foil Spectroscopy* (Proceedings of the Conference, Gatlinburg, Tenn., September 1975), ed. I. A. Sellin and D. J. Pegg, Plenum, New York, 1976.

Pegg, D. J., S. B. Elston, J. P. Forester, P. M. Griffin, H. C. Hayden, R. S. Peterson, R. S. Thoe, and I. A. Sellin, "Lifetimes and Transition Rates for Allowed In-Shell Transitions in Highly Stripped Sulfur," p. 166 in *Atomic Physics 5* (Proceedings of the Fifth International Conference on Atomic Physics, Berkeley, California, July 1976), ed. R. Marrus, M. Prior, and H. Sugart, Plenum, New York, 1977.

Pegg, D. J., S. B. Elston, P. M. Griffin, H. C. Hayden, J. P. Forester, R. S. Thoe, R. S. Peterson, and I. A. Sellin, "Radiative Lifetimes and Transition Probabilities for Electric Dipole $\Delta n = 0$ Transitions in Highly Stripped Sulfur Ions," *Phys. Rev. A* 14, 1036–41 (1976).

Pegg, D. J., S. B. Elston, P. M. Griffin, H. C. Hayden, J. P. Forester, R. S. Thoe, R. S. Peterson, and I. A. Sellin, "Dipole Oscillator Strengths for $\Delta n = 0$ Transitions in Highly Ionized Sulfur," *Phys. Lett.* 58A, 349 (1976).

Pegg, D. J., H. H. Haselton, R. S. Thoe, P. M. Griffin, M. D. Brown, and I. A. Sellin, "Autoionizing States Formed in Na^+ + He and Mg^+ + He Collisions at 70 keV±," p. 312 in *Proceedings, Ninth International Conference on Physics of Electronics and Atomic Collisions, Seattle, Washington, July 1975*, ed. J. S. Risley and R. Geballe, University of Washington Press, Seattle, 1975.

Pegg, D. J., H. H. Haselton, R. S. Thoe, P. M. Griffin, M. D. Brown, and I. A. Sellin, "Optically Inaccessible Core Excited States of Li and Na," *Phys. Lett.* 50A, 447 (1975).

Pegg, D. J., H. H. Haselton, R. S. Thoe, P. M. Griffin, M. D. Brown, and I. A. Sellin, "Core Excited Autoionizing States in the Alkalis," *Phys. Rev. A* 12, 1330 (1975).

Peter, J., C. Ngo, F. Plasil, B. Tamain, M. Berlanger, and F. Hanappe, "Quasi-Fission and Other Strongly Damped Collisions between ^{63}Cu Ions and ^{197}Au Nuclei," *Nucl. Phys.* A279, 110–24 (1977).

Peter, J., C. Ngo, F. Plasil, B. Tamain, F. Hanappe, and M. Berlanger, "Inelastic Collisions between Heavy Ions (Ar, Cu) and a Heavy Target (Au)," pp. 119–21 in *Proceedings of the International Workshop on Gross Properties of Nuclei and Nuclear Excitations IV, Hirschegg, Kleinwalsertal, Austria, January 1976*, Institut für Kernphysik, Technische Hochschule Darmstadt, 1976.

Peterson, R. S., S. B. Elston, I. A. Sellin, R. Laubert, F. K. Chen, and C. A. Peterson, "Strong Isotope Dependence of K-Vacancy Production in Slow Ne^+-Ne Collisions," *Phys. Rev. Lett.* 37, 984–86 (1976).

Peterson, R. S., R. S. Thoe, H. Hayden, S. B. Elston, J. P. Forester, K.-H Liao, P. M. Griffin, D. J. Pegg, I. A. Sellin, and R. Laubert, "Differences in the Production of Noncharacteristic Radiation in Solid and Gas Targets," pp. 497–504 in vol. II of *Beam Foil Spectroscopy* (Proceedings of the Conference, Gatlinburg, Tenn., September 1975), ed. I. A. Sellin and D. J. Pegg, Plenum, New York, 1976.

Pichevar, M., J. Delaunay, B. Delaunay, H. J. Kim, Y. El Masri, and J. Vervier, "High Spin States in ^{60}Ni," *Nucl. Phys. A* 264, 132–50 (1976).

Piercey, R. B., A. V. Ramayya, J. H. Hamilton, R. M. Ronningen, R. L. Robinson, and H. J. Kim, "Band Structure in ^{74}Se," p. 83 in *Proceedings, European Conference on Nuclear Physics with Heavy Ions, Caen, France, September 1976*, ed. B. Fernandez et al., European Physical Society, 1976.

Piercey, R. B., A. V. Ramayya, R. M. Ronningen, J. H. Hamilton, R. L. Robinson, and H. J. Kim, "Evidence for an Octupole Rotational Band in ^{74}Se," *Phys. Rev. Lett.* 37, 496–98 (1976).

Piercey, R. B., A. V. Ramayya, R. M. Ronningen, J. H. Hamilton, R. L. Robinson and H. J. Kim, "Evidence for an Octupole Rotational Band in ^{74}Se," p. 196 in *Proceedings, International Conference on Selected Topics in Nuclear Structure, Dubna, U.S.S.R., June 1976*, Joint Institute for Nuclear Research, 1976.

Preedom, B. M., C. W. Darden, R. D. Edge, T. Marks, M. J. Saltmarsh, K. Gabathuler, E. E. Gross, C. A. Ludemann, P. Y. Bertin, M. Blecher, K. Gotow, J. Alster, R. L. Burman, J. P. Perroud, R. P. Redwine, B. Gopler, V. R. Gibbs, and E. L. Lomon, "The Deuteron *D*-State and the $\pi^+ + d \rightarrow pp + p$ Reaction," *Phys. Lett.* **65B**, 31-34 (1976).

Preedom, B. M., M. J. Saltmarsh, C. A. Ludemann, and J. Alster, "The Response of Plastic Scintillator to Stopping Protons in the Energy Range 70 to 100 MeV," *Nucl. Instrum. Methods* **133**, 311-14 (1976).

Rainis, A. E., K. S. Toth, and C. R. Bingham, "Isomerism in the New $N+81$ Isotope, ^{147}Dy," *Phys. Rev. C* **13**, 1609-16 (1976).

Raman, S. (invited paper), "General Survey of Applications Which Require Nuclear Data," pp. 39-112 in *Proceedings, IAEA Meeting on Transactinium Isotope Nuclear Data, Karlsruhe, Germany, November 1975*, IAEA-186, 1976.

Raman, S. (invited paper), "Some Activities in the United States Concerning the Physics Aspects of Actinide Waste Recycling," pp. 201-14 in *Proceedings, IAEA Meeting on Transactinium Isotope Nuclear Data, Karlsruhe, Germany, November 1975*, IAEA-186, 1976.

Raman, S., R. L. Auble, J. B. Ball, E. Newman, J. C. Wells, Jr., and J. Lin, "Levels in ^{144}Nd from the ^{143}Nd(d,p) and the ^{146}Nd(p,t) Reactions," *Phys. Rev. C* **14**, 1381-88 (1976).

Rickertsen, L. D., and G. R. Satchler, "On the Single-Folding Model for Heavy-Ion Potentials," p. 5 in *Proceedings, European Conference on Nuclear Physics with Heavy Ions, Caen, France, September 1976*, ed. B. Fernandez et al., European Physical Society, 1976.

Rickertsen, L. D., and G. R. Satchler, "On the Single-Folding Model for Heavy-Ion Potentials," *Phys. Lett.* **66B**, 9-10 (1977).

Rickertsen, L. D., G. R. Satchler, R. G. Stokstad, and R. M. Wieland, "Macroscopic Folded Form Factors for ^{12}C + ^{12}C Inelastic Scattering," pp. 733-40 in vol. II of *Proceedings, Symposium on Macroscopic Features of Heavy-Ion Collisions, Argonne, Illinois, April 1976*, Contributed Papers, ANL PHY-76-2, 1976.

Robinson, R. L., J. K. Bair, C. H. Johnson, P. H. Stelson, W. B. Dress, and C. M. Jones, "Cross Sections for the Ni, Cu, Zn(^{16,18}O,xn) Reactions Near the Coulomb Barrier," *Phys. Rev. C* **14**, 2126-32 (1976).

Robinson, R. L., H. J. Kim, J. B. McGrory, G. J. Smith, W. T. Milner, R. O. Sayer, J. C. Wells, Jr., and J. Lin, "High-Spin States in ^{42}Ca," *Phys. Rev. C* **13**, 1922-35 (1976).

Robinson, R. L., H. J. Kim, R. O. Sayer, J. C. Wells, Jr., and R. M. Ronningen, "High-Spin States in ^{70}Ge," p. 91 in *Proceedings, European Conference on Nuclear Physics with Heavy Ions, Caen, France, September 1976*, ed. B. Fernandez et al., European Physical Society, 1976.

Ronningen, R. M., A. V. Ramayya, J. H. Hamilton, W. Lourens, J. Lange, H. K. Carter, and R. O. Sayer, "Mean Life of the 854-keV O_2 State in ^{74}Se and the Coexistence Model," *Nucl. Phys.* **A261**, 439-44 (1976).

Saltmarsh, M. J., and J. A. Horak (invited paper), "A Large-Volume Intense Neutron Source for CTR Materials Studies," pp. 380-91 in *Proceedings, International Conference on Radiation Test Facilities for the CTR Surface and Materials Program, Argonne, Illinois, July 1975*, ANL-CTR-75-4, 1975.

Samuelson, L., W. H. Kelly, R. L. Auble, and W. C. McHarris, "Nuclear Data Sheets for $A = 104$," *Nucl. Data Sheets* **18**, 125-65 (June 1976).

Sarantites, D. G., J. H. Barker, M. L. Halbert, D. C. Hensley, R. A. Dayras, E. Eichler, N. R. Johnson, and S. A. Gronemeyer, "Gamma-Ray Multiplicities in Evaporation Residues Formed in Bombardments of ^{150}Nd by ^{20}Ne," *Phys. Rev. C* **14**, 2138-57 (1976).

Sastry, K. S. R., A. V. Ramayya, R. S. Lee, J. H. Hamilton, R. L. Mlekodaj, and N. R. Johnson, "Cyromagnetic Ratio of the First 2^+ Excited State in ^{126}Se," *Nucl. Phys.* **A273**, 61-68 (1976).

Satchler, G. R. (invited paper), "Potential Model Description of Heavy-Ion Elastic and Inelastic Scattering," pp. 33-63 in vol. I of *Proceedings, Symposium on Macroscopic Features of Heavy-Ion Collisions, Argonne, Illinois, April 1976*, ANL/PHY-76-2, 1976.

Satchler, G. R., "^{16}O + ^{28}Si: Deep or Shallow Potentials," *Nucl. Phys.* **A279**, 493-501 (1977).

Satchler, R., and W. G. Love, "A New Interaction for Heavy-Ion Scattering," *Phys. Lett.* 65B, 415-18 (1976).

Schmidt, A. G., R. L. Mlekodaj, E. L. Robinson, F. T. Avignone III, J. Lin, G. M. Gowdy, J. L. Wood, and R. W. Fink, "New Isomers of ^{195,197}Tl and the Departure of the $h_{9/2}$ Intruder State," *Phys. Lett.* 66B, 133-35 (1977).

Schmidt-Ott, W. D., and K. S. Toth, "Decay Rates for Doubly-Even $N = 84$ Alpha Emitters and the Subshell Closure at $Z = 64$," *Phys. Rev. C* 13, 2574-76 (1976).

Schmorak, M. R., "Nuclear Data Sheets for $A = 244$-262 (even-A)," *Nucl. Data Sheets* 17, 391-484 (March 1976).

Schmorak, M. R., "Nuclear Data Sheets for $A = 249$-263 (odd-A)," *Nucl. Data Sheets* 18, 389-461 (July 1976).

Schmorak, M. R., "Nuclear Data Sheets for $A = 232, 236, 240$," *Nucl. Data Sheets* 20, 165-252 (February 1977).

Schmorak, M. R., "Nuclear Data Sheets for $A = 231$," *Nucl. Data Sheets* 21, 91-116 (May 1977).

Schmorak, M. R., "Nuclear Data Sheets for $A = 235$," *Nucl. Data Sheets* 21, 117-51 (May 1977).

Schmorak, M. R., "Nuclear Data Sheets for $A = 239$," *Nucl. Data Sheets* 21, 153-200 (May 1977).

Schmorak, M. R., and M. J. Martin, "The Nuclear Data Project Data Bank," pp. 33-35 in *Proceedings, ERDA Symposium on X- and Gamma-Ray Sources and Applications, Ann Arbor, Michigan, May 1976*, ed. H. C. Griffin et al., ERDA CONF-760539, 1976.

Sellin, I. A., "Applications of Beam Foil Spectroscopy to Atomic Collisions in Solids," *Nucl. Instrum. Methods* (Proceedings of the Sixth International Conference on Atomic Collisions in Solids, Amsterdam, Netherlands, September 1975). 132, 397-404 (1976).

Sellin, I. A., "Highly Ionized Ions," p. 215 in vol. 12 of *Advances in Atomic and Molecular Physics*, Academic Press, New York, 1976.

Sellin, I. A., "Applications of Beam-Foil Spectroscopy to Atomic Collisions in Solids," *Nucl. Instrum. Methods* 132, 397 (1976).

Sellin, I. A., "The Measurement of Autoionizing Ion Levels and Lifetimes by Projectile Electron Spectroscopy," pp. 265-97 in *Topics in Modern Physics: Beam-Foil Spectroscopy*, ed. S. Bashkin, Springer-Verlag, New York, 1976.

Sellin, I. A., and D. J. Pegg, eds., *Beam Foil Spectroscopy* (Proceedings of the Conference, Gatlinburg, Tenn., September 1975), Plenum, New York, vols. 1 and 2, 987 pp., 1976.

Shamu, R. E., Ch. Lagrange, E. M. Bernstein, J. J. Ramirez, T. Tamura, and C. Y. Wong, "Quadrupole Deformation Parameters of ^{148,152,154}Sm Determined from Neutron Total Cross Sections," *Phys. Lett.* 61B, 29-32 (1976).

Sparks, C. J., Jr., S. Raman, H. L. Yakel, R. V. Gentry, and M. O. Krause, "Search with Synchrotron Radiation for Superheavy Elements in Giant-Halo Inclusions," *Phys. Rev. Lett.* 38, 205-8 (1977).

Stelson, P. H. (invited paper), "Future of Physics with Heavy Ions," *IEEE Trans. Nucl. Sci.* (Proceedings of the International Conference on Heavy-Ion Sources, Gatlinburg, Tenn., October 1975), NS-23(2), 1162-65 (1976).

Stelson, P. H. (invited paper), "The Atomic Physics Potential of New Accelerators," pp. 401-17 in vol. 1 of *Beam Foil Spectroscopy* (Proceedings of the Conference, Gatlinburg, Tenn., September 1975), ed. I. A. Sellin and D. J. Pegg, Plenum, New York, 1976.

Stokstad, R. G., J. Gomez del Campo, J. A. Biggerstaff, A. H. Snell, and P. H. Stelson, "Fusion of ^{14}N + ^{12}C at Energies up to 178 MeV," *Phys. Rev. Lett.* 36, 1529-31 (1976).

Stokstad, R. G., J. Gomez del Campo, J. A. Biggerstaff, A. H. Snell, and P. H. Stelson, "Fusion of ^{14}N + ^{12}C at High Energies," pp. 795-802 in vol. II of *Proceedings, Symposium on Macroscopic Features of Heavy-Ion Collisions, Argonne, Illinois, April 1976*, ANL/PHY-76-2, 1976.

Stokstad, R. G., D. C. Hensley, and A. H. Snell, "A Position-Sensitive ΔE-E Telescope," *Nucl. Instrum. Methods* 141, 499-504 (1977).

Stokstad, R. G., Z. E. Switkowski, R. A. Dayras, and R. M. Wieland, "Measurements of Fusion Cross Sections for Heavy-Ion Systems at Very Low Energies," *Phys. Rev. Lett.* 37, 888–90 (1976).

Switkowski, Z. E., R. G. Stokstad, and R. M. Wieland, "Measurement of Fusion Cross Sections for $^{14}N + {}^{14}N$ and $^{12}C + {}^{16}O$ at Low Energies," *Nucl. Phys.* A274, 202–22 (1976).

Switkowski, Z. E., R. G. Stokstad, and R. M. Wieland, "^{14}N Fusion with ^{12}C and ^{16}O at Sub-Barrier Energies," *Nucl. Phys.* A279, 502–16 (1977).

Tamagawa, H. I. Alexeff, C. M. Jones, N. H. Lazar, and P. D. Miller, "Use of the Hot-Electron Mirror Machine Interem as a High-Z Ion Source," *IEEE Trans. Nucl. Sci.* (Proceedings of the International Conference on Heavy-Ion Sources, Gatlinburg, Tenn., October 1975), NS-23(2), 994–98 (1976).

Tamain, B., F. Plasil, C. Ngo, J. Peter, M. Berlanger, and F. Hanappe, "On the Energy Dependence of Quasi-Fission," *Phys. Rev. Lett.* 36, 18–20 (1976).

Thoe, R. S., R. S. Peterson, I. A. Sellin, K. H. Liao, D. J. Pegg, J. P. Forester, and P. M. Griffin, "Polarization Measurements of the Noncharacteristic Radiation Emitted from Collision between High-Energy Al Ions," *Phys. Lett.* 56A, 89 (1976).

Thoe, R. S., I. A. Sellin, K. H. Liao, R. S. Peterson, D. J. Pegg, J. P. Forester, and P. M. Griffin, "Angular Distribution Studies of Noncharacteristic X Radiation," pp. 477–82 in vol. II of *Beam Foil Spectroscopy* (Proceedings of the Conference, Gatlinburg, Tenn., September 1975), ed. I. A. Sellin and D. J. Pegg, Plenum, New York, 1976.

Thornton, S. T., D. E. Gustafson, J. L. C. Ford, Jr., K. S. Toth, and D. C. Hensley, "Inelastic Scattering and Transfer Reactions from ^{12}C Ions on ^{90}Zr," *Phys. Rev. C* 13, 1502–9 (1976).

Thornton, S. T., T. C. Schweizer, D. E. Gustafson, J. L. C. Ford, Jr., and M. J. LeVine, "Nuclear Structure Study of ^{141}Nd, ^{143}Nd, and ^{143}Pm by ^{3}C-Induced Reactions on ^{142}Nd," *Phys. Rev. C* 13, 1936–43 (1976).

Thornton, S. T., T. C. Schweizer, D. E. Gustafson, J. L. C. Ford, Jr., and M. J. LeVine, "Nuclear and Coulomb Deformation Parameters of ^{142}Nd," *Nucl. Phys.* A270, 428–36 (1976).

Toth, K. S., "Nuclear Data Sheets for $A = 226$," *Nucl. Data Sheets* 20, 119–37 (February 1977).

Toth, K. S., J. L. C. Ford, Jr., G. R. Satchler, E. E. Gross, D. C. Hensley, S. T. Thornton, and T. C. Schweizer, "Measurements and Analysis of the $^{208}Pb(^{12}C, {}^{11}C)$, $(^{12}C, {}^{11}B)$, and $(^{12}C, {}^{14}C)$ Reactions," *Phys. Rev. C* 14, 1471–83 (1976).

Toth, K. S., M. A. Ijaz, J. Lin, E. L. Robinson, B. O. Hannah, E. H. Spejewski, J. D. Cole, J. H. Hamilton, and A. V. Ramayya, "Observation of Alpha Decay in Thallium Nuclei, Including the New Isotopes ^{184}Tl and ^{185}Tl," *Phys. Lett.* 63B, 150–53 (1976).

Tuttle, W. K., III, P. H. Stelson, R. L. Robinson, W. T. Milner, F. K. McGowan, S. Raman, and W. K. Dagenhart, "Coulomb Excitation of $^{113,115}In$," *Phys. Rev. C* 13, 1036–48 (1976).

Vernon, G. A., G. Stucky, and T. A. Carlson, "Comprehensive Study of Satellite Structure in the Photoelectron Spectra of Transition Metal Compounds," *Inorg. Chem.* 15, 278–84 (1976).

Weigmann, H., R. L. Macklin, and J. A. Harvey, "Isobaric Analogue Impurities from Neutron Capture and Transmission by Magnesium," *Phys. Rev.* 14, 1328–35 (1976).

Wells, J. C., Jr., R. L. Robinson, H. J. Kim, and J. L. C. Ford, Jr., "Absolute Cross Sections for $^{61}Ni(^{16}O,3n)^{74}Kr$," *Phys. Rev. C* 13, 2588 (1976).

Wheeler, R. M., R. P. Chaturvedi, J. L. Duggan, J. Tricomi, and P. D. Miller, "*K* X-Ray Production Cross Sections for Fourteen Elements from Calcium to Palladium for Incident Carbon Ions," *Phys. Rev. A* 13, 958–64 (1976).

Wieland, R. M., R. G. Stokstad, G. R. Satchler, and L. D. Rickertsen, "Analysis of $^{12}C + {}^{12}C$ Scattering: Deep or Shallow Potentials?" *Phys. Rev. Lett.* 37, 1458–60 (1976).

Wong, C. Y., "Limits of the Nuclear Viscosity Coefficient in the Liquid Drop Model," *Phys. Lett.* 61B, 321–23 (1976).

Wong, C. Y., "Primordial Superheavy Element 126," *Phys. Rev. Lett.* 37, 664–66 (1976).

Wong, C. Y., "On the Schrödinger Equation in Fluid Dynamical Form," *J. Math. Phys.* 17, 1008–10 (1975).

Wong, C. Y., "On the Thomas-Fermi Approximation of the Kinetic Energy Density," *Phys. Lett.* 63B, 395–98 (1976).

Wong, C. Y., and K. S. Low, "Time-Dependent Hartree-Fock Formalism with Phenomenological Dissipation," pp. 38-40 in *Proceedings, International Workshop IV on Gross Properties of Nuclei and Nuclear Excitations, Hirschegg, Austria, January 1976*, Technische Hochschule Darmstadt Report No. AED CONF-76 015 000, 1976.

Wong, C. Y., J. A. Maruhn, and T. A. Welton, "Comparison of Nuclear Hydrodynamics and Time-Dependent Hartree-Fock Results," *Phys. Lett.* 66B, 19–22 (1977).

Wong, C. Y., and H. H. K. Tang (invited paper), "Vibrational Frequency of a Nonconducting Charged Liquid Drop," pp. 79–84 in *Proceedings, International Colloquium on Drops and Bubbles, Pasadena, California, August 1974*, ed. D. J. Collins, M. S. Plesset, and M. M. Saffren, U.S. Government Printing Office, 1976.

Wong, C. Y., T. A. Welton, and J. A. Maruhn, "Dynamics of Nuclear Fluid: II. Normal Sound, Spin Sound, Isospin Sound, and Spin-Isospin Sound," *Phys. Rev. C* 15, 1558–70 (1977).

Wood, J. L., G. M. Gowdy, R. W. Fink, D. A. McClure, M. S. Rapaport, R. A. Braga, E. H. Spejewski, R. L. Mlekodaj, H. K. Carter, A. G. Schmidt, J. D. Cole, A. V. Ramayya, J. H. Hamilton, H. Kawakami, E. F. Zganjar, C. R. Bingham, L. L. Riedinger, A. C. Kahler, L. L. Collins, E. L. Robinson, J. Lin, B. D. Kern, J. L. Weil, K. S. R. Sastry, F. T. Avignone, M. A. Ijaz, and K. S. Toth, "Recent Work at UNISOR on Neutron-Deficient Au, Hg, and Tl Nuclei in the Mass Range $184 \leq A \leq 197$," pp. 364–66 in *Proceedings, Third International Conference on Nuclei Far from Stability, Cargese, Corsica, France, May 1976*, ed. R. Klapisch, CERN Report 76-13, 1976.

Worsham, R. E., and J. E. Mann, "A Liquid-Helium Cryostat for a Superconducting Objective and Cold Stage," pp. 532–33 in *Proceedings, Thirty-fourth Annual Meeting of the Electron Microscopy Society of America, Miami Beach, Florida, August 1976*, Claitor's Publishing Division, Baton Rouge, Louisiana, 1976.

Zucker, A., and J. B. Ball (invited paper), "The Heavy-Ion Accelerator Project at Oak Ridge," pp. 36–42 in vol. II of *Proceedings, Fourth All-Union National Conference on Particle Accelerators, Moscow, U.S.S.R., November 1974*, ed. A. A. Vaselov, U.S.S.R. Academy of Sciences, 1975.

THESES

Barker, M. D., "Exploratory Studies in the Mass Region $A = 60$–80 Far from Stability," B.S. degree, Emory University, June 1976.

Dagenhart, W. K., "Coulomb Excitation Studies of ^{114}Sn," Ph.D. dissertation, University of Tennessee, March 1977.

Gowdy, G. M., "Decay Scheme Studies of Neutron-Deficient Odd-Mass Thallium Isotopes and the Systematics of the Odd-Mass Mercury Levels," Ph.D. dissertation, Georgia Institute of Technology, December 1976.

Hillis, D. L., "Shape Effects in the Elastic and Inelastic Scattering of 70.4-MeV ^{12}C Ions from the Even Neodymium Isotopes," Ph.D dissertation, University of Tennessee, March 1976.

Tung, Cheng-May, "Electron Charge Density Distributions Surrounding Impurities in Gold," Ph.D. dissertation, Louisiana State University, August 1976.

ANNUAL REPORT

Stelson, P. H., *Physics Division Annual Progress Report for the Period Ending December 31, 1975*, ORNL-5137 (May 1976).

TOPICAL REPORTS

Barnett, C. F., H. B. Gilbody, E. W. McDaniel, J. A. Ray, E. Ricci, E. W. Thomas, and I. Wilker, *Atomic Data for Controlled Fusion*, ORNL-5206 (February 1977).

Barnett, C. F., H. B. Gilbody, E. W. McDaniel, J. A. Ray, E. Ricci, E. W. Thomas, and I. Wilker, *Atomic Data for Controlled Fusion*, ORNL-5207 (February 1977).

Dabbs, J. W. T., *The Nuclear Fuel Cycle and Actinide Wastes: Cross Section Needs and Recent Measurements*, ORNL/TM-30 (August 1976).

Dalton, Bill, *Statistical Shell-Model Level Density Computer Code Description and User's Manual*, ORNL/TM-5486 (July 1976).

Ford, J. L. C., Jr., H. A. Enge, J. R. Erskine, D. L. Hendrie, and M. J. LeVine, *A Magnetic Spectrograph for the Holifield Heavy-Ion Research Facility*, ORNL/TM-5687 (January 1977).

Larson, D. C., J. A. Harvey, and N. W. Hill, *Measurement of the Neutron Total Cross Section of Sodium from 32 keV to 37 MeV*, ORNL/TM-5614 (October 1976).

Larson, D. C., C. H. Johnson, J. A. Harvey, and N. W. Hill, *Measurement of the Neutron Total Cross Section of Fluorine from 5 eV to 20 MeV*, ORNL/TM-5612 (October 1976).

Macklin, R. L., *Electrostatic Energy Storage*, ORNL/TM-5529 (September 1976).

Martin, M. J., ed., *Nuclear Decay Data for Selected Radionuclides*, ORNL-5114 (March 1976).

Saltmarsh, M. J., C. A. Ludemann, C. B. Fulmer, and R. C. Styles, *Characteristics of an Intense Neutron Source Based on the d + Be Reaction*, ORNL/TM-5696 (November 1976).

Saltmarsh, M. J., and R. E. Worsham, *INGRID—A Proposal for an Intense Neutron Generator for Radiation-Induced Damage Studies in the CTR Materials Program*, ORNL/TM-5233 (January 1976).

ARTICLES PENDING PUBLICATION AS OF MAY 1, 1977

Allen, B. J., J. W. Boldeman, A. R. de L. Musgrove, and R. L. Macklin, "Resonance Neutron Capture in the Isotopes of Titanium," *Nuclear Physics*.

Allen, B. J., A. R. de L. Musgrove, J. W. Boldeman, and R. L. Macklin, "Valence Neutron Capture in ^{54}Fe," *Nuclear Physics*.

Amsden, A. A., N. J. Ginocchio, F. H. Harlow, J. R. Nix, M. Danos, E. C. Halbert, and R. K. Smith, Jr., "Comparison of Macroscopic and Microscopic Calculations of High-Energy ^{20}Ne + ^{238}U," *Physical Review Letters*.

Andersen, O., R. Bauer, G. B. Hagemann, M. L. Halbert, B. Herskind, M. Neiman, H. Oeschler, and H. Ryde, "A Study of γ-Decay Modes from High Angular Momentum Nuclear States by High-Order Multiplicity Measurements," *Nuclear Physics A*.

Appleton, B. R., R. H. Ritchie, J. A. Biggerstaff, T. S. Noggle, S. Datz, C. D. Moak, and H. Verbeek, "Energetic Heavy-Ion Channeling as an Experimental Technique for Simulating Radiative Electron Capture by Plasma and Impurity Ions in a CTR Type Plasma," *Proceedings, International Conference on Surface Effects in Controlled Fusion Devices, San Francisco, California, February 1976*.

Ball, J. B. (invited paper), "A New Generation of Heavy-Ion Facilities," *IEEE Trans. Nucl. Sci.* (Proceedings of the 1977 Particle Accelerator Conference, Chicago, Ill., March 1977).

Ball, J. B., "The Use of Cyclotrons as Energy Boosters for Electrostatic Accelerators," *Proceedings, Second International Conference on Electrostatic Accelerator Technology, Strasbourg, France, May 1977*.

Ball, J. B., J. A. Martin, J. A. Biggerstaff, C. M. Jones, R. S. Lord, and R. L. Robinson, "The Holifield Heavy-Ion Research Facility at Oak Ridge," *Proceedings, Conference on Nuclear Physics with Heavy Ions, Caen, France, September 1976*.

Barnett, C. F. (invited paper), "Compilation and Evaluation of Atomic and Molecular Data Relevant to Controlled Fusion Research," *Proceedings, IAEA Conference on Atomic Data for Fusion, Culham, England, November 1976*.

Barnett, C. F., "Controlled Fusion Atomic Data Center," *Transactions of the American Nuclear Society*.

Becker, R. L., and J. A. Smith, "Is There a Central Hole in the Alpha Particle?" *Nuclear Physics*.

Boldeman, J. W., B. J. Allen, M. J. Kenny, A. R. de L. Musgrove, and R. L. Macklin, "Valence and Doorway State Effects in Neutron Capture Near Closed Shells," *Proceedings, Third National Soviet Conference on Neutron Physics, Kiev, U.S.S.R., June 1975*.

Boldeman, J. W., B. J. Allen, A. R. de L. Musgrove, and R. L. Macklin, "The Neutron Capture Cross Section of ^{89}Y," *Nuclear Physics*.

Butler, G. W., D. G. Perry, L. P. Remsberg, A. M. Poskanzer, J. B. Natowitz, and F. Plasil, "Observation of the New Nuclides ^{17}Ne, ^{31}Mg, ^{34}Al, and ^{39}P," *Physical Review Letters*.

Carlson, T. A., "Hot Atom Chemistry," *Encyclopedia of Physics*, ed. Rita G. Lerner and George L. Trigg, Dowden, Hutchinson, and Ross, Stroudsburg, Pa.

Carlson, T. A., and C. W. Nestor, "Calculation of *K* and *L* X Rays for Elements of $Z = 95$ to 130," *Atomic Data and Nuclear Data Tables*.

Chen, F. K., G. Lapicki, R. Laubert, S. B. Elston, R. S. Peterson, and I. A. Sellin, "Projectile Charge-State Dependence in *K*-Shell Ionization of Neon, Silicon, and Argon," *Physics Letters*.

Cowan, J. J., and E. T. Arakawa, "Artificial Polarization Anomalies from Holographic Gratings," *Journal of Optics* (Communications).

Crandall, D. H. (invited paper), "Electron Capture by Multicharged Ions," *IEEE Trans. Nucl. Sci.* (Proceedings of the Fourth Conference on the Use of Small Accelerators, Denton, Texas, October 1976).

Crandall, D. H., "Atomic Reactions in Very High Temperature Plasmas," *Proceedings, Third International Symposium on Plasma Chemistry, Limoges, France, July 1977.*

Crandall, D. H., P. O. Taylor, and R. A. Phaneuf, "Electron Impact Ionization of C-IV and N-V," *Proceedings, Tenth International Conference on Physics of Electronic and Atomic Collisions, Paris, France, July 1977.*

Cusson, R. Y., J. A. Maruhn, and H. W. Meldner, "Quantal Theory of Heavy-Ion Collisions Using a Three-Dimensional Time-Dependent Hartree-Fock Scheme," *Annals of Physics.*

Dagenhart, W. K., P. H. Stelson, F. K. McGowan, R. L. Robinson, W. T. Milner, S. Raman, and W. K. Tuttle III, "Coulomb Excitation of ^{115}Sn," *Nuclear Physics.*

Davies, K. T. R., R. A. Managan, J. R. Nix, and A. J. Sierk, "Rupture of the Neck in Nuclear Fission," *Physical Review.*

Dayras, R. A., R. G. Stokstad, D. C. Hensley, M. L. Halbert, C. B. Fulmer, A. H. Snell, R. L. Robinson, D. G. Sarantites, and L. Westerberg, "Pre-Scission Cooling in Strongly Damped Collisions," *Physical Review Letters.*

Dress, W. B., T. A. Carlson, F. H. Ward, and G. L. Nyberg, "Polarized HeI Radiation for Surface Studies," *Proceedings, Thirty-seventh Conference on Physical Electronics, Stanford, California, June 1977.*

Eagle, R., N. M. Clarke, R. J. Griffiths, C. B. Fulmer, and D. C. Hensley, "Inelastic Scattering of ^{3}He from Samarium Isotopes at 53 MeV," *Physical Review C.*

Ewbank, W. B., "Computer Processing of 'Free-Text' Keyword Strings," *Proceedings, Fifth International CODATA Conference, Boulder, Colorado, June 1976.*

Ewbank, W. B., "Evaluated Nuclear Structure Data File (ENSDF) for Basic and Applied Research," *Proceedings, Fifth International CODATA Conference, Boulder, Colorado, June 1976.*

Ewbank, W. B. (invited paper), "Evaluated Nuclear Structure Data File (ENSDF) for Basic and Applied Research," *Transactions of the American Nuclear Society.*

Feng, Da Hsuan, W. W. Eidson, R. F. Kollarits, C. C. Foster, N. M. O'Fallon, S. A. Gronemeyer, C. B. Fulmer, and D. C. Hensley, "Energy Dependence of Back-Angle Alpha Scattering to the Octupole Unnatural Parity State in ^{24}Mg," *Physical Review C.*

Fowler, J. L., book review—*Gamma-Ray Astronomy: Nuclear Transition Region* (E. L. Chupp, D. Reidel Publishing Company, 1976), *American Scientist.*

Gomez del Campo, J., J. L. C. Ford, Jr., R. L. Robinson, M. E. Ortiz, A. Dacal, and E. Andrade, "Yrast Levels in ^{12}C(^{15}N,α) Resonance," *Physical Review Letters.*

Goodman, C. D., J. Rapaport, D. Bainum, and C. Brient, "Large, Time-Compensated Scintillation Counters for High-Energy Neutron Time-of-Flight Measurements," *Nuclear Instruments and Methods.*

Halbert, E. C., J. B. McGrory, G. R. Satchler, and J. Speth, "Hadronic Excitation of the Giant Resonance Region of ^{208}Pb," *Proceedings, Symposium on Highly Excited States in Nuclei, Jülich, Germany, September 1975.*

Hayden, H. C., and R. S. Thoe, "Least-Squares Deconvolution Method for Spectroscopic Data," *Proceedings, Tenth International Conference on the Physics of Electronic and Atomic Collisions, Paris, France, July 1977.*

Horen, D. J., "Nuclear Spectra," *Encyclopedia of Science and Technology*, McGraw-Hill, New York.

Horen, D. J., J. A. Harvey, and N. W. Hill, "First Observation of ($s+d$)-Wave Admixture in Low-Energy Elastic Neutron Scattering," *Physics Letters.*

Horen, D. J., J. A. Harvey, and N. W. Hill, "Giant Magnetic Dipole States in ^{208}Pb Observed in the ^{207}Pb + n Reaction," *Physical Review Letters.*

Hudson, E. D., and M. L. Mallory, "Heavy-Ion Source Support Gas Mixing Experiments," *IEEE Trans. Nucl. Sci.* (Proceedings of the 1977 Particle Accelerator Conference, Chicago, Ill., March 1977).

Hunter, R. C., L. L. Riedinger, D. L. Hillis, C. R. Bingham, and K. S. Toth, "Levels in ^{164}Yb from ^{164}Lu Decay," *Physical Review*.

Huray, P. G., C. M. Tung, F. E. Obenshain, and J. O. Thomson, "Character of the Charge Density Distribution Surrounding Impurities in Gold Metal," *Proceedings, International Conference on the Applications of the Mössbauer Effect, Corfu, Greece, September 1976.*

Hutchinson, D. P., "ORNL Plasma Diagnostic Research," *Proceedings of the Society of Photo-Optical Instrumentation Engineers, SPIE/SPSE Technical Symposium East, Reston, Virginia, April 1977.*

Hutchinson, D. P., and K. L. Vander Sluis, "Design of a High-Power Submillimeter Oscillator-Amplifier System," *Proceedings, Second International Conference and Winter School on Submillimeter Waves and Their Applications, San Juan, Puerto Rico, December 1976.*

Ijaz, M. A., C. R. Bingham, H. K. Carter, E. L. Robinson, and K. S. Toth, "Further Study of ^{196}Tl Alpha Decay," *Physical Review C.*

Judish, J. P., C. M. Jones, F. K. McGowan, W. T. Milner, and P. Z. Peebles, Jr., "Measurements of the Low-Temperature rf Surface Resistance of Lead at Frequencies from 136 to 472 MHz," *Physical Review B.*

Lauber, R., R. S. Peterson, J. P. Forester, K. H. Liao, P. M. Griffin, H. Hayden, S. B. Elston, D. J. Pegg, R. S. Thoe, and I. A. Sellin, "Differences in the Production of Noncharacteristic Radiation in Gaseous and Solid Targets," *Physical Review Letters.*

Love, W. G., T. Terasawa, and G. R. Satchler, "A Dynamic Polarization Potential for Coulomb Excitation Effects on Heavy-Ion Scattering," *Physical Review Letters.*

Love, W. G., T. Terasawa, and G. R. Satchler, "A Dynamic Polarization Potential for Heavy-Ion Scattering," *Nuclear Physics.*

Love, W. G., T. Terasawa, and G. R. Satchler, "Coulomb Excitation Effects on Heavy-Ion Elastic Scattering," *Proceedings, Meeting on Heavy-Ion Collisions, Pikeville, Tennessee, June 1977.*

Macklin, R. L., and J. Halperin, "^{232}Th(n,γ) Cross Section from 2.6 800 keV," *Nuclear Science and Engineering.*

Macklin, R. L., J. Halperin, and R. R. Winters, "Neutron Capture by ^{208}Pb at Stellar Temperatures," *Astrophysical Journal.*

Martin, J. A., J. B. Ball, E. D. Hudson, R. S. Lord, G. S. McNeilly, and S. W. Mosko, "Design Status of a Separated-Sector Cyclotron Booster Accelerator for the HHIRF," *IEEE Trans. Nucl. Sci.* (Proceedings of the 1977 Particle Accelerator Conference, Chicago, Ill., March 1977).

Martin, M. J., ed., "Nuclear Decay Data for Selected Radionuclides Appendix," *A Manual of Radioactivity Measurements Procedures*, National Council on Radiation Protection and Measurements.

Maruhn, J. A., "FC RGEN: A Fast Fourier Transform Program Generator," *Computer Physics Communications.*

Maruhn, J. A., C. Y. Wong, and T. A. Welton, "Nuclear Collisions in a One-Dimensional Fluid-Dynamical Calculation," *Physics Letters B.*

Maruhn-Rezwani, V., K. T. R. Davies, and S. E. Koonin, "Time-Dependent Hartree-Fock Calculations for ^{14}N + ^{12}C Reactions," *Physics Letters.*

Mateja, J. F., C. P. Browne, C. E. Moss, and J. B. McGrory, "Level Structure of ^{53}Mn from a ^{54}Mn(t,p)^{53}Mn Reaction Study and a Mixed-Configuration Shell Model Calculation," *Physical Review.*

McDaniel, F. D., J. L. Duggan, G. Basbas, P. D. Miller, and G. Lapicki, "Projectile Charge-State Dependence of *K*-Shell Ionization by Silicon Ions: A Comparison of Coulomb Ionization Theories for Direct Ionization and Electron Capture with X-Ray Production Data," *Physical Review*.

McGowan, F. K., W. T. Milner, R. O. Sayer, R. L. Robinson, and P. H. Stelson, "Coulomb Excitation of ^{182,184,186}W and ^{166}Er with ^{4}He and ^{16}O Ions," *Nuclear Physics*.

McGrory, J. B. (invited paper), "Shell Model Calculations of Electromagnetic Observables of Nuclei in the *sd*-Shell Region," *Proceedings, International Conference on Gamma-Ray Transition Probabilities, Delhi, India, November 1974*.

Monk, C. D., "Sources of Protons," *McGraw-Hill Encyclopedia of Science and Technology*, 4th ed., Daniel N. Lapedes, ed., McGraw-Hill, New York.

Monk, C. D., "Channeling in Solids," *McGraw-Hill Encyclopedia of Science and Technology*, 4th ed., Daniel N. Lapedes, ed., McGraw-Hill, New York.

Monk, C. D. (invited paper), "Accelerator-Based Atomic Physics Experiments: An Overview," *IEEE Trans. Nucl. Sci.* (Proceedings of the Fourth Conference on Applications of Small Accelerators, Denton, Tex., October 1976).

Mosko, S. W., E. D. Hudson, R. S. Lord, D. C. Hensley, and J. A. Biggerstaff, "Magnetic Field Measuring System for Remapping the ORIC Magnetic Field," *IEEE Trans. Nucl. Sci.* (Proceedings of the 1977 Particle Accelerator Conference, Chicago, Ill., March 1977).

Mosko, S. W., J. D. Rylander, and G. K. Schulze, "ORIC RF System—Preparation for HHIRF," *IEEE Trans. Nucl. Sci.* (Proceedings of the 1977 Particle Accelerator Conference, Chicago, Ill., March 1977).

Musgrove, A. R. de L., B. J. Allen, J. W. Boldeman, and R. L. Macklin, "Nonstatistical Effects in the Radiative Capture Cross Sections of the Neodymium Isotopes," *Nuclear Physics*.

Musgrove, A. R. de L., B. J. Allen, J. W. Boldeman, and R. L. Macklin, "Nonstatistical Neutron Capture in ^{140}Ce," *Nuclear Physics*.

Musgrove, A. R. de L., B. J. Allen, J. W. Boldeman, and R. L. Macklin, "keV Neutron Resonance Capture in ^{137}Ba," *Australian Journal of Physics*.

Musgrove, A. R. de L., B. J. Allen, and R. L. Macklin, "Resonant Neutron Capture in ^{139}La," *Nuclear Physics*.

Musgrove, A. R. de L., J. W. Boldeman, B. J. Allen, J. A. Harvey, and R. L. Macklin, "High-Resolution Neutron Transmission and Capture for ^{91}Zr," *Nuclear Physics*.

Musgrove, A. R. de L., J. A. Harvey, and W. M. Good, "Neutron Resonance Parameters of ^{90}Zr below 300 keV," *Nuclear Physics*.

Nann, H., E. Kashy, D. Mueller, A. Saha, and S. Raman, "Mass of ^{57}Ni," *Physical Review*.

Nathan, A. M., J. W. Olness, E. K. Warburton, and J. B. McGrory, "Yrast Decay Schemes from Hl + ^{48}Ca Fusion-Evaporation Reactions. I: $^{54-56}$Mn, ^{56}Cr, and ^{52,53}V," *Physical Review*.

Olson, R. E., A. Salop, R. A. Phaneuf, and F. W. Meyer, "Electron Loss by Atomic and Molecular Hydrogen in Collisions with ^{3}He^{2+} and ^{4}He^{+}," *Physical Review A*.

Pegg, D. J., "Beam-Foil Spectroscopy," *Scientific American*.

Pegg, D. J., J. P. Forester, S. B. Elston, P. M. Griffin, K.-O. Groeneveld, R. S. Peterson, R. S. Thoe, C. R. Vane, and I. A. Sellin, "The Splitting and Oscillator Strengths for the $2s^2S$-$2p^2p^0$ Doublet in Lithium-like Sulfur," *Astrophysical Letters*.

Pegg, D. J., J. P. Forester, C. R. Vane, S. B. Elston, P. M. Griffin, K.-O. Groeneveld, R. S. Peterson, R. S. Thoe, and I. A. Sellin, "Oscillator Strengths for $\Delta n + 0$ Dipole Transitions in Li- and Be-like Sulfur: Comparisons with Recent Relativistic Calculations," *Physical Review Letters*.

Pegg, D. J., P. M. Griffin, B. M. Johnson, K. W. Jones, J. L. Cecchi, and T. H. Kruse, "Field-Free Intensity Modulations and 'Yrast' Cascades in Decay Studies of the $n + 3$ Levels of Sodium-like Copper," *Physical Review Letters.*

Peterson, R. S., F. K. Chen, S. B. Elston, J. P. Forester, P. M. Griffin, H. C. Hayden, R. Laubert, C. A. Peterson, R. S. Thoe, C. R. Vane, and I. A. Sellin, "Neon Characteristic X-Ray Production in Neon-Neon Collisions as a Function of Incident Projectile Charge State," *Proceedings, Tenth International Conference on the Physics of Electronic and Atomic Collisions, Paris, France, July 1977.*

Petitt, G. A., and F. E. Obenshain, "Perturbed Angular Correlation of $^{111}Cd^m$ in Nickel-Cadmium Ferrites," *Physical Review B.*

Petitt, G. A., and F. E. Obenshain, "Time Differential Perturbed Angular Correlations Using ^{161}Dy," *Physical Review B.*

Phaneuf, R. A., F. W. Meyer, R. H. McKnight, and D. H. Crandall, "Electron Transfer between Multicharged Ions and Atomic Hydrogen," *Proceedings, Tenth International Conference on Physics of Electron and Atomic Collisions, Paris, France, July 1977.*

Phaneuf, R. A., F. W. Meyer, R. H. McKnight, R. E. Olson, and A. Salop, "Electron Capture and Impact Ionization Cross Sections of N^{+4} in Atomic Hydrogen," *Journal of Physics B* (Letter).

Plasil, F., "De-excitation of Compound Nuclei with High Angular Momenta," *Physical Review* (Communications).

Plasil, F., "Fusion in Kr Bombardments of Medium-Mass Nuclei," *Proceedings, Fifteenth International Winter Meeting on Nuclear Physics, Bormio, Italy, January 1977.*

Rapaport, M. S., R. W. Fink, L. L. Collins, and L. L. Riedinger, "Isomerism in ^{197}Pb," *Physical Review C.*

Reiss, H., H. V. Klapdor, G. Rosner, J. L. C. Ford, Jr., and S. T. Thornton, "Enhanced ^9Be Production in the $^{14}N + {}^{11}B$ Reaction," *Nuclear Physics.*

Roberto, J. B., C. E. Klabunde, J. M. Williams, R. R. Coltman, Jr., M. Saltmarsh, and C. B. Fulmer, "Damage Production by High-Energy *d*-Be Neutrons in Cu, Nb, and Pt at 4.2° K," *Applied Physics Letters.*

Ronningen, R. M., J. H. Hamilton, A. V. Ramayya, L. L. Riedinger, G. Garcia-Bermudez, J. Lange, W. Lourens, L. Varnell, R. L. Robinson, P. H. Stelson, and J. L. C. Ford, Jr., "Reduced Transition Probabilities of Vibrational States in Deformed Rare-Earth Nuclei," *Proceedings, International Conference on Gamma-Ray Transition Probabilities, Delhi, India, November 1974.*

Ronningen, R. M., J. H. Hamilton, A. V. Ramayya, L. Varnell, G. Garcia-Bermudez, J. Lange, W. Lourens, L. L. Riedinger, R. L. Robinson, P. H. Stelson, and J. L. C. Ford, Jr., "Reduced Transition Probabilities of Vibrational States in $^{154-160}Gd$ and $^{176-180}Hf$," *Physical Review.*

Ronningen, R. M., R. B. Piercey, A. V. Ramayya, J. H. Hamilton, S. Raman, P. H. Stelson, and W. K. Dagenhart, "Coulomb Excitation of 2^+ and 3^- States in ^{192}Pt and ^{194}Pt," *Physical Review C.*

Saltmarsh, M. J., C. A. Ludemann, C. B. Fulmer, and R. C. Styles, "Characteristics on an Intense Neutron Source Based on the D + Be Reaction," *Nuclear Instruments and Methods.*

Saltmarsh, M. J., C. A. Ludemann, C. B. Fulmer, and R. C. Styles (invited paper), "Neutron Yields and Dosimetry for Be(*d*,*n*) and Li(*d*,*n*) Neutron Sources at $E_d = 40$ MeV," *Proceedings, International Specialists Symposium on Neutron Standards and Applications, Gaithersburg, Maryland, March 28-31, 1977.*

Satchler, G. R. (invited paper), "The Study of Giant Resonances in Nuclei by Inelastic Scattering," *Proceedings of the International School of Physics "Enrico Fermi," Varenna, Italy, July-August 1976.*

Satchler, G. R., M. L. Halbert, N. M. Clarke, E. E. Gross, C. B. Fulmer, A. Scott, M. D. Cohler, D. C. Hensley, C. A. Ludemann, J. G. Cramer, M. S. Zisman, and R. M. DeVries, "Heavy-Ion Elastic Scattering II: 142-MeV ^{16}O on ^{28}Si, ^{59}Co, and ^{60}Ni," *Nuclear Physics.*

Sayer, R. O., "Semi-Empirical Formulas for Heavy-Ion Stripping Data," *Proceedings, Second International Conference on Electrostatic Accelerator Technology, Strasbourg, France, May 1977.*

Schmorak, M. R., "The Nuclear Data Project Data Bank," *Proceedings, ERDA Symposium on X- and Gamma-Ray Sources and Applications, Ann Arbor, Michigan, May 1976.*

Schumann, S., S. B. Elston, C. R. Vance, J. P. Forester, P. M. Griffin, D. J. Pegg, I. A. Sellin, R. S. Thoe, and J. J. Wright, "Spin-Dependent Excitation of Autoionizing States of Li Produced in Collisions with Noble Gas Targets," *Proceedings, Tenth International Conference on the Physics of Electronic and Atomic Collisions, Paris, France, July 1977.*

Sellin, I. A., S. B. Elston, J. P. Forester, P. M. Griffin, D. J. Pegg, R. S. Peterson, R. S. Thoe, C. R. Vane, J. J. Wright, and K.-O. Groeneveld, "Recoil Ion Spectroscopy in the XUV Soft X-Ray Region Following Heavy-Ion Impact on Thin Gas Targets," *Proceedings, Tenth International Conference on the Physics of Electronic and Atomic Collisions, Paris, France, July 1977.*

Sellin, I. A., S. B. Elston, J. P. Forester, P. M. Griffin, D. J. Pegg, R. S. Peterson, R. S. Thoe, C. R. Vane, J. J. Wright, K.-O. Groeneveld, R. Laubert, and F. Chen, "Production of Soft X-Ray-Emitting Slow Multiply Charged Ions: Recoil Ion Spectroscopy," *Physics Letters A.*

Stelson, P. H., "Coulomb Excitation," *McGraw-Hill Encyclopedia of Science and Technology*, 4th ed., Daniel N. Lapedes, ed., McGraw-Hill, New York.

Stokstad, R. G., R. A. Dayras, J. Gomez del Campo, P. H. Stelson, C. Olmer, and M. S. Zisman, "Measurements of the Fusion of $^{12}C + {}^{14}N$ and the Liquid-Drop Limit for ^{26}Al," *Physics Letters.*

Thoe, R. S., R. S. Peterson, D. J. Pegg, J. P. Forester, P. M. Griffin, H. C. Hayden, and I. A. Sellin, "Polarization Measurements on Noncharacteristic Radiations Emitted in Energetic Heavy-Ion Atom Collisions," *Physical Review A.*

Tricomi, J., J. L. Duggan, F. D. McDaniel, P. D. Miller, R. P. Chaturvedi, R. M. Wheeler, J. Lin, K. A. Kuenhold, L. A. Rayburn, and S. J. Cipolla, "*K* Shell X-Ray Production in Ge, Rb, Y, Zr, and Ag by ^{14}N Ion Impact," *Physical Review.*

Van der Borg, K., M. N. Harakeh, S. Y. van der Werf, A. van der Woude, and F. E. Bertrand, "A High-Resolution Study of the Giant Resonance Region in ^{28}Si by Inelastic Alpha-Particle Scattering," *Physics Letters.*

Vane, C. R., I. A. Sellin, F. Chen, S. B. Elston, J. P. Forester, P. M. Griffin, K.-O. Groeneveld, R. Laubert, D. J. Pegg, R. S. Peterson, R. S. Thoe, and J. J. Wright, "High-Resolution Studies of Extensive Ne *L*-Shell Excitation by Energetic Heavy-Ion Impact," *Proceedings, Tenth International Conference on the Physics of Electronic and Atomic Collisions, Paris, France, July 1977.*

Wagner, G. J., K. T. Knopfle, G. Mairle, P. Doll, H. Hafner, and J. L. C. Ford, Jr., "A Strong Effect of Isospin Mixing in ^{16}O," *Physical Review Letters.*

Wells, G. W., "The Heavy-Ion Simulated Neutron Damage Facility at Oak Ridge National Laboratory," *Proceedings, Fourth Conference on Application of Small Accelerators, Denton, Texas, October 1976.*

Welton, T. A., "Optimized Programs for Testing Image Processing Algorithms," *Proceedings, Thirty-fifth Annual Meeting of the Electron Microscopy Society of America, Boston, Massachusetts, August 1977.*

Wong, C. Y., "Quantum Stress Tensor and Density Oscillations," *Physical Review Letters.*

Wong, C. Y., "Some Nuclear Spin and Isospin Properties in the Hydrodynamical Model," *Physics Letters.*

Wong, C. Y., and J. A. McDonald, "Dynamics of Nuclear Fluid III: General Considerations on the Kinetic Theory of Quantum Fluids," *Physical Review.*

Worsham, R. E., "Field Emission Gun for a 150-kV CTEM," *Proceedings, Analytical Electron Microscopy Workshop, Ithaca, New York, August 1976.*

Worsham, R. E., and J. E. Mann, "A Liquid-Helium Cryostat for a Superconducting Objective and Cold Stage," *Proceedings, Sixth European Congress on Electron Microscopy, Jerusalem, Israel, September 1976.*

9. Papers Presented at Scientific and Technical Meetings

Prepared by Wilma L. Stair

American Physical Society Meeting (Topical Conference on Diagnostics of High-Temperature Plasmas), Knoxville, Tennessee, January 7-9, 1976

D. P. Hutchinson and K. L. Vander Sluis, "Development of a Far-Infrared Laser for Ion Thomson Scattering," *Bull. Am. Phys. Soc.* 21, 848 (1976).

International Workshop IV on Gross Properties of Nuclei and Nuclear Excitations, Hirschegg, Austria, January 12-17, 1976

C. Y. Wong and K. S. Low, "Time-Dependent Hartree-Fock Formalism with Phenomenological Dissipation."

International Research Workshop on Atomic, Molecular, and Solid-State Theory, Sanibel Island, Florida, January 15-17, 1976

T. A. Carlson (invited talk), "Use of Quantum Chemistry in Photoelectron Spectroscopy."

Annual Symposium on Applied Vacuum Science and Technology, Tampa, Florida, February 2-4, 1976

J. W. Johnson, "Evaluation of Vacuum Components for Beam Lines for the ORNL 25-MV Heavy-Ion Accelerator."

American Physical Society Meeting, New York, New York, February 2-5, 1976

C. D. Goodman, W. R. Wharton, and D. C. Hensley, "The Reaction $^{14}C(^6Li,^6He)^{14}N$ and the Distribution of Gamow-Teller Strength," *Bull. Am. Phys. Soc.* 21, 82 (1976).

M. A. Ijaz, K. S. Toth, J. Lin, and F. L. Robinson, "Alpha-Decay Studies of Thallium and Mercury Isotopes with $A \leq 186$," *Bull. Am. Phys. Soc.* 21, 96 (1976).

D. C. Kocher and F. E. Bertrand, "Study of the Giant Resonance Region in ^{208}Pb via the (p,p') Reaction," *Bull. Am. Phys. Soc.* 21, 30 (1976).

R. Mehta, J. L. Duggan, F. D. McDaniel, G. Monigold, P. D. Miller, R. P. Chaturvedi, R. M. Wheeler, K. Kuenhold, J. Lin, and L. A. Rayburn, "Production of K X Rays by 4- to 38-MeV Boron Ions Incident on Selected Elements from Cu to Sr," *Bull. Am. Phys. Soc.* 21, 33 (1976).

G. A. Petitt and F. E. Obenshain, "DPAC Measurements with ^{161}Dy in Gd_2O_3 at High Temperature," *Bull. Am. Phys. Soc.* 21, 22 (1976).

International Conference on Surface Effects in Controlled Fusion Devices, San Francisco, California, February 16-20, 1976

B. R. Appleton, R. H. Ritchie, J. A. Biggerstaff, T. S. Noggle, S. Datz, C. D. Moak, and H. Verbeek, "Energetic Heavy-Ion Channeling as an Experimental Technique for Simulating Radiative Electron Capture by Plasma and Impurity Ions in a CTR Type Plasma."

Workshop on Electron Microscopy of Biological Materials at Atomic Resolution, Pacific Grove, California, March 16–19, 1976

T. A. Welton (invited talk), "Theoretical Simulations."

Symposium on Macroscopic Features of Heavy-Ion Collisions, Argonne, Illinois, April 1–3, 1976

J. P. Bondorf, P. J. Siemens, H. Feldmeier, S. Garpman, and E. C. Halbert, "Classical Microscopic Description of Fast Heavy-Ion Collisions."

M. L. Halbert, R. G. Stokstad, R. L. Ferguson, F. E. Obenshain, D. C. Hensley, A. H. Snell, F. Plasil, and F. Pleasonton, "Strongly Damped Collisions of ^{20}Ne on Ni."

J. A. Maruhn, R. Y. Cusson, and R. K. Smith, "T.D.H.F. Study of the Reaction ^{16}O + ^{16}O at Finite Impact Parameters in Three Dimensions."

L. D. Rickertsen, G. R. Satchler, R. M. Wieland, and R. G. Stokstad, "Macroscopic Folding Form Factors for ^{12}C-^{12}C Inelastic Scattering."

G. R. Satchler (invited talk), "Potential Model Description of Heavy-Ion Elastic and Inelastic Scattering."

R. G. Stokstad, J. Gomez del Campo, J. A. Biggerstaff, A. H. Snell, and P. H. Stelson, "The Fusion of ^{14}N + ^{12}C at High Energies."

American Chemical Society Meeting (Division of Nuclear Chemistry and Technology), New York, New York, April 4–9, 1976

K. S. Toth (invited talk), "Alpha Decay Systematics for Elements with $50 < Z < 83$."

Workshop on Deep Inelastic Processes and Compound Nucleus Formation in Heavy-Ion Reactions, Stony Brook, Long Island, New York, April 23–25, 1976

F. Plasil (invited talk), "Fission and Fusion Induced with Ar, Cu, and Kr Ions."

R. G. Stokstad (invited talk), "Studies of Deep Inelastic Reactions at the ORIC."

American Physical Society Meeting, Washington, D.C., April 26–29, 1976

G. D. Alton, M. Reeves, and W. R. Garrett, "Optical-Model Analysis of Electron and Positron Scattering from Atomic Hydrogen," *Bull. Am. Phys. Soc.* 21, 574 (1976).

J. B. Ball, C. B. Fulmer, and R. L. Robinson, "Light-Particle Emission from Heavy-Ion Reactions," *Bull. Am. Phys. Soc.* 21, 680 (1976).

J. E. Bayfield, P. M. Koch, L. D. Gardner, I. A. Sellin, D. J. Pegg, R. S. Peterson, D. H. Crandall, and M. L. Mallory, "Single and Double Electron Transfer in B^{q+} (q + 2, 3, 4) Collisions with He, Ar, and H_2," *Bull. Am. Phys. Soc.* 21, 549 (1976).

R. L. Becker and N. M. Larson, "Second-Order Brueckner Calculations for ^{40}Ca," *Bull. Am. Phys. Soc.* 21, 640 (1976).

F. E. Bertrand (invited talk), "Excitation of New Giant Resonances in Nuclei by Inelastic Scattering," *Bull. Am. Phys. Soc.* 21, 678 (1976).

F. E. Bertrand, D. C. Kocher, and E. E. Gross, "Inelastic Proton Excitation of Giant Resonances in *sd*-Shell Nuclei," *Bull. Am. Phys. Soc.* 21, 516 (1976).

R. R. Carlton, S Raman, and G. G. Slaughter, "Capture Gamma Rays from ^{122}Sn + n and ^{124}Sn + n Systems," *Bull. Am. Phys. Soc.* 21, 634 (1976).

T. P. Cleary, J. L. C. Ford, Jr., J. Gomez del Campo, E. E. Gross, D. C. Hensley, K. S. Toth, and S. T. Thornton, "Single-Particle Transfer Reactions Induced by ^{12}C on ^{208}Pb," *Bull. Am. Phys. Soc.* 21, 579 (1976).

L. L. Collins, L. L. Riedinger, G. D. O'Kelley, C. R. Bingham, J. L. Wood, R. W. Fink, E. H. Spejewski, and H. K. Carter, "Triaxial Band in ^{195}Tl," *Bull. Am. Phys. Soc.* 21, 559 (1976).

J. W. T. Dabbs (invited talk), "The Nuclear Fuel Cycle and Actinide Wastes: Cross-Section Needs and Recent Measurements," *Bull. Am. Phys. Soc.* 21, 507 (1976).

S. Datz, P. F. Dittner, J. Gomez del Campo, P. D. Miller, and J. A. Biggerstaff, "Screening by Bound *K* Electrons in Electric Stopping," *Bull. Am. Phys. Soc.* 21, 689 (1976).

R. A. Dayras, M. L. Halbert, D. C. Hensley, C. B. Fulmer, and R. G. Stokstad, "Deep-Inelastic Collisions in the $^{12}C + ^{63}Cu$ Reactions," *Bull. Am. Phys. Soc.* 21, 606 (1976).

S. B. Elston, D. J. Pegg, P. M. Griffin, J. P. Forester, H. C. Hayden, R. S. Peterson, R. S. Thoe, and I. A. Sellin, "Lifetimes and Spectra of Highly Ionized Sulfur," *Bull. Am. Phys. Soc.* 21, 626 (1976).

H. Feldmeier, K. T. R. Davies, V. Maruhn-Rezwani, S. E. Koonin, S. J. Krieger, and J. W. Negele, "Time-Dependent Hartree-Fock Calculations for $^{16}O + ^{16}O$ and $^{40}Ca + ^{40}Ca$ Reactions," *Bull. Am. Phys. Soc.* 21, 511 (1976).

J. L. C. Ford, Jr., R. L. Robinson, P. H. Stelson, J. Gomez del Campo, M. E. Ortiz, A. Dacal, and S. T. Thornton, "Coherence Widths in ^{28}Si Measured by the $^{12}C(^{16}O,\alpha)$ Reaction," *Bull. Am. Phys. Soc.* 21, 679 (1976).

J. L. Fowler, C. H. Johnson, and N. W. Hill, "Resonant States of ^{209}Pb from Neutron Total Cross-Section Measurements," *Bull. Am. Phys. Soc.* 21, 537 (1976).

C. B. Fulmer, D. C. Hensley, S. Raman, A. H. Snell, P. H. Stelson, R. G. Stokstad, and R. M. Wieland, "$^{12}C + ^{12}C$ Transfer Reactions," *Bull. Am. Phys. Soc.* 21, 579 (1976).

J. Gomez del Campo and R. G. Stokstad, "Monte-Carlo Caiculations of Evaporation Residues from the $^{14}N + ^{12}C$ Reaction," *Bull. Am. Phys. Soc.* 21, 657 (1976).

G. M. Gowdy, J. L. Wood, R. W. Fink, E. F. Zganjar, and A. G. Schmidt, "Systematics of the Levels in the Neutron-Deficient Odd-Mass Mercuries," *Bull. Am. Phys. Soc.* 21, 559 (1976).

E. E. Gross, T. P. Cleary, D. C. Hensley, R. G. Stokstad, K. S. Toth, and E. V. Hungerford, "Decay-in-Flight Measurements of Alpha Activity," *Bull. Am. Phys. Soc.* 21, 681 (1976).

M. L. Halbert, R. G. Stokstad, D. C. Hensley, F. E. Obenshain, F. Plasil, R. L. Ferguson, and F. Pleasonton, "Deep Inelastic Reactions Induced by 164- and 173-MeV ^{20}Ne or Ni," *Bull. Am. Phys. Soc.* 21, 607 (1976).

J. A. Harvey, J. Halperin, N. W. Hill, and S. Raman, "(n,α) and (n,p) Measurements on ^{59}Ni," *Bull. Am. Phys. Soc.* 21, 536 (1976).

D. C. Hensley, R. G. Stokstad, M. L. Halbert, R. A. Dayras, and C. B. Fulmer, "Deep Inelastic Reactions Induced by 113-MeV ^{16}O Bombardment of Ni," *Bull. Am. Phys. Soc.* 21, 606 (1976).

D. J. Horen, J. A. Harvey, C. H. Johnson, and N. W. Hill, "$(d + s)$-Wave Admixture in the 256.25-keV Resonance in $^{207}Pb + n$," *Bull. Am. Phys. Soc.* 21, 582 (1976).

P. G. Huray, C. M. Tung, J. O. Thomson, and F. E. Obenshain, "Electron Charge Density Distributions Surrounding Impurity Atoms in Gold Metal," *Bull. Am. Phys. Soc.* 21, 566 (1976).

A. C. Kahler, C. R. Bingham, L. L. Riedinger, R. L. Mlekodaj, A. G. Schmidt, J. L. Wood, R. W. Fink, and J. H. Hamilton, "Decay of ^{193}Pb," *Bull. Am. Phys. Soc.* 21, 559 (1976).

H. J. Kim, R. L. Robinson, W. K. Tuttle III, R. Ronningen, R. O. Sayer, and J. C. Wells, Jr., "^{50}Cr High-Spin States," *Bull. Am. Phys. Soc.* 21, 680 (1976).

F. D. McDaniel, J. L. Duggan, J. Tricomi, P. D. Miller, K. A. Kuenhold, F. Elliott, J. Lin, R. M. Wheeler, and R. P. Chaturvedi, "X-Ray Production for ^{14}N Ions Incident on Thin Targets of Elements from Ti to Zn." *Bull. Am. Phys. Soc.* 21, 650 (1976).

J. A. McDonald and C. Y. Wong, "General Considerations on the Kinetic Theory of Nuclear Fluid." *Bull. Am. Phys. Soc.* 21, 560 (1976).

R. L. Mlekodaj, E. H. Spejewski, H. K. Carter, and A. G. Schmidt, "Target-Ion Sources for Mass Separators On-Line with Heavy-Ion Beams." *Bull. Am. Phys. Soc.* 21, 611 (1976).

G. Monigold, F. D. McDaniel, J. L. Duggan, R. Mheta, P. D. Miller, J. Lin, K. A. Kuenhold, R. P. Chaturvedi, R. M. Wheeler, C. J. Cipolla, and L. A. Rayburn, "*K*-Shell X-Ray Production Cross Sections of Selected Elements P to Ni for 0.4–3.8 MeV/amu ^{10}B Ions." *Bull. Am. Phys. Soc.* 21, 651 (1976).

C. Ngo, S. Ouichaoui, J. Peter, F. Plasil, B. Tamain, M. Berlanger, and F. Hanappe, "Quasi-fission from ^{197}Au + ^{40}Ar at 220 MeV," *Bull. Am. Phys. Soc.* 21, 606 (1976).

D. J. Pegg (invited talk), "Beam-Foil Studies of Highly Ionized Atoms," *Bull. Am. Phys. Soc.* 21, 508 (1976).

D. J. Pisano, K. W. Jones, P. Griffin, D. Pegg, I. Sellin, T. Kruse, and S. Bashkin, "Beam-Foil Radiative Lifetime Measurements in SiIX-SiXII," *Bull. Am. Phys. Soc.* 21, 689 (1976).

S. Raman, G. G. Slaughter, and R. F. Carlton, "The ^{118}Sn$(n,\gamma)^{119}$Sn Reaction," *Bull. Am. Phys. Soc.* 21, 634 (1976).

A. D. Ray, F. D. McDaniel, J. L. Duggan, J. Tricomi, P. D. Miller, J. Lin, L. A. Rayburn, and F. Elliott, "*L*-Shell X-Ray Production in Sm, Gd, Ho, Yb, Au, and Pb by Incident 7- to 35-MeV ^{14}N Ions," *Bull. Am. Phys. Soc.* 21, 650 (1976).

R. L. Robinson and J. K. Bair, "Total Reaction Cross Section near the Coulomb Barrier for ^{16,18}O, Cu, Zn Systems," *Bull. Am. Phys. Soc.* 21, 680 (1976).

A. G. Schmidt, G. M. Gowdy, R. W. Fink, and C. R. Bingham, "The Decay of Mass-Separated ^{197}Tl," *Bull. Am. Phys. Soc.* 21, 559 (1976).

M. Schmorak, "Alpha-Decay Systematics for the Heavy Nuclides," *Bull. Am. Phys. Soc.* 21, 583 (1976).

R. G. Stokstad, J. Gomez del Campo, A. H. Snell, J. A. Biggerstaff, and P. H. Stelson, "The Fusion of ^{14}N + ^{12}C at Energies up to $E(^{14}\text{N}) = 178$ MeV," *Bull. Am. Phys. Soc.* 21, 656 (1976).

R. G. Stokstad, D. C. Hensley, and A. H. Snell, "A Position-Sensitive ΔE-E Counter Telescope," *Bull. Am. Phys. Soc.* 21, 657 (1976).

R. S. Thoe, J. P. Forester, D. J. Pegg, R. S. Peterson, K. H. Liao, and I. A. Sellin, "Radiative Electron Capture Cross Sections for High-Energy Al-Al and Al-C Collisions," *Bull. Am. Phys. Soc.* 21, 650 (1976).

R. S. Thoe, J. P. Forester, R. S. Peterson, D. J. Pegg, P. M. Griffin, K. H. Liao, and I. A. Sellin, "Characteristic *K* X-Ray Production from High-Energy Al-Al Collisions," *Bull. Am. Phys. Soc.* 21, 650 (1976).

K. S. Toth, J. L. C. Ford, Jr., G. R. Satchler, E. E. Gross, D. C. Hensley, S. T. Thornton, and T. C. Schweizer, "Analysis for the (^{12}C,^{13}C) and (^{12}C,^{11}B) Reactions Induced by ^{12}C on ^{208}Pb," *Bull. Am. Phys. Soc.* 21, 579 (1976).

G. J. Wagner, K. T. Knopfle, G. Mairle, J. L. C. Ford, Jr., and S. T. Thornton, "A Puzzling Case of Strong Isospin Mixing in ^{16}O," *Bull. Am. Phys. Soc.* 21, 514 (1976).

J. C. Wells, Jr., S. Raman, and G. G. Slaughter, "Energy Levels in ^{146}Nd from Resonance Neutron Capture in Gamma-Ray Measurements," *Bull. Am. Phys. Soc.* 21, 657 (1976).

R. M. Wieland, R. G. Stokstad, G. R. Satchler, and L. D. Rickertsen, "Analysis of ^{12}C + ^{12}C Elastic Scattering with Folded-Model Potentials," *Bull. Am. Phys. Soc.* 21, 578 (1976).

C. Y. Wong (invited talk), "Dynamics of Nuclear Fluid in Heavy-Ion Collisions," *Bull. Am. Phys. Soc.* 21, 530 (1976).

Ninth International Conference on Electromagnetic Isotope Separators and Related Ion Accelerators, Kibbutz, Kiryat Anavim, Israel, May 10–13, 1976

H. K. Carter, E. H. Spejewski, R. L. Mlekodaj, A. G. Schmidt, F. T. Avignone, C. R. Bingham, R. A. Braga, J. D. Cole, A. V. Ramayya, E. L. Robinson, K. S. R. Sastry, and E. F. Zganjar, "The UNISOR ISOL Data Acquisition."

R. L. Mlekodaj, E. H. Spejewski, H. K. Carter, and A. G. Schmidt, "The UNISOR Integrated Target-Ion Source."

ERDA Symposium on X- and Gamma-Ray Sources and Applications, Ann Arbor, Michigan, May 19–21, 1976

M. R. Schmorak and M. J. Martin, "The Nuclear Data Project Data Bank."

Third International Conference on Nuclei Far from Stability, Cargèse, Corsica, France, May 19–26, 1976

J. D. Cole, J. H. Hamilton, A. V. Ramayya, K. S. Toth, M. A. Ijaz, E. L. Robinson, J. Lin, W. H. Brantley, K. S. R. Sastry, P. V. G. Rao, E. H. Spejewski, and R. L. Mlekodaj, "New Isotope ^{184}Tl and the Excited Deformed Band in ^{184}Hg."

J. L. Wood, R. W. Fink, E. F. Zganjar, R. L. Mlekodaj, L. L. Riedinger, and C. R. Bingham, "The Structure of Neutron-Deficient Odd-Mass Nuclei in the Au, Tl Region: Evidence for Coexisting Triaxial Shapes and a Two-Component Pairing Force."

J. L. Wood, G. M. Gowdy, R. W. Fink, D. A. McClure, M. S. Rapaport, R. A. Braga, E. H. Spejewski, R. L. Mlekodaj, H. K. Carter, A. G. Schmidt, J. D. Cole, A. V. Ramayya, J. H. Hamilton, H. Kawakami, E. F. Zganjar, C. R. Bingham, L. L. Riedinger, A. C. Kahler, L. L. Collins, E. L. Robinson, J. Lin, B. D. Kern, J. L. Weil, K. S. R. Sastry, F. T. Avignone, M. A. Ijaz, and K. S. Toth, "Recent Work at UNISOR on Neutron-Deficient Au, Hg, and Tl Nuclei in the Mass Range $184 \leqslant A \leqslant 197$."

E. F. Zganjar, G. M. Gowdy, J. L. Wood, R. W. Fink, A. G. Schmidt, H. K. Carter, R. L. Mlekodaj, and E. H. Spejewski, "The Structure of the Light Odd-Neutron Hg and Pt Nuclei."

Southeast Electron Microscopy Society Meeting, Orlando, Florida, May 21–22, 1976

R. E. Worsham, J. E. Mann, E. G. Richardson, and N. F. Ziegler, "A 150-kV High-Coherence Microscope."

1976 National Computer Conference, New York, New York, June 7–10, 1976

C. A. Ludemann, "Raise Your Hand if You Know What CAMAC Is!"

American Nuclear Society Meeting, Toronto, Canada, June 13–18, 1976

R. L. Auble, "The NDP Nuclear Structure Information System."

M. J. Saltmarsh, "*d*-Li Neutron Sources Application to the CTR Materials Program."

International Conference on Selected Topics in Nuclear Structure, Dubna, U.S.S.R., June 15–19, 1976

A. P. deLima, B. van Nooijen, R. M. Ronningen, H. Kawakami, J. H. Hamilton, A. V. Ramayya, R. B. Piercey, R. L. Robinson, H. J. Kim, and W. K. Tuttle, "High-Spin States and Possible Band Crossings in ^{74}Ge."

R. B. Piercey, A. V. Ramayya, R. M. Ronningen, J. H. Hamilton, R. L. Robinson, and H. J. Kim, "Evidence for an Octupole Rotational Band in ^{74}Se."

Gordon Research Conference on Nuclear Chemistry, New London, New Hampshire, June 21–25, 1976

F. Plasil (invited talk), "Quasi-fission and Compound Nucleus Reactions."

K. S. Toth (invited talk), "Heavy-Element Production at Dubna and Elsewhere: What Are We Learning?"

International Conference on Radial Shape of Nuclei, Cracow, Poland, June 22–25, 1976

G. Bagieu, A. J. Cole, R. deSwiniarski, C. B. Fulmer, D. H. Koang, and G. Mariolopoulos, "Optical-Model Analysis of 41-MeV Alpha Particles Scattering from ^{28,29,30}Si and ^{27}Al and Nuclear Matter Distribution."

Fifth International CODATA Conference, Boulder, Colorado, June 28–July 1, 1976

W. B. Ewbank, "Computer Processing of 'Free-Text' Keyword Strings."

W. B. Ewbank, "Evaluated Nuclear Structure Data File (ENSDF) for Basic and Applied Research."

International Conference on the Interaction of Neutrons with Nuclei, Lowell, Massachusetts, July 6–9, 1976

J. W. T. Dabbs, N. W. Hill, C. E. Bemis, and S. Raman, "Fission Cross-Section Measurements on ^{244}Cm and ^{243}Cm."

J. L. Fowler (invited talk), "Neutrons and Energy."

J. A. Harvey, "Neutron Resonances: Neutron Reaction Mechanisms and Nuclear Structure."

D. J. Horen, J. A. Harvey, and N. W. Hill, "Resonances in ^{207}Pb + n Including $d + s$ Wave Admixture."

C. H. Johnson, S. K. Penny, J. K. Bair, and C. M. Jones, "Competition of Gamma-Ray and Neutron Emission above the Sn(p,n) Thresholds."

S. F. Mughabghab, A. I. Namenson, G. G. Slaughter, and S. Raman, "Search for Nonstatistical Effects in ^{174}Yb(n,γ)^{175}Yb."

S. F. Mughabghab, O. Wasson, G. G. Slaughter, and S. Raman, "Determination of Parity of ^{95}Mo Resonances with Low-Energy Gamma Rays."

S. Raman, N. W. Hill, J. Halperin, and J. A. Harvey, "Angular Anisotropy in the ^{6}Li(n,α)^{3}H Reaction in the eV and keV Energy Region."

R. R. Winters, E. D. Earle, J. A. Harvey, and R. L. Macklin, "The Neutron Strength Functions and Radiation Widths of ^{209}Tl Resonances."

Fifth International Conference on Atomic Physics, Berkeley, California, July 26–30, 1976

C. F. Barnett (invited talk), "Role of Impurities in Magnetically Confined High-Temperature Plasmas."

J. E. Bayfield, P. M. Koch, L. D. Gardner, I. A. Sellin, D. J. Pegg, R. S. Peterson, and D. H. Crandall, "An Experimental Survey of Electron Transfer in keV Collisions of Multiply Charged Ions with Atomic Hydrogen."

D. J. Pegg, S. B. Elston, J. P. Forester, P. M. Griffin, H. C. Hayden, R. S. Peterson, I. A. Sellin, and R. S. Thoe, "Lifetimes and Transition Rates for Allowed 'In-Shell' Transitions in Highly Stripped Sulfur."

Enrico Fermi International School of Physics, Varenna, Italy, July 26–August 7, 1976

G. R. Satchler (lecture series), "The Study of Giant Resonances in Nuclei by Inelastic Scattering."

Gordon Research Conference on Particle Solid Interactions, Andover, New Hampshire, August 2–6, 1976

C. F. Barnett (invited talk), "CTR Fusion Research."

Analytical Electron Microscopy Workshop, Ithaca, New York, August 3–6, 1976

R. E. Worsham, "Field Emission Gun for a 150-kV CTEM."

Thirty-fourth Annual Meeting Electron Microscopy Society of America, Miami, Florida, August 9–13, 1976

T. A. Welton (invited talk), "Clean Calculations for Dirty Data: Fourier Optics for the Practicing Electron Microscopist."

T. A. Welton, "Synthetic Electron Micrographs for the Study of Reconstruction Algorithms."

R. E. Worsham and J. E. Mann, "A Liquid-Helium Cryostat for a Superconducting Objective and Cold Stage."

European Conference on Nuclear Physics with Heavy Ions, Caen, France, September 6–10, 1976

J. B. Ball, J. A. Martin, J. A. Biggerstaff, C. M. Jones, R. S. Lord, and R. L. Robinson, "The Holifield Heavy-Ion Research Facility at Oak Ridge."

A. P. de Lima, J. H. Hamilton, A. V. Ramayya, R. van Nooijen, R. M. Ronningen, H. Kawakami, R. B. Piercey, R. L. Robinson, H. J. Kim, W. K. Tuttle, and L. K. Peker, "Anomalous Behavior of Yrast States in ^{74}Ge."

H. J. Kim, R. L. Robinson, W. K. Tuttle III, R. Ronninger, R. O. Sayer, and J. C. Wells, Jr., "^{50}Cr High-Spin States."

S. Koonin, V. Maruhn-Rezwani, K. T. R. Davies, H. Feldmeier, S. J. Krieger, and J. W. Negele, "Microscopic Calculation of Energy Loss in Heavy-Ion Collisions."

W. G. Love and G. R. Satchler, "A New Interaction for Heavy-Ion Scattering."

R. B. Piercey, A. V. Ramayya, J. H. Hamilton, R. M. Ronningen, R. L. Robinson, and H. J. Kim, "Band Structure in ^{74}Se."

L. D. Rickertsen and G. R. Satchler, "On the Single-Folding Model for Heavy-Ion Potentials."

R. L. Robinson, H. J. Kim, R. O. Sayer, J. C. Wells, Jr., and R. M. Ronningen, "High-Spin States in ^{70}Ge."

International Conference on the Applications of the Mössbauer Effect, Corfu, Greece, September 13–17, 1976

P. G. Huray, C. M. Tung, F. E. Obenshain, and J. O. Thomson, "Character of the Charge Density Distribution Surrounding Impurities in Gold Metal."

Sixth European Congress on Electron Microscopy, Jerusalem, Israel, September 14–20, 1976

R. E. Worsham and J. E. Mann, "A Liquid-Helium Cryostat for a Superconducting Objective and Cold Stage."

Optical Society of America Meeting, Tucson, Arizona, October 17–21, 1976

J. J. Cowan, "Holography with Optical Guided Waves."

J. J. Cowan, "Blazed and High-Line Density Holographic Gratings Produced by Use of Optical Guided Waves."

Fourth Conference on Use of Small Accelerators in Research, Teaching, and Industrial Applications (APS Topical Conference), Denton, Texas, October 25–27, 1976

D. H. Crandall (invited talk), "Electron Capture by Multicharged Ions," *Bull. Am. Phys. Soc.* 21, 1327 (1976).

K. A. Kuenhold, J. L. Duggan, F. D. McDaniel, A. D. Ray, A. Zander, and P. D. Miller (invited talk), "Production of *L* X Rays by 9.5- to 41.8-MeV Fluorine Ions Incident on Six Elements from Pr to Bi."

C. D. Moak (invited talk), "Accelerator-Based Atomic Physics Experiments: An Overview," *Bull. Am. Phys. Soc.* 21, 1320 (1976).

G. Monigold, F. D. McDaniel, J. L. Duggan, R. Mehta, R. Rice, and P. D. Miller (invited talk), "*K*-Shell X-Ray Production Cross Sections of Selected Elements Al to Ni for 4.0 to 38.0 MeV," *Bull. Am. Phys. Soc.* 21, 1323 (1976).

I. A. Sellin (invited talk), "Overcoming the Doppler Limitation in Beam-Foil Experiments by Target Ion Spectroscopy," *Bull. Am. Phys. Soc.* 21, 1333 (1976).

G. F. Wells, "The Heavy-Ion Simulated Neutron Damage Facility at Oak Ridge National Laboratory," *Bull. Am. Phys. Soc.* 21, 1341 (1976).

American Physical Society Meeting, East Lansing, Michigan, October 28–30, 1976

B. Anderson, A. Baldwin, J. Knudson, T. Witten, R. Madey, C. D. Goodman, D. E. Bainum, J. Rapaport, and C. C. Foster, "Neutron Spectra at 9.3° from ^{9}Be(p,n) and ^{13}C(p,n) Reaction at 61.8 MeV," *Bull. Am. Phys. Soc.* 21, 978 (1976).

G. Bagieu, A. J. Cole, R. de Swiniarski, D. H. Koang, G. Mariolopoulo., C. B. Fulmer, and I.. D. Rickertsen, "45-MeV ^{3}He Elastic Scattering from ^{27}Al, ^{28,29,30}Si," *Bull. Am. Phys. Soc.* 21, 986 (1976).

F. T. Baker, A. Scott, T. P. Cleary, J. L. C. Ford, Jr., E. E. Gross, and D. C. Hensley, "Inelastic ^{12}C Scattering from ^{194}Pt," *Bull. Am. Phys. Soc.* 21, 970 (1976).

M. D. Barker, J. D. Galambos, A. C. Rester, H. Kawakami, A. deLima, R. M. Ronningen, J. H. Hamilton, H. K. Carter, R. L. Mlekodaj, and E. H. Spejewski, "Exploratory Studies in the Mass Region $A = 60$ to 80 Far from Stability," *Bull. Am. Phys. Soc.* 21, 968 (1976).

K. R. Cordell, S. T. Thornton, L. C. Dennis, T. C. Schweizer, J. L. C. Ford, Jr., and J. Gomez del Campo, "Excitation Functions of the ^{12}C(^{14}N,α)^{22}Na Reaction," *Bull. Am. Phys. Soc.* 21, 970 (1976).

C. D. Goodman, M. B. Greenfield, C. A. Goulding, and C. C. Foster, "A Beam Swinger for Neutron Time-of-Flight Experiments at IUCF," *Bull. Am. Phys. Soc.* 21, 1007 (1976).

E. E. Gross, T. P. Cleary, J. L. C. Ford, Jr., D. C. Hensley, and K. S. Toth, "Nuclear Shapes from ^{20}Ne + ^{208}Pb," *Bull. Am. Phys. Soc.* 21, 985 (1976).

E. D. Hudson and M. L. Mallory, "Enhancement of Cyclotron Beam Intensity by Using an Easily Ionized Support Gas in the Ion Source," *Bull. Am. Phys. Soc.* 21, 988 (1976).

M. A. Ijaz, K. S. Toth, J. Lin, E. L. Robinson, C. R. Bingham, and H. K. Carter, "Observation of Alpha Decay in ^{184,185,186,187}Tl," *Bull. Am. Phys. Soc.* 21, 975 (1976).

C. H. Johnson, J. K. Bair, C. M. Jones, S. K. Penny, and D. W. Smith, "P-Wave Size Resonances Observed by 2.6- to 7-MeV Protons Incident on Isotopes of Sn," *Bull. Am. Phys. Soc.* 21, 987 (1976).

N. R. Johnson, S. W. Yates, R. M. Ronningen, R. D. Hichwa, L. L. Riedinger, and A. C. Kahler, "Properties of ^{164}Er in the Band Crossing Region," *Bull. Am. Phys. Soc.* 21, 984 (1976).

A. C. Kahler, L. L. Riedinger, P. Hubert, N. R. Johnson, E. Eichler, R. L. Robinson, and G. J. Smith, "In-Beam Spectroscopy of ^{191,193}Tl," *Bull. Am. Phys. Soc.* 21, 976 (1976).

H. Kawakami, P. A. deLima, R. M. Ronningen, J. H. Hamilton, A. V. Ramayya, R. L. Robinson, and H. J. Kim, "Level Structure of ^{65}Ga," *Bull. Am. Phys. Soc.* 21, 968 (1976).

C. H. King, B. A. Brown, T. L. Khoo, E. Eichler, N. R. Johnson, A. C. Kahler, L. L. Riedinger, and A. G. Schmidt, "High-Spin States in ^{146,147,148,149}Sm," *Bull. Am. Phys. Soc.* 21, 1004 (1976).

W. G. Love, "Microscopic Description of Sn(p,n) Reactions," *Bull. Am. Phys. Soc.* 21, 963 (1976).

D. Malbrough, R. D. Edge, C. W. Darden, T. Marks, B. M. Preedom, F. E. Bertrand, E. E. Gross, C. A. Ludemann, M. J. Saltmarsh, R. L. Burman, R. P. Redwine, K. Gotow, and M. Moinester, "Measurements of Pion-Nuclear Elastic Scattering at Low Energies," *Bull. Am. Phys. Soc.* 21, 983 (1976).

M. L. Mallory, K. W. Fischer, and E. D. Hudson, "Space Charge Beam Loss in Heavy-Ion Cyclotrons," *Bull. Am. Phys. Soc.* 21, (1976).

G. S. McNeilly, E. D. Hudson, R. S. Lord, S. W. Mosko, J. E. Mann, K. N. Fischer, J. A. Martin, and J. B. Ball, "Development Studies on a Separated-Sector Cyclotron for Phase II of the Holifield Heavy-Ion Research Facility," *Bull. Am. Phys. Soc.* 21, 989 (1976).

H. Nann, A. Saha, and S. Raman, "The ^{59}Ni(p,t)^{57}Ni Reaction," *Bull. Am. Phys. Soc.* 21, 967 (1976).

A. V. Ramayya, J. D. Cole, J. H. Hamilton, H. Kawakami, E. H. Spejewski, and K. S. R. Sastry, "Shape Isomerism in ^{184}Hg," *Bull. Am. Phys. Soc.* 21, 975 (1976).

R. L. Robinson, H. J. Kim, R. O. Sayer, J. C. Wells, and R. M. Ronningen, "High-Spin States in ^{76}Ge," *Bull. Am. Phys. Soc.* 21, 968 (1976).

R. M. Ronningen, R. B. Piercey, R. S. Grantham, J. H. Hamilton, A. V. Ramayya, B. van Nooijen, H. Kawakami, C. Maguire, L. L. Riedinger, and W. K. Dagenhart, "$E2$ and $E4$ Moments in ^{160,162}Dy, ^{162,164}Er, and ^{172}Yb," *Bull. Am. Phys. Soc.* 21, 985 (1976).

R. M. Ronningen, R. B. Piercey, A. V. Ramayya, J. H. Hamilton, W. K. Dagenhart, S. Raman, and P. H. Stelson, "Coulomb Excitation of ^{192,194}Pt," *Bull. Am. Phys. Soc.* 21, 976 (1976).

S. T. Thornton, L. C. Dennis, K. R. Cordell, R. C. Schweizer, P. G. Lookadoo, J. L. C. Ford, Jr., and J. Gomez del Campo, "^{12}C(^{12}C,α)^{20}Ne Reaction Excitation Functions," *Bull. Am. Phys. Soc.* 21, 970 (1976).

C. Y. Wong, "On the Primordial Superheavy Element 126," *Bull. Am. Phys. Soc.* 21, 981 (1976).

IAEA Conference on Atomic Data for Fusion, Culham, England, November 1–5, 1976

C. F. Barnett (invited talk), "Compilation and Evaluation of Atomic and Molecular Data Relevant to Controlled Fusion Research."

Symposium of Northeastern Accelerator Personnel (SNEAP 1976), Tallahassee, Florida, November 3–5 (1976)

J. W. Johnson, "Recent Vacuum Work at Oak Ridge."

Southeastern Section Meeting of the American Physical Society, Virginia Beach, Virginia, November 11–13, 1976

T. A. Carlson and C. W. Nestor, Jr., "Calculation of K and L X-Ray Energies for Elements from $Z = 95$ to 130," *Bull. Am. Phys. Soc.* 22, 487 (1977).

R. L. Mlekodaj (invited talk), "Technological Advances at UNISOR," *Bull. Am. Phys. Soc.* 22, 488 (1977).

W. G. Nettles, R. Beraud, J. D. Cole, J. H. Hamilton, A. V. Ramayya, E. H. Spejewski, and K. S. R. Sastry, "Decay of ^{184}Hg to ^{184}Au," *Bull. Am. Phys. Soc.* 22, 488 (1977).

R. B. Piercey, J. H. Hamilton, R. M. Ronningen, A. V. Ramayya, R. L. Robinson, and H. J. Kim, "Ode to an Unidentified Isotope," *Bull. Am. Phys. Soc.* 22, 488 (1977).

K. S. Toth and M. A. Ijaz (invited talk), "Alpha Decay for Isotopes with $Z < 83$: Recent Experiments at UNISOR," *Bull. Am. Phys. Soc.* 22, 488 (1977).

American Physical Society Meeting, San Francisco, California, November 15–19, 1976

H. J. Kim, P. H. Stelson, J. E. Bayfield, P. M. Koch, and L. D. Gardner, "Electron-Capture Cross Sections for Multiply-Charged ^{56}Fe Ions Incident on Atomic Hydrogen Targets," post-deadline paper.

American Physical Society Meeting, Lincoln, Nebraska, December 6–8, 1976

D. H. Crandall, P. O. Taylor, and R. A. Phaneuf, "Electron Impact Ionization of C^{+3}," *Bull. Am. Phys. Soc.* 21, 1256 (1976).

J. P. Forester, D. J. Pegg, S. B. Elston, P. M. Griffin, K.-O. Groeneveld, R. S. Peterson, R. S. Thoe, C. R. Vane, and I. A. Sellin, "Radiative Lifetimes and Oscillator Strength for the $n = 2$ States of Be-like Sulfur," *Bull. Am. Phys. Soc.* 21, 1253 (1976).

F. D. McDaniel, J. L. Duggan, R. K. Rice, R. Mehta, B. D. Payne, G. C. Monigold, O. W. Holland, D. E. Johnson, P. D. Miller, L. A. Rayburn, A. Zander, K. A. Kuenhold, R. M. Wheeler, R. P. Chaturvedi, and S. J. Cipolla, "Evidence for K-Shell Charge Exchange for ^{28}Si Ions Penetrating Thin Solid Targets," *Bull. Am. Phys. Soc.* 21, 1248 (1976).

R. S. Peterson, S. B. Elston, I. A. Sellin, R. Laubert, F. K. Chen, and C. A. Peterson, "Mass Dependence of Ne K X-Ray Yields from Ne^{+}-Ne Collisions at keV Energies," *Bull. Am. Phys. Soc.* 21, 1248 (1976).

R. A. Phaneuf and R. H. McKnight, "Charge Transfer Collisions of N^{3+} with Atomic and Molecular Hydrogen," *Bull. Am. Phys. Soc.* 21, 1266 (1976).

I. A. Sellin (invited talk), "High Ionization-Excitation States of Ne^{q+} Ions and Their Mass-Dependent Symmetric Collision Interactions," *Bull. Am. Phys. Soc.* 21, 1250 (1976).

P. H. Stelson (invited talk), "The Atomic Physics Potential of New Accelerators," *Bull. Am. Phys. Soc.* 21, 1260 (1976).

P. O. Taylor, R. A. Phaneuf, G. H. Dunn, and D. H. Crandall, "Electron Impact Excitation Cross Sections for C^{3+} from a Crossed-Beams Measurement," *Bull. Am. Phys. Soc.* 21, 1256 (1976).

C. R. Vane, D. J. Pegg, S. B. Elston, J. P. Forester, P. M. Griffin, K.-O. Groeneveld, R. S. Peterson, R. S. Thoe, and I. A. Sellin, "A Beam-Foil Study of the $2s^2 2p^2 {}^1p^1$ Doublet in Li-like Sulfur," *Bull. Am. Phys. Soc.* 21, 1252 (1976).

Second International Conference and Winter School on Submillimeter Waves and Their Applications, San Juan, Puerto Rico, December 6–10, 1976

D. P. Hutchinson and K. L. Vander Sluis, "Design of a High-Power Submillimeter Oscillator-Amplifier System."

Fifteenth International Winter Meeting on Nuclear Physics, Bormio, Italy, January 17–22, 1977

F. Plasil (invited talk), "Fusion and Other Strongly Damped Collisions in Kr Bombardments of Medium-Mass Nuclei."

American Physical Society Meeting, Chicago, Illinois, February 7–10, 1977

Y. A. Ellis and K. S. Toth, "Alpha Systematics for the $214 \leqslant A \leqslant 242$ Region," *Bull. Am. Phys. Soc.* 22, 54 (1977).

J. L. Fowler, J. A. Cookson, M. Hussian, C. A. Uttley, and R. B. Schwartz, "Angular Distribution of Neutron-Proton Scattering at 27.3 MeV," *Bull. Am. Phys. Soc.* 22, 53 (1977).

S. Raman (invited talk), "Search for Superheavy Elements with Synchrotron Radiation," *Bull. Am. Phys. Soc.* 22, 71 (1977).

Conference on Atomic Processes in High-Temperature Plasmas (American Physical Society Topical Conference), Knoxville, Tennessee, February 16–18, 1977

D. H. Crandall (invited talk), "Atomic Collision Cross Sections for Plasma Applications."

T. H. Kruse, J. L. Cecchi, B. M. Johnson, K. W. Jones, P. M. Griffin, and D. J. Pegg, "Decay Studies of the $n + 3$ States of Sodium-like Copper Using Foil Excitation."

F. W. Meyer and R. A. Phaneuf, "Charge Transfer Collisions of Multicharged Carbon, Nitrogen, and Oxygen Ions with Atomic and Molecular Hydrogen."

I. A. Sellin (invited talk), "Contributions of Beam-Foil Spectroscopy to *f*-Value Measurements on Ions of Interest in High-Temperature Plasmas."

German Physical Society Meeting, Munster, West Germany, March 11, 1977

J. Fink, G. Czjek, H. Schmidt, K. Tomala, and F. E. Obenshain, "Measurement of Local Susceptibility and Moments in Alloys of Pd-Ni with ^{61}Ni."

1977 IEEE Particle Accelerator Conference, Chicago, Illinois, March 16–18, 1977

J. B. Ball (invited talk), "A New Generation of Heavy-Ion Facilities," *Bull. Am. Phys. Soc.* 22, 135 (1977).

E. D. Hudson and M. L. Mallory, "Heavy-Ion Source Support Gas Mixing Experiments," *Bull. Am. Phys. Soc.* 22, 175 (1977).

J. A. Martin, J. B. Ball, E. D. Hudson, R. S. Lord, J. E. Mann, G. S. McNeilly, and S. W. Mosko, "Design Status of a Separated-Sector Cyclotron Booster Accelerator for the Holifield Heavy-Ion Research Facility," *Bull. Am. Phys. Soc.* 22, 153 (1977).

S. W. Mosko, E. D. Hudson, R. S. Lord, and J. A. Biggerstaff, "Magnetic Field Measuring System for Remapping the ORIC Magnetic Field," *Bull. Am. Phys. Soc.* 22, 145 (1977).

S. W. Mosko, J. D. Rylander, and G. K. Schulze, "ORIC RF System—Preparation for HHIRF," *Bull. Am. Phys. Soc.* 22, 162 (1977).

American Chemical Society Meeting, New Orleans, Louisiana, March 21–24, 1977

C. E. Bemis, Jr., R. L. Ferguson, F. Plasil, R. J. Silva, Frances Pleasonton, and R. L. Hahn, "Heavy-Ion Reactions and Fission in the Actinide and Transactinide Region."

R. L. Hahn, K. S. Toth, F. Hubert, and P. F. Dittner, "Transfer Reaction Studies: The Production of ^{243,244}Cf in Reactions of ^{239}Pu with ^{12}C, ^{16}O, ^{20}Ne, and ^{14}N."

F. Plasil (invited talk), "Heavy-Ion Reactions and Fission in the Actinide and Transactinide Region."

American Physical Society Meeting, San Diego, California, March 21–24, 1977

D. H. Crandall (invited talk), "Atomic Collision Cross Section for Plasma Impurities," *Bull. Am. Phys. Soc.* 22, 251 (1977).

Joint German and Dutch Physical Society Meeting, Konstanz, Germany, March 21–26, 1977

E. E. Gross, T. P. Cleary, J. L. C. Ford, Jr., D. C. Hensley, and K. S. Toth, "Multistep Processes in ^{20}Ne + ^{208}Pb Scattering."

Nordic Symposium on Atomic and Molecular Transition Probabilities, Lund, Sweden, March 28–29, 1977

D. J. Pegg, P. M. Griffin, S. B. Elston, J. P. Forester, K.-O. Groeneveld, H. C. Hayden, R. S. Peterson, R. S. Thoe, C. R. Vane, and I. A. Sellin, "$\Delta n + 0$ Transitions in Highly Ionized Ions."

International Specialists Symposium on Neutron Standards and Applications, Gaithersburg, Maryland, March 28–31, 1977

M. J. Saltmarsh, C. A. Ludemann, C. B. Fulmer, and R. C. Styles (invited talk), "Neutron Yields and Dosimetry for Be(d,n) and Li(d,n) Neutron Sources at E_d + 40 MeV."

American Physical Society Meeting, Washington, D.C., April 25–28, 1977

C. E. Bemis, Jr., R. L. Ferguson, R. J. Silva, F. Plasil, G. D. O'Kelley, R. L. Hahn, D. C. Hensley, E. K. Hulet, and R. W. Lougheed, "Production and Decay of ^{202}105 and Spontaneous Fission Properties of ^{262}105-^{262}104," *Bull. Am. Phys. Soc.* 22, 611 (1977).

C. R. Bingham, R. W. Lide, J. A. Vrba, L. L. Riedinger, H. K. Carter, R. L. Mlekodaj, E. H. Spejewski, R. A. Braga, W. R. Western, and R. W. Fink, "Decay of Mass-Separated ^{200}Po," *Bull. Am. Phys. Soc.* 22, 546 (1977).

F. K. Chen, G. Lapicki, R. Laubert, S. B. Elston, R. S. Peterson, and I. A. Sellin, "Projectile Charge-State Dependence in K-Shell Ionization of Neon, Silicon, and Argon Cases by Lithium Projectiles," *Bull. Am. Phys. Soc.* 22, 655 (1977).

T. P. Cleary, J. L. C. Ford, Jr., E. E. Gross, D. C. Hensley, C. R. Bingham, and J. Vrba, "Mutual Excitation of ^{22}Ne and ^{126}Te in Inelastic Scattering," *Bull. Am. Phys. Soc.* 22, 564 (1977).

S. Datz, P. F. Dittner, J. A. Biggerstaff, J. Gomez del Campo, P. D. Miller, and C. D. Moak, "K-Shell Vacancy Effects on Charge States of 50- to 60-MeV Cl Ions Emerging from Solids," *Bull. Am. Phys. Soc.* 22, 624 (1977).

R. A. Dayras, R. G. Stokstad, M. L. Halbert, D. C. Hensley, A. H. Snell, R. L. Robinson, C. B. Fulmer, D. G. Sarantites, and L. Westerberg, "Gamma-Ray Multiplicity in DI Reactions," *Bull. Am. Phys. Soc.* 22, 593 (1977).

S. B. Elston, C. R. Vane, J. P. Forester, D. J. Pegg, I. A. Sellin, and S. R. Schumann, "Production of Core-Excited States of Li and Li^+ in Collisions with Gas Targets," *Bull. Am. Phys. Soc.* 22, 655 (1977).

R. L. Ferguson, F. E. Obenshain, F. Plasil, F. Pleasonton, and A. H. Snell, "Reactions Induced by 155-MeV ^{20}Ne Bombardment of ^{45}Tl," *Bull. Am. Phys. Soc.* 22, 593 (1977).

J. L. C. Ford, Jr., J. Gomez del Campo, R. L. Robinson, D. Shapira, E. Aguilera, E. Andrade, A. Dacal, A. Menchaca-Rocha, and M. E. Ortiz, "Yrast Levels in ^{27}Al Suggested by Resonance Structure in the ^{12}C(^{15}N,α) Reaction," *Bull. Am. Phys. Soc.* 22, 630 (1977).

Linda Fugate, J. C. Wells, Jr., R. O. Sayer, R. L. Robinson, H. J. Kim, W. T. Milner, and G. J. Smith, "Lifetimes of Levels in ^{64}Zn via the ^{51}V(^{16}O,$p2n$)^{64}Zn Reaction," *Bull. Am. Phys. Soc.* 22, 565 (1977).

J. Gomez del Campo, J. K. Bair, P. D. Miller, and P. H. Stelson, "Measurements of Total Neutron Yields for the ^{12}C + ^{12}C, ^{12}C, ^{13}C, and ^{13}C + ^{13}C Systems," *Bull. Am. Phys. Soc.* 22, 628 (1977).

C. D. Goodman, F. E. Bertrand, R. Madey, B. Anderson, A. Baldwin, J. Knudson, T. Whitten, J. Rapaport, D. Bainum, M. B. Greenfield, and C. C. Foster, "Charge Exchange Reactions ^{12}C(p,n)^{12}N and ^{28}Si(p,n)^{28}P," *Bull. Am. Phys. Soc.* 22, 544 (1977).

M. L. Halbert, R. A. Dayras, F. Plasil, R. L. Ferguson, and D. G. Sarantites, "Fusion Cross Sections for 175-MeV ^{20}Ne on ^{150}Nd," *Bull. Am. Phys. Soc.* 22, 630 (1977).

D. J. Horen and J. A. Harvey, "Giant Magnetic Dipole States in ^{208}Pb," *Bull. Am. Phys. Soc.* 22, 543 (1977).

C. H. Johnson and A. Galonsky, "Anomalous A Dependence ($90 < A < 130$) for the Absorptive Potential for Protons below the Coulomb Barrier," *Bull. Am. Phys. Soc.* 22, 544 (1977).

A. C. Kahler, L. L. Riedinger, N. R. Johnson, R. L. Robinson, A. Visvanathan, and E. F. Zganjar, "High-Spin States in ^{185}Au," *Bull. Am. Phys. Soc.* 22, 615 (1977).

D. J. Malbrough, R. D. Edge, C. W. Darden, B. M. Preedom, F. E. Bertrand, T. P. Cleary, E. E. Gross, C. A. Ludemann, R. L. Burman, R. P. Redwine, K. Gotow, and M. A. Moinester, "Pion-Nuclear Elastic Scattering at 50 MeV," *Bull. Am. Phys. Soc.* 22, 525 (1977).

F. D. McDaniel, G. Basbas, J. L. Duggan, P. D. Miller, and G. Lapicki, "Projectile Cross Sections Inferred from Measurements of Target X-Ray Production," *Bull. Am. Phys. Soc.* 22, 656 (1977).

F. Milder, M. Blecher, K. Gotow, D. Jenkins, P. Roberson, F. E. Bertrand, T. P. Cleary, E. E. Gross, C. A. Ludemann, C. W. Darden, R. D. Edge, B. M. Preedom, T. Marks, D. Malbrough, R. L. Burman, R. P. Redwine, and M. Moinester, "Pion-Nuclear Inelastic Scattering at 50 MeV," *Bull. Am. Phys. Soc.* 22, 525 (1977).

D. J. Pegg, P. M. Griffin, B. M. Johnson, K. W. Jones, J. L. Cecchi, and T. H. Kruse, "Lifetime Measurements in Cu XIX," *Bull. Am. Phys. Soc.* 22, 609 (1977).

G. A. Petitt and F. E. Obenshain, "Perturbed Angular Correlation of ^{111}Cd" in Nickel-Cadmium Ferrites," *Bull. Am. Phys. Soc.* 22, 573 (1977).

F. Plasil, "Angular Momentum Effects in the De-excitation of Compound Nuclei with High Angular Momenta," *Bull. Am. Phys. Soc.* 22, 646 (1977).

S. Raman, M. Mizumoto, R. L. Macklin, G. G. Slaughter, G. L. Morgan, J. Halperin, G. T. Chapman, and R. R. Winters, "Location of Dipole and Quadrupole Strengths in ^{208}Pb via the ^{207}Pb(n,γ) Reaction," *Bull. Am. Phys. Soc.* 22, 542 (1977).

S. Raman, C. J. Sparks, Jr., R. V. Gentry, M. O. Krause, H. L. Yakel, and E. Ricci, "A Search with Synchrotron Radiation for Superheavy Elements in Giant Halo," *Bull. Am. Phys. Soc.* 22, 611 (1977).

A. C. Rester, J. B. Ball, and R. L. Auble, "^{74,76}Ge(p,t) Reactions with 35-MeV Protons," *Bull. Am. Phys. Soc.* 22, 544 (1977).

D. G. Sarantites, L. Westerberg, J. H. Barker, R. A. Dayras, M. L. Halbert, and D. C. Hensley, "Gamma-Ray Multiplicities from the Decay of ^{170}Yb Compound Nuclei at Excitation Energies of 67–94 MeV Formed in Reactions of ^{4}He + ^{166}Er and ^{20}Ne + ^{150}Nd," *Bull. Am. Phys. Soc.* 22, 630 (1977).

M. Schmorak, "Level Structure of ^{233}U," *Bull. Am. Phys. Soc.* 22, 644 (1977).

I. A. Sellin, C. R. Vane, S. B. Elston, J. P. Forester, P. M. Griffin, D. J. Pegg, R. S. Peterson, and R. S. Thoe, "Recoil Ion Spectroscopy: Reduction of Doppler Shifts and Spreads in Fast-Beam Experiments," *Bull. Am. Phys. Soc.* 22, 610 (1977).

D. Shapira, R. deVries, M. Clover, R. Cherry, and R. N. Boyd, "Excitation Functions and Angular Distributions for ^{12}C + ^{16}O Scattering," *Bull. Am. Phys. Soc.* 22, 629 (1977).

R. G. Stokstad, R. A. Dayras, J. Gomez del Campo, and P. H. Stelson, "Fusion of ^{14}N + ^{12}C and the Liquid-Drop Limit," *Bull. Am. Phys. Soc.* 22, 628 (1977).

H. H. K. Tang and C. Y. Wong, "Two-Dimensional and Three-Dimensional Nuclear Hydrodynamical Calculations," *Bull. Am. Phys. Soc.* 22, 645 (1977).

K. S. Toth, P. Singh, C. R. Bingham, H. K. Carter, M. A. Ijaz, and D. C. Sousa, "Decay Studies of Neutron-Deficient Holmium Isotopes," *Bull. Am. Phys. Soc.* 22, 614 (1977).

C. R. Vane, S. B. Elston, I. A. Sellin, J. P. Forester, P. M. Griffin, D. J. Pegg, R. S. Peterson, R. S. Thoe, J. Wright, K.-O. Groeneveld, R. Laubert, and F. Chen, "Lower Limits on Resolved Neon *L*-Shell Excitation Cross Sections by Impact of 1.5 MeV A ~ S^{12+} Cl^{12+} Ions," *Bull. Am. Phys. Soc.* 22, 609 (1977).

A. Visvanathan, E. F. Zganjar, M. A. Grimm, J. L. Wood, R. W. Fink, A. C. Kahler, L. L. Riedinger, E. L. Robinson, and H. K. Carter, "Decay of Mass-Separated ^{187}Tl, ^{187}Hg and the Structure of ^{183}Au," *Bull. Am. Phys. Soc.* 22, 615 (1977).

J. A. Vrba, L. L. Riedinger, C. R. Bingham, E. L. Robinson, B. O. Hannah, E. H. Spejewski, R. L. Mlekodaj, and H. K. Carter, "Decay of ^{196}Pb," *Bull. Am. Phys. Soc.* 22, 546 (1977).

M. P. Webb, F. E. Obenshain, R. L. Ferguson, F. Plasil, F. Pleasonton, A. H. Snell, and H. Nakahara, "Strongly Damped Reactions in the ^{20}Ne + ^{96}Zr System at 166 MeV," *Bull. Am. Phys. Soc.* 22, 594 (1977).

J. C. Wells, Jr., S. Raman, and G. G. Slaughter, "Neutron Capture Gamma-Ray Studies of Levels in ^{57}Fe and ^{59}Fe," *Bull. Am. Phys. Soc.* 22, 528 (1977).

L. Westerberg, D. G. Sarantites, R. A. Goldworm, J. H. Barker, M. L. Halbert, R. A. Dayras, and D. C. Hensley, "Decay of ^{170}Yb Compound Nuclei at 132 MeV of Excitation Formed in Reactions of ^{20}Ne with ^{150}Nd, and ^{12}C with ^{158}Gd," *Bull. Am. Phys. Soc.* 22, 630 (1977).

10. General Information

Prepared by R. L. Macklin, B. F. McHargue, and W. L. Stair

PERSONNEL ASSIGNMENTS

During 1976-77 the Physics Division was host to guests from abroad as well as from the United States. Some of these were short-term assignments, variously sponsored by different organizations and institutions. Physics Division staff members have also been the guests of laboratories located outside the United States.

Research Participants from Abroad

E. F. Aguilera-Reyes—Instituto Nacional de Energia Nuclear, Mexico

E. I. Andrade—Universidad Nacional Autonoma, Mexico

A. A. Dacal—Ciudad Universitaria, Mexico

H. T. Feldmeier—Technische Hochschule, Darmstadt, West Germany

J. Gomez del Campo—National University of Mexico (now an ORNL employee)

K.-O. Groeneveld—University of Tennessee (on leave from Universität Frankfurt, Frankfurt am Main, West Germany)

H. B. Gilbody—Queen's University, Belfast, Northern Ireland

G. D. James—Atomic Energy Research Establishment, Harwell, England

Vida Maruhn—University of Frankfurt, Frankfurt, Germany (now an ORNL employee)

R. A. A. Menchaca—University of Mexico

M. Mizumoto—Japan Atomic Energy Research Institute, Tokai-Mura, Japan; Oak Ridge Electron Linear Accelerator Program

M. A. Moinester—Los Alamos Scientific Laboratory at LAMPF (on leave from Tel Aviv University, Israel)

H. Nakahara—Tokyo Metropolitan University, Tokyo, Japan

G. L. Nyberg—Latrobe University, Bundoora, Australia

S. M. E. Ortiz—Universidad Nacional Autonoma, Mexico

Cleide Renner—Instituto de Energia Atomica, Sao Paulo, Brazil

S. R. Schumann—University of Tennessee (on leave from J. W. Goethe Universität, Frankfurt am Main, West Germany

T. Terasawa—University of Tokyo, Japan

H. Verheul—Natuurkundig Laboratorium der Vrije Universiteit, Amsterdam, Netherlands

A. van der Woude—Kernfysisch Versneller Instituut der Rijksuniversiteit, Groningen, Netherlands

Herman Weigmann—Central Bureau for Nuclear Measurements (CBNM), Euratom, Geel, Belgium

Research Participants from United States Institutions

Visiting scientists participate in the activities of the Physics Division under a variety of auspices. Many are sponsored in part under programs of Oak Ridge Associated Universities (listed separately). Others, in addition to support from their home institutions, are aided by ORNL subcontracts, ERDA contracts, various grants, and awards. Their research at ORNL is generally in collaboration with staff members.

Ali Abdel-Ghany Antar—University of Connecticut

George Auchampaugh—Los Alamos Scientific Laboratory

P. M. Bakshi—Boston College

J. H. Barker—St. Louis University

J. E. Bayfield—Pittsburgh University

C. R. Bingham—University of Tennessee

M. Blecher—Virginia Polytechnic Institute and State University

H. G. Blosser—Michigan State University

D. A. Bromley—Yale University

D. A. Brown—Michigan State University

W. M. Bugg—University of Tennessee

R. F. Carlton—Middle Tennessee State University

H. K. Carter—Oak Ridge Associated Universities

G. T. Condo—University of Tennessee

R. Y. Cusson—Duke University

P. J. Daly—Purdue University

D. M. Drake—Los Alamos Scientific Laboratory

S. B. Elston—University of Tennessee

John Felvinci—Columbia University

L. D. Gardner—Pittsburgh University

J. B. Garg—State University of New York at Albany

F. A. Grimm—University of Tennessee

D. C. Gregory—Joint Institute for Laboratory Astrophysics

S. Gronemeyer—Washington University

M. W. Guidry—University of Tennessee

H. Haelppi—Purdue University

E. L. Hart—University of Tennessee

T. Handler—University of Tennessee

H. C. Hayden—University of Connecticut

P. G. Huray—University of Tennessee

J. Jastrzebski—Indiana University

B. R. Junker—University of Georgia

A. C. Kahler—University of Tennessee

Constance Kalbach—University of Tennessee

T. L. Khoo—Michigan State University

C. H. King—Michigan State University

R. F. King—self, ORNL retiree

P. M. Koch—Yale University

J. D. Larson—self

Bernd Luers—Columbia University

J. J. Malanify—Los Alamos Scientific Laboratory

D. J. Malbrough—University of South Carolina

E. R. Marshalek—Notre Dame University

E. W. McDaniel—Georgia Institute of Technology

R. H. McKnight—University of Virginia

Ed Melkonian—Columbia University

F. L. Milder—Virginia Polytechnic Institute and State University

R. L. Mlekodaj—Oak Ridge Associated Universities

T. J. Morgan—Wesleyan University

Ron Nelson—Los Alamos Scientific Laboratory

P. Z. Peebles—University of Tennessee

D. J. Pegg—University of Tennessee

Frances Pleasonton—self, ORNL retiree

S. Popick—Purdue University

C. A. Rester—Tennessee Technological University

L. L. Riedinger—University of Tennessee

R. Ronningen—Vanderbilt University

A. Russek—University of Connecticut

S. K. Saha—Purdue University

A. G. Schmidt—Oak Ridge Associated Universities

I. A. Sellin—University of Tennessee

J. A. Smith—Yale University

A. H. Snell—self, ORNL retiree

P. C. Simms—Purdue University

E. H. Spejewski—Oak Ridge Associated Universities

R. M. Tate—University of Tennessee (with Instrumentation and Controls Division)

P. O. Taylor—Joint Institute for Laboratory Astrophysics

R. S. Thoe—University of Tennessee

E. W. Thomas—Georgia Institute of Technology

J. R. Thompson—University of Tennessee

J. O. Thomson—University of Tennessee

S. T. Thornton—University of Virginia

L. Westerberg—Washington University

R. M. Wieland—Franklin and Marshall College

L. Wilets—University of Washington

J. J. Wright—University of New Hampshire

S. W. Yates—University of Kentucky

Undergraduates

J. D. Bell—Earlham College

H. E. Doughty II—University of Tennessee

C. A. Gossett—DePauw University

M. W. Howard—University of Tennessee

C. M. Manning—University of Tennessee

R. L. Monday—University of Tennessee

H. A. Scott—Cornell University

V. D. Vandergriff—University of Tennessee

Staff Assignments

F. E. Bertrand—Groningen Cyclotron Laboratory, Kernfysisch Versneller Instituut, Groningen, Netherlands, June-September 1976 and May 1977

E. E. Gross—Grenoble Cyclotron Laboratory, Grenoble, France, February-May 1977

D. P. Hutchinson—Kurchatov Institute, Moscow, U.S.S.R., May-June 1977

N. R. Johnson—Institute de Physique Nucleaire, Orsay, France, and Centre D'Etudes Nucleaires de Bordeaux, Bordeaux, France, February-March 1977

R. L. Macklin—Los Alamos Scientific Laboratory, July-August 1976

M. L. Mallory—Michigan State University; began two-year assignment in July 1976

J. B. McGrory—Continued loan assignment to Program Planning and Analysis Office begun in October 1975

C. D. Moak—Completed in March 1976 a 13-month assignment including seven months at the Institute of Physics, University of Aarhus, Denmark, and six months at the Daresbury Laboratory, Daresbury, England

M. J. Saltmarsh—Began a loan assignment with the ORNL Fusion Energy Division October 1976

Personnel Changes

J. R. Beene—Nuclear Data Project; began a two-year postdoctoral appointment in November 1976

J. A. Benjamin—Hoiifield Heavy-Ion Research Facility; began a two-year appointment in August 1976

T. P. Cleary—Oak Ridge Isochronous Cyclotron; began a one-year postdoctoral appointment in August 1976

J. J. Cowan—Infrared Spectroscopy Program; transferred from Health Physics Division to Physics Division in July 1976

R. A. Dayras—Oak Ridge Isochronous Cyclotron; continued a two-year postdoctoral appointment begun in October 1975

J. Gomez del Campo—Van de Graaff Laboratory; began a two-year appointment in May 1976

W. W. Harris—Electron Microscopy Program; transferred from Physics Division to Metals and Ceramics Division in March 1976

D. C. Kocher—Nuclear Data Project; transferred from Physics Division to Environmental Sciences Division in September 1976

M. B. Marshall—Oak Ridge Isochronous Cyclotron; retired in February 1977

J. A. Maruhn—Theoretical Physics Program; continued a temporary appointment begun in September 1974

Vida Maruhn—Theoretical Physics Program; began one-year part-time employment in August 1976

F. W. Meyer—CTR-Related Atomic Physics Program; began a two-year appointment in September 1976

R. A. Phaneuf—CTR-Related Atomic Physics Program; transferred from Thermonuclear Division to Physics Division in October 1976 for two-year appointment

Frances Pleasonton—Physics of Fission Program; retired in December 1976

L. D. Rickertsen—Theoretical Physics Program; completed a two-year postdoctoral appointment in July 1976

D. Shapira—Van de Graaff Laboratory; began a two-year postdoctoral appointment in September 1976

M. P. Webb—Nuclear Data Project and Heavy-Ion Program; began a two-year postdoctoral appointment in December 1976

RESEARCH PARTICIPANTS UNDER CONTRACT ARRANGEMENT WITH OAK RIDGE ASSOCIATED UNIVERSITIES

Under arrangements with Oak Ridge Associated Universities ("S" contracts and "U" contracts), 86 university or college faculty members and students visited the Physics Division for consultation and collaboration during 1976-77. These individuals and their affiliation are listed below:

William J. Atkinson, Jr., University of Alabama at Birmingham

Frank T. Avignone III, University of South Carolina

Nestor Azziz, University of Puerto Rico at Mayaguez

F. Todd Baker, University of Georgia

James H. Barker, Saint Louis University

Stephen Bart, University of Houston

Stanley Bashkin, University of Arizona

James E. Bayfield, University of Pittsburgh

Robert A. Braga, Georgia Institute of Technology

William H. Brantley, Furman University

Lynn B. Bridwell, Murray State University

David A. Brisson, North Carolina State University

Ram P. Chaturvedi, State University of New York at Cortland

Sam Cipolla, Creighton University

Jerald D. Cole, Vanderbilt University

Kathryn R. Cordell, University of Virginia

Philip W. Coulter, University of Alabama

John G. Cramer, University of Washington

Frederick L. Culp, Tennessee Technological University

Lawrence C. Dennis, University of Virginia

Ralph DeVries, University of Rochester

Robert R. Doering, University of Virginia

Jerry P. Draayer, Louisiana State University

Jerome L. Duggan, North Texas State University

Richard W. Fink, Georgia Institute of Technology

John D. Fox, Florida State University

Thomas A. Girard, University of South Carolina

David A. Goldberg, University of Maryland

John D. Gressett, North Texas State University

Marvin A. Grimm, Jr., Georgia Institute of Technology

Suzanne A. Gronemeyer, Washington University

Joseph H. Hamilton, Vanderbilt University

Bernie O. Hannah, University of Alabama at Birmingham

Richard D. Hichwa, Vanderbilt University

Ed V. Hungerford III, University of Houston

M. A. Ijaz, Virginia Polytechnic Institute and State University

Hirokane Kawakami, Vanderbilt University

Kirby W. Kemper, Florida State University

Bernard D. Kern, University of Kentucky

Quentin Kessel, University of Connecticut

Stephen J. Krieger, University of Illinois

Kenneth A. Kuenhold, University of Tulsa

Krishna Kumar, Vanderbilt University

Roman Laubert, New York University

Robert S. Lee, Vanderbilt University

Jung Lin, Tennessee Technological University

Phillip G. Lookadoo, University of Virginia

W. G. Love, University of Georgia

Alan D. MacKellar, University of Kentucky

Charles F. Maguire, Vanderbilt University

Donald A. McClure, Georgia Institute of Technology

Floyd D. McDaniel, North Texas State University

Martin R. Meder, Georgia State University

Thomas F. Parkinson, Virginia Polytechnic Institute and State University

Bobby D. Payne, Jr., North Texas State University

Rodney B. Piercey, Vanderbilt University

W. T. Pinkston, Vanderbilt University

Arthur R. Quinton, University of Massachusetts

A. V. Ramayya, Vanderbilt University

Venugopala Rao, Emory University

Meir S. Rapaport, Georgia Institute of Technology

Louis A. Rayburn, University of Texas at Arlington

Alfred C. Rester, Jr., Emory University
Roger Rice, North Texas State University
Edward Lee Robinson, University of Alabama at Birmingham
Demetrios G. Sarantites, Washington University
Kandula S. R. Sastry, University of Massachusetts
Thomas C. Schweizer, University of Virginia
Alan Scott, University of Georgia
Enrique Silberman, Fisk University
Paramjit Singh, Virginia Polytechnic Institute and State University
Robert K. Smith, Jr., Duke University
David C. Sousa, Eastern Kentucky University
Arvel D. Toten, Jr., North Texas State University
Ashok Visvanathan, Louisiana State University
Thomas A. Walkiewicz, Edinboro State College
Jesse L. Weil, University of Kentucky
John C. Wells, Jr., Tennessee Technological University
Warren R. Western, Georgia Institute of Technology
Richard M. Wheeler, State University of New York at Cortland
Bryan H. Wildenthal, Michigan State University
Ron R. Winters, Denison University
John L. Wood, Georgia Institute of Technology
Steven W. Yates, University of Kentucky
Arlen R. Zander, East Texas State University
Edward F. Zganjar, Louisiana State University

Undergraduate Research Trainees

Terry C. Awes, University of Wisconsin
David F. Chernoff, Yale University
Cheryl A. Houser, Pennsylvania State University
Robert A. Managan, Rice University
Richard T. Snodgrass, Carleton College
Robert C. Styles, Berry College
D. M. Thomas, Emory University
Walter H. Thompson III, University of Southwestern Louisiana
David E. Toodle, Samford University
Larry E. Williams, University of Tennessee

GRADUATE THESIS RESEARCH

During 1976–77, Physics Division staff and associates served as advisors or supervisors for 16 students engaged in thesis research. All projects listed below were carried out with facilities operated at least in part by the Division.

Ph.D. Thesis Research

Candidate	Advisor(s)	Thesis title or field of research
A. V. Ahmed, Vanderbilt University	R. L. Robinson	In-Beam Gamma-Ray Spectroscopy of ^{39}K
W. K. Dagenhart, University of Tennessee	P. H. Stelson	Coulomb Excitation of ^{115}Sn (degree conferred March 1977)
A. P. DeLima, Vanderbilt University	R. L. Robinson	High-Spin States in ^{68,72}Ge
E. J. Fisher, University of Pittsburgh	D. H. Crandall and C. F. Barnett	Charge Exchange in Multiply Charged Ion Collisions
J. P. Forester, University of Tennessee	D. J. Pegg, University of Tennessee	Lifetimes and Spectra of Multicharged Ions Using Beam-Foil Excitation

Candidate	Advisor(s)	Thesis title or field of research
G. M. Gowdy, Georgia Institute of Technology	E. J. Spejewski and N. R. Johnson	Decay Scheme Studies of Neutron-Deficient Odd-Mass Thallium Isotopes and the Systematics of the Odd-Mass Mercury Levels (degree conferred December 1976)
M. A. Grimm, Georgia Institute of Technology	E. J. Spejewski and R. L. Mlekodaj	Shape Coexistence near the $Z = 82$ Closed Shell
D. L. Hillis, University of Tennessee	E. E. Gross	Shape Effects in the Elastic and Inelastic Scattering of 70.4-MeV ^{12}C Ions from the Even Neodymium Isotopes (degree conferred March 1976)
R. S. Peterson, University of Tennessee	I. A. Sellin, University of Tennessee	Collision and Structure Experiments on Low-Energy Multiply Charged Ions
R. Piercy, Vanderbilt University	R. L. Robinson	High-Spin States in ^{74}Se
P. J. Singh, Virginia Polytechnic Institute and State University	K. S. Toth; M. A. Ijaz, Virginia Polytechnic Institute and State University	Investigation of Single-Particle States in Dysprosium Nuclei
Henry H. K. Tang, Yale University	C. Y. Wong and D. A. Bromley (Yale)	Dynamics of Nuclear Fluid
Cheng-May Tung, University of Tennessee	F. Obenshain	Isomer Shift Studies in Dilute Au Alloys (degree conferred August 1976)
C. R. Vane University of Tennessee	I. A. Sellin, University of Tennessee	Heavy-Ion Atomic Collisions
J. A. Vrba, University of Tennessee	C. R. Bingham and E. E. Gross	Inelastic Scattering of Heavy Ions
	Master's Thesis Research	
David Brisson, North Carolina State	C. F. Barnett	A Cesium Heat-Pipe Neutral Particle Spectrometer
	Bachelor's Thesis Research	
M. D. Barker, Emory University	E. H. Spejewski and H. K. Carter	Exploratory Studies in the Mass Region $A = 60$ to 80 Far from Stability (degree conferred June 1976)

MISCELLANEOUS PROFESSIONAL ACTIVITIES OF DIVISIONAL PERSONNEL

Staff members are frequently involved in professional work incidental to their primary laboratory responsibilities. For example, a majority of the professional staff act as referees for over two dozen journals, principally the *Physical Review*, *Physical Review Letters*, and *Nuclear Physics*, and many review proposals for funding organizations. Other activities include those listed below.

J. B. Ball—member of program committee for Nuclear Physics Division of APS; member of organizing committee for 2d International Conference on Electrostatic Accelerator Technology (Strasbourg); member of ORNL Landscape and Architecture Committee; member of ad hoc committee on Guidelines for Management and Control of Construction Projects at ORNL

C. F. Barnett—Research Advisory Committee for ERDA-EMFE; consultant to IAEA on atomic data; organized APS Topical Conference on Atomic Physics in High-Temperature Plasmas, Knoxville, Tennessee, February 16, 1977; member of committee to review a National Research Plasma Facility, ERDA Security Review Board, and ERDA advisors committee on Neutral Injection Heating

R. L. Becker—lecturer, University of Tennessee; reviewer of research proposals for the Division of Physical Sciences of ERDA and for the National Science Foundation

F. E. Bertrand—chairman, Indiana University Cyclotron Facility Users Group; member, LAMPF Users Group, IUCF Advisory Committee for Five-Year Development Plan

T. A. Carlson—joint editor-in-chief of the *Journal of Electron Spectroscopy*; chairman of 1976 Gordon Conference on Electron Spectroscopy; advisor to 1977 Nobel Prize Committee

D. H. Crandall—member of local committee for the APS Topical Conference on Atomic Physics in High-Temperature Plasmas, Knoxville, Tennessee, February 16, 1977.

J. W. T. Dabbs—Registered Professional Engineer (Tennessee No. 11,475) October 1976; University Relations Coordinator for the ORAU and ORNL Summer Student Trainee, Faculty Research Participant, and Exceptional Graduate Student summer programs, 1975-77 and for the GLCA Science Program, 1976; moderator, Breeder Reactor Workshop, April 16, 1977, sponsored by Scientists and Engineers for Appalachia and the University of Tennessee

E. Eichler (Chemistry Division) Physics Division Seminar Chairman; Heavy-Ion Laboratory Users Group Liaison Officer

W. B. Ewbank—Research Advisor for Great Lakes Colleges Association Science Semester (September–December 1976).

J. L. C. Ford—member, HHIRF Users Group Executive Committee; member, LBL SuperHILAC, Brookhaven National Laboratory, and Indiana Cyclotron Facility Users Groups

J. L. Fowler—part-time professor, University of Tennessee; organizer of 1979 Conference on Nuclear Cross Sections and Technology

C. B. Fulmer—safety officer and radiation control officer for Physics Division; instructor for ORNL Personnel Development Programs

C. D. Goodman—chairman of the ORNL Science and Technology Colloquium; Physics Division Quality Assurance Coordinator; member of Indiana University Cyclotron Users Group; chairman of the Nominating Committee, IUCF Users Group

P. M. Griffin—member, Users Group of Brookhaven National Laboratory

J. A. Harvey—labor coordinator for the Physics Division; Physics Division coordinator for ORNL Awards Committee; secretary-treasurer of the Division of Nuclear Physics of the American Physical Society (1967-77); member, organizing committee of the 1976 International Conference on the Interactions of Neutrons with Nuclei; member of the editorial board of the Atomic and Nuclear Data Tables

N. R. Johnson (Chemistry Division)—member of the ORIC Planning Committee; member of HHIF Users Liaison Group; ORIC Scheduling Coordinator

C. M. Jones—member, Program Committee, 1977 Particle Accelerator Conference

H. J. Kim Neutron Spectrometer Section chairperson, 1976 Experimental Apparatus Working Groups, Holifield Heavy-Ion Research Facility; local committee member, 1977 Conference on Atomic Processes in High-Temperature Plasma, Knoxville, Tennessee, February 16, 1977

C. A. Ludemann Physics Division representative, Union Carbide Nuclear Division Affirmative Action Program; member, LAMPF Users Group

F. K. McGowan member, editorial board of Atomic Data and Nuclear Data Tables

J. B. McCrory ORNL Ad Hoc Committee on Long-Range ADP Acquisition; Physics Division ORIC Scheduling Committee; on leave to Program Planning and Analysis Group

R. L. Macklin Physics Division Technology Utilization Coordinator; member of Criticality Safety Approvals Committee, ORGDP

J. A. Martin chairman, Meetings Committee of Technical Activities Board of IEEE; chairman, Technical Committee on Accelerators and member of Administrative Committee of the IEEE Nuclear and Plasma Sciences Society; deputy member, International Organizing Committee, World Electrotechnical Congress, Moscow, June 1977; member, Editorial Advisory Board of Particle Accelerators; consultant, National Science Foundation Physics Section as member of Visiting Committees for Indiana University Cyclotron Project and Columbia University Synchrotron Improvement Project; member, Organizing Committee for the 1976 Particle Accelerator Conference, Chicago, Illinois; member, International Organizing Committee for VIIIth International Conference on Cyclotrons and Their Applications to be held at Indiana University, September 1978; member, Lawrence Berkeley Laboratory Accelerator Division Review Committee

J. A. Maruhn lecturer, University of Tennessee

H. W. Morgan faculty member of Fisk University Infrared Spectroscopy Institute; member of Board of Trustees of Cordell Hull Foundation for International Education; member of Board of Directors of Tennessee Partners of the Americas, and Chairman of Committee for Scientific Exchange; Senior Research Associate, Department of Natural Sciences, Hollins College; local-section lecturer, American Chemical Society

S. W. Mosko – member, ERDA Electrical Safety Criteria Committee; member, Program Committee of 1977 Particle Accelerator Conference, Chicago, Illinois; Board of Directors, Oak Ridge Section IEEE

F. E. Obenshain – part-time professor, University of Tennessee

F. Plasil – chairman, ORNL Graduate Fellow Selection Panel; Lawrence Berkeley Laboratory SuperHILAC Users Executive Committee; Cochairman Physics Division Seminars; Vice-Chairman 1977 Gordon Conference on Nuclear Chemistry; member LAMPF Users Association

R. L. Robinson liaison officer and chairman of the Nominating Committee for the Users Group of the Holifield Heavy-Ion Research Facility

M. J. Saltmarsh member, LAMPF Advisory Committee, LAMPF; member, American Society for Testing Materials Subcommittee E10.08 (Procedures for Radiation Damage Simulation)

G. R. Satchler member, Executive Committee, Division of Nuclear Physics, American Physical Society; member, Program Committee, Division of Nuclear Physics, American Physical Society; member, editorial board of Atomic Data and Nuclear Data Tables

P. A. Staats staff member, Fisk University Infrared Spectroscopy Institute; participated in organization of and directed laboratory portion of Twenty-seventh Annual Fisk Infrared Institute, Vanderbilt University, Nashville, Tennessee, July 26–30, 1976; Physics Division Quality Assurance Coordinator

P. H. Stelson part-time faculty member, Department of Physics, University of Tennessee; associate editor of *Nuclear Physics;* member, advisory committee for the ORNL Instrumentation and Controls Division

R. G. Stokstad member, Ad Hoc Panel on the Future of Nuclear Science (CNS-NAS); member, SuperHILAC Program Advisory Committee

K. S. Toth chairman, UNISOR Scheduling Committee; Major Nuclear Chemistry Facilities Committee of the American Chemical Society; acting member, UNISOR Executive Committee

T. A. Welton part-time consultant to the ORGDP Gas Centrifuge Program; part-time professor and colloquium chairman, University of Tennessee Physics Department

PHYSICS DIVISION SEMINARS

Physics Division seminars were held once a week on the average. The seminar cochairmen during the period were W. B. Dress, E. Eichler (Chemistry Division), and F. Plasil. The seminars listed below are announced to the entire Laboratory in the ORNL Technical Calendar. In addition, groups within the Division hold meetings of more specialized interest, such as the Nuclear Research coffee meetings on alternate Wednesday afternoons, the Theoretical Circus on Fridays, Atomic Physics seminars, and ORELA seminars.

Date	Speaker and affiliation	Topic
1/13/76	D. L. Hillis, Physics Division, ORNL	Shape Effects in the Elastic and Inelastic Scattering of 70-MeV ^{12}C Ions from the Even Neodymium Nuclei
1/16/76	Eric Sheldon, University of Lowell, Lowell, Massachusetts	Neutron Scattering Studies by the University of Lowell Nuclear Group
1/19/76	Yvon LeBeyec, Institute of Nuclear Physics, Orsay, France	Complete Fusion in Heavy-Ion-Induced Reactions: Production of Neutron-Deficient Isotopes
1/22/76	Ken Toth, Physics Division, ORNL	Window Overlooking the Volga or a Five-Month Assignment in Dubna
1/22/76	Michael P. Webb, University of Washington, Seattle	Elastic and Deeply Inelastic Scattering of ^{86}Kr from ^{208}Pb and ^{139}La
1/29/76	Dan Dill, Boston University, Boston, Massachusetts	Recent Theoretical Developments in Photoelectron Cross Sections of Molecules
2/24/76	P. J. Moffa, Brookhaven National Laboratory, Upton, New York	Heavy-Ion Reaction Studies – Localization and Inelastic Scattering
2/26/76	J. O. Rasmussen, Lawrence Berkeley Laboratory and Chemistry Division, University of California, Berkeley	Classical Equations of Motion Approach to Heavy-Ion Collisions
3/11/76	Dag Horn, Massachusetts Institute of Technology, Cambridge	Fusion Studies of ^{32}S on ^{58}Ni
3/17/76	V. Schmidt, University of Freiburg, Freiburg, West Germany	Double Photoionization in the Outer Shell of Rare Gases
3/31/76	Ulrich Mosel, University of Giessen, Giessen, West Germany	Thermal Properties of Nuclei
4/1/76	M. W. Guidry, Lawrence Berkeley Laboratory, Berkeley, California	Reduced Transition Probabilities for High-Spin States
4/7/76	Helga G. Kalinowski, Hahn-Meitner Institute, Berlin, West Germany	Heavy-Ion Collisions in a Classical Model Including Single Particle Surface Friction
4/8/76	Steven Young, University of California at Los Angeles	Multiple Diffraction Expansion for Intermediate Energy Nuclear Reaction
4/9/76	Dan Shapira, University of Rochester, Rochester, New York	The Rochester Heavy-Ion Counter in Recent Experiments
4/9/76	S. M. Perez, University of Oxford	Sum Rules for Nucleon Spectroscopic Factors
4/12/76	W. E. Cleveland, Louisiana State University, Baton Rouge	Structure of ^{194}Pt

Date	Speaker and affiliation	Topic
4/22/76	Reginald Ronningen, Vanderbilt University/ORNL	Recent Coulomb Excitation Studies in the Rare-Earth Region
5/3/76	Hans Jörg Mang, Technical University of Munich, Germany	A Single-Particle Model for Rotational States
5/4/76	M. E. Hamm, Texas A & M University, College Station, Texas	Nuclear Spectroscopy with Heavy-Ion-Induced Multi-Nucleon Transfer Reactions
5/13/76	M. Danos, National Bureau of Standards, Washington, D.C.	Nuclear Shock Waves: Yes and No
5/13/76	Burke Ritchie, University of Alabama, University	Theory of the Angular Distribution of Molecular Photoelectrons
6/7/76	Arnold R. Bodmer, Argonne National Laboratory, Argonne, Illinois	Classical Microscopic Calculations of High-Energy Collisions of Heavy Ions
6/8/76	L. Wilets, University of Washington, Seattle	Semiclassical Calculation of the Nuclear Many-Body Problem for Heavy-Ion Collisions
6/22/76	P. J. Twin, University of Liverpool	Gamma-Ray Spectroscopy in Ni and Zn Isotopes
6/24/76	R. Y. Cusson, Duke University, Durham, North Carolina	Three-Dimensional Time-Dependent Hartree-Fock Calculations of Heavy-Ion Reactions
6/29/76	R. Babinet C.E.N. de Saclay, France	Deep Inelastic Collisions – The Approach to Equilibrium in the $^{40}Ar + ^{58}Ni$ System
7/1/76	J. R. Bird, Australian AEC Research Establishment, Lucas Heights	Recent Developments in Prompt Nuclear Analysis
7/8/76	G. Siegert, Institut Laue Langevin, Grenoble, France	Current Research at the Institut Laue Langevin and Recent Fission Charge Distribution Results
7/12/76	V. G. Soloviev, Joint Institute of Nuclear Research, Dubna	Some Aspects of Nuclear Reaction Theory
7/12/76	V. I. Lushchikov, Joint Institute of Nuclear Research, Dubna	Ultra-Cold Neutrons
7/14/76	A. M. Lane, AERE, Harwell	Theoretical Approaches to Giant Multipoles
7/15/76	James Byrne, University of Sussex	Measuring the Neutron Lifetime
7/22/76	P. Colombani, Lawrence Berkeley Laboratory, Berkeley, California, and Institute of Nuclear Physics, Orsay, France	Subcoulomb-Fission Induced by Xe and Kr Ions
9/23/76	Michael Howard, Lawrence Livermore Laboratory, Livermore, California	Heavy-Ion Reactions of Astrophysical Interest
9/30/76	Alan Goodman, Tulane University, New Orleans, Louisiana	Microscopic Calculations of Backbending in Nuclei
10/1/76	John Zabolitzky, University of Bochum, West Germany	Many-Body Theory and Mesonic Degrees of Freedom in Finite Nuclei
10/7/76	Z. Switkowski, Niels Bohr Institute, Copenhagen, Denmark	Sub-Barrier Heavy-Ion Fusion
10/14/76	Cleland H. Johnson, ORNL	Observation of Single-Particle Proton States Quasibound by the Coulomb Potential

Date	Speaker and affiliation	Topic
11/3/76	J. A. Cookson, AERE, Harwell	Analysis Using Focused Beams of Nuclear Particles, with Comments on Search for Superheavy Elements
1/6/77	Aaron Galonsky, Michigan State University, East Lansing	Giant Fermi and Giant Gamow-Teller Transitions in (p,n) Reactions
1/13/77	Dave Crandall, ORNL	Atomic Collision Cross Sections for Plasma Application
1/17/77	Reinhard Simon, Lawrence Berkeley Laboratory, Berkeley, California	Experimental Studies of High-Spin Nuclear States
1/27/77	E. L. Hart, University of Tennessee, Knoxville	Quarks with Color, Flavor, and Charm
2/3/77	Taro Tamura, University of Texas, Austin	Multi-Step Direct-Reaction Treatment of Deep Inelastic Reactions
2/10/77	H. C. Britt, Los Alamos Scientific Laboratory, Los Alamos, New Mexico	Fission Studies Using Direct Reactions
2/24/77	Peggy L. Dyer, University of Washington, Seattle	Angular Momentum Transfer in the $^{86}Kr + ^{209}Bi$ Reaction
3/3/77	I. Sellin, University of Tennessee, Knoxville	Highly Ionized Ions and Their Symmetric Collision Interactions
3/10/77	Fred R. Mynatt, Neutron Physics Division, ORNL	The Accelerator Breeder as an Alternate to the LMFBR
3/24/77	I. Y. Lee, University of California, Berkeley	Coulomb Excitation of Pt Isotopes with Xe Beam
3/25/77	R. Y. Cusson, Duke University, Durham, North Carolina	Quantal Theory of Heavy-Ion Collisions Using a 3-Dimensional TDHF Scheme
3/31/77	C. J. Herrlander, Michigan State University, East Lansing	High-Spin States and Quadrupole Interaction in the Lead Region
4/5/77	J. W. Hugg, Stanford University, Stanford, California	Nuclear Moments of Conjugate Nuclei
4/7/77	O. F. Nemets, Institute of Nuclear Research of the Ukrainian SSR, Kiev	Measurement of g Factors of Excited States
4/13/77	A. Faessler, Kernforschungsanlage Jülich, West Germany	Spins, High Spins, and Very High Spins in Nuclei
4/21/77	G. T. Garvey, Argonne National Laboratory, Argonne, Illinois	Are There Any First-Class Experiments on Second-Class Currents?
5/2/77	D. J. Malbrough, University of South Carolina, Columbia	π^+-Nucleus Elastic Scattering at Low Energies
5/3/77	L. Peker, Vrije Universiteit, Amsterdam, Netherlands	Backbending and the $g_{9/2}$ Shell
5/9/77	C. Mahaux, Université de Liège, Liège, Belgium	Calculation of the Complex Optical-Model Potential from a Realistic Nucleon-Nucleon Interaction
5/19/77	S. Raman, Physics Division, ORNL	Where Have All the $M1$ Strengths Gone in ^{208}Pb?

COLLOQUIA AND SEMINARS PRESENTED AT OTHER INSTITUTIONS

Staff members of the Physics Division and other scientists associated with the Division frequently receive invitations to present seminars and colloquia at institutions both in the United States and abroad. Partial support for some of the requests was provided through the Traveling Lecture Program (TLP) administered by Oak Ridge Associated Universities.

Following is a list of seminars and colloquia presented in 1976-77:

G. D. Alton - Murray State University, February 11, 1976, "Ion Sources"

J. B. Ball - University of Rochester, September 17, 1976, "The User Mode in Nuclear Physics"; Case Western Reserve University, November 18, 1976, "Heavy-Ion Research and the New Accelerator Facility at Oak Ridge"; Michigan State University, February 18, 1977, "Status Report on the Heavy-Ion Facility at Oak Ridge"

C. F. Barnett - Battelle Research Laboratory, February 6, 1976, "The Role of Atomic Physics in the Controlled Thermonuclear Research Program"

F. E. Bertrand - Institut für Kernphysik, Jülich, West Germany, May 24, 1976, "The New Giant Resonances"; Max-Planck-Institut für Kernphysik, Heidelberg, West Germany, May 26, 1976, "Excitation of Giant Resonances via Inelastic Scattering"; Institut de Physique Nucleaire, Orsay, France, May 31, 1976, "The New Giant Resonances"; Niels Bohr Institute, Copenhagen, Denmark, June 21, 1976, "The Giant Quadrupole Resonance 1976"; Kernfysisch Versneller Instituut, Groningen, Netherlands, July 21, 1976, "The Nuclear Continuum - Theory and Experiment"; Kernfysisch Versneller Instituut, Groningen, Netherlands, August 10, 1976, "The New Giant Resonances"

T. A. Carlson - Auburn University, January 12, 1976, "Angular Distribution in Photoelectron Spectroscopy"; Research Institute of Physics - Stockholm, May 12, 1977, "Angular Distribution in Photoelectron Spectroscopy"; University of Linköping, May 16, 1977, "Angular Distribution in Photoelectron Spectroscopy"; Los Alamos Laboratory Colloquium, June 28, 1977, "Electron Spectroscopy and Its Applications"

D. H. Crandall - Stanford Research Laboratory, October 29, 1976, "Collision Cross Sections for Plasma Applications"; Regional Meeting of Society for Physics Students, Murray, Kentucky, April 16, 1977, "Atomic Physics Processes in High-Temperature Plasmas - Fusion and Astrophysics"

J. L. Fowler - University of Tennessee, April 21, 1976, "Resonance Structure of ^{208}Pb from Neutron Scattering"; Vanderbilt University, October 16, 1976, "Nuclear Physics and Energy"; University of Tennessee, May 9, 1977, "Neutron-Proton Scattering and Nucleon-Nucleon Interaction"

C. B. Fulmer - Drexel University, April 30, 1976, "Some Heavy-Ion Experiments at Oak Ridge"

Jorge Gomez del Campo - University of North Carolina, March 24, 1977, "Fusion Reactions of ^{12}C with ^{14}N"

E. E. Gross - Iowa State University, March 22, 1976, "Heavy-Ion Research at the ORIC"; University of Strasbourg, Strasbourg, France, June 3; University of Göttingen, Göttingen, West Germany, June 6; Institute for Nuclear Physics, Jülich, Germany, June 8; Niels Bohr Institute, Copenhagen, Denmark, June 13; University of Groningen, Groningen, Netherlands, week of June 18.

M. L. Halbert - Washington University, Department of Chemistry, December 9, 1976, "Strongly Damped Collisions of Heavy Ions"

J. A. Harvey - Lowell University, October 20, 1976, "Fast Neutron Physics (Basic and Applied) at the ORELA"

D. P. Hutchinson—University of Mississippi, February 25-26, 1976, "Design of High-Power Sub-Millimeter Lasers for Plasma Diagnostics" and "The Tokomak, a Promising Fusion Device"; Medical University of South Carolina, November 17, 1976, "The Tokomak, a Promising Fusion Device"; The Citadel, November 17, 1976, "The Development of High-Power, Far-Infrared Lasers for Plasma Diagnostics"; Hardin-Simmons University, February 21, 1977, "The Tokomak, a Promising Fusion Device"; Vanderbilt University, March 25, 1977, "The Development of High Power for Infrared Lasers"; University of Puerto Rico, Mayaguez, April 6, 1977, "The Tokomak, a Promising Fusion Device"

J. W. Johnson—Florida State University, November 3-5, 1976, "Evaluation of Vacuum Components for Beam Lines for the ORNL 25-MV Heavy-Ion Accelerator"

N. R. Johnson—William and Mary College, February 7, 1976, "High Angular Momentum States in Nuclei"; American Chemical Society, New York, April 5-9, 1976, "$B(E2)$ Information on High-Spin Rotational States from Doppler-Shift Lifetime Measurements"; Brookhaven National Laboratory, April 13, 1976, "Coulomb Excitation and Lifetime Measurements of High Angular Momentum States in Deformed Nuclei"; Emory University, May 18, 1976, "Properties of High Angular Momentum States in Deformed Nuclei" (TLP); University of Kentucky, February 8, 1977, "New Insight into the Properties of High Angular Momentum States in Nuclei"; University of Paris, South Orsay, France, February 24, 1977, "Report on the Heavy-Ion Accelerator Project at Oak Ridge"; University of Bordeaux, Bordeaux, France, March 11, 1977, "Properties of ^{164}Er in the Backbend Region" and "Report on the Heavy-Ion Accelerator Project at Oak Ridge"; Research Institute of Physics, Stockholm, Sweden, March 16, 1977, "Report on the Heavy-Ion Accelerator Project at Oak Ridge" and "Lifetime and Coulomb Excitation Measurements on High Angular Momentum States in Deformed Nuclei"

C. H. Johnson—University of Kentucky, October 15, 1976, "Unbound Single-Particle Proton States in Tin: The First Observation of Energy-Dependent Size Resonances"; University of Minnesota, October 25, 1976, "Unbound Single-Particle Proton States in Tin: The First Observation of Energy-Dependent Size Resonances"

R. L. Macklin—Los Alamos Scientific Laboratory, August 5, 1976, "Neutron Capture at the ORELA"

J. A. Maruhn—Michigan State University, March 31, 1976, "Non-Head-on Collisions of ^{16}O + ^{16}O in a TDHF Description"; University of Frankfurt, Germany, February 19, 1977, "The Time-Dependent Hartree-Fock Model of Heavy-Ion Collisions" and "Hydrodynamical Calculations for Heavy-Ion Collisions"

C. D. Moak—Institute of Physics, University of Aarhus, Denmark, February 1976, "Nanosecond Ion Pulse Detection for Tandem Accelerators"; University of Witwatersrand, Johannesburg, South Africa, March 1976, "The Accelerator Atomic Physics Program at ORNL"; Australian National University, Canberra, Australia, March 1976, "Heavy-Ion Charge States"

H. W. Morgan—Tennessee Technological Institute, February 26, 1976; Armstrong State College, March 16, 1976; Coastal Empire Section, ACS,[1] March 17, 1976; South Carolina Section, ACS,[1] March 18, 1976; Ball State University, June 21, 1976; Dayton Section, ACS,[1] February 8, 1977; Marietta College,[1] February 9, 1977; Fairmont College,[1] February 10, 1977; West Virginia State College,[1] February 10, 1977; Central Ohio Section, ACS,[1] February 11, 1977, "Coherent Light and Holography" (Lectures sponsored by American Chemical Society lecture program[1]); Sloan-Kettering Research Institute, February 8, 1976; Loyola University, November 16, 1977, "Sub-millimeter Waves"

F. E. Obenshain—Auburn University, February 27, 1976, "The Mössbauer Effect: Studies of Hyperfine Interactions in Metals and Alloys" (TLP); University of Alabama, February 25, 1976, "Experimental Test of Weyl's Gauge Invariant Geometry" (TLP); Florida Technological University (TLP), April 13, 1976; Florida A & M University, April 14, 1976, "The Mössbauer Effect: Studies of Hyperfine Interactions in Metals and Alloys" (TLP)

F. Plasil—C.E.N., Saclay, September 15, 1976, "Réactions Induites par ^{86}Kr"; G.S.I., Darmstadt, West Germany, January 14, 1977, "Heavy-Ion Experiments at Oak Ridge and Berkeley"

S. Raman—Los Alamos Scientific Laboratory, July 22, 1976, and Livermore Laboratory, July 29, 1976, "An Overview of the Research Program at the ORELA"; University of Tennessee, November 9, 1976; Lawrence Berkeley Laboratory, December 14, 1976; Brookhaven National Laboratory, January 11, 1977; Vanderbilt University (TLP), February 11, 1977; Louisiana State University, February 25, 1977; Michigan State University, February 28, 1977; Florida State University (TLP), March 4, 1977; and Georgia State University (TLP), April 18, 1977, "Search for Superheavy Elements"

L. D. Rickertsen—Murray State University, April 19, 1976, "Computer Simulation of Nuclear Heavy-Ion Scattering"

R. L. Robinson—The Citadel, February 9, 1976, "The Heavy-Ion Accelerator Facility at ORNL"

M. J. Saltmarsh—The Institute of Experimental Nuclear Physics, Karlsruhe Nuclear Center, Germany, February 16, 1977, "*d*,Li Neutron Sources"

G. R. Satchler—Daresbury Laboratory, England, September 1, 1976, "Giant Resonances" and "Heavy-Ion Scattering"; International School of Physics "Enrico Fermi," Varenna, Italy, July 26-August 7, 1976, "The Study of Giant Resonances in Nuclei by Inelastic Scattering"

E. J. Spejewski—Florida State University, December 2, 1976, "The Study of Nuclei Far from Stability"

R. G. Stokstad—Yale University, July 26, 1976, "Fusion of $^{12}C + {}^{14}N$ and the Liquid Drop Limit"; California Institute of Technology, November 17, 1976, "Fusion of Light Nuclei"; Chalk River Nuclear Laboratories, January 26, 1977, "Fusion Reactions with Light Nuclei"; Laboratoire de Physique Nucleaire, Universite de Montreal, January 27, 1977, "The Question of Intermediate Resonances"; Washington University, February 10, "Fusion of Light Nuclei at High Energies"; University of Rochester, April 20, 1977, "Pre-Scission Cooling in Strongly Damped Collisions"

K. S. Toth—Virginia Polytechnic Institute and State University, April 7, 1977, "Heavy-Element Research at Dubna, Berkeley, and Elsewhere"

T. A. Welton—University of South Carolina, February 5, 1976, "Seeing Atoms with the Computer"

C. Y. Wong—McGill University, April 13, 1976, "Dynamics of Nuclear Fluid in Heavy-Ion Collisions"; College of William and Mary, September 24, 1976, "Nuclear Fluid Dynamics"; University of Tennessee, February 1, 1977, "Schrödinger Equation Revisited"

[1]Out of the country at the time of the 1976 meeting.

ANNUAL INFORMATION MEETING

The 1976 Physics Division Information Meeting was held on June 9 and 10. Members of the Advisory Committee were:

C. K. Bockelman, Yale University
R. E. Chrien, Brookhaven National Laboratory
Alexander Dalgarno, Center for Astrophysics
H. A. Enge, Massachusetts Institute of Technology
J. R. Nix, Los Alamos Scientific Laboratory
H. E. Wegner,[1] Brookhaven National Laboratory

[1]Out of the country at the time of the 1976 meeting.